Investigation of haematopoietic stem cell homing post-transplantation, using an in *vitro* model of the bone marrow/vasculature interface

SULTAN ALMALKI

This thesis is submitted in partial fulfilment of the requirements of the University of the West of England for the degree of Doctor of Philosophy in Biomedical Science

Faculty of Health and Applied Sciences, University of the West of England

June 25, 2021

I. Author's declaration

This Report is submitted in fulfilment of the requirements of the PhD Project, and except where duly acknowledged or referenced it is entirely my own work. It has not been submitted, either in whole or in part, for any other award at the University of the West of England or elsewhere.

Signed ..... Date .../..../…

June 25, 2021

II. Project supervisors' declaration

We confirm that we have read this Project Report and that the work it describes was undertaken under my supervision.

Dr Ruth Morse
Senior Lecturer in Biomedical Sciences (Human & Clinical Genetics)
University of the West of England, Bristol
Faculty of Health and Life Sciences
Tel: 0117-3282022
Email: ruth.morse@uwe.ac.uk

Signed ..... Date ...../...../.....

Dr Elizabeth Anderson
Senior Lecturer in Haematology
University of the West of England, Bristol
Faculty of Health and Life Sciences
Tel: 0117-3287627
Email: Elizabeth3.Anderson@uwe.ac.uk

Signed ..... Date ...../...../.....

III. Abstract

Homing of haematopoietic stem cells (HSCs) to the bone marrow (BM) niches after transplantation (HSCT) is controlled by chemotactic signalling released from the BM microenvironment. This process is incompletely understood, but some factors are known, such as stromal cell-derived factor 1 alpha (SDF-1 α). Studies have shown that HSCs naturally mobilise to sites of ischaemic injury and since the BM microenvironment is hypoxic, it has been theorised that the mandatory conditioning chemotherapy for HSCT might play a role in stem cell homing, by producing an "injury" in the hypoxic BM. This injury leads to the release of chemotactic factors which might induce HSCs to traffic to the BM niches. This combination of chemotherapy and hypoxia in the BM microenvironment is often underestimated *in vitro*; however, adding the hypoxia element might provide a novel candidate that previously has been overlooked.

A novel model of HSC homing has been developed, using HL-60 cells as HSC equivalent, which traffic through a vasculature endothelium (HMEC-1) on a hanging transwell insert, to reach the BM (HS-5) in hypoxia and compared to normoxic conditions. Transmigrated HL-60 cells were monitored under the influence of SDF-1 or conditioned medium (C.M.) from HS-5 after treatment with clinically relevant doses and low intensity conditioning therapy (melphalan, carmustine, etoposide and cytarabine) and targeted therapies (ibrutinib and imatinib) in hypoxic and normoxic environments.

Herein, peptide-based chemokine signalling factors released by HS-5 post-chemotherapy exposure were explored using proteomics analysis. HS-5 C.M. were analysed after treatment with a combination of conditioning therapy (BEAM) in hypoxia and normoxia to identify the chemokines accounting for the functional effects of the cell secretome. For the first time, this approach led to the recognition

of distinct functions associated with HS-5 secretome according to the treatment conditions. In hypoxia, 25 proteins were upregulated, predominantly related to stress and response to hypoxia. For BEAM treatment plus hypoxia 31 proteins were upregulated, evidencing a secretome linked to stress, hypoxia, angiogenesis, localisation, cell migration and vascular permeability. These findings suggest that conditioning therapy might be strongly involved in manipulating vascular endothelium and facilitating HSCs trafficking.

In addition, some candidate proteins were obtained as a recombinant and tested in the transmigration model. MMP-1, MMP-3 and AMOT were investigated for their ability to act as inducers for HL-60 transmigration. Both MMP-1 and MMP-3 were shown to affect the barrier integrity by loosening the endothelial membrane; MMP-1 was shown to have an extra role in inducing HL-60 trafficking actively. Conversely, AMOT was shown to affect the endothelium integrity without inducing HL-60 trafficking. However, both MMPs and AMOT were shown to have more potency in combination with SDF-1α.

Finally, several proteins were upregulated after exposing HS-5 to conditioning therapy and hypoxia, suggesting that HSC homing is a complex process that involves several factors aside from SDF-1α. These factors might be effective inducers for HSCs homing to the BM microenvironment for a limited time, which can be utilised to infuse the donated graft to have better engraftment.

IV. Acknowledgement

It is my great pleasure to acknowledge many people who made this work possible. This work could not have been accomplished without the support and encouragement of my supervisors, Dr Ruth Morse and Dr Elizabeth Anderson. I would like to thank them for their valuable support; despite an extremely busy eventful few years, they were able to make time to discuss my research extensively, giving valuable suggestions and constructive criticism. They have provided a perfect balance of project guidance and support while still allowing me the freedom to work and progress the project independently, which has been optimum for my development as a researcher, and I am very grateful for everything they have done.

I am also very much thankful to all technical staff of CRIB lab with no exception, for the assistance and technical guidance during my research. I am grateful to Dr David Patton, for his help with scanning electron microscopy.

Besides, I would like to express my appreciation to all my research team members and colleagues, particularly the PhD students, for their sustained support and valuable guidance throughout my research programme.

I would like to thank my family for their unconditional support and believe in my ability to accomplish my full potential; without their support, I would have been distressed and lose track of my goals.

I am very much grateful for the Saudi cultural bureau and King Abdullah medical city for giving me this opportunity and sponsoring my scholarship.

V. Table of contents

VI. List of Figures

VII. List of Tables

VIII. Abbreviations

˚C	Degrees Celsius
Ab	Antibody
ADM	Adrenomedullin
AGM	Aorta-gonad-mesonephros
ANGPTL4	Angiopoietin-related protein 4
ANXA2	Annexin A2
ASCT	Autologous stem cell transplant
ATCC	American Type Culture Collection
ATP	Adenosine triphosphate
BEAM	Carmustine (BiCNU®), Etoposide, Cytarabine (Ara-C), Melphalan)
BM	Bone marrow
BM-MSC	Bone marrow mesenchymal stem cell
BMEC	Bone marrow endothelial cells
C.M.	Conditioned medium
C.L.	Cell lysate
CLP	Common lymphoid progenitor
C1P	Ceramide-1-phosphate
CAM	Cell adhesion molecule
CCL20	C-C Motif Chemokine Ligand 20
CCR6	C-C chemokine receptor type 6
CD	Cluster of differentiation
CFU-F	Colony forming unit fibroblast

cm	Centimetre
CMP	Common myeloid progenitor
CXCL12	C-X-C Motif Chemokine Ligand 12
DMEM-HG	Dulbecco's Modified Eagle Medium high glucose
DMSO	Dimethyl sulphoxide
DNA	Deoxyribonucleic acid
EDTA	Ethylenediaminetetraacetic acid
ELISA	Enzyme Linked Immunosorbent Assay
F-12K	Kaighn's Modification of Ham's F-12 Medium
FBS	Foetal bovine serum
FDR	False discovery rate
FGF-4	Endothelium-derived fibroblast growth factor 4
FITC	Fluorescein isothiocyanate
G-CSF	Granulocyte colony stimulating factor
g/dl	Grams per decilitre
g/L	Grams per litre
GM-CSF	Granulocyte-macrophage colony stimulating factor
GMP	Granulocyte‐macrophage progenitor
GVHD	Graft versus host disease
GVL	Graft versus leukaemia effect
HL-60	Human leukaemia cell line
HLA-DR	Human Leukocyte Antigen – DR isotype
HMEC-1	Human Microvascular Endothelial Cell line-1
HPCs	Haematopoietic progenitor cells

Hrs	Hour (s)
HS-5	Human bone marrow stromal cell lines
HSCs	Haematopoietic stem cells
HSCT	Haematopoietic stem cell transplantation
HUVEC	Human umbilical vein endothelial cells
I.U	International unit
Ig	Immunoglobulin
IL	Interleukin
ISCT	International Society for Cellular Therapy
KL	Kit ligand
LFA-1	Lymphocyte function associated antigen-1
LMPP	Lymphoid-primed multipotent progenitor
LOXL2	Lysyl oxidase homolog 2
M-CSF	Macrophage colony stimulating factor
MEP	Megakaryocyte-erythroid progenitor
Min	Minute(s)
MIP-1α	Macrophage inflammatory protein-1 alpha
mmol/L	Millimoles per litre
MMP	Matrix metallopeptidase
MPPs	Multipotential progenitors
MSC	Mesenchymal stem cell
nM	Nanomolar
PB	Peripheral blood
PET	Polyethylene terephthalate

pg/ml	Picograms per millilitre
PLOD1	Procollagen-lysine, 2-oxoglutarate 5-dioxygenase 1
PLOD2	Procollagen-lysine, 2-oxoglutarate 5-dioxygenase 2
PSGL-1	P-selectin glycoprotein ligand 1
RBC	Red blood cells
S1P	Sphingosine-1-phosphate
SD	The standard deviation of the mean
SDF-1	Stromal cell-derived factor 1
sKITL	Soluble KIT ligand
SNOs	Osteoblasts expressing spindle-shaped N-cadherin
STC1	Stanniocalcin-1
STC2	Stanniocalcin-2
TBI	Total body irradiation
U/ml	International unit per millilitre
UCB	Umbilical cord blood
UTP	Uridine triphosphate
VCAM-1	Vascular cell adhesion molecule 1
VEGFA	Vascular endothelial growth factor-A
VLA-4	Very late antigen 4
WBC	White blood cells
µg	Microgram
µg/ml	Micrograms per millilitre
µl	Microlitre
µM	Micro molar

µm	Micrometre
Ω cm^2	Ohm Square Centimeter

Chapter 1: Introduction

1.1 Bone marrow structure and function

Bone marrow (BM) is one of the largest organs in the body, consisting of spongy and soft connective tissues located within the trabecular areas of long and flat bone cavities. It is the most important site of blood cells production (haematopoiesis; Figure 1-1) that starts from the 6th to 7th month of foetal life, which then shifts to be the primary site of haematopoiesis during childhood and adult life (Kawahara, 2007; Hoffbrand and Moss, 2011). Haematopoiesis may be divided into two developmental processes; primitive haematopoiesis and definitive haematopoiesis. Primitive haematopoiesis begins at embryonic days 18-20 through week 8 in which the first human haematopoietic cells, including primitive erythroid cells and monocytes/macrophages, are produced in the blood islands of the yolk sac and the embryo proper (Ivanovs *et al*., 2017; Julien, El Omar and Tavian, 2016). After the onset of cardiac contractions at day 21 and later stages of embryogenesis, yolk sac-derived haematopoietic cells are circulated throughout the developing embryo. Primitive haematopoietic cells can then be found in the major arteries of the embryo, including the vitelline artery and the ventral wall of the dorsal aorta from days 27-42 (Ivanovs *et al*., 2017). On the other hand, definitive haematopoiesis occurs after primitive haematopoiesis, in which haematopoietic stem cells (HSCs) can be generated at different anatomical sites involving the vasculature. Definitive haematopoietic progenitors can be produced in the aorta-gonad-mesonephros (AGM) region of the embryo proper, usually occurring in the dorsal aorta (Kumar, D'Souza and Thakur, 2019). However, the AGM region is considered as the primary site of definitive haematopoiesis throughout the mid-stage gestational development. Subsequently, the foetal liver replaces the yolk sac and AGM region as the main haematopoietic site,

besides the spleen and lymph nodes. In a fully developed embryo, HSCs migrate to the foetal liver temporarily and finally expand in the BM to initiate definitive haematopoiesis and self-renewal during postnatal and adult life (Zambidis *et al*., 2005). During childhood, the most common haematopoiesis sites are the proximal ends of long bones, primarily the femur, tibia and fibula (Mahajan et al., 2015). In adults, haematopoiesis transitions to the pelvis, sternum, cranium and vertebrae (Hayman *et al*., 2011).

Bone marrow consists of a meshwork of bone trabeculae containing haematopoietic (red marrow) and fat (yellow marrow) cells. The ratio between these two elements depends on the age and activity of bone marrow in response to various physiological stimuli. However, marrow cellularity is roughly inversely proportional to age (Małkiewicz and Dziedzic, 2012). Thus, newborns have higher cellular bone marrow and hence more haematopoietically active marrow, compared to older individuals. The composition of the bone marrow microenvironment is complex; it includes multiple different cell populations that have been shown to participate in normal haematopoietic stem and progenitor cell support. HSCs, the precursor of all blood cells, are characterised by their self-renewal, and capacity to differentiate into single or multiple types of daughter cells. HSCs normally reside in close association with bone marrow osteoblasts in the endosteal niche (osteoblastic niche) and in proximity to BM sinusoidal vessels (vascular niche). HSCs undergo lineage commitments and extensive proliferation, until reaching full differentiation (Figure 1-1; MacLean, Lo Celso and Stumpf, 2017). HSCs have the potential to differentiate into several lymphoid and myeloid haematopoietic cell lineages, and to provide a future supply of functionally differentiated mature blood cells. However, developmental pathways of lymphoid and myeloid lineages are controlled tightly by several transcription factors

as a response to growth and conditions such as haemorrhage or disease (Kondo, 2010). The lineage branches in the haematopoietic hierarchical system starts with long-term haematopoietic stem cells (LT-HSCs) which give rise to short-term haematopoietic stem cells (ST-HSCs) which then commit into multipotent progenitors (MPPs). At this point, part of these MPPs start to branch and commit into common myeloid progenitors (CMP) which can further differentiate into megakaryocyte-erythrocyte progenitors (MEP) and granulocyte-macrophage progenitors (GMP). On the other hand, some of the MPPs differentiate into the common lymphoid progenitor (CLP) via lymphoid-primed multipotent progenitors (LMPP) and give rise to mature dendritic cells, T- and B-cells, and NK cells (MacLean, Lo Celso and Stumpf, 2017; Singh and Cancelas, 2020).

However, recent trends in technologies have identified other lineages and alternate pathways; thus, it might be wrong to think of a committed or stable cell lineage. Several alternative pathways have been discovered by recent studies, challenging the classical models of the adult haematopoietic hierarchy. HSCs were shown to differentiate directly into erythroid and megakaryocyte lineages, bypassing the oligopotent progenitor's CMP intermediate stage as demonstrated by Notta *et al*., (2016) in their newly developed cell-sorting scheme. This finding was supported by another study by Velten *et al*., (2017) of human HSCs, showing that unilineage-restricted cells might emerge directly from a "Continuum of LOw primed UnDifferentiated haematopoietic stem- and progenitor cells" (CLOUD-HSPCs). A recent study by Belluschi *et al*., (2018) showed that in humans, the first lineage restriction events occur within the HSC's compartment in which myelo-lymphoid committed cells with no erythroid differentiation capacity were generated. However, in murine models, it was long observed that HSCs can differentiate into LMPP lacking

any megakaryocyte-erythroid potential with downregulation of megakaryocyte-erythroid genes and upregulation of common lymphoid genes as cells progress from HSCs to LMPPs (Månsson *et al*., 2007). On the other hand, myeloid-restricted progenitors which are lineage-committed to megakaryocytes, megakaryocyte-erythroid cells, or common myeloid cells were found in the phenotypically defined HSC compartment together with HSCs as demonstrated by Yamamoto *et al*., (2013). However, this observation in murine models might be applicable for humans; in 2011, a gene expression study by Novershtern *et al*., showed that transcriptional state of the megakaryocyte/erythrocytes was maintained in some of the early progenitors, suggesting a close relationship between HSCs and early progenitors of the megakaryocyte/erythrocytes in which lineage specification of the erythroid and megakaryocyte might occur early in the hierarchy at either the stem or multipotential progenitor stage.

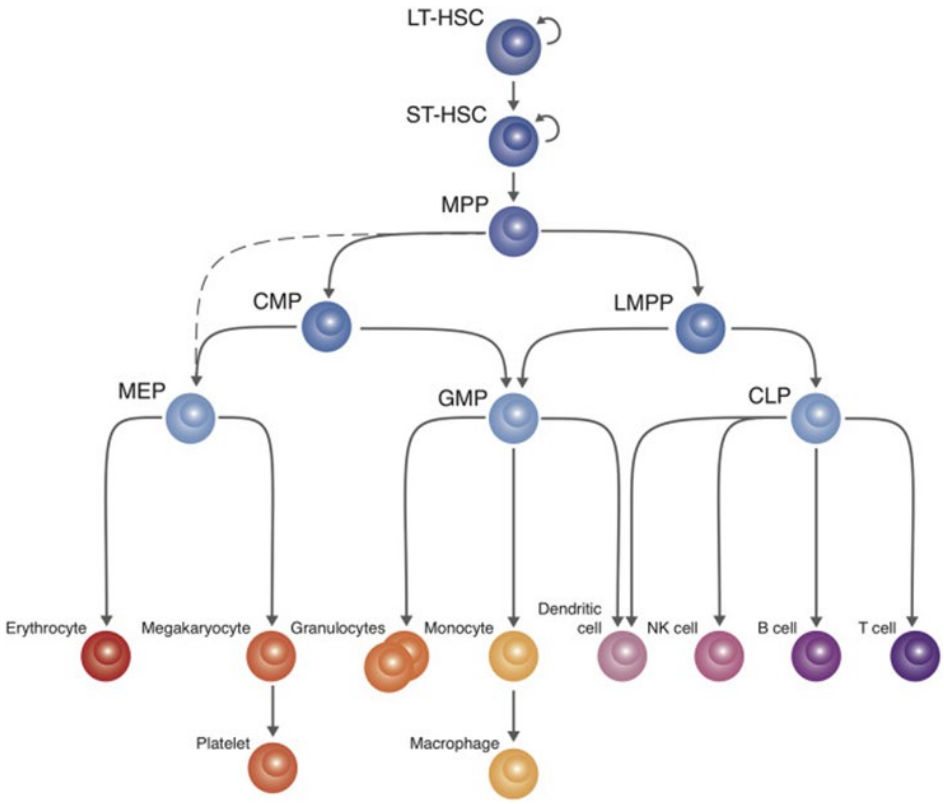

Figure 1-1 Haematopoiesis; general concept of blood cell formation.

All cellular blood components are derived from pluripotent HSCs which reside in specialised niches. Cellular differentiation starts from the stem cell via committed haematopoietic progenitors which are restricted in their developmental potential. Putative transition indicated by dashed arrow. LT, long term; ST, short term; HSCs, haematopoietic stem cells; CLP, common lymphoid progenitor; CMP, common myeloid progenitor; GMP, granulocyte-macrophage progenitor; LMPP, lymphoid-primed multipotent progenitor; MEP, megakaryocyte-erythroid progenitor; NK, natural killer. (MacLean, Lo Celso and Stumpf, 2017).

1.2 Bone marrow microenvironment and stem cell niche

The microenvironment of the BM is a complex structure, composed of different cellular components (osteoblast, osteocyte, adipocyte, fibroblast and haematopoietic cells) and extracellular matrix proteins (Panaroni *et al.*, 2014). It is formed by mesenchymal stem cells (MSCs) which are multipotent stem cells with trilineage differentiation capacity into osteoblasts, chondrocytes and adipocytes. HSCs commonly reside in specialised niches within the adult BM; a stem-cell niche can be defined as a spatial structure in which stem cells are contained and maintained by allowing self-renewal in the absence of differentiation (Wilson and Trumpp, 2006).

Those niches are composed of a specific population of cells that play an essential role in regulating adult stem cell self-renewal and differentiation. Osteoblasts and haematopoietic cells are closely associated in the bone marrow, suggesting a combined relationship between the two. Quiescent and slow-cycling HSCs have been identified close to the endosteal surface in the trabecular bone, making a reservoir of HSCs that can be mobilised and restore the haematopoiesis in response to tissue injury, whereas, HSCs located at the perivascular side are more active (Levesque *et al*., 2010; Asada *et al*., 2017; Mendelson and Frenette, 2014). HSCs also interact with other stromal cells, including endothelial cells as part of the vascular niche. The vascular niche promotes proliferation, differentiation, and short-term HSCs which have limited self-renewal activity (Levesque *et al*., 2010). Endosteal bone surfaces are lined with stromal cells called 'osteoblasts expressing spindle-shaped N-cadherin' (SNOs) which maintain quiescence and prevent differentiation of attached HSCs in the quiescent and self-renewing endosteal niche; these niches are maintaining long-term dormant and self-renewing HSCs. In response to injury, quiescent HSCs might be activated and recruited to the vascular niche. Self-renewing HSCs produce MPPs either by divisional or environmental asymmetry, and provide the vascular niche with new HSCs. In the vascular niche, HSCs promote differentiation to megakaryocytes, erythrocytes and other myeloid cells. MPPs can give rise to all haematopoietic lineages, including B-cell precursors and T-cell precursors. B-cell precursors can attach to CXCL12-expressing stromal cells through the CXCR4 receptor, and T-cell precursors migrate to the thymus to promote T-cell maturation (Wilson & Trumpp, 2006). Deficiency in either CXCL12 or CXCR4 leads to a decrease in cell retention in the BM and mobilization of B-cell precursors to the blood circulation (Nie *et al*., 2004).

The balance that controls between self-renewal and differentiation of HSCs in the

bone marrow is mediated by several factors (Figure 1-2). When the level of stromal cell-derived factor 1 (SDF-1; also known as CXCL12) in the BM microenvironment reduces, a portion of the HSC daughter cells leave the niche and begin to mobilise to the circulation (Wang and Ema, 2016). However, HSC mobilisation might occur due to downregulation of receptors like CXCR4 and Robo4, as demonstrated by Smith-Berdan *et al.* (2011). Conversely, HSC homing is the reverse of mobilisation, occurring in response to elevated levels of SDF-1 in the microenvironment (Wang and Ema, 2016). Recruitment of haematopoietic progenitor cells (HPCs) to the vascular niche may depend on endothelium-derived fibroblast growth factor 4 (FGF-4) and SDF-1. An elevated level of FGF-4 and oxygen concentration might play a fundamental role in recruitment, proliferation, and differentiation of HSCs/HPCs as they progress from the osteoblastic niche to the vascular niche. FGF-4 and oxygen concentration gradients increase as the cells progress from the osteoblastic niche to the vascular niche (Yin and Li, 2006). However, it has been observed that the BM *in vivo* is a hypoxic environment (Spencer *et al*., 2014; Nombela-Arrieta and Silberstein, 2014). Under stress conditions like thrombocytopenia, SDF-1 and vascular endothelial growth factor (VEGF) activate matrix metallopeptidase 9 (MMP-9), which converts membrane-associated Kit ligand into soluble Kit ligand (sKitL). This process, in turn, promotes HSCs entry into the cell cycle, mobilisation to the vascular niche, and differentiation (Avraham *et al*., 1994; Heissig *et al.*, 2002).

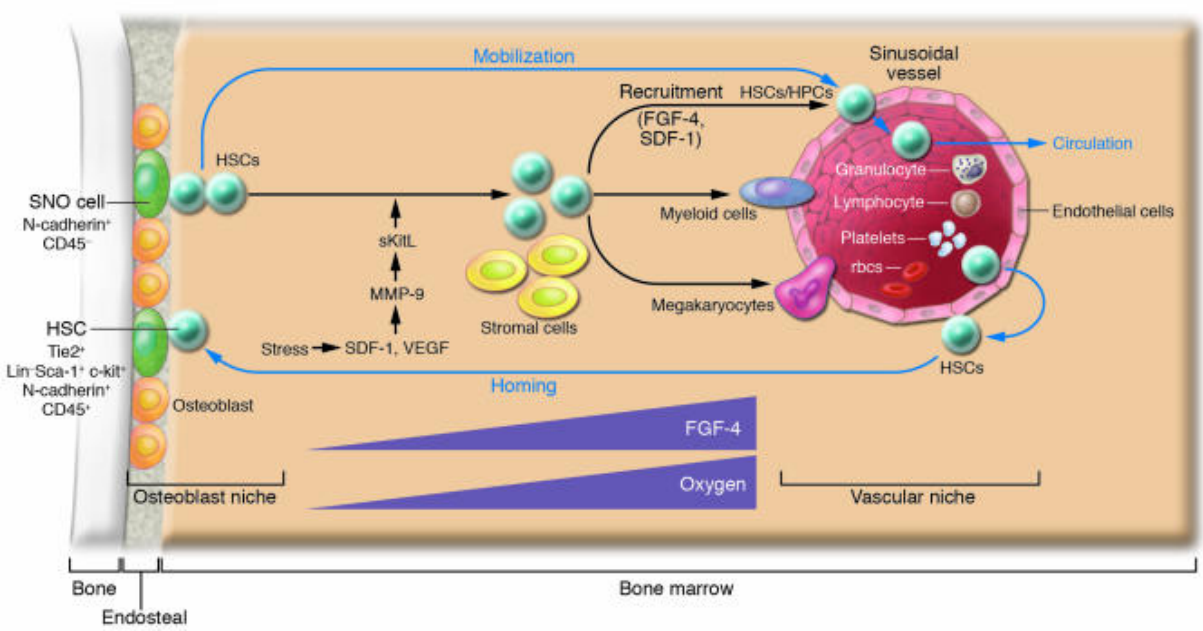

Figure 1-2: BM niche signalling controlling HSCs.

The balance between self-renewal and differentiation of HSCs in the bone marrow niches is mediated by several factors; normally HSCs reside in the osteoblastic or vascular niche, and in response to reduced levels of SDF-1 in the BM microenvironment, they will begin to mobilise and circulate. Higher FGF-4 and oxygen concentration gradients as the cells progress from the osteoblastic niche to the vascular niche might enhance recruitment, proliferation, and differentiation of HSCs/HPCs. During stress like thrombocytopenia, SDF-1 and VEGF activate MMP-9, which converts membrane-associated Kit ligand into soluble Kit ligand (sKitL) and promotes HSCs entry into the cell cycle, mobilisation to the vascular niche, and differentiation. Homing is the reverse of mobilisation, occurring in response to higher levels of SDF-1 in the BM microenvironment, cited from Yin and Li (2006).

1.2.1 The vascular niche and its role in stem cell homing

The BM vascular niche provides a barrier between the haematopoietic compartment and the peripheral circulation; it has the potential to regulate haematopoiesis and maintains the self-renewal of HSCs including motility, trans-endothelial migration, haematopoietic differentiation and maintenance of HSC trafficking inside or outside the BM (Chute *et al*., 2007). Interaction between HSCs and bone marrow endothelial cells (BMEC) allows for adherence of HSCs to the vascular endothelium, tethering, then rolling and transendothelial migration (Figure 1-3), which involves several molecules summarised in Table 1-1. BMEC direct HSC to the marrow and slow cell movement under the shear stress of blood flow result in tethering and rolling of HSC along the endothelium, however, in sinusoidal vessels the

shear stress is low which aids the homing process (Perlin, Sporrij and Zon, 2017).

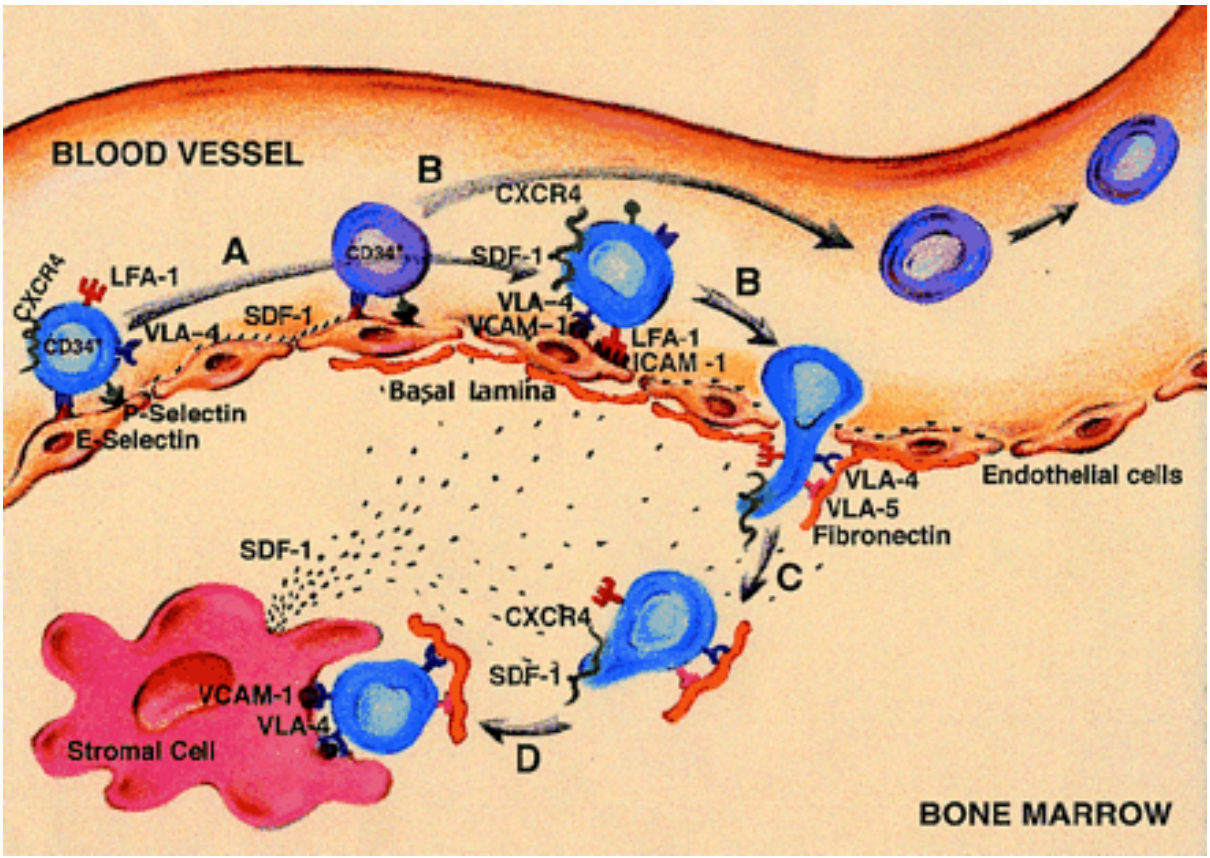

Figure 1-3: Stem cell trans-endothelial migration.

(A) Initial capture and rolling of HSCs expressing endothelial E and P selectins are mediated predominantly by the interaction of selectin molecules to the endothelium. SDF-1 activates CXCR4 HSCs secreted from BM endothelial cells and trigger LFA-1/ICAM-1 and VLA-4/VCAM-1 interactions to support firm adhesion to endothelial cells. (B) HSCs expressing insufficient levels of CXCR4 will detach and return to the bloodstream. (C) In response to SDF-1, CXCR4 HSCs will migrate between the endothelial cells using VLA-4 and VLA-5 integrin receptors to fibronectin (FN). (D) Transmigrated HSCs will reach stromal cells expressing VCAM-1 in stem cell niches. (Peled *et al*., 2000).

Table 1-1: Molecules involved in HSCs mobilisation, transendothelial migration, differentiation and maintenance in the BM.

Molecules	**Function**
Endothelial FGF-4	Supports adhesion of megakaryocytes to BMECs, induce the expression of adhesion molecules, including VLA-4 expressed by megakaryocytes and VCAM-1 expressed by BMECs (Avraham *et al*., 1994).
SDF-1α	Expressed by BMECs, induces the transendothelial migration, plays a key role in HSCs differentiation, retention in the bone marrow, quiescence, and repopulating activity (Peled *et al*., 1999).
Jagged 1	Notch signalling receptor (ligand) expressed by BMECs control HSC self-renewal and

	differentiation during haematopoietic stress conditions (Lilly *et al.,* 2011).
VCAM-1	Expressed by BMECs induces the expression of adhesion molecules (Avraham *et al*., 1994).
G-CSF	Mobilisation of HSCs (Lapidot *et al*., 2002).
Tie2	Cell-surface receptor mediates HSC adhesion to osteoblasts, maintaining quiescence in osteoblastic niche, angiopoietins receptor (Arai *et al*.,2004).
SCF	HSCs maintenance in BM niches (Ding *et al*.,2012)
E- and P-selectin	Enhances HSC quiescence and self-renewal potential and promotes HSC proliferation (Winkler *et al*. 2012).
Gp130	Cytokine receptor for IL-6 family; regulation of haematopoiesis (Yao *et al*., 2005).
PTN	Induces HSC regeneration (Himburg *et al*., 2005).
α- and β-integrins	Mediate cell adhesion and migration (Katayama *et al*., 2003).
Sialomucins and CD44 isoforms	Play a vital role in the initial adhesion and tethering of stem cells to bone marrow endothelial cells (Xia *et al*., 2004; Lapidot & Kollet, 2005).

Interaction between HSCs and bone marrow endothelial cell (BMEC) involves several molecules; fibroblast growth factor 4 (FGF-4), the stromal cell derived factor-1 (SDF-1α), vascular cell adhesion molecule 1 (VCAM-1), granulocyte-colony stimulating factor (G-CSF), stem cell factor (SCF), glycoprotein 130 (Gp130), pleiotrophin (PTN).

1.2.2 Haematopoietic stem cell homing

Homing of transplanted HSCs to the BM is a multi-step process involving the interaction of transplanted cells with bone marrow sinusoidal endothelial cells and transmigration through the vascular endothelium. This fundamental process is controlled by multiple cell adhesion molecule–ligand interactions. Several adhesion molecules are expressed by HSCs, including α- and β-integrins, which are heterodimeric transmembrane molecules that mediate cell adhesion and migration, and sialomucins and CD44 isoforms which play a vital role in the initial adhesion and tethering of stem cells to bone marrow endothelial cells (Xia *et al*., 2004; Lapidot & Kollet, 2005). The bone marrow sinusoidal endothelial cells express E-selectin, P-selectin and P-selectin glycoprotein ligand 1 (PSGL-1), one of the membrane-bound C-type lectins that bind to cell surface glycosylated ligands expressed on HSCs (Yang *et al*., 1999). The supportive interaction of E- and P-selectin with glycosylated ligands mediate the initial tethering and rolling of stem cells along the endothelial wall (Katayama *et al*., 2003). Once the stem cell has tethered to the endothelial membrane, chemoattractants such as SDF-1 then induces an intracellular signalling cascade leading to integrin activation (Wright *et al*., 2002). To produce firm

adhesion, α4β1 integrin binds to cognate receptors on endothelial cells, particularly VCAM-1, allowing the stem cell to migrate through the endothelium (Avraham *et al*., 1994).

While there is some knowledge regarding chemical messengers that can encourage HSC to home (Ahmadzadeh *et al*., 2015), it is a multifactorial process involving the BM of the patient, the donated HSC as well as endothelial cells of the blood vessel walls in which HSC cross to the BM niche. Signalling underlying this process, however, is incompletely understood. Several molecules identified to date include:

Chemokines: SDF-1, is expressed highly in the BM and associated cells. SDF-1 is a potent chemoattractant for HSCs and has been demonstrated to regulate cell adhesion, survival and cell cycle status (Mendez-Ferrer *et al*., 2008).

Receptors: Two receptors for SDF-1 on HSCs have been identified; CXCR4 and CXCR7 (Lilly, Johnson and Bunce, 2011). The presence of CXCR4 on the cell surface promotes migration and homing of HSCs into the BM niche (Ma, Jones and Springer, 1999; Wang and Knaut, 2014). CXCR7 is the second high-affinity receptor for SDF-1 but does not link to signalling pathways for migration (Zabel *et al*., 2011). Pre-treatment of umbilical cord blood (UCB) to enhance receptor expression, has been shown to enhance homing to the BM (Marquez-Curtis *et al*., 2011; Ratajczak and Suszynska, 2016).

Ligands and adhesion molecules: HSCs attach to endothelial cells of the blood vessel via adhesion molecules, before trafficking through vessel walls to reach the BM. Several adhesion molecules are involved in these migratory pathways including; the integrins α4β1 (VLA-4; which binds to VCAM-1 [CD106] and fibronectin) and αLβ2 (LFA-1; which binds to ICAM-1 [CD54]); L-selectin (CD62-L) which binds CD34 found on both endothelial cells and HSC; and the glycoprotein CD44 on HSC which binds to hyaluronate and other extracellular matrix proteins (Colvin *et al*., 2007).

Other elements influencing homing of HSCs to the bone marrow include some bioactive lipids, including sphingosine-1-phosphate (S1P) and ceramide-1-phosphate (C1P) which induce homing (Kim *et al*., 2012). Conditioning of mice for transplantation resulted in enhanced levels of these lipids in the BM. C1P also stimulates the secretion of SDF-1 from BM-derived fibroblasts (Kim *et al*., 2012). Adenosine triphosphate (ATP) and uridine triphosphate (UTP) also act as chemotactic molecules (Di Virgilio *et al*., 2001). UTP treatment up-regulates several adhesion-related genes such as *GLG1*, *RAC2*, *CD44*, *CD164* and *SELPLG* (Rossi *et al*., 2007). HSC may also respond to ion gradients (e.g. Ca^{2+} or H^{+}) by employing calcium- or proton-sensing receptors, respectively (Levesque, Helwani and Winkler, 2010).

1.3 Haematopoietic stem cell transplantation (HSCT)

For patients with malignant and nonmalignant haematologic diseases HSC transplantation (HSCT) remains as one of the most important therapeutic approaches. However, in some malignancies like chronic lymphocytic leukemia (CLL) it might be the only potentially curative option (Kerbauy *et al*., 2007; McClanahan & Gribben, 2014). HSCT became relatively safe due to advances in transplantation technology and supportive care practices, together with expanding stem cell sources. However, HSCT is still associated with morbidity and mortality especially in older patients (Okamoto, 2017). The most common indications for autologous HSCT treatment are myeloma and malignant lymphoma while the main indications for allogeneic HSCT are acute myeloblastic leukaemia, lymphoblastic leukaemia, dysmyelopoietic syndrome, chronic myeloblastic leukaemia refractory to tyrosine kinase inhibitors, then lymphoid malignancies and nonmalignant disorders (Hong and Deeg, 1994; Holowiecki, 2008; Majhail *et al*., 2015).

Such patients usually undergo conditioning therapy, prior to transplantation, which comprises high or reduced intensity conditioning chemotherapy, with or without total body irradiation. This therapy clears the patient of haematopoietic cells, including their disease; it also makes space in the BM for the new incoming donated HSC and immunosuppresses the patient to reduce the risk of graft rejection (Liso *et al*., 2017). Patients are allowed a few days for residual chemotherapy to leave the body, depending on the conditioning regimen, and then new HSCs are infused intravenously with the aim that the HSC will find the BM due to homing messages released from the BM microenvironment (Gyurkocza and Sandmaier, 2014).

It is well documented that the BM microenvironment becomes damaged due to chemotherapy (Kemp *et al.*, 2010; Georgiou *et al.*, 2010), so it is reasonable to suggest that damage or injury to the BM releases novel messengers for homing of HSC. These messengers include chemotactic factors which induce stem cells to traffic to the site of the injury in order to repair it. Cell death releases bioactive lipids like sphingosine-1-phosphate (S1P) and ceramide-1-phosphate (C1P) (Kim *et al.*, 2011), as well as prostaglandins and leukotrienes, and chemotherapeutic injury has also been shown to induce the release of cytokines from the BM including SDF-1 (Ponomaryov *et al.*, 2000). A successful HSCT can be identified as sustained engraftment of the transplanted HSC after making their way to the BM niches. Engraftment can be monitored when blood testing of the patient reveals the presence of chimerism in which donor and recipient haematopoietic cells may coexist (Servais *et al.,* 2013). Complete chimerism occurs when all cells are of donor origin; however, a high percentage of donor chimerism (90% to 95%) is associated with improved event-free survival (Brown, 2018). The main considerable parameters of engraftment are neutrophil and platelet recovery; a patient needs to have an absolute neutrophil count of more than 500 x 10^6/L for the first three consecutive days, and a platelet

count of more than 20,000/µL without transfusion support for seven successive days (Chang *et al.*, 2009). However, neutrophil engraftment occurs first, and platelet engraftment might appear 1-3 weeks later, depending on the donor and HSC source (Brown, 2018). After engraftment, new blood cells including WBC, RBC, then platelets, start to populate the vasculature. These cells' absence is life-threatening, and patients can only survive with blood product support, which is not an indefinite option, carrying intrinsic risks itself (Gyurkocza and Sandmaier, 2014). Due to myeloablative conditioning regimens, HSCT patients remain dependent on RBC and platelet transfusions until engraftment of these cell lines occurs. However, plasma and cryoprecipitate transfusions might not be required because the production of coagulation factors are not typically affected by HSCT (Cohn, 2015). However, transfusion-related complications like transfusion-associated graft versus host disease (TA-GVHD), passenger lymphocyte syndrome (PLS) and pure red cell aplasia (PRCA) are still very common in transfusion dependant HSCT candidates (Cohn, 2015). Whilst HSCT is well established and widely used, the first option in therapy is usually drugs that control the disease, rather than a transplant to cure the disease because HSCT is still difficult and potentially associated with unwanted side effects (McClanahan & Gribben, 2014). While most patients do well with HSCT, resulting in complete remission of their disease, for many, the outcome is not successful. For example, graft failure may be as high as 13% with a single HLA mismatched related donor vs 0% with HLA identical sibling donor (Hasegawa *et al*., 2003). Graft failure is a serious complication of HSCT defined as either lack of initial engraftment of the graft (primary graft failure) or loss of donor cells after initial engraftment (secondary graft failure) (Hutt, 2018). Factors associated with graft failure include HLA disparity like HLA-mismatched grafts, ABO mismatching in the donor/recipient pair, type of conditioning regimen like reduced-intensity conditioning, the initial diagnosis of the

recipient like severe aplastic anaemia, haemoglobinopathies and myeloid disorders, stem cell source employed, low stem cell dose, graft manipulation like T-cell depletion, female donor grafts for male recipients and underlying disease of the recipients (Ozdemir and Civriz Bozdağ, 2018).

Approximately 75% of all leukaemias occur in the elderly who are less tolerant of the toxicity of conditioning therapy and less likely to have an identical sibling donor. Thus, the risk of killing the patient is too high to warrant HSCT as a cure as the primary therapy, when good life quality can be achieved through disease control using small/targeted molecules (McClanahan & Gribben, 2014). HSCT becomes the only option when the malignancy progresses and mutates to a crisis state, where it is unresponsive to further drug therapy. Patients are at risk of death primarily through toxicity from high dose chemotherapy, as well as the failure of new stem cells to engraft into the BM, and as a result, patients succumb to lack of blood production concomitant with no immune system to protect them from infection (Mateos *et al*., 2013; Wahid, 2013). Patients in the pre-engraftment phase are at high risk of bacterial infections, including coagulase-negative staphylococci, viridans group streptococci and facultative gram-negative bacteria. Herpes simplex virus and fungal infections such as *Candida* and *Aspergillus spp* are common in this phase. However, at the post-engraftment phase infections are predominately caused by cytomegalovirus (CMV), varicella-zoster virus (VZV), adenovirus and *Aspergillus spp*. (Srinivasan *et al*., 2013; Pereira, Pouch and Scully, 2018). Nevertheless, there are arguments suggesting that some patients could do better with HSCT as a therapy early in their disease, instead of waiting until their leukaemia reaches a crisis with HSCT being the only option left (Johny *et al*., 2006). It is argued that if HSCT was improved, where toxicity was reduced and engraftment of new HSC was guaranteed, then an early HSCT could be of most benefit to the patient.

1.3.1 Alternative sources of HSC:

There are three recognised sources of HSC: BM, peripheral blood (PB) and UCB. BM is extracted by syringe from the iliac crest. PB mobilised HSC is where donors are administered drugs or growth factors to release HSC into the vasculature; these HSC are collected from the peripheral blood through apheresis. The most commonly used agents for HSC mobilisation are granulocyte colony stimulating factor (G-CSF), granulocyte-macrophage colony stimulating factor (GM-CSF), Plerixafor and stem cell factor (SCF) (Hopman and DiPersio, 2014). UCB is collected after a normal healthy delivery. After the afterbirth is collected and confirmed complete, the placenta is placed in an elevated position with the umbilical cord hanging below, then a syringe is placed into the umbilical cord vein, and the remaining blood which is rich in HSC is collected and used for HSCT (Ruggeri, 2016). Each of these sources can be given as an autologous (patient's own cells) or allogeneic (cells from another donor) transplant, with the former being highly unlikely to be rejected, and the latter having a high risk of rejection, thus, requiring tissue type matching and immunosuppression (Claude Gorin, 2016). In the case of leukaemia, donation of HSC means that you are donating a new immune system to the patient. Immune cells in the donated HSC, particularly T lymphocytes, have the capacity to recognise the patient as foreign and can attack the patient's cells. This rejection of the patient via donated cells is termed graft versus host disease (GVHD) and is also life-threatening (Negrin, 2015). Although donated HSCs are normally T cell-depleted to avoid this sort of outcome, it still can result in GVHD. However, it has been shown that patients who suffer GVHD have a much lower risk of leukaemic relapse, suggestive of the new HSC recognising the leukaemia cells as a foreign and destroying them, which is termed the graft versus leukaemia effect (GVL). Research shows that GVL benefits the patient, providing the GVHD is not too severe (Negrin,

2015). The different sources of HSC have helped identify some factors that help or hinder transplantation. For example, BM allows the procurement of a plentiful supply of HSC to enable engraftment; however, originating from adults (donors are 18-60 yrs) means they are immunologically competent and high risk for GVHD. Similarly, PB HSC are plentiful and cause GVHD, but engraft better. PB-HSCT results in faster engraftment; neutrophil and platelet recovery occurred significantly faster after transplantation because large numbers of CD34+ cells can be obtained and extensive manipulation of the graft is possible without losing too many haematopoietic cells (Schmitz *et al*., 2002). UCB is least likely to cause GVHD, but this results in reduced GVL. UCB also engrafts less successfully, and with low HSC numbers, UCB transplants are usually limited to children or small adults. Recently, UCB transplant to larger adults has been achieved by pooling UCB donations; low immunogenicity makes this feasible, but engraftment is still a problem. Nowadays, less BM is used in transplants compared to PB and UCB, however, it is more likely that UCB will become widely accepted despite being affected by religious and cultural differences, and hence, UCB transplantation needs to improve. The key parameters of HSC sources are summarised in Table 1-2.

Table 1-2 Comparison of the BM, PB and UCB stem cell sources.

	UCB	**PB**	**BM**
Risk for the donor	None	Yes	Yes
Duration of searching (month)	≤1	3-6	3-6
Factors limiting the engraftment	Low cell count	HLA match	HLA match
Dominant factor affecting the outcome	Engraftment failure, delayed immune recovery	GVHD	GVHD
Minimal HLA match	4/6	9/10	9/10
Risk for GVHD	Low	High	High
Acute	Low	High	High
Chronic	Low	Higher	High
DLI possibility	None	Possible	Possible
Post-transplant infection risk	Higher	High	High
Immunotherapy possibility	None	Yes	Yes

There is no risk for donors for UCB; UCB are easily sourced, and HLA matching is less stringent because GVHD is low. However, engraftment is poorer, and there is limited use of UCB as immunotherapy and returning to the donor for lymphocytes to promote GVL is not an option (DLI; donor lymphocyte infusion). Risk of infection is also higher (Sirinoglu Demiriz, Tekgunduz and Altuntas, 2012)

1.3.2 Pre-transplantation conditioning regimens

Conditioning regimens are a crucial component of allogeneic and autologous HSCT, administered before the HSC infusion. Conditioning regimens have been classified as high dose (myeloablative), reduced intensity, and nonmyeloablative (Giralt *et al*., 2009). Regimens were predominantly dependent on dose intensity, assuming that high dose chemotherapy and radiotherapy would eliminate malignant disease and infusion of HSC would then restore haematopoiesis (Barrett and Savani, 2006). However, as the contribution of GVL effects to the success of allogeneic HSCT was discovered over time, many investigators lowered the dose of radiation and chemotherapeutic agents in the conditioning regimen. Subsequently, this resulted in a significant change in the implemented conditioning strategies and expanded the eligibility measures to include more patient categories (Gyurkocza and Sandmaier, 2014).

Myeloablative regimens comprise single or multiple doses of alkylating agents, with or without total body irradiation (TBI) leading to complete BM ablation and prevention of autologous haematologic recovery. In contrast, reduced intensity regimens relied on ≥ 30% reduced-intensity alkylating agents or TBI, which resulted in prolonged cytopenias, and subsequently, require HSC support. Whereas, nonmyeloablative regimens, relied mostly on immunosuppressive drugs causing minimal cytopenias, and do not require HSC support (Gyurkocza and Sandmaier, 2014). Most commonly used myeloablative, reduced intensity, and nonmyeloablative regimens are summarised in Table 1-3.

Table 1-3 Summary of myeloablative, reduced intensity, and nonmyeloablative regimens include doses and duration of treatment.

Myeloablative	Total dose (days)	**Reduced-intensity**	Total dose (days)	**Nonmyeloablative**	Total dose (days)
Cy/TBI Cy (mg/kg) TBI (Gy)	 120 (-6, -5) 12-14 (-3 to -1)	**Flu/Mel** Flu (mg/m^2) Mel (mg/m^2)	 150 (-7 to -3) 140 (-2, -1)	**Flu/TBI** Flu (mg/m^2) TBI (Gy)	 90 (-4 to -2) 2 (0)
Bu/Cy Bu (mg/kg) Cy (mg/kg)	 16 (-7 to -4) 120 (-3 to -2)	**Flu/Bu** Flu (mg/m^2) Bu (mg/kg)	 150 (-9 to -5) 8-10 (-6 to -4)	**TLI/ATG** TLI (Gy) ATG	 8 (-11 to -1) 2 (0)
***BACT** BCNU (mg/m^2) Ara-C (mg/m^2) Cy (mg/kg) 6-Thioguanine (mg/m^2)	 200 (-6) 800 (-5 to -2) 50 (-5 to -2) 800 (-5 to -2)	**Flu/Cy** Flu (mg/m^2) Cy (mg/kg)	 150 (-7 to -3) 140 (-2, -1)	**TBI** TBI (Gy)	 1-2 (0)
****BEAM** BCNU (mg/m^2) Etoposide (mg/m^2) Ara-C (mg/m^2) Melphalan (mg/m^2)	 300 (-6) 800 (-5 to -2) 800 (-5 to -2) 140 (-1)	**Flu/Bu/TTP** Flu (mg/m^2) Bu (mg/kg) Thiotepa (mg/m^2)	 150 (-7 to -5) 8 (-6 to -4) 5 (-3)		
TBI/VP TBI (Gy) Etoposide (mg/kg)	 12-13.2 (-7 to -4) 60 (-3)				
AC/TBI Ara-C (g/m^2) TBI (Gy)	 36 (-9 to -4) 12 (-3 to -1)				
Mel/TBI Melphalan (mg/m^2) TBI (Gy)	 110-140 10-14				
Cy/VP/TBI Cy (mg/kg) Etoposide (mg/kg) TBI (Gy)	 120 (-6, -5) 30-60 (-4) 12-13.8 (-3 to -1)				
TBI/TTP/Cy TBI (Gy) Thiotepa (mg/kg) Cy (mg/kg)	 13.8 (-9 to -6) 10 (-5, -4) 120 (-3, -2)				
Bu/Cy/Mel Bu (mg/kg) Cy (mg/kg) Mel (mg/m^2)	 16 (-7 to -4) 120 (-3, -2) 140 (-1)				
ATG: anti-thymocyte globulin, **Bu**: busulfan, **Cy**: cyclophosphamide, **Flu**: fludarabin, **Mel**: melphalan, **TBI**: total body irridation, **TLI**: total lymphoid irridation, **TTP**: thiotepa, **VP**: etoposide, **Ara-C**: cytarabine (cytosine arabinoside), **BCNU**: carmustine. ***BACT:** (carmustine, cytarabine, cyclophosphamide and 6-thioguanine), ****BEAM**: (carmustine, etoposide, cytarabine and melphalan), Data sourced from (Atilla, Ataca Atilla and Demirer, 2017).					

1.4 Models of endothelial barriers (Boyden chamber assays)

The Boyden chamber assay was introduced initially by Boyden in 1962 (Chen, 2005) and is also known as filter membrane migration assay, transwell migration assay, or chemotaxis assay. It was first used for the analysis of leukocyte chemotaxis (Boyden, 1962). The basic principle of this assay is based on a chamber of two medium-filled compartments separated by a microporous membrane, usually PET membrane (polyethylene terephthalate) with specific pore sizes, 3µm, 5µm, 8µm and 12µm which can be selected based on the size and behaviour of the cells to be tested. Cells are placed in the upper compartment of the insert and are allowed to migrate through the pores of the membrane insert into the lower chamber, in which chemotactic agents are present. After incubation for a specific time, the membrane between the two compartments is removed carefully, fixed and stained, and the number of cells that have migrated to the lower side of the membrane is monitored and tested. In this research, this approach will be utilised and modified by adding other cellular components, including an endothelial cell layer, bone marrow stromal cells and HPC. Optimal cell culture conditions will be determined in which the three cell lines will be co-cultured in an attempt to simulate the BM microenvironment. Although the BM microenvironment might be very complex, containing multiple cellular compartments interacting with specific signalling pathways, this approach might be considered as a valuable tool to understand how cells communicate inside the BM under various conditions. This research was aimed to establish a co-culture *in vitro* model that can be used to measure the capacity of HSC to home to the BM. This co-culture model will be utilised in the presence and absence of chemotherapy versus targeted/small molecule therapies, under normoxic and hypoxic conditions.

1.5 General hypothesis

Chemotherapy is mandatory for HSCT to induce engraftment; it usually induces BM injury leading to release of homing factors like that seen under ischaemic conditions. The combination of chemotherapy with hypoxia in the BM might induce production of homing elements which might represent a 'help' signal to the transplanted SC to come to reside in the BM niches. The combination of chemotherapy with hypoxia is often ignored *in vitro*, and adding the hypoxia element might provide a novel candidate that previously has been overlooked. It will be possible to identify and then induce these novel messengers using novel therapies to improve the outcome of HSCT, through promoting higher engraftment but lower toxicity.

1.6 Aims and Objectives

1. **To Build a model of the BM/endothelium interface.**

a) To build an *in vitro* model of the BM/blood vessel/HPCs interaction where a human BM mesenchymal stem cell line (HS-5) will be grown in the base of the culture well, a vascular endothelial cell line (HUVEC or HMEC-1) will be grown as a layer in a cell culture insert and a haematopoietic progenitor cell equivalent (HL-60) will be placed in the insert above the endothelial cells. Inserts can be placed directly above HS-5 cells or alternatively use HS-5 conditioned media (C.M.) to induce trafficking. The ability of the HL-60 to traffic through the endothelium and reach the lower compartment will be indicative of “trafficking and homing” and will be monitored using cell tracking dyes.

b) To optimise the model for culture conditions in order to allow cells to grow together in one environment. This will involve testing culture media and supplementation.

c) To validate homing using recombinant cytokines (e.g. SDF-1α) to demonstrate that HL-60 can traverse the endothelium and reach the lower compartment of the inserts.

2. To measure the capacity of HPC to home to the BM in the *in vitro* model in the presence and absence of chemotherapy versus targeted therapies, under normoxic and hypoxic conditions

a) To explore the ability of chemotherapy to induce homing by pre-exposing HS-5 to clinically relevant doses of standard conditioning therapy, and then monitoring the ability and speed at which HL-60 can cross the endothelial barrier. Drugs will include carmustine, etoposide, cytarabine and melphalan.

b) To test the ability of HL-60 to traverse the endothelial barrier using targeted therapies, typically used in the treatment of leukaemia. Drugs will include imatinib and ibrutinib.

c) Both (a) and (b) will be performed under hypoxic and normoxic conditions.

3. Determine and measure the release of novel homing factors under normoxic versus hypoxic conditions.

Identify homing factor proteins released from HS-5 by comparing hypoxic versus normoxic conditions when treated with standard conditioning therapy. Protein detection will be achieved utilising the proteomics service at the University of Bristol.

4. To assess the expression of surface adhesion molecules on the endothelium after exposure to identified homing factors.

Treatment of endothelium with homing factors will be explored to assess upregulated adhesion molecules (e.g. E-and P-selectin). A concentration range will be utilised to test the theory that adhesion will be higher at the point of

injury, as a signal to the HSC to bind. Measurement of HL-60 traversing the barrier under these conditions will also be investigated.

Chapter 2: Materials and methods

2.1 Cell lines and maintenance

All cell lines unless otherwise stated were from American Type Culture Collection (ATCC). Two vascular endothelial cell lines were obtained, human umbilical vein endothelial cell line (HUVEC) and human microvascular endothelial cell line-1 (HMEC-1). BM stromal cell line (HS-5) was obtained to represent BM MSCs in the model. The leukaemia cell line (HL-60) was obtained to be used as a haematopoietic progenitor cell (HPC). HL-60 cells express the chemokine receptor CXCR4, which can be induced by stromal cell-derived factor-1α (SDF-1α) to initiate the transmigration process. Neuroblastoma cell line (SH-SY5Y) was obtained and used as a model for neural cell function and differentiation. All media used to propagate cells were supplemented with heat inactivated foetal bovine serum (FBS; 10%), L-glutamine (2 mM), penicillin (100 U/mL) and streptomycin (100 µg/mL); additional supplements were added as indicated in Table 2-1, cells were maintained at 37°C and 5% CO_2, and medium was changed every 3-4 days. Additional information about the respective cell lines is detailed in Table 2-1.

Table 2-1 Cell lines used in this study.

Cell line	Type	Source	Growth medium - Basal medium and additional supplements **	Role in this study	Doubling time (DT)	Seeding density	Origins
HUVEC	Umbilical vein endothelial cell line (adherent)	ATCC	F-12K (ATCC) 0.1 mg/ml heparin, 0.03 mg/ml endothelial cell growth supplement (ECGS) 10% heat inactivated FBS 100 U / ml penicillin and 100 µg/ml streptomycin	Endothelial cell	5-6 days	$2x10^5/cm^2$	Normal endothelial primary cell derived from the vein of a normal human umbilical cord. HUVEC cells are non-transformed.
HMEC-1	Microvascular endothelial cell line (adherent)	ATCC	MCDB 131 (ATCC) 10ng/mL epidermal growth factor (EGF), 1 µg/mL hydrocortisone 10% heat inactivated FBS 100 U/ml penicillin and 100 µg/ml streptomycin	Endothelial cell	20-25 hours	$5x10^5/cm^2$	From human foreskin, transfected with pSVT vector, a pBR-322 based plasmid containing the coding region for Simian virus 40A gene product, large T antigen (Ades, *et al.*, 1992).
HS-5	BM stromal cell line (adherent)	ATCC	DMEM-HG 10% heat inactivated FBS 100 U / ml penicillin and 100 µg / ml streptomycin	BM MSCs	40-45 hours	$2x10^5/cm^2$	From a 30-year-old Caucasian male and immortalised by transduction with the human papilloma virus- 16 E6/E7 genes (Roecklein & Torok-Storb, 1995).
HL-60	Leukaemic cell line (suspension)	ATCC	RPMI 1640 10% heat inactivated FBS 100 U / ml penicillin and 100 µg/ml streptomycin	Haematopoietic progenitor cell (HPC)	30-35 hours	$3x10^5/ml$	From peripheral blood leukocytes obtained by leukopheresis of a 36-year-old Caucasian female with acute promyelocytic leukaemia (Gallagher et al., 1979).
SH-SY5Y	Neural cell line (adherent)	Collaborator*	DMEM-HG 10% heat inactivated FBS 100 U/ml penicillin and 100µg/ml streptomycin	Neural cell	25-30 hours	$2x10^5/cm^2$	From a metastatic bone tumour biopsy from a 4-year-old female child suffering from neuroblastoma (Ross, Spengler and Biedler, 1983).

* Generous gift from Prof. Myra Conway at University of the West of England (Bristol, UK), ** All additional supplements were from Sigma Aldrich (Dorset, UK).

2.2 General Methods

2.2.1 Thawing of cryopreserved cell lines

Cell lines were transferred from liquid nitrogen and first quickly thawed in a 37°C water bath. Just before the ice completely melted, the vial was thawed by adding a thaw medium of 20% FBS in cell line basal medium in a dropwise manner to fill the vial. The contents of the cryovial were transferred into a 15ml tube and made up to the 10ml mark using 1ml aliquots of the wash medium (basal medium) and subsequent mixing over a 10-minute period. The wash medium and centrifugation step (5 minutes; 230 x g) ensures removal of dimethylsulphoxide (DMSO) from the cells. The supernatant was removed, and the washing step repeated before reconstituting in growth medium, performing a cell count using trypan blue, and seeding cells at the required density.

2.2.2 Cryopreservation of cell lines

Cell lines were cryopreserved for future use by centrifugation (300 x g for 10 minutes) and removal of all medium from the cell pellet. Cells were resuspended in a solution of 25% FBS, 10% DMSO and 65% cell line growth medium at a concentration of 1-2 x 10^6 cells per mL. Cells were firstly resuspended in 50:50 FBS: cell growth medium at twice the final required density of cells. Then an 80% cell line growth medium /20% DMSO solution was added drop-wise over ice until a 1:1 mix of the two solutions was achieved, thus halving the cell concentrations for freezing. Cell suspensions were then added to cryovials at 1ml per vial. These were then placed in a cryopreserving chamber (‘Mr Frosty’; Sigma) containing isopropanol (Sigma) which reduced the

temperature gradually (1°C per 1 minute) at -80°C for 24 hours before being transferred to liquid nitrogen for storage.

2.2.3 Trypsinisation of adherent cells

Trypsinogen (trypsin), was used to dissociate the cells from the 75 cm^2 flask. When the adherent cells (see Table 2.1) had reached 80-90% confluence, the medium was removed from the flask and the cells were washed once with phosphate buffered saline (PBS). Then, 2-3 ml of trypsin (0.25% trypsin–EDTA solution; Gibco) was added to the flask and incubated at 37°C for 5-10 minutes. After incubation, the cells were microscopically checked to see if they had detached from the flask. The cells were then added to a 15mL tube containing 2-3 mL medium supplemented with heat inactivated FBS (10%) and centrifuged at 300 x g for 10 mins. Cells were then counted and seeded at the relevant density.

2.2.4 Trypan blue exclusion assay for cell viability and cell counting

The trypan blue dye exclusion assay is used to determine the number of viable and dead cells present in a cell suspension. The principle of this test is based on the fact that live cells with intact cell membranes can exclude trypan blue, whereas dead cells take up the dye. A viable cell will have a clear cytoplasm whereas a nonviable cell will have a blue cytoplasm. An aliquot of cell suspension was collected into a microcentrifuge tube, and diluted with 0.4% trypan blue dye to obtain a 1: 2 to 1:20 dilution and mixed properly by pipetting. An aliquot of 10 µL of the mixture was then counted using a haemocytometer counter, or LUNA-FLTM Dual Fluorescence Cell Counter, (Logos Biosystems Inc.

USA). Percentage of viable cells was calculated by dividing the number of viable cells by the total number of cells and multiplying by 100.

2.2.5 Light and phase contrast microscopy

Light microscopy was used to examine cell proliferation and cell transmigration, and phase contrast microscopy was used to examine endothelial monolayer formation during model development. Images were taken using a Nikon Eclipse TE300 microscope and a Nikon Coolpix 950 camera.

2.2.6 Induction of hypoxic conditions

Cells were incubated in a humidified hypoxic Modular Incubator Chamber (MIC-101; Billups-Rothenberg, USA), a self-contained and sealed chamber that fits inside existing laboratory incubators. After cleaning and sterilisation of the hypoxia chamber, cell culture plates were placed inside the chamber. To maintain humidity, the chamber was humidified by placing 20 mL of sterile water in an uncovered petri dish inside the chamber. After sealing the chamber properly, it was purged at a rate of 40-50 L/min for 2 minutes using a gas mixture containing; 1% O_2 / 5% CO_2 / 94% N_2 (BOC, UK) and placed inside the laboratory incubator for 24 hours.

2.3 Establishment of the transmigration model

Creating a vascular barrier is a crucial element in this model. Endothelial cells should make a tight junction between each other without any gaps to prevent any transmigration, except when induced to loosen junctions to allow passage of relevant cells. Optimal seeding density should be determined in order to

create a barrier mimicking the vasculature. Two cell lines were used, HUVEC and HMEC-1. Formation of endothelial layer was monitored by light microscopy (2.2.5) and trans-endothelial electrical resistance (TEER). Formed endothelium was also visualised by scanning electron microscopy (SEM).

2.3.1 Trans-endothelial electrical resistance (TEER)

Trans-endothelial electrical resistance (TEER) is a quantitative technique to measure the integrity of tight junction dynamics in cell culture models of endothelial monolayers. The basic principle is based on measuring ohmic resistance across an endothelial monolayer as evidence of complete confluence over the insert (Lea, 2015). For TEER measurements, STX chopstick dual electrodes of the Millicell® ERS-2 Voltohmmeter were used (Milipore®, Merck Millipore, UK) with one electrode placed in the upper compartment and the other in the lower compartment and the electrodes were separated by the cellular monolayer (Figure 2-1). Both the upper and the lower compartments contain culture medium; the shorter electrode should not be in contact with the cell layer, and the electrodes are held steady at a 90° angle to the plate insert. Triplicate readings were obtained for each insert including a blank insert which contained media only without cells. Measurements then were averaged, and the blank reading was subtracted from each reading.

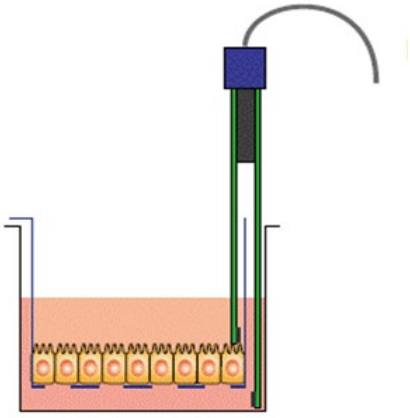

Figure 2-1 Trans-endothelial electrical resistance (TEER) measurement.

Representation of the electrode placed in a tissue culture insert, the shorter tip of the electrode should not be in contact with the cell layer, while the long tip should just touch the bottom of the outer chamber. Picture cited from Lea (2015).

2.3.2 Scanning electron microscopy of endothelial monolayer

HMEC-1 were seeded at 3.0 x 10^5, 4.0 x 10^5 and 5.0 x 10^5 in 12 well 8 μm pore inserts (Milipore®, Merck Millipore, UK); after 24 hours inserts were fixed and dehydrated (Appendix 1). Membranes of dried inserts were cut to appropriate size and attached to sample holders to be examined by electron microscopy to check that pores were covered by endothelial cells. Images were taken with the FEI Quanta 650 FEG scanning electron microscope.

2.3.3 Establishment of a HUVEC monolayer.

The cells were diluted to give 0.1×10^6 cells/cm^2 (culture insert growth surface area 1.1 cm^2) suspended in 1 mL F-12K culture medium and added to 8μm Millicell polyethylene terephthalate membrane hanging trans-well inserts for 12-well plates (Milipore®, Merck Millipore, UK). A confluent monolayer formation over the insert was monitored by light microscopy to confirm that none of the HUVEC cells transmigrated to the lower chamber of each well. HUVEC monolayer barrier integrity was measured by TEER (section 2.3.1).

2.3.4 Establishment of HMEC-1 monolayer and optimisation of seeding density

HMEC-1 were seeded at different densities in 12 well 8 μm pore inserts: 1.0 x 10^5, 1.5 x 10^5, 2.0 x 10^5, 2.5 x 10^5, 3.0 x 10^5, 3.5 x 10^5, 4.0 x 10^5, 4.5 x 10^5, 5.0 x 10^5, 5.5 x 10^5 and 6.0 x 10^5 cell/cm^2 suspended in 1 mL MCDB 131 culture medium. TEER was measured (section 2.3.1) for the HMEC-1 at 24 and 48 hours for each insert. A confluent monolayer formation over the insert was monitored by light microscopy to confirm that none of the HMEC-1 cells transmigrated to the lower chamber of each well. HMEC-1 monolayer barrier integrity was measured by TEER (section 2.3.1).

2.3.5 Optimisation of culture medium for the model

This step aimed to reduce the variables that might interfere with transmigration; a tolerable medium for all cells should be selected to run the test without any effect on the viability of cells and integrity of the barrier. The proliferation rate of HS-5 in DMEM-HG (High glucose Dulbecco's Modified Eagle's Medium), MCDB 131, RPMI 1640 (Roswell Park Memorial Institute Medium 1640) and F-12K was measured. HS-5 were seeded at 4.0×10^4 cells/cm^2 in a T25 flask containing 7 mL of growth medium. After 96 hours, HS-5 cells were trypsinised (section 2.2.3) and counted (section 2.2.4).

The proliferation rate of HMEC-1 in MCDB 131, RPMI 1640 and DMEM-HG was measured. The cells were seeded at 2.0×10^4 cells/cm^2 in a T25 flask containing 7 mL of growth medium and kept for 48 hours, after which cells were trypsinised and counted.

2.3.6 Assessment of membrane integrity during media change

Following culture medium testing as described in section 2.3.5, the optimal medium for co-culture was determined to be RPMI 1640 (see chapter 3, section 3.5.10 for results). This section describes assessment of membrane integrity following establishment of the barrier in basal medium, followed by medium change to RPMI 1640 for co-culture and transmigration experiments.

Maintaining the integrity of the barrier is crucial for the model; this step was performed to check the possible effect of changing the medium from MCDB 131 to RPMI 1640 on TEER measurement of the HMEC-1 monolayer. Inserts with established barriers were washed three times with fresh medium (RPMI 1640) before adding RPMI 1640 for running the experiment. This step was made to determine if the barrier was affected by changing the medium, washing or depletion of nutrients in the culture medium. The washing step might affect the integrity of the monolayer by disturbing the cells on the inserts. To rule out depletion of nutrients, inserts were tested for any changes on the TEER after removal and replacement of the same medium with and without PBS wash (see chapter 3, section 3.5.10 for results).

2.3.7 Validating transmigration in the co-culture model

HMEC-1 cells were diluted to give 0.5×10^6 cells/cm^2 (culture insert growth surface area 1.1 cm^2) resuspended in 1 mL MCDB 131 and added to 8µm Millicell trans-well inserts for 12-well plates (Milipore®, Merck Millipore, UK). A confluent monolayer formation over the insert was monitored by light microscopy, integrity of the membrane was evaluated by TEER monolayer as described in sections 2.3.3 and 2.3.4. After 24 hours from seeding, inserts were washed gently in RPMI 1640 and transferred to new plates. An aliquot of 2 mL of complete RPMI 1640 medium was added to the lower compartments of the inserts supplemented with 200 and 400 ng/ml SDF-1α (positive control; Sigma Aldrich, UK), 100% conditioned medium from untreated and treated HS-5 or 2 mL of complete RPMI 1640 supplemented with any potential inducer of interest. After 2 hours, HL-60 were then added to the upper compartment of each insert (3.0×10^5 cells/insert) that contained a confluent layer of HMEC-1, and volumes were adjusted to 1 mL in each insert. Negative control inserts were seeded with 3.0×10^5 cells/insert without the HMEC-1 barrier in RPMI-1640 medium. After 24 hours of incubation in normoxia or hypoxia (section 2.2.6), samples were collected from the lower compartments for transmigration cell counts using a haemocytometer.

2.3.8 Cell tracker labelling

CellTracker™ Oregon Green™ 488 Carboxy-DFFDA, SE (Thermo Scientific, UK) was dissolved in DMSO to a final concentration of 10 mM. The stock solution was diluted to a final working concentration of 0.5-25 µM in serum-free RPMI 1640 and warmed to 37°C. HL-60 cells were harvested by centrifugation at 500 x g for 3 minutes and supernatant was aspirated. Cells were resuspended gently in the pre-warmed CellTracker™ working solution and incubated for 45 minutes at 37°C and 5% CO_2. Cells

were then centrifuged at 500 x g for 3 minutes to remove the CellTracker™ working solution. Cells were then resuspended gently in RPMI 1640 and maintained for 24 hours at 37°C and 5% CO_2 before further use.

2.3.9 SH-SY5Y culture conditions and differentiation

To differentiate SH-SY5Y neuroblastoma cell line into 'neurons' for hypoxia induction, cells were seeded into a 6 well plate at 1×10^6 cells per well suspended in DMEM-HG supplemented with 10 µM Synthetic Retinoid ec23® (Amsbio, UK), 3% FBS, 2 mM L-glutamine, 100 U/mL penicillin and 100 µg/mL streptomycin at 37°C and 5% CO_2. The medium was changed every 2 days for 3 cycles, and the last change of medium was replaced with complete RPMI 1640. Cells were incubated in normoxia and hypoxia (section 2.2.6), and conditioned medium was collected after 24 hours.

2.4 Flow cytometry

HS-5 cells were cultured at 1 x 10^6 cells per 25 cm^2 flask, in different culture media including: DMEM-HG, RPMI 1640, and F-12K. After 7 days, HS-5 were trypsinised (section 2.2.3) to be washed and evaluated for percent positivity and relative expression of MSCs markers; CD44, CD73, CD90 and CD105. Cell samples (1.5 x 10^5) were washed in PBS and centrifuged at 500 x g for 5 mins to remove any residual medium before being resuspended in 100 µL stain buffer (Becton Dickinson, Oxford, UK) and stained with each antibody or isotype control for 45 minutes at 4 °C (Tables 2.2 and 2.3). Subsequently excess antibody was washed off with PBS by centrifugation at 500 x g for 3 minutes before cells were fixed in fixative buffer (Becton Dickinson, Oxford, UK). Cells were analysed by flow cytometry (BD Accuri™ C6 cytometer; Becton Dickinson, Oxford, UK). Cells were gated to exclude debris based on forward and side scatter properties; analysis was based on collecting 10,000

events through the gate (Figure 2-2). Cells were stained with anti-CD44, anti-CD73, anti-CD90, anti-CD105, and isotype controls (Tables 2.2; 2.3) (all Becton Dickinson Biosciences, Oxford, UK).

Table 2-2 antibodies for flow cytometry.

Antibody	Isotype	Conjugate	Vol. per test
Anti-Human CD44	Mouse IgG2b, κ	Phycoerythrin (PE)	20 µL
Anti-Human CD73	Mouse IgG1, κ	Phycoerythrin (PE)	5 µL
Anti-Human CD90	Mouse IgG1, κ	Fluorescein isothiocyanate (FITC)	5 µL
Anti-Human CD105	Mouse IgG1, κ	Phycoerythrin (PE)	5 µL

Table 2-3 Isotype controls for flow cytometry.

Antibody	Isotype	Conjugate	Vol. per test
Mouse IgG2b κ Isotype Control	Mouse IgG2b, κ	Phycoerythrin (PE)	20 µL
Mouse IgG1, κ Isotype Control	Mouse IgG1, κ	Fluorescein isothiocyanate (FITC)	5 µL
Mouse IgG1, κ Isotype Control	Mouse IgG1, κ	Phycoerythrin (PE)	5 µL

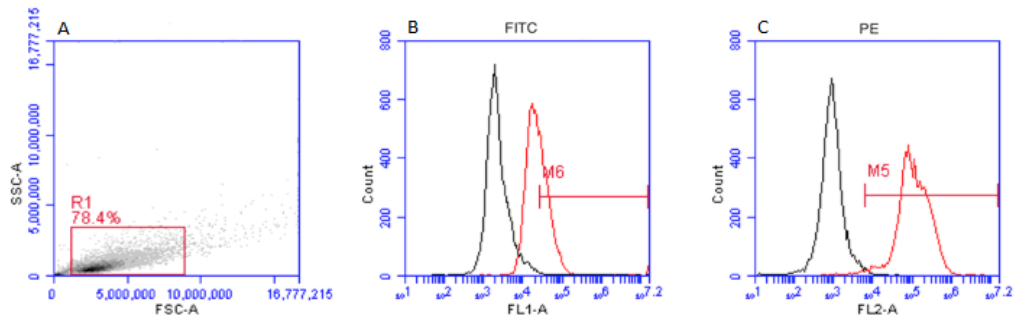

Figure 2-2 HS-5 gating in flow cytometer.

HS-5 were gated based on forward scatter and side scatter properties (A). FITC labelled cell signals were resolved on channel FL1 (anti-CD90) (B). PE labelled signals were resolved on channel FL2 (anti-CD44, anti-CD73 and anti-CD105) (C). Gating strategy in the first dot plot was used to select a uniform population of cells and to eliminate duplicate gating. Positive threshold was selected to exclude the isotype control peak and to eliminate the signal produced by non-specific binding and background signal.

2.5 *In vitro* HS-5 treatment

2.5.1 Treatment of HS-5 with chemotherapeutic and targeted therapeutic agents

HS-5 were seeded in a 6-well tissue culture plate at $1x10^6$ cells per well resuspended in DMEM-HG. Cells were incubated under normal culture conditions at 37°C and 5% CO_2 for 24 hours to enable adherence to the plate, at which point the medium was changed to complete RPMI 1640 supplemented with chemotherapeutic and targeted therapeutic agents according to the tables below (Table 2-4; Table 2-5). Cells were then incubated in normal culture conditions in normoxia or hypoxia (section 2.2.6) for 24 hours. After 24 hours, the medium was replaced by fresh complete RPMI 1640 and re-incubated in normal culture conditions in normoxia or hypoxia for 24 hours. Media were then harvested and used in the transmigration model.

Table 2-4 Chemotherapeutic agents (BEAM).

High and low concentrations were used in this study; plasma concentrations were based on the published literature.

Drug	Group	High Conc.	Low Conc.	Plasma Conc.
Melphalan	Alkylating agent	32.8 μM	16.4 μM	32.8 μM (Andrews, 2015)
Carmustine	Alkylating agent	7.8 μM	3.9 μM	7.8 μM (Henner, *et al*., 1986)
Etoposide	Topoisomerase inhibitor	10 μM	5 μM	10 μM (Teixeira, *et al*., 2009)
Cytarabine (Ara-C)	Antimetabolite	10 μM	5 μM	10 μM (Hu, *et al*., 2011)

Table 2-5 Targeted therapies.

High and low concentrations were used in this study; recommended concentrations were based on the supplier's recommendation. Targeted therapies were obtained from Stratech (UK)

Drug	Group	High Conc.	Low Conc.	Recommended Conc.
Imatinib Mesylate	Antineoplastic Agent, Tyrosine Kinase Inhibitor	3.4 μM	1.7 μM	1.7 μM
Ibrutinib	Antineoplastic Agent, Tyrosine Kinase Inhibitor	4.6 μM	2.3 μM	2.3 μM

2.5.2 Treatment of HS-5 with inhibitors

HS-5 were seeded in a 6-well tissue culture plate at $1x10^6$ cells per well resuspended in DMEM-HG. Cells were incubated at normal culture conditions of 37°C and 5% CO_2 for 24 hours to enable adherence to the plate, at which point the medium was changed to complete RPMI 1640 supplemented with inhibitor drugs according to the Table below (Table 2-6). Cells were then incubated in normal culture conditions at 37°C and 5% CO_2 for 24 hours. After 24 hours, the medium was replaced by fresh complete RPMI 1640 and re-incubated in normal culture conditions for 24 hours. Medium was then harvested and used in the transmigration model.

Table 2-6 Inhibitors used for HS-5 treatment.

High and low concentrations were used in this study; plasma concentrations were based on the published literature.

Drug	Target	High Conc.	Low Conc.	Recommended Conc.
Aspirin	Cyclooxygenase-1 and 2 (COX-1 and 2) inhibitor	10 mM	5 mM	N/A
Cycloheximide (CHX)	Protein synthesis inhibitor	10 mM	5 mM	10 mM (Liu et al., 2017a)
Salicylate	Cyclooxygenase-1 and 2 (COX-1 and 2) inhibitor	10000 μM	20μM	4000 μM (Alfonso *et al.*, 2014)

2.6 Proteomic analysis

2.6.1 Protein quantification assay

Conditioned medium from treated cells was collected as described in section 2.5.1, and the protein level was measured using Pierce™ Coomassie (Bradford)

Protein Assay Kit (Thermo Scientific, UK). Samples and standards were prepared according to the manufacturer's protocol. In brief, 150 µL of standard and unknown samples were pipetted into appropriate microplate wells (Corning 96 well, clear) in triplicate including diluent as a blank. Coomassie Reagent (150 µL) was added to each well and mixed on a plate shaker for 30 seconds. The plate was then incubated for 10 minutes at room temperature (RT). The absorbance was measured using a FLUOstar OPTIMA (BMG Labtech, Germany) plate reader at a wavelength of 580 nm. Measurements were averaged, and the blank was subtracted from all standards and unknown samples. The standard curve was prepared by plotting the averaged blank subtracted measurement for each standard versus its concentration in µg/ml. The protein concentration estimate for each unknown sample was determined using the equation of the standard curve.

2.6.2 Proteomic analysis and identification of paracrine factors in HS-5 C.M. under normoxia and hypoxia

HS-5 samples were prepared in two groups; untreated and BEAM (carmustine (BiCNU®), etoposide, cytarabine (Ara-C), melphalan) treated, each group was tested in normoxia and hypoxia to make the following subgroups: untreated normoxia, untreated hypoxia, BEAM treated in normoxia and BEAM treated in hypoxia; each subgroup contained three biological repeats. Cells were seeded in a 6-well tissue culture plate at $1x10^6$ cells per well resuspended in DMEM-HG. Cells were incubated at normal culture conditions of 37°C and 5% CO_2 for 24 hours to enable adherence to the plate, at which point the medium was changed to complete RPMI 1640 supplemented with combination chemotherapeutic agents (melphalan 8.2µM, carmustine 1.9µM, etoposide 2.5µM, cytarabine 2.5µM). Cells were then incubated

at normal culture conditions in normoxia or hypoxia (section 2.2.6) for 24 hours. After 24 hours, the medium was replaced by serum free RPMI 1640 and re-incubated in normal culture conditions in normoxia or hypoxia for 24 hours; the conditioned medium was then collected.

2.6.3 Proteomic samples processing and analysis

Samples of conditioned medium (C.M.) for proteomic analysis were sent to the proteomic service unit at the University of Bristol. Protein extracts isolated from C.M. were reduced, alkylated and digested overnight (Appendix 2). Samples were labelled with the tandem mass tags (TMT) Reagents (TMT10plex Mass Tag Labelling; Thermo Scientific ™, USA) and then mixed before sample fractionation and clean-up. Labelled samples were analysed by high resolution Orbitrap LC-MS/MS (Thermo Scientific ™, USA) before data analysis to identify peptides and quantify reporter ion relative abundance.

Raw data was processed in Proteome Discoverer™ Software (Thermo Scientific ™, USA), a package developed for protein identification and quantification from large proteomics datasets obtained through high-resolution mass-spectrometry. Results were obtained as a Microsoft data sheet which was then converted to .txt format. Results were then analysed in Perseus (release 1.6.2.2 and release 1.6.5.0).

2.6.4 Loading results data into Perseus

Perseus software is a framework for the data annotation and statistical analysis of proteomics data obtained through high-resolution mass spectrometry (http://www.perseus-framework.org/), (Tyanova, *et al*., 2016; Tyanova and Cox, 2018). Results were obtained as a Microsoft Excel datasheet which was then

converted to .txt format. Data were uploaded to Perseus through the main upload menu > Generic upload > result group selected. Data were filtered to remove contaminants (e.g. anything indicated to be of non-human origin); Processing > Filter > Filter category > Contaminant > Remove matching rows. Data also were filtered based on valid and numerical values, so all proteins without valid and numerical values were removed. After that, data columns were named according to experimental design based on testing conditions of the samples, for example (untreated normoxia, untreated hypoxia, treated normoxia and treated hypoxia). Data then were visualised using a Volcano plot and heat map to determine the significantly changed proteins, from which upregulated proteins were determined.

To match proteins matrices from different experimental conditions, proteins matched by accessions, common candidate proteins between matrices were determined based on a numeric Venn diagram.

Enrichment analysis of protein groups was made utilising Protein Analysis Through Evolutionary Relationships (PANTHER) classification system (release 14.1) (Mi *et al*., 2018). Protein to protein interactions, including direct (physical) and indirect (functional) associations were determined through STRING database (version 11) (Szklarczyk *et al*., 2019).

2.7 Recombinant proteins in the transmigration model

Candidate proteins selected from proteomic analysis were obtained as recombinant proteins (Table 2.7). These proteins were tested in the transmigration model to evaluate their effects on HL-60 transmigration. The model was established as described in section 2.3.7; recombinant proteins were added to the lower compartments of each insert mixed with complete RPMI 1640. Additional inserts

were tested alongside as a negative control without barrier as well as positive controls with SDF-1α.

Table 2-7 recombinant proteins.

MMP-1 and MMP-3 concentration was based on *in vitro* approximations. AMOT concentration was based on ELISA results.

Protein	Conc.	Supplier
Matrix Metalloproteinase-1 (MMP-1)	50ng/mL	Sigma Aldrich
Matrix Metalloproteinase-1 (MMP-3)	50ng/mL	Sigma Aldrich
*Angiomotin (AMOT)	1ng/mL	Bio-Techne

* A recombinant protein with GST-tag at the N-terminal corresponding to the amino acids 1 - 675 of Human AMOT full-length ORF dissolved in 200 µl of 50 mM Tris-HCl, 10 mM reduced glutathione.

Amino Acid Sequence:
(MPRAQPSSASYQPVPADPFAIVSRAQQMVEILSDENRNLRQELEGCYEKVARLQKVETEIQRVSEAYENLVKSSSKREALEKAMRNKLEGEIRRMHDFNRDLRERLETANK QLAEKEYEGSEDTRKTISQLFAKNKESQREKEKLEAELATARSTNEDQRRHIEIRDQALSNAQAKVVKLEEELKKKQVYVDKVEKMQQALVQLQAACEKREQLEHRLRTRLER ELESLRIQQRQGNCQPTNVSEYNAAALMELLREKEERILALEADMTKWEQKYLEENVMRHFALDAAATVAAQRDTTVISHSPNTSYDTALEARIQKEEEEILMANKRCLDM EGRIKTLHAQIIEKDAMIKVLQQRSRKEPSKTEQLSCMRPAKSLMSISNAGSGLLSHSSTLTGSPIMEEKRDDKSWKGSLGILLGGDYRAEYVPSTPSPVPPSTPLLSAHSKTGS RDCSTQTERGTESNKTAAVAPISVPAPVAAAATAAAITATAATITTTMVAAAPVAVAAAAAPAAAAAPSPATAAATAAAVSPAAAGQIPAAASVASAAAVAPSAAAAAAAV QVAPAAPAPVPAPALVPVPAPAAAQASAPAQTQAPTSAPAVAPTPAPTPTPAVAQAEVPASPATGPGPHRLSIPSLTCNPDKTDGPVFHSNTLERKTPIQILGQEPDAEMV EYLI)

2.8 Estimation of angiomotin (AMOT) levels by ELISA

HS-5 C.M. samples were prepared as described in section 2.6.2, media were then harvested, and cells were trypsinized and resuspended in PBS to be lysed by ultrasonication four times (1 minute at 20kHz). Samples were then preserved at -20°C until further testing.

Samples were tested for AMOT levels by Angiomotin (AMOT) Sandwich ELISA Kit (Biorbyt, UK), Cat#: orb437894, with a minimum sensitivity of 0.112ng/mL, and a detection range from 0.312 to 20ng/ml. Samples and reagents were processed according to the manufacturer's instructions. In brief, 100µL of standard, unknown samples (C.M. and cell lysates (C.L.)) and blank were added into appropriate antibody coated microplate wells in triplicate, and the plate was incubated for 2 hours at 37°C. The liquid was removed from each well, 100µL of Detection Reagent A working solution were added to each culture well, and the plate was incubated in the dark for

1 hour at 37°C. After 1 hour, the solution was aspirated, and wells were washed with 300µL of 1× Wash Solution three times. After the last wash, the remaining liquid from all wells was completely removed by tapping the plate onto absorbent paper. Subsequently, 100µL of Detection Reagent B working solution were added to each well, and the plate was incubated in the dark for 1 hour at 37°C. After 1 hour, the solution was aspirated, and wells were washed with 300µL of 1× Wash Solution three times. Substrate Solution (90µL) was added to each well, and the plate was incubated for 20 minutes at 37°C. Finally, 50µL of Stop Solution were added to each well, and the liquid was mixed by tapping the side of the plate. Measurements of the microplate's O.D. was taken using the FLUOstar OPTIMA (BMG Labtech, Germany) plate reader at wavelength of 450nm ± 10nm. O.D. measurements were averaged, and the blank was subtracted from all other standards and unknown samples. The standard curve was prepared by plotting the average blank subtracted measurement for each standard versus its concentration in ng/ml. The concentration of AMOT in the samples was then determined by comparing the O.D. of the samples to the standard curve.

2.9 Immunocytochemistry

HMEC-1 cells were seeded into sterilised flexiPERM culture chambers (Figure 2.3) attached to slides at $2x10^5$ cells/cm^2, each well is $\cong$ 0.7cm^2 and incubated in normal culture conditions. After 24 hours, the medium was replaced with fresh MCDB 131 supplemented with SDF-1α at 400ng/mL, MMP-1 at 50ng/ml, MMP-3 at 50ng/mL or AMOT at 1ng/mL in independent culture well, and re-incubated in normal culture conditions for 24 hours. Medium and attached culture chambers were removed gently, and slides were washed once with sterile PBS prior to fixation with 4% (w/v)

paraformaldehyde (PFA) (Sigma, UK) for 15 minutes at RT. Subsequently, slides were washed three times with sterile PBS and then blocked with 10% (w/v) FBS/PBS for 60 minutes (Gibco, UK). Slides were then incubated overnight with primary antibody prepared in the blocking buffer at the appropriate concentration at 4°C (Table 2-8). Antibodies were selected from different species origin in order to test both antigens at the same time.

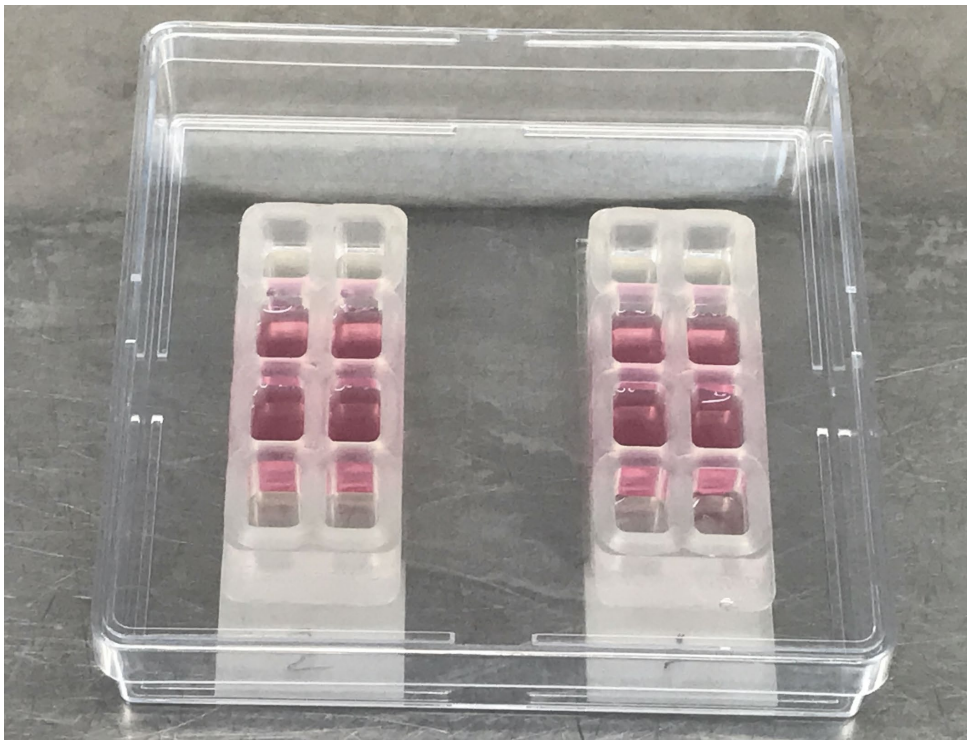

Figure 2-3: FlexiPERM culture chambers.

FlexiPERM is a removable culture chamber made of silicone. It can stick to slides due to its naturally adhesive underside without glue, creating multiple growth chambers for cells.

Table 2-8 Primary antibodies for immunocytochemistry.

Antibody	Clone	Isotype	Supplier	Working conc.
Anti-CD62E	1.2B6	Mouse monoclonal IgG1	Abcam, UK	2.5 µg/mL
Anti-CD62P	EPR1444(2)(B)	Rabbit monoclonal IgG	Abcam, UK	2.5 µg/mL

After this, slides were washed three times for 5 minutes in PBS and incubated in the dark with the appropriate secondary antibody at the recommended concentration, at RT (Table 2-9). Following antibody attachment, slides were washed a further three

times and then incubated for 5 minutes in 4',6-diamidino-2-phenylindole (DAPI; 1:10,000) nuclear counterstain. Slides were then washed with PBS a further three times for 5 minutes and were visualised using the fluorescence microscope (Leica, Germany) and images acquired using Leica Confocal Software (Leica, Germany). Images were processed using ImageJ 1.52k (National Institutes of Health, USA).

Table 2-9 Secondary antibodies for immunocytochemistry.

Antibody	Conjugation	Supplier	Working conc.
Rat monoclonal Anti-Mouse IgG1 H&L	(FITC)	Abcam, UK	1 mg/mL
Donkey Anti-Rabbit IgG H&L	(Texas Red ®)	Abcam, UK	1 mg/mL

2.10 Wound healing assay

HMEC-1 cells were seeded at $2x10^5$ cells/cm^2 into sterilised flexiPERM culture chambers attached to slides and incubated in normal culture conditions as described in section (2.9). After 24 hours, the medium was replaced with fresh MCDB 131 supplemented with SDF-1α at 400ng/mL. HMEC-1 cell migration to the area between the culture wells was monitored after 24 and 48 hours.

2.11 Statistical Analysis

Experiments were performed three times unless otherwise stated. Results are presented as the mean ± standard deviation (SD) of at least three biological repeats. Statistical analysis of the data was performed using one-way ANOVA and two-way ANOVA. A p-value of 0.05 or below was considered significant. Graphical presentation of significant differences was identified as * $p < 0.05$, ** $p < 0.01$, *** $p < 0.001$ and **** $p < 0.001$. Graphical representation was performed using GraphPad Prism software.

CHAPTER 3: Development and optimisation of the transmigration model

3.1 Background

The transmigration model development process was based on the Boyden chamber assays which was originally introduced by Boyden (1962); also known as the filter membrane migration assay, transwell migration assay, or chemotaxis assay. It was first used for the analysis of leukocyte chemotaxis. The basic principle of this assay is based on a chamber of two culture medium-filled compartments separated by a microporous membrane, usually polyethylene terephthalate (PET) membrane with specific pore sizes (3µm, 5µm, 8µm and 12µm), which can be selected based on the size and behaviour of the cells to be tested. Cells are placed in the upper compartment of the insert and are allowed to migrate through the pores of the membrane insert into the lower chamber, in which chemotactic agents are present. After incubation for a specific time, the number of cells that have migrated to the lower side of the membrane will be monitored and tested. In this research, this approach was utilised and modified by adding other cellular components including an endothelial cell layer, bone marrow stromal cells (HS-5) and HL-60 as haematopoietic progenitor cells (Figure 3-1). Optimal cell culture conditions were determined in which cell lines were co-cultured in an attempt to simulate the BM microenvironment. Although the *in vivo* BM/blood vessel/HSC might be very complex, containing multiple cellular compartments interacting with specific signalling pathways, this approach might provide a valuable tool to understand how cells communicate inside the BM under various conditions.

Establishment of a tolerable setting for all candidate cell lines to proliferate normally without losing any of their functionality was a key element in the model. This part of the study focused on finding suitable conditions to create the

transmigration model. Determining the proliferation rate of each cell line was essential to adjust the experimental design and to reduce the variables that might interfere with transmigration. The initial part of developing the transmigration model was to establish an endothelial monolayer; endothelial cells should make a tight junction between each other without any gaps to prevent any transmigration, except when induced to loosen junctions to allow passage of relevant cells (Ganguly *et al*., 2012). Optimal seeding density should be determined in order to create a barrier mimicking the vasculature. Two cell lines were used, HUVEC and HMEC-1 (Lidington *et al*., 1999). HMEC-1 has a doubling time (D.T.) of 76 hours and ability to maintain endothelial characteristics up to 95 passages (Ades *et al*., 1992). It also expresses endothelial cell-surface molecules including CD31 and CD36 and expresses the cell adhesion molecules ICAM-1 and CD44 which play a vital role in the initial adhesion and tethering of stem cells to vascular endothelial cells (Ades *et al*., 1992).

The mesenchymal stem cell HS-5 was used to represent the bone marrow stroma; it appears to be fibroblastoid in shape and secretes significant levels of granulocyte colony-stimulating factor (G-CSF), granulocyte-macrophage-CSF (GM-CSF), macrophage-CSF (M-CSF), Kit ligand (KL), macrophage-inhibitory protein-1 alpha, interleukin-6 (IL-6), IL-8, and IL-11. HS-5 also supports proliferation of haematopoietic progenitor cells when co-cultured in serum-deprived medium with no exogenous factors (Roecklein & Torok-Storb, 1995). The HS-5 can take up to 36 hours to double under standard conditions as described by Trivanovic *et al.* (2015).

The HL-60 cell line was used as haematopoietic progenitor cell (HPCs). HL-60 has been used in a number of studies to characterise leukocyte-endothelial interactions (Chang *et al*., 2016; Zhu *et al*., 2017); in this study the HL-60 cell line was used to validate the transmigration process through the endothelium. HL-60 cells express the

chemokine receptor CXCR4 inducible by SDF-1α to initiate the transmigration process.

3.2 Aims

The aim was to establish an *in vitro* co-culture model of the blood vessel endothelial cells/HPC interaction, where endothelial cells were grown as a layer in a cell culture insert and HPC cell line was placed in the basket above the endothelium, and the ability of the HPC to traffic through the endothelial monolayer was monitored as an indication of 'trafficking and homing'. The chemoattractant SDF-1α was used as a positive control to confirm the ability of HL-60 to traffic through the endothelium and to confirm that the model will work under the co-culture conditions.

3.3 Methods

3.3.1 Culture medium

All cell culture procedures were carried out, as described in section 2.1. The range of culture medium for each of the cell lines is outlined in section 2.1.

3.3.2 Microscopy

Light microscopy was used to examine the morphology and cell growth of all cell lines (section 2.2.). SEM was used to confirm adherence of the endothelial cells to the inserts and to confirm that pores are covered with cells (section 2.4.2).

3.3.3 Trans-endothelial electrical resistance (TEER)

TEER was used to assess the endothelial cell membrane integrity (section 2.3.1).

3.3.4 Flow cytometry

Flow cytometry was used to assess HS-5 MSCs markers; CD44, CD73, CD90 and CD105 in different media (section 2.4).

3.4 Development and general design of the transmigration model

Building the *in vitro* transmigration model was initially based on co-culture of all the three cell lines together in one environment, in which the BM mesenchymal stem cell line HS-5 was grown in the base of the culture well, the vascular endothelial cell line was grown as a layer in a cell culture insert and the HL-60 cell line was placed in the basket above the endothelial monolayer (Figure 3-1 A). This approach was possible only if one tolerable medium for all cells was identified without affecting the viability of the cells and integrity of the endothelial barrier. An alternative approach was by maintaining and expanding each cell line in its optimal culture condition separately, then during the test the vascular endothelial cell line was grown as a layer in a cell culture insert and the HL-60 cell line was added to the basket above the endothelial monolayer. Conditioned medium from the BM mesenchymal stem cell line HS-5 was placed in the base of the culture well to induce transmigration (Figure 3-1 B).

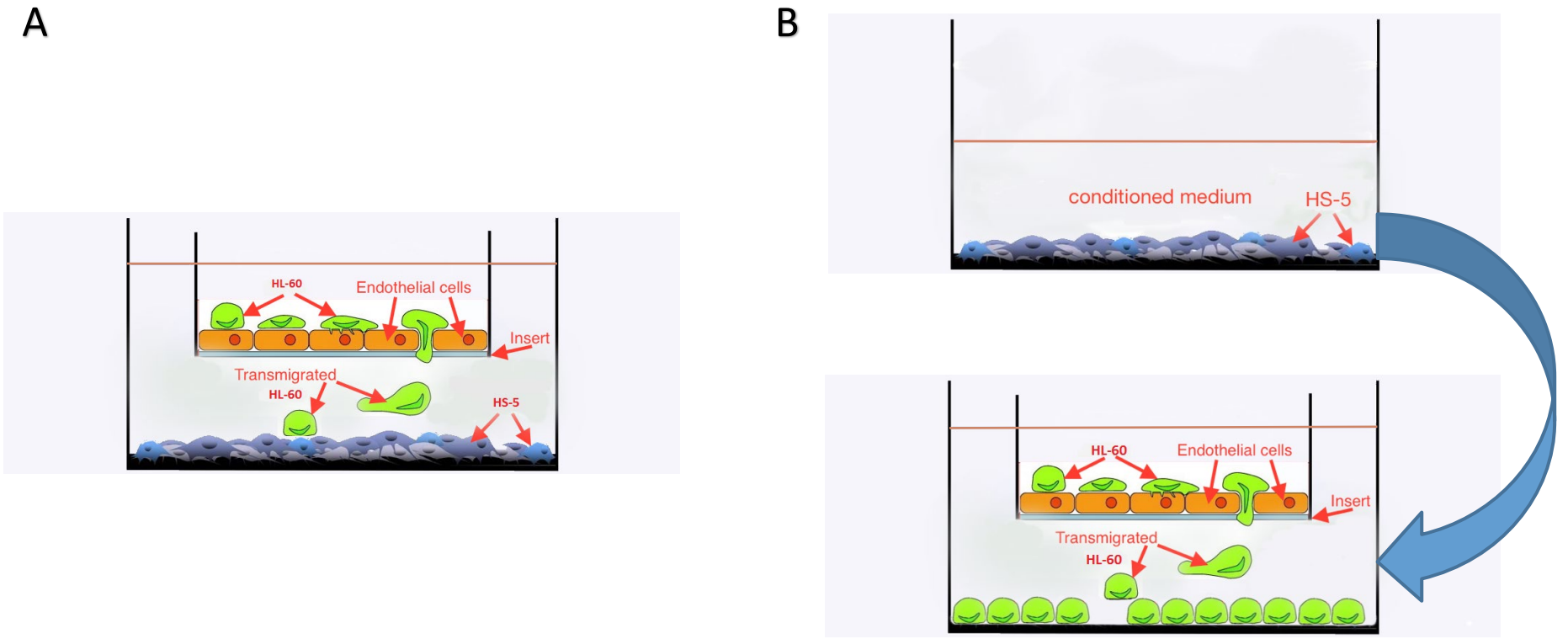

Figure 3-1 Transmigration co-culture model.

(A) Co-culture all the three cell lines together in one environment, HL-60, HS-5 and endothelial cells. (B) Co-culture the vascular endothelial cell line and the HL-60 cell line; conditioned medium from BM mesenchymal stem cell line HS-5, is added in the base of the culture well. Straight line represents medium level.

3.5 Results and discussion

3.5.1 Comparing endothelial cell lines as a model of the vasculature

HUVEC and HMEC-1 were compared in terms of morphology, growth and proliferation rate, and ability to demonstrate a suitable membrane ohmic resistance to create an endothelial barrier.

3.5.1.1 The HUVEC monolayer showed slow growth with slightly increased TEER

HUVEC were seeded at three different densities: 1.5 x 10^5, 2.5 x 10^5 and 3.5 x10^5 cell/cm^2 in a 12 well culture plate. The HUVEC monolayer formation was monitored, and images were taken using phase-contrast microscopy after 24 and 48 hours. Some gaps between cells were observed even with high seeding density in all wells; the cells just lie over each other in some areas, and the number of floating cells was high (Figure 3-2). The presence of gaps between cells might interfere with the tightness of the endothelial monolayer, which might affect the process of transmigration.

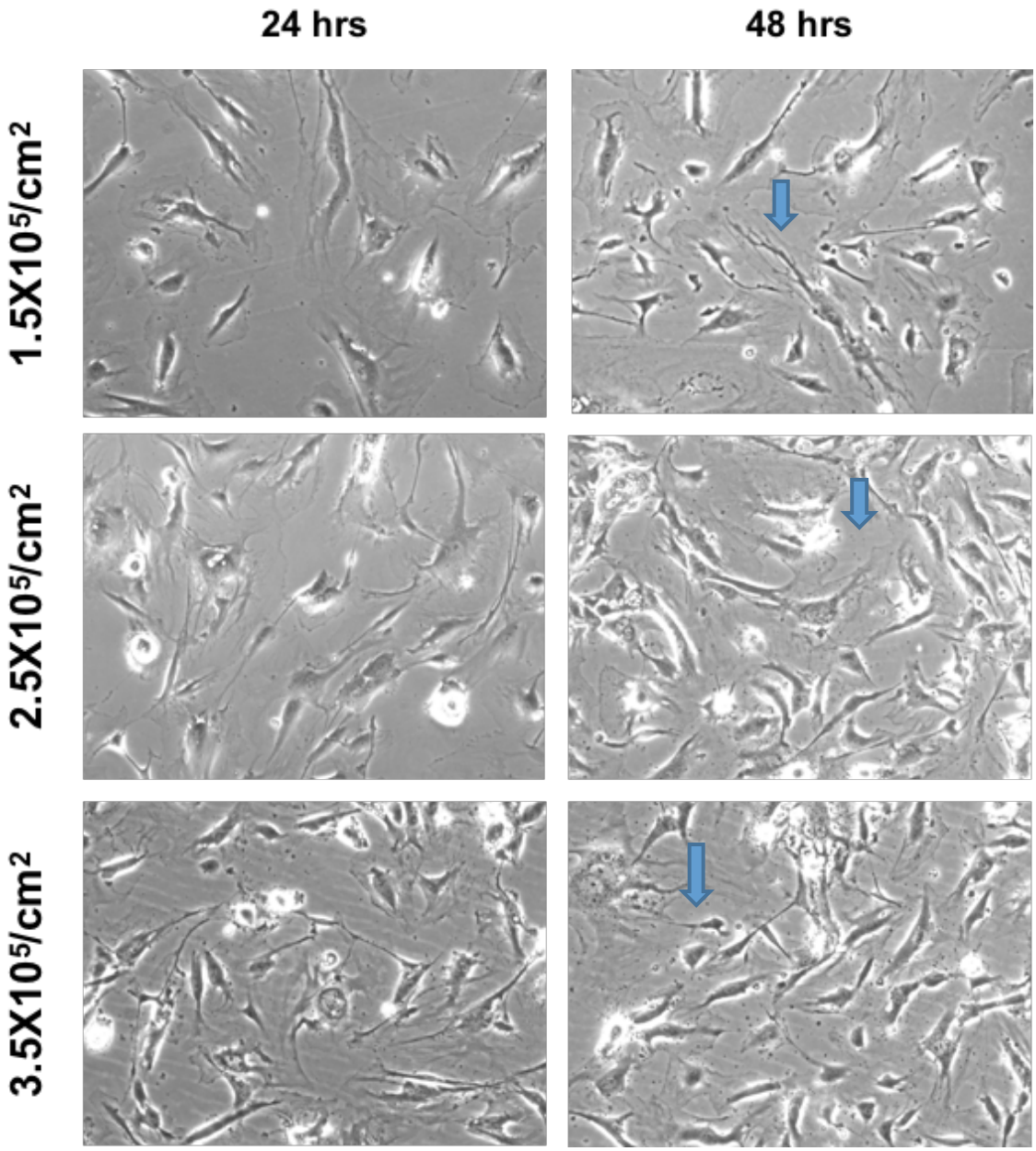

Figure 3-2 HUVEC cells at 24 and 48 hours from seeding in 12 well culture plate.

Growth rate was slow; cells make a layer of endothelium, gaps between cells were observed (arrowed). Pictures were captured using a Nikon inverted phase-contrast microscope under 20X objectives. Results are representative of n=3.

Ohmic resistance was measured for the HUVEC cells' monolayer on 8µm Millicell PET membrane hanging trans-well inserts at different time points. The cell monolayer started to show some resistance after 72 hours. Proliferation rate of HUVEC was slow; growth of the cells was not enough to cover the surface of

the insert and create a suitable TEER resistance level. Based on this finding the HUVEC cell line was excluded from the development process of the transmigration model due to long maintenance time.

The HUVEC cell line growth was very slow especially during the first two weeks from resurrection. None of the HUVEC cells transmigrated across the inserts; this finding might propose using the 8µm pore size for the co-culture of the cell lines as this will give the HSCs enough space to transmigrate to the lower chamber of the insert, but not the HUVEC. There was a slight increase of ohmic resistance of the HUVEC cells' monolayer after 72 hours (Figure 3-3), which might indicate the beginning of formation of tight junctions between cells in order to make an endothelial layer. Generally, formation of endothelium will increase the electrical resistance of the monolayer. Ohmic resistance of a confluent HUVEC monolayer might reach an average of 74 Ω cm^2 (Man *et al.*, 2008). The generation of appropriate resistance will play an integral role in understanding how drugs might compromise this barrier and perhaps increase or decrease the capacity for HSC to cross. To improve endothelialisation, the inserts might be coated with collagen type I together with fibronectin which was described by Sgarioto *et al.*, (2012). Collagen and fibronectin coated surfaces have an enhanced adhesion property that is more suitable for the growth and proliferation of HUVEC as well as reducing floating cells. A high seeding density might be helpful in such conditions as well, and it might reduce the time to reach confluence rather than waiting for the HUVEC to grow and spread over the insert. Seeding the insert initially with enough cells to cover the inserts' seeding area might facilitate HUVEC monolayer formation in a shorter time especially during co-culture stage. Conversely, the HMEC-1 cell line proliferated fast

enough to make a confluent monolayer and was taken forward for further co-culture experiments.

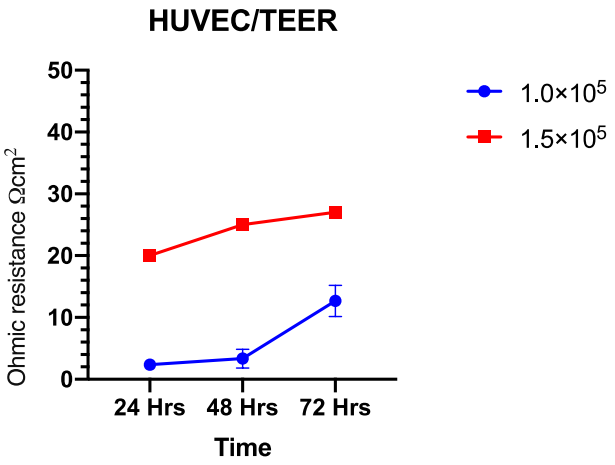

Figure 3-3 Ohmic resistance of HUVEC monolayer.

HUVEC cell line was seeded at 1.0 × 10^5 cells/cm^2 and 1.5 × 10^5 cells/cm^2 suspended in 1 ml of medium and added to collagen coated 8µm Millicell hanging trans-well inserts for 12-well plates (2mL of medium was added to the lower compartment). Collagen was used to improve adherence, endothelialisation and to reduce the gaps between cells. Ohmic resistance TEER was measured for the HUVEC at 24, 48 and 72 hours. (Collagen coated blank insert resistance: 70 Ωcm^2). Readings represent resistance after subtracting blank insert resistance. Results are presented as average TEER value ± S.D. for n=3 for seeding at 1.0 × 105 cells/cm^2 and n=1 for seeding at 1.5 × 10^5 cells/cm^2.

3.5.1.2 HMEC-1 demonstrate a suitable proliferation rate, morphological features and coverage of the insert

HMEC-1 was seeded at different densities in a 24 well plate: 1.0 x 10^5, 1.5 x 10^5, 2.0 x 10^5, 2.5 x 10^5, 3.0 x 10^5, 3.5 x 10^5, 4.0 x 10^5, 4.5 x 10^5 and 5.0 x 10^5 cell/cm^2. The HMEC-1 monolayer formation was monitored, and images were taken using phase contrast microscopy after 24 and 48 hours (Figure 3-4, 5 and 6). The HMEC-1 cells in culture appear more consistent, showing spindle-shaped elongated cells at low seeding density after 24 hours. Cells started to adopt cobblestone morphology as seeding density was elevated to reach 5.0 x 10^5. After 24 hours, cobblestone morphology started to appear at the lower seeding density 3.5 x 10^5 and above. In both cases cells did not overgrow on top of one

another. Seeding density was elevated gradually to determine the optimal cell count to create a barrier within 24 hours.

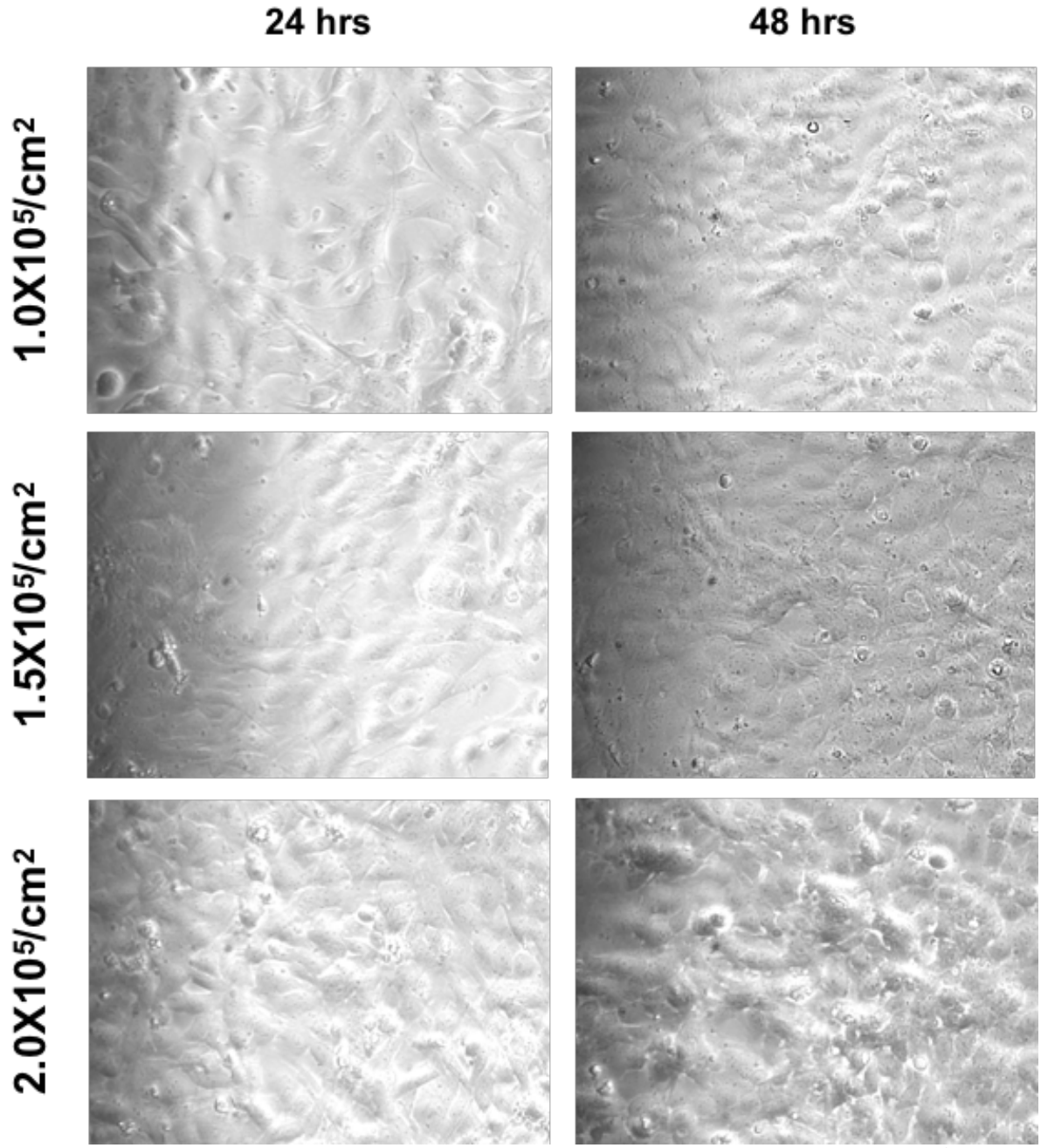

Figure 3-4 HMEC-1 cells at 24 and 48 hours from seeding at 1.0 x 10^5, 1.5 x 10^5 and 2.0 x 10^5 cells/cm^2 in a 24 well plate.

Cells started to make a layer of endothelium. Pictures were captured using a Nikon inverted phase contrast microscope under 20X objectives. Results are representative of n=3.

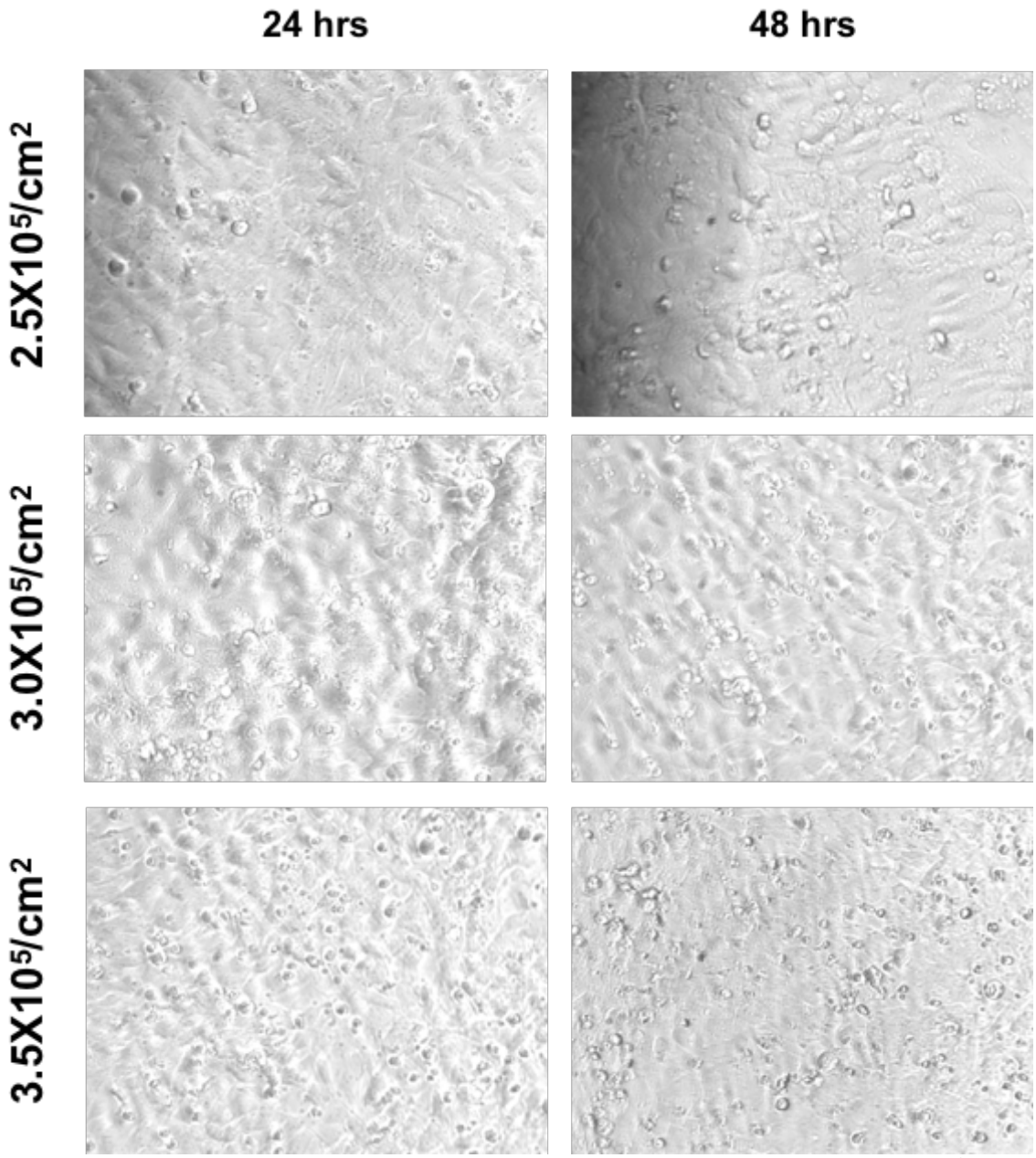

Figure 3-5 HMEC-1 cells at 24 and 48 hours from seeding at 2.5 x 10^5, 3.0 x 10^5 and 3.5 x 10^5 cells/cm^2 in a 24 well plate.

Cells make a layer of endothelium. Pictures were captured using a Nikon inverted phase contrast microscope under 20X objectives. Results are representative of n=3.

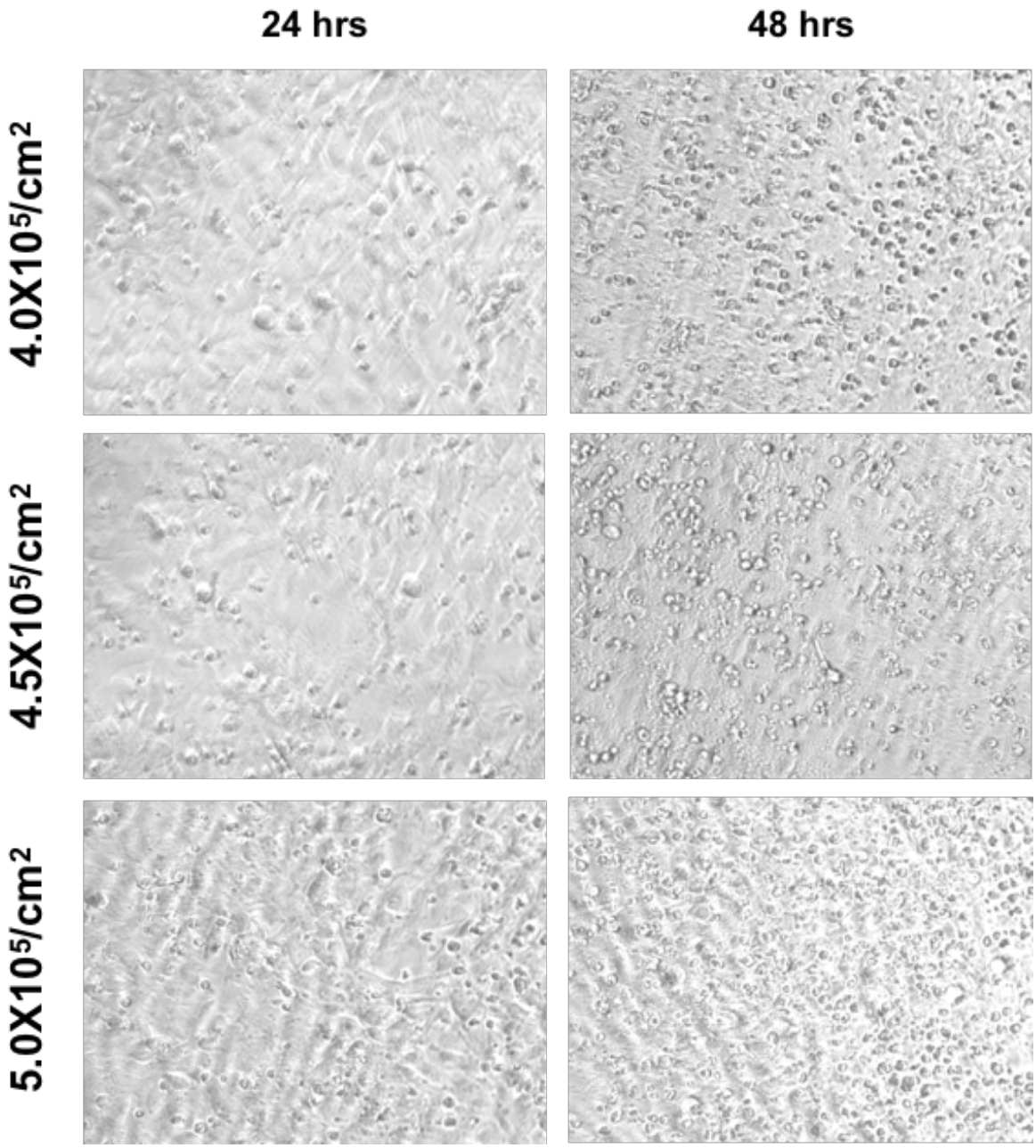

Figure 3-6 HMEC-1 cells at 24 and 48 hours from seeding 4.0 x 10^5, 4.5 x 10^5 and 5.0 x 10^5 cells/cm^2 in a 24 well plate.

Cells make a layer of endothelium. Pictures were captured using a Nikon inverted phase contrast microscope under 20X objectives. Results are representative of n=3.

Scanning electron microscopy showed that the HMEC-1 cells tend to cover the pores of the insert (Figure 3-7).

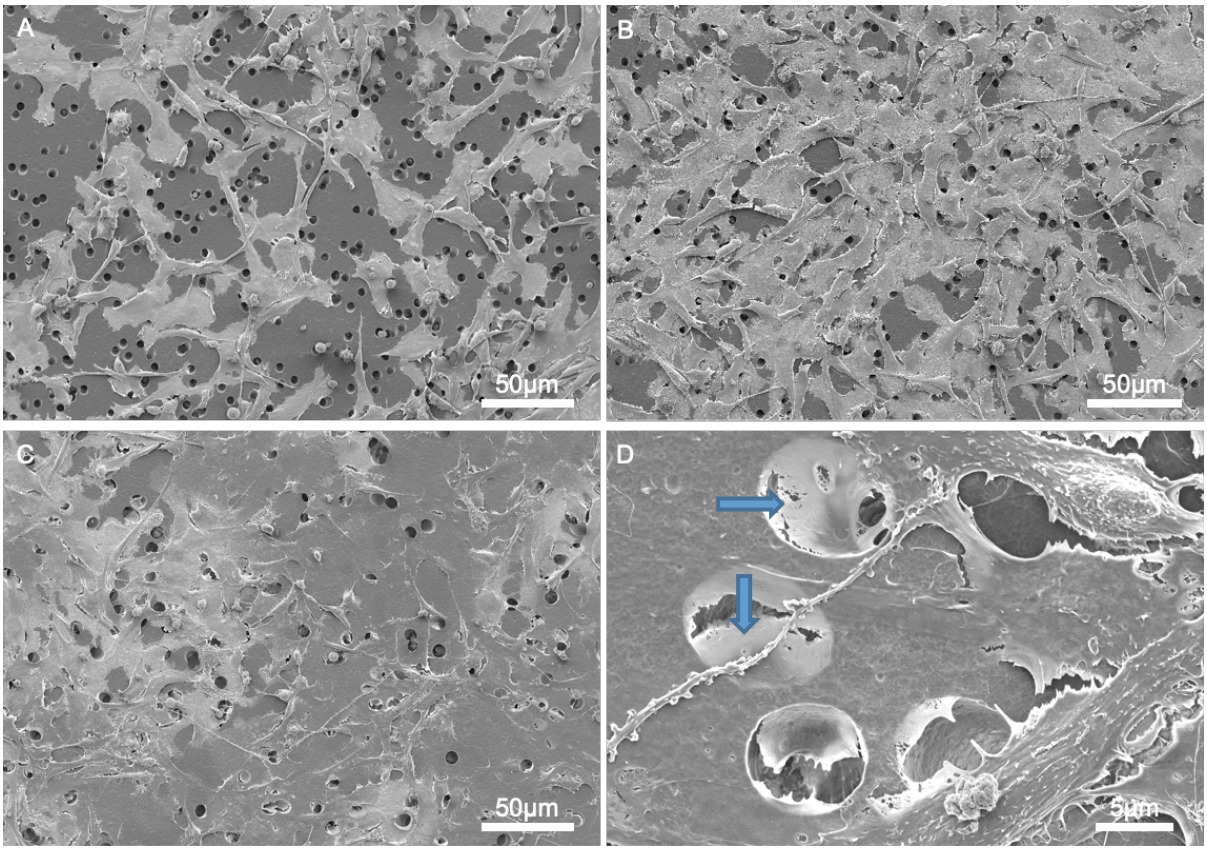

Figure 3-7 Scanning electron microscopy SEM of the HMEC-1.

HMEC-1 was seeded at 3.0 x 10^5 (A), 4.0 x 10^5 (B) and 5.0 x 10^5 (C and D) in 12 well 8 µm pore inserts, images were taken with the FEI Quanta 650 FEG scanning electron microscope after 24 hours, cells appear more confluent at high seeding density, pores of the inserts were covered by the endothelial layer (arrowed) (D). Results represent n=1.

Ohmic resistance was measured for the HMEC-1 at 24 and 48 hours (Figure 3-8). TEER values increased depending on two factors: the seeding density and the incubation time. Measurements reached their highest level after 24 hours at a seeding density of 5.0 x 10^5 which might suggest this seeding density created the best endothelial monolayer. After 48 hours, TEER values tend to be more stable even for lower seeding densities starting from 3.5 x 10^5 and above.

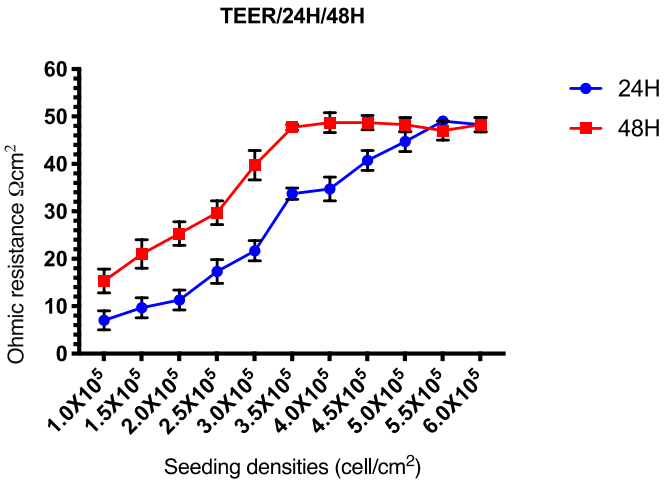

Figure 3-8 HMEC-1 TEER at different seeding densities.

HMEC-1 were seeded at 1.0 x 10^5, 1.5 x 10^5, 2.0 x 10^5, 2.5 x 10^5, 3.0 x 10^5, 3.5 x 10^5, 4.0 x 10^5, 4.5 x 10^5, 5.0 x 10^5, 5.5 x $10^5$and 6.0 x 10^5 cells/cm^2 in 12 well 8 μm pore inserts: Blank insert resistance is 70 Ω cm^2. Results are presented as average TEER value ± S.D. at 24 and 48 hours for n=3.

HMEC-1 tend to proliferate normally in different media, with a significant increase in doubling time in DMEM-HG (Figure 3-9). This step was made to measure the effect of exposing the endothelium to different culture conditions and to evaluate any interfering factor that might affect the integrity of the membrane itself and interfere with transmigration.

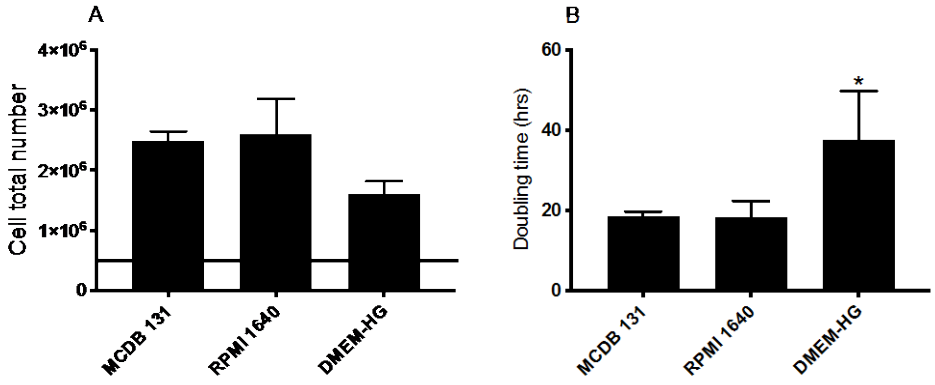

Figure 3-9 HMEC-1 proliferation rate in different media

HMEC-1 proliferation rate (A) and doubling time (B) in MCDB 131, RPMI 1640 and DMEM-HG. Cells were seeded at 2.0×10^4 cells/cm^2 in a T25 flask and counted after 48 hours. The horizontal line represents the initial seeding density. Results are presented as average cell count ± S.D. for n=3. Statistical significance is indicated as * p<0.05. Statistical analysis was done using one-way ANOVA test.

3.5.2 HS-5 maintains its characteristics in different media

The HS-5 cell line was cultured in four different types of complete media (including the recommended medium of DMEM-HG) to determine the optimal medium for cell growth that allows a normal proliferation rate of the HS-5 cell line. Each alternative medium was compared with the recommended medium by the cell supplier. The total cell number and doubling time was compared in each medium 96 hours after seeding. Among the different types of media, the highest growth potential and shortest doubling time was demonstrated in F-12K, since cell number was significantly higher compared to that of the recommended medium (p < 0.001; Figure 3-10). F-12K contains additional supplements such as ECGS as described in Table 2-1. Although the recommended medium for HS-5 is DMEM-HG, cells showed similar growth and proliferation rates in MCDB 131 and RPMI 1640. The final yield after 96 hours of culture was compared to the initial seeding density. The results indicated that all three alternative media could support HS-5 proliferation.

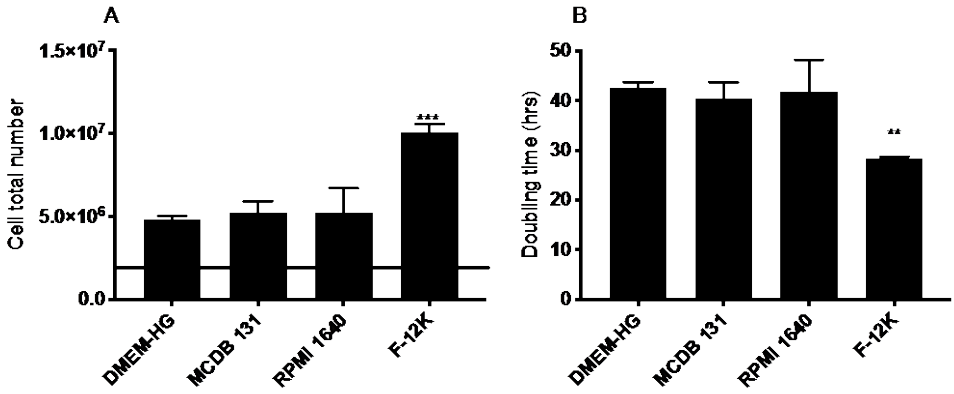

Figure 3-10 HS-5 Proliferation rate in different media.

HS-5 proliferation rate (A) and doubling time (B) in DMEM-HG, MCDB 131, RPMI 1640 and F-12K. Cells were seeded at 4.0×10^4 cells/cm^2 in a T25 flask and counted after 96 hours. The horizontal line represents the initial seeding density. Results are presented as average cell count ± S.D. for n=3. Statistical significance is indicated as **p < 0.01 and ***p < 0.001. Statistical analysis was done using one-way ANOVA test.

3.5.3 Comparing the stromal cell line morphological changes in different media

The HS-5 cell line was seeded at 1 x 10^6 per 25 cm^2 flask. After 72 hours, images were taken using phase contrast microscopy (Figure 3-11). HS-5 generally formed a confluent layer of fibroblast-like cells in all media. More floating HS-5 cells were observed in DMEM-HG. Viability was high in all media, which might indicate that floating cells are viable. Conversely, HS-5 cells were more endothelial-like in the F-12K and MCDB 131 media; cells were flatter in shape and appeared to be more adhesive. A study by Janeczek Portalska *et al.*, (2012) showed that human MSCs derived from bone marrow acquire several endothelial-like characteristics when cultured in endothelial cell growth supplements; these characteristics include differentiation into cells with an endothelial gene expression profile and morphology when seeded on Matrigel and ability to create a capillary network in 3D culture both *in vitro* and *in vivo* conditions. Constituents of each growth medium might have an influence on cells' shape and differentiation. Floating cells might indicate the presence of a subset of non-adherent HS-5 cells, which might have different proliferation capacity and different CD markers positivity and expression.

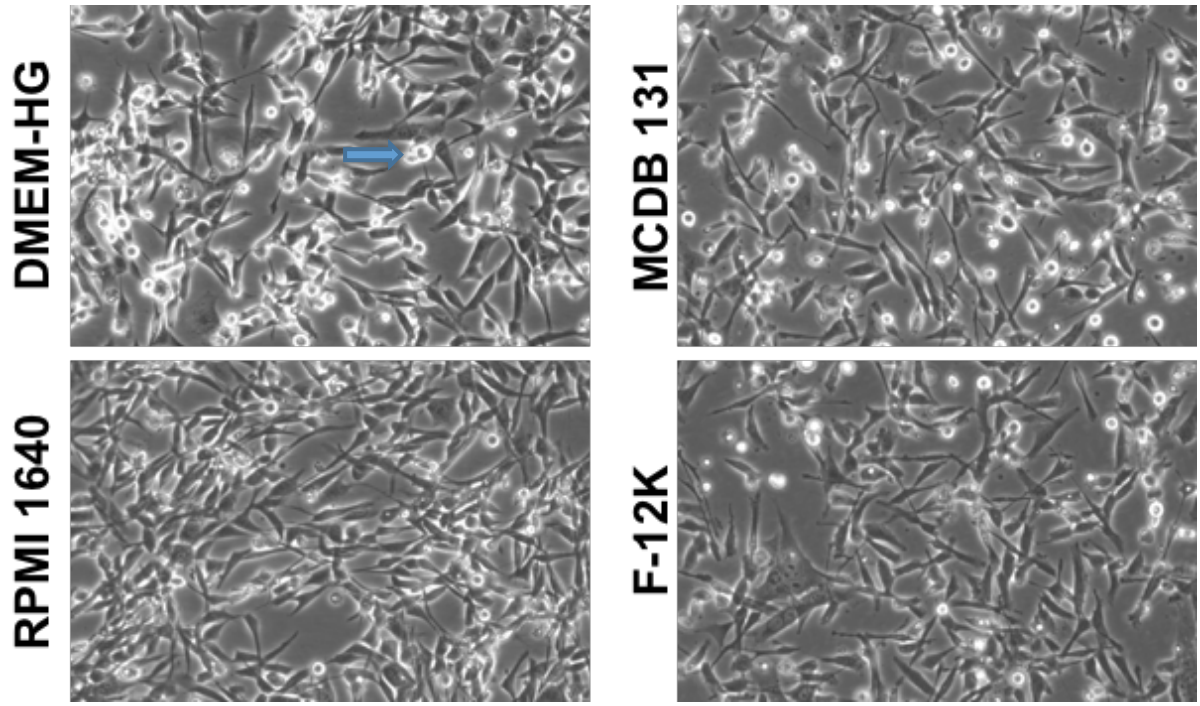

Figure 3-11 morphology in different culture media.

The HS-5 cell line was seeded at $1X10^6$ per 25 cm^2 flask. After 72 hours, images were taken using phase contrast microscopy. Pictures were captured using a Nikon inverted phase contrast microscope under 20X objectives. HS-5 forms a confluent layer of fibroblast-like cells in all media, cells were more endothelial like in F-12K and MCDB 131, more floating cells were observed in DMEM-HG medium (arrowed). Results represent three biological repeats.

3.5.4 HS-5 maintain expression of mesenchymal stem cell CD markers

HS-5 were tested for the percent positivity and expression of four MSCs CD markers (CD44, CD73, CD90 and CD105) after seven days from seeding (as described in section 2.4). Percent positivity for CD markers of HS-5 cells was determined and compared to that in the recommended medium (DMEM-HG). It was observed that each medium has a relatively different effect on HS-5 marker percent positivity (Figure 3-12 A). For CD44, the percent positivity was reduced by 26% in F-12K and by 2% in RPMI 1640 compared to DMEM-HG (p<0.0001 and p<0.05) respectively. CD73 percent positivity was reduced by 10% in RPMI 1640 compared to DMEM-HG (p<0.0001). CD90 percent positivity was also reduced in both F-12K and RPMI 1640 medium compared to DMEM-HG. CD105 percent positivity was significantly reduced especially in RPMI 1640 (p<0.0001), although, its average positivity was low in HS-5, especially in late passages as shown in Figure 3-12.

Median fluorescence intensity (MFI) was measured for each CD marker (Figure 3-11 B). Although, the percent positivity of some markers was relatively high in all media like in CD44, median fluorescence intensity was variable. For example, for CD44, the highest fluorescence intensity was observed in F-12K medium. For the CD 105 marker with extremely low percent positivity, MFI was only detectable, which might indicate that expression of the CD marker on the cells deemed positive was high.

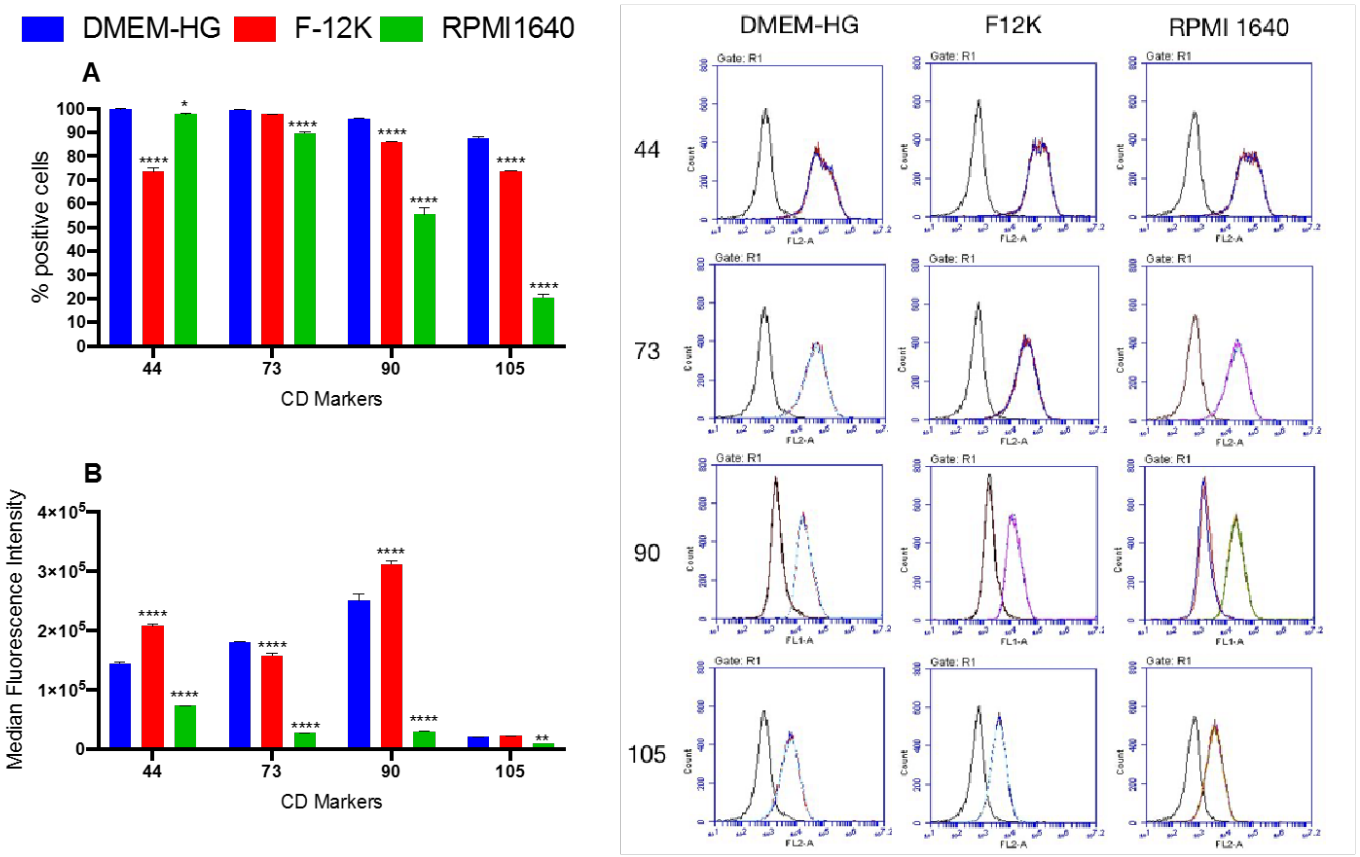

Figure 3-12 Percent positivity (A) and median fluorescence intensity (B) of CD44, CD73, CD90 and CD105.

Results are presented as percent average positivity and median fluorescence intensity ± S.E. for n=3. Overlays of histograms showing the fluorescence signal of HS-5 cells (right) compared to the isotype control (left). Statistical significance is indicated as * $p<0.05$ and **** $p<0.0001$. Statistical analysis was done using two-way ANOVA test.

However, primary stromal cells are highly positive (more than 95%) for all the four markers. According to Dominici *et al*., (2006), primary MSCs must express CD105, CD73 and CD90, and lack expression of CD45, CD34, CD14, CD19 and Human Leukocyte Antigen D Related (HLA-DR) surface molecules. The current results showed that HS-5 was positive for all stromal markers in all three media, although CD105 was low in RPMI 1640; however, percent positivity was lower than expected for CD44, CD73 and CD90 also. A study by Li *et al*., (2014), demonstrated that in primary MSCs, the percent positivity of each antigen was >99% positive for CD44, CD73, CD90 and CD105. They have used cells at passage 3 from BM, adipose tissue, umbilical cord Wharton's jelly and placenta. Different sources of MSCs might have different levels of percent positivity and expression of these markers; HS-5 originate from the BM and should agree with their findings. Although the current findings showed that HS-5 fulfilled the minimal criteria for MSC's characterisation and displayed a similar phenotype in all media, changes in CD markers might represent an alteration in the functionality of HS-5 in this model. CD44 is multifunctional class I integral transmembrane glycoprotein that is widely expressed on a number of cells in the BM with varying functions (Sackstein *et al*., 2008; Ponta, Sherman and Herrlich, 2003). CD73 is an ecto-5'-nucleotidase, which is known to be involved in BM stromal signal transduction in the haematopoietic compartment of bone marrow (Barry *et al*., 2001), and MSCs migration (Ode *et al*., 2011). CD90 marker is also called Thy-1 protein which plays an important role in cell adhesion. In primary BM-MSCs, it has been demonstrated that a reduction in CD90 expression results in increased differentiation of MSCs (Moraes *et al*., 2016). According to Trivanovic *et al*., (2015), MSCs derived from different tissues, exhibit a high degree of variability regarding biological properties related to their self-renewal and differentiation

capacity as well as percent positivity of mesenchymal markers. CD105 showed low positivity, though MFI was detectable, which might indicate that expression of the CD marker on the positive cells was high. Variation of CD105, (also known as endoglin), percent positivity might indicate a subpopulation of HS-5. In a murine model, CD105 negative mMSCs define a new multipotent subpopulation with distinct differentiation and immunomodulatory capacities (Anderson *et al.*, 2013). Low expression of CD105 might be associated with lineage differentiation capacity, as it has been demonstrated that down-regulation of CD105 is associated with multilineage differentiation in cord blood MSCs (Jin *et al*., 2009). According to the International Society for Cellular Therapy (ISCT), multipotent mesenchymal stromal cells (MSC) must maintain three criteria: adherence to plastic in standard culture conditions, (though some cells were floating), express CD105, CD73 and CD90, and lack expression of CD45, CD34, CD14, CD19 and HLA-DR surface molecules and ability to differentiate into osteoblasts, adipocytes, chondroblasts *in vitro* (Dominici *et al*., 2006). In general, some of these criteria were maintained in this study, like plastic adherence and mesenchymal marker expression but differentiation potential was not tested. However, HS-5 represents immortalised BM-MSCs and should retain its original characterisation to maintain its functionality. As HS-5 is an immortalised version of the BM, it is reasonable to assume that all of its characteristics are likely to be identical.

To test the expansion stability of the HS-5, it was tested also for the percent positivity and expression of MSCs CD markers in different passages (3, 5, 7 and 9) after 7 days from seeding in DMEM-HG (Figure 3-13). Passages 7 showed a significant reduction of CD105 percent positivity ($p<0.0001$), while, passage 9 showed a significant reduction of both CD73 and CD105 ($p<0.0001$), which might suggest that HS-5 could lose both MSCs markers with extended passaging.

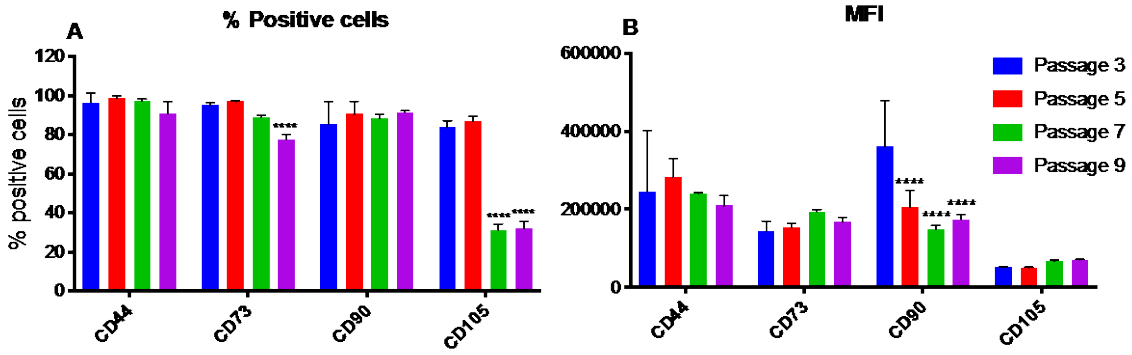

Figure 3-13 Percent positivity (A) and median fluorescence intensity (B) of CD44, CD73, CD90 and CD105.

HS-5 cells were cultured at 1 x 10^6 cells per 25 cm^2 flask, in DMEM-HG. HS-5 were tested for the percent positivity and expression of four MSCs CD markers (CD44, CD73, CD90 and CD105) after 7 days from seeding. Results are presented as percent average positivity and median fluorescence intensity ± S.D. for n=3. Statistical significance is indicated as **** $p<0.0001$. Statistical analysis was done using two-way ANOVA test.

3.5.5 HL-60 proliferation and exponential stage

The human promyelocytic cell line HL-60 is considered as a fast-growing cell line with a doubling time of 34 hours; this might influence the count of transmigrated cells in the model. Determination of the exponential stage of HL-60 proliferation was made to adjust the timing of the model setup. HL-60 was seeded at 1.0 × 10^5 and 2.0 × 10^5 cells/ml suspended in 5ml of RPMI 1640 complete medium and added to a T25 flask. Cell count was measured at different time points (Figure 3-14). Results indicated that at the seeded densities, HL-60 did not achieve the exponential phase of cell growth until 24hrs

post-seeding. However, HL-60 continued to proliferate exponentially to reach 2.0x10^6/mL in which proliferation was stabilised.

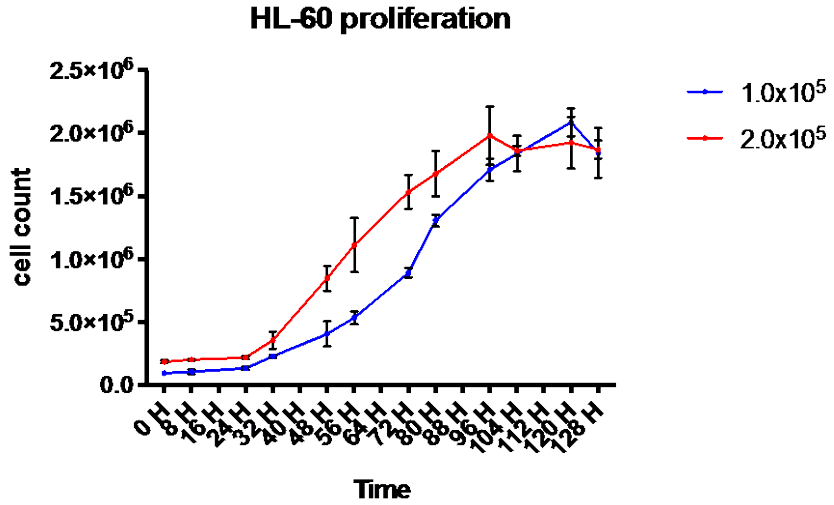

Figure 3-14 HL-60 proliferation and exponential phase.

HL-60 was seeded at 1.0 × 10^5 and 2.0 × 10^5 cells/ml suspended in 5ml of RPMI 1640 complete medium and added to a T25 flask. Cells were counted between 0 to 128 hours at different time points. HL-60 began exponential phase of growth at 24 hours. Results are presented as average cell count ± S.D. for n=3.

After determining the exponential phase of the HL-60, the proliferation rate was tested with, and without 10% FBS. Presence of the FBS as a constituent of the medium added to the base of the inserts might influence the transmigration process of HL-60 cell. Providing that HL-60 can survive without serum, this effect might be excluded by using serum free medium in the base of the inserts. Proliferation rate of HL-60 was tested with and without serum. Cells were seeded at 2.0 × 10^5 cells/ml suspended in 5ml of RPMI 1640 with and without FBS and added to a T25 flask. Cell count was measured at different time points (Figure 3-15). Results indicated that HL-60 proliferation was reduced significantly (p<0.0001) without FBS. HL-60 growth stopped, suggesting that serum is mandatory for HL-60; survival of the transmigrated HL-60 might be affected in the serum free medium, which might then alter the total cell count.

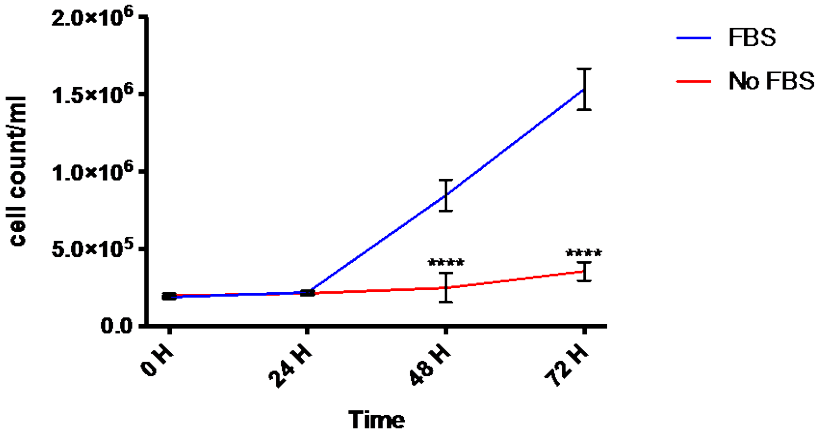

Figure 3-15 HL-60 proliferation and exponential phase.

HL-60 was seeded at 2.0×10^5 cells/ml suspended in 5ml of RPMI 1640 with and without FBS and added to a T25 flask. Cells were counted at 0, 24, 48 and 72 hours. HL-60 started to proliferate after 24 hours with FBS but not without FBS. HL-60 proliferation was reduced significantly without FBS. Results are presented as average cell count/ml ± S.D. for n=3. Statistical significance is indicated as **** $p<0.0001$. Statistical analysis was done using two-way ANOVA test.

3.5.6 Validation of the transmigration across endothelial monolayer

The transmigration model was initialised by creating an HMEC-1 barrier in the insert as described in section 2.3.4, HL-60 were labelled with cell tracker at 2.0 µM as described in section 2.3.8, placing HL-60 within the insert, and establishing capacity of the barrier to hinder transmigration (in the absence of inducers), and capacity of HL-60 to migrate (under the influence of inducers). Figure 3.16 A, demonstrates that in the absence of an HEMC-1 barrier, that HL-60 will easily cross the insert unhindered whereas in the presence of an HMEC-1 barrier, very few HL-60 are able to cross the barrier, demonstrating the production of a tight barrier. When SDF-1α was added to the well below the insert, there was a statistically significant increase in HL-60 trafficking across the barrier ($p<0.01$), and similarly a non-significant increase of HL-60 trafficking was seen with HS-5 conditioned medium in the base of the well. Plates were read on a SpectraMax M2 Microplate reader (Molecular Devices, U.K.) after removing the inserts. Figure 3.16 B, demonstrated that fluorescence intensity was

significantly increased (p<0.0001) in the well with SDF-1α added compared to that without SDF-1α added. The highest fluorescence intensity was observed in the well without HMEC-1 barrier also, indicating that HL-60 cells were able to cross the inserts easily.

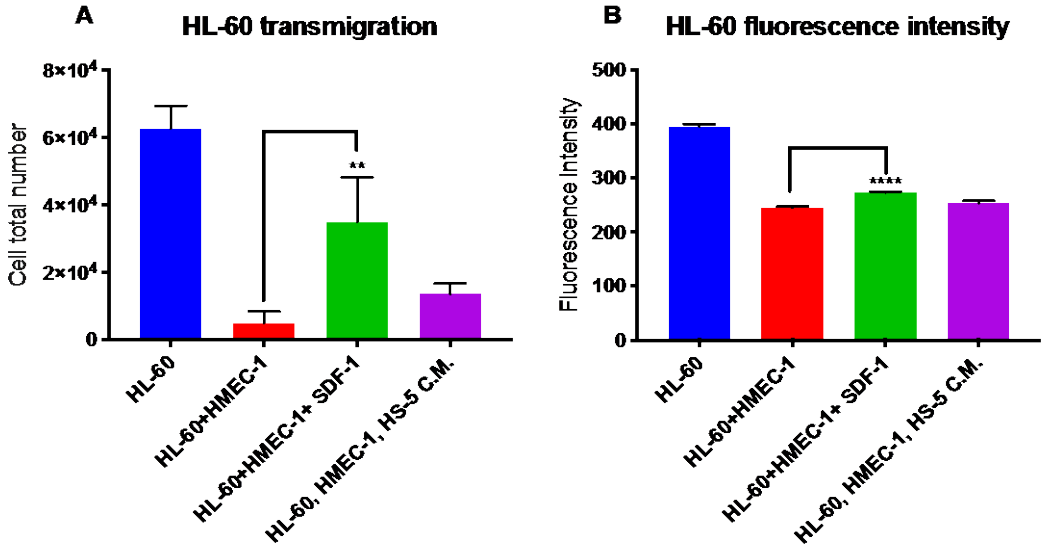

Figure 3-16 Transmigrated HL-60 cell count and fluorescence intensity.

HL-60 were seeded at 3.0 x 10^5 cells/insert in 8 μm pore inserts that contain a confluent layer of HMEC-1; control inserts were seeded with 3.0 x 10^5 cells/insert in 1ml of RPMI 1640 without HMEC-1. The lower compartments of the inserts were supplemented as follows: 2 ml of RPMI 1640 only, 2 ml of MCDB 131 only, 2 ml of MCDB 131 supplemented with 200 ng/ml SDF-1 and 2ml of 1:1 MCDB 131/HS-5 conditioned medium (HS-5 C.M.) respectively. Transmigrated HL-60 cell count (A) and fluorescence intensity (B) were monitored. Results are presented as average cell count and average fluorescence intensity ± S.D. for n=3. Statistical significance is indicated as ** p<0.01 and **** p<0.0001. Statistical analysis was done using one-way ANOVA test.

3.5.7 HL-60/HS-5 adhesion assay

As HL-60 was demonstrated to be influenced by HS-5 C.M. (section 3.5.6), an adhesion assay was employed to confirm that trafficking of HL-60 was due to inducers in the HS-5 C.M., and not due to gravity. The HL-60 cells were labelled with CellTrace™ Oregon Green™ (Carboxy-DFFDA, SE) at 2.0 μM as described in section 2.3.8. HS-5 cells (5×10^5 cells/well) were seeded onto 12-well plates 24 hours prior to experiments and incubated at 37°C with 5% CO_2. HL-60 at 3.0 x 10^5 cells/insert were co-cultured with HS-5 in 8 μm pore inserts (HL-60 upper

compartment/HS-5 lower compartment). After 24 hours, the inserts were removed, and HS-5 cells were washed three times with medium and scanned under the fluorescent microscope to visualise adherent HL-60 (Figure 3-17). Images showed that HL-60 cells were attached to the HS-5 firmly and not affected by the washing process.

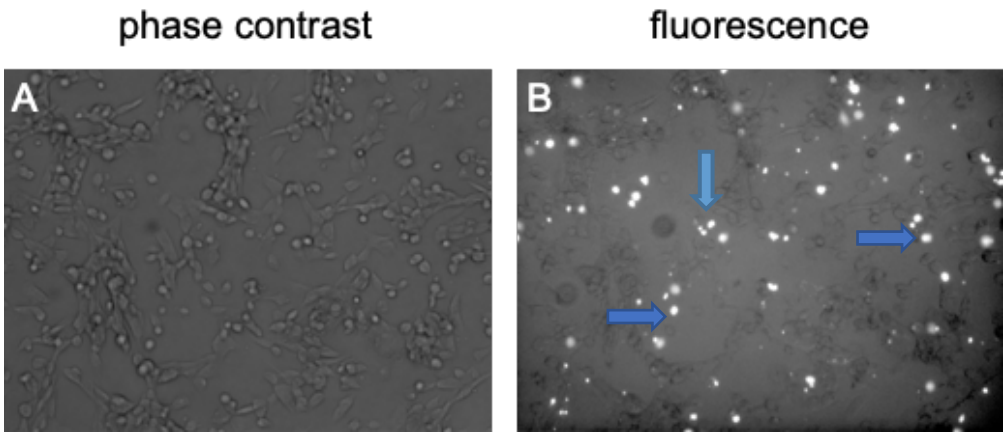

Figure 3-17 Adherent HL-60 to HS-5.

Images represent scanning the same field with phase contrast (A) and fluorescent microscopes (B). Images showed that transmigrated HL-60 were firmly adhered to HS-5 after 3 times wash with medium (arrowed). Results are representative of n=3

3.5.8 Cytotoxic effects of the cell tracker on the HL-60

Using a fluorescence marker to track the transmigrated HL-60 might be associated with toxicity and reduced viability. This cell tracker was dissolved in DMSO which is known to induce HL-60 differentiation at a concentration around 1.3% (Schacher et al., 2000; Jacob et al., 2002). To study this effect, the HL-60 cell line was labelled with CellTrace™ Oregon Green™ 488 (Carboxy-DFFDA, SE; section 2.3.8) at 0.5 µM, 1.0 µM, 5 µM, 10 µM, 17.5 µM and seeded at 2.0×10^4 cells/ml suspended in 2 ml of medium and added to 12-well plates. The DMSO levels at these concentrations are 0.005%, 0.01%, 0.05%, 0.1% and 0.17% respectively. In addition, cells were tested with DMSO only at 0.25% as the

highest concentration of DMSO included within the recommended range of the dye (5-25µM). Cell viability and cell count was measured after 24, 48 and 72 hours (Figure 3-18). Results indicated that viability was non-significantly reduced at all concentrations of the dye and DMSO ($p>0.05$). Moreover, expansion of the HL-60 was reduced compared to untreated cells (Figure 3-18 D). HL-60 is a fast growing cell line and expected to double in around 34 hours as previously shown in Figure 3-14. A sharp drop of proliferation was observed with DMSO (vehicle for the cell tracker) suggesting that cell tracker might interfere with the HL-60 proliferation.

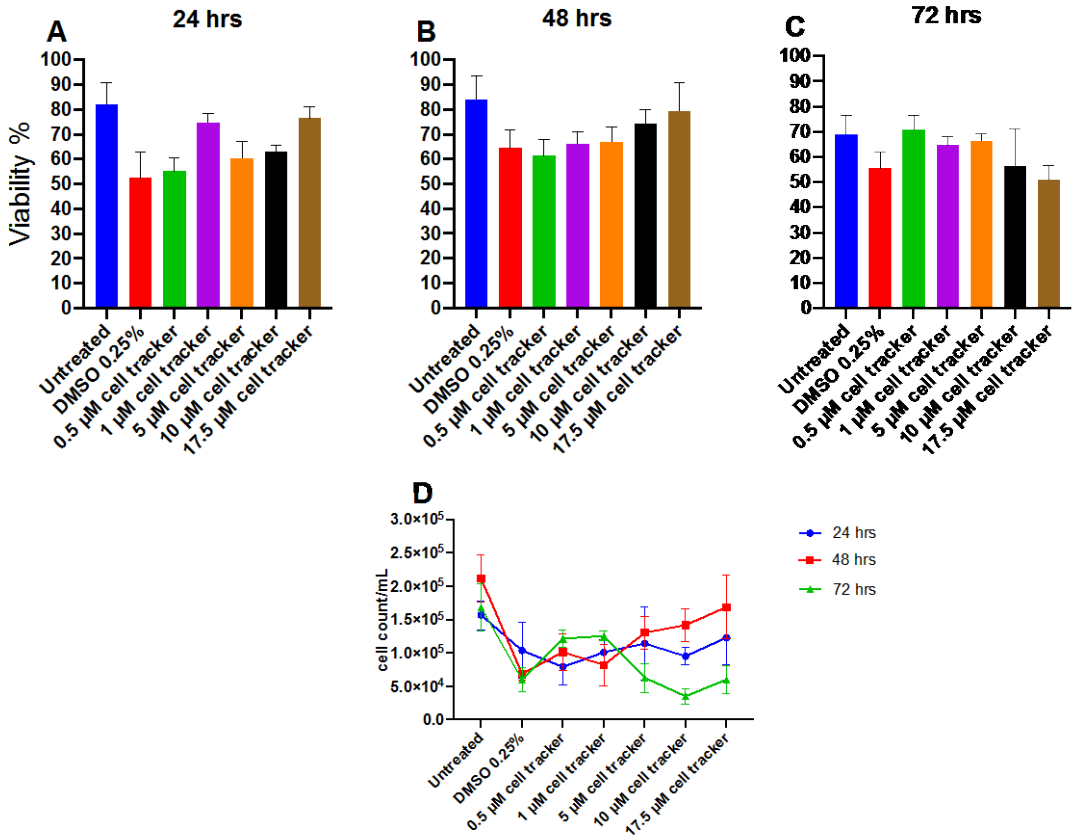

Figure 3-18: HL-60 viability with the cell tracker at 0.5 µM, 1.0 µM, 5 µM, 10 µM, 17.5 µM.

HL-60 cells viability after 24 hours (A), 48 hours (B) and 72 hours (C); results are presented as average cell viability ±S.D. Proliferation of HL-60 at the same time points (D), results are presented as average cell count ±S.D. for n=3. Non-significant reduction of HL-60 viability at all concentrations. Statistical analysis was done using one-way ANOVA test.

3.5.9 Optimisation of culture medium for the model

Each of the three cell lines required different culture medium, which was not conducive to culturing all of them together. Thus, establishing which culture medium would best support all three cell lines without compromising their culture conditions was needed. Presence of more than one culture medium might interfere with the transmigration process by introducing extra variables to the assay environment. To reduce variables during the assay, a suitable medium needed to be selected to maintain all for co-culture and treatment. A tolerable medium for all cells should be selected to run the model without any effect on the viability of cells and the integrity of the barrier. Based on results in sections 3.3, 3.4 and 3.5, RPMI 1640 was the medium of choice to maintain the three cell lines (HS-5, HMEC-1 and HL-60) for co-culture. It has been shown that RPMI 1640 maintained HS-5 characteristics and supported HL-60 proliferation, so it will be an appropriate choice if proved to be a suitable medium for HMEC-1 as an alternative for the costly MCDB 131.

3.5.10TEER measurements after changing the medium from MCDB 131 to RPMI 1640 with or without RPMI 1640 wash

Maintaining the integrity of the barrier is crucial for the model; this step was performed to check the possible effect of changing the medium from MCDB 131 to RPMI 1640 on TEER measurement of the HMEC-1 monolayer. Inserts used were washed three times with fresh medium (RPMI 1640) before adding RPMI 1640 for experimenting. To investigate whether any effect might be caused by this process, membrane integrity was evaluated by measuring the TEER for each insert (Figure 3-19). Medium was replaced by either RPMI 1640 or MCDB 131

for comparison. Part of the inserts was washed three times in RPMI 1640 before adding the new medium. TEER was measured before, and immediately at the time of replacing the medium, and at further time points as indicated in Figure 3-19. TEER value raised at the time of medium replacement for all inserts, however, for the inserts washed in RPMI 1640, TEER remained steady (Figure 3-19 A). A sharp drop of TEER was observed after one hour for all inserts, which then started to recover after 2 hours.

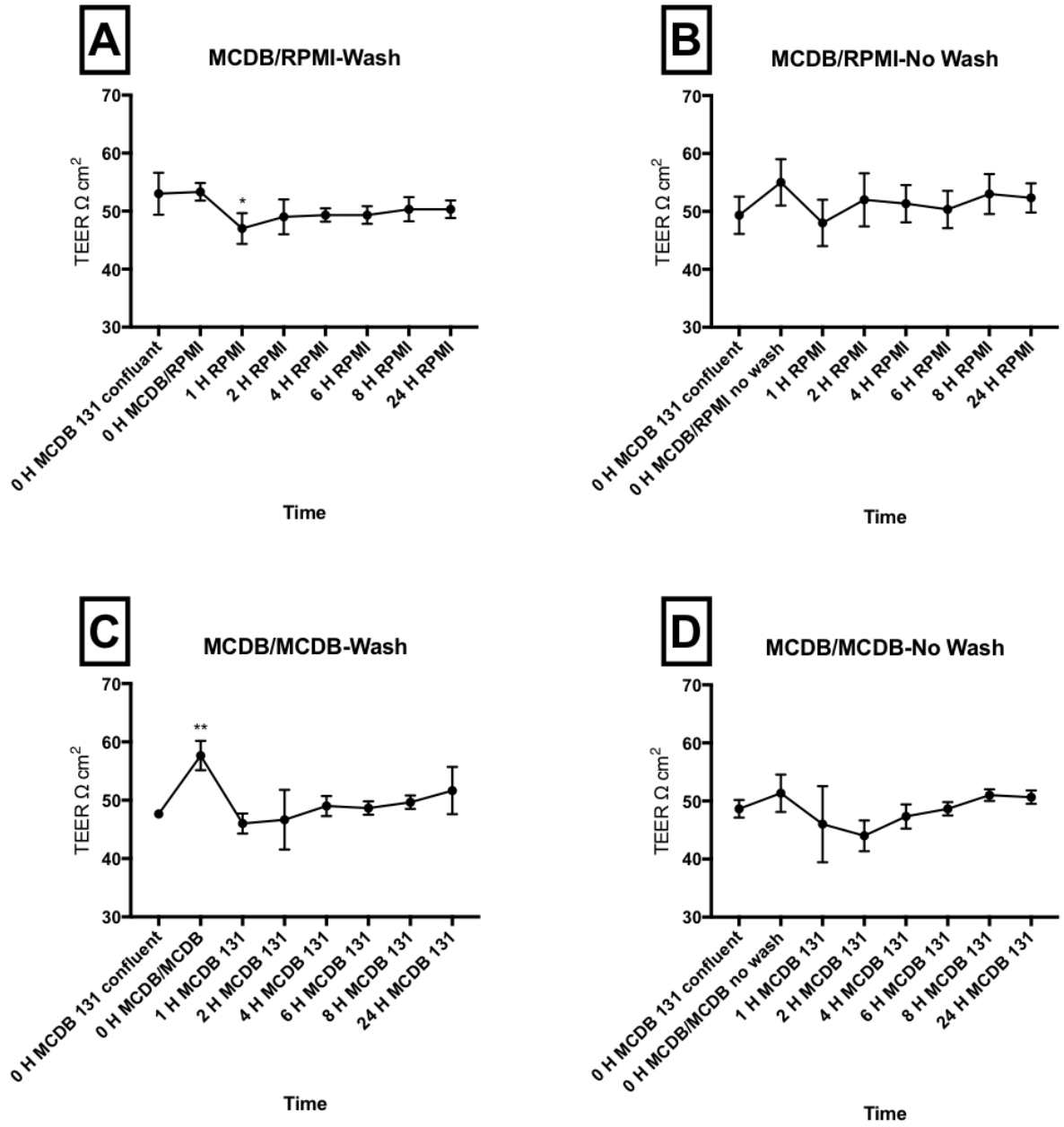

Figure 3-19 TEER measurements of HMEC-1 monolayer after changing the medium to RPMI 1640 with and without wash.

HMEC-1 were seeded at 5.0 x 10^5 cells/cm^2 suspended in MCDB 131 in 12 well 8 μm pore inserts. After 24 hours, medium was replaced in each HMEC-1 insert to RPMI 1640 or MCDB 131; A and B, medium changed to RPMI 1640 with and without wash respectively; C and D, medium changed to MCDB 131 with and without wash respectively. TEER was measured at different time points: 0-hour, 1 hour, 2 hours, 4 hours, 6 hours, 8 hours and 24 hours. Results are presented as average TEER value ± S.D. for n=3. Statistical significance is indicated as * $p<0.05$ and ** $p < 0.01$. Statistical analysis was done using one-way ANOVA test.

The washing step, which was made initially to remove any residual MCDB 131 medium from the inserts, might affect the integrity of the monolayer by

disturbing the cells. Some slight changes in TEER measurement were observed mainly during the first two hours. TEER measurement can be affected by several factors like small changes in temperature or culture medium composition, as shown by van der Helm *et al*., (2016). A study by Ferruzza *et al*., (2013) showed that maintaining Caco-2 cells monolayers in MITO+ ™ serum extender resulted in significantly lower TEER values when compared to complete DMEM-HG supplemented with 10% FBS. Temperature of the added culture medium might affect the TEER values, which is conversely proportional to temperature as shown by Matter and Balda, (2003). This might explain the increase in TEER value at the time of replacing the media and why it recovered after one hour of incubation at 37°C, which might be due to equilibration from room temperature to 37°C after incubation. A group of researchers have tried to address these variations on TEER measurements according to variation in temperature in which a mathematical method has been developed to correct TEER values (Blume *et al*., 2010).

A further step was made to investigate the possible effect of the medium constituents, and to rule out disturbing the barrier monolayer during the washing process. Inserts were tested for any changes on the TEER after removal and then, re-using the same medium, with and without PBS wash (Figure 3-20). Washing with PBS was used to remove any residual MCDB 131 medium from the inserts and introduce physical stress to the endothelium. A non-significant drop of TEER was observed immediately after PBS wash, whereas TEER value tended to remain more stable for the inserts tested without washing. This finding might suggest that barrier was not disturbed by the washing process; the variation on TEER values might be due to constituents of the medium itself, especially during the first two hours post-medium change. Therefore, it was recommended to

keep the inserts for at least two hours after changing the medium from MCDB 131 to RPMI 1640 to stabilise the endothelial barrier before adding the HL-60 for transmigration experiments.

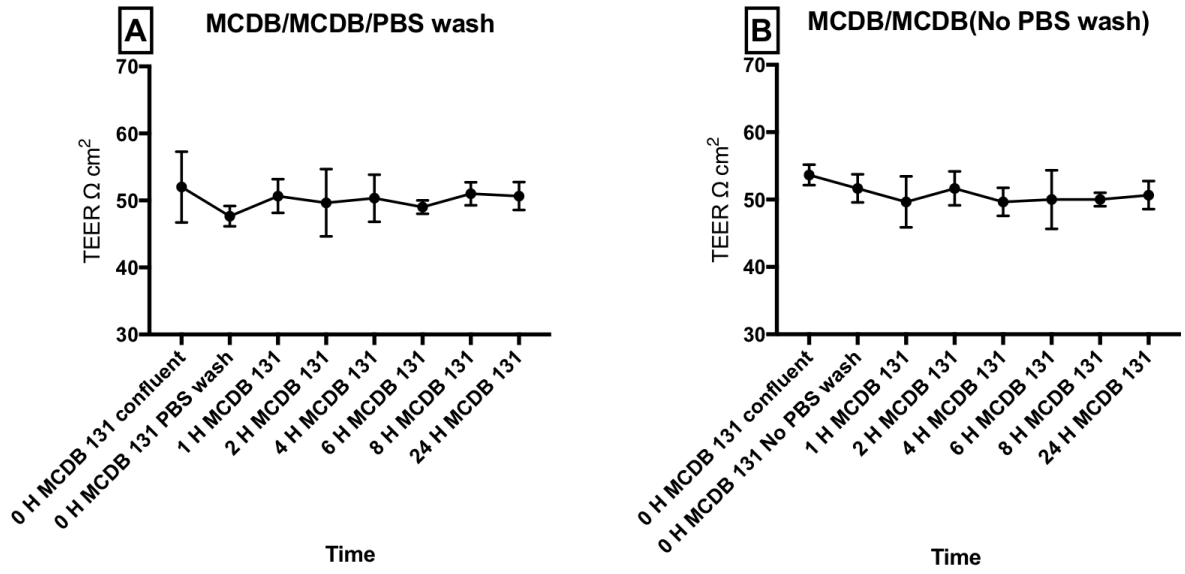

Figure 3-20 TEER measurements of HMEC-1 monolayer after PBS wash compared to that without wash.

HMEC-1 were seeded at 5.0 x 10^5 cells/cm^2 suspended in MCDB 131 in 12 well 8 μm pore inserts. After 24 hours, (A), inserts were removed from each well, washed with PBS and returned back to the same well without medium change. (B), inserts were removed from each well and returned back to the same well without medium change. TEER was measured at different time points: 0-hour, 1 hour, 2 hours, 4 hours, 6 hours, 8 hours and 24 hours. No significant change was observed. Results are presented as average TEER value ± S.D. for n=3. Statistical analysis was done using one-way ANOVA test.

3.5.11 TEER measurements of HMEC-1 with SDF-1α at different concentrations

Transmigration of HL-60 cells through the HMEC-1 monolayer were induced by SDF-1, as shown in Figure 3-16. Therefore, it was theorised that SDF-1 might affect the tight junction between HMEC-1 cells leading to unbinding of adjacent cells and creating some gaps between cells. The purpose of this test was to study the direct effect of SDF-1α concentration on the HMEC-1 monolayer. No significant change was observed on the TEER value (Figure 3-21). Adding SDF-1α

directly to the HMEC-1 endothelial layer did not show any change in membrane integrity at all concentrations. It is well known that CXCR4 is expressed on HMEC-1 cells as described by Ades *et al*., (1992) and Volin *et al*., (1998). This protein acts as a cytokine receptor for SDF-1α. However, several studies showed that treating endothelium with SDF-1α can raise TEER, inhibit the endothelial hyperpermeability and induce an angiogenic effect (Kobayashi *et al*., 2014; Mirshahi *et al*., 2000). In this study, SDF-1α treatment did not increase or decrease TEER value, suggesting that membrane integrity remained steady. An increase in endothelial barrier function was not visible because TEER value was at its upper limit.

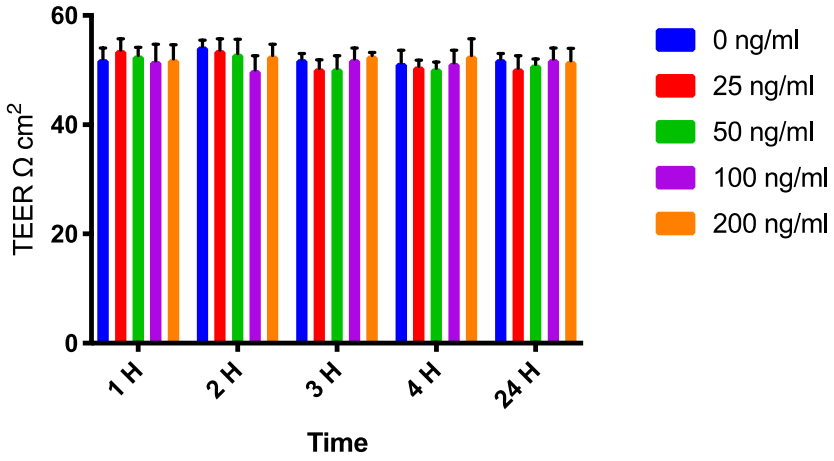

Figure 3-21 TEER measurements of the HMEC-1 monolayer with SDF-1α at different concentrations.

HMEC-1 were seeded at 5.0 x 10^5 cells/cm^2 suspended in MCDB 131 in 12 well 8 μm pore inserts. After 24 hours SDF-1α was added to the upper compartment of each HMEC-1 insert at different concentrations: 25 ng/ml, 50 ng/ml, 100 ng/ml and 200 ng/ml. TEER was measured at different time points: 1 hour, 2 hours, 3 hours, 4 hours and 24 hours. The SDF-1α concentration has no direct effect on the tight junction between HMEC-1cells. Results are presented as average TEER value ± S.D. for n=3. Statistical analysis was done using one-way ANOVA test.

3.5.12 HL-60 Transmigration with SDF-1/HS-5 conditioned medium (C.M.) in RPMI 1640

Since RPMI was proven to support all three cell lines in the model, the model was retested for HL-60 transmigration using RPMI 1640 medium only (Figure 3-22). HMEC-1 was seeded into the insert as described in section 2.3.7, at a seeding density of 5.0 x 10^5 cells/cm^2 in 12 well 8 µm pore inserts and maintained in MCDB 131 for 24 hours, and then transferred to RPMI 1640. After two hours, the TEER was measured, and HL-60 was added to each insert at 3.0x 10^5 cells/insert to check for transmigration under the influence of HS-5 C.M. TEER was measured for each insert to confirm the barrier integrity before adding HL-60. Results indicated that SDF-1α at 200 and 400 ng/ml produced a significant increase in HL-60 trafficking across the barrier (p<0.01 and p<0.0001) respectively. Similarly, a significant increase of HL-60 trafficking was seen with HS-5 C.M. in the base of the wells compared to the inserts without SDF-1 and HS-5 C.M. (p<0.001). This result suggests that changing the medium to RPMI 1640 is not affecting HL-60 transmigration, and it is suitable to be used as an alternative to support all three cell lines in the model.

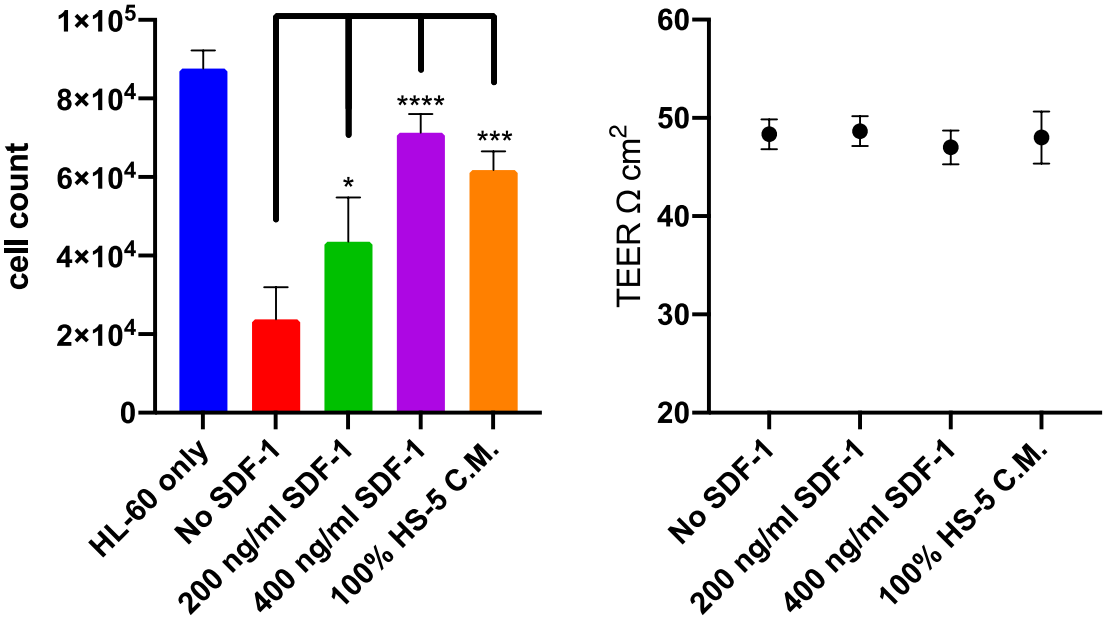

Figure 3-22 Transmigrated HL-60 cell count in RPMI 1640.

HL-60 were seeded at 3.0x 10^5 cells/insert in 8 μm pore inserts that contained a confluent layer of HMEC-1. The lower compartments of the inserts were supplemented as follows: 2 ml of RPMI 1640 only, 2 ml of RPMI 1640 supplemented with 200 ng/ml SDF-1, 2 ml of RPMI 1640 supplemented with 400 ng/ml SDF-1α, 2ml of 100% HS-5 C.M. Control inserts were seeded with 3.0 x 10^5 cells/insert in 2ml of RPMI-1640 without HMEC-1. Transmigrated HL-60 cells were counted, and TEER was monitored. Statistical significance is indicated as * $p<0.05$, *** $p<0.001$ and **** $p<0.0001$. Results are presented as average cell count ± S.D. for n=3. Statistical analysis was done using one-way ANOVA test.

3.6 Conclusion

The optimal settings of the transmigration model were concluded based on the results detailed within this chapter. The initial step of the development of the model was to establish a confluent layer of endothelium on the transwell inserts. HUVEC proliferation was very slow, taking up to 6 days to produce a confluent barrier, which extended the preparation time for each experiment. Although, HUVEC was a suitable option in several transmigration studies (Buffone, Anderson and Hammer, 2018; Ebrahim and Leach, 2015; Yan *et al.*, 2011), batch lots of HUVEC are heterogeneous

since they are derived from different sources. HUVEC are primary cells, and there is a limit on how many population doublings and passaging that can be achieved, in which several batches of HUVEC might be required. This is not only causing a large expense but also produces variability into the transmigration model as they will potentially be from different sources with different genetics.

On the other hand, HMEC-1 proliferate faster as a cell line, are homogeneous and provide an indefinite supply of cells from the same source and provide the required TEER measurement to create an endothelial barrier in a relatively short period of time. This finding fits with the timeframe of the transmigration model. The required seeding density of HMEC-1 was 5.0 x 10^5 cell/cm^2 to create a confluent monolayer on the inserts in 24 hours. HMEC-1 was able to tolerate a medium change to RPMI 1640, which was the medium of choice to perform the model, as it was able to support proliferation and functionality of all three cell lines. The concluded general approach for the transmigration model was by initially maintaining each cell line separately in their optimal culture conditions, followed by HMEC-1 grown as a monolayer in a cell culture insert and the HL-60 cell line added to the insert above the endothelial monolayer. C.M. from HS-5 was placed in the base of the culture well to induce transmigration. Transmigration was possible without all three cell lines being in the same co-culture. The model was established as described in section 2.3.7.

The availability of an *in vitro* model to study cell migration is essential to allow a better understanding of the *in vivo* underlying biological mechanisms. Other studies have used different settings and different cell combinations employing the same principle of the Boyden chamber and trafficking through the endothelium. Since the Boyden chamber was introduced, a wide range of assays to analyse chemokinetic and chemotactic cell migration has been developed utilising endothelial barriers like

HMEC-1. For example, HMEC-1 was used by Guo *et al*. (2009) to study monocyte transendothelial migration after treating the endothelial monolayer with tumour necrosis factor-α (TNFα) for 6 hours. Another study by Al-Sowayan *et al*. (2017) utilised HMEC-1 to study migration of chorionic mesenchymal stem cells (CMSC) through an activated endothelial cell monolayer using lipopolysaccharide (LPS) treatment and hypoxic conditioning.

The model presented in this study for HPCs endothelial interaction is highly reproducible, can be high-throughput, and can be adapted to integrate the complexities of the BM microenvironment, and chemoattractant signalling controls the HPCs trafficking in and out of the BM niches.

Chapter 4: Effect of chemotherapy and targeted therapy on HPC transmigration

4.1 Background

Part of the preparation for HSCT is administration of a conditioning regimen in which the patient will receive doses of total body irradiation (TBI) and chemotherapeutic agents that are toxic to the body. This process will provide sufficient immunoablation to prevent graft rejection and provide a space for the transplanted cells by killing the malignant host cells. It is well documented that the BM microenvironment becomes damaged due to chemotherapy (Kemp *et al.*, 2010; Georgiou *et al.*, 2010), so it is reasonable to suggest that damage or injury to the BM releases novel messengers for homing of HSC. These messengers include chemotactic factors which induce stem cells to traffic to the site of the injury in order to repair it. HSC have been observed to traffic and home to sites of injury of the myocardium after cardiac arrest, and the brain after ischaemic stroke (Czeiger *et al.*, 2011; Kavanagh & Kalia; 2011). It was suggested that molecules released due to this injury appear to have chemoattractant properties, and notably this predominantly occurs due to hypoxic conditions.

This part of the study included cell treatment and injury induction of the HS-5 cells. HS-5 was treated with chemotherapy used in BEAM regimen and treated with targeted therapy typically used to treat leukaemia, like imatinib and ibrutinib as described in section 2.5. Cells were incubated in normoxia or hypoxia, HS-5 C.M. was then used in the transmigration model to explore chemotherapy's capability to promote homing and cellular communication between these cells. Within a transplant setting, the BM and blood vessels would be systemically exposed to such drugs, whereas the donated HSCs would not. We theorise that chemotherapy alone cannot promote localisation for HSC to home to the correct place; otherwise, HSCs

would adhere to the entire vasculature. Instead, localised communication between BM and endothelial cells likely promotes exclusive messenger or adhesion molecule expression, which may be subjected to a concentration gradient becoming more diluted as we move away from the site of injury. The BM microenvironment is hypoxic as described by Chow *et al.*, (2001), so it is reasonable to suggest that damage or injury to the BM, heart and brain release novel hypoxia-induced messengers for homing of HSC.

Homing of HSCs from peripheral blood through the circulation to the BM stem cell niches is enforced by chemotactic factors released in the BM microenvironment by BM cells that chemoattract HSCs. These chemotactic factors might be peptide-based like chemokines or growth factors, bioactive phosphosphingolipids like sphingosine-1-phosphate (S1P) or ceramide-1-phosphate (C1P), or extracellular nucleotides like ATP or UTP (Ratajczak and Abdelbaset-Ismail, 2016; Ratajczak *et al*., 2012). All these factors are upregulated in the BM after myeloablative conditioning therapies for HSCT as reviewed by Ratajczak *et al*. (2012).

To evaluate the role of proteins and bioactive lipid released by HS-5, adherent monolayers were treated with aspirin and cycloheximide (CHX) to inhibit the production of proteins and bioactive lipid production. Aspirin impairs the biosynthesis of all prostanoids through the irreversible inhibition of both COX1 and COX2 (Lucotti *et al*., 2019), while CHX is a protein synthesis inhibitor in eukaryotes which has been shown to inhibit translation elongation through binding to the E-site of the 60S ribosomal unit and interfering with deacetylated tRNA (Schneider-Poetsch *et al*., 2010; Klinge *et al.*, 2011).

4.2 Aims

The aims were to induce injury of HS-5 by exposure to clinically relevant doses of chemotherapy and targeted therapy to explore release of novel hypoxia-induced

messengers and their effect on HSC movement across the endothelium. Conditioned culture medium containing these messengers from HS-5 was used to induce transmigration of HL-60 in normoxic and hypoxic conditions.

Conditioned medium was used “neat” and through serial dilutions to investigate a concentration gradient away from the injury.

4.3 Methods

4.3.1 Cell Culture

All cell culture procedures were carried out, as described in section 2.1. HS-5 were seeded and treated, as described in section 2.6.2.

4.3.2 Microscopy

Light microscopy was used to examine the morphology and cell growth of all cell lines, as described in section 2.2.

4.3.3 Trans-endothelial electrical resistance (TEER)

TEER was used to assess the endothelial cell membrane integrity (section 2.3.1).

4.3.4 Transmigration analysis

All transmigration assays and insert preparations were carried out as described in section 2.3.7. Hypoxic conditions were induced as described in section 2.2.6.

4.4 Results

4.4.1 HL-60 Transmigration is increased depending on HS-5 C.M. concentration.

Transmigration of HL-60 was affected significantly by the concentration gradient of HS-5 C.M.; a higher transmigration of HL-60 was observed with higher percentage of HS-5 C.M., whereas dilution of HS-5 C.M. to 50% and 25% showed significant reduction of HL-60 transmigration (Figure 4-1). Generally, the total cell counts of the transmigrated HL-60 were directly proportional to HS-5 C.M. concentrations. SDF-1α was used as a positive control to validate transmigration of HL-60. The total cell

counts of the transmigrated HL-60 were directly proportional to SDF-1α concentrations. Transmigrated HL-60 cell count induced by 100% HS-5 C.M. was nearly at the same level of transmigration induced by 400 ng/ml SDF-1α. However, transmigration induced by 75% HS-5 C.M. was higher than that induced by 200 ng/ml SDF-1α.

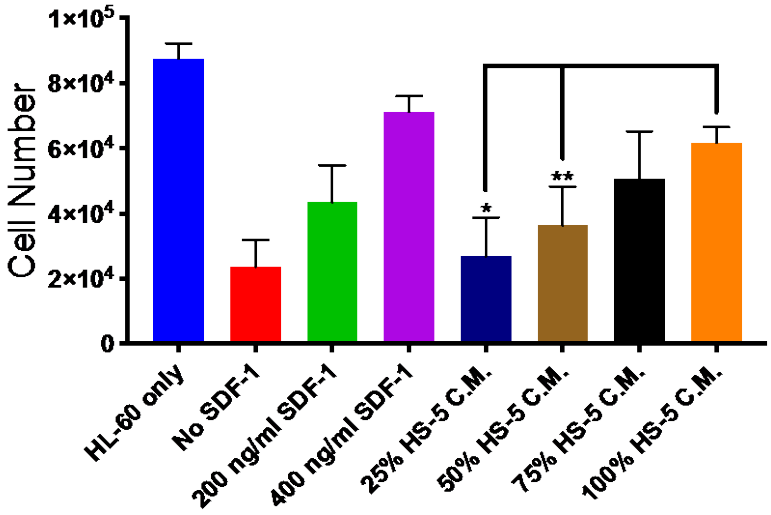

Figure 4-1 HL-60 transmigration at different percentage of HS-5 C.M.

HL-60 were seeded at 3.0x 10^5 cells/insert in 8 μm pore inserts that contain a confluent layer of HMEC-1, the lower compartments of the inserts were supplemented as follows: 2 ml of RPMI 1640 only, 2 ml of RPMI 1640 supplemented with 200 ng/ml SDF-1, 2 ml of RPMI 1640 supplemented with 400 ng/ml SDF-1α, 2ml of 100% HS-5 C.M., 2ml of 75% HS-5 C.M., 2ml of 50% HS-5 C.M. and 2ml of 25% HS-5 C.M. Control inserts were seeded with 3.0 x 10^5 cells/insert in 2ml of RPMI-1640 without HMEC-1. Transmigrated HL-60 cells were counted. Statistical significance is indicated as * $p<0.05$ and ** $p<0.01$. Results are presented as average cell count ± S.D. for n=3. Statistical analysis was done using one-way ANOVA test.

4.4.2 Hypoxia-induced HL-60 transmigration

Transmigration of HL-60 was affected by induction of hypoxic conditions (section 2.2.6). Hypoxic HL-60 showed enhanced transmigration across the endothelium (Figure 4-2). HL-60 was maintained in hypoxia for 24 hours in which 3.0 x 10^5 cells were used in each insert. RPMI 1640 (2 mL) was added to the lower compartments supplemented with 200 ng/ml and 400 ng/ml SDF-1α. Transmigration

of hypoxia-maintained HL-60 was non-significantly enhanced in all inserts with HMEC-1 monolayer with and without SDF-1α.

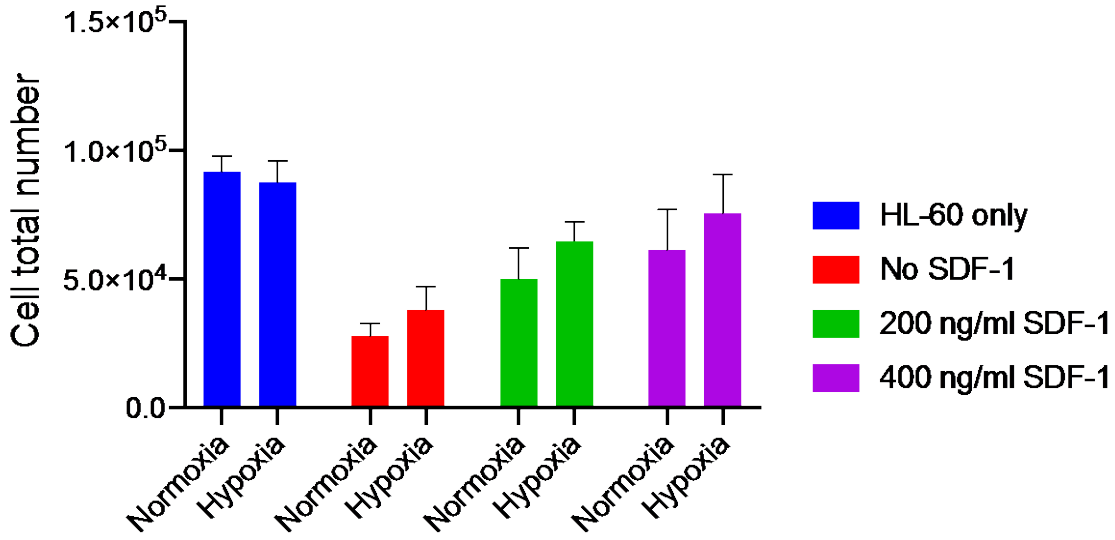

Figure 4-2 Hypoxia pre-conditioned HL-60 transmigration,

HL-60 were maintained in hypoxia for 24 hours and seeded at 3.0x 10^5 cells/insert in 8 μm pore inserts that contain a confluent layer of HMEC-1, the lower compartments of the inserts were supplemented as follows: 2 ml of RPMI 1640 supplemented with 200 ng/ml SDF-1α and 2 ml of RPMI 1640 supplemented with 400 ng/ml SDF-1α. Transmigrated HL-60 cells were counted after 24 hours. Results are presented as average cell count ± S.D. for n=3. Statistical analysis was done using two-way ANOVA test.

4.4.3 Chemotherapy and targeted therapy treatments

HS-5 was treated with clinically relevant and low doses of chemotherapy to test the hypothesis that chemotherapeutic damage or injury to the BM might release novel messengers for homing of HSC. C.M. of HS-5 were harvested and used in the transmigration model to induce HL-60 transmigration.

4.4.4 Chemotherapy treated HS-5 C.M. does not increase trafficking in hypoxia and normoxia

HS-5 were treated as described in section 2.5.1. Briefly, HS-5 were treated at clinically relevant doses for 2 hours (Figure 4-3) or 24 hours (Figure 4-4), and also at 50% lower intensity doses for 24 hours (Figure 4-5). Treatments were conducted in

hypoxia and normoxia for HS-5 cells only. During the transmigration analysis, the whole model was monitored in hypoxia and normoxia. Transmigrated HL-60 cells were counted in the lower compartment of each insert. Chemotherapy treated HS-5 C.M. did not raise HL-60 trafficking above the level of untreated HS-5 C.M ($p>0.05$). Melphalan and ara-C raised the trafficking by 15.5% and 29.5% respectively under hypoxia compared to normoxia for the 2 hours treated HS-5 (Figure 4-3). Conversely, melphalan treated HS-5 C.M. reduced trafficking significantly for the 24 hours treatment in both normoxia ($p<0.05$) and hypoxia ($p<0.01$) compared to untreated HS-5; in addition, trafficking was higher in hypoxia versus normoxia by 55% for melphalan. Generally, there was a non-significant trend towards lower trafficking with hypoxia for all drugs except melphalan for the 24 hrs treatment (Figure 4-4).

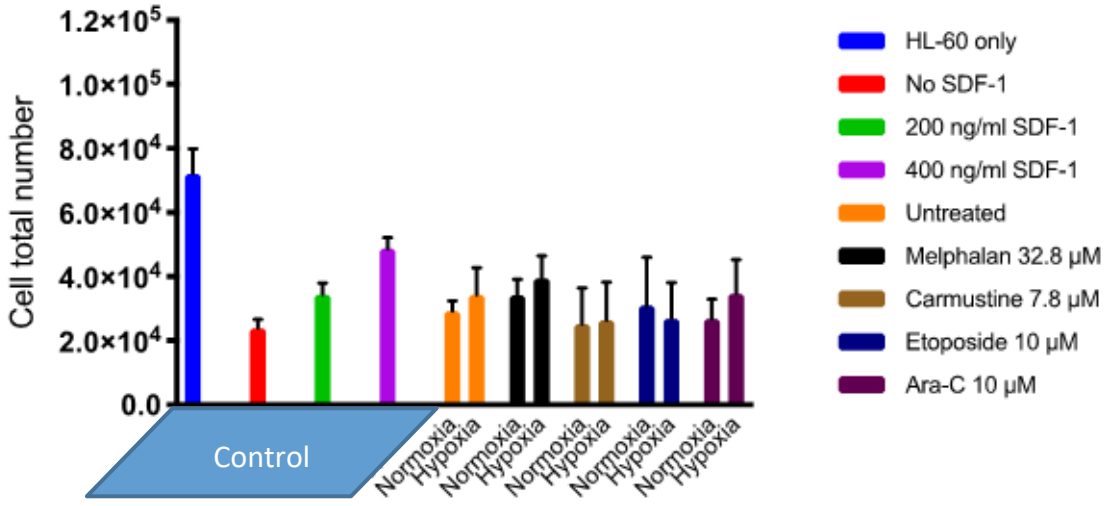

Figure 4-3 Transmigration of HL-60 at clinically relevant doses (2 hours treatment).

HS-5 C.M. were collected after 2 hours treatment and then used to induce transmigration. HL-60 were seeded at 3.0x 10^5 cells/insert in 8 µm pore inserts that contain a confluent layer of HMEC-1; the lower compartments of the inserts were supplemented as follows: 2 ml of RPMI 1640 only, 2 ml of RPMI 1640 supplemented with 200 ng/ml SDF-1α, 2 ml of RPMI 1640 supplemented with 400 ng/ml SDF-1, 2ml of 100% HS-5 C.M. treated with clinically relevant dose chemotherapy in normoxic and hypoxic conditions. Control inserts were seeded with 3.0 x 10^5 cells/insert in 1ml of RPMI 1640 without HMEC-1. All controls are untreated maintained in normoxia. Control bars represent inserts seeded with HL-60 only without HMEC-1 (blue), inserts seeded with HL-60 on top of HMEC-1 without SDF-1α (red) inserts seeded with HL-60 on top of HMEC-1 with SDF-1α in the lower compartment at 200 ng/ml and 400 ng/ml (green and purple) respectively. Transmigrated HL-60 cells were counted after 24 hours. Results are presented as average cell count ± S.D. for n=3. Statistical analysis was done using two-way ANOVA test.

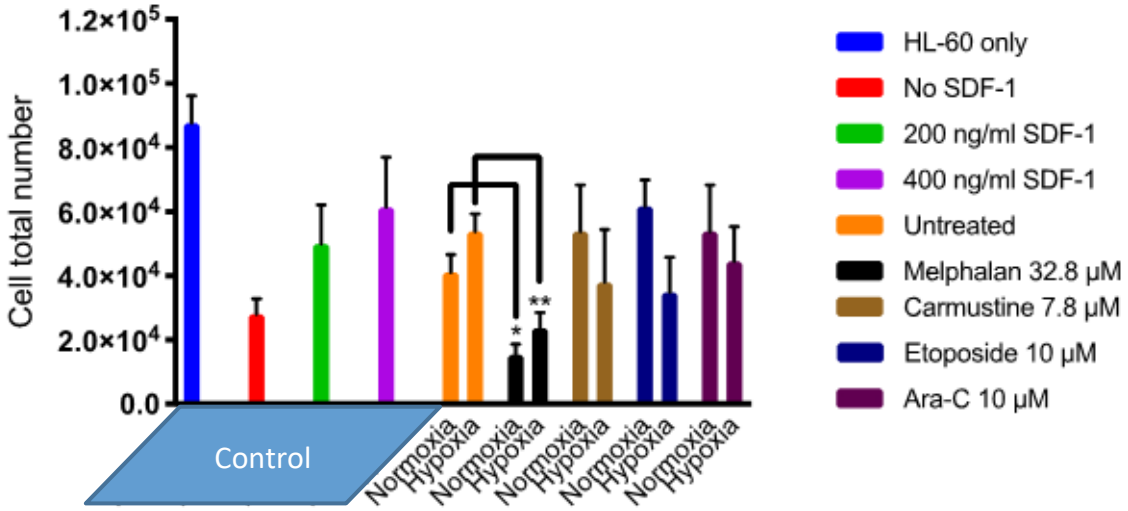

Figure 4-4 Transmigration of HL-60 at clinically relevant doses (24 hours treatment).

HL-60 were seeded at 3.0x 10^5 cells/insert in 8 µm pore inserts that contain a confluent layer of HMEC-1, the lower compartments of the inserts were supplemented as follows: 2 ml of RPMI 1640 only, 2 ml of RPMI 1640 supplemented with 200 ng/ml SDF-1α, 2 ml of RPMI 1640 supplemented with 400 ng/ml SDF-1, 2ml of 100% HS-5 C.M. treated with clinically relevant dose chemotherapy in normoxic and hypoxic conditions. Control inserts were seeded with 3.0 x 10^5 cells/insert in 1ml of RPMI 1640. All controls are untreated maintained in normoxia. Control bars represent inserts seeded with HL-60 only without HMEC-1 (blue), inserts seeded with HL-60 on top of HMEC-1 without SDF-1α (red) inserts seeded with HL-60 on top of HMEC-1 with SDF-1α in the lower compartment at 200 ng/ml and 400 ng/ml (green and purple) respectively. Transmigrated HL-60 cells were counted after 24 hours. Statistical significance is indicated as* $p<0.05$ and ** $p<0.01$. Results are presented as average cell count ± S.D. for n=3. Statistical analysis was done using two-way ANOVA test.

The 50% reduced intensity treated HS-5 C.M. did not affect trafficking significantly (Figure 4-5), with no increase in trafficking noted except for etoposide treatment which showed a minor acceleration of trafficking in normoxic conditions compared to untreated. Melphalan and ara-C raised the trafficking by 22.7% and 31.4% respectively with hypoxia compared to normoxia. Conversely, carmustine and etoposide lowered trafficking by 24% and 29.6% respectively in hypoxia compared to normoxia. However, controls results were variable in each of these treatments. Consequently, this might limit the conclusions that can be drawn.

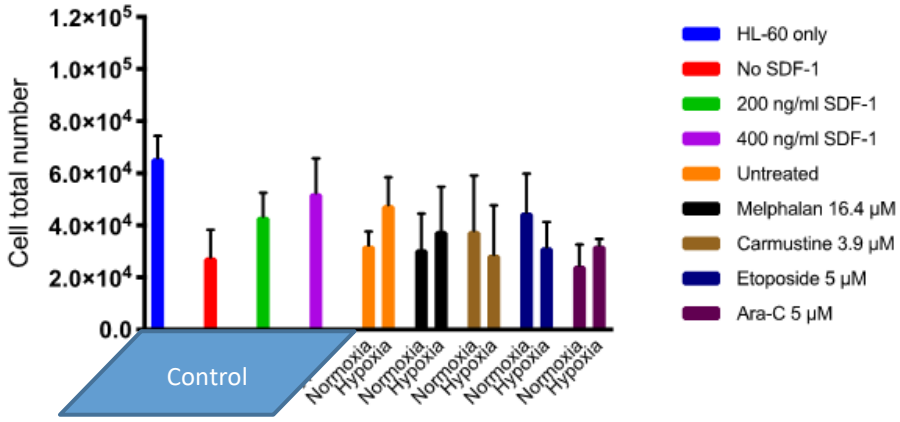

Figure 4-5 Transmigration of HL-60 at 50% lower doses (24 hours treatment).

HL-60 were seeded at 3.0x 10^5 cells/insert in 8 µm pore inserts that contain a confluent layer of HMEC-1, the lower compartments of the inserts were supplemented as follows: 2 ml of RPMI 1640 only, 2 ml of RPMI 1640 supplemented with 200 ng/ml SDF-1α, 2 ml of RPMI 1640 supplemented with 400 ng/ml SDF-1, 2ml of 100% HS-5 C.M. treated with clinically relevant dose chemotherapy in normoxic and hypoxic conditions. Control inserts were seeded with 3.0 x 10^5 cells/insert in 1ml of RPMI 1640. All controls are untreated maintained in normoxia. Control bars represent inserts seeded with HL-60 only without HMEC-1 (blue), inserts seeded with HL-60 on top of HMEC-1 without SDF-1α (red) inserts seeded with HL-60 on top of HMEC-1 with SDF-1α in the lower compartment at 200 ng/ml and 400 ng/ml (green and purple) respectively. Transmigrated HL-60 cells were counted after 24 hours. Results are presented as average cell count ± S.D. for n=3. Statistical analysis was done using two-way ANOVA test.

4.4.5 Targeted therapies can induce trafficking compared to chemotherapy

HS-5 were treated with imatinib and ibrutinib, as described in section 2.5.1. DMSO was used as a vehicle for the drugs at a maximum concentration of 0.1 %. HS-5 C.M. was collected after treatment and used in the transmigration model. Imatinib treatment at the recommended dose induced trafficking significantly under normoxic conditions by 62% ($p<0.001$) compared to untreated HS-5 cells. Ibrutinib treatment increased trafficking in hypoxia by 47% ($p<0.01$) (Figure 4-6). Increasing the doses of imatinib and ibrutinib by 100% showed enhanced trafficking by 45% and 49% respectively in normoxia compared to untreated HS-5 cells (Figure 4-7). However, trafficking of HL-60 was enhanced but not to the same level when HS-5 was treated with the recommended doses (imatinib 1.7µM and ibrutinib 2.3µM) ($p<0.05$) (Figure 4-7). In both cases, the controls produced the same level of HL-60 trafficking.

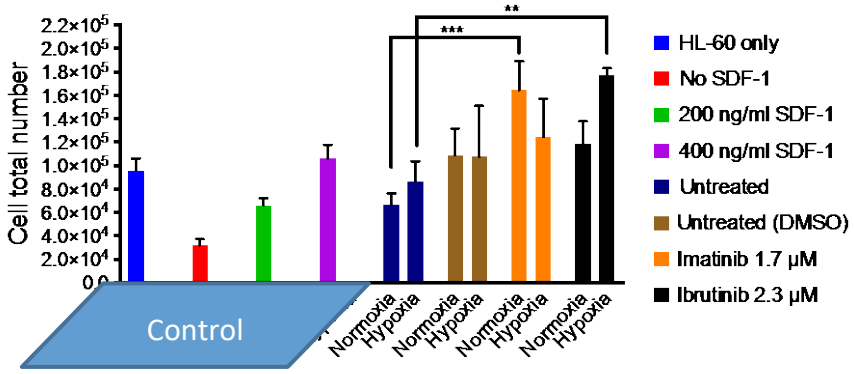

Figure 4-6 HL-60 transmigration with targeted therapy.

HS-5 C.M. was collected after treatment of HS-5 with imatinib and ibrutinib for 24 hours. Two ml of the C.M. were added to the lower compartments of the test inserts to induce trafficking. HL-60 were seeded at 3.0x 10^5 cells/insert in 8 μm pore inserts that contained a confluent layer of HMEC-1. DMSO was used as a solvent for the drugs, so additional inserts were involved in which HS-5 was treated with DMSO. Tests were conducted in normoxia and hypoxia. Imatinib increased transmigration in normoxia while ibrutinib increased transmigration in hypoxia. No significant changes were observed with DMSO (0.1 %). Transmigrated HL-60 cells were counted after 24 hours. Control inserts were seeded with 3.0 x 10^5 cells/insert in 1ml of RPMI 1640. All controls are untreated maintained in normoxia. Control bars represent inserts seeded with HL-60 only without HMEC-1 (blue), inserts seeded with HL-60 on top of HMEC-1 without SDF-1α (red) inserts seeded with HL-60 on top of HMEC-1 with SDF-1α in the lower compartment at 200 ng/ml and 400 ng/ml (green and purple) respectively. Statistical significance is indicated as** p<0.01 and *** p<0.001. Results are presented as average cell count ± S.D. for n=3. Statistical analysis was done using two-way ANOVA test.

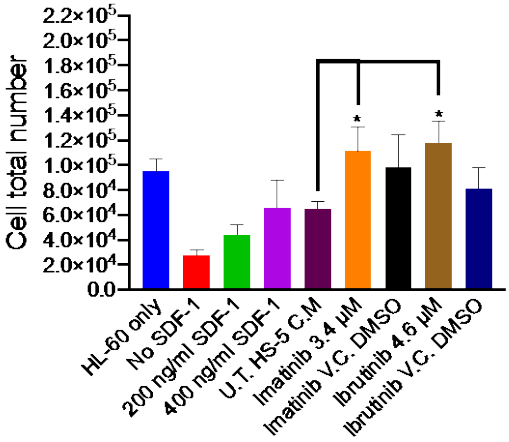

Figure 4-7 HL-60 transmigration with 100% elevated targeted therapy in normoxia.

HS-5 C.M. was collected after treatment of HS-5 with imatinib and ibrutinib for 24 hrs. Two ml of the C.M. were added to the lower compartments of the test inserts to induce trafficking. HL-60 were seeded at 3.0x 10^5 cells/insert in 8 μm pore inserts that contained a confluent layer of HMEC-1. DMSO was used as a solvent for the drugs, so additional inserts were involved in which HS-5 was treated with DMSO at the same level as drugs. No additional effect was observed in imatinib while the double dose of ibrutinib seems to increase trafficking. No significant changes were observed with DMSO V.C. treatment. Transmigrated HL-60 cells were counted after 24 hours. Control inserts were seeded with 3.0 x 10^5 cells/insert in 1ml of RPMI 1640. All controls are untreated maintained in normoxia. Control bars represent inserts seeded with HL-60 only without HMEC-1 (blue), inserts seeded with HL-60 on top of HMEC-1 without SDF-1α (red) inserts seeded with HL-60 on top of HMEC-1 with SDF-1α in the lower compartment at 200 ng/ml and 400 ng/ml (green and purple) respectively. Statistical significance is indicated as** p<0.01. Results are presented as average cell count ± S.D. for n=3. Statistical analysis was done using one-way ANOVA test.

DMSO as a vehicle had no significant effect on transmigration (Figure 4-8). To exclude the effect of FBS, transmigration was assessed after adding FBS (10%) to the lower compartment of the inserts, no significant changes were observed (Figure 4-9).

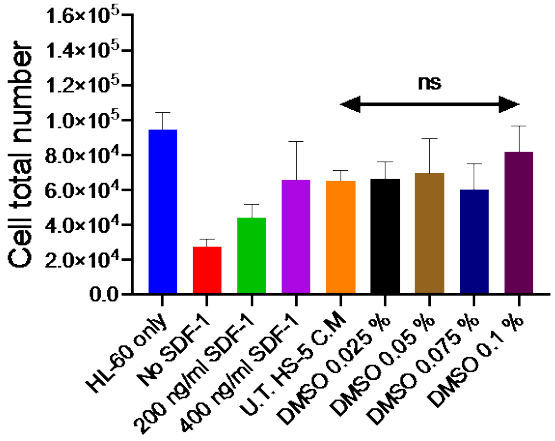

Figure 4-8 Transmigration of HL-60 with DMSO treated HS-5 C.M.

HS-5 was treated with DMSO at 0.025% to 0.1%. HL-60 were seeded at 3.0x 10^5 cells/insert in 8 μm pore inserts that contained a confluent layer of HMEC-1. No significant changes were induced by DMSO treated HS-5 C.M. Control inserts were seeded with 3.0 x 10^5 cells/insert in 1ml of RPMI 1640. All controls are untreated maintained in normoxia. Control bars represent inserts seeded with HL-60 only without HMEC-1 (blue), inserts seeded with HL-60 on top of HMEC-1 without SDF-1α (red) inserts seeded with HL-60 on top of HMEC-1 with SDF-1α in the lower compartment at 200 ng/ml and 400 ng/ml (green and purple) respectively. Transmigrated HL-60 cells were counted after 24 hours. Results are presented as average cell count ± S.D. for n=3. Statistical analysis was done using one-way ANOVA test.

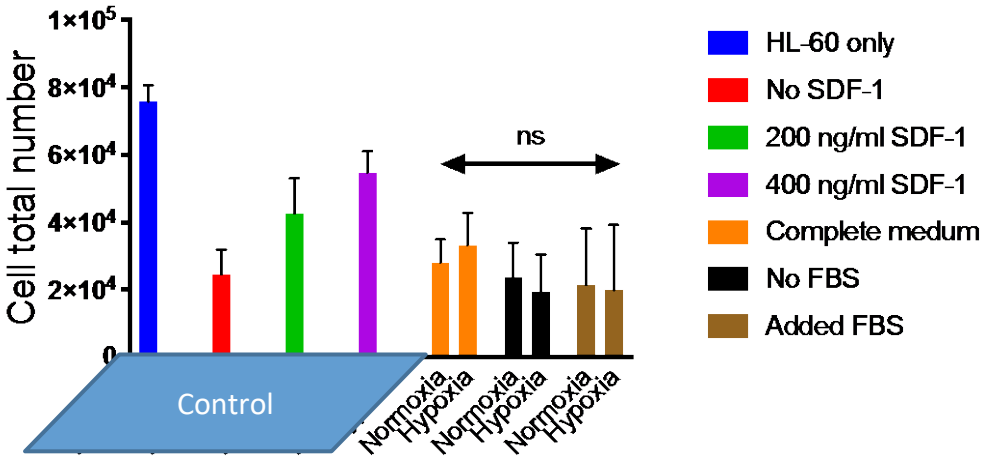

Figure 4-9 Transmigration of HL-60 after adding FBS at 10 %.

FBS was added to the lower compartments of the model at 10%. HL-60 were seeded at 3.0x 10^5 cells/insert in 8 μm pore inserts that contained a confluent layer of HMEC-1. Tests were conducted in normoxia and hypoxia. No significant changes were induced by adding FBS. Control inserts were seeded with 3.0 x 10^5 cells/insert in 1ml of RPMI 1640. All controls are untreated maintained in normoxia. Control bars represent inserts seeded with HL-60 only without HMEC-1 (blue), inserts seeded with HL-60 on top of HMEC-1 without SDF-1α (red) inserts seeded with HL-60 on top of HMEC-1 with SDF-1α in the lower compartment at 200 ng/ml and 400 ng/ml (green and purple) respectively. Transmigrated HL-60 cells were counted after 24 hours. Results are presented as average cell count ± S.D. for n=3. Statistical analysis was done using two-way ANOVA test.

4.4.6 Differentiated neural cell C.M. induced trafficking

The human neuroblastoma cell line (SH-SY5Y) was differentiated by Synthetic Retinoid ec23® (section 2.3.8); conditioned medium was collected after incubating the cells in normoxia and hypoxia for 24 hours. This C.M. (neural C.M.) was then used to test the theory that ischaemic injury to the neural cells might produce chemoattractant factors as a signal for HPCs. Hypoxia-incubated SH-SY5Y C.M. showed a non-significant enhancement of HL-60 transmigration across the endothelium. Transmigration increased by 22% compared to normoxia-maintained SH-SY5Y cells (Figure 4-10).

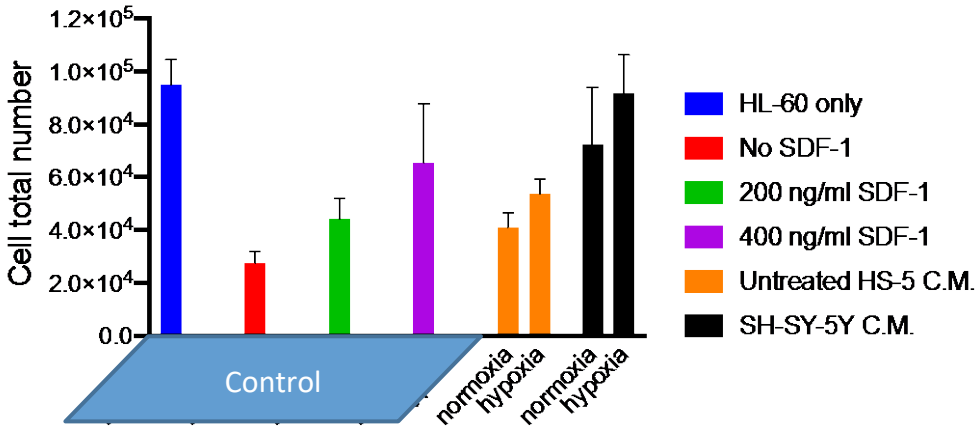

Figure 4-10 Transmigrated HL-60 with SHSY-5Y C.M.

HL-60 were seeded at 3.0x 10^5 cells/insert in 8 μm pore inserts that contain a confluent layer of HMEC-1. Tests were conducted in normoxia and hypoxia. Transmigrated HL-60 cells were counted after 24 hours. Control bars represent inserts seeded with HL-60 only without HMEC-1 (blue), inserts seeded with HL-60 on top of HMEC-1 without SDF-1α (red) inserts seeded with HL-60 on top of HMEC-1 with SDF-1α in the lower compartment at 200 ng/ml and 400 ng/ml (green and purple) respectively. Results are presented as average cell count ± S.D. for n=3. Statistical analysis was done using two-way ANOVA test.

4.4.7 Treatment of HS-5 with inhibitors of protein and bioactive lipid production

HS-5 was treated with CHX and aspirin (section 2.5.2); CHX was used at 5 μg/ml and 10 μg/ml (Liu *et al.*, 2017a), and protein production was measured prior to

transmigration assessment. Protein production by HS-5 was reduced significantly at both concentrations, most notably at 10 µg/ml ($p<0.0001$) (Figure 4-11).

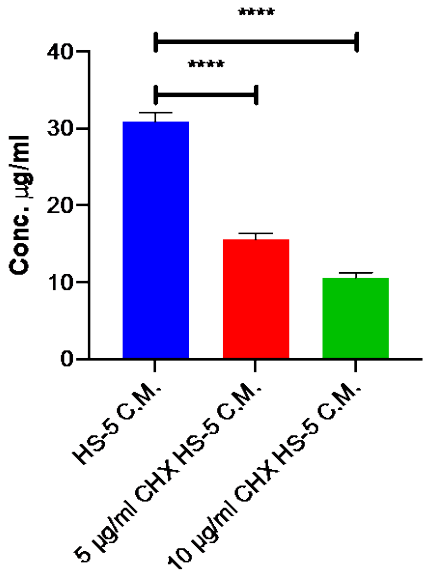

Figure 4-11 Protein concentration of CHX treated HS-5 C.M.

HS-5 was seeded at 1.0x 10^6cells/ well approximately 10^5 cell/cm^2 in 2 ml of RPMI 1640 supplemented with 5µg/ml and 10 µg/ml CHX; media was collected after 24 hours and protein concentration was measured by Bradford assay. Statistical significance is indicated as**** p<0.0001. Results are presented as average concentration ± S.D. for n=3. Statistical analysis was done using one-way ANOVA test.

CHX-treated HS-5 C.M. at both doses showed 32% and 46% less trafficking of HL-60 compared to untreated HS-5 C.M. ($p<0.05$ and $p<0.005$) respectively. (Figure 4-12). Aspirin-treated HS-5 C.M. also showed less trafficking of HL-60, aspirin was used as both acetylsalicylic acid (ASA), and as salicylate, the end product of aspirin hydrolysis (Vane and Botting, 2003). HS-5 were treated with aspirin at 5 mM and 10 mM while salicylate was used at different concentrations (20 µM, 1000 µM, 4000 µM and 10000 µM) (Figure 4-13). ASA treatment at 10 mM showed significant inhibition of trafficking of HL-60, while salicylate showed a trend towards inhibition, with 0.8-fold decrease at 20 µM ($p>0.05$). Escalating the dose of salicylate to 1000 µM and higher showed

significant inhibition of HL-60 transmigration (p<0.001), however no further improvement on this inhibition was achieved above 1000 µM (p>0.05).

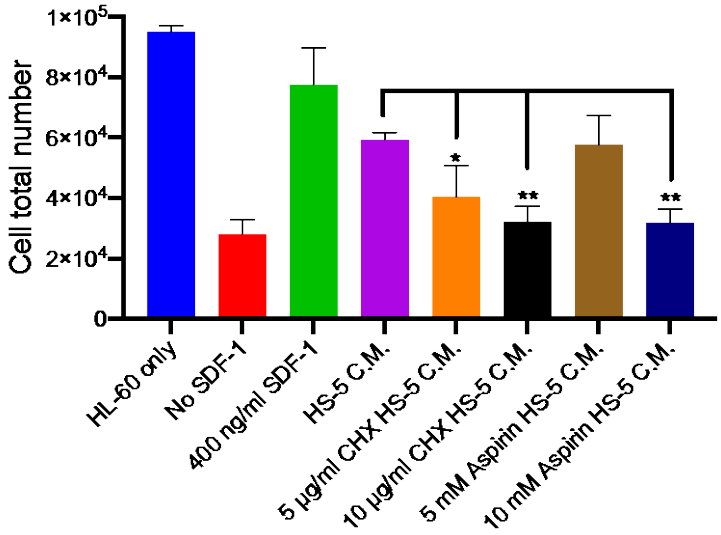

Figure 4-12 Transmigration of HL-60 with CHX and aspirin treated HS-5 C.M.

HS-5 was treated with CHX at 5µg/ml and 10 µg/ml and with aspirin at 5 mM and 10 mM. HL-60 were seeded at 3.0x 10^5 cells/insert in 8 µm pore inserts that contained a confluent layer of HMEC-1. Transmigrated HL-60 cells were counted after 24 hours. Statistical significance is indicated as* p<0.05 and ** p<0.005 Results are presented as average cell count ± S.D. for n=3. Statistical analysis was done using one-way ANOVA test.

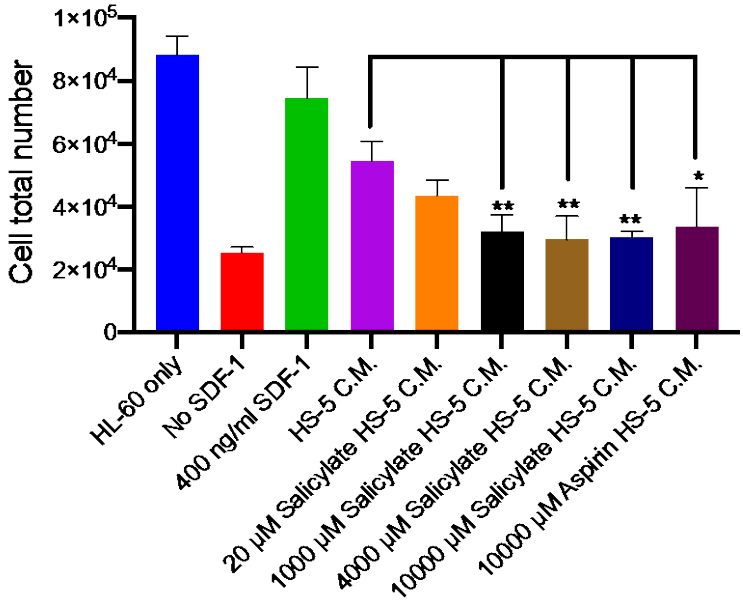

Figure 4-13 Transmigration of HL-60 with aspirin and salicylate treated HS-5 C.M.

HS-5 was treated with salicylate at 20 µM, 1000 µM, 4000 µM and 10000 µM, and with aspirin at 10000 µM. HL-60 were seeded at 3.0x 10^5 cells/insert in 8 µm pore inserts that contained a confluent layer of HMEC-1. Transmigrated HL-60 cells were counted after 24 hours. Statistical significance is indicated as* p<0.05 and ** p<0.01 Results are presented as average cell count ± S.D. for n=3. Statistical analysis was done using one-way ANOVA test.

4.5 Discussion

In this part of the study, it has been demonstrated that HS-5 C.M. could induce transmigration of HL-60 (Figure 4-1), suggesting that HS-5 cells are producing elements that play a crucial role in stem cell chemoattraction. It is well demonstrated that HS-5 protect leukaemia cells from chemo- and targeted therapies (Garrido *et al*., 2001; Beaulieu *et al*., 2011; Kuckertz *et al*., 2012; Chen *et al*., 2015; Podszywalow-Bartnicka *et al*., 2018; Zhou *et al*., 2018).

In addition to studying the effect of HS-5 C.M. as a stromal cell in this model, HS-5 C.M. was diluted to lower concentrations to investigate the impact of the concentration gradient (Figure 4-1). HS-5 C.M. showed more efficiency to cause transmigration in undiluted concentration (100%) than the diluted medium. This finding might suggest that the chemoattractant's effect might be localised in an area of the endothelium close to the injury site, in which adhesion molecules might be activated and allow for HPC to attach. This finding might also explain the localisation effect of chemoattractant on the endothelial sinusoidal cell membrane, as otherwise, chemoattractant signals might move with the bloodstream to other parts of the body, leading to stem cell attachment at different locations.

HSC transmigration across the endothelium is a process whereby stem cells respond to gradients of chemoattractants, migrating towards high concentration gradients and lodging within specific tissue areas inside the BM microenvironment. Interactions between transplanted cells and the BM microvascular endothelium are dependent on several factors, including some elements released by the BM stromal cell itself (Asri *et al*., 2016).

HL-60 transmigration through the endothelium monolayer was induced by SDF-1α (Figure 4-1). The capacity of haematopoietic progenitor cells (HPCs) to respond to chemoattractant stimulation is essential in the validation of the model.

SDF-1α is long known to be produced by many types of stromal cells, including those from the BM (Aiuti *et al.*, 1997). SDF-1α was showed to increase in actin polymerisation and in polarisation of the actin cytoskeleton in HL-60 cells as described by Voermans *et al.* (2001).

Transmigration of HL-60 was slightly enhanced by the induction of hypoxic conditioning of the model (Figure 4-2), pre-conditioning of HL-60 in hypoxia showed induction of transmigration and response to SDF-1α. Low oxygen concentration might induce high expression of the CXCR4 in different cell types including monocytes, monocyte-derived macrophages, tumour-associated macrophages, endothelial cells, and cancer cells, and is paralleled by increased chemotactic responsiveness to SDF-1α (Schioppa *et al*., 2003). For HL-60, it is most likely that hypoxia does not affect the expression of CXCR4 as shown by Seo *et al*. (2007). They demonstrated that CXCR4 transcriptional levels in HL-60 were neither significantly increased nor decreased under hypoxia and there was no decrease in the surface expression of CXCR4 in HL-60 cultured in 1% O_2 for 24 hours, however HL-60 migration toward SDF-1α was reduced through blocking Akt activation without the reduction in the expression levels of CXCR4 (Seo *et al*., 2007). Conversely, a recent study by Mohammadali *et al*. (2018) showed that mild hypoxia with 5% O_2 tension significantly increases CXCR4 gene expression after seven days of incubation.

In this study, enhanced response to SDF-1α might be not directly related to HL-60 cells; it might be related to induced overexpression of adhesion molecules on the endothelium after exposure to 1% O_2 hypoxia and SDF-1α. A study by Befani and Liakos (2017) demonstrated that exposure of HMEC-1 to hypoxia at 1% O_2 caused a reduction in their proliferation rate and enhanced expression of αv, β1, β3, and β5 integrins. Both α- and β-integrins are long known to mediate cell adhesion and

migration (Katayama *et al*., 2003). Whereas, SDF-1α was showed to stimulate HMEC-1 cell proliferation and reduced apoptosis (Ho *et al*., 2010).

The CXCR4/SDF-1 complex activates several pathways that mediate chemotaxis and migration. The function of the CXCR4/SDF-1 complex is to promote homing and engraftment of CD34+ cells within the recipient BM (Asri *et al*., 2016; Peled *et al*., 2000; Vagima *et al*., 2011). SDF-1 transcription is partially controlled by hypoxia inducible factor-1 (HIF-1), and upregulated by hypoxia during vascular injury (Aiuti *et al*., 1997; Ceradini and Gurtner, 2005; Tu *et al*., 2016).

Chemotherapy treatment of the stromal cell HS-5 showed no significant improvement of transmigration (Figure 4-3). Treating HS-5 with plasma concentration equivalents to clinically relevant doses for 2 hours and 24 hours did not improve transmigration significantly ($p>0.05$). Melphalan treated HS-5 C.M. inhibited transmigration of HL-60 in the 24 hours treatment in normoxia and hypoxia ($p<0.05$) and ($p<0.01$) respectively (Figure 4-4). Other chemotherapeutic drugs, carmustine, etoposide and ara-C, showed slightly reduced transmigration particularly in hypoxia ($p>0.05$). This finding might be in line with that described by Seo *et al.* (2007), who showed that hypoxia might reduce SDF-1α dependant transmigration of HL-60. It is commonly known these chemotherapeutic agents can induce injury to stromal cells (May *et al*., 2018). Melphalan and ara-C were demonstrated to affect viability of both HS-5 and primary MSC when treated with a similar range of chemotherapy as described by Schmidmaier *et al*. (2006).

On the other hand, 50% reduced chemotherapy treated HS-5 C.M. did not improve transmigration (Figure 4-5) compared to untreated HS-5. Reducing the intensities of chemotherapeutic agents by 50% was done to reduce the cytotoxic effect of the standard doses in which HS-5 might produce more reliable signals to induce transmigration. Although HS-5 had been washed three times after each treatment,

residual drug carryover cannot be excluded, which might have affected the viability of HL-60. *In vitro* treatment conditions of cells are different from *in vivo* models which might affect the outcome in many ways. Simulating BEAM *in vivo* treatment (Table 1-3) might be difficult to implement *in vitro*.

Conversely, targeted therapies appear to have more effects on transmigration than cytotoxic chemotherapy (Figures 4-6 and 4-7). Imatinib treated HS-5 C.M. improved HL-60 transmigration in normoxia, while for ibrutinib it was more effective in hypoxia. Imatinib mesylate is a member of the class of small molecule tyrosine kinase inhibitors with an ATP-competitive selective inhibition of Bcr-Abl kinase (Cismowski, 2007). Imatinib specifically blocks the Bcr-Abl fusion protein kinase resulting from the Philadelphia chromosomal translocation which is the major cause of chronic myelogenous leukemia (CML), as well as activated c-Kit mutants in gastrointestinal stromal tumours (GIST) (Deininger and Druker 2003). Few studies have investigated the direct effect of imatinib on the stromal cells. It has been demonstrated to affect the proliferation of MSCs *in vitro* in a dose dependent manner (Melzer *et al*., 2004). The effect was partly independent of platelet-derived growth factor receptors (PDGF-R) and c-kit signalling and related to the proliferative status of the cells as described by Melzer *et al*. (2004). This inhibitory effect was demonstrated also by Soares *et al*. (2013) mainly in fibroblast MSCs in an *in vitro* murine model.

Ibrutinib treatment showed improved transmigration in hypoxia ($p<0.05$), and in normoxia after increasing the dose by 100% from 2.3µM to 4.6µM. This finding might suggest that the effect of ibrutinib on HS-5 is dose-dependent. Ibrutinib is a small molecule which serves as an irreversible inhibitor of Bruton's tyrosine kinase (BTK), and is used to treat B cell malignancy, most notably chronic lymphocytic leukaemia (CLL) (Parmar, Patel and Pinilla-Ibarz, 2014). There are no evidences in the literature to suggest that ibrutinib directly affects stromal cells. However, MSCs were

demonstrated to not protect CLL cells from the apoptosis induced by ibrutinib (Trimarco *et al*., 2015). In this context, improved HL-60 transmigration might be due to induction of hypoxia. However, the possible effects of the interfering elements like FBS and DMSO as a vehicle for the drugs were eliminated (Figures 4-8 and 4-9). There were no significant changes in transmigration after adding FBS and also in DMSO treated HS-5. HS-5 is the only part of this model exposed to targeted therapies; after each treatment, HS-5 were washed three times to remove any residual drug, however residual drug effect on the other cellular components of the model cannot be excluded.

HL-60 transmigration was assessed towards hypoxic maintained differentiated neural cells (Figure 4-10). Differentiated SH-SY5Y C.M. showed enhanced transmigration of HL-60, especially with hypoxia-treated cells. Some reports suggested that ischaemic stroke might activate and mobilise haematopoietic stem cells in the BM. In 2015, Courties *et al*. showed that ischaemic stroke activates the haematopoietic system at its most upstream point in a murine model. Daughter cell differentiation was shifted towards the myeloid lineage within four days following stroke. Shortly after brain injury, haematopoietic stem cells enter the cell cycle, giving rise to inflammatory monocytes, neutrophils, and their progenitors (Courties *et al*., 2015).

Several factors are involved in HSCs trafficking and homing to the site of injury; in HSCT settings, the BM microenvironment is known to release chemotactic factors including peptide-based chemokines (Zhang and Lodish, 2008) and bioactive phosphosphingolipids (Juarez *et al*., 2012). Here we have demonstrated that treating HS-5 with CHX inhibits protein biosynthesis significantly (Figures 4-11) in a concentration-dependent manner, and subsequently, C.M. produced from these HS-5 were effective at reducing HL-60 transmigration in the model (Figure 4-12). This might suggest that the majority of the chemotactic factors released by HS-5 are, or

are signalled by, peptide-based chemokines. In this context, besides being directed to receptors on HPC, cytokines might affect homing indirectly by influencing HPC and microvascular endothelium to over-express specific adhesion molecules to which trafficking cells might bind. Denning-Kendall *et al*. (2003) demonstrated that cytokine expansion culture of cord blood CD34+ cells with stem cell factor (SCF), Flt-3-ligand (Flt-3), thrombopoietin (TPO) and G-CSF, induced marked and sustained changes in adhesion receptor and CXCR4 expressions.

Besides protein-based signalling and adhesion molecules, bioactive lipids are also known to play a role in transmigration (Juarez *et al*., 2012). Inhibition of biosynthesis of bioactive phosphosphingolipids by aspirin showed significant inhibition of HL-60 transmigration (Figure 4-13). ASA-treated (10 mM) HS-5 C.M. showed significant inhibition of HL-60, while salicylate treatment started to show a significant inhibition at a concentration above 10 mM, which might suggest that aspirin can be metabolised by HS-5. Inhibition of bioactive lipid biosynthesis reduced HL-60 trafficking through the endothelium (Figure 4-13). Bioactive lipids S1P and C1P have emerged as potent chemoattractants for a variety of cells, being upregulated in damaged tissues, in response to organ and tissue injuries (Drukala *et al*., 2012); as side effects of radio-chemotherapy (Kim *et al*., 2012; Schneider *et al*., 2013); or hypoxia related to acute myocardial infarction or stroke leading to stem cell mobilisation (Nagareddy *et al*., 2014; Karapetyan *et al*., 2013). In 2015, Adamiak *et al*. reported a defect in homing and engraftment in BM expressed S1P-deficient ($Sphk1^{-/-}$) mice when transplanted with haematopoietic cells from wild type normal control mice and floxed CXCR4 ($CXCR4^{fl/fl}$). They also supported the concept that, in addition to the SDF-1/CXCR4 axis, other chemotactic axes like S1P might be strongly involved in HCS homing and engraftment to the bone marrow.

4.6 Conclusion

In conclusion, myeloablative therapy is essential for HSCT to promote homing and engraftment. In this model, we have demonstrated that it does not affect HL-60 transmigration compared to the targeted therapies studied here. This might be associated with the used treatment approach involving drug concentration and exposure time; however, simulating the *in vivo* treatment approach might be challenging to achieve in this *in vitro* model. Targeted therapy was shown to induce trafficking, which might be due to the reduced toxicity of the used drugs and the influence of hypoxia on the co-culture model. Inhibiting biosynthesis of proteins and bioactive lipids showed a reduced transmigration of HL-60, which might suggest that both are essential for HPCs trafficking. Inhibiting biosynthesis of proteins was shown to be more effective, which might suggest that the majority of chemoattractants are peptide-based, which will be investigated in the next chapter.

Chapter 5: Proteomic analyses of conditioned media from chemotherapy exposed stromal cells, and validation of identified secreted proteins

5.1 Background

Stromal cells play a crucial role in the BM microenvironment. Besides their ability to differentiate into several cell types (Ohishi and Schipani, 2010; Han *et al*., 2017) and their importance in regenerative medicine, tissue engineering and immune modulation (Naji *et al*., 2019), stromal cells also deliver various proteins to protect haematopoietic cells and to promote drug resistance (Liu *et al*., 2019). Alterations of protein expression upon exposing stromal cells to 'injury' are typically associated with cell to cell signal transduction, and regulation of cellular functions in the BM. Conditioned medium derived from BM-MSCs have therapeutic effects, by secreting factors that affect the regulation of angiogenesis, protect tissues and reduce inflammation in the presence of ischaemic tissue injury. In HSCT settings, combining HSCs with MSCs might improve engraftment and reduce graft failure (MacMillan *et al*., 2009; Liu *et al*., 2017b; Wu *et al*., 2014; Xiong *et al*., 2014). It has been demonstrated that *ex vivo* expanded BM-derived MSCs from HLA-mismatched unrelated or haploidentical donors, combined with HSC from PBSC or CB are effective in treating engraftment failure after HSCT. This combination therapy has an improved effect on neutrophil reconstruction.

It is well accepted that stromal cells play a role in the chemotactic process of SC homing after transplant due to exposing the mesenchymal compartment of the BM to the pre-conditioning regimen and inducing stromal cells to produce homing factors like that seen under ischaemic conditions. This study hypothesised that the combination of chemotherapy with hypoxia in the BM might induce production of

homing elements which might represent a 'help' signal to the transplanted SC to come to reside in the BM niches. The combination of chemotherapy with hypoxia is often ignored *in vitro*, and adding the hypoxia element might provide a novel candidate that previously had been overlooked.

In this part of the study, HS-5 cells were utilised as a stromal cell compartment. The HS-5 cells were tested untreated under normoxic and hypoxic conditions, and also treated with chemotherapy (BEAM) under normoxic and hypoxic conditions. HS-5 C.M. were harvested (section 2.6.2) in a standard way to avoid variation in seeding density and volume, which might affect the concentration of the secreted proteins. After proteomics data analysis, some of the candidate upregulated proteins were obtained as recombinant proteins and tested in the transmigration model to evaluate the ability to induce transmigration of HL-60 and also to evaluate the effect of these proteins on the endothelial monolayer of HMEC-1 in terms of key adhesion molecules expression. Selection of proteins for further analyses was made depending on two factors. Upregulated proteins are highly likely to affect the transmigration process mostly if they originate from or act on extracellular space or cell membrane. Selected proteins shall be functionally associated with endothelial membrane integrity or associated with the cell migration process. However, downregulated proteins might affect transmigration, but it will be challenging to implement this effect on the current model.

5.2 Aims

To expose the stromal cell line HS-5 to a combination of conditioning chemotherapy (BEAM) in normoxic and hypoxic conditions. The HS-5 cell line was used as untreated, under normoxic and hypoxic conditions, and was subject to conditioning chemotherapy (BEAM) in normoxic and hypoxic conditions. Conditioned media from HS-5 were collected and analysed with LC-MS/MS. Affected paracrine peptide-based

factors were obtained as recombinant proteins and tested in the transmigration model.

5.3 Methods

5.3.1 Cell culture and BEAM treatment

HS-5 were seeded and treated, as described in section 2.6.2.

5.3.2 Protein quantification assay

C.M. from treated HS-5 was collected as described in section 2.5.1, and the samples' protein levels were measured using Bradford assay as described in section 2.6.1.

5.3.3 Proteomic samples processing and analysis

Samples of chemotherapy exposed HS-5 C.M. for proteomics analysis were sent to the proteomic service unit at the University of Bristol and processed as described in section 2.6.3.

5.3.4 Loading results data into Perseus and data filtration

Results were obtained as a Microsoft Excel datasheet, which was then converted to a tab-delimited .txt format. Data were uploaded to Perseus and processed as described in section 2.6.4. TMT proteome data were obtained as a .txt file. Data were processed and analysed using the Perseus software platform as described by Tyanova and colleagues (Tyanova *et al*., 2016; Tyanova and Cox 2018). Filtering strategies were implemented by excluding contaminants and non-valid values. Contaminants usually are from non-human origin, while non-valid values represent protein intensity measurements of 0 in the raw data set. This usually occurs due to sample complexity and variation (or stochasticity) in sampling from one run to another (O'Rourke *et al*., 2019). Depending on the nature of the values, with proteins having very low expression levels in one of the samples, filtering was implemented based on a minimum number of valid values of 1 in at least one sample. Before data analysis,

relative peptide abundance was group-wise median normalised (Tyanova *et al*., 2016; Tyanova and Cox 2018). Peptide relative abundance shows the abundances of the sample values before scaling and normalisation. Evaluation of cellular function and location of over-represented gene ontology (GO) biological processes of proteins was performed using Panther Protein ANalysis THrough Evolutionary Relationships (www.pantherdb.org) and a Fisher's Exact with FDR multiple test correction. To display protein interactions, selected proteins were uploaded into String database Search Tool for the Retrieval of Interacting Genes (www.string-db.og).

5.3.5 Recombinant proteins in the transmigration model

Candidate proteins selected from proteomics analysis were obtained as recombinant proteins and tested in the transmigration model as described in section 2.7.

5.3.6 Estimation of AMOT level by ELISA

Samples of chemotherapy exposed HS-5 C.M. were collected as described in section 2.5.1. Samples were tested for AMOT levels, as described in section 2.8.

5.3.7 Immunocytochemistry

HMEC-1 samples were prepared and tested for E- & P-selectin after exposure to candidate proteins selected from proteomics analysis as described in section 2.9.

5.3.8 Wound healing assay

Wound healing assay was performed for the HMEC-1 samples under the influence of SDF-1α as described in section 2.10.

5.4 Results

5.4.1 Protein quantification assay

HS-5 cells were tested at four different conditions; untreated normoxia, untreated hypoxia, BEAM normoxia and BEAM hypoxia, as described in 2.6.2. Briefly, HS-5 was treated with a combination of chemotherapeutic agents (melphalan 8.2µM, carmustine 1.9µM, etoposide 2.5µM, cytarabine 2.5µM) for 24 hours, and C.M. was collected. All samples of HS-5 C.M. were tested for protein levels by Bradford assay before TMT labelling (Figure: 5-1). Protein levels should be 25-100µg in each sample for each labelling reaction as recommended in the TMT 10plex protocol.

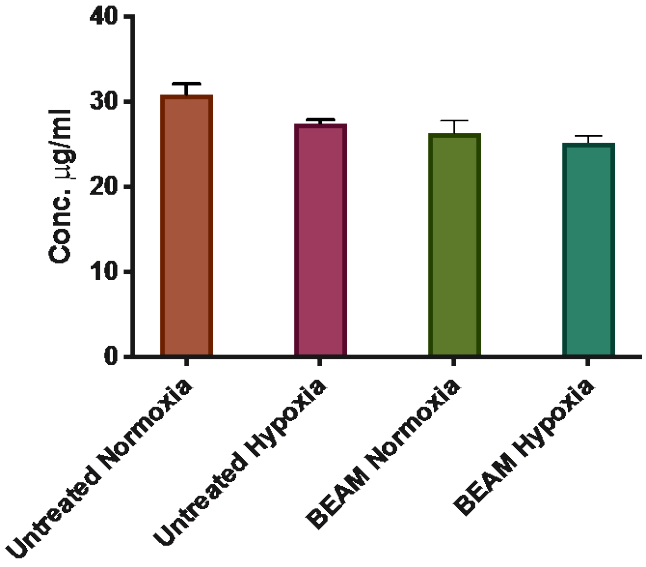

Figure 5-1 Total protein levels in proteomics samples.

HS-5 C.M. from proteomics analysis were tested for protein levels by Bradford assay. Results are presented as average protein concentration ± S.D. for n=3.

5.4.2 Untreated hypoxia versus normoxia

Results were obtained as protein relative abundance in the samples, for the first group of samples (untreated hypoxia vs normoxia). Seven hundred sixty-seven proteins were identified after data filtering; complete proteins accessions are listed in the supplementary data (appendix 3); of these 137 proteins were significantly changed (Figure 5-2), 25 proteins were upregulated (Table 5-1), and 112 proteins were downregulated in hypoxia; accessions are listed in supplementary data appendix 4. Analysis was based on a volcano plot which visualises the results of a t-test to determine significant data points with a permutation-based false discovery rate (FDR) calculation (Tyanova *et al*., 2016; Tyanova and Cox 2018). A specific focus was given to proteins upregulated in hypoxia; 25 proteins were upregulated in hypoxia vs normoxia as shown in Figure 5-3. A two-dimensional hierarchical heatmap of the 25 upregulated proteins was generated based on median–normalised protein abundance in each sample.

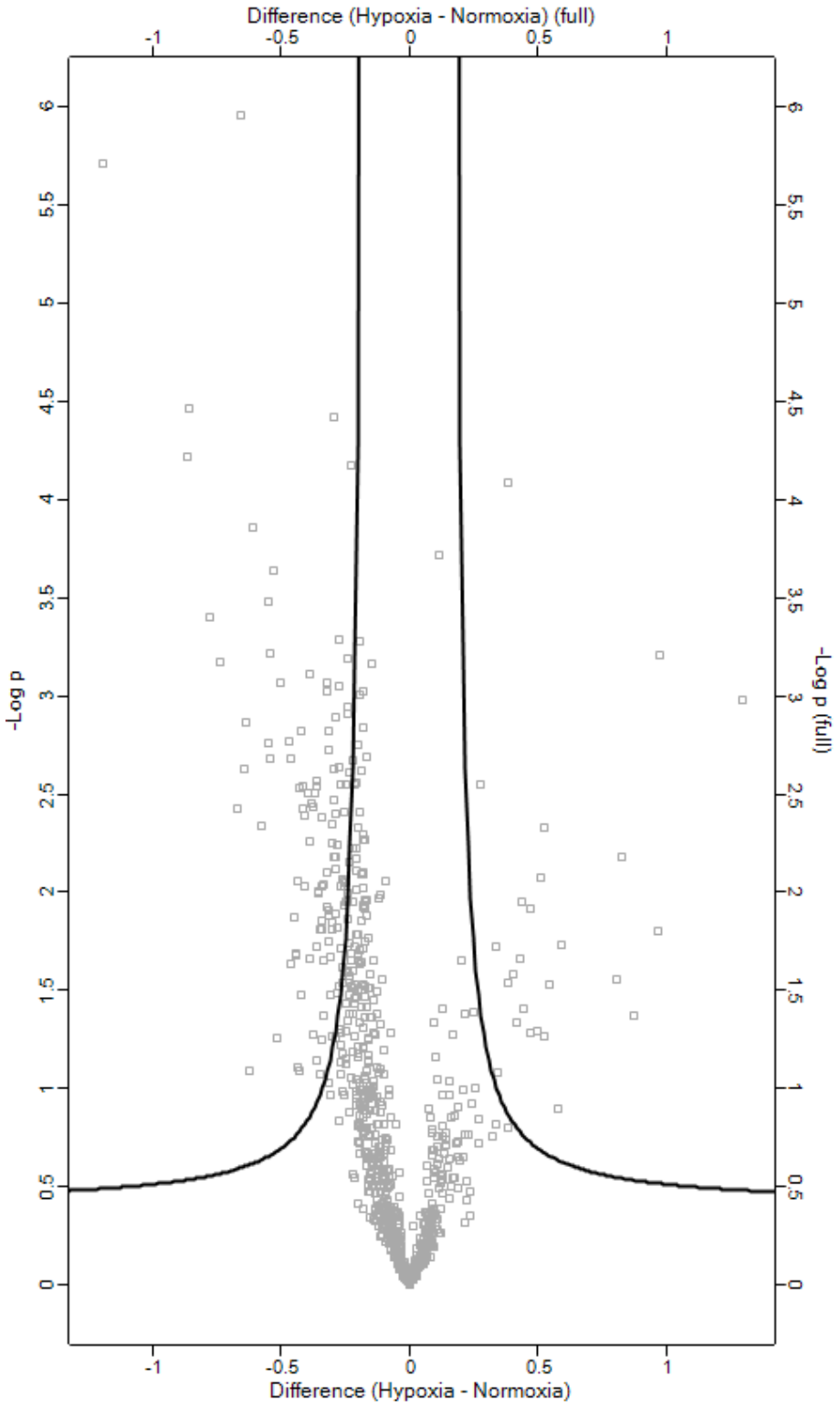

Figure 5-2 Volcano plots of group-wise comparisons of hypoxia vs normoxia affected proteins.

The solid lines indicate the Student t-test Benjamini–Hochberg FDR 5% and s0:0.2; the data points above the solid lines represent proteins whose abundance was significantly changed; left side downregulated, right side upregulated. Upregulated IDs are in Table 5-1.

Table 5-1 Upregulated proteins in hypoxia vs normoxia.

GN=Gene Name, PE=Protein Existence which is the numerical value describing the evidence for the existence of the protein, SV=Sequence Version which is the version number of the sequence, -log *P* = -log p value for Student t-test Benjamini–Hochberg, Diff.= Difference in average protein abundance.

Accession	Description		-log *P*	Diff.
A0A024QYT5	SERPINE1	Serpin peptidase inhibitor, clade E (Nexin, plasminogen activator inhibitor type 1), member 1, isoform CRA_b (GN=SERPINE1 PE=3 SV=1)	1.80	0.97
P19338	NCL	Nucleolin (GN=NCL PE=1 SV=3)	1.41	0.45
B2R6I6	STC1	cDNA, FLJ92965, highly similar to *Homo sapiens* stanniocalcin 1 (STC1), mRNA (PE=2 SV=1)	1.53	0.55
A0A024R4H0	PLOD1	Procollagen-lysine 1, 2-oxoglutarate 5-dioxygenase 1, isoform CRA_a (GN=PLOD1 PE=4 SV=1)	1.29	0.50
Q9Y4K0	LOXL2	Lysyl oxidase homolog 2 (GN=LOXL2 PE=1 SV=1)	2.18	0.83
O76061	STC2	Stanniocalcin-2 (GN=STC2 PE=1 SV=1)	1.54	0.38
M1VKI3	SDC4-ROS1_S4	Tyrosine-protein kinase receptor (GN=SDC4-ROS1_S4; R32 PE=2 SV=1)	3.21	0.97
O00469	PLOD2	Procollagen-lysine,2-oxoglutarate 5-dioxygenase 2 (GN=PLOD2 PE=1 SV=2)	1.08	0.34
A0A024R5Z7	ANXA2	Annexin (GN=ANXA2 PE=3 SV=1)	2.55	0.28
Q9BY76	ANGPTL4	Angiopoietin-related protein 4 (GN=ANGPTL4 PE=1 SV=2)	2.98	1.30
P04141	CSF2	Granulocyte-macrophage colony-stimulating factor (GN=CSF2 PE=1 SV=1)	1.66	0.43
A0A024RDR0	HMGB1	High-mobility group box 1, isoform CRA_a (GN=HMGB1 PE=4 SV=1)	1.92	0.47
G3V4U0	FBLN5	Fibulin-5 (GN=FBLN5 PE=1 SV=1)	1.28	0.47
P35318	ADM	ADM (GN=ADM PE=1 SV=1)	2.33	0.53
P19957	PI3	Elafin (GN=PI3 PE=1 SV=3)	1.56	0.80
Q9H1E3	NUCKS1	Nuclear ubiquitous casein and cyclin-dependent kinase substrate 1 (GN=NUCKS1 PE=1 SV=1)	2.08	0.51
A2A2V4	VEGFA	Vascular endothelial growth factor A (GN=VEGFA PE=1 SV=1)	1.95	0.44
Q6UXH9	PAMR1	Inactive serine protease PAMR1 (GN=PAMR1 PE=1 SV=1)	1.59	0.41
P62906	RPL10A	60S ribosomal protein L10a (GN=RPL10A PE=1 SV=2)	1.33	0.42
H0YBI8	VEGFA	Vascular endothelial growth factor A (Fragment) (GN=VEGFA PE=1 SV=1)	1.73	0.59
P35659	DEK	Protein DEK (GN=DEK PE=1 SV=1)	1.37	0.87
O43570	CA12	Carbonic anhydrase 12 (GN=CA12 PE=1 SV=1)	1.27	0.52
P05023	ATP1A1	Sodium/potassium-transporting ATPase subunit alpha-1 (GN=ATP1A1 PE=1 SV=1)	0.90	0.58
Q86U86	PBRM1	Protein polybromo-1 (GN=PBRM1 PE=1 SV=1)	4.09	0.39
O60882	MMP-20	Matrix metalloproteinase-20 (GN=MMP20 PE=1 SV=3)	1.72	0.34

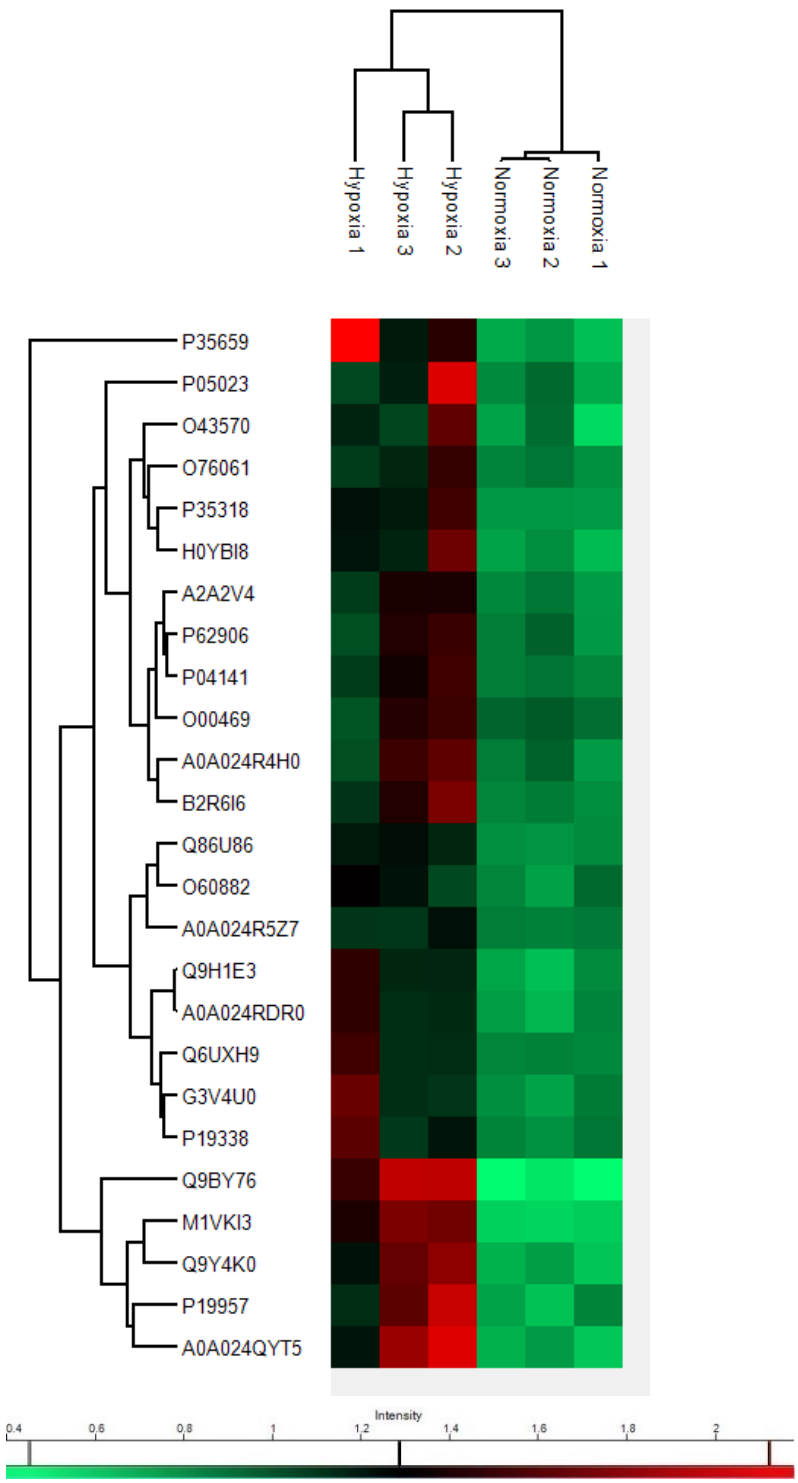

Figure 5-3 Two-dimensional hierarchical heatmap of 25 upregulated proteins in hypoxia vs normoxia.

Abundance was significantly upregulated (Student t test Benjamini–Hochberg with FDR 5%). Log2-transformed expression values were median–normalised for each biological replicate. Hierarchical clustering was performed, with columns representing C.M. samples and rows representing individual proteins (green, low expression; red, high expression).

Evaluation of over-represented GO biological processes and cellular component of proteins was performed using Panther platform (Mi *et al*., 2018). Out of the 25 upregulated proteins, the number of mapped genes was 15 genes, with a total of 22 processes hits and nine cellular component hits. Some protein IDs were not mapped to a corresponding protein record in the Panther platform. These unmapped proteins include A0A024QYT5, B2R6I6, A0A024R4H0, M1VKI3, A0A024R5Z7, A0A024RDR0, G3V4U0, A2A2V4 and H0YBI8.

The percent of gene hit against the total number of genes and percent of gene hit against the total number of processes hits are presented in Figure 5-4 and Table 5-2. When looking at the biological processes of the proteins, all of them had different functions. Cellular process, metabolic process and biological regulation were shown to be enriched in the overall upregulated hypoxia proteome. Cellular process generally includes communication between cells which occurs at the cellular level, while, the metabolic process includes anabolism and catabolism, by which cells transform chemical substances. Biological regulation includes the modulation of the cellular function and biological process (Mi *et al*., 2018).

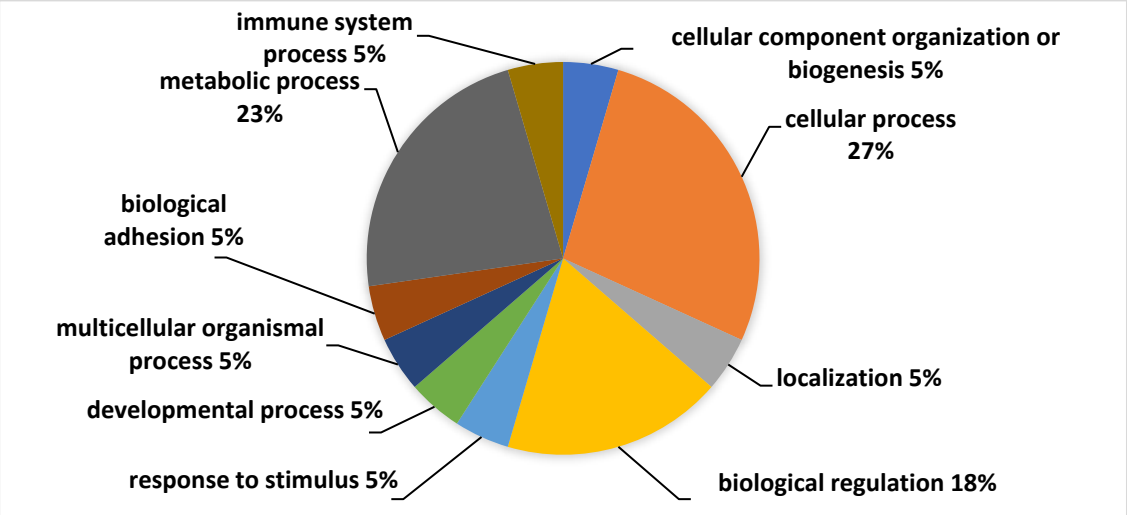

Figure 5-4 Hypoxia vs Normoxia Panther GO-Slim Biological Process of upregulated proteins.

Enrichment analysis showed that cellular process, metabolic process and biological regulation were enriched in hypoxia.

Table 5-2 Hypoxia vs Normoxia Panther GO-Slim Biological Process associated with mapped proteins IDs of upregulated proteins.

Panther GO-Slim Biological Process	Accession	Protein name
Cellular component organisation or biogenesis	P62906	60S ribosomal protein L10a
Cellular process	Q9Y4K0	Lysyl oxidase homolog 2
	P35659	Protein DEK
	Q86U86	Protein polybromo-1
	O60882	Matrix metalloproteinase-20
	Q9BY76	Angiopoietin-related protein 4
	O76061	Stanniocalcin-2
	O00469	Procollagen-lysine,2-oxoglutarate 5-dioxygenase 2
Localisation	P05023	Sodium/potassium-transporting ATPase subunit alpha-1
Biological regulation	P35659	Protein DEK
	P05023	Sodium/potassium-transporting ATPase subunit alpha-1
	P19338	Nucleolin
	O76061	Stanniocalcin-2
Response to stimulus	Q6UXH9	Inactive serine protease PAMR1
Developmental process	O60882	Matrix metalloproteinase-20
Multicellular organismal process	O60882	Matrix metalloproteinase-20
Biological adhesion	Q9BY76	Angiopoietin-related protein 4
Metabolic process	P19957	Elafin
	P19338	Nucleolin
	Q9H1E3	Nuclear ubiquitous casein and cyclin-dependent kinase substrate 1
	Q86U86	Protein polybromo-1
	O60882	Matrix metalloproteinase-20
	O00469	Procollagen-lysine,2-oxoglutarate 5-dioxygenase 2
Immune system process	P04141	Granulocyte-macrophage colony-stimulating factor

These proteins were run in the STRING platform (Szklarczyk *et al*., 2019) for further analysis of protein-protein interaction and functional enrichment analysis. Functional enrichment confirmed that no relevant functional pathway was associated with these proteins, even though the majority of differently secreted proteins are associated with biological regulation. For example, 12 proteins were released in response to stress (FDR: 0.0029) which include: ADM, ANGPTL4, CSF2, HMGB1, LOXL2, NUCKS1, PLOD1, PLOD2, SERPINE1, STC1, STC2 and VEGFA. Eight of these proteins were released particularly in response to hypoxia which included: ADM, ANGPTL4, LOXL2, PLOD1, PLOD2, STC1, STC2 and VEGFA. Moreover, five proteins were found to be regulating endothelial cell migration which included: HMGB1, LOXL2, VEGFA,

SERPINE1 and STC1. Six proteins were associated with angiogenesis which included: ANGPTL4, ANXA2, LOXL2, NCL, SERPINE1 and VEGFA.

The locations of the proteins were from the extracellular space origin, protein-containing complex inside the cells, cell membrane and cellular organelle (Figure 5-5; Table 5-3). Although samples were conditioned medium, some proteins originated from inside the cells. These proteins might be released in response to, or as a result of hypoxic conditions.

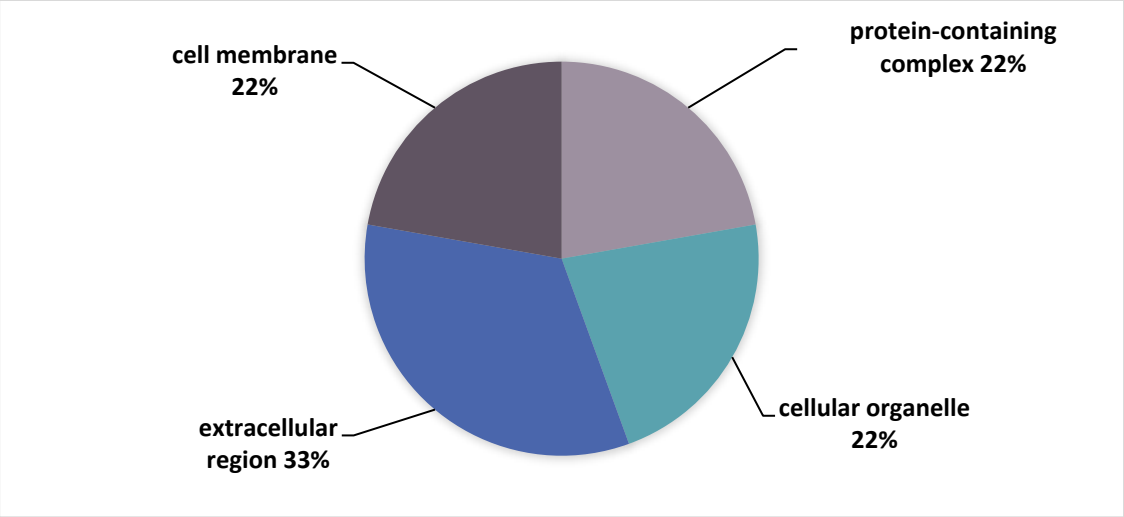

Figure 5-5 Hypoxia vs Normoxia Panther GO-Slim Cellular Component of upregulated proteins.

The majority of the proteins were from the extracellular region of the cells; remaining proteins were from cell membrane, protein-containing complex and cellular organelle.

Table 5-3 Hypoxia vs Normoxia Panther GO-Slim Cellular Component of upregulated proteins, shows origins of mapped proteins and IDs of upregulated proteins.

Panther GO-Slim Cellular Component	Accession	Protein name
Protein-containing complex	P19338	Nucleolin
	Q86U86	Protein polybromo-1
Cellular organelle	P35659	Protein DEK
	Q86U86	Protein polybromo-1
Extracellular region	Q9Y4K0	Lysyl oxidase homolog 2
	P04141	Granulocyte-macrophage colony-stimulating factor
	Q9BY76	Angiopoietin-related protein 4
Cell membrane	P05023	Sodium/potassium-transporting ATPase subunit alpha-1
	P62906	60S ribosomal protein L10a

The STRING analysis showed that 12 proteins were from the extracellular region including ADM, ANGPTL4, ANXA2, CSF2, FBLN5, HMGB1, LOXL2, PAMR1, PI3, SERPINE1, STC1 and VEGFA. The STRING protein-protein interaction networks of hypoxia vs normoxia (Figure 5-6) showed that 22 out of 25 upregulated proteins were mapped. Proteins have a high level of interactions among themselves, which might indicate that the proteins are at least partially biologically connected, as a group. The protein-protein interaction (PPI) enrichment *p*-value was 4.54×10^{-8}. VEGFA and SERPINE1 showed a high level of interactions with other proteins. VEGFA is essential for the survival of HSCs in the hypoxic BM niches, as shown by Rehn *et al*., (2011). SERPINE1 is essential for fibrinolysis and cell migration; it has been shown to promote the recruitment and polarisation of M2 monocytes/macrophages through different structural domains (Kubala *et al*., 2018).

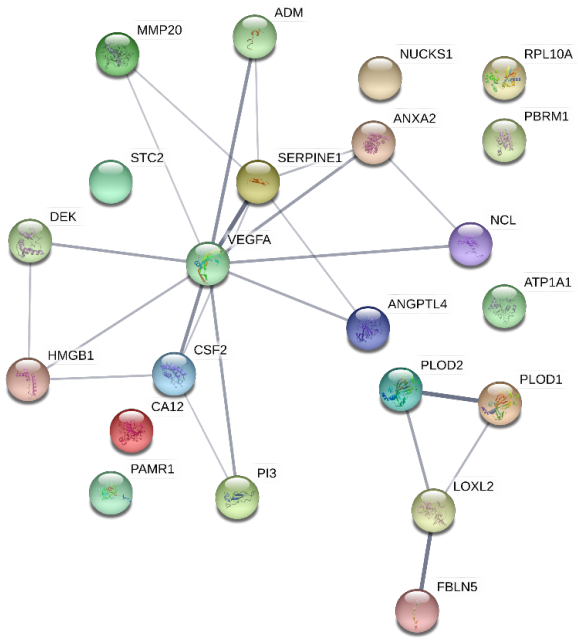

Figure 5-6 STRING analysis reveals protein interaction networks of 22 out of 25 upregulated protein in Hypoxia vs Normoxia.

Interactions of the identified proteins were mapped by searching the STRING database version 11.0 with a confidence cut-off of 0.4. In the resulting protein association network, proteins are presented as nodes which are connected by lines whose thickness represents the confidence level. Coloured nodes are query proteins and first shell of interactors; empty nodes are proteins of unknown 3D structure, filled nodes indicate some 3D structure is known or predicted.

As mentioned earlier in this section, 112 proteins were downregulated in hypoxia; these are listed in the supplementary data (appendix 4) and presented in Figure 5-7. These proteins mostly originated from the cytoplasmic region of the cells, and are involved in several pathways, including cytokine-cytokine receptor interaction.

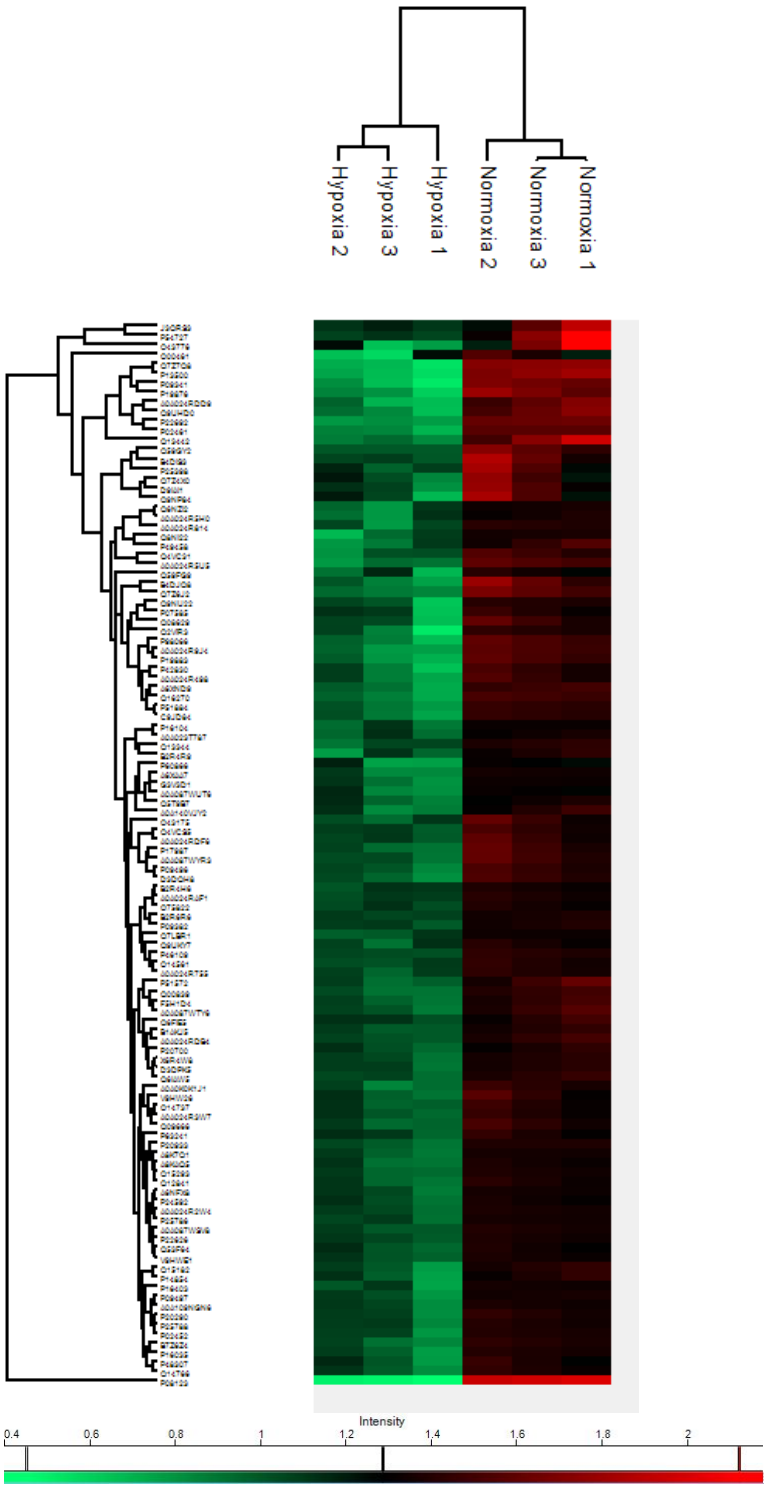

Figure 5-7 Two-dimensional hierarchical heatmap of 112 downregulated proteins in Hypoxia vs Normoxia.

Abundance was significantly downregulated (Student t-test Benjamini–Hochberg with FDR 5%). Log2-transformed expression values were median–normalised for each biological replicate. Hierarchical clustering was performed, with columns representing C.M. samples and rows representing individual proteins (green, low expression; red, high expression).

5.4.3 BEAM treated Hypoxia vs Normoxia

The second group of samples was BEAM treated; treatments were conducted in normoxia and hypoxia as described in section 2.6.2. After data filtering, 1661 proteins were identified; complete protein accessions are listed in the supplementary data (Appendix 5). Based on the volcano plot (Figure 5-8) analysis showed that 1080 proteins were significantly changed, with 31 proteins upregulated (Table 5-4) and 1049 proteins downregulated in hypoxia, listed in the supplementary data (Appendix 6). Focusing on upregulated proteins in hypoxia vs normoxia, a two-dimensional hierarchical heatmap of the 31 upregulated proteins was generated based on median-normalised protein abundance in each sample (Figure 5-9).

Further analysis of the upregulated proteins was conducted in the Panther database, to link protein IDs with gene families and determine their related functional subfamilies. Further analysis was also made utilising the STRING platform to determine protein-protein interaction networks and functional enrichment analysis.

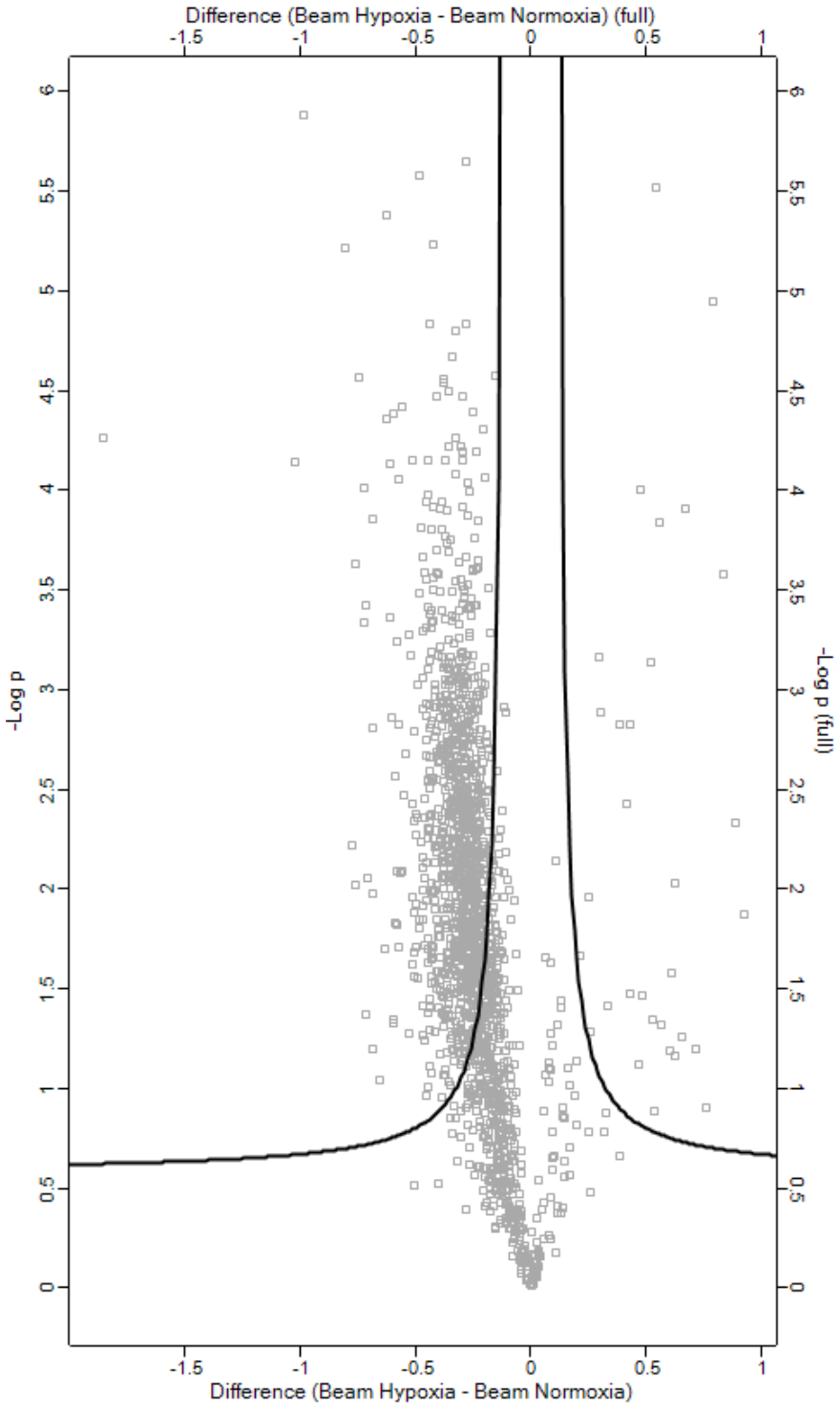

Figure 5-8 Volcano plots of group-wise comparisons of Hypoxia vs Normoxia affected proteins from BEAM treated HS-5 cells.

The dashed lines indicate the Student t-test Benjamini–Hochberg F.D.R. 1% and s0:0.1; the data points above the dashed lines represent proteins whose abundance was significantly changed; left side downregulated, right side upregulated. Upregulated IDs are in Table 5-4.

Table 5-4 Upregulated proteins in BEAM treated HS-5 in Hypoxia vs Normoxia.

GN=Gene Name, PE=Protein Existence which is the numerical value describing the evidence for the existence of the protein, SV=Sequence Version which is the version number of the sequence, -log *P* = -log *p* value for Student t-test Benjamini–Hochberg, Diff.= Difference in average protein abundance.

Accession	Description		-log *p*	Diff.
Q53G75	MMP-1	Matrix metalloproteinase 1 preproprotein variant (Fragment) (PE=2 SV=1)	1.48	0.43
O00469	PLOD2	Procollagen-lysine,2-oxoglutarate 5-dioxygenase 2 (GN=PLOD2 PE=1 SV=2)	3.58	0.84
A0A024QYT5	SERPINE1	Serpin peptidase inhibitor, clade E (Nexin, plasminogen activator inhibitor type 1), member 1, isoform CRA_b (GN=SERPINE1 PE=3 SV=1)	1.66	0.21
Q6FHV6	ENO2	ENO2 protein (GN=ENO2 PE=1 SV=1)	3.17	0.30
B2R6I6	STC1	cDNA, FLJ92965, highly similar to Homo sapiens stanniocalcin 1 (STC1), mRNA (PE=2 SV=1)	2.89	0.30
A0A024R4H0	PLOD1	Procollagen-lysine 1, 2-oxoglutarate 5-dioxygenase 1, isoform CRA_a (GN=PLOD1 PE=4 SV=1)	2.83	0.39
Q6FHC9	STC2	STC2 protein (Fragment) (GN=STC2 PE=2 SV=1)	5.52	0.54
Q647J8		Granulocyte-macrophage colony stimulating factor 2 (PE=2 SV=1)	2.34	0.89
B4DZR0		cDNA FLJ55529, highly similar to Heat shock 70 kDa protein 4L (PE=2 SV=1)	1.47	0.48
P35318	ADM	ADM (GN=ADM PE=1 SV=1)	4.01	0.47
D3DRR6	ITIH2	Inter-alpha (Globulin) inhibitor H2, isoform CRA_a (GN=ITIH2 PE=4 SV=1)	1.35	0.53
Q597H1	TRG14	Transformation-related protein 14 (GN=TRG14 PE=2 SV=1)	3.90	0.67
A2A2V4	VEGFA	Vascular endothelial growth factor A (GN=VEGFA PE=1 SV=1)	3.84	0.56
P78556	CCL20	C-C motif chemokine 20 (GN=CCL20 PE=1 SV=1)	2.43	0.42
P58107	EPPK1	Epiplakin (GN=EPPK1 PE=1 SV=3)	3.14	0.53
P19957	PI3	Elafin (GN=PI3 PE=1 SV=3)	4.94	0.79
A5Y5A3		PC1/MRPS28 fusion protein (PE=2 SV=1)	1.96	0.25
Q9BY76	ANGPTL4	Angiopoietin-related protein 4 (GN=ANGPTL4 PE=1 SV=2)	1.12	0.47
A0A0Y0J542	VEGFA	Vascular endothelial growth factor A121 (Fragment) (PE=2 SV=1)	2.83	0.43
Q9NXJ5	PGPEP1	Pyroglutamyl-peptidase 1 (GN=PGPEP1 PE=1 SV=1)	0.90	0.76
Q07812	BAX	Apoptosis regulator BAX (GN=BAX PE=1 SV=1)	1.41	0.34
B4E1C2	KNG1	Kininogen 1, isoform CRA_b (GN=KNG1 PE=2 SV=1)	1.17	0.63
A0A024R2W4	DAG1	Dystroglycan 1 (Dystrophin-associated glycoprotein 1), isoform CRA_a (GN=DAG1 PE=4 SV=1)	0.88	0.54
A8K6A8		cDNA FLJ76304, highly similar to Homo sapiens ADAM metallopeptidase with thrombospondin type 1 motif, 4 (ADAMTS4), mRNA (PE=2 SV=1)	1.28	0.26
Q9H8Y1	VRTN	Vertnin (GN=VRTN PE=1 SV=1)	1.87	0.93
Q4VCS5	AMOT	Angiomotin (GN=AMOT PE=1 SV=1)	1.58	0.61
A4D218	MAD1L1	MAD1 mitotic arrest deficient-like 1 (Yeast) (GN=MAD1L1 PE=4 SV=1)	1.32	0.57
A0A087WYC6	DNAH11	Dynein heavy chain 11, axonemal (GN=DNAH11 PE=1 SV=1)	1.20	0.72
Q15643	TRIP11	Thyroid receptor-interacting protein 11 (GN=TRIP11 PE=1 SV=3)	1.19	0.60
Q9NVN8	GNL3L	Guanine nucleotide-binding protein-like 3-like protein (GN=GNL3L PE=1 SV=1)	1.26	0.66
A0A087X256	WASHC4	WASH complex subunit 4 (GN=WASHC4 PE=1 SV=1)	2.03	0.63

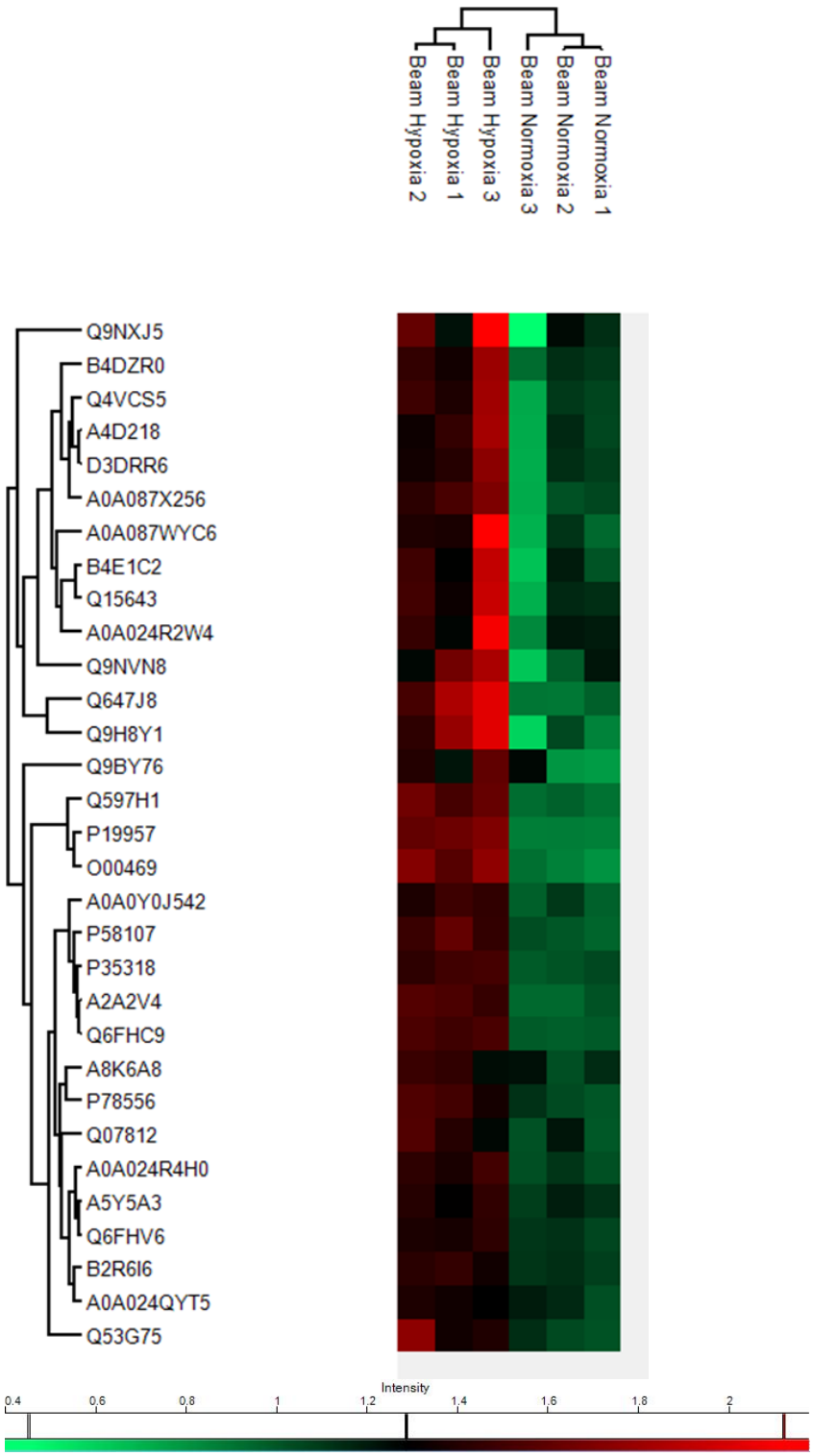

Figure 5-9 Two-dimensional hierarchical heatmap of upregulated proteins in BEAM treated HS-5 under hypoxia vs normoxia.

Abundance was significantly downregulated (Student t-test Benjamini–Hochberg with FDR 5%). Log2-transformed expression values were median–normalised for each biological replicate. Hierarchical clustering was performed, with columns representing C.M. samples and rows representing individual proteins (green, low expression; red, high expression).

Upregulated peptides were evaluated in the Panther platform; the number of mapped protein IDs were linked to 12 genes out of 31 protein IDs, with a total of 19 processes hits and nine cellular component hits of genes. Cellular process, metabolic process and biological regulation were shown to be enriched in the overall upregulated proteome (Figure 5-10; Table 5-5). Unmapped IDs (not found in Panther) include: Q53G75, A0A024QYT5, Q6FHV6, B2R6I6, A0A024R4H0, Q6FHC9, Q647J8, B4DZR0, D3DRR6, Q597H1, A2A2V4, A5Y5A3, A0A0Y0J542, B4E1C2, A0A024R2W4, A8K6A8, A4D218, A0A087WYC6, A0A087X256.

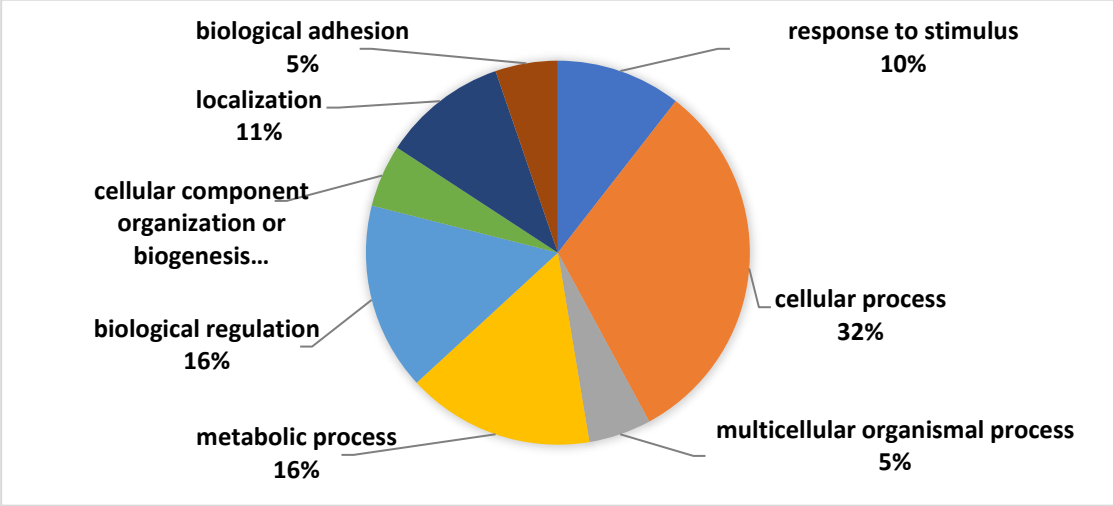

Figure 5-10 BEAM treated HS-5 cells under hypoxia vs normoxia. Panther GO-Slim Biological Process of upregulated proteins in BEAM treated hypoxia vs normoxia.

Table 5-5 BEAM treated HS-5 cells under hypoxia vs normoxia. Panther GO-Slim Biological Process associated with mapped upregulated protein IDs.

Panther GO-Slim Biological Process	Accession	Protein name
Response to stimulus	P58107	Epiplakin
	P78556	C-C motif chemokine 20
Cellular process	Q9BY76	Angiopoietin-related protein 4
	Q07812	Apoptosis regulator BAX
	Q4VCS5	Angiomotin
	P58107	Epiplakin
	P78556	C-C motif chemokine 20
	P58107	Epiplakin
Multicellular organismal process	P78556	C-C motif chemokine 20
Metabolic process	P19957	Elafin
	O00469	Procollagen-lysine,2-oxoglutarate 5-dioxygenase 2
	Q9NXJ5	Pyroglutamyl-peptidase 1
Biological regulation	P78556	C-C motif chemokine 20
	Q9H8Y1	Vertnin
	O00469	Procollagen-lysine,2-oxoglutarate 5-dioxygenase 2
Cellular component organisation or biogenesis	P58107	Epiplakin
Localisation	Q4VCS5	Angiomotin
	P78556	C-C motif chemokine 20
Biological adhesion	Q9BY76	Angiopoietin-related protein 4

The origin of proteins was predominantly from cellular organelles inside the cells, the extracellular region and cellular membrane (Figure 5-11; Table 5-6). Hypoxia and chemotherapy together might have induced the stromal cells to release these proteins to the C.M.

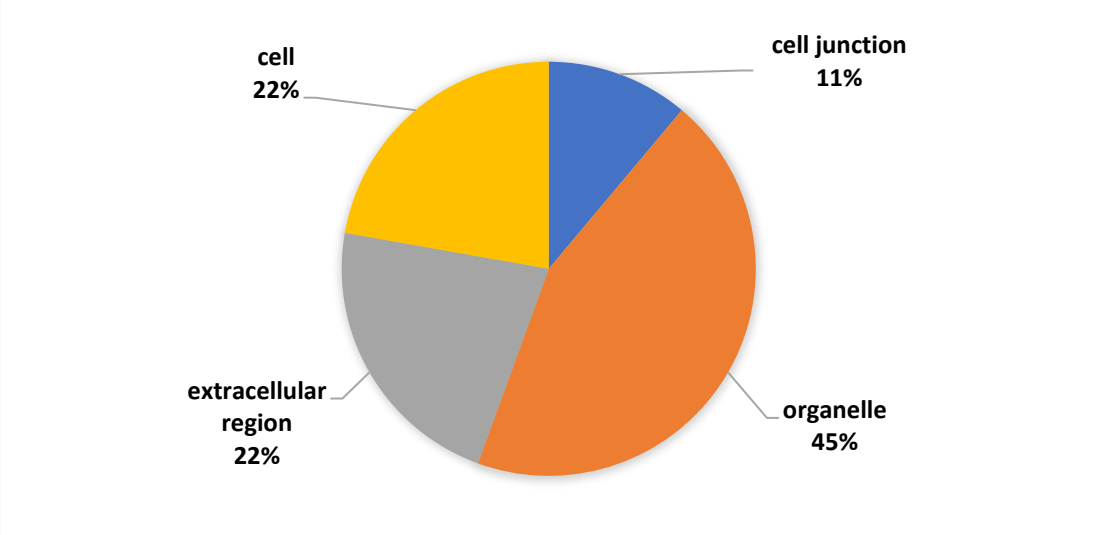

Figure 5-11 BEAM treated hypoxia vs normoxia Panther GO-Slim Cellular Component of upregulated proteins.

Table 5-6 BEAM treated hypoxia vs normoxia Panther GO-Slim Cellular Component of upregulated proteins associated with mapped proteins and IDs of upregulated proteins

Panther GO-Slim Cellular Component	Accession	Protein name
Cell junction	Q4VCS5	Angiomotin
Cellular organelle	Q07812	Apoptosis regulator BAX
	Q4VCS5	Angiomotin
	O00469	Procollagen-lysine,2-oxoglutarate 5-dioxygenase 2
	Q9NVN8	Guanine nucleotide-binding protein-like 3-like protein
Extracellular region	P78556	C-C motif chemokine 20
	O00469	Procollagen-lysine,2-oxoglutarate 5-dioxygenase 2
Cell membrane	Q4VCS5	Angiomotin
	P58107	Epiplakin

The STRING analysis of protein-protein interaction and functional enrichment analysis of BEAM treated hypoxia vs normoxia upregulated proteins was done to have further insight into the functions of these proteins as a group and how they might interact with each other. The results showed that these proteins are in general associated with stress, hypoxia, angiogenesis, cell migration, and vascular permeability. Further details of the biological processes associated with these proteins are listed in Table 5-7.

Table 5-7 STRING analysis discovery of protein-protein interactions and biological processes associated with the 31 proteins secreted by BEAM treated hypoxia vs normoxia HS-5.

Biological Process	Gene count	Background gene count	FDR	Matching proteins
Response to Stress	10	3267	0.0052	ADM, ANGPTL4, BAX, CCL20, EPPK1, PLOD1, PLOD2, SERPINE1, STC2, VEGFA
Regulation of Localisation	8	2524	0.0156	AMOT, BAX, CCL20, EPPK1, GNL3L, SERPINE1, STC2, VEGFA
Circulatory System Development	7	807	0.0006	ADM, AMOT, ANGPTL4, BAX, SERPINE1, TRIP11, VEGFA
Response to External Stimulus	7	1857	0.0147	ADM, AMOT, CCL20, PI3, SERPINE1, STC2, VEGFA
Response to Hypoxia	6	288	0.00017	ADM, ANGPTL4, PLOD1, PLOD2, STC2, VEGFA
Blood Vessel Morphogenesis	6	381	0.00022	ADM, AMOT, ANGPTL4, BAX, SERPINE1, VEGFA
Regulation of Angiogenesis	5	277	0.0006	ADM, AMOT, ANGPTL4, SERPINE1, VEGFA
Regulation of Cell Migration	5	753	0.0118	AMOT, CCL20, EPPK1, SERPINE1, VEGFA
Positive Regulation of Angiogenesis	4	162	0.0011	ADM, ANGPTL4, SERPINE1, VEGFA
Positive Regulation of Cell Migration	4	452	0.0144	AMOT, CCL20, SERPINE1, VEGFA
Cell Migration	4	812	0.0494	AMOT, BAX, CCL20, VEGFA
Regulation of Vascular Permeability	3	34	0.00061	ADM, AMOT, VEGFA
Vasculogenesis	3	65	0.002	ADM, AMOT, VEGFA
Positive Regulation of Leukocyte Migration	3	127	0.0077	CCL20, SERPINE1, VEGFA
Negative Regulation of Vascular Permeability	2	13	0.0041	ADM, AMOT
Negative Regulation of Endothelial Cell Apoptotic Process	2	28	0.0105	ANGPTL4, SERPINE1
Positive Regulation of Blood Vessel Endothelial Cell Migration	2	55	0.0226	AMOT, VEGFA
Positive Regulation of Leukocyte Chemotaxis	2	91	0.0383	SERPINE1, VEGFA
Negative Regulation of Angiogenesis	2	99	0.043	AMOT, SERPINE1

The STRING analysis of these proteins secreted by BEAM treated hypoxia vs normoxia HS-5 showed that they are primarily related to the HIF-1 signalling pathway, EGFR tyrosine kinase inhibitor resistance and p53 signalling pathway (Table 5-8). Protein-protein interaction networks of the BEAM hypoxia vs normoxia (Figure 5-12) showed that 17 out of 31 upregulated proteins were mapped. Generated networks (Figure 5-

12) of proteins have a high level of interactions among themselves, which might indicate that the proteins are at least partially biologically connected, as a group. Protein-protein interaction (PPI) enrichment *p*-value is 2.96×10^{-4}. VEGFA and SERPINE1 showed a high level of interactions with other proteins in this group. VEGFA is essential for the survival of HSCs in the hypoxic BM niches and SERPINE1 is essential for fibrinolysis and cell migration of M2 monocytes/macrophages as previously mentioned.

Table 5-8 STRING analysis discovery of KEGG Pathways associated with the 31 proteins secreted by BEAM treated hypoxia vs normoxia HS-5. KEGG; Kyoto Encyclopedia of Genes and Genomes.

KEGG Pathway (Kyoto Encyclopedia of Genes and Genomes)	Gene count	Background gene count	FDR	Matching proteins
HIF-1 signaling pathway	3	98	0.006	ENO2, SERPINE1, VEGFA
EGFR tyrosine kinase inhibitor resistance	2	78	0.0294	BAX, VEGFA
p53 signaling pathway	2	68	0.0294	BAX, SERPINE1

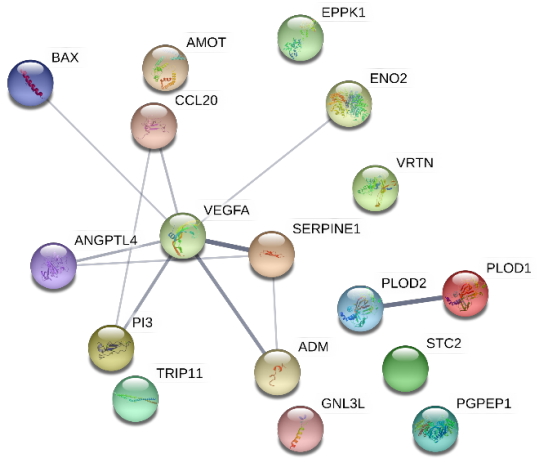

Figure 5-12 STRING analysis reveals protein interaction networks of 17 out of 31 upregulated protein in BEAM treated normoxia vs hypoxia.

Interactions of the identified proteins were mapped by searching the STRING database version 11.0 with a confidence cut-off of 0.4. In the resulting protein association network, proteins are presented as nodes which are connected by lines whose thickness represents the confidence level. Coloured nodes are query proteins and first shell of interactors; empty nodes are proteins of unknown 3D structure, filled nodes are where some 3D structure is known or predicted.

5.4.4 Common proteins in the two groups of untreated and BEAM treated samples in hypoxia vs normoxia.

In order to determine which proteins were common to the two groups of samples (untreated hypoxia vs normoxia) and (BEAM treated hypoxia vs normoxia), the proteome of the untreated C.M. was matched with the BEAM treated group C.M. using the Perseus software. Five hundred and nineteen proteins were common to the two sample groups listed in supplementary Appendix 7; (Figure 5-13). These proteins were differentially expressed in all samples after excluding non-common proteins. The rationale for comparing common proteins was finding a group of candidate proteins expressed in all samples, to be able to follow the effect of the implemented test condition on each identified protein.

Figure 5-13 Venn diagram of common identified proteins to the two sample groups. (Untreated hypoxia vs normoxia) and (BEAM treated hypoxia vs normoxia).

A volcano plot of the untreated hypoxia vs normoxia group of the common proteins (Figure 5-14) showed that 15 proteins were upregulated (Table 5-9). For the BEAM

treated group of samples, a volcano plot (Figure 5-15) showed that 11 proteins were upregulated in hypoxia (Table 5-10).

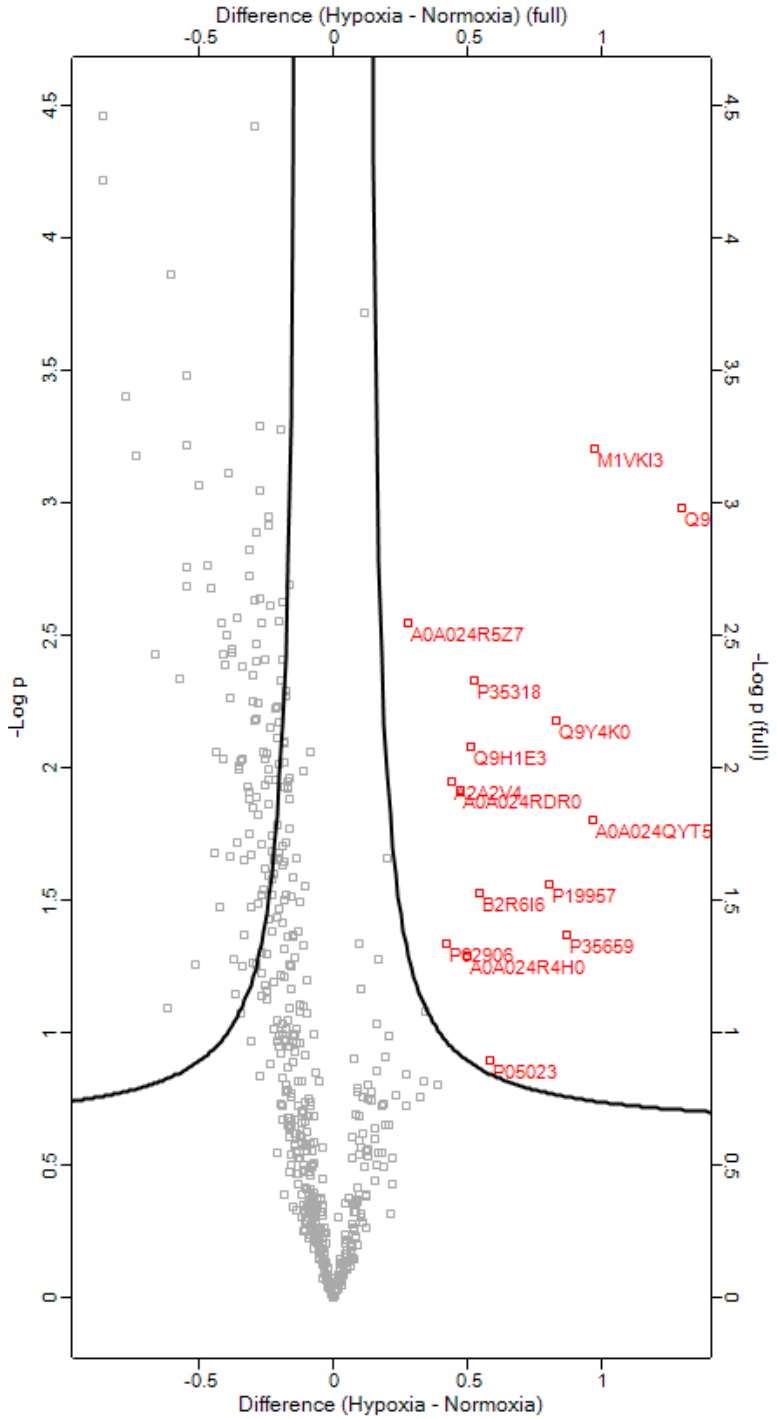

Figure 5-14 Volcano plots of group-wise comparisons of common proteins to the two groups of samples in hypoxia vs normoxia affected proteins.

The dashed lines indicate the Student t-test Benjamini–Hochberg F.D.R. 5% and s0:0.1; the data points above the dashed lines represent proteins whose abundance was significantly changed; left side downregulated, right side upregulated. Upregulated IDs are in Table 5-9.

Table 5-9 Upregulated proteins of common proteins to the two groups of samples in hypoxia vs normoxia.

GN=Gene Name, PE=Protein Existence which is the numerical value describing the evidence for the existence of the protein, SV=Sequence Version which is the version number of the sequence, -log *P* = -log *p* value for Student t-test Benjamini–Hochberg, Diff.= Difference in average protein abundance.

Accession	Description	-Log *p*	Diff.
A0A024QYT5	Serpin peptidase inhibitor, clade E (Nexin, plasminogen activator inhibitor type 1), member 1, isoform CRA_b (GN=SERPINE1 PE=3 SV=1)	1.80	0.97
B2R6I6	cDNA, FLJ92965, highly similar to *Homo sapiens* stanniocalcin 1 (STC1), mRNA (PE=2 SV=1)	1.53	0.55
A0A024R4H0	Procollagen-lysine 1, 2-oxoglutarate 5-dioxygenase 1, isoform CRA_a (GN=PLOD1 PE=4 SV=1)	1.29	0.50
Q9Y4K0	Lysyl oxidase homolog 2 (GN=LOXL2 PE=1 SV=1)	2.18	0.83
M1VKI3	Tyrosine-protein kinase receptor (GN=SDC4-ROS1_S4; R32 PE=2 SV=1)	3.21	0.97
A0A024R5Z7	Annexin OS=Homo sapiens GN=ANXA2 PE=3 SV=1	2.55	0.28
Q9BY76	Angiopoietin-related protein 4 (GN=ANGPTL4 PE=1 SV=2)	2.98	1.30
A0A024RDR0	High-mobility group box 1, isoform CRA_a (GN=HMGB1 PE=4 SV=1)	1.92	0.47
P35318	ADM (GN=ADM PE=1 SV=1)	2.33	0.53
P19957	Elafin (GN=PI3 PE=1 SV=3)	1.56	0.80
Q9H1E3	Nuclear ubiquitous casein and cyclin-dependent kinase substrate 1 (GN=NUCKS1 PE=1 SV=1)	2.08	0.51
A2A2V4	Vascular endothelial growth factor A (GN=VEGFA PE=1 SV=1)	1.95	0.44
P62906	60S ribosomal protein L10a (GN=RPL10A PE=1 SV=2)	1.33	0.42
P35659	Protein DEK (GN=DEK PE=1 SV=1)	1.37	0.87
P05023	Sodium/potassium-transporting ATPase subunit alpha-1 (GN=ATP1A1 PE=1 SV=1)	0.90	0.58

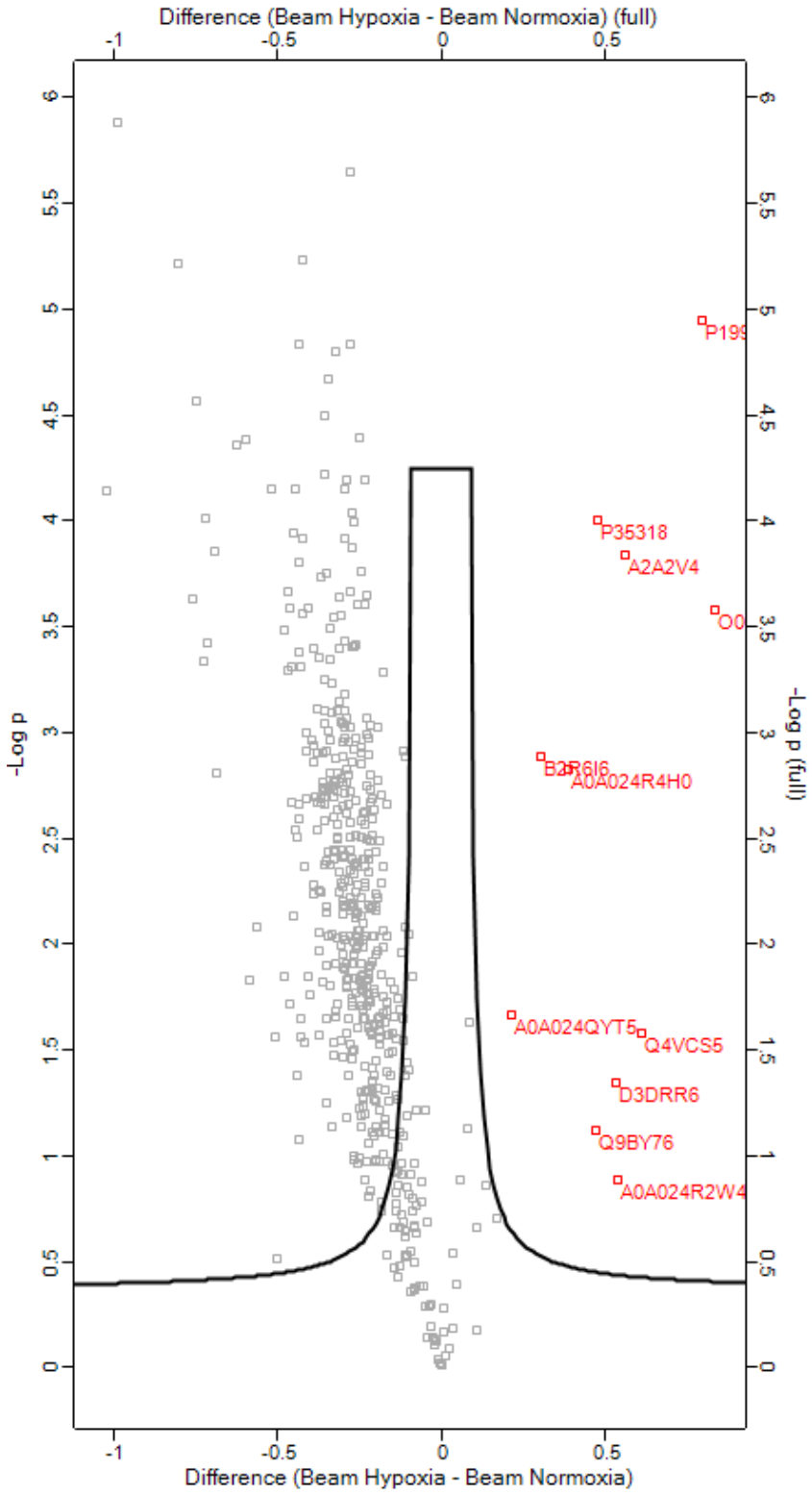

Figure 5-15 Volcano plots of group-wise comparisons of common proteins to the two groups of samples in BEAM treated hypoxia vs normoxia affected proteins.

The dashed lines indicate the Student t-test Benjamini–Hochberg F.D.R. 5% and s0:0.1; the data points above the dashed lines represent proteins whose abundance was significantly changed; left side upregulated, right side downregulated. Upregulated IDs are in Table 5-10.

Table 5-10 Upregulated proteins of common proteins to the two groups of samples in BEAM treated hypoxia vs normoxia.

GN=Gene Name, PE=Protein Existence which is the numerical value describing the evidence for the existence of the protein, SV=Sequence Version which is the version number of the sequence, -log *P* = -log *p* value for Student t-test Benjamini–Hochberg, Diff.= Difference in average protein abundance.

Accession	Description	-Log *p*	Diff.
A0A024QYT5	Serpin peptidase inhibitor, clade E (Nexin, plasminogen activator inhibitor type 1), member 1, isoform CRA_b (GN=SERPINE1 PE=3 SV=1)	1.66	0.21
B2R6I6	cDNA, FLJ92965, highly similar to *Homo sapiens* stanniocalcin 1 (STC1), mRNA (PE=2 SV=1)	2.89	0.30
A0A024R4H0	Procollagen-lysine 1, 2-oxoglutarate 5-dioxygenase 1, isoform CRA_a (GN=PLOD1 PE=4 SV=1)	2.83	0.39
O00469	Procollagen-lysine,2-oxoglutarate 5-dioxygenase 2 (GN=PLOD2 PE=1 SV=2)	3.58	0.84
Q9BY76	Angiopoietin-related protein 4 (GN=ANGPTL4 PE=1 SV=2)	1.12	0.47
P35318	ADM (GN=ADM PE=1 SV=1)	4.01	0.47
P19957	Elafin (GN=PI3 PE=1 SV=3)	4.94	0.79
A2A2V4	Vascular endothelial growth factor A (GN=VEGFA PE=1 SV=1)	3.84	0.56
D3DRR6	Inter-alpha (Globulin) inhibitor H2, isoform CRA_a (GN=ITIH2 PE=4 SV=1)	1.35	0.53
A0A024R2W4	Dystroglycan 1 (Dystrophin-associated glycoprotein 1), isoform CRA_a (GN=DAG1 PE=4 SV=1)	0.88	0.54
Q4VCS5	Angiomotin (GN=AMOT PE=1 SV=1)	1.58	0.61

5.4.5 Protein selection for transmigration analysis

In order to deduce protein functions from GO, enrichment analysis of only upregulated extracellular and cell membrane proteins was performed. Based on the results of proteins upregulated in the BEAM treated hypoxia vs normoxia, a particular focus was given to proteins involved in endothelial cell function, proliferation and cell migration. For example, matrix metallopeptidase (MMPs), particularly MMP-1 and MMP-3, were common in all samples (Figure 5-16). MMP-1 was significantly upregulated in hypoxia vs normoxia, and the preproprotein variant of MMP-1 was significantly upregulated in BEAM treated hypoxia samples as previously shown in section 5.4.3. However, relative to the common protein trend, MMP-1 was upregulated in hypoxia and downregulated in normoxia. Conversely, MMP-3 was downregulated in BEAM treated hypoxia samples compared to BEAM treated normoxia samples, but generally followed the common proteins trend in the BEAM

treated samples since the majority of the proteins were downregulated in hypoxia compared with normoxia samples. Another example of membrane related protein is angiomotin (AMOT) which was significantly upregulated in BEAM treated hypoxia samples compared with BEAM treated normoxia samples as previously shown in section 5.4.3. However, the AMOT profile was against the overall trend of the common proteins in both BEAM treated conditions, being much higher expression in hypoxic and lower expression in normoxic samples than the majority of the common proteins. These three proteins were selected for further testing and obtained as a recombinant to be tested in the transmigration model.

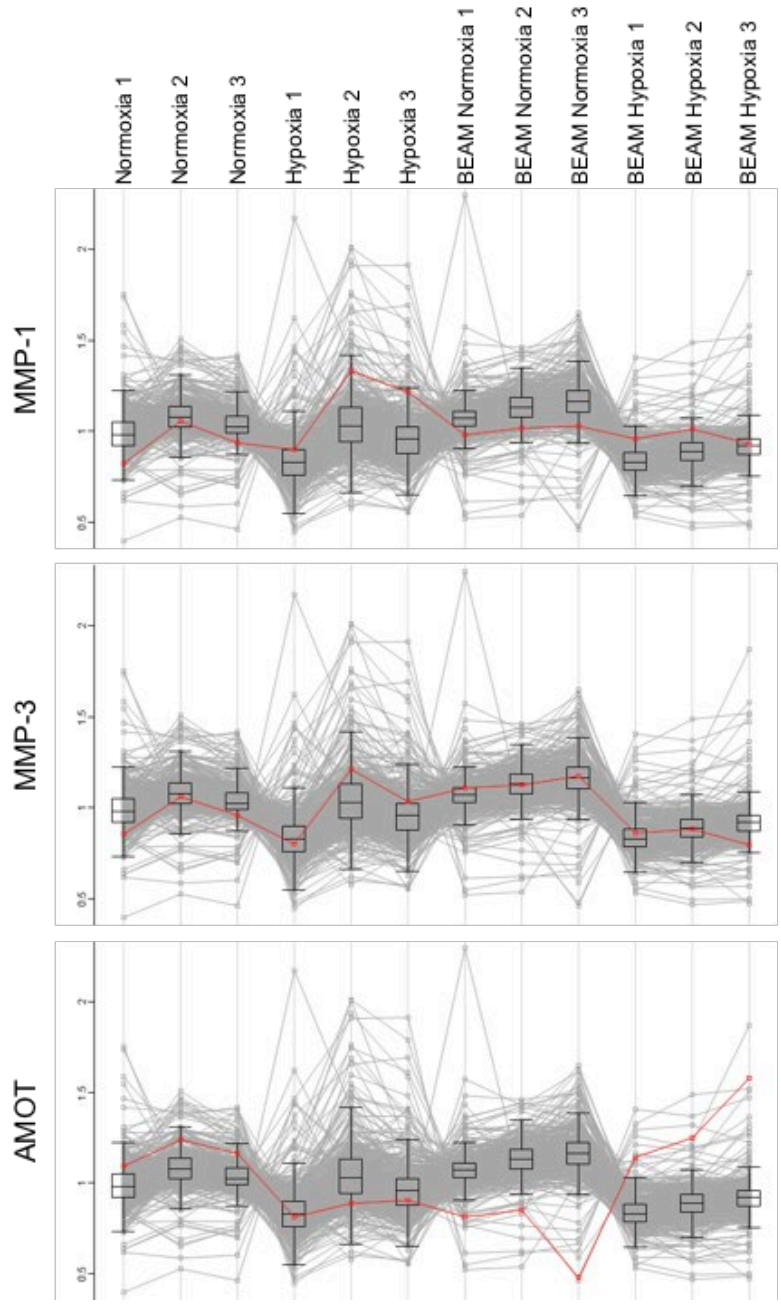

Figure 5-16 Profile plots of MMP-1, MMP-3, and AMOT.

Profile plots of MMP-1, MMP-3, and AMOT. Results are represented as median–normalised protein abundance for each biological replicate. The red lines represent the proteins of interest in each plot (MMP-1, MMP-3, and AMOT). Box plots represent distribution and central tendency of median–normalised protein abundance for the common proteins. MMP-1 is upregulated in hypoxic samples, MMP-3 was downregulated in BEAM treated hypoxic compared to BEAM normoxic samples but followed the overall trend of common proteins, and AMOT was upregulated in the BEAM with hypoxia compared to BEAM treated normoxic samples and was expressed against the overall trend of common proteins.

5.4.5.1 Matrix metalloproteinases (MMP-1 and MMP-2) affect TEER values

The HMEC-1 monolayer was established as described in section 2.3.4. Briefly, cells were seeded in 12 well 8 µm pore inserts at 5.0 x 10^5cell/cm^2 suspended in 1 mL MCDB 131. After 24 hours, MMP-1 and MMP-3 were added to the upper compartment of the inserts at different concentrations, as shown in Figure 5-18. TEER was measured at different time points: 0-hour, 1 hour, 24 hours and 48 hours. Inserts with MMP-1 added showed a sharp drop of TEER values after one hour at all concentrations compared to that with no MMP-1 added (Figure 5-17). TEER value started to recover after 24 and 48 hours especially at high concentrations of MMP-1, (150 ng/ml and 200 ng/ml), however, for the two lower concentrations, (50 ng/ml and 100 ng/ml), the TEER resistance remained less than the control. This inferred that lower MMP-1 levels might be conducive to relaxing the endothelial barrier. However, MMP-1 was used at a concentration higher than the normal range which is 2.2-22.9 ng/mL, whereas for MMP-3 the normal range is 15-72 ng/ml (Masuhara *et al*., 2002).

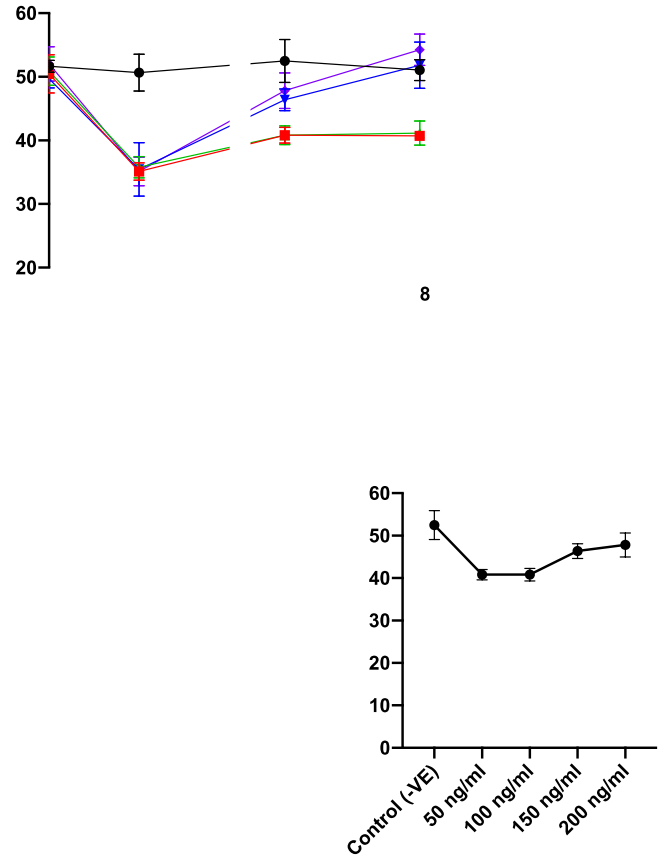

Figure 5-17 TEER measurements of HMEC-1 monolayer with MMP-1 at different concentrations.

HMEC-1 were seeded at 5.0 x 10^5 cell/cm^2 suspended in MCDB 131 in 12 well 8 µm pore inserts. After 24 hours MMP-1 was added to the upper compartment of each HMEC-1 insert at different concentrations: 0 ng/ml (control), 50 ng/ml, 100 ng/ml, 150 ng/ml and 200 ng/ml. TEER was measured at different time points: 0-hour, 1 hour, 24 hours and 48 hours. Results are presented as average TEER value ± SE for n=3.

For the inserts with MMP-3 added, the TEER measurement showed a sharp drop during the first one hour after adding MMP-3 at all concentrations (Figure 5-18). After 24 hours, the HMEC-1 barrier started to show increased resistance again with MMP-3 concentrations at 150 ng/ml and 200 ng/ml, which then continued to increase gradually to reach the control level after 48 hours. Conversely, inserts with concentrations added at 50 ng/ml and 100 ng/ml, resistance increased slightly but not to the control level, which might suggest that lowered MMP-3 levels might be conducive to reduce the tightness of the endothelial barrier.

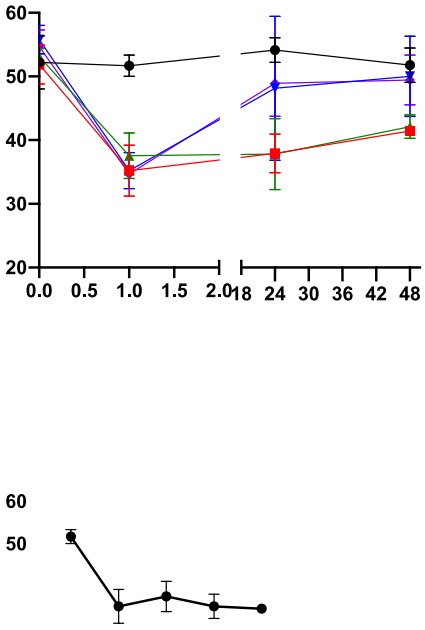

Figure 5-18 TEER measurements of HMEC-1 monolayer with MMP-3 at different concentrations.

HMEC-1 were seeded at 5.0 x 10^5 cell/cm^2 suspended in MCDB 131 in 12 well 8 µm pore inserts. After 24 hour MMP-3 was added to the upper compartment of each HMEC-1 insert at different concentrations: 0 ng/ml (control), 50 ng/ml, 100 ng/ml, 150 ng/ml and 200 ng/ml. TEER was measured at different time points: 0-hour, 1 hour, 24 hours and 48 hours. Results are presented as average TEER value ± SE for n=3.

5.4.5.2 MMPs induce HL-60 trafficking

To study the effects of MMP-1 and MMP-3 on HL-60 trafficking through the endothelium, both MMPs were used in the transmigration model with and without SDF-1. Both MMP-1 and MMP-3 significantly increased HL-60 trafficking, especially in combination with SDF-1 (p<0.0001 and p<0.001) respectively (Figure 5-19). MMP-1 showed more potency in combination with SDF-1; trafficking of HL-60 rose steeply compared to the untreated inserts. MMP-3 showed a slightly enhanced trafficking,

which was improved when combined with SDF-1. Both MMP-1 and MMP-3 were shown to affect the barrier integrity, they seem to affect the barrier by loosening the barrier junctions. Therefore, it is most likely that they simply loosen the barrier and allow the SDF-1 to pull the cells through. However, MMP-3 did not increase HL-60 transmigration above that for the inserts with no barrier, whereas for MMP-1, more cells transmigrated compared to no barrier inserts, which infers that MMP-1 might have some extra role to actively induce trafficking, more than just loosening the barrier. MMP-1 was able to induce this increase of transmigration without the SDF-1 being added, which might deduce that it could be an inducer, whereas MMP-3 most likely loosens the barrier only.

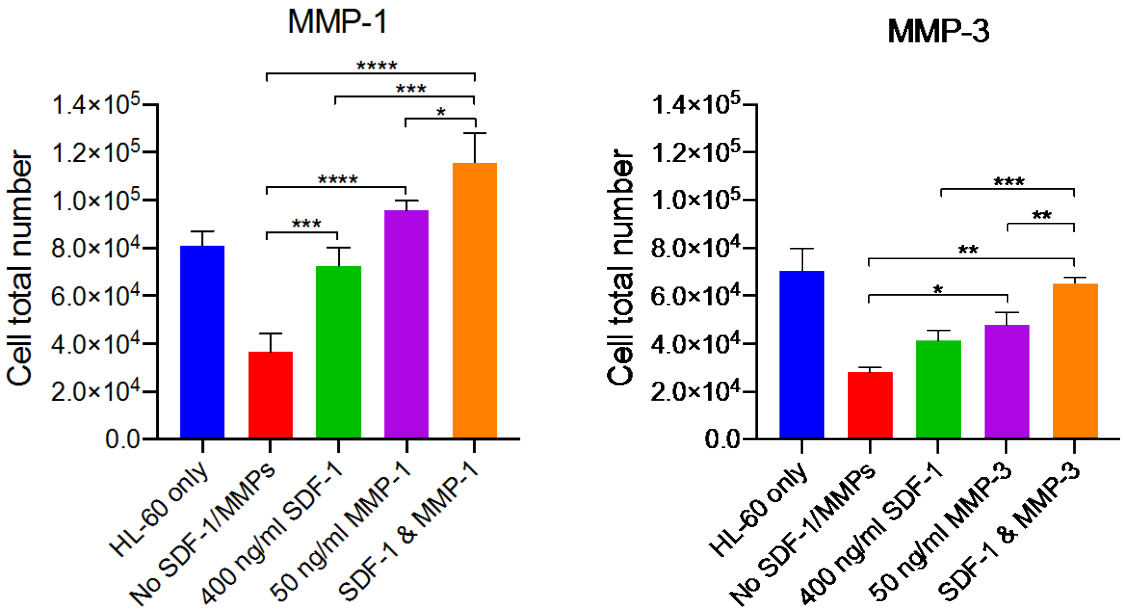

Figure 5-19 HL-60 transmigration with the influence of MMPs.

HL-60 were seeded at 3.0x 10^5 cells/insert in 8 µm pore inserts that contain a confluent layer of HMEC-1, the lower compartments of the inserts were supplemented as follows: 2 ml of RPMI 1640 only, 2 ml of RPMI 1640 supplemented with 400 ng/ml SDF-1, 2 ml of RPMI 1640 supplemented with 50 ng/ml MMP-1 or MMP-3, 2 ml of RPMI 1640 supplemented with 50 ng/ml MMP-1 or MMP-3 and 400 ng/ml SDF-1. Control inserts were seeded with 3.0 x 10^5 cells/insert in 2ml of RPMI-1640 without HMEC-1. Transmigrated HL-60 cells were counted. Statistical significance is indicated as * $p<0.05$, ** $p<0.001$, *** $p<0.001$ and**** $p<0.0001$. Results are presented as average cell count transmigrated to the base of the well ± S.D. for n=3. Statistical analysis was done using one-way ANOVA test.

5.4.5.3 Angiomotin (AMOT) levels in HS-5 C.M. and HS-5 C.L.

HS-5 samples were prepared and treated with BEAM as described in section 2.6.2. Samples were prepared in four groups; untreated normoxia, untreated hypoxia, treated normoxia and treated hypoxia; each group contained three biological repeats. C.M. and cell lysate (C.L.) samples were then prepared and tested for AMOT by ELISA, as described in section 2.8. Detected concentrations of AMOT ranged from 0.2 ng/mL to just over 0.4 ng/mL as shown in Figure 5-20. The highest levels were observed in normoxic untreated C.L., and normoxic treated C.M. samples. For untreated samples, the AMOT might be getting sequestered within the cells in normoxic conditions, and may not be particularly increased in expression, whereas for BEAM treated samples, there appears to be similar levels for hypoxia for both medium and lysate, but AMOT may be released into the medium under BEAM treated normoxic conditions which is the opposite of untreated samples.

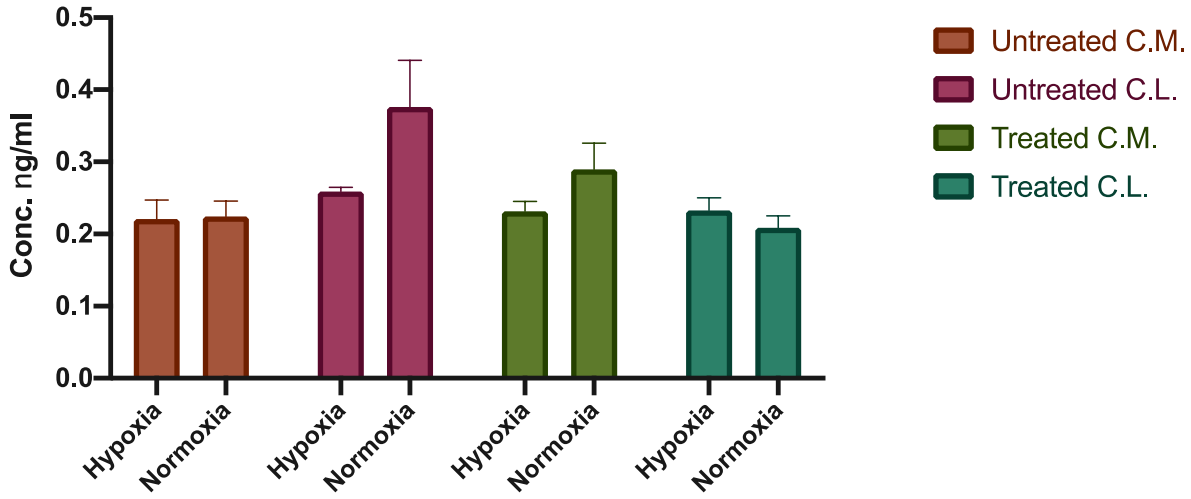

Figure 5-20 AMOT concentrations in HS-5 C.M. and corresponding C.L.

After treating HS-5 with chemotherapy (BEAM), media were then harvested, and the cells were trypsinised and resuspended in PBS to be lysed by ultrasonication 4 times (1 minute at 20kHz). Samples of C.M. and CL were tested by ELISA for AMOT concentration. Results are presented as average cell count ± S.D. for n=3.

5.4.5.4 AMOT affects the HMEC-1 membrane integrity

The HMEC-1 monolayer was established as described in section 2.3.4 in 12 well 8 µm pore inserts. Cells were seeded at 5.0 x 10^5 cells/cm^2 suspended in 1 mL MCDB 131. After 24 hours AMOT was added to the upper compartment of the inserts at different concentrations (0.2 to 1.0 ng/mL) as described in section 2.8. TEER was measured at different time points: 0-hour, 1 hour, 24 hours and 48 hours. A sharp drop of TEER values was observed after one hour at all concentrations compared to that with no AMOT added (Figure 5-21). This sharp drop was dose dependent, with the higher doses recovering more dramatically than the lower doses and exceeding the TEER of the control. However, TEER values started to recover when measured again after 24 and 48 hours at all concentrations to reach control levels or above. In HSCT settings, this effect might occur soon after conditioning, which might shorten the time before the barrier is back to normal and before the HSC are infused.

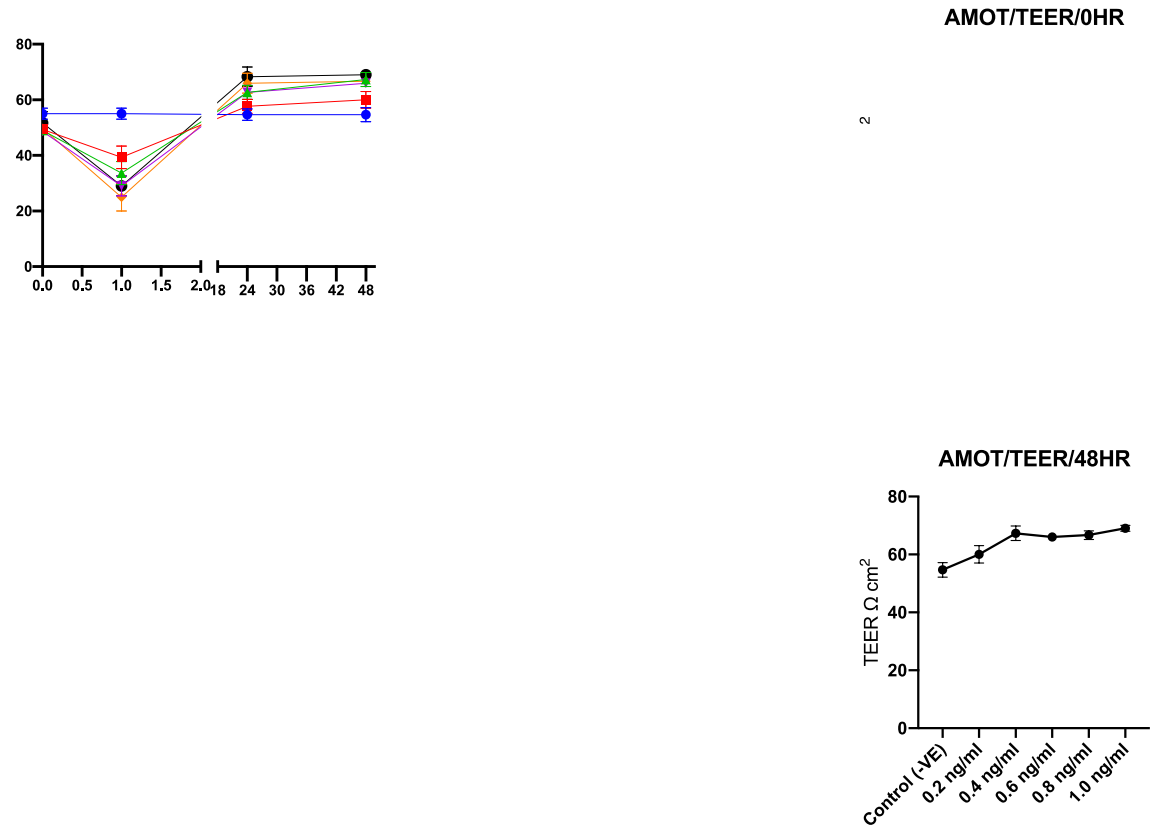

Figure 5-21 TEER measurements of HMEC-1 monolayer with MMP-3 at different concentrations.

HMEC-1 were seeded at 5.0 x 10^5 cells/cm^2 suspended in MCDB 131 in 12 well 8 µm pore inserts. After 24 hours AMOT was added to the upper compartment of each HMEC-1 insert at different concentrations: 0 ng/ml (control), 0.2 ng/ml, 0.4 ng/ml, 0.6 ng/ml, 0.8 ng/ml and 1.0 ng/ml. TEER was measured at different time points: 0 hour, 1 hour, 24 hours and 48 hours. Results are presented as average TEER value ± S.D. for n=3.

Recombinant AMOT was obtained in reduced glutathione (GSH) containing buffer, which might affect endothelial membrane integrity at high concentrations. To exclude the effect of GSH, TEER values were assessed after adding GSH only to the inserts in corresponding concentrations to that in the AMOT solution (Figure 5-22). TEER was evaluated every 2 hours to understand more about the sharp drop shown in the data above. GSH showed a slight change in the endothelial membrane resistance, which then recovered after 6 hours. A concentration dependant sharp drop of TEER value was observed after one hour, predominantly caused by AMOT, which lasted only for 8 hours then started to recover and reach control levels.

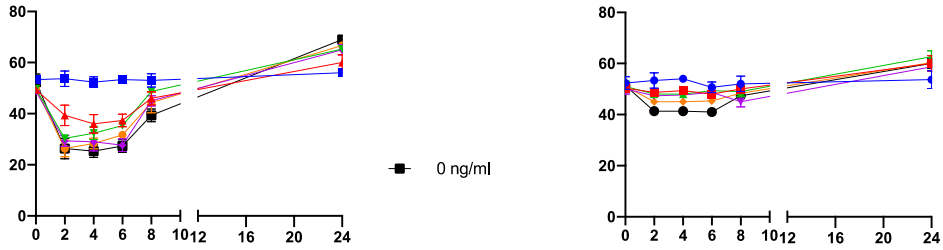

Figure 5-22 TEER measurements of HMEC-1 monolayer with AMOT and GSH at different concentrations.

HMEC-1 were seeded at 5.0 x 10^5 cells/cm^2 suspended in MCDB 131 in 12 well 8 µm pore inserts. After 24 hours AMOT and GSH were added to the upper compartment of the inserts at different concentrations. TEER was measured at different time points. Results are presented as average TEER value ± S.D. for n=3.

5.4.5.5 AMOT did not affect HL-60 transmigration

To study the effect of AMOT on HL-60 trafficking through the endothelium, AMOT was investigated in the transmigration model. AMOT did not show any significant increase in HL-60 trafficking by itself (Figure 5-23). Similarly, adding AMOT to HS-5 C.M. did not improve HL-60 trafficking when compared with C.M. without AMOT.

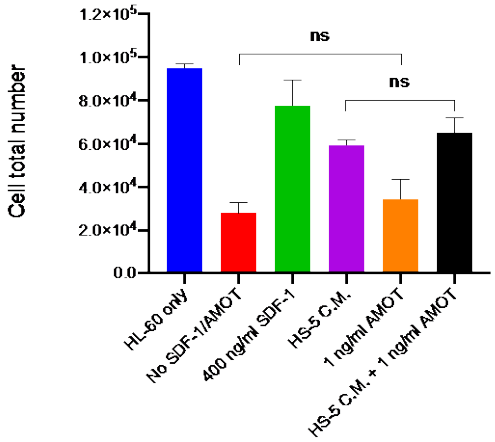

Figure 5-23 HL-60 transmigration with AMOT.

HL-60 were seeded at 3.0x 10^5 cells/insert in 8 µm pore inserts that contain a confluent layer of HMEC-1, 2 ml of RPMI 1640 were added to the lower compartments of the inserts supplemented as follows: RPMI 1640 only (No SDF-1 or AMOT), 400ng/ml SDF-1, 100% HS-5 C.M. (RPMI 1640), 1 ng/ml AMOT and 100% HS-5 C.M. containing 1 ng/ml AMOT. Control inserts were seeded with 3.0 x 10^5 cells/insert in 2ml of RPMI-1640 without HMEC-1. Transmigrated HL-60 cells

were counted. Results are presented as average cell count ± S.D. for n=3. Statistical analysis was done using one-way ANOVA test.

5.4.6 Immunocytochemistry and wound healing assay

To evaluate the effect of SDF-1α, MMP-1, MMP-3 and AMOT on the HMEC-1 endothelial monolayer, it has been theorised that they might act as specific inducers to activate and enhance the expression of adhesion molecules rather than to loosen the barrier. So, adhesion molecules like E and P selectin expression were explored for evidence of barrier activation and initiation of transmigration.

Cells were stained with human E-selectin (CD62E) and P-selectin (CD62P) antibody after exposing the endothelium to SDF-1α, MMP-1, MMP-3 and AMOT. E-selectin and P-selectin are known to be expressed by endothelial cells, and one or both are required for efficient homing of HSC to BM. Slides containing endothelial cells were prepared and stained, as described in section 2.9. Preconditioning of the endothelial membrane with SDF-1α for 24 hours showed an increased expression of both E and P selectin (Figure 5-24). This finding might be in line with what was observed before, of SDF-1α not affecting the barrier integrity; it instead induces the expression of adhesion molecules. In general, relative to the control, E and P selectins were raised in all treatments. Lower intensities of both E and P-selectin were observed for MMP-3 and AMOT preconditioned slides compared with SDF-1α. Conversely, the endothelial membrane showed elevated levels of P-selectin upon exposure to MMP-1, but neither selectin, and particularly E selectin, was not as raised for MMP1 as for the other treatments.

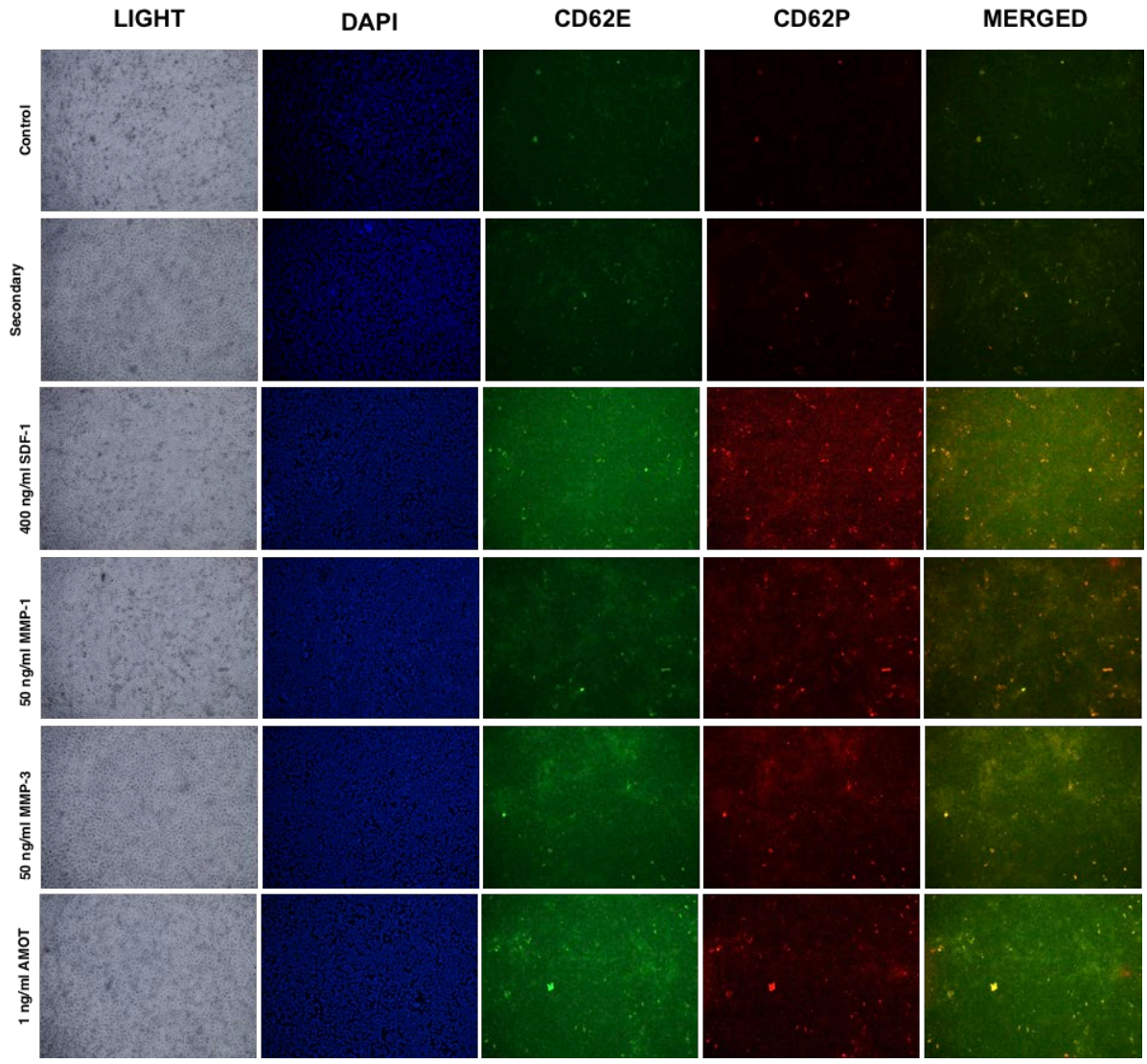

Figure 5-24 E & P-selectin expression on HMEC-1 upon preconditioning with SDF-1α, MMP-1, MMP-3 and AMOT.

HMEC-1 cells were allowed to spread on slides and then incubated with SDF-1α (400ng/mL), MMP-1 (50ng/ml), MMP-3 (50ng/mL) or AMOT (1ng/mL) using sterilised flexiPERM culture chambers for 24 hours, fixed with paraformaldehyde and immunostained with anti-CD62E and anti-CD62P antibodies followed by FITC-coupled (green) and texas red-coupled (red) secondary antibodies (red) and counterstained with DAPI. Images were acquired with a fluorescence microscope.

The wound-healing assay was done as described in section 2.10 and employed as a technique to investigate the effect of SDF-1α on HMEC-1 migration and formation of monolayers, which were monitored after 24 hours and 48 hours. SDF-1α was previously shown to not affect the TEER value of HMEC-1 as described in section 3.5.11. HMEC-1 were cultured with or without SDF-1α added to the culture medium

in order to determine the rate of migration into the scratched area (Figure 5-25). SDF-1α induced HMEC-1 cell migration to the area between the culture wells. SDF-1α showed strong chemotaxis of endothelial cells and promoted endothelialisation rather than hindered the endothelium.

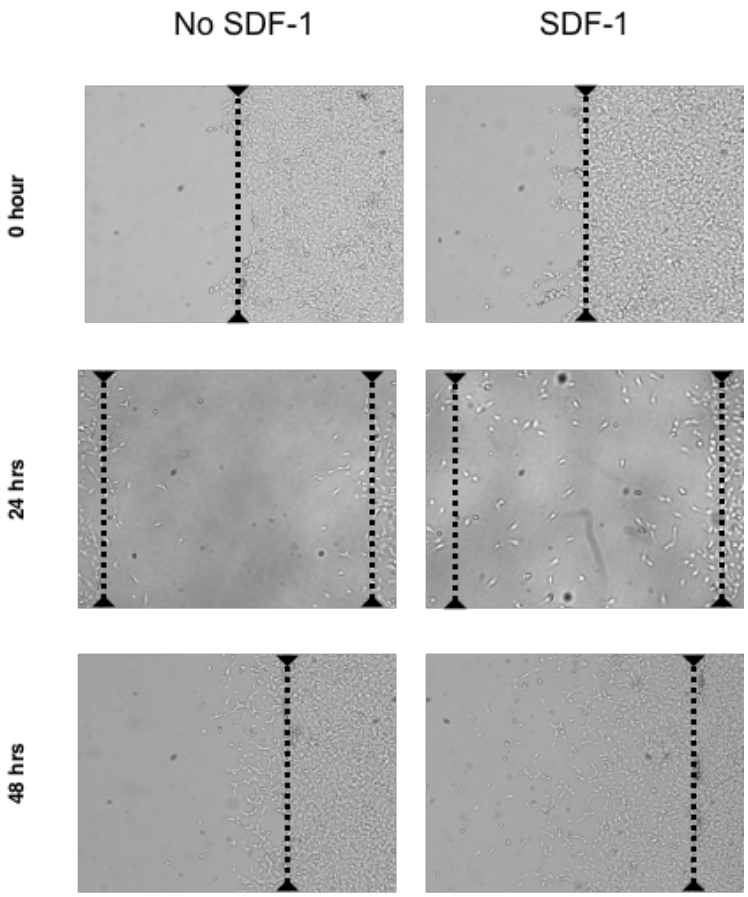

Figure 5-25 Wound healing assay of HMEC-1 with and without SDF-1.

HMEC-1 cells were seeded into sterilised flexiPERM culture chambers attached to slides at $2x10^5$ cells/cm^2; each well is approximately 0.7cm^2 and incubated in standard culture conditions. After 24 hours medium was replaced with fresh MCDB 131 supplemented with or without SDF-1α (400ng/mL). HMEC-1 cell migration to the area between the culture wells was monitored after 24hrs and 48 hrs. Dotted lines represent the borders of the culture wells.

5.5 Discussion

5.5.1 Differential secretome analysis of hypoxia vs normoxia HS-5 C.M.

LCMS/MS analysis was performed to identify differentially secreted proteins between untreated hypoxic HS-5 C.M. and untreated normoxic HS-5 C.M. Three C.M. samples

of each condition were analysed representing three biological repeats. Seven hundred and sixty-seven proteins were qualified after data filtering, of which 137 proteins were significantly changed. Out of these, 25 proteins were upregulated, and 112 proteins were downregulated in hypoxia. Particular focus was given to the upregulated proteins, listed in Table 5-1. Using this list as an input in the Panther platform showed that cellular processes, metabolic processes and biological regulation were enriched as biological processes associated with these proteins in the overall upregulated hypoxia proteome. These proteins originated from the extracellular space, protein-containing complex inside the cells, cell membrane and cellular organelles inside the cells. This observation might suggest that the release of these factors to the C.M. came as a response to hypoxia.

The STRING analysis of these factors indicated that 8 proteins have distinct functions and they were released particularly in response to hypoxia which includes: ADM, ANGPTL4, LOXL2, PLOD1, PLOD2, STC1, STC2 and VEGFA. This result came in line with the previous report by Hu *et al*., (2014). They demonstrated that LOXL2, VEGFA, SERPINE1, STC1 and ANGPTL4 were upregulated in severe hypoxia in MSCs. Half of these proteins were found to be regulating endothelial cell migration which includes: LOXL2, VEGFA, SERPINE1 and STC1 in addition to HMGB1 as indicated in this study. However, some of these proteins are linked to angiogenesis including ANXA2, LOXL2, SERPINE1 and VEGFA in addition to NCL and ANGPTL4 as indicated before.

ANXA2 is crucial for regulating HSCs homing and binding to the BM microenvironment as demonstrated by Jung *et al*., (2007) in an animal model. Also, VEGFA is essential for the survival of HSCs in the hypoxic BM niches, as shown by Rehn *et al*., (2011). Hypoxia is an essential component of the BM microenvironment and the HSCs niches, suggesting that release of these proteins as a response to hypoxia might play a role in the development and maintenance of the HSC niche.

5.5.2 Differential secretome analysis of BEAM treated hypoxia vs normoxia HS-5 C.M.

The second group of samples was BEAM treated, and LCMS/MS analysis was performed to identify differentially secreted proteins between BEAM treated hypoxic HS-5 C.M. and BEAM treated normoxic HS-5 C.M. Three C.M. samples were analysed for each of the two conditions (BEAM normoxia and BEAM hypoxia). After data filtering, 1661 proteins were identified, of which 1080 proteins were significantly changed, with 31 proteins upregulated and 1049 proteins downregulated in BEAM treated hypoxia. Cellular processes, metabolic processes and biological regulation were shown to be enriched in the overall upregulated proteome after Panther analysis. The origin of proteins was predominantly from cellular organelles inside the cells, extracellular region and cellular membrane.

The STRING analysis of these factors indicated that most of the proteins linked to stress, hypoxia, angiogenesis, localisation, cell migration, and vascular permeability as listed in Table 5-7. One of the key biological processes of interest is positive regulation of cell migration which linked to AMOT, CCL20, SERPINE1 and VEGFA. AMOT plays a central role in tight junctions and controls cell proliferation and migration of many cell types (Brunner *et al*., 2020).

CCL20 acts as a ligand for C-C chemokine receptor CCR6. Binding of CCL20 to CCR6 leads to activation and induction of a strong chemotactic response shown to induce T-cell migration (Armas-González *et al*., 2018). SERPINE1 also known as plasminogen activator inhibitor-1 (PAI-1) interacts with vitronectin (VN) to promote fibrinolysis and cell migration (Czekay *et al*., 2011). PAI-1 has been shown to promote the recruitment and polarisation of M2 monocytes/macrophages through different structural domains (Kubala *et al*., 2018).

The differentially upregulated proteins secreted by BEAM treated hypoxic HS-5 are primarily related to the HIF-1 signalling pathway, EGFR tyrosine kinase inhibitor resistance and the p53 signalling pathway including ENO2, SERPINE1, VEGFA and BAX. HS-5 might be releasing these factors as cellular stress responses due to exposure to chemotherapy and hypoxia. Cells respond to stress in several ways ranging from activation of pathways that support the cell's survival or to provoke programmed cell death that eliminates damaged cells (Fulda *et al*., 2010).

Based on the results of the proteins upregulated in the BEAM treated hypoxic samples, MMP-1 preproprotein variant was among the significantly upregulated proteins. However, MMP-1 was slightly upregulated in hypoxia and in BEAM treated hypoxic samples as previously shown in section 5.4.3. Conversely, MMP-1 alternative protein, MMP-2 MMP-3, MMP-14 and MMP-27 were downregulated in BEAM treated hypoxia samples.

Matrix metalloproteinases (MMPs) have been demonstrated to have complementary roles in developmental HSPC production and migration (Theodore *et al*., 2017). MMP-2 and MMP-9, for example were demonstrated to modulate processes critical to successful transplantation of HSPC (Shirvaikar, Marquez-Curtis and Janowska-Wieczorek, 2012; Liu *et al*., 2020)

5.5.3 Transmigration analysis of the candidate proteins

Based on the results of proteins upregulated in the BEAM treated hypoxia vs normoxia, a particular focus was given to proteins involved in endothelial cell function, proliferation and cell migration. MMP-1, MMP-3 and AMOT were selected for further testing and obtained in recombinant form to be tested in the transmigration model.

Both MMP-1 and MMP-3 were shown to affect the barrier integrity by loosening the endothelial membrane; additionally, MMP-1 was shown to have an extra role in inducing HL-60 trafficking actively. Conversely, AMOT was shown to affect the endothelium integrity without induction of HL-60 trafficking. However, both MMPs and AMOT were showed to have more potency in combination with SDF-1α.

MMP-1 is an interstitial collagenase which can cleave interstitial collagens I, II, III, VII and X as reviewed by Cawston (2013). MMP-3 is stromelysin-1 which can cleave type III, IV, VII, IX and X collagen, gelatin, elastin, laminin, proteoglycan core proteins, pro-MMP-1, and fibronectin (Nagase, Visse and Murphy, 2006). MMP-1 and MMP-3 are endopeptidases which can degrade various components of the extracellular matrix and basement membrane. However, reduction in TEER value after exposing the endothelial membrane to these peptidases might be attributed to loosening the interaction between the cells. In this study, MMP-1 showed potency to induce active transmigration without SDF-1, suggesting that it might have the ability to induce HL-60 trafficking. MMP-1 was shown to induce the migration of human BM-MSCs toward human glioma *in vivo* and *in vitro* as described by Ho *et al.* (2009; 2014). MMP-1 usually acts on protease-activated receptor 1 (PAR1) as a protease agonist, cleaving the PAR1 at the proper site to generate PAR1-dependent Ca^{2+} signals and migration in the cancer cell (Boire *et al*., 2005). In the BM, PAR1 signalling was shown to regulate the retention and recruitment of endothelial protein C receptor (EPCR)-expressing HSCs and enhance CXCL12-CXCR4-induced motility (Gur-Cohen *et al*., 2015). Therefore, MMP-1 might have a role to play in HSCs trafficking to the BM, exerted by proteolytic ability or through activation of signalling pathways which might need further investigation.

On the other hand, AMOT showed a dose-dependent sharp drop on TEER, which lasted for almost 8 hours; the higher doses recovered more dramatically than lower

doses and exceeded the TEER of the control. AMOT did not show a significant improvement in HL-60 transmigration across the barrier. AMOT is angiomotin which acts as a receptor for angiostatin that regulates endothelial cell migration and tube formation (Ernkvist *et al*., 2009; Troyanovsky *et al*., 2001). Despite its low expression in the BM (Moleirinho, Guerrant and Kissil, 2014), AMOT was differentially over-represented after treating HS-5 with BEAM in hypoxia, and it was not clear how it might be involved in HL-60 trafficking. However, it was shown to play a role in signalling pathways regulated by small G-proteins and the Hippo-YAP pathway which can modulate cell proliferation, differentiation, and migration (Moleirinho, Guerrant and Kissil, 2014).

Immunocytochemistry showed that exposing the HMEC-1 membrane to SDF-1α for 24 hours increased expression of both E and P selectin. This finding suggests that SDF-1α might not affect the barrier integrity, it rather induces the expression of adhesion molecules. Lower intensities of both E and P-selectin were observed for MMP-3 and AMOT preconditioned slides. However, the endothelial membrane showed increased expression of P-selectin upon exposure to MMP-1. SDF-1α was shown to upregulate E-selectin expression in the human microvascular endothelial cell (Liu *et al*., 2010; Liu *et al*., 2016).

5.6 Conclusion

This study has shown changes in a wide range of peptide-based chemokine signalling factors caused by hypoxia and chemotherapy exposure. Proteomics analysis of untreated normoxia vs hypoxia HS-5 C.M. showed that in hypoxia, 25 proteins were upregulated, predominantly related to stress and response to hypoxia. On the other hand, for BEAM treatment plus hypoxia, 31 proteins were upregulated, evidencing a secretome linked to stress, hypoxia, angiogenesis, localisation, cell migration and

vascular permeability. These findings suggest that conditioning therapy might be strongly involved in manipulating the vascular endothelium and facilitating HSCs trafficking. Some proteins like MMP-1 and MMP-3 were shown to affect the barrier integrity by loosening the endothelial membrane with high potency in combination with SDF-1α. Since all these factors were affected or upregulated in the BM after BEAM conditioning and hypoxia, a more complex picture of HSC homing has emerged involving several candidates, which might support homing through chemotactic and proteolytic activity, and in some situations activating cellular pathways. Aside from SDF-1α, other potential factors like MMP-1 might play a critical role that requires further investigation. In HSCT settings, the effects of these factors might occur soon after conditioning, which may be utilised to perform the transplant and infuse the HSCs.

Chapter 6 Final discussion

6.1 Summary of the findings

Engraftment is the process by which transplanted HSCs make their way to home to the BM niches where they can find optimal conditions to survive and proliferate to generate all haematopoietic cell subsets (Servais *et al*., 2013). The main important parameters of engraftment are neutrophil and platelet recovery; a patient needs to have an absolute neutrophil count of more than 500 x 10^6/L for the first three consecutive days, and a platelet count of more than 20,000/µL without transfusion support for seven successive days (Chang *et al*., 2009). The homing process relies on intracellular signalling and interaction between HSC and microvascular endothelium, mediated by chemokines, chemokine receptors, adhesion molecules, and proteases, all of which promote HSC adhesion and transmigration (Perlin, Sporrij and Zon, 2017). The general aims of this study were initially to develop an *in vitro* model for the BM microenvironment simulating the interactions between BM/blood vessel/HPCs as described in chapter 3. The model was then used to investigate the effect of chemotherapy and targeted therapy on the transmigration process after treating HS-5 as BM MSCs with standard doses in normoxia and hypoxia as shown in chapter 4. Finally, the proteins secreted by HS-5 post-chemotherapy treatment were investigated and some candidate proteins were examined in detail in the *in vitro* transmigration model as shown in chapter 5.

To address the aims of this study, an *in vitro* co-culture model of BM/blood vessel/HPCs was developed for investigating the effects of conditioning chemotherapy exposure on HPC trafficking. The primary step of building the co-culture model was to select a suitable endothelial barrier where cells can form a membrane of confluent cells in the culture inserts. Two cell lines were evaluated;

HUVEC and HMEC-1 in terms of proliferation rate, formation of suitable barrier and practicality of extended use. Both cell lines are well established and have been used in several studies as an endothelial model to investigate and characterise endothelial functionality. HUVEC is closely similar to the BM vasculature, but batches of HUVEC are heterogeneous since they are derived from different human beings. However, HMEC-1 proliferate faster and provide the required TEER measurement to create an endothelial barrier in a relatively shorter period of time (Ades *et al*., 1992). HMEC-1 demonstrate a suitable proliferation rate, morphological features and coverage of the insert after 24 hours from seeding at $5x10^5/cm^2$ as shown in section 3.5.1. SEM revealed that HMEC-1 cells had covered the pores of the insert and did not transmigrate through the insert, and the pores of the insert were small enough to hold the endothelial cells in the upper compartment. Here it was important that there was enough space within the inserts to allow for HMEC-1 cell growth over 24 hours yet also sufficient cells for making a confluent endothelium at certain time points. For HMEC-1, HS-5 and HL-60, proliferation rate and morphology were monitored in a range of culture media (F12K, MCDB 131, DMEM-HG and RPMI 1640) as required, to select the medium that best sustains all the cell types in the transmigration model, as each of these cell types have different requirements and supplements for their growth. Furthermore, MSC's CD markers were assessed for HS-5 (section 3.5.4). The initial setup of the transmigration model involved mixed culture medium; RPMI 1640 for HL-60, MCDB 131 for HMEC-1 and DMEM-HG for HS-5. Presence of more than one culture medium might interfere with the transmigration process by introducing extra variables to the assay environment. To reduce variables during the assay, a suitable medium might be selected to maintain all cell lines, especially for co-culture and treatment. RPMI 1640 was shown to be the best option for all cell types, although it is not commonly used to propagate endothelial cells. However, some researchers

have demonstrated that RPMI 1640 can support HMEC-1 growth and proliferation (Dodmane *et al*., 2015). The morphological characteristics and MSC's CD markers of HS-5 were unchanged in RPMI 1640, and the cells exhibited a fibroblast-like morphology. However, it was shown that HS-5 could lose some MSCs markers with extended passaging, such as CD73 and CD105 (section 3.5.4). A further step of optimisation was excluding any effects due to medium change to RPMI 1640 from the original medium of HMEC-1. This step was made to determine if the barrier was affected by changing media, washing or depletion of nutrients in the culture medium. The results showed that contents of the new medium are the reason for the variation on TEER measurement, especially during the first two hours. Therefore, inserts should be kept for at least two hours before adding HL-60 to stabilise the endothelial membrane. The overall settings of the transmigration model were concluded based on the previously mentioned results. It was possible to induce trafficking of HL-60 with SDF-1α, which appears to not compromise the endothelial membrane. Transmigration was possible without all three cell lines being in the same co-culture. The general approach was by maintaining each cell line separately in optimal conditions, HMEC-1 was grown as a layer in a cell culture insert, and the HL-60 cell line was added to the insert above the endothelial monolayer. C.M. from HS-5 was placed in the base of the culture well to induce transmigration.

This transmigration model is considered an *in vitro* two-dimensional (2D) cell co-culture system; it is highly reproducible and can be used for long-term assays and is easy to interpret due to its simplicity. However, 2D culture systems have many limitations, such as the disturbance of interactions between the cellular and extracellular environments, variations in cell morphology, and cell's polarity. Therefore, 2D models can't mimic the exact *in vivo* condition. However, the model developed in this study used multiple cell lines in the same environment, which might

overcome these issues to some extent and provide better cellular interactions and communications.

On the other hand, three-dimensional culture (3D) systems were developed to overcome the issues with 2D culture systems. According to Kapałczyńska *et al*. (2018), 3D models can be divided into three types depending on the mode of cell culture: suspension cultures on non-adherent plates, cultures in concentrated medium or gel-like substances and cultures on a scaffold. These culture systems provide a better environment for cells and proper interactions of cell-cell and cell-extracellular environment, and preserve the cell morphology and genes similar to an *in vivo* environment. Yet these 3D culture systems are associated with several disadvantages. It is challenging to extract cells for further analysis, especially for the scaffold and gel culture system. Furthermore, they are expensive and time-consuming compared to 2D systems (Kapałczyńska *et al*., 2018). One example of the advanced 3D culture systems is dynamic perfusion culture systems. In this system, the culture medium continually circulates through the cell retention device containing cell–polymer constructs made of a porous structure retained in a bioreactor. Cells are retained inside the retention device while fresh medium is added and products of interest and waste products are removed (Kurtis Kasper and Mikos, 2013).

Following the establishment of the transmigration model, chemotherapeutic agents currently used in the conditioning regimens of SCT were used to investigate their effects on HL-60 transmigration. This was addressed by treating HS-5 cells, cultured independently, with a standard dose of chemotherapy and then collecting the C.M. from HS-5 to be used in the transmigration model. To highlight the importance of hypoxia in the BM, all treatments and the subsequent transmigration investigations were conducted in both normoxia and hypoxia. The BM microenvironment contains a mixture of many different cell types, interacting with each other in hypoxic

conditions. It has been observed that the BM *in vivo* is a hypoxic environment (Chow *et al*., 2001; Parmar *et al*., 2007). This was an important aspect to investigate as many previous studies have not taken this into consideration.

Transmigration of HL-60 was first evaluated against SDF-1α and a range of HS-5 C.M. concentrations. The total cell counts of transmigrated HL-60 was affected significantly by the concentration gradient of HS-5 C.M.; higher transmigration rate was observed with a higher percentage of HS-5 C.M., this supports the idea that HS-5 can release chemotactic factors which can induce trafficking of HL-60. This result was in concordance with the HL-60 adhesion assay (chapter 3) in which HL-60 cells traffic towards HS-5 in the co-culture without endothelial cells. Furthermore, increasing transmigration, with increasing C.M. concentration, might indicate that chemoattractant signals from the BM is a localised effect within the vascular niches in which stem cell transmigration can occur.

Transmigration of HL-60 was also affected by induction of hypoxic conditions; maintaining HL-60 in hypoxia for 24 hours before adding to the transmigration model accelerated HL-60 transmigration across the endothelium in response to SDF-1α. Low oxygen concentration might induce high expression of the CXCR4 in different cell types including monocytes, monocyte-derived macrophages, tumour-associated macrophages, endothelial cells, and cancer cells, which is paralleled by increased chemotactic responsiveness to SDF-1 α (Schioppa *et al*., 2003). For HL-60, it is most likely that hypoxia does not affect the expression of CXCR4 as shown by Seo *et al*., in 2007. They demonstrated that CXCR4 transcription levels of HL-60 was neither significantly increased nor decreased under hypoxia and there was no decrease in the surface expression of CXCR4 in HL-60 cultured under 1 % O_2 for 24 hrs which might then affect migration of HL-60 cells toward SDF-1α. Seo's findings might contradict with our findings here of HL-60 response to hypoxia and enhanced transmigration,

however it is possible that other chemoattractants might also play an important role which are affected by hypoxia, but as yet unidentified. Conversely, a recent study by Mohammadali *et al*., (2018) showed that mild hypoxia with 5% O_2 tension has significantly increased CXCR4 gene expression of human cord blood CD34+ cells after seven days of incubation. Enhanced response to SDF-1α under hypoxia might not be directly related to HL-60 cells; instead it might be related to induced overexpression of adhesion molecules on the endothelium, and improved chemotaxis. The CXCR4/SDF-1 complex activates several pathways that mediate chemotaxis and migration (Umezawa *et al*., 2017). Its function is to promote homing and engraftment of CD34+ cells within the recipient BM as shown by Peled *et al*., (2000). SDF-1 transcription is partially controlled by hypoxia-inducible factor-1 (HIF-1), upregulated by hypoxia during vascular injury (Aiuti *et al*., 1997; Ceradini and Gurtner, 2005; Tu *et al*., 2016).

Preconditioning HS-5 independently with a range of conditioning therapy including melphalan, carmustine, etoposide and cytarabine (Ara-c) did not improve trafficking of HL-60 compared to the untreated HS-5 C.M.; only melphalan and Ara-c raised the trafficking slightly in hypoxia for the two hours treatment of HS-5, while for the 24 hours treatment, melphalan showed a significantly reduced trafficking. Reducing the intensity of the chemotherapeutic agents by 50% also did not affect trafficking; there was no increase in trafficking except with etoposide, which showed a slight increase of trafficking in normoxia. It is well known that these chemotherapeutic agents might induce injury to the stromal cells. Melphalan and Ara-C were demonstrated to affect the viability of both HS-5 and primary MSC when treated with a similar range of chemotherapy as described by Schmidmaier *et al*., (2006). However, in this study, HS-5 cells were treated with each of the chemotherapeutic agents independently, in an attempt to reduce cytotoxicity. Simulating the *in vivo* treatment with BEAM as

described in Table 1-3 might be difficult to accomplish in an *in vitro* model. It was suggested that molecules released due to this injury appear to have chemoattractant properties, yet it might also not be strong enough to induce transmigration in the current model. *In vitro* treatment conditions of cells are different from *in vivo* models which might affect the outcome in many ways. It is almost impossible to establish the same conditions as *in vivo*, due to variations in the timelines of conditioning therapy, consideration about the *in vivo* metabolism, consideration of the half-life of the drugs, and also about the bioavailable portion of the drugs (i.e. some will bind to proteins).

A better understanding of these novel molecules will help to understand the possible effects of these treatments and also improve the outcome for patients who undergo SCT.

Treating HS-5 with targeted therapies like imatinib and ibrutinib showed different results; imatinib improved transmigration of HL-60 in normoxia while ibrutinib was more effective in hypoxia, and also in normoxia after increasing the dose by 100%. Imatinib and ibrutinib are tyrosine kinase inhibitors that, respectively, target the BCR-ABL1 fusion protein (O'Brien *et al*., 2003) and the Bruton's tyrosine kinase (BTK) (Byrd *et al*., 2015). However, in the current model, HS-5 is the only compartment treated with these targeted therapies, and it is not clear how HS-5 metabolised imatinib and ibrutinib.

Further attempts to explore the nature of the chemoattractant molecules released by HS-5 post-chemotherapy treatment was by inhibiting the biosynthesis of proteins and phospholipids by CHX and aspirin, respectively. Inhibiting protein biosynthesis was shown as a potent inhibitor of HL-60 transmigration. Treating HS-5 with CHX inhibits protein biosynthesis significantly in a concentration-dependent manner, and subsequently, C.M. produced from these HS-5 were effective at reducing HL-60 transmigration in the model, suggesting that the majority of the chemotactic factors

released by HS-5 are, or are signalled by, peptide-based chemokines. Similarly, inhibition of biosynthesis of bioactive phosphosphingolipids by aspirin showed a significant inhibition of HL-60 transmigration. This suggests that both types of molecules may work in concert to effect transmigration and that perhaps more attention should be paid to the role of phospholipids.

To explore the peptide-based chemokine signalling factors released by HS-5 post-chemotherapy exposure, proteomics analysis was conducted for the HS-5 C.M. after treating the cells with a combination of conditioning therapy (BEAM). Samples were tested in two groups; untreated and treated, and each group of samples were prepared in normoxia and hypoxia. Results were obtained as protein relative abundance in each sample, and for the first group of samples (untreated hypoxia vs normoxia), 767 proteins were identified after filtration; of these 137 proteins were significantly changed, 25 proteins were upregulated and 112 proteins were downregulated in hypoxia. Within the second group of samples (BEAM treated hypoxia vs normoxia), 1661 proteins were identified, of which 1080 proteins were significantly changed, with 31 proteins upregulated and 1049 proteins downregulated in hypoxia.

To determine the common proteins to the two groups of samples, the proteome of the untreated C.M. were matched with BEAM treated group C.M. using the Perseus software. Five hundred and nineteen proteins were common to the two sample groups. Eleven proteins were upregulated in hypoxia, and 15 proteins were upregulated with BEAM and hypoxia. Further analysis of only upregulated extracellular and membrane proteins was performed. For example, MMP-1 and MMP-3 were common in all samples. MMP-1 was slightly upregulated in hypoxia while MMP-3 was downregulated in BEAM treated hypoxia samples relative to BEAM normoxia samples, although it followed the general trends for the common proteins.

Another example of a membrane related protein is AMOT, which was significantly upregulated in BEAM treated hypoxia samples. These three proteins were selected for further investigation and obtained as a recombinant protein and tested in the transmigration model. MMP-1 and MMP-3 reduced TEER values and affected membrane integrity, and subsequently, induced trafficking of HL-60, especially in combination with SDF-1α. MMP-1 was shown to have an extra role in inducing HL-60 trafficking actively. Conversely, AMOT did not show any significant increase in HL-60 trafficking by itself; only when used in combination with HS-5 C.M. was HL-60 trafficking improved.

The effect of SDF-1α, MMP-1, MMP-3 and AMOT on the HMEC-1 endothelial monolayer was investigated; cells were assessed in terms of E-selectin (CD62E) and P-selectin (CD62P) expression by immunocytochemistry after exposing the endothelium to the recombinant proteins. E-selectin and P-selectin are known to be expressed by endothelial cells, and one or both are required for efficient homing of HSCs to BM. SDF-1α showed increased expression of both E & P selectin. Conversely, the endothelial membrane showed an elevated level of P-selectin only, upon exposure to MMP-1. Lower intensities of both E- and P-selectin were observed in MMP-3 and AMOT preconditioned slides. Moreover, SDF-1α showed strong chemotaxis for endothelial cells in the wound-healing assay, which was employed as a technique to determine the migration capacity of HMEC-1.

6.2 Limitations of the study

It is important to indicate that this study has limitations which may have had an impact on the results. It has predominantly been undertaken with the use of immortalised cell lines. All cells types used in the development of the transmigration model were immortalised cell lines. It might be more relevant if primary cells from a healthy individual were used. For example, primary CD34+ cells from umbilical cord

blood or peripheral blood might provide more insight into the stem cells' trafficking. Nonetheless, it might be possible to highlight the effect of hypoxia on response to chemotactic signalling (Mantel *et al*., 2015). Moreover, some other endothelial cells might provide a suitable barrier, like human bone marrow microvascular endothelial cell (BMEC) (Rafii *et al*., 1994) and the immortalised version (BMEC-1) with primary cell characteristics (Candal *et al*., 1996). However, primary cells might be difficult to maintain, take a longer time to grow and have passage limitations, therefore, further optimisation of this model might be required. This study has looked at the effects of conditioning chemotherapy (BEAM) and targeted therapies on the stromal cell line HS-5 in an attempt to understand the possible chemoattractant signals produced by the BM that might induce HPC trafficking. In order to increase the clinical relevance of the co-culture model, it was tested in normoxic and hypoxic conditions.

Additionally, this study has looked at the peptide-based chemokine signalling factors released by HS-5 post-chemotherapy exposure in normoxia and hypoxia through proteomics analysis. It might be useful to investigate other elements influencing homing of HSCs to the BM including some bioactive lipids. This study has demonstrated that inhibition of lipid biosynthesis leads to inhibition of HL-60 transmigration. Bioactive lipids like S1P and C1P are known to induce homing of HSCs (Kim *et al*., 2012).

6.3 Future directions

This study provides a basis for building a reproducible transmigration model simulating the BM microenvironment involving interaction of multiple cells. There is much scope to explore other cell lines and primary cells, like primary BM MSCs, BMEC and CD34+ cells. With suitable ethical approval and further optimisation, other primary cells might be investigated.

This study provides some novel findings and an interesting basis for further research. The results described here highlight the role of BM MSCs in the BM microenvironment. Proteomics analysis of HS-5 provides several potential candidate proteins like vascular endothelial growth factor A (VEGFA) and C-C motif chemokine 20 (CCL20). VEGFA mediates the differentiation of endothelial cells (Ge *et al*., 2018), and CCL20 mediates homing of mesenchymal stromal cells to the site of injury (Kallmeyer and Pepper, 2015; Honczarenko *et al*., 2006). With additional time and funding, there is much scope to expand the investigation in this area. Many other conditioning therapy chemotherapeutic combinations might also be investigated within this *in vitro* transmigration model with a range of MMPs and cytokines implicated in HSCs trafficking as well as other candidate molecules detected. Indeed, it may be possible to identify key cross-reactivity between chemoattractant molecules and determine which therapies are most effective in inducing this trafficking. Such understanding might eventually be exploited in future therapies.

6.4 Conclusion

This study was conducted to achieve four main aims. Firstly, to establish an *in vitro* model of the BM/endothelium/HPCs interface. Secondly, to measure the capacity of HPCs to traffic through the endothelium in the *in vitro* model with and without conditioning therapy, under normoxic and hypoxic conditions. Thirdly, to determine the release of novel homing factors under normoxic versus hypoxic conditions. Finally, to measure the expression of surface adhesion molecules on the endothelium after exposure to identified homing factors. The general goal of this study was to aid in the understanding of the molecular processes that might improve the engraftment of HSCs and reduce the toxicity of chemotherapy.

It was hypothesised that chemotherapy is important for HSCT to induce engraftment; it usually induces BM injury leading to release of homing factors like that seen under ischaemic conditions. It will be possible to identify and then induce these novel messengers using novel therapies to improve the outcome of HSCT, through promoting higher engraftment but lower toxicity.

In this study, a multicellular *in vitro* transmigration model was developed to provide a further understanding of the cellular communication in the BM microenvironment. Here it has been demonstrated that SDF-1α can induce transmigration of HPCs HL-60 through the HMEC-1 monolayer. C.M. produced from chemotherapy-treated HS-5 did not improve HL-60 trafficking; conversely, targeted therapies showed some improvement.

While SDF-1α remains the most effective known inducer for HSCs trafficking, this work indicates some other possible candidates released by stromal cells in the BM. Here it has been demonstrated that MMP-1 and MMP-3 might play a role in HSCs/HPCs trafficking through the endothelium. This study has demonstrated that MMP-1 and MMP-3 were able to improve the transmigration of HL-60; additionally, transmigration was higher in combination with SDF-1α. HSC homing is a multi-step process controlled by several factors, not only chemokines such as SDF-1α.

References:

Adamiak, M., Borkowska, S., Wysoczynski, M., Suszynska, M., Kucia, M., Rokosh, G., Abdel-Latif, A., Ratajczak, J. and Ratajczak, M.Z. (2015) Evidence for the involvement of sphingosine-1-phosphate in the homing and engraftment of hematopoietic stem cells to bone marrow. *Oncotarget* [online]. 6 (22), pp.18819-18828.

Ades, E.W., Candal, F.J., Swerlick, R.A., George, V.G., Summers, S., Bosse, D.C. and Lawley, T.J. (1992) HMEC-1: establishment of an immortalized human microvascular endothelial cell line. *The Journal of Investigative Dermatology* [online]. 99 (6), pp.683-690.

Ahmadzadeh, A., Kast, R.E., Ketabchi, N., Shahrabi, S., Shahjahani, M., Jaseb, K. and Saki, N. (2015) Regulatory effect of chemokines in bone marrow niche. *Cell and Tissue Research* [online]. 361 (2), pp.401-410.

Aiuti, A., Webb, I.J., Bleul, C., Springer, T. and Gutierrez-Ramos, J. (1997) The chemokine SDF-1 is a chemoattractant for human CD34+ hematopoietic progenitor cells and provides a new mechanism to explain the mobilization of CD34+ progenitors to peripheral blood. *The Journal of Experimental Medicine* [online]. 185 (1), pp.111-120.

Alfonso, L., Ai, G., Spitale, R.C. and Bhat, G.J. (2014) Molecular targets of aspirin and cancer prevention. *British Journal of Cancer* [online]. 111 (1), pp.61-67.

Al-Sowayan, B., Keogh, R.J., Abumaree, M., Georgiou, H.M. and Kalionis, B. (2017) The effect of endothelial cell activation and hypoxia on placental chorionic mesenchymal stem/stromal cell migration. *Placenta* [online]. 59 pp.131-138.

Anderson P, Carrillo-Gálvez AB, García-Pérez A, Cobo M, Martín F. (2013) CD105 (Endoglin)-Negative Murine Mesenchymal Stromal Cells Define a New Multipotent Subpopulation with Distinct Differentiation and Immunomodulatory Capacities. *Plos One* [online]. 8 (10). doi: 10.1371/journal.pone.0076979

Arai, F., Hirao, A., Ohmura, M., Sato, H., Matsuoka, S., Takubo, K., Ito, K., Koh, G.Y. and Suda, T. (2004) Tie2/angiopoietin-1 signaling regulates hematopoietic stem cell quiescence in the bone marrow niche. *Cell* [online]. 118 (2), pp.149-161.

Armas-González, E., Domínguez-Luis, M.J., Díaz-Martín, A., Arce-Franco, M., Castro-Hernández, J., Danelon, G., Hernández-Hernández, V., Bustabad-Reyes, S., Cantabrana, A., Uguccioni, M. and Díaz-González, F. (2018) Role of CXCL13 and CCL20 in the recruitment of B cells to inflammatory foci in chronic arthritis. *Arthritis Research & Therapy* [online]. 20 (1). doi:10.1186/s13075-018-1611-2.

Asada, N., Takeishi, S. and Frenette, P.S. (2017) Complexity of bone marrow hematopoietic stem cell niche. *International Journal of Hematology* [online]. 106 (1), pp.45-54.

Asri, A., Sabour, J., Atashi, A. and Soleimani, M. (2016) Homing in hematopoietic stem cells: focus on regulatory role of CXCR7 on SDF1a/CXCR4 axis. *EXCLI Journal* [online]. 15 pp.134-143.

Atilla, E., Ataca Atilla, P. and Demirer, T. (2017) A Review of Myeloablative vs Reduced Intensity/Non-Myeloablative Regimens in Allogeneic Hematopoietic Stem Cell Transplantations. *Balkan Medical Journal* [online]. 34 (1), pp.1-9.

Avraham, H., Banu, N., Scadden, D.T., Abraham, J. and Groopman, J.E. (1994) Modulation of megakaryocytopoiesis by human basic fibroblast growth factor. *Blood* [online]. 83 (8), pp.2126-2132.

Barrett, A.J. and Savani, B.N. (2006) Stem cell transplantation with reduced-intensity conditioning regimens: a review of ten years experience with new transplant concepts and new therapeutic agents. *Leukemia* [online]. 20 (10), pp.1661-1672.

Barry, F., Boynton, R., Murphy, M. and Zaia, J. (2001) The SH-3 and SH-4 Antibodies Recognize Distinct Epitopes on CD73 from Human Mesenchymal Stem Cells. *Biochemical and Biophysical Research Communications* [online]. 289(2), pp. 519-524.

Beaulieu, A., Poncin, G., Belaid-Choucair, Z., Humblet, C., Bogdanovic, G., Lognay, G., Boniver, J. and Defresne, M.P. (2011) Leptin reverts pro-apoptotic and antiproliferative effects of alpha-linolenic

acids in BCR-ABL positive leukemic cells: involvement of PI3K pathway. *PloS One* [online]. 6 (10). doi: 10.1371/journal.pone.0025651.

Beauregard, P. and Blajchman, M.A. (1994) Hemolytic and pseudo-hemolytic transfusion reactions: an overview of the hemolytic transfusion reactions and the clinical conditions that mimic them. *Transfusion Medicine Reviews* [online]. 8 (3), pp.184-199.

Befani, C. and Liakos, P. (2017) Hypoxia upregulates integrin gene expression in microvascular endothelial cells and promotes their migration and capillary-like tube formation. *Cell Biology International* [online]. 41 (7), pp.769-778.

Belluschi, S., Calderbank, E.F., Ciaurro, V., Pijuan-Sala, B., Santoro, A., Mende, N., Diamanti, E., Sham, K.Y.C., Wang, X., Lau, W.W.Y., Jawaid, W., Göttgens, B. and Laurenti, E. (2018) Myelo-lymphoid lineage restriction occurs in the human haematopoietic stem cell compartment before lymphoid-primed multipotent progenitors. *Nature Communications* [online]. 9 (1). Doi:10.1038/s41467-018-06442-4.

Blume, L.F., Denker, M., Gieseler, F. and Kunze, T. (2010) Temperature corrected transepithelial electrical resistance (TEER) measurement to quantify rapid changes in paracellular permeability. *Die Pharmazie* [online]. 65 (1), pp.19-24.

Boire, A., Covic, L., Agarwal, A., Jacques, S., Sherifi, S. and Kuliopulos, A. (2005) PAR1 Is a Matrix Metalloprotease-1 Receptor that Promotes Invasion and Tumorigenesis of Breast Cancer Cells. *Cell* [online]. 120 (3), pp.303-313.

Boyden, S. (1962) The chemotactic effect of mixtures of antibody and antigen on polymorphonuclear leucocytes. *The Journal of Experimental Medicine* [online]. 115 pp.453-466.

Brunner, P., Hastar, N., Kaehler, C., Burdzinski, W., Jatzlau, J. and Knaus, P. (2020) AMOT130 drives BMP-SMAD signaling at the apical membrane in polarized cells. *Molecular Biology of the Cell* [online]. 31 (2), pp.118-130.

Buffone, A., Anderson, N.R. and Hammer, D.A. (2018) Migration against the direction of flow is LFA-1-dependent in human hematopoietic stem and progenitor cells. *Journal of Cell Science* [online]. 131 (1). doi:10.1242/jcs.205575.

Byrd, J.C., Furman, R.R., Coutre, S.E., Burger, J.A., Blum, K.A., Coleman, M., Wierda, W.G., Jones, J.A., Zhao, W., Heerema, N.A., Johnson, A.J., Shaw, Y., Bilotti, E., Zhou, C., James, D.F. and O'Brien, S. (2015) Three-year follow-up of treatment-naive and previously treated patients with CLL and SLL receiving single-agent ibrutinib. *Blood* [online]. 125 (16), pp.2497-2506.

Callahan, M.K., Williams, K.A., Kivisäkk, P., Pearce, D., Stins, M.F. and Ransohoff, R.M. (2004) CXCR3 marks CD4+ memory T lymphocytes that are competent to migrate across a human brain microvascular endothelial cell layer. *Journal of Neuroimmunology* [online]. 153 (1–2), pp.150-157.

Campioni, D., Lanza, F., Moretti, S., Dominici, M., Punturieri, M., Pauli, S., Hofinann, T., Horwitz, E. and Castoldi, G.L. (2003) Functional and immunophenotypic characteristics of isolated CD105+ and fibroblast+ stromal cells from AML: implications for their plasticity along endothelial lineage. *Cytotherapy* [online]. 5 (1), pp.66-79.

Candal, F.J., Rafii, S., Parker, J.T., Ades, E.W., Ferris, B., Nachman, R.L. and Kellar, K.L. (1996) BMEC-1: a human bone marrow microvascular endothelial cell line with primary cell characteristics. *Microvascular Research* [online]. 52 (3), pp.221-234.

Cawston, T. E. (2013) Chapter 152 - Matrix Metallopeptidase-1/Interstitial Collagenase. *Handbook of Proteolytic Enzymes* (Third Edition) [online]. pp.718-725.

Ceradini, D. J. and Gurtner, G. C. (2005) Homing to Hypoxia: HIF-1 as a Mediator of Progenitor Cell Recruitment to Injured Tissue. *Trends in Cardiovascular Medicine* [online]. 15(2), pp.57-63.

Chang, C., Hale, S.J., Cox, C.V., Blair, A., Kronsteiner, B., Grabowska, R., Zhang, Y., Cook, D., Khoo, C.P., Schrader, J.B., Kabuga, S.B., Martin-Rendon, E. and Watt, S.M. (2016) Junctional Adhesion Molecule-A Is Highly Expressed on Human Hematopoietic Repopulating Cells and Associates with the Key Hematopoietic Chemokine Receptor CXCR4. *Stem Cells* [online]. 34 (6), pp.1664-1678.

Chang, Y., Xu, L., Liu, D., Liu, K., Han, W., Chen, Y., Yu-Wang, Chen, H., Wang, J., Zhang, X., Zhao, X. and Huang, X. (2009) Platelet Engraftment in Patients with Hematologic Malignancies following Unmanipulated Haploidentical Blood and Marrow Transplantation: Effects of CD34+ Cell Dose and Disease Status. *Biology of Blood and Marrow Transplantation* [online]. 15 (5), pp.632-638.

Chen, L.S., Bose, P., Cruz, N.D., Jiang, Y., Wu, Q., Thompson, P.A., Feng, S., Kroll, M.H., Qiao, W., Huang, X., Jain, N., Wierda, W.G., Keating, M.J. and Gandhi, V. (2018) A pilot study of lower doses of ibrutinib in patients with chronic lymphocytic leukemia. *Blood* [online]. 132 (21), pp.2249-2259.

Chen, P., Huang, H., Wu, J., Lu, R., Wu, Y., Jiang, X., Yuan, Q. and Chen, Y. (2015) Bone marrow stromal cells protect acute myeloid leukemia cells from anti-CD44 therapy partly through regulating PI3K/Akt-p27(Kip1) axis. *Molecular Carcinogenesis* [online]. 54 (12), pp.1678-1685.

Chow, D.C., Wenning, L.A., Miller, W.M. and Papoutsakis, E.T. (2001) Modeling pO(2) distributions in the bone marrow hematopoietic compartment. I. Krogh's model. *Biophysical Journal* [online]. 81 (2), pp.675-684.

Chute, J.P., Muramoto, G.G., Salter, A.B., Meadows, S.K., Rickman, D.W., Chen, B., Himburg, H.A. and Chao, N.J. (2007) Transplantation of vascular endothelial cells mediates the hematopoietic recovery and survival of lethally irradiated mice. *Blood* [online]. 109 (6), pp.2365-2372.

Cismowski, M.J. (2007) Imatinib. In: Enna, S.J. and Bylund, D.B., eds. (2007) xPharm: The *Comprehensive Pharmacology Reference* [online]. New York: Elsevier, pp.1-7.

Claude Gorin, N. (2016) Autologous stem cell transplantation versus alternative allogeneic donor transplants in adult acute leukemias. *Seminars in Hematology* [online]. 53 (2), pp.103-110.

Cohn, C.S. (2015) Transfusion support issues in hematopoietic stem cell transplantation. Cancer Control: *Journal of the Moffitt Cancer Center* [online]. 22 (1), pp.52-59.

Colvin, G.A., Lambert, J., Dooner, M.S., Cerny, J. and Quesenberry, P.J. (2007) Murine allogeneic in vivo stem cell homing. *Journal of Cellular Physiology* [online]. 211 (2), pp.386-391.

Courties, G., Herisson, F., Sager, H.B., Heidt, T., Ye, Y., Wei, Y., Sun, Y., Severe, N., Dutta, P., Scharff, J., Scadden, D.T., Weissleder, R., Swirski, F.K., Moskowitz, M.A. and Nahrendorf, M. (2015) Ischemic stroke activates hematopoietic bone marrow stem cells. *Circulation Research* [online]. 116 (3), pp.407-417.

Czeiger, D., Dukhno, O., Douvdevani, A., Porat, Y., Shimoni, D., Fulga, V., Ament, J.D. and Shaked, G. (2011) Transient Extremity Ischemia Augments CD34+ Progenitor Cell Availability. *Stem Cell Reviews and Reports* [online]. 7 (3), pp.639-645.

Czekay, R., Wilkins-Port, C., Higgins, S.P., Freytag, J., Overstreet, J.M., Klein, R.M., Higgins, C.E., Samarakoon, R. and Higgins, P.J. (2011) PAI-1: An Integrator of Cell Signaling and Migration. *International Journal of Cell Biology* [online]. 2011. doi: 10.1155/2011/562481.

Denning-Kendall, P., Singha, S., Bradley, B. and Hows, J. (2003) Cytokine expansion culture of cord blood CD34+ cells induces marked and sustained changes in adhesion receptor and CXCR4 expressions. *Stem Cells* (Dayton, Ohio) [online]. 21 (1), pp.61-70.

Deininger, M.W.N. and Druker, B.J. (2003) Specific Targeted Therapy of Chronic Myelogenous Leukemia with Imatinib. *Pharmacological Reviews* [online]. 55 (3), pp.401-423.

Di Virgilio, F., Chiozzi, P., Ferrari, D., Falzoni, S., Sanz, J.M., Morelli, A., Torboli, M., Bolognesi, G. and Baricordi, O.R. (2001) Nucleotide receptors: an emerging family of regulatory molecules in blood cells. *Blood* [online]. 97 (3), pp.587-600.

Ding, L., Saunders, T.L., Enikolopov, G. and Morrison, S.J. (2012) Endothelial and perivascular cells maintain haematopoietic stem cells. *Nature* [online]. 481 (7382), pp.457-462.

Dodmane, P. R., Arnold, L. L., Pennington, K. L., Singh, R. K., Cardoso, A. P. F. and Cohen, S. M. (2015) Effect of trivalent arsenicals on cell proliferation in mouse and human microvascular endothelial cells. *Toxicology Reports* [online]. 2, pp. 833-837.

Dominici, M., Le Blanc, K., Mueller, I., Slaper-Cortenbach, I., Marini, F., Krause, D., Deans, R., Keating, A., Prockop, D. and Horwitz, E. (2006) Minimal criteria for defining multipotent mesenchymal

stromal cells. The International Society for Cellular Therapy position statement. *Cytotherapy* [online]. 8 (4), pp.315-317.

Drukala, J., Paczkowska, E., Kucia, M., Mlynska, E., Krajewski, A., Machalinski, B., Madeja, Z. and Ratajczak, M.Z. (2012) Stem cells, including a population of very small embryonic-like stem cells, are mobilized into peripheral blood in patients after skin burn injury. *Stem Cell Reviews and Reports* [online]. 8 (1), pp.184-194.

Ebrahim, N.A. and Leach, L. (2015) Temporal studies into attachment, VE-cadherin perturbation, and paracellular migration of human umbilical mesenchymal stem cells across umbilical vein endothelial monolayers. *Stem Cells and Development* [online]. 24 (4), pp.426-436.

Ernkvist, M., Luna Persson, N., Audebert, S., Lecine, P., Sinha, I., Liu, M., Schlueter, M., Horowitz, A., Aase, K., Weide, T., Borg, J.P., Majumdar, A. and Holmgren, L. (2009) The Amot/Patj/Syx signaling complex spatially controls RhoA GTPase activity in migrating endothelial cells. *Blood* [online]. 113 (1), pp.244-253.

Ferruzza, S., Rossi, C., Sambuy, Y. and Scarino, M.L. (2013) Serum-reduced and serum-free media for differentiation of Caco-2 cells. *Altex* [online]. 30 (2), pp.159-168.

Fischer, L.J., McIlhenny, S., Tulenko, T., Golesorkhi, N., Zhang, P., Larson, R., Lombardi, J., Shapiro, I. and DiMuzio, P.J. (2009) Endothelial Differentiation of Adipose-Derived Stem Cells: Effects of Endothelial Cell Growth Supplement and Shear Force. *Journal of Surgical Research* [online]. 152 (1), pp.157-166.

Fukuda, K., Koshihara, Y., Oda, H., Ohyama, M. and Ooyama, T. (1988) Type V collagen selectively inhibits human endothelial cell proliferation. *Biochemical and Biophysical Research Communications* [online]. 151 (3), pp.1060-1068.

Fulda, S., Gorman, A.M., Hori, O. and Samali, A. (2010) Cellular Stress Responses: Cell Survival and Cell Death. *International Journal of Cell Biology* [online]. 2010. Doi: 10.1155/2010/214074.

Gallagher, R., Collins, S., Trujillo, J., McCredie, K., Ahearn, M., Tsai, S., Metzgar, R., Aulakh, G., Ting, R., Ruscetti, F. and Gallo, R. (1979) Characterization of the continuous, differentiating myeloid cell line (HL-60) from a patient with acute promyelocytic leukemia. *Blood* [online]. 54 (3), pp.713-733.

Ganguly, A., Zhang, H., Sharma, R., Parsons, S. and Patel, K.D. (2012) Isolation of human umbilical vein endothelial cells and their use in the study of neutrophil transmigration under flow conditions. *Journal of Visualized Experiments*, 66 (e4032). doi: 10.3791/4032.

Garrido, S.M., Appelbaum, F.R., Willman, C.L. and Banker, D.E. (2001) Acute myeloid leukemia cells are protected from spontaneous and drug-induced apoptosis by direct contact with a human bone marrow stromal cell line (HS-5). *Experimental Hematology* [online]. 29 (4), pp.448-457.

Ge, Q., Zhang, H., Hou, J., Wan, L., Cheng, W., Wang, X., Dong, D., Chen, C., Xia, J., Guo, J., Chen, X. and Wu, X. (2018) VEGF secreted by mesenchymal stem cells mediates the differentiation of endothelial progenitor cells into endothelial cells via paracrine mechanisms. *Molecular Medicine Reports* [online]. 17 (1), pp.1667-1675.

Georgiou, K.R., Foster, B.K. and Xian, C.J. (2010) Damage and recovery of the bone marrow microenvironment induced by cancer chemotherapy - potential regulatory role of chemokine CXCL12/receptor CXCR4 signalling. *Current Molecular Medicine* [online]. 10 (5), pp.440-453.

Giralt, S., Ballen, K., Rizzo, D., Bacigalupo, A., Horowitz, M., Pasquini, M. and Sandmaier, B. (2009) Reduced-intensity conditioning regimen workshop: defining the dose spectrum. Report of a workshop convened by the center for international blood and marrow transplant research. Biology of Blood and Marrow Transplantation: *Journal of the American Society for Blood and Marrow Transplantation* [online]. 15 (3), pp.367-369.

Guo, Y.L., Bai, R., Chen, C.X., Liu, D.Q., Liu, Y., Zhang, C.Y. and Zen, K. (2009) Role of junctional adhesion molecule-like protein in mediating monocyte transendothelial migration. *Arteriosclerosis, Thrombosis, and Vascular Biology* [online]. 29 (1), pp.75-83.

Gur-Cohen, S., Itkin, T., Chakrabarty, S., Graf, C., Kollet, O., Ludin, A., Golan, K., Kalinkovich, A., Ledergor, G., Wong, E., Niemeyer, E., Porat, Z., Erez, A., Sagi, I., Esmon, C.T., Ruf, W. and Lapidot, T.

(2015) PAR1 signaling regulates the retention and recruitment of EPCR-expressing bone marrow hematopoietic stem cells. *Nature Medicine* [online]. 21 (11), pp.1307-1317.

Gyurkocza, B. and Sandmaier, B.M. (2014) Conditioning regimens for hematopoietic cell transplantation: one size does not fit all. *Blood* [online]. 124 (3), pp.344-353.

Hagmann, S., Moradi, B., Frank, S., Dreher, T., Kämmerer, P.W., Richter, W. and Gotterbarm, T. (2013) Different culture media affect growth characteristics, surface marker distribution and chondrogenic differentiation of human bone marrow-derived mesenchymal stromal cells. *BMC Musculoskeletal Disorders* [online]. 14 pp.223-223.

Han, I., Kwon, B.S., Park, H.K. and Kim, K.S. (2017) Differentiation Potential of Mesenchymal Stem Cells Is Related to Their Intrinsic Mechanical Properties. *International Neurourology Journal* [online]. 21 (Suppl 1), pp.24-31.

Hasegawa, W., Lipton, J.H., Messner, H.A., Jamal, H., Yi, Q.L., Daly, A.S., Kotchetkova, N. and Kiss, T.L. (2003) Influence of one human leukocyte antigen mismatch on outcome of allogeneic bone marrow transplantation from related donors. *Hematology* (Amsterdam, Netherlands) [online]. 8 (1), pp.27-33.

Hass, R., Kasper, C., Böhm, S. and Jacobs, R. (2011) Different populations and sources of human mesenchymal stem cells (MSC): A comparison of adult and neonatal tissue-derived MSC. *Cell Communication and Signaling: CCS* [online]. 9. Doi:10.1186/1478-811X-9-12.

Hayman, J.A., Callahan, J.W., Herschtal, A., Everitt, S., Binns, D.S., Hicks, R.J. and Mac Manus, M. (2011) Distribution of proliferating bone marrow in adult cancer patients determined using FLT-PET imaging. *International Journal of Radiation Oncology, Biology, Physics* [online]. 79 (3), pp.847-852.

Heissig, B., Hattori, K., Dias, S., Friedrich, M., Ferris, B., Hackett, N.R., Crystal, R.G., Besmer, P., Lyden, D., Moore, M.A., Werb, Z. and Rafii, S. (2002) Recruitment of stem and progenitor cells from the bone marrow niche requires MMP-9 mediated release of kit-ligand. *Cell* [online]. 109 (5), pp.625-637.

Henner, W.D., Peters, W.P., Eder, J.P., Antman, K., Schnipper, L. and Frei, E.,3rd (1986) Pharmacokinetics and immediate effects of high-dose carmustine in man. *Cancer Treatment Reports* [online]. 70 (7), pp.877-880.

Himburg, H.A., Muramoto, G.G., Daher, P., Meadows, S.K., Russell, J.L., Doan, P., Chi, J.T., Salter, A.B., Lento, W.E., Reya, T., Chao, N.J. and Chute, J.P. (2010) Pleiotrophin regulates the expansion and regeneration of hematopoietic stem cells. *Nature Medicine* [online]. 16 (4), pp.475-482.

Ho, I.A.W., Chan, K.Y.W., Ng, W., Guo, C.M., Hui, K.M., Cheang, P. and Lam, P.Y.P. (2009) Matrix metalloproteinase 1 is necessary for the migration of human bone marrow-derived mesenchymal stem cells toward human glioma. *Stem Cells* (Dayton, Ohio) [online]. 27 (6), pp.1366-1375.

Ho, I.A.W., Yulyana, Y., Sia, K.C., Newman, J.P., Guo, C.M., Hui, K.M. and Lam, P.Y.P. (2014) Matrix metalloproteinase-1-mediated mesenchymal stem cell tumor tropism is dependent on crosstalk with stromal derived growth factor 1/C-X-C chemokine receptor 4 axis. *The FASEB Journal* [online]. 28 (10), pp.4359-4368.

Ho, T. K., Tsui, J., Xu, S., Leoni, P., Abraham, D. J. and Baker, D. M. (2010) Angiogenic effects of stromal cell-derived factor-1 (SDF-1/CXCL12) variants in vitro and the in vivo expressions of CXCL12 variants and CXCR4 in human critical leg ischemia. *Journal of Vascular Surgery* [online]. 51(3), pp. 689-699.

Hoffbrand, A.V. & Moss, P.A.H., ed. (2011) Essential Haematology. 6th ed. Oxford: Blackwell.

Holowiecki, J. (2008) Indications for hematopoietic stem cell transplantation. *Polskie Archiwum Medycyny Wewnetrznej* [online]. 118 (11), pp.658-663.

Honczarenko, M., Le, Y., Swierkowski, M., Ghiran, I., Glodek, A.M. and Silberstein, L.E. (2006) Human bone marrow stromal cells express a distinct set of biologically functional chemokine receptors. *Stem Cells* (Dayton, Ohio) [online]. 24 (4), pp.1030-1041.

Hong, D.S. and Deeg, H.J. (1994) Hemopoietic stem cells: sources and applications. *Medical Oncology* (Northwood, London, England) [online]. 11 (2), pp.63-68.

Hopman, R.K. and DiPersio, J.F. (2014) Advances in stem cell mobilization. *Blood Reviews* [online]. 28 (1), pp.31-40.

Hu, S., Niu, H., Inaba, H., Orwick, S., Rose, C., Panetta, J.C., Yang, S., Pounds, S., Fan, Y., Calabrese, C., Rehg, J.E., Campana, D., Rubnitz, J.E. and Baker, S.D. (2011) Activity of the multikinase inhibitor sorafenib in combination with cytarabine in acute myeloid leukemia. *Journal of the National Cancer Institute* [online]. 103 (11), pp.893-905.

Hu, X., Wu, R., Shehadeh, L.A., Zhou, Q., Jiang, C., Huang, X., Zhang, L., Gao, F., Liu, X., Yu, H., Webster, K.A. and Wang, J. (2014) Severe hypoxia exerts parallel and cell-specific regulation of gene expression and alternative splicing in human mesenchymal stem cells. *BMC Genomics* [online]. 15 pp.303-303.

Hutt, D. (2018) Engraftment, Graft Failure, and Rejection. In: Kenyon, M. and Babic, A. (eds) The European Blood and Marrow Transplantation Textbook for Nurses: *Under the Auspices of EBMT* [online]. Cham (CH): EBMT and the Author(s), pp.259-270.

Hwang, J.H., Kim, S.W., Park, S.E., Yun, H.J., Lee, Y., Kim, S. and Jo, D.Y. (2006) Overexpression of stromal cell-derived factor-1 enhances endothelium-supported transmigration, maintenance, and proliferation of hematopoietic progenitor cells. *Stem Cells and Development* [online]. 15 (2), pp.260-268.

Ivanovs, A., Rybtsov, S., Ng, E.S., Stanley, E.G., Elefanty, A.G. and Medvinsky, A. (2017) Human haematopoietic stem cell development: from the embryo to the dish. *Development* [online]. 144 (13), pp.2323-2337.

Jacob, C., Leport, M., Szilagyi, C., Allen, J. M., Bertrand, C. and Lagente, V. (2002) DMSO-treated HL60 cells: a model of neutrophil-like cells mainly expressing PDE4B subtype. *International Immunopharmacology* [online]. 2(12), pp. 1647-1656.

Janeczek Portalska, K., Leferink, A., Groen, N., Fernandes, H., Moroni, L., van Blitterswijk, C. and de Boer, J. (2012) Endothelial Differentiation of Mesenchymal Stromal Cells. *PLoS ONE*, 7 (10). doi: 10.1371/journal.pone.0046842.

Jazwiec, B., Solanilla, A., Grosset, C., Mahon, F.X., Dupouy, M., Pigeonnier-Lagarde, V., Belloc, F., Schweitzer, K., Reiffers, J. and Ripoche, J. (1998) Endothelial cell support of hematopoiesis is differentially altered by IL-1 and glucocorticoids. *Leukemia* [online]. 12 (8), pp.1210-1220.

Jin, H.J., Park, S.K., Oh, W., Yang, Y.S., Kim, S.W. and Choi, S.J. (2009) Down-regulation of CD105 is associated with multi-lineage differentiation in human umbilical cord blood-derived mesenchymal stem cells. *Biochemical and Biophysical Research Communications* [online]. 381 (4), pp.676-681.

Johny, A., Song, K.W., Nantel, S.H., Lavoie, J.C., Toze, C.L., Hogge, D.E., Forrest, D.L., Sutherland, H.J., Le, A., Nitta, J.Y., Barnett, M.J., Smith, C.A., Shepherd, J.D. and Nevill, T.J. (2006) Early stem cell transplantation for refractory acute leukemia after salvage therapy with high-dose etoposide and cyclophosphamide. Biology of Blood and Marrow Transplantation: *Journal of the American Society for Blood and Marrow Transplantation* [online]. 12 (4), pp.480-489.

Juarez, J.G., Harun, N., Thien, M., Welschinger, R., Baraz, R., Pena, A.D., Pitson, S.M., Rettig, M., DiPersio, J.F., Bradstock, K.F. and Bendall, L.J. (2012) Sphingosine-1-phosphate facilitates trafficking of hematopoietic stem cells and their mobilization by CXCR4 antagonists in mice. *Blood* [online]. 119 (3), pp.707-716.

Julien, E., El Omar, R. and Tavian, M. (2016) Origin of the hematopoietic system in the human embryo. *FEBS Letters* [online]. 590 (22), pp.3987-4001.

Jung, Y., Wang, J., Song, J., Shiozawa, Y., Wang, J., Havens, A., Wang, Z., Sun, Y., Emerson, S.G., Krebsbach, P.H. and Taichman, R.S. (2007) Annexin II expressed by osteoblasts and endothelial cells regulates stem cell adhesion, homing, and engraftment following transplantation. *Blood* [online]. 110 (1), pp.82-90.

Kallmeyer, K. and Pepper, M.S. (2015) Homing properties of mesenchymal stromal cells. *Expert Opinion on Biological Therapy* [online]. 15 (4), pp.477-479.

Kapałczyńska, M., Kolenda, T., Przybyła, W., Zajączkowska, M., Teresiak, A., Filas, V., Ibbs, M., Bliźniak, R., Łuczewski, Ł and Lamperska, K. (2018) 2D and 3D cell cultures - a comparison of different types of cancer cell cultures. *Archives of Medical Science: AMS* [online]. 14 (4), pp.910-919.

Karapetyan, A.V., Klyachkin, Y.M., Selim, S., Sunkara, M., Ziada, K.M., Cohen, D.A., Zuba-Surma, E., Ratajczak, J., Smyth, S.S., Ratajczak, M.Z., Morris, A.J. and Abdel-Latif, A. (2013) Bioactive lipids and cationic antimicrobial peptides as new potential regulators for trafficking of bone marrow-derived stem cells in patients with acute myocardial infarction. *Stem Cells and Development* [online]. 22 (11), pp.1645-1656.

Katayama, Y., Hidalgo, A., Furie, B.C., Vestweber, D., Furie, B. and Frenette, P.S. (2003) PSGL-1 participates in E-selectin-mediated progenitor homing to bone marrow: evidence for cooperation between E-selectin ligands and alpha4 integrin. *Blood* [online]. 102 (6), pp.2060-2067.

Kavanagh, D.P. and Kalia, N. (2011) Hematopoietic stem cell homing to injured tissues. *Stem Cell Reviews and Reports* [online]. 7 (3), pp.672-682.

Kawahara, R. (2007) Hematopoiesis. In: Enna, S.J. and Bylund, D.B., (eds) *xPharm: The Comprehensive Pharmacology Reference* [online]. New York: Elsevier, pp.1-5.

Kemp, K., Morse, R., Wexler, S., Cox, C., Mallam, E., Hows, J. and Donaldson, C. (2010) Chemotherapy-induced mesenchymal stem cell damage in patients with hematological malignancy. *Annals of Hematology* [online]. 89 pp.701-13.

Kerbauy, D.M., Gooley, T.A., Sale, G.E., Flowers, M.E., Doney, K.C., Georges, G.E., Greene, J.E., Linenberger, M., Petersdorf, E., Sandmaier, B.M., Scott, B.L., Sorror, M., Stirewalt, D.L., Stewart, F.M., Witherspoon, R.P., Storb, R., Appelbaum, F.R. and Deeg, H.J. (2007) Hematopoietic cell transplantation as curative therapy for idiopathic myelofibrosis, advanced polycythemia vera, and essential thrombocythemia. Biology of Blood and Marrow Transplantation: *Journal of the American Society for Blood and Marrow Transplantation* [online]. 13 (3), pp.355-365.

Kim, C.H., Wu, W., Wysoczynski, M., Abdel-Latif, A., Sunkara, M., Morris, A., Kucia, M., Ratajczak, J. and Ratajczak, M.Z. (2012) Conditioning for hematopoietic transplantation activates the complement cascade and induces a proteolytic environment in bone marrow: a novel role for bioactive lipids and soluble C5b-C9 as homing factors. *Leukemia* [online]. 26 (1), pp.106-116.

Klinge, S., Voigts-Hoffmann, F., Leibundgut, M., Arpagaus, S. and Ban, N. (2011) Crystal Structure of the Eukaryotic 60S Ribosomal Subunit in Complex with Initiation Factor 6. *Science* [online]. 334 (6058), pp.941-948.

Kobayashi, K., Sato, K., Kida, T., Omori, K., Hori, M., Ozaki, H. and Murata, T. (2014) Stromal cell-derived factor-1alpha/C-X-C chemokine receptor type 4 axis promotes endothelial cell barrier integrity via phosphoinositide 3-kinase and Rac1 activation. *Arteriosclerosis, Thrombosis, and Vascular Biology* [online]. 34 (8), pp.1716-1722.

Köhler, T., Plettig, R., Wetzstein, W., Schaffer, B., Ordemann, R., Nagels, H.O., Ehninger, G. and Bornhäuser, M. (1999) Defining optimum conditions for the ex vivo expansion of human umbilical cord blood cells. Influences of progenitor enrichment, interference with feeder layers, early-acting cytokines and agitation of culture vessels. *Stem Cells* (Dayton, Ohio) [online]. 17 (1), pp.19-24.

Kondo, M. (2010) Lymphoid and myeloid lineage commitment in multipotent hematopoietic progenitors. *Immunological Reviews* [online]. 238 (1), pp.37-46.

Kopp, H.G., Avecilla, S.T., Hooper, A.T. and Rafii, S. (2005) The bone marrow vascular niche: home of HSC differentiation and mobilization. *Physiology* (Bethesda, Md.) [online]. 20 pp.349-356.

Kubala, M.H., Punj, V., Placencio-Hickok, V., Fang, H., Fernandez, G.E., Sposto, R. and DeClerck, Y.A. (2018) Plasminogen Activator Inhibitor-1 Promotes the Recruitment and Polarization of Macrophages in Cancer. *Cell Reports* [online]. 25 (8), pp.2177-2191.e7.

Kuckertz, M., Patz, M., Veldurthy, A., Gehrke, I., Claasen, J., Frenzel, L.P., Wendtner, C.M., Hallek, M. and Krause, G. (2012) Comparison of the effects of two kinase inhibitors, sorafenib and dasatinib, on chronic lymphocytic leukemia cells. *Onkologie* [online]. 35 (7-8), pp.420-426.

Kumar, A., D'Souza, S.S. and Thakur, A.S. (2019) Understanding the Journey of Human Hematopoietic Stem Cell Development. *Stem Cells International* [online]. 2019. doi: 10.1155/2019/2141475.

Kurtis Kasper, M.S., F. and Mikos, A.G. (2013) Chapter II.6.3 - Tissue Engineering Scaffolds. In: Ratner, B.D., Hoffman, A.S., Schoen, F.J. and Lemons, J.E., eds. (2013) *Biomaterials Science* (Third Edition) [online]. Academic Press, pp.1138-1159.

Lapidot, T., Dar, A. and Kollet, O. (2005) How do stem cells find their way home? *Blood* [online]. 106 (6), pp.1901-1910.

Lapidot, T. and Petit, I. (2002) Current understanding of stem cell mobilization: the roles of chemokines, proteolytic enzymes, adhesion molecules, cytokines, and stromal cells. *Experimental Hematology* [online]. 30 (9), pp.973-981.

Laviola, L., Orlando, M.R., Incalza, M.A., Caccioppoli, C., Melchiorre, M., Leonardini, A., Cignarelli, A., Tortosa, F., Labarbuta, R., Martemucci, S., Pacelli, C., Cocco, T., Perrini, S., Natalicchio, A. and Giorgino, F. (2013) TNFα signals via p66(Shc) to induce E-Selectin, promote leukocyte transmigration and enhance permeability in human endothelial cells. *PloS One* [online]. 8 (12). doi: 10.1371/journal.pone.0081930.

Levesque, J.P., Helwani, F.M. and Winkler, I.G. (2010) The endosteal 'osteoblastic' niche and its role in hematopoietic stem cell homing and mobilization. *Leukemia* [online]. 24 (12), pp.1979-1992.

Li, B., Bailey, A.S., Jiang, S., Liu, B., Goldman, D.C. and Fleming, W.H. (2010) Endothelial cells mediate the regeneration of hematopoietic stem cells. *Stem Cell Research* [online]. 4 (1), pp.17-24.

Li, X., Bai, J., Ji, X., Li, R., Xuan, Y. and Wang, Y. (2014) Comprehensive characterization of four different populations of human mesenchymal stem cells as regards their immune properties, proliferation and differentiation. *International Journal of Molecular Medicine* [online]. 34 (3), pp.695-704.

Lidington, E.A., Moyes, D.L., McCormack, A.M. and Rose, M.L. (1999) A comparison of primary endothelial cells and endothelial cell lines for studies of immune interactions. *Transplant Immunology* [online]. 7 (4), pp.239-246.

Lilly, A.J., Johnson, W.E. and Bunce, C.M. (2011) The haematopoietic stem cell niche: new insights into the mechanisms regulating haematopoietic stem cell behaviour. *Stem Cells International* [online]. 2011. doi:10.4061/2011/274564.

Liso, A., Neri, M., Maglietta, F., La Russa, R. and Turillazzi, E. (2017) Hematopoietic Stem Cell Transplantation: A Bioethical Lens. *Stem Cells International* [online]. 2017. doi:10.1155/2017/1286246.

Liu, R., Wang, Y., Li, B., Wang, H., Guan, F., Tan, Z. and Li, X. (2019) Screening differentially expressed proteins from co-cultured hematopoietic cells and bone marrow-derived stromal cells by quantitative proteomics (SILAC) method. *Clinical Proteomics* [online]. 16. doi: 10.1186/s12014-019-9249-x.

Liu, Y., Ding, L., Zhang, B., Deng, Z., Han, Y., Wang, S., Yang, S., Fan, Z., Zhang, J., Yan, H., Han, D., He, L., Yue, W., Wang, H., Li, Y. and Pei, X. (2020) Thrombopoietin enhances hematopoietic stem and progenitor cell homing by impeding matrix metalloproteinase 9 expression. *Stem Cells Translational Medicine* [online]. 9 (6), pp.661-673.

Liu, Z., Gao, L., Wang, P., Xie, Z., Cen, S., Li, Y., Wu, X., Wang, L., Su, H., Deng, W., Wang, S., Li, D., Li, J., Ouyang, Y., Wu, Y. and Shen, H. (2017a) TNF-α Induced the Enhanced Apoptosis of Mesenchymal Stem Cells in Ankylosing Spondylitis by Overexpressing TRAIL-R2. *Stem Cells International* [online]. 2017. doi: 10.1155/2017/4521324.

Liu, Z., Tian, R., An, W., Zhuge, Y., Li, Y., Shao, H., Habib, B., Livingstone, A.S. and Velazquez, O.C. (2010) Identification of E-selectin as a novel target for the regulation of postnatal neovascularization: implications for diabetic wound healing. *Annals of Surgery* [online]. 252 (4), pp.625-634.

Liu, Z., Tian, R., Li, Y., Zhang, L., Shao, H., Yang, C. and Velazquez, O.C. (2016) SDF-1α-induced dual pairs of E-selectin/ligand mediate endothelial progenitor cell homing to critical ischemia. *Scientific Reports* [online]. 6 (1). doi: 10.1038/srep34416.

Liu, Z., Zhang, Y., Xiao, H., Yao, Z., Zhang, H., Liu, Q., Wu, B., Nie, D., Li, Y., Pang, Y., Fan, Z., Li, L., Jiang, Z., Duan, F., Li, H., Zhang, P., Gao, Y., Ouyang, L., Yue, C., Xie, M., Shi, C., Xiao, Y. and Wang, S. (2017b) Cotransplantation of bone marrow-derived mesenchymal stem cells in haploidentical hematopoietic stem cell transplantation in patients with severe aplastic anemia: an interim

summary for a multicenter phase II trial results. *Bone Marrow Transplantation* [online]. 52 (5), pp.704-710.

Lozito, T.P., Kuo, C.K., Taboas, J.M. and Tuan, R.S. (2009) Human mesenchymal stem cells express vascular cell phenotypes upon interaction with endothelial cell matrix. *Journal of Cellular Biochemistry* [online]. 107 (4), pp.714-722.

Lucotti, S., Cerutti, C., Soyer, M., Gil-Bernabé, A.M., Gomes, A.L., Allen, P.D., Smart, S., Markelc, B., Watson, K., Armstrong, P.C., Mitchell, J.A., Warner, T.D., Ridley, A.J. and Muschel, R.J. (2019) Aspirin blocks formation of metastatic intravascular niches by inhibiting platelet-derived COX-1/thromboxane A2. *The Journal of Clinical Investigation* [online]. 129 (5), pp.1845-1862.

Ma, Q., Jones, D. and Springer, T.A. (1999) The chemokine receptor CXCR4 is required for the retention of B lineage and granulocytic precursors within the bone marrow microenvironment. *Immunity* [online]. 10 (4), pp.463-471.

MacLean, A.L., Lo Celso, C. and Stumpf, M.P.H. (2017) Concise Review: Stem Cell Population Biology: Insights from Hematopoiesis. *Stem Cells* [online]. 35 (1), pp.80-88.

MacMillan, M.L., Blazar, B.R., DeFor, T.E. and Wagner, J.E. (2009) Transplantation of ex-vivo culture-expanded parental haploidentical mesenchymal stem cells to promote engraftment in pediatric recipients of unrelated donor umbilical cord blood: results of a phase I–II clinical trial. *Bone Marrow Transplantation* [online]. 43 (6), pp.447-454.

Mahajan, M.M., Cheng, B., Beyer, A.I., Mulvaney, U.S., Wilkinson, M.B., Fomin, M.E. and Muench, M.O. (2015) A quantitative assessment of the content of hematopoietic stem cells in mouse and human endosteal-bone marrow: a simple and rapid method for the isolation of mouse central bone marrow. *BMC Hematology* [online]. 15 pp.9-7.

Majhail, N.S., Farnia, S.H., Carpenter, P.A., Champlin, R.E., Crawford, S., Marks, D.I., Omel, J.L., Orchard, P.J., Palmer, J., Saber, W., Savani, B.N., Veys, P.A., Bredeson, C.N., Giralt, S.A. and LeMaistre, C.F. (2015) Indications for Autologous and Allogeneic Hematopoietic Cell Transplantation: Guidelines from the American Society for Blood and Marrow Transplantation.

Biology of Blood and Marrow Transplantation: *Journal of the American Society for Blood and Marrow Transplantation* [online]. 21 (11), pp.1863-1869.

Małkiewicz, A. and Dziedzic, M. (2012) Bone marrow reconversion - imaging of physiological changes in bone marrow. *Polish Journal of Radiology* [online]. 77 (4), pp.45-50.

Man, S., Ubogu, E.E., Williams, K.A., Tucky, B., Callahan, M.K. and Ransohoff, R.M. (2008) Human brain microvascular endothelial cells and umbilical vein endothelial cells differentially facilitate leukocyte recruitment and utilize chemokines for T cell migration. *Clinical & Developmental Immunology* [online]. 2008. doi: 10.1155/2008/384982.

Månsson, R., Hultquist, A., Luc, S., Yang, L., Anderson, K., Kharazi, S., Al-Hashmi, S., Liuba, K., Thorén, L., Adolfsson, J., Buza-Vidas, N., Qian, H., Soneji, S., Enver, T., Sigvardsson, M. and Jacobsen, S.E. (2007) Molecular evidence for hierarchical transcriptional lineage priming in fetal and adult stem cells and multipotent progenitors. *Immunity* [online]. 26 (4), pp.407-419.

Mantel, C.R., O'Leary, H.A., Chitteti, B.R., Huang, X., Cooper, S., Hangoc, G., Brustovetsky, N., Srour, E.F., Lee, M.R., Messina-Graham, S., Haas, D.M., Falah, N., Kapur, R., Pelus, L.M., Bardeesy, N., Fitamant, J., Ivan, M., Kim, K.S. and Broxmeyer, H.E. (2015) Enhancing Hematopoietic Stem Cell Transplantation Efficacy by Mitigating Oxygen Shock. *Cell* [online]. 161 (7), pp.1553-1565.

Marquez-Curtis, L., Turner, A.R., Sridharan, S., Ratajczak, M.Z. and Janowska-Wieczorek, A. (2011) The ins and outs of hematopoietic stem cells: studies to improve transplantation outcomes. *Stem Cell Reviews and Reports* [online]. 7 (3), pp.590-607.

Masuhara, K., Nakai, T., Yamaguchi, K., Yamasaki, S. and Sasaguri, Y. (2002) Significant increases in serum and plasma concentrations of matrix metalloproteinases 3 and 9 in patients with rapidly destructive osteoarthritis of the hip. *Arthritis & Rheumatism* [online]. 46 (10), pp.2625-2631.

Mateos, M.K., O'Brien, T.A., Oswald, C., Gabriel, M., Ziegler, D.S., Cohn, R.J., Russell, S.J., Barbaric, D., Marshall, G.M. and Trahair, T.N. (2013) Transplant-related mortality following allogeneic hematopoeitic stem cell transplantation for pediatric acute lymphoblastic leukemia: 25-year retrospective review. *Pediatric Blood & Cancer* [online]. 60 (9), pp.1520-1527.

Matter, K. and Balda, M.S. (2003) Functional analysis of tight junctions. *Methods* (San Diego, Calif.) [online]. 30 (3), pp.228-234.

May, J.E., Donaldson, C., Gynn, L. and Morse, H.R. (2018) Chemotherapy-induced genotoxic damage to bone marrow cells: long-term implications. *Mutagenesis* [online]. 33 (3), pp.241-251.

McClanahan, F. and Gribben, J. (2014) Transplantation in chronic lymphocytic leukemia: does it still matter in the era of novel targeted therapies? *Hematology/Oncology Clinics of North America* [online]. 28 (6), pp.1055-1071.

Melzer, D., Neumann, U., Ebell, W., Seeger, K., Neuhaus, P., Gaedicke, G., Brummendorf, T.H. and Scheding, S. (2004) Imatinib Mesylate (STI571) Considerably Affects Normal Human Bone Marrow Stromal Cell Growth in Vitro. *Blood* [online]. 104 (11). doi: 10.1182/blood.V104.11.2330.2330.

Mendelson, A. and Frenette, P.S. (2014) Hematopoietic stem cell niche maintenance during homeostasis and regeneration. *Nature Medicine* [online]. 20 (8), pp.833-846.

Mendez-Ferrer, S., Lucas, D., Battista, M. and Frenette, P.S. (2008) Haematopoietic stem cell release is regulated by circadian oscillations. *Nature* [online]. 452 (7186), pp.442-447.

Mendez-Ferrer, S., Michurina, T.V., Ferraro, F., Mazloom, A.R., Macarthur, B.D., Lira, S.A., Scadden, D.T., Ma'ayan, A., Enikolopov, G.N. and Frenette, P.S. (2010) Mesenchymal and haematopoietic stem cells form a unique bone marrow niche. *Nature* [online]. 466 (7308), pp.829-834.

Mi, H., Muruganujan, A., Ebert, D., Huang, X. and Thomas, P.D. (2018) PANTHER version 14: more genomes, a new PANTHER GO-slim and improvements in enrichment analysis tools. *Nucleic Acids Research* [online]. 47 pp. D419-D426.

Minter, A.J., Dawes, J. and Chesterman, C.N. (1992) Effects of heparin and endothelial cell growth supplement on haemostatic functions of vascular endothelium. *Thrombosis and Haemostasis* [online]. 67 (6), pp.718-723.

Mirshahi, F., Pourtau, J., Li, H., Muraine, M., Trochon, V., Legrand, E., Vannier, J., Soria, J., Vasse, M. and Soria, C. (2000) SDF-1 activity on microvascular endothelial cells: consequences on angiogenesis in in vitro and in vivo models. *Thrombosis Research* [online]. 99 (6), pp.587-594.

Mohammadali, F., Abroun, S. and Atashi, A. (2018) Mild hypoxia and human bone marrow mesenchymal stem cells synergistically enhance expansion and homing capacity of human cord blood CD34+ stem cells. *Iranian Journal of Basic Medical Sciences* [online]. 21 (7), pp.709-716.

Moleirinho, S., Guerrant, W. and Kissil, J. L. (2014) The Angiomotins – From discovery to function. *FEBS Letters* [online]. 588(16), pp. 2693-2703.

Moraes, D.A., Sibov, T.T., Pavon, L.F., Alvim, P.Q., Bonadio, R.S., Da Silva, J.R., Pic-Taylor, A., Toledo, O.A., Marti, L.C., Azevedo, R.B. and Oliveira, D.M. (2016) A reduction in CD90 (THY-1) expression results in increased differentiation of mesenchymal stromal cells. *Stem Cell Research & Therapy* [online]. 7 (1). doi: 10.1186/s13287-016-0359-3.

Nagareddy, P.R., Asfour, A., Klyachkin, Y.M. and Abdel-Latif, A. (2014) A novel role for bioactive lipids in stem cell mobilization during cardiac ischemia: new paradigms in thrombosis: novel mediators and biomarkers. *Journal of Thrombosis and Thrombolysis* [online]. 37 (1), pp.24-31.

Nagase, H., Visse, R. and Murphy, G. (2006) Structure and function of matrix metalloproteinases and TIMPs. *Cardiovascular Research* [online]. 69 (3), pp.562-573.

Naji, A., Eitoku, M., Favier, B., Deschaseaux, F., Rouas-Freiss, N. and Suganuma, N. (2019) Biological functions of mesenchymal stem cells and clinical implications. *Cellular and Molecular Life Sciences* [online]. 76 (17), pp.3323-3348.

Negrin, R.S. (2015) Graft-versus-host disease versus graft-versus-leukemia. *Hematology Am Soc Hematol Educ Program.* [online]. 2015 pp.225-230.

Nie, Y., Waite, J., Brewer, F., Sunshine, M.J., Littman, D.R. and Zou, Y.R. (2004) The role of CXCR4 in maintaining peripheral B cell compartments and humoral immunity. *The Journal of Experimental Medicine* [online]. 200 (9), pp.1145-1156.

Nombela-Arrieta, C. and Silberstein, L.E. (2014) The science behind the hypoxic niche of hematopoietic stem and progenitors. *Hematology* [online]. 2014 (1), pp.542-547.

Notta, F., Zandi, S., Takayama, N., Dobson, S., Gan, O.I., Wilson, G., Kaufmann, K.B., McLeod, J., Laurenti, E., Dunant, C.F., McPherson, J.D., Stein, L.D., Dror, Y. and Dick, J.E. (2016) Distinct routes of lineage development reshape the human blood hierarchy across ontogeny. *Science* [online]. 351 (6269). doi: 10.1126/science.aab2116.

Novershtern, N., Subramanian, A., Lawton, L.N., Mak, R.H., Haining, W.N., McConkey, M.E., Habib, N., Yosef, N., Chang, C.Y., Shay, T., Frampton, G.M., Drake, A.C.B., Leskov, I., Nilsson, B., Preffer, F., Dombkowski, D., Evans, J.W., Liefeld, T., Smutko, J.S., Chen, J., Friedman, N., Young, R.A., Golub, T.R., Regev, A. and Ebert, B.L. (2011) Densely interconnected transcriptional circuits control cell states in human hematopoiesis. *Cell* [online]. 144 (2), pp.296-309.

O'Brien, S.G., Guilhot, F., Larson, R.A., Gathmann, I., Baccarani, M., Cervantes, F., Cornelissen, J.J., Fischer, T., Hochhaus, A., Hughes, T., Lechner, K., Nielsen, J.L., Rousselot, P., Reiffers, J., Saglio, G., Shepherd, J., Simonsson, B., Gratwohl, A., Goldman, J.M., Kantarjian, H., Taylor, K., Verhoef, G., Bolton, A.E., Capdeville, R., Druker, B.J. and IRIS Investigators (2003) Imatinib compared with interferon and low-dose cytarabine for newly diagnosed chronic-phase chronic myeloid leukemia. *The New England Journal of Medicine* [online]. 348 (11), pp.994-1004.

Ode, A., Kopf, J., Kurtz, A., Schmidt-Bleek, K., Schrade, P., Kolar, P., Buttgereit, F., Lehmann, K., Hutmacher, D., Duda, G. and Kasper, G. (2011) CD73 and CD29 concurrently mediate the mechanically induced decrease of migratory capacity of mesenchymal stromal cells. *European Cells and Materials* [online]. 22 pp.26-42.

Ohishi, M. and Schipani, E. (2010) Bone marrow mesenchymal stem cells. *Journal of Cellular Biochemistry* [online]. 109 (2), pp.277-282.

Okamoto, S. (2017) Current indication for hematopoietic cell transplantation in adults. *Hematology/Oncology and Stem Cell Therapy* [online]. 10 (4), pp.178-183.

O'Rourke, M., B., Town, S.E.L., Dalla, P.V., Bicknell, F., Koh Belic, N., Violi, J.P., Steele, J.R. and Padula, M.P. (2019) What is normalization? the strategies employed in top-down and bottom-up proteome analysis workflows. *Proteomes* [online]. 7 (3). doi: 10.3390/proteomes7030029.

Ozdemir, Z.N. and Civriz Bozdağ, S. (2018) Graft failure after allogeneic hematopoietic stem cell transplantation. Transfusion and Apheresis Science: Official Journal of the World Apheresis Association: *Official Journal of the European Society for Haemapheresis* [online]. 57 (2), pp.163-167.

Panaroni, C., Tzeng, Y., Saeed, H. and Wu, J.Y. (2014) Mesenchymal progenitors and the osteoblast lineage in bone marrow hematopoietic niches. *Current Osteoporosis Reports* [online]. 12 (1), pp.22-32.

Parmar, K., Mauch, P., Vergilio, J., Sackstein, R. and Down, J.D. (2007) Distribution of hematopoietic stem cells in the bone marrow according to regional hypoxia. *Proc Natl Acad Sci USA* [online]. 104 (13). doi: 10.1073/pnas.0701152104.

Parmar, S., Patel, K. and Pinilla-Ibarz, J. (2014) Ibrutinib (imbruvica): a novel targeted therapy for chronic lymphocytic leukemia. P & T: *A Peer-Reviewed Journal for Formulary Management* [online]. 39 (7), pp.483-519.

Peled, A., Grabovsky, V., Habler, L., Sandbank, J., Arenzana-Seisdedos, F., Petit, I., Ben-Hur, H., Lapidot, T. and Alon, R. (1999) The chemokine SDF-1 stimulates integrin-mediated arrest of CD34(+) cells on vascular endothelium under shear flow. *The Journal of Clinical Investigation* [online]. 104 (9), pp.1199-1211.

Peled, A., Kollet, O., Ponomaryov, T., Petit, I., Franitza, S., Grabovsky, V., Slav, M.M., Nagler, A., Lider, O., Alon, R., Zipori, D. and Lapidot, T. (2000) The chemokine SDF-1 activates the integrins LFA-1, VLA-4, and VLA-5 on immature human CD34+ cells: role in transendothelial/stromal migration and engraftment of NOD/SCID mice. *Blood* [online]. 95 (11), pp.3289-3296.

Pereira, M.R., Pouch, S.M. and Scully, B. (2018) Infections in Allogeneic Stem Cell Transplantation. *Principles and Practice of Transplant Infectious Diseases* [online]. 2018. pp.209-226.

Perlin, J.R., Sporrij, A. and Zon, L.I. (2017) Blood on the tracks: hematopoietic stem cell-endothelial cell interactions in homing and engraftment. *Journal of Molecular Medicine* (Berlin, Germany) [online]. 95 (8), pp.809-819.

Podszywalow-Bartnicka, P., Kominek, A., Wolczyk, M., Kolba, M.D., Swatler, J. and Piwocka, K. (2018) Characteristics of live parameters of the HS-5 human bone marrow stromal cell line cocultured with the leukemia cells in hypoxia, for the studies of leukemia-stroma cross-talk. Cytometry.Part A: *The Journal of the International Society for Analytical Cytology* [online]. 93 (9), pp.929-940.

Ponta, H., Sherman, L. and Herrlich, P.A. (2003) CD44: from adhesion molecules to signalling regulators. *Nature Reviews.Molecular Cell Biology* [online]. 4 (1), pp.33-45.

Rafii, S., Shapiro, F., Rimarachin, J., Nachman, R.L., Ferris, B., Weksler, B., Moore, M.A. and Asch, A.S. (1994) Isolation and characterization of human bone marrow microvascular endothelial cells: hematopoietic progenitor cell adhesion. *Blood* [online]. 84 (1), pp.10-19.

Ratajczak, M. Z. and Abdelbaset-Ismail, A. (2016) Chapter 2 - Stem Cell Homing. *In Situ Tissue Regeneration* [online]. pp. 21-34.

Ratajczak, M.Z., Lee, H., Wysoczynski, M., Wan, W., Marlicz, W., Laughlin, M.J., Kucia, M., Janowska-Wieczorek, A. and Ratajczak, J. (2010) Novel insight into stem cell mobilization-plasma sphingosine-1-phosphate is a major chemoattractant that directs the egress of hematopoietic stem progenitor cells from the bone marrow and its level in peripheral blood increases during mobilization due to activation of complement cascade/membrane attack complex. *Leukemia* [online]. 24 (5), pp.976-985.

Ratajczak, M.Z. and Suszynska, M. (2016) Emerging Strategies to Enhance Homing and Engraftment of Hematopoietic Stem Cells. *Stem Cell Reviews and Reports* [online]. 12 (1), pp.121-128.

Ratajczak, M.Z., Kim, C., Janowska-Wieczorek, A. and Ratajczak, J. (2012) The expanding family of bone marrow homing factors for hematopoietic stem cells: stromal derived factor 1 is not the only player in the game. *The Scientific World Journal* [online]. 2012. doi: 10.1100/2012/758512.

Rehn, M., Olsson, A., Reckzeh, K., Diffner, E., Carmeliet, P., Landberg, G. and Cammenga, J. (2011) Hypoxic induction of vascular endothelial growth factor regulates murine hematopoietic stem cell function in the low-oxygenic niche. *Blood* [online]. 118 (6), pp.1534-1543.

Roecklein, B.A. and Torok-Storb, B. (1995) Functionally distinct human marrow stromal cell lines immortalized by transduction with the human papilloma virus E6/E7 genes. *Blood* [online]. 85 (4), pp.997-1005.

Ross, R.A., Spengler, B.A. and Biedler, J.L. (1983) Coordinate morphological and biochemical interconversion of human neuroblastoma cells. *Journal of the National Cancer Institute* [online]. 71 (4), pp.741-747.

Rossi, L., Manfredini, R., Bertolini, F., Ferrari, D., Fogli, M., Zini, R., Salati, S., Salvestrini, V., Gulinelli, S., Adinolfi, E., Ferrari, S., Di Virgilio, F., Baccarani, M. and Lemoli, R.M. (2007) The extracellular nucleotide UTP is a potent inducer of hematopoietic stem cell migration. *Blood* [online]. 109 (2), pp.533-542.

Ruggeri, A. (2016) Alternative donors: cord blood for adults. *Seminars in Hematology* [online]. 53 (2), pp.65-73.

Sackstein, R., Merzaban, J.S., Cain, D.W., Dagia, N.M., Spencer, J.A., Lin, C.P. and Wohlgemuth, R. (2008) Ex vivo glycan engineering of CD44 programs human multipotent mesenchymal stromal cell trafficking to bone. *Nature Medicine* [online]. 14 (2), pp.181-187.

Schacher, D.H., VanHoy, R.W., Liu, Q., Arkins, S., Dantzer, R., Freund, G.G. and Kelley, K.W. (2000) Developmental Expression of Insulin Receptor Substrate-2 During Dimethylsulfoxide-Induced Differentiation of Human HL-60 Cells. *The Journal of Immunology* [online]. 164 (1), pp.113-120.

Schioppa, T., Uranchimeg, B., Saccani, A., Biswas, S.K., Doni, A., Rapisarda, A., Bernasconi, S., Saccani, S., Nebuloni, M., Vago, L., Mantovani, A., Melillo, G. and Sica, A. (2003) Regulation of the chemokine receptor CXCR4 by hypoxia. *The Journal of Experimental Medicine* [online]. 198 (9), pp.1391-1402.

Schmidmaier, R., Baumann, P., Emmerich, B. and Meinhardt, G. (2006) Evaluation of chemosensitivity of human bone marrow stromal cells--differences between common chemotherapeutic drugs. *Anticancer Research* [online]. 26 (1A), pp.347-350.

Schmitz, N., Beksac, M., Hasenclever, D., Bacigalupo, A., Ruutu, T., Nagler, A., Gluckman, E., Russell, N., Apperley, J.F., Gorin, N.C., Szer, J., Bradstock, K., Buzyn, A., Clark, P., Borkett, K., Gratwohl, A. and European Group for Blood and Marrow Transplantation (2002) Transplantation of mobilized peripheral blood cells to HLA-identical siblings with standard-risk leukemia. *Blood* [online]. 100 (3), pp.761-767.

Schneider, G., Bryndza, E., Abdel-Latif, A., Ratajczak, J., Maj, M., Tarnowski, M., Klyachkin, Y.M., Houghton, P., Morris, A.J., Vater, A., Klussmann, S., Kucia, M. and Ratajczak, M.Z. (2013) Bioactive lipids S1P and C1P are prometastatic factors in human rhabdomyosarcoma, and their tissue levels increase in response to radio/chemotherapy. *Molecular Cancer Research: MCR* [online]. 11 (7), pp.793-807.

Schneider-Poetsch, T., Ju, J., Eyler, D.E., Dang, Y., Bhat, S., Merrick, W.C., Green, R., Shen, B. and Liu, J.O. (2010) Inhibition of eukaryotic translation elongation by cycloheximide and lactimidomycin. *Nature Chemical Biology* [online]. 6 (3), pp.209-217.

Schutyser, E., Su, Y., Yu, Y., Gouwy, M., Zaja-Milatovic, S., Van Damme, J. and Richmond, A. (2007) Hypoxia enhances CXCR4 expression in human microvascular endothelial cells and human melanoma cells. *European Cytokine Network* [online]. 18 (2), pp.59-70.

Seo, Y., Koh, S. H., Kang, H. J., Shin, H. Y., Jeong, G. and Ahn, H. S. (2007) Hypoxia inhibits the SDF-1-dependent migration of human leukemic cell line HL-60 via blocking of Akt activation. *Biochemical and Biophysical Research Communications* [online]. 364(2), pp. 388-394.

Servais, S., Beguin, Y. and Baron, F. (2013) Emerging drugs for prevention of graft failure after allogeneic hematopoietic stem cell transplantation. *Expert Opinion on Emerging Drugs* [online]. 18 (2), pp.173-192.

Sgarioto, M., Vigneron, P., Patterson, J., Malherbe, F., Nagel, M.D. and Egles, C. (2012) Collagen type I together with fibronectin provide a better support for endothelialization. *Comptes Rendus Biologies* [online]. 335 (8), pp.520-528.

Shirvaikar, N., Marquez-Curtis, L. and Janowska-Wieczorek, A. (2012) Hematopoietic Stem Cell Mobilization and Homing after Transplantation: The Role of MMP-2, MMP-9, and MT1-MMP. *Biochemistry Research International* [online]. 2012. doi: 10.1155/2012/685267.

Singh, A. K. and Cancelas, J. A. (2020) Gap Junctions in the Bone Marrow Lympho-Hematopoietic Stem Cell Niche, Leukemia Progression, and Chemoresistance. *International Journal of Molecular Sciences* [online]. 21(3). doi:10.3390/ijms21030796.

Sirinoglu Demiriz, I., Tekgunduz, E. and Altuntas, F. (2012) What Is the Most Appropriate Source for Hematopoietic Stem Cell Transplantation? Peripheral Stem Cell/Bone Marrow/Cord Blood. *Bone Marrow Research* [online]. 2012. doi: 10.1155/2012/834040.

Smith-Berdan, S., Nguyen, A., Hassanein, D., Zimmer, M., Ugarte, F., Ciriza, J., Li, D., García-Ojeda, M.E., Hinck, L. and Forsberg, E.C. (2011) Robo4 Cooperates with Cxcr4 to Specify Hematopoietic Stem Cell Localization to Bone Marrow Niches. *Cell Stem Cell* [online]. 8 (1), pp.72-83.

Soares, P.B., Jeremias, T.S., Alvarez-Silva, M., Licinio, M.A., Santos-Silva, M. and Vituri, C.L. (2013) In vitro inhibitory effects of imatinib mesylate on stromal cells and hematopoietic progenitors from bone marrow. *Brazilian Journal of Medical and Biological Research* [online]. 46 (1), pp.39-51.

Sotiropoulou, P.A., Perez, S.A., Salagianni, M., Baxevanis, C.N. and Papamichail, M. (2006) Characterization of the optimal culture conditions for clinical scale production of human mesenchymal stem cells. *Stem Cells* (Dayton, Ohio) [online]. 24 (2), pp.462-471.

Spencer, J.A., Ferraro, F., Roussakis, E., Klein, A., Wu, J., Runnels, J.M., Zaher, W., Mortensen, L.J., Alt, C., Turcotte, R., Yusuf, R., Côté, D., Vinogradov, S.A., Scadden, D.T. and Lin, C.P. (2014) Direct measurement of local oxygen concentration in the bone marrow of live animals. *Nature* [online]. 508 (7495), pp.269-273.

Srinivasan, A., Wang, C., Srivastava, D.K., Burnette, K., Shenep, J.L., Leung, W. and Hayden, R.T. (2013) Timeline, epidemiology, and risk factors for bacterial, fungal, and viral infections in children and adolescents after allogeneic hematopoietic stem cell transplantation. Biology of Blood and Marrow Transplantation: *Journal of the American Society for Blood and Marrow Transplantation* [online]. 19 (1), pp.94-101.

Szklarczyk, D., Gable, A.L., Lyon, D., Junge, A., Wyder, S., Huerta-Cepas, J., Simonovic, M., Doncheva, N.T., Morris, J.H., Bork, P., Jensen, L.J. and Mering, C.V. (2019) STRING v11: protein-protein association networks with increased coverage, supporting functional discovery in genome-wide experimental datasets. *Nucleic Acids Research* [online]. 47 (D1), pp. D607-D613.

Teixeira, A.C., Dos Santos, R.A., Poersch, A., Carrara, H.H.A., de Andrade, J.M. and Takahashi, C.S. (2009) DNA repair in Etoposide-induced DNA damage in lymphocytes of breast cancer patients and healthy women. *International Journal of Clinical and Experimental Medicine* [online]. 2 (3), pp.280-288.

Theodore, L.N., Hagedorn, E.J., Cortes, M., Natsuhara, K., Liu, S.Y., Perlin, J.R., Yang, S., Daily, M.L., Zon, L.I. and North, T.E. (2017) Distinct Roles for Matrix Metalloproteinases 2 and 9 in Embryonic Hematopoietic Stem Cell Emergence, Migration, and Niche Colonization. *Stem Cell Reports* [online]. 8 (5), pp.1226-1241.

Trimarco, V., Ave, E., Facco, M., Chiodin, G., Frezzato, F., Martini, V., Gattazzo, C., Lessi, F., Giorgi, C.A., Visentin, A., Castelli, M., Severin, F., Zambello, R., Piazza, F., Semenzato, G. and Trentin, L. (2015) Cross-talk between chronic lymphocytic leukemia (CLL) tumor B cells and mesenchymal stromal cells (MSCs): implications for neoplastic cell survival. *Oncotarget* [online]. 6 (39), pp.42130-42149.

Trivanović, D., Jauković, A., Popović, B., Krstić, J., Mojsilović, S., Okić-Djordjević, I., Kukolj, T., Obradović, H., Santibanez, J.F. and Bugarski, D. (2015) Mesenchymal stem cells of different origin: Comparative evaluation of proliferative capacity, telomere length and pluripotency marker expression. *Life Sciences* [online]. 141 pp.61-73.

Troyanovsky, B., Levchenko, T., Månsson, G., Matvijenko, O. and Holmgren, L. (2001) Angiomotin: an angiostatin binding protein that regulates endothelial cell migration and tube formation. *The Journal of Cell Biology* [online]. 152 (6), pp.1247-1254.

Tu, T.C., Nagano, M., Yamashita, T., Hamada, H., Ohneda, K., Kimura, K. and Ohneda, O. (2016) A Chemokine Receptor, CXCR4, Which Is Regulated by Hypoxia-Inducible Factor 2α, Is Crucial for Functional Endothelial Progenitor Cells Migration to Ischemic Tissue and Wound Repair. *Stem Cells and Development* [online]. 25 (3), pp.266-276.

Tyanova, S. and Cox, J. (2018) Perseus: A Bioinformatics Platform for Integrative Analysis of Proteomics Data in Cancer Research. In: von Stechow, L., ed. (2018) Cancer Systems Biology: Methods and Protocols [online]. New York, NY: *Springer* New York, pp.133-148.

Tyanova, S., Temu, T., Sinitcyn, P., Carlson, A., Hein, M.Y., Geiger, T., Mann, M. and Cox, J. (2016) The Perseus computational platform for comprehensive analysis of (prote)omics data. *Nature Methods* [online]. 13 (9), pp.731-740.

Umezawa, Y., Akiyama, H., Okada, K., Ishida, S., Nogami, A., Oshikawa, G., Kurosu, T. and Miura, O. (2017) Molecular mechanisms for enhancement of stromal cell-derived factor 1-induced chemotaxis by platelet endothelial cell adhesion molecule 1 (PECAM-1). *The Journal of Biological Chemistry* [online]. 292 (48), pp.19639-19655.

Vagima, Y., Lapid, K., Kollet, O., Goichberg, P., Alon, R. and Lapidot, T. (2011) Pathways implicated in stem cell migration: the SDF-1/CXCR4 axis. *Methods in Molecular Biology* (Clifton, N.J.) [online]. 750 pp.277-289.

van der Helm, M. W., Odijk, M., Frimat, J.P., van der Meer, A. D., Eijkel, J.C.T., van den Berg, A. and Segerink, L.I. (2016) Direct quantification of transendothelial electrical resistance in organs-on-chips. *Biosensors & Bioelectronics* [online]. 85 pp.924-929.

Vane, J.R. and Botting, R.M. (2003) The mechanism of action of aspirin. *Thrombosis Research* [online]. 110 (5-6), pp.255-258.

Velten, L., Haas, S.F., Raffel, S., Blaszkiewicz, S., Islam, S., Hennig, B.P., Hirche, C., Lutz, C., Buss, E.C., Nowak, D., Boch, T., Hofmann, W., Ho, A.D., Huber, W., Trumpp, A., Essers, M.A.G. and Steinmetz, L.M. (2017) Human haematopoietic stem cell lineage commitment is a continuous process. *Nature Cell Biology* [online]. 19 (4), pp.271-281.

Verhoeckx K, Cotter P, López-Expósito I, Kleiveland C, Lea T, Mackie A, Requena T, Swiatecka D, Wichers H, editors. (2015) The Impact of Food Bioactives on Health: *In Vitro and Ex Vivo Models* [online]. Cham: Springer International Publishing, pp.95-102.

Vittorio, O., Jacchetti, E., Pacini, S. and Cecchini, M. (2013) Endothelial differentiation of mesenchymal stromal cells: when traditional biology meets mechanotransduction. *Integrative Biology: Quantitative Biosciences from Nano to Macro* [online]. 5 (2), pp.291-299.

Voermans, C., Anthony, E. C., Mul, E., van der Schoot, E. and Hordijk, P. (2001) SDF-1–induced actin polymerization and migration in human hematopoietic progenitor cells. *Experimental Hematology* [online]. 29(12), pp. 1456-1464.

Volin, M.V., Joseph, L., Shockley, M.S. and Davies, P.F. (1998) Chemokine receptor CXCR4 expression in endothelium. *Biochemical and Biophysical Research Communications* [online]. 242 (1), pp.46-53.

Wahid, S.F. (2013) Indications and outcomes of reduced-toxicity hematopoietic stem cell transplantation in adult patients with hematological malignancies. *International Journal of Hematology* [online]. 97 (5), pp.581-598.

Wang, J. and Knaut, H. (2014) Chemokine signaling in development and disease. *Development* (Cambridge, England) [online]. 141 (22), pp.4199-4205.

Wang, Z. and Ema, H. (2016) Mechanisms of self-renewal in hematopoietic stem cells. *International Journal of Hematology* [online]. 103 (5), pp.498-509.

Wilson, A. and Trumpp, A. (2006) Bone-marrow haematopoietic-stem-cell niches. *Nature Reviews Immunology* [online]. 6 (2), pp.93-106.

Winkler, I.G., Barbier, V., Nowlan, B., Jacobsen, R.N., Forristal, C.E., Patton, J.T., Magnani, J.L. and Levesque, J.P. (2012) Vascular niche E-selectin regulates hematopoietic stem cell dormancy, self renewal and chemoresistance. *Nature Medicine* [online]. 18 (11), pp.1651-1657.

Wright, N., Hidalgo, A., Rodriguez-Frade, J.M., Soriano, S.F., Mellado, M., Parmo-Cabanas, M., Briskin, M.J. and Teixido, J. (2002) The chemokine stromal cell-derived factor-1 alpha modulates alpha 4 beta 7 integrin-mediated lymphocyte adhesion to mucosal addressin cell adhesion molecule-1 and fibronectin. *Journal of Immunology* (Baltimore, Md.: 1950) [online]. 168 (10), pp.5268-5277.

Wu, Y., Cao, Y., Li, X., Xu, L., Wang, Z., Liu, P., Yan, P., Liu, Z., Wang, J., Jiang, S., Wu, X., Gao, C., Da, W. and Han, Z. (2014) Cotransplantation of haploidentical hematopoietic and umbilical cord mesenchymal stem cells for severe aplastic anemia: Successful engraftment and mild GVHD. *Stem Cell Research* [online]. 12(1), pp. 132-138.

Xia, L., McDaniel, J.M., Yago, T., Doeden, A. and McEver, R.P. (2004) Surface fucosylation of human cord blood cells augments binding to P-selectin and E-selectin and enhances engraftment in bone marrow. *Blood* [online]. 104 (10), pp.3091-3096.

Xiong, Y., Fan, Q., Huang, F., Zhang, Y., Wang, Y., Chen, X., Fan, Z., Zhou, H., Xiao, Y., Xu, X., Dai, M., Xu, N., Sun, J., Xiang, P., Huang, X. and Liu, Q. (2014) Mesenchymal Stem Cells versus Mesenchymal Stem Cells Combined with Cord Blood for Engraftment Failure after Autologous Hematopoietic Stem Cell Transplantation: A Pilot Prospective, Open-Label, Randomized Trial. *Biology of Blood and Marrow Transplantation* [online]. 20(2), pp. 236-242.

Yamamoto, R., Morita, Y., Ooehara, J., Hamanaka, S., Onodera, M., Rudolph, K.L., Ema, H. and Nakauchi, H. (2013) Clonal analysis unveils self-renewing lineage-restricted progenitors generated directly from hematopoietic stem cells. *Cell* [online]. 154 (5), pp.1112-1126.

Yan, X., Liu, B., Lu, S.H., Ge, M.L., Li, X.X. and Zheng, Y.Z. (2011) The effects of stem cell factor on proliferation, transmigration, capillary tube formation of endothelial cells and on the chemotaxis of CD133(+) cells. *Zhonghua Xueyexue Zazhi* [online]. 32 (5), pp.326-330.

Yang, J., Hirata, T., Croce, K., Merrill-Skoloff, G., Tchernychev, B., Williams, E., Flaumenhaft, R., Furie, B.C. and Furie, B. (1999) Targeted gene disruption demonstrates that P-selectin glycoprotein ligand 1 (PSGL-1) is required for P-selectin-mediated but not E-selectin-mediated neutrophil rolling and migration. *The Journal of Experimental Medicine* [online]. 190 (12), pp.1769-1782.

Yao, L., Yokota, T., Xia, L., Kincade, P.W. and McEver, R.P. (2005) Bone marrow dysfunction in mice lacking the cytokine receptor gp130 in endothelial cells. *Blood* [online]. 106 (13), pp.4093-4101.

Yildirim, S., Boehmler, A.M., Kanz, L. and Mohle, R. (2005) Expansion of cord blood CD34+ hematopoietic progenitor cells in coculture with autologous umbilical vein endothelial cells (HUVEC) is superior to cytokine-supplemented liquid culture. *Bone Marrow Transplantation* [online]. 36 (1), pp.71-79.

Yin, T. and Li, L. (2006) The stem cell niches in bone. *The Journal of Clinical Investigation* [online]. 116 (5), pp.1195-1201.

Zabel, B.A., Lewén, S., Berahovich, R.D., Jaén, J.C. and Schall, T.J. (2011) The novel chemokine receptor CXCR7 regulates trans-endothelial migration of cancer cells. *Molecular Cancer* [online]. 10 (1). doi: 10.1186/1476-4598-10-73.

Zambidis, E.T., Peault, B., Park, T.S., Bunz, F. and Civin, C.I. (2005) Hematopoietic differentiation of human embryonic stem cells progresses through sequential hematoendothelial, primitive, and definitive stages resembling human yolk sac development. *Blood* [online]. 106 (3), pp.860-870.

Zhang, C.C. and Lodish, H.F. (2008) Cytokines regulating hematopoietic stem cell function. *Current Opinion in Hematology* [online]. 15 (4), pp.307-311.

Zhou, L., Zhang, Y., Sampath, D., Leverson, J., Dai, Y., Kmieciak, M., Nguyen, M., Orlowski, R.Z. and Grant, S. (2018) Flavopiridol enhances ABT-199 sensitivity in unfavourable-risk multiple myeloma cells in vitro and in vivo. *British Journal of Cancer* [online]. 118 (3), pp.388-397.

Zhu, L., Xiao, M., Chen, Y., Wang, L., Luo, X., Yuan, X., Ren, J., Chen, Z., Hu, J. and Yang, T. (2017) In vitro effects of reprogramming factors on the expressions of pluripotent genes and CD34 gene in human acute promyelocytic leukemia HL-60 cells. *Genomics* [online]. 109(5), pp. 331-335.

Appendices:

Appendix 1

Preparation of dry samples for SEM using (hexamethyldisilazane) HMDS

1. Fixation

- Fix samples in 4% glutaraldehyde in PBS buffer (8.4ml PBS + 1.6ml 25% glutaraldehyde)
- Leave for 1 hr at room temperature (or 24hrs in the fridge)
- Rinse in PBS buffer three times

2. Dehydration

- 5min. in 20% ethanol
- 5min. in 30% ethanol
- 5min. in 50% ethanol
- 5min. in 70% ethanol
- 5min. in 80% ethanol
- 5min. in 90% ethanol
- 5min. in 100% ethanol
- 5min. in 100% ethanol
- 5min. in 100% ethanol
- 5min. in 100% ethanol / HMDS (2:1)
- 5min. in 100% ethanol / HMDS (2:2)
- 5min. in 100% ethanol / HMDS (1:2)
- 5min. in 100% HMDS
- 5min. in 100% HMDS
- 5min. in 100% HMDS

3. Remove specimen from HMDS and place on filter paper in a petri dish and leave in fume hood until dry.

Appendix 2

Proteomic samples processing and analysis

TMT Labelling

An equal volume of six samples per experiment were digested with trypsin (2.5µg trypsin per 100µg protein; 37°C, overnight), labelled with Tandem Mass Tag (TMT) six plex reagents according to the manufacturer's protocol (Thermo Fisher Scientific, Loughborough, UK) and the labelled samples pooled.

The pooled sample was evaporated to dryness, resuspended in 5% formic acid and then desalted using SepPak cartridges according to the manufacturer's instructions (Waters, Milford, Massachusetts, USA). Eluate from the SepPak cartridge was again evaporated to dryness and resuspended in 1% formic acid prior to analysis by nano-LC MSMS using an Orbitrap Fusion Tribrid Mass Spectrometer.

Nano-LC Mass Spectrometry

The pooled TMT-labelled sample was fractionated using an Ultimate 3000 nano-LC system in line with an Orbitrap Fusion Tribrid mass spectrometer (Thermo Scientific). In brief, peptides in 1% (vol/vol) formic acid were injected onto an Acclaim PepMap C18 nano-trap column (Thermo Scientific). After washing with 0.5% (vol/vol) acetonitrile 0.1% (vol/vol) formic acid, peptides were resolved on a 250 mm × 75 µm Acclaim PepMap C18 reverse phase analytical column (Thermo Scientific) over a 150 min organic gradient, using 6 gradient segments (5-9% solvent B over 2min., 9-25% B over 94min., 25-60% B over 23min., 60-90% B over 5min., held at 90% B for 5min and then reduced to 1% B over 2min.) with a flow rate of 300 nl min^{-1}. Solvent A was 0.1% formic acid and Solvent B was aqueous 80% acetonitrile in 0.1% formic acid. Peptides were ionized by nano-electrospray ionization at 2.0kV using a stainless-steel emitter with an internal diameter of 30 µm (Thermo Scientific) and a capillary temperature of 275°C.

All spectra were acquired using an Orbitrap Fusion Tribrid mass spectrometer controlled by Xcalibur 2.0 software (Thermo Scientific) and operated in data-dependent acquisition mode using an SPS-MS3 workflow. FTMS1 spectra were collected at a resolution of 120 000, with an automatic gain control (AGC) target of 400 000 and a maximum injection time of 100ms. Precursors were filtered with an intensity range from 5000 to 1E20, according to charge state (to include charge states 2-6) and with monoisotopic precursor selection. Previously interrogated precursors were excluded using a dynamic window (60s +/-10ppm). The MS2 precursors were isolated with a quadrupole mass filter set to a width of 1.2m/z. ITMS2 spectra were collected with an AGC target of 10 000, with maximum injection time of 70ms and CID collision energy of 35%.

For FTMS3 analysis, the Orbitrap was operated at 30 000 resolution with an AGC target of 50 000 and a maximum injection time of 105ms. Precursors were fragmented by high energy collision dissociation (HCD) at a normalised collision energy of 55% to ensure maximal TMT reporter ion yield. Synchronous Precursor Selection (SPS) was enabled to include up to 5 MS2 fragment ions in the FTMS3 scan.

Data Analysis

The raw data files were processed and quantified using Proteome Discoverer software v2.1 (Thermo Scientific) and searched against the UniProt Human database (downloaded 14/09/17: 140000 entries) using the SEQUEST algorithm. Peptide precursor mass tolerance was set at 10ppm, and MS/MS tolerance was set at 0.6Da. Search criteria included oxidation of methionine (+15.9949) as a variable modification and carbamidomethylation of cysteine (+57.0214) and the addition of the

TMT mass tag (+229.163) to peptide N-termini and lysine as fixed modifications. Searches were performed with full tryptic digestion and a maximum of two missed cleavage sites were allowed. The reverse database search option was enabled and all data was filtered to satisfy false discovery rate (FDR) of 5%.

Appendix 3

Proteins identified after data filtering in untreated hypoxia vs normoxia samples, 767 proteins were identified GN=Gene Name, PE=Protein Existence which is the numerical value describing the evidence for the existence of the protein, SV=Sequence Version which is the version number of the sequence.

Accession	Description	-log P	Diff.
V9HWA9	Epididymis secretory sperm binding protein Li 62p GN=HEL-S-62p PE=2 SV=1	0.92	0.18
P08123	Collagen alpha-2(I) chain GN=COL1A2 PE=1 SV=7	5.71	1.20
P12109	Collagen alpha-1(VI) chain GN=COL6A1 PE=1 SV=3	0.11	0.04
P03956	Interstitial collagenase GN=MMP1 PE=1 SV=3	0.65	-0.21
A0A024R462	Fibronectin 1, isoform CRA_n GN=FN1 PE=4 SV=1	0.14	0.04
J3QSU6	Tenascin GN=TNC PE=1 SV=1	0.00	0.00
V9HWB4	Epididymis secretory sperm binding protein Li 89n GN=HEL-S-89n PE=2 SV=1	0.84	-0.27
V9HW22	Epididymis luminal protein 33 GN=HEL-S-72p PE=2 SV=1	0.06	-0.02
P06733	Alpha-enolase GN=ENO1 PE=1 SV=2	0.16	-0.05
P21333	Filamin-A GN=FLNA PE=1 SV=4	0.14	0.03
P11047	Laminin subunit gamma-1 GN=LAMC1 PE=1 SV=3	0.40	0.09
Q14766	Latent-transforming growth factor beta-binding protein 1 GN=LTBP1 PE=1 SV=4	1.93	0.32
P12814	Alpha-actinin-1 GN=ACTN1 PE=1 SV=2	0.26	-0.07
P10809	60 kDa heat shock protein, mitochondrial GN=HSPD1 PE=1 SV=2	1.46	0.22
P07900	Heat shock protein HSP 90-alpha GN=HSP90AA1 PE=1 SV=5	0.18	-0.03
P02452	Collagen alpha-1(I) chain GN=COL1A1 PE=1 SV=5	1.88	0.32
G3XAI2	Laminin subunit beta-1 GN=LAMB1 PE=1 SV=1	0.28	0.08
P08254	Stromelysin-1 GN=MMP3 PE=1 SV=2	0.17	-0.06
C9JD84	Latent-transforming growth factor beta-binding protein 1 GN=LTBP1 PE=1 SV=1	2.53	0.43
P12110	Collagen alpha-2(VI) chain GN=COL6A2 PE=1 SV=4	0.22	0.07
P13639	Elongation factor 2 GN=EEF2 PE=1 SV=4	0.32	0.07
P08238	Heat shock protein HSP 90-beta GN=HSP90AB1 PE=1 SV=4	0.12	-0.04
V9HWE1	Epididymis luminal protein 113 GN=HEL113 PE=2 SV=1	2.55	0.25
P07996	Thrombospondin-1 GN=THBS1 PE=1 SV=2	0.36	-0.09
O43707	Alpha-actinin-4 GN=ACTN4 PE=1 SV=2	0.22	-0.08
P08253	72 kDa type IV collagenase GN=MMP2 PE=1 SV=2	0.05	0.02
P35579	Myosin-9 GN=MYH9 PE=1 SV=4	1.53	0.18
A0A024R498	Serpin peptidase inhibitor, clade E (Nexin, plasminogen activator inhibitor type 1), member 2, isoform CRA_b GN=SERPINE2 PE=3 SV=1	2.06	0.44
P02545	Prelamin-A/C GN=LMNA PE=1 SV=1	2.11	0.21
P35556	Fibrillin-2 GN=FBN2 PE=1 SV=3	1.43	0.25
Q15149	Plectin GN=PLEC PE=1 SV=3	0.37	0.05
A0A024QYT5	Serpin peptidase inhibitor, clade E (Nexin, plasminogen activator inhibitor type 1), member 1, isoform CRA_b GN=SERPINE1 PE=3 SV=1	1.80	-0.97
A0A0A0MQS9	Laminin subunit alpha-4 GN=LAMA4 PE=1 SV=1	0.48	0.10
V9HWB8	Pyruvate kinase GN=HEL-S-30 PE=1 SV=1	0.27	0.05
A0A024R718	Pre-B-cell colony enhancing factor 1, isoform CRA_a GN=PBEF1 PE=4 SV=1	0.02	0.01
B2R7Y0	cDNA, FLJ93654, highly similar to Homo sapiens serpin peptidase inhibitor, clade B (ovalbumin), member 2 (SERPINB2), mRNA PE=2 SV=1	0.32	-0.10
P35555	Fibrillin-1 GN=FBN1 PE=1 SV=3	0.76	0.16
D3DTX7	Collagen, type I, alpha 1, isoform CRA_a GN=COL1A1 PE=4 SV=1	0.33	0.10
P05120	Plasminogen activator inhibitor 2 GN=SERPINB2 PE=1 SV=2	0.27	-0.13
V9HWK2	Epididymis luminal protein 114 GN=HEL114 PE=2 SV=1	0.30	-0.09
V9HW88	Calreticulin, isoform CRA_b GN=HEL-S-99n PE=2 SV=1	0.51	0.07
Q59EN5	Prosaposin variant (Fragment) PE=2 SV=1	1.02	0.17
O00391	Sulfhydryl oxidase 1 GN=QSOX1 PE=1 SV=3	0.04	0.01
E7EUF1	Ectonucleotide pyrophosphatase/phosphodiesterase family member 2 GN=ENPP2 PE=1 SV=1	0.17	-0.05
V9HW80	Epididymis luminal protein 220 GN=HEL-S-70 PE=1 SV=1	0.22	0.05
Q59E93	Aminopeptidase (Fragment) PE=2 SV=1	0.65	-0.19

Q12841	Follistatin-related protein 1 GN=FSTL1 PE=1 SV=1	2.25	0.30
P00558	Phosphoglycerate kinase 1 GN=PGK1 PE=1 SV=3	0.35	-0.09
P34932	Heat shock 70 kDa protein 4 GN=HSPA4 PE=1 SV=4	0.10	0.02
A0A0S2Z3Y1	Lectin galactoside-binding soluble 3 binding protein isoform 1 (Fragment) GN=LGALS3BP PE=2 SV=1	0.18	0.07
P19338	Nucleolin GN=NCL PE=1 SV=3	1.41	-0.45
V9HWD6	Epididymis secretory protein Li 1 GN=HEL-S-1 PE=2 SV=1	0.11	0.03
Q53G35	Phosphoglycerate mutase (Fragment) PE=2 SV=1	0.56	-0.13
P26038	Moesin GN=MSN PE=1 SV=3	0.37	-0.09
P60174	Triosephosphate isomerase GN=TPI1 PE=1 SV=3	0.48	0.11
P05231	Interleukin-6 GN=IL6 PE=1 SV=1	0.55	0.14
B5BUB5	Autoantigen La (Fragment) GN=SSB PE=2 SV=1	1.20	0.10
P63104	14-3-3 protein zeta/delta GN=YWHAZ PE=1 SV=1	0.02	0.01
Q15113	Procollagen C-endopeptidase enhancer 1 GN=PCOLCE PE=1 SV=2	0.06	0.02
P62258	14-3-3 protein epsilon GN=YWHAE PE=1 SV=1	0.11	0.04
Q8N1C8	HSPA9 protein (Fragment) GN=HSPA9 PE=2 SV=1	0.27	0.06
Q53EM5	Transketolase variant (Fragment) PE=2 SV=1	0.04	-0.01
P68104	Elongation factor 1-alpha 1 GN=EEF1A1 PE=1 SV=1	0.68	0.11
P35442	Thrombospondin-2 GN=THBS2 PE=1 SV=2	1.22	0.27
E9PK54	Heat shock cognate 71 kDa protein (Fragment) GN=HSPA8 PE=1 SV=8	0.56	0.07
A0A0C4DFU2	Superoxide dismutase GN=SOD2 PE=1 SV=1	0.16	-0.05
P23142	Fibulin-1 GN=FBLN1 PE=1 SV=4	0.95	0.20
P30101	Protein disulfide-isomerase A3 GN=PDIA3 PE=1 SV=4	0.21	-0.06
A0A0G2JIW1	Heat shock 70 kDa protein 1B GN=HSPA1B PE=1 SV=1	0.12	-0.02
P14625	Endoplasmin GN=HSP90B1 PE=1 SV=1	0.64	-0.12
P02461	Collagen alpha-1(III) chain GN=COL3A1 PE=1 SV=4	3.86	0.61
P51858	Hepatoma-derived growth factor GN=HDGF PE=1 SV=1	1.85	0.18
P68363	Tubulin alpha-1B chain GN=TUBA1B PE=1 SV=1	1.25	0.16
D3YTG3	Target of Nesh-SH3 GN=ABI3BP PE=1 SV=1	0.23	-0.08
P48307	Tissue factor pathway inhibitor 2 GN=TFPI2 PE=1 SV=1	1.48	0.31
P49321	Nuclear autoantigenic sperm protein GN=NASP PE=1 SV=2	1.95	0.17
A8K3K1	cDNA FLJ78096, highly similar to Homo sapiens actin, alpha, cardiac muscle (ACTC), mRNA PE=2 SV=1	0.26	0.05
A0A024R8S5	Protein disulfide-isomerase GN=P4HB PE=2 SV=1	0.24	0.07
A8K7Q1	cDNA FLJ77770, highly similar to Homo sapiens nucleobindin 1 (NUCB1), mRNA PE=2 SV=1	2.40	0.29
P04406	Glyceraldehyde-3-phosphate dehydrogenase GN=GAPDH PE=1 SV=3	1.21	0.18
P26022	Pentraxin-related protein PTX3 GN=PTX3 PE=1 SV=3	0.73	-0.27
D3DQH8	Secreted protein, acidic, cysteine-rich (Osteonectin), isoform CRA_a GN=SPARC PE=4 SV=1	2.54	0.41
B4DUV1	Fibulin-1 PE=2 SV=1	1.09	0.17
B2R983	cDNA, FLJ94267, highly similar to Homo sapiens glutathione S-transferase omega 1 (GSTO1), mRNA PE=2 SV=1	0.04	0.01
P67936	Tropomyosin alpha-4 chain GN=TPM4 PE=1 SV=3	2.41	0.19
J3KPS3	Fructose-bisphosphate aldolase GN=ALDOA PE=1 SV=1	0.28	-0.07
B2R6I6	cDNA, FLJ92965, highly similar to Homo sapiens stanniocalcin 1 (STC1), mRNA PE=2 SV=1	1.53	-0.55
P00338	L-lactate dehydrogenase A chain GN=LDHA PE=1 SV=2	0.30	0.12
P19883	Follistatin GN=FST PE=1 SV=2	2.76	0.55
E9PK25	Cofilin-1 GN=CFL1 PE=1 SV=1	1.47	0.20
O00299	Chloride intracellular channel protein 1 GN=CLIC1 PE=1 SV=4	0.58	0.12
A0A024R374	Cathepsin B, isoform CRA_a GN=CTSB PE=3 SV=1	0.79	0.17
Q5TA02	Glutathione S-transferase omega-1 (Fragment) GN=GSTO1 PE=1 SV=1	0.38	0.13
B4DPQ0	Complement C1r subcomponent GN=C1R PE=1 SV=1	0.66	0.12
A0A140VJC8	Testicular tissue protein Li 2 PE=2 SV=1	0.65	0.12
Q16610	Extracellular matrix protein 1 GN=ECM1 PE=1 SV=2	0.80	0.16
P61981	14-3-3 protein gamma GN=YWHAG PE=1 SV=2	0.01	0.00
P22626	Heterogeneous nuclear ribonucleoproteins A2/B1 GN=HNRNPA2B1 PE=1 SV=2	2.95	0.24

A0A0S2Z4G4	Tropomyosin 3 isoform 1 (Fragment) GN=TPM3 PE=2 SV=1	1.78	0.20
Q5U077	L-lactate dehydrogenase GN=LDHB PE=2 SV=1	0.91	0.19
P26641	Elongation factor 1-gamma GN=EEF1G PE=1 SV=3	0.08	-0.02
Q14112	Nidogen-2 GN=NID2 PE=1 SV=3	0.68	0.17
B4DTH2	cDNA FLJ61165, highly similar to Fibronectin PE=2 SV=1	0.03	-0.01
P27348	14-3-3 protein theta GN=YWHAQ PE=1 SV=1	0.26	0.06
B3KQF4	cDNA FLJ90373 fis, clone NT2RP2004606, highly similar to Metalloproteinase inhibitor 1 PE=2 SV=1	0.67	0.19
P07737	Profilin-1 GN=PFN1 PE=1 SV=2	1.26	0.29
A0A024R1N4	X-ray repair complementing defective repair in Chinese hamster cells 6 (Ku autoantigen, 70kDa), isoform CRA_a GN=XRCC6 PE=4 SV=1	0.82	0.10
A0A024R1A3	Testicular secretory protein Li 63 GN=UBE1 PE=2 SV=1	0.10	0.03
P15121	Aldose reductase GN=AKR1B1 PE=1 SV=3	0.22	-0.05
Q32Q12	Nucleoside diphosphate kinase GN=NME1-NME2 PE=1 SV=1	0.26	0.05
B4DLV7	Rab GDP dissociation inhibitor PE=2 SV=1	0.37	-0.09
P80723	Brain acid soluble protein 1 GN=BASP1 PE=1 SV=2	0.68	0.09
Q16658	Fascin GN=FSCN1 PE=1 SV=3	0.00	0.00
A0A0D9SF54	Spectrin alpha chain, non-erythrocytic 1 GN=SPTAN1 PE=1 SV=1	0.48	0.15
A0A024RAZ7	Heterogeneous nuclear ribonucleoprotein A1, isoform CRA_b GN=HNRPA1 PE=4 SV=1	2.22	0.22
A0A024R4K3	Malate dehydrogenase GN=MDH2 PE=2 SV=1	0.13	0.03
V9HW31	ATP synthase subunit beta GN=HEL-S-271 PE=1 SV=1	1.59	0.24
P25786	Proteasome subunit alpha type-1 GN=PSMA1 PE=1 SV=1	2.41	0.26
Q9P2E9	Ribosome-binding protein 1 GN=RRBP1 PE=1 SV=4	0.40	0.06
Q6IAW5	CALU protein GN=CALU PE=2 SV=1	2.82	0.31
A0A024R755	Calumenin, isoform CRA_a GN=CALU PE=4 SV=1	2.64	0.28
A0A140VK56	Transaldolase PE=2 SV=1	0.52	-0.13
Q09666	Neuroblast differentiation-associated protein AHNAK GN=AHNAK PE=1 SV=2	2.38	0.34
P27695	DNA-(apurinic or apyrimidinic site) lyase GN=APEX1 PE=1 SV=2	0.66	-0.09
A0A0A0MTS2	Glucose-6-phosphate isomerase (Fragment) GN=GPI PE=1 SV=1	0.34	-0.09
B4DJ30	cDNA FLJ61290, highly similar to Neutral alpha-glucosidase AB PE=2 SV=1	0.75	-0.13
B7ZKY6	Membrane metallo-endopeptidase GN=MME PE=2 SV=1	1.17	-0.11
A8K7F6	cDNA FLJ78244, highly similar to Homo sapiens eukaryotic translation initiation factor 4A, isoform 1 (EIF4A1), mRNA PE=2 SV=1	0.18	0.03
F4ZW66	NF110b PE=2 SV=1	0.05	0.01
A0A024RB85	Proliferation-associated 2G4, 38kDa, isoform CRA_a GN=PA2G4 PE=4 SV=1	0.11	0.02
A0A0C4DGB5	Calpastatin GN=CAST PE=1 SV=1	2.69	0.17
P48594	Serpin B4 GN=SERPINB4 PE=1 SV=2	0.22	-0.08
E7EQR4	Ezrin GN=EZR PE=1 SV=3	0.74	0.11
Q9Y4L1	Hypoxia up-regulated protein 1 GN=HYOU1 PE=1 SV=1	0.50	-0.16
Q03252	Lamin-B2 GN=LMNB2 PE=1 SV=4	1.65	0.19
P09936	Ubiquitin carboxyl-terminal hydrolase isozyme L1 GN=UCHL1 PE=1 SV=2	0.51	0.10
D3DQ70	SERPINE1 mRNA binding protein 1, isoform CRA_d GN=SERBP1 PE=4 SV=1	1.34	0.24
A0A087WVQ6	Clathrin heavy chain GN=CLTC PE=1 SV=1	0.20	0.06
P20700	Lamin-B1 GN=LMNB1 PE=1 SV=2	2.06	0.26
A0A0S2Z491	Nucleophosmin isoform 2 (Fragment) GN=NPM1 PE=2 SV=1	1.00	-0.26
P13010	X-ray repair cross-complementing protein 5 GN=XRCC5 PE=1 SV=3	0.45	0.04
P37802	Transgelin-2 GN=TAGLN2 PE=1 SV=3	0.99	0.15
E7EMB3	Calmodulin-2 GN=CALM2 PE=1 SV=1	0.32	0.04
A0A024RDB4	Heterogeneous nuclear ribonucleoprotein D (AU-rich element RNA binding protein 1, 37kDa), isoform CRA_c GN=HNRPD PE=4 SV=1	3.02	0.32
P39687	Acidic leucine-rich nuclear phosphoprotein 32 family member A GN=ANP32A PE=1 SV=1	1.04	-0.16
A8K690	cDNA FLJ76863, highly similar to Homo sapiens stress-induced-phosphoprotein 1 (Hsp70/Hsp90-organizing protein) (STIP1), mRNA PE=2 SV=1	1.78	0.21
P28799	Granulins GN=GRN PE=1 SV=2	1.65	0.23
J3KQ32	Obg-like ATPase 1 GN=OLA1 PE=1 SV=1	0.41	-0.09
P19876	C-X-C motif chemokine 3 GN=CXCL3 PE=1 SV=1	3.18	0.74

A0A024R1K7	Tyrosine 3-monooxygenase/tryptophan 5-monooxygenase activation protein, eta polypeptide, isoform CRA_b GN=YWHAH PE=3 SV=1	0.31	0.04
P09382	Galectin-1 GN=LGALS1 PE=1 SV=2	2.91	0.24
B4DJQ5	cDNA FLJ59211, highly similar to Glucosidase 2 subunit beta PE=2 SV=1	0.96	0.14
A0A024R895	SET translocation (Myeloid leukemia-associated), isoform CRA_b GN=SET PE=3 SV=1	0.99	-0.21
P67809	Nuclease-sensitive element-binding protein 1 GN=YBX1 PE=1 SV=3	1.29	0.07
Q99715	Collagen alpha-1(XII) chain GN=COL12A1 PE=1 SV=2	0.04	-0.01
O94985	Calsyntenin-1 GN=CLSTN1 PE=1 SV=1	0.01	0.00
A4QPB0	IQ motif containing GTPase activating protein 1 GN=IQGAP1 PE=1 SV=1	0.29	0.04
P14543	Nidogen-1 GN=NID1 PE=1 SV=3	0.68	0.17
Q5U0B9	Stem cell growth factor;lymphocyte secreted C-type lectin PE=2 SV=1	0.78	-0.09
P15531	Nucleoside diphosphate kinase A GN=NME1 PE=1 SV=1	0.28	-0.11
P12004	Proliferating cell nuclear antigen GN=PCNA PE=1 SV=1	0.82	0.13
A0A024R4H0	Procollagen-lysine 1, 2-oxoglutarate 5-dioxygenase 1, isoform CRA_a GN=PLOD1 PE=4 SV=1	1.29	-0.50
Q14767	Latent-transforming growth factor beta-binding protein 2 GN=LTBP2 PE=1 SV=3	1.72	0.18
P49767	Vascular endothelial growth factor C GN=VEGFC PE=1 SV=1	0.99	0.19
Q9Y4K0	Lysyl oxidase homolog 2 GN=LOXL2 PE=1 SV=1	2.18	-0.83
Q00888	Pregnancy-specific beta-1-glycoprotein 4 GN=PSG4 PE=2 SV=3	0.33	-0.08
B4DJQ8	cDNA FLJ55694, highly similar to Dipeptidyl-peptidase 1 (EC 3.4.14.1) PE=2 SV=1	2.34	0.58
P25789	Proteasome subunit alpha type-4 GN=PSMA4 PE=1 SV=1	1.63	0.19
P61604	10 kDa heat shock protein, mitochondrial GN=HSPE1 PE=1 SV=2	2.29	0.18
A8K7T0	Kynureninase GN=KYNU PE=2 SV=1	0.00	0.00
B0YJ88	Radixin GN=RDX PE=2 SV=1	1.45	0.14
Q92626	Peroxidasin homolog GN=PXDN PE=1 SV=2	0.35	0.10
A0A0K0K1K4	Proteasome subunit alpha type GN=HEL-S-276 PE=2 SV=1	1.66	0.20
P23284	Peptidyl-prolyl cis-trans isomerase B GN=PPIB PE=1 SV=2	1.36	0.15
P31150	Rab GDP dissociation inhibitor alpha GN=GDI1 PE=1 SV=2	0.05	-0.01
Q53F64	Heterogeneous nuclear ribonucleoprotein AB isoform a variant (Fragment) PE=2 SV=1	1.99	0.24
P07437	Tubulin beta chain GN=TUBB PE=1 SV=2	0.33	0.10
P13667	Protein disulfide-isomerase A4 GN=PDIA4 PE=1 SV=2	1.39	-0.25
A0A024R962	HCG40889, isoform CRA_b GN=hCG_40889 PE=4 SV=1	0.97	0.18
Q92688	Acidic leucine-rich nuclear phosphoprotein 32 family member B GN=ANP32B PE=1 SV=1	0.79	-0.09
P68371	Tubulin beta-4B chain GN=TUBB4B PE=1 SV=1	0.07	0.01
B2R8Z8	cDNA, FLJ94136, highly similar to Homo sapiens synaptotagmin binding, cytoplasmic RNA interacting protein (SYNCRIP), mRNA PE=2 SV=1	0.41	0.11
V9HWC7	Epididymis secretory sperm binding protein Li 128m GN=HEL-S-128m PE=2 SV=1	0.03	0.01
P16035	Metalloproteinase inhibitor 2 GN=TIMP2 PE=1 SV=2	2.03	0.34
Q01469	Fatty acid-binding protein, epidermal GN=FABP5 PE=1 SV=3	0.50	0.16
P07585	Decorin GN=DCN PE=1 SV=1	1.25	0.34
B8ZWD9	Diazepam binding inhibitor, splice form 1D(2) GN=DBI PE=2 SV=1	1.50	0.13
Q15293	Reticulocalbin-1 GN=RCN1 PE=1 SV=1	2.63	0.29
A0A024R9J4	Nephroblastoma overexpressed gene, isoform CRA_a GN=NOV PE=4 SV=1	3.22	0.55
Q9Y266	Nuclear migration protein nudC GN=NUDC PE=1 SV=1	0.10	-0.02
Q59FF0	EBNA-2 co-activator variant (Fragment) PE=2 SV=1	0.39	0.07
Q13185	Chromobox protein homolog 3 GN=CBX3 PE=1 SV=4	0.58	0.09
P06899	Histone H2B type 1-J GN=HIST1H2BJ PE=1 SV=3	0.01	0.00
P16403	Histone H1.2 GN=HIST1H1C PE=1 SV=2	1.67	0.31
B4DR52	Histone H2B PE=2 SV=1	0.22	0.08
B2R9U2	Peptidylprolyl isomerase PE=2 SV=1	0.04	0.01
V9HWH9	Protein S100 GN=HEL-S-43 PE=2 SV=1	0.73	0.09
P20618	Proteasome subunit beta type-1 GN=PSMB1 PE=1 SV=2	1.02	0.18
Q99497	Protein DJ-1 GN=PARK7 PE=1 SV=2	1.38	0.22
B3KT93	Polyadenylate-binding protein PE=2 SV=1	0.02	0.01
Q16270	Insulin-like growth factor-binding protein 7 GN=IGFBP7 PE=1 SV=1	3.07	0.50
P62805	Histone H4 GN=HIST1H4A PE=1 SV=2	0.18	0.07
Q5EC54	Heterogeneous nuclear ribonucleoprotein K transcript variant GN=HNRPK PE=2 SV=1	1.51	0.22

B7Z6Z4	Myosin light polypeptide 6 GN=MYL6 PE=1 SV=1	2.56	0.36
A3R0T7	Liver histone H1e PE=2 SV=1	0.97	0.26
P21291	Cysteine and glycine-rich protein 1 GN=CSRP1 PE=1 SV=3	1.59	0.15
O76061	Stanniocalcin-2 GN=STC2 PE=1 SV=1	1.54	-0.38
E9KL48	Epididymis tissue sperm binding protein Li 18mP GN=GLUD1 PE=2 SV=1	0.36	0.08
A0A140VJW2	Stathmin PE=2 SV=1	1.28	0.13
J3KQE5	GTP-binding nuclear protein Ran (Fragment) GN=RAN PE=1 SV=1	0.59	0.08
P63241	Eukaryotic translation initiation factor 5A-1 GN=EIF5A PE=1 SV=2	1.86	0.24
V9HW62	Lactoylglutathione lyase GN=HEL-S-74 PE=2 SV=1	0.11	0.03
P23526	Adenosylhomocysteinase GN=AHCY PE=1 SV=4	0.02	0.00
Q14566	DNA replication licensing factor MCM6 GN=MCM6 PE=1 SV=1	0.91	0.11
E7EVA0	Microtubule-associated protein GN=MAP4 PE=1 SV=1	1.07	0.10
A0A1S5UZ07	Talin-1 GN=TLN1 PE=2 SV=1	0.58	0.10
P40925	Malate dehydrogenase, cytoplasmic GN=MDH1 PE=1 SV=4	0.19	-0.06
B2RBR9	cDNA, FLJ95650, highly similar to Homo sapiens karyopherin (importin) beta 1 (KPNB1), mRNA PE=2 SV=1	0.58	0.15
Q59ER5	WD repeat-containing protein 1 isoform 1 variant (Fragment) PE=2 SV=1	0.10	-0.03
A0A024R1A4	Ubiquitin-conjugating enzyme E2L 3, isoform CRA_a GN=UBE2L3 PE=3 SV=1	2.27	0.18
A0A087WTP3	Far upstream element-binding protein 2 GN=KHSRP PE=1 SV=1	1.95	0.22
Q15691	Microtubule-associated protein RP/EB family member 1 GN=MAPRE1 PE=1 SV=3	0.56	0.10
Q9BTY2	Plasma alpha-L-fucosidase GN=FUCA2 PE=1 SV=2	0.14	0.06
Q9BRK5	45 kDa calcium-binding protein GN=SDF4 PE=1 SV=1	1.41	0.17
P68431	Histone H3.1 GN=HIST1H3A PE=1 SV=2	0.03	0.01
A0A024R319	Laminin, beta 2 (Laminin S), isoform CRA_a GN=LAMB2 PE=4 SV=1	0.81	-0.34
M1VKI3	Tyrosine-protein kinase receptor GN=SDC4-ROS1_S4;R32 PE=2 SV=1	3.21	-0.97
Q6YHK3	CD109 antigen GN=CD109 PE=1 SV=2	0.04	-0.01
A0A140VJT8	Testicular tissue protein Li 164 PE=2 SV=1	0.31	-0.06
Q15084	Protein disulfide-isomerase A6 GN=PDIA6 PE=1 SV=1	0.35	0.04
A0A109NGN6	Proteasome subunit alpha type PE=2 SV=1	1.82	0.28
P23246	Splicing factor, proline- and glutamine-rich GN=SFPQ PE=1 SV=2	1.50	0.19
O60361	Putative nucleoside diphosphate kinase GN=NME2P1 PE=5 SV=1	0.82	0.05
A0A0B4J2C3	Translationally-controlled tumor protein GN=TPT1 PE=1 SV=1	1.60	0.22
P52907	F-actin-capping protein subunit alpha-1 GN=CAPZA1 PE=1 SV=3	0.06	-0.03
A5PLM9	Cathepsin L1 GN=CTSL1 PE=2 SV=1	0.33	0.09
P29966	Myristoylated alanine-rich C-kinase substrate GN=MARCKS PE=1 SV=4	0.85	0.07
A0A024R3W7	Eukaryotic translation elongation factor 1 beta 2, isoform CRA_a GN=EEF1B2 PE=3 SV=1	2.18	0.28
P09341	Growth-regulated alpha protein GN=CXCL1 PE=1 SV=1	3.40	0.78
P11717	Cation-independent mannose-6-phosphate receptor GN=IGF2R PE=1 SV=3	0.06	-0.01
E9PAV3	Nascent polypeptide-associated complex subunit alpha, muscle-specific form GN=NACA PE=1 SV=1	1.36	0.17
P16070	CD44 antigen GN=CD44 PE=1 SV=3	1.92	0.17
Q549N0	Cofilin 2 (Muscle), isoform CRA_a GN=CFL2 PE=1 SV=1	0.06	-0.03
B2R7W4	cDNA, FLJ93632, highly similar to Homo sapiens heterogeneous nuclear ribonucleoprotein R (HNRPR), mRNA PE=2 SV=1	0.07	0.02
P25788	Proteasome subunit alpha type-3 GN=PSMA3 PE=1 SV=2	1.89	0.29
A0A0B4U5E3	Granulocyte-colony stimulating factor (Fragment) PE=2 SV=1	1.16	0.25
P42830	C-X-C motif chemokine 5 GN=CXCL5 PE=1 SV=1	1.87	0.45
F4ZW62	NF45 PE=1 SV=1	0.32	-0.09
O00622	Protein CYR61 GN=CYR61 PE=1 SV=1	0.36	0.09
P52209	6-phosphogluconate dehydrogenase, decarboxylating GN=PGD PE=1 SV=3	0.67	0.16
O43493	Trans-Golgi network integral membrane protein 2 GN=TGOLN2 PE=1 SV=2	3.27	0.19
P04083	Annexin A1 GN=ANXA1 PE=1 SV=2	0.20	-0.04
B1AK88	Capping protein (Actin filament) muscle Z-line, beta, isoform CRA_d GN=CAPZB PE=1 SV=1	0.21	-0.07
P41250	Glycine--tRNA ligase GN=GARS PE=1 SV=3	0.35	0.09
P06703	Protein S100-A6 GN=S100A6 PE=1 SV=1	1.10	0.11
A2RUM7	Ribosomal protein L5 GN=RPL5 PE=2 SV=1	0.32	0.05

A0A087WSV8	Nucleobindin 2, isoform CRA_b GN=NUCB2 PE=1 SV=1	3.29	0.27
O00468	Agrin GN=AGRN PE=1 SV=5	0.23	0.09
A8K9A4	cDNA FLJ75154, highly similar to Homo sapiens heterogeneous nuclear ribonucleoprotein C (C1/C2), mRNA PE=2 SV=1	1.33	0.11
A0A024QZS4	Peptidyl-prolyl cis-trans isomerase GN=PPIF PE=3 SV=1	1.60	0.24
A0A024R6W0	Aspartate aminotransferase GN=GOT2 PE=4 SV=1	1.55	0.11
G3V5Z7	Proteasome subunit alpha type GN=PSMA6 PE=1 SV=1	0.72	0.13
A0A024RDD9	C-X-C motif chemokine GN=CXCL2 PE=3 SV=1	2.63	0.64
P16402	Histone H1.3 GN=HIST1H1D PE=1 SV=2	0.61	0.13
P07686	Beta-hexosaminidase subunit beta GN=HEXB PE=1 SV=3	1.26	0.16
P16401	Histone H1.5 GN=HIST1H1B PE=1 SV=3	0.67	0.15
A8K4B1	cDNA FLJ77984, highly similar to Homo sapiens serpin peptidase inhibitor, clade B (ovalbumin), member 7 (SERPINB7), mRNA PE=2 SV=1	0.63	-0.20
A8K651	cDNA FLJ75700, highly similar to Homo sapiens complement component 1, q subcomponent binding protein (C1QBP), nuclear gene encoding mitochondrial protein, mRNA PE=2 SV=1	0.99	0.08
Q06481	Amyloid-like protein 2 GN=APLP2 PE=1 SV=2	0.54	-0.10
Q16531	DNA damage-binding protein 1 GN=DDB1 PE=1 SV=1	1.77	0.16
A0A0C4DG17	40S ribosomal protein SA GN=RPSA PE=1 SV=1	1.03	0.19
B7Z8Z6	DNA helicase PE=2 SV=1	0.16	0.06
Q4W4Y1	Dopamine receptor interacting protein 4 GN=DRIP4 PE=2 SV=1	0.03	-0.01
A8K2N0	cDNA FLJ77835, highly similar to Homo sapiens complement component 1, s subcomponent (C1S), transcript variant 2, mRNA PE=2 SV=1	0.95	0.16
E5RJD8	Tubulin-specific chaperone A GN=TBCA PE=1 SV=1	1.99	0.11
P24592	Insulin-like growth factor-binding protein 6 GN=IGFBP6 PE=1 SV=1	1.95	0.24
B2RDY9	Adenylyl cyclase-associated protein PE=2 SV=1	0.23	0.05
Q07954	Prolow-density lipoprotein receptor-related protein 1 GN=LRP1 PE=1 SV=2	0.02	0.01
Q6FIC5	Chloride intracellular channel protein GN=CLIC4 PE=2 SV=1	0.04	0.01
A8K329	cDNA FLJ76656, highly similar to Homo sapiens scaffold attachment factor B (SAFB), mRNA PE=2 SV=1	1.93	0.17
P30044	Peroxiredoxin-5, mitochondrial GN=PRDX5 PE=1 SV=4	0.54	0.16
Q9Y2J2	Band 4.1-like protein 3 GN=EPB41L3 PE=1 SV=2	1.14	0.16
A8K7E0	cDNA FLJ76911, highly similar to Homo sapiens biglycan (BGN), mRNA PE=2 SV=1	0.80	0.18
B2R5M8	Isocitrate dehydrogenase [NADP] PE=2 SV=1	0.86	-0.17
P05387	60S acidic ribosomal protein P2 GN=RPLP2 PE=1 SV=1	0.17	0.05
Q15582	Transforming growth factor-beta-induced protein ig-h3 GN=TGFBI PE=1 SV=1	0.26	-0.08
P02795	Metallothionein-2 GN=MT2A PE=1 SV=1	0.77	0.16
P54727	UV excision repair protein RAD23 homolog B GN=RAD23B PE=1 SV=1	1.26	0.51
P30050	60S ribosomal protein L12 GN=RPL12 PE=1 SV=1	0.05	0.00
P28074	Proteasome subunit beta type-5 GN=PSMB5 PE=1 SV=3	0.93	0.19
Q14019	Coactosin-like protein GN=COTL1 PE=1 SV=3	0.13	0.04
P16152	Carbonyl reductase [NADPH] 1 GN=CBR1 PE=1 SV=3	0.26	-0.07
O00469	Procollagen-lysine,2-oxoglutarate 5-dioxygenase 2 GN=PLOD2 PE=1 SV=2	1.08	-0.34
G3V3D1	Epididymal secretory protein E1 (Fragment) GN=NPC2 PE=1 SV=1	1.85	0.30
A0A024R713	Dihydrolipoyl dehydrogenase GN=DLD PE=3 SV=1	0.70	0.11
Q96CG8	Collagen triple helix repeat-containing protein 1 GN=CTHRC1 PE=1 SV=1	0.73	-0.19
Q59EA2	Coronin (Fragment) PE=2 SV=1	0.37	-0.06
P52926	High mobility group protein HMGI-C GN=HMGA2 PE=1 SV=1	0.74	-0.14
O14786	Neuropilin-1 GN=NRP1 PE=1 SV=3	0.19	-0.07
A8K3S1	Glucosamine-6-phosphate isomerase PE=2 SV=1	0.08	-0.02
Q6LAF9	Cathepsin B (Fragment) PE=2 SV=1	0.77	-0.23
P07205	Phosphoglycerate kinase 2 GN=PGK2 PE=1 SV=3	0.11	-0.04
A0A024R5Z7	Annexin GN=ANXA2 PE=3 SV=1	2.55	-0.28
B2R6S5	UMP-CMP kinase GN=CMPK PE=2 SV=1	0.07	-0.03
O60568	Procollagen-lysine,2-oxoglutarate 5-dioxygenase 3 GN=PLOD3 PE=1 SV=1	1.38	-0.22
Q9UKY7	Protein CDV3 homolog GN=CDV3 PE=1 SV=1	1.94	0.26
A0A024RA52	Proteasome subunit alpha type GN=PSMA2 PE=1 SV=1	1.50	0.20

O75369	Filamin-B GN=FLNB PE=1 SV=2	0.91	0.21
P26639	Threonine--tRNA ligase, cytoplasmic GN=TARS PE=1 SV=3	0.97	0.15
Q6FI13	Histone H2A type 2-A GN=HIST2H2AA3 PE=1 SV=3	0.29	0.10
P16188	HLA class I histocompatibility antigen, A-30 alpha chain GN=HLA-A PE=1 SV=2	3.16	0.15
H0YMD1	Low-density lipoprotein receptor GN=LDLR PE=1 SV=1	0.68	0.07
O15460	Prolyl 4-hydroxylase subunit alpha-2 GN=P4HA2 PE=1 SV=1	0.44	-0.16
B2ZZ86	Collagen type V alpha 1 GN=COL5A1 PE=2 SV=1	0.19	0.06
V9HW37	Epididymis secretory protein Li 69 GN=HEL-S-69 PE=1 SV=1	0.00	0.00
Q6IQ30	Polyadenylate-binding protein GN=PABPC4 PE=2 SV=1	0.39	0.12
B3KXY9	cDNA FLJ46359 fis, clone TESTI4049786, highly similar to Hexokinase-1 (EC 2.7.1.1) PE=2 SV=1	0.41	0.12
Q4LE64	NUMA1 variant protein (Fragment) GN=NUMA1 variant protein PE=2 SV=1	0.86	0.18
P07954	Fumarate hydratase, mitochondrial GN=FH PE=1 SV=3	0.77	0.13
P55060	Exportin-2 GN=CSE1L PE=1 SV=3	0.29	0.10
A0A0K0K1J1	Cystatin GN=HEL-S-2 PE=2 SV=1	2.50	0.37
J3QQX2	Rho GDP-dissociation inhibitor 1 GN=ARHGDIA PE=1 SV=1	0.56	0.10
Q9UNN8	Endothelial protein C receptor GN=PROCR PE=1 SV=1	0.26	0.11
V9HWA6	Epididymis luminal protein 32 GN=HEL32 PE=2 SV=1	1.38	0.13
A8K8F0	cDNA FLJ76436 PE=2 SV=1	0.32	0.08
P49720	Proteasome subunit beta type-3 GN=PSMB3 PE=1 SV=2	0.17	0.03
Q8N7G1	Purine nucleoside phosphorylase PE=2 SV=1	0.22	0.05
A8K335	cDNA FLJ76254, highly similar to Homo sapiens gamma-glutamyl hydrolase (GGH), mRNA PE=2 SV=1	0.41	0.09
A0A140VKA6	Testis secretory sperm-binding protein Li 233m PE=2 SV=1	0.01	0.00
A0A024RBB7	Nucleosome assembly protein 1-like 1, isoform CRA_a GN=NAP1L1 PE=3 SV=1	0.25	0.03
A0A023T6R1	Mago nashi protein GN=FLJ10292 PE=2 SV=1	0.14	-0.03
P50990	T-complex protein 1 subunit theta GN=CCT8 PE=1 SV=4	0.13	0.03
E9PRY8	Elongation factor 1-delta GN=EEF1D PE=1 SV=1	0.64	0.17
B2RDF5	cDNA, FLJ96587, highly similar to Homo sapiens SUMO-1 activating enzyme subunit 2 (UBA2), mRNA PE=2 SV=1	0.31	-0.06
A0A024R7B7	CDC37 cell division cycle 37 homolog (S. cerevisiae), isoform CRA_a GN=CDC37 PE=4 SV=1	0.61	0.12
O75390	Citrate synthase, mitochondrial GN=CS PE=1 SV=2	0.28	-0.07
P52888	Thimet oligopeptidase GN=THOP1 PE=1 SV=2	0.38	-0.12
Q76LA1	CSTB protein GN=CSTB PE=2 SV=1	1.70	0.19
X6R8A1	Carboxypeptidase GN=CTSA PE=1 SV=1	0.62	0.14
P54819	Adenylate kinase 2, mitochondrial GN=AK2 PE=1 SV=2	0.54	0.11
A0A0S2Z4Z9	Non-POU domain containing octamer-binding isoform 1 (Fragment) GN=NONO PE=2 SV=1	0.67	0.10
A6XND9	Beta-2-microglobulin PE=2 SV=1	2.77	0.47
P15018	Leukemia inhibitory factor GN=LIF PE=1 SV=1	0.07	0.03
Q9BY76	Angiopoietin-related protein 4 GN=ANGPTL4 PE=1 SV=2	2.98	-1.30
B4DIV8	cDNA FLJ56402, highly similar to Tripeptidyl-peptidase 1 (EC 3.4.14.9) PE=2 SV=1	0.99	0.26
P25391	Laminin subunit alpha-1 GN=LAMA1 PE=1 SV=2	0.05	-0.01
Q13838	Spliceosome RNA helicase DDX39B GN=DDX39B PE=1 SV=1	0.00	0.00
A0A140VK69	Aspartate aminotransferase PE=2 SV=1	0.05	0.01
P04141	Granulocyte-macrophage colony-stimulating factor GN=CSF2 PE=1 SV=1	1.66	-0.43
B4DRM3	cDNA FLJ54492, highly similar to Eukaryotic translation initiation factor 4B PE=2 SV=1	2.06	0.09
P26583	High mobility group protein B2 GN=HMGB2 PE=1 SV=2	0.77	-0.14
P18065	Insulin-like growth factor-binding protein 2 GN=IGFBP2 PE=1 SV=2	0.27	-0.11
A0A0K0K1L8	Epididymis secretory sperm binding protein Li 129m GN=HEL-S-129m PE=2 SV=1	0.35	0.07
P13500	C-C motif chemokine 2 GN=CCL2 PE=1 SV=1	4.22	0.86
P54725	UV excision repair protein RAD23 homolog A GN=RAD23A PE=1 SV=1	3.02	0.18
Q16881	Thioredoxin reductase 1, cytoplasmic GN=TXNRD1 PE=1 SV=3	0.02	0.01
B7Z9B1	cDNA FLJ52398, highly similar to Cadherin-13 PE=2 SV=1	1.74	0.23
A0A024RDR0	High-mobility group box 1, isoform CRA_a GN=HMGB1 PE=4 SV=1	1.92	-0.47
P17096	High mobility group protein HMG-I/HMG-Y GN=HMGA1 PE=1 SV=3	0.32	-0.08

D9IAI1	Epididymis secretory protein Li 34 GN=PEBP1 PE=2 SV=1	1.47	0.42
Q5U000	Cathepsin Z PE=2 SV=1	1.62	0.26
G3V4U0	Fibulin-5 GN=FBLN5 PE=1 SV=1	1.28	-0.48
B7Z6S9	Glucosylceramidase PE=2 SV=1	0.08	0.03
H0YLF3	Beta-2-microglobulin (Fragment) GN=B2M PE=1 SV=1	1.53	0.21
A0A024R6D4	Enhancer of rudimentary homolog GN=ERH PE=3 SV=1	2.09	0.18
B3KUY2	Prostaglandin E synthase 3 (Cytosolic), isoform CRA_c GN=PTGES3 PE=2 SV=1	2.02	0.18
A2A274	Aconitate hydratase, mitochondrial GN=ACO2 PE=1 SV=1	0.20	-0.09
B2RAQ9	Proteasome subunit beta type PE=2 SV=1	3.00	0.19
Q96D15	Reticulocalbin-3 GN=RCN3 PE=1 SV=1	1.29	0.14
O75942	Major prion protein GN=PRNP PE=3 SV=2	1.68	0.20
A0A140VK72	Testis secretory sperm-binding protein Li 199a PE=2 SV=1	0.15	-0.04
P49588	Alanine--tRNA ligase, cytoplasmic GN=AARS PE=1 SV=2	0.15	-0.03
B4DPD5	Ubiquitin thioesterase PE=2 SV=1	0.53	-0.07
B2R7P8	cDNA, FLJ93545, highly similar to Homo sapiens 5-aminoimidazole-4-carboxamide ribonucleotide formyltransferase/IMP cyclohydrolase (ATIC), mRNA PE=2 SV=1	0.35	-0.08
Q09028	Histone-binding protein RBBP4 GN=RBBP4 PE=1 SV=3	0.28	0.09
Q4LE58	eIF4G1 variant protein (Fragment) GN=EIF4G1 variant protein PE=2 SV=1	0.00	0.00
B4DHQ3	Phosphoserine aminotransferase PE=2 SV=1	0.32	-0.08
Q15181	Inorganic pyrophosphatase GN=PPA1 PE=1 SV=2	0.50	0.14
A0A024R8W0	DEAD (Asp-Glu-Ala-Asp) box polypeptide 48, isoform CRA_a GN=DDX48 PE=3 SV=1	0.97	-0.13
P50454	Serpin H1 GN=SERPINH1 PE=1 SV=2	0.83	0.19
A0A024RDF6	Heterogeneous nuclear ribonucleoprotein D-like, isoform CRA_a GN=HNRPDL PE=4 SV=1	2.10	0.32
Q59FR8	Galectin (Fragment) PE=2 SV=1	0.09	-0.02
P36957	Dihydrolipoyllysine-residue succinyltransferase component of 2-oxoglutarate dehydrogenase complex, mitochondrial GN=DLST PE=1 SV=4	1.02	0.22
O43405	Cochlin GN=COCH PE=1 SV=1	1.07	0.17
O14980	Exportin-1 GN=XPO1 PE=1 SV=1	1.08	0.12
A0A024R608	Ribosomal protein, large, P1, isoform CRA_a GN=RPLP1 PE=3 SV=1	1.88	0.16
V9HW26	ATP synthase subunit alpha GN=HEL-S-123m PE=1 SV=1	1.86	0.34
P28070	Proteasome subunit beta type-4 GN=PSMB4 PE=1 SV=4	1.96	0.24
P35318	ADM GN=ADM PE=1 SV=1	2.33	-0.53
B4DPV7	cDNA FLJ54534, highly similar to Homo sapiens cysteinyl-tRNA synthetase (CARS), transcript variant 3, mRNA PE=2 SV=1	0.13	-0.03
A0A1C7CYX9	Dihydropyrimidinase-related protein 2 GN=DPYSL2 PE=1 SV=1	0.38	0.06
Q15631	Translin GN=TSN PE=1 SV=1	0.21	-0.07
P78371	T-complex protein 1 subunit beta GN=CCT2 PE=1 SV=4	0.18	-0.07
Q15019	Septin-2 GN=SEPT2 PE=1 SV=1	0.64	0.16
A0A0C4DFX3	EMILIN-1 GN=EMILIN1 PE=1 SV=1	0.37	0.05
Q9HAV7	GrpE protein homolog 1, mitochondrial GN=GRPEL1 PE=1 SV=2	1.93	0.18
Q6EMK4	Vasorin GN=VASN PE=1 SV=1	0.65	0.17
P10644	cAMP-dependent protein kinase type I-alpha regulatory subunit GN=PRKAR1A PE=1 SV=1	1.72	0.21
Q8NBJ5	Procollagen galactosyltransferase 1 GN=COLGALT1 PE=1 SV=1	1.28	-0.17
P30084	Enoyl-CoA hydratase, mitochondrial GN=ECHS1 PE=1 SV=4	0.97	0.21
P38159	RNA-binding motif protein, X chromosome GN=RBMX PE=1 SV=3	0.89	0.15
Q00839	Heterogeneous nuclear ribonucleoprotein U GN=HNRNPU PE=1 SV=6	3.11	0.39
Q13011	Delta(3,5)-Delta(2,4)-dienoyl-CoA isomerase, mitochondrial GN=ECH1 PE=1 SV=2	0.36	-0.04
K7EL20	Eukaryotic translation initiation factor 3 subunit G (Fragment) GN=EIF3G PE=1 SV=8	1.48	0.24
Q8NBS9	Thioredoxin domain-containing protein 5 GN=TXNDC5 PE=1 SV=2	1.52	0.27
P19957	Elafin GN=PI3 PE=1 SV=3	1.56	-0.81
P21399	Cytoplasmic aconitate hydratase GN=ACO1 PE=1 SV=3	0.20	-0.09
Q15366	Poly(rC)-binding protein 2 GN=PCBP2 PE=1 SV=1	0.35	0.11
B4DT31	cDNA FLJ53425, highly similar to Far upstream element-binding protein 1 PE=2 SV=1	0.23	0.04
P23396	40S ribosomal protein S3 GN=RPS3 PE=1 SV=2	0.24	0.08
Q9H1E3	Nuclear ubiquitous casein and cyclin-dependent kinase substrate 1 GN=NUCKS1 PE=1 SV=1	2.08	-0.51
A2A2V4	Vascular endothelial growth factor A GN=VEGFA PE=1 SV=1	1.95	-0.44

A0A0A7E7X3	Aminopeptidase (Fragment) GN=ERAP1 PE=2 SV=1	0.16	0.06
A0A023T787	RNA-binding protein 8A GN=RBM8 PE=2 SV=1	2.06	0.26
Q969H8	Myeloid-derived growth factor GN=MYDGF PE=1 SV=1	1.34	-0.10
A0A087X1N8	Serpin B6 GN=SERPINB6 PE=1 SV=1	0.64	-0.16
A0A087X1Z3	Proteasome activator complex subunit 2 GN=PSME2 PE=1 SV=1	0.46	0.09
H0Y8C6	Importin-5 (Fragment) GN=IPO5 PE=1 SV=1	0.36	-0.08
Q99536	Synaptic vesicle membrane protein VAT-1 homolog GN=VAT1 PE=1 SV=2	0.08	0.03
B2R780	cDNA, FLJ93320, highly similar to Homo sapiens angiopoietin-like 2 (ANGPTL2), mRNA PE=2 SV=1	0.53	0.12
P30048	Thioredoxin-dependent peroxide reductase, mitochondrial GN=PRDX3 PE=1 SV=3	0.12	0.04
P62316	Small nuclear ribonucleoprotein Sm D2 GN=SNRPD2 PE=1 SV=1	2.56	0.21
O75396	Vesicle-trafficking protein SEC22b GN=SEC22B PE=1 SV=4	0.50	0.11
V9HW12	Epididymis secretory sperm binding protein Li 2a GN=HEL-S-2a PE=2 SV=1	0.26	-0.07
Q15436	Protein transport protein Sec23A GN=SEC23A PE=1 SV=2	0.09	-0.03
P00492	Hypoxanthine-guanine phosphoribosyltransferase GN=HPRT1 PE=1 SV=2	0.23	0.06
F8W031	Uncharacterized protein (Fragment) PE=1 SV=1	1.69	0.23
P34897	Serine hydroxymethyltransferase, mitochondrial GN=SHMT2 PE=1 SV=3	2.17	0.20
P22692	Insulin-like growth factor-binding protein 4 GN=IGFBP4 PE=1 SV=2	5.96	0.66
Q7Z7Q8	C-C motif chemokine GN=MCP-3 PE=3 SV=1	4.46	0.86
A0A024R904	Calcyclin binding protein, isoform CRA_a GN=CACYBP PE=4 SV=1	0.48	-0.24
A0A087WYR3	Tumor protein D54 GN=TPD52L2 PE=1 SV=1	2.50	0.40
A0A140VJL8	Inositol-1-monophosphatase PE=2 SV=1	0.73	-0.18
Q9UHV9	Prefoldin subunit 2 GN=PFDN2 PE=1 SV=1	0.47	0.13
A0A140VJY2	Testicular tissue protein Li 209 PE=2 SV=1	1.81	0.35
Q8TDQ7	Glucosamine-6-phosphate isomerase 2 GN=GNPDA2 PE=1 SV=1	0.26	0.04
A0A087WUZ3	Spectrin beta chain GN=SPTBN1 PE=1 SV=1	1.37	0.15
B2R960	cDNA, FLJ94230, highly similar to Homo sapiens thioredoxin-like 1 (TXNL1), mRNA PE=2 SV=1	0.24	0.07
P17987	T-complex protein 1 subunit alpha GN=TCP1 PE=1 SV=1	2.39	0.41
Q15907	Ras-related protein Rab-11B GN=RAB11B PE=1 SV=4	0.12	0.03
O43175	D-3-phosphoglycerate dehydrogenase GN=PHGDH PE=1 SV=4	1.99	0.35
Q6UXH9	Inactive serine protease PAMR1 GN=PAMR1 PE=1 SV=1	1.59	-0.41
P98066	Tumor necrosis factor-inducible gene 6 protein GN=TNFAIP6 PE=1 SV=2	2.68	0.55
E9KL35	Epididymis tissue sperm binding protein Li 3a PE=1 SV=1	1.04	0.14
Q86UD1	Out at first protein homolog GN=OAF PE=2 SV=1	0.67	0.13
B9EKV4	Aldehyde dehydrogenase 9 family, member A1 GN=ALDH9A1 PE=2 SV=1	0.15	-0.05
Q99584	Protein S100-A13 GN=S100A13 PE=1 SV=1	1.01	0.14
H7C2I1	Protein arginine N-methyltransferase 1 GN=PRMT1 PE=1 SV=1	0.93	0.11
A0A0U1RRM4	Polypyrimidine tract-binding protein 1 GN=PTBP1 PE=1 SV=1	0.53	0.13
Q13283	Ras GTPase-activating protein-binding protein 1 GN=G3BP1 PE=1 SV=1	1.00	0.18
Q96AY3	Peptidyl-prolyl cis-trans isomerase FKBP10 GN=FKBP10 PE=1 SV=1	0.73	0.20
Q9UNZ2	NSFL1 cofactor p47 GN=NSFL1C PE=1 SV=2	0.01	0.00
P07814	Bifunctional glutamate/proline--tRNA ligase GN=EPRS PE=1 SV=5	0.53	0.13
Q00688	Peptidyl-prolyl cis-trans isomerase FKBP3 GN=FKBP3 PE=1 SV=1	0.31	0.08
A0A140VJK1	Testicular tissue protein Li 75 PE=2 SV=1	0.99	0.19
P31153	S-adenosylmethionine synthase isoform type-2 GN=MAT2A PE=1 SV=1	0.29	0.06
O15347	High mobility group protein B3 GN=HMGB3 PE=1 SV=4	0.01	0.00
A6XAA7	Gremlin GN=GREM1 PE=2 SV=1	2.04	0.33
Q59G24	Activated RNA polymerase II transcription cofactor 4 variant (Fragment) PE=2 SV=1	0.76	-0.32
D3DRR6	Inter-alpha (Globulin) inhibitor H2, isoform CRA_a GN=ITIH2 PE=4 SV=1	0.65	0.17
A8KAP9	cDNA FLJ78448, highly similar to Homo sapiens argininosuccinate synthetase (ASS), transcript variant 1, mRNA PE=2 SV=1	1.96	0.17
P0C0S5	Histone H2A.Z GN=H2AFZ PE=1 SV=2	0.99	0.21
J3KQ18	D-dopachrome decarboxylase GN=DDT PE=1 SV=1	1.66	0.14
P58546	Myotrophin GN=MTPN PE=1 SV=2	1.13	0.25
P05362	Intercellular adhesion molecule 1 GN=ICAM1 PE=1 SV=2	0.11	0.03

A8K6Q8	cDNA FLJ75881, highly similar to Homo sapiens transferrin receptor (p90, CD71) (TFRC), mRNA PE=2 SV=1	0.05	-0.03
A0A140VJW5	Testicular tissue protein Li 192 PE=2 SV=1	0.06	-0.02
Q9P0L0	Vesicle-associated membrane protein-associated protein A GN=VAPA PE=1 SV=3	1.05	0.21
P41091	Eukaryotic translation initiation factor 2 subunit 3 GN=EIF2S3 PE=1 SV=3	1.44	0.21
A0A0A0MSW4	Phosphatidylinositol transfer protein beta isoform GN=PITPNB PE=1 SV=1	0.97	-0.16
A8KAQ5	cDNA FLJ77404, highly similar to Homo sapiens small nuclear ribonucleoprotein 70kDa polypeptide (RNP antigen) (SNRP70), transcript variant 1, mRNA PE=2 SV=1	2.12	0.29
Q9NRN5	Olfactomedin-like protein 3 GN=OLFML3 PE=2 SV=1	0.01	0.00
Q9BRA2	Thioredoxin domain-containing protein 17 GN=TXNDC17 PE=1 SV=1	1.75	0.17
Q53FN7	BZW1 protein variant (Fragment) PE=2 SV=1	3.72	-0.12
P62495	Eukaryotic peptide chain release factor subunit 1 GN=ETF1 PE=1 SV=3	0.74	0.08
G3V180	Dipeptidyl peptidase 3 GN=DPP3 PE=1 SV=1	0.14	-0.08
B2R9K8	cDNA, FLJ94440, highly similar to Homo sapiens chaperonin containing TCP1, subunit 6A (zeta 1)(CCT6A), mRNA PE=2 SV=1	0.73	0.20
P53675	Clathrin heavy chain 2 GN=CLTCL1 PE=1 SV=2	0.06	0.03
P30479	HLA class I histocompatibility antigen, B-41 alpha chain GN=HLA-B PE=1 SV=1	0.96	0.16
P25398	40S ribosomal protein S12 GN=RPS12 PE=1 SV=3	1.28	0.37
Q13151	Heterogeneous nuclear ribonucleoprotein A0 GN=HNRNPA0 PE=1 SV=1	0.26	0.08
Q08629	Testican-1 GN=SPOCK1 PE=1 SV=1	1.69	0.44
A0A024R1S8	LIM and SH3 protein 1, isoform CRA_b GN=LASP1 PE=4 SV=1	0.06	-0.02
P62906	60S ribosomal protein L10a GN=RPL10A PE=1 SV=2	1.33	-0.42
Q13344	Fus-like protein (Fragment) PE=2 SV=1	2.72	0.31
P09496	Clathrin light chain A GN=CLTA PE=1 SV=1	2.45	0.38
D3DPK5	SH3 domain binding glutamic acid-rich protein like 3, isoform CRA_a (Fragment) GN=SH3BGRL3 PE=4 SV=1	2.24	0.28
G5EA09	Syndecan binding protein (Syntenin), isoform CRA_a GN=SDCBP PE=1 SV=1	0.85	-0.16
P55010	Eukaryotic translation initiation factor 5 GN=EIF5 PE=1 SV=2	1.04	-0.11
Q9HCU0	Endosialin GN=CD248 PE=1 SV=1	0.84	0.28
B2R5W3	Poly [ADP-ribose] polymerase PE=2 SV=1	1.20	0.18
Q96FQ6	Protein S100-A16 GN=S100A16 PE=1 SV=1	0.65	0.14
P14866	Heterogeneous nuclear ribonucleoprotein L GN=HNRNPL PE=1 SV=2	0.14	-0.07
H0YBI8	Vascular endothelial growth factor A (Fragment) GN=VEGFA PE=1 SV=1	1.73	-0.59
P62304	Small nuclear ribonucleoprotein E GN=SNRPE PE=1 SV=1	0.29	0.11
Q99471	Prefoldin subunit 5 GN=PFDN5 PE=1 SV=2	1.05	0.17
Q5T9B7	Adenylate kinase isoenzyme 1 GN=AK1 PE=1 SV=1	1.71	0.27
Q9UN70	Protocadherin gamma-C3 GN=PCDHGC3 PE=1 SV=1	0.50	0.08
Q15257	Serine/threonine-protein phosphatase 2A activator GN=PTPA PE=1 SV=3	0.54	-0.13
Q9Y3F4	Serine-threonine kinase receptor-associated protein GN=STRAP PE=1 SV=1	0.43	-0.22
Q2VIR3	Putative eukaryotic translation initiation factor 2 subunit 3-like protein GN=EIF2S3L PE=5 SV=2	1.64	0.46
I3L0A0	HCG2044781 GN=TMEM189-UBE2V1 PE=3 SV=1	0.03	-0.01
Q5KU26	Collectin-12 GN=COLEC12 PE=1 SV=3	0.82	0.20
Q8NI22	Multiple coagulation factor deficiency protein 2 GN=MCFD2 PE=1 SV=1	1.72	0.36
A8K8U1	cDNA FLJ77762, highly similar to Homo sapiens cullin-associated and neddylation-dissociated 1 (CAND1), mRNA PE=2 SV=1	0.12	-0.07
Q9H2G2	STE20-like serine/threonine-protein kinase GN=SLK PE=1 SV=1	1.52	0.17
B4E3D4	cDNA FLJ56293, highly similar to Transmembrane glycoprotein NMB PE=2 SV=1	0.21	-0.07
A0A024RBS2	60S acidic ribosomal protein P0 GN=RPLP0 PE=3 SV=1	0.85	-0.09
B2RCP7	cDNA, FLJ96197, highly similar to Homo sapiens connective tissue growth factor (CTGF), mRNA PE=2 SV=1	0.55	0.08
P55786	Puromycin-sensitive aminopeptidase GN=NPEPPS PE=1 SV=2	0.80	-0.39
Q59F66	DEAD box polypeptide 17 isoform p82 variant (Fragment) PE=2 SV=1	0.17	-0.05
P28072	Proteasome subunit beta type-6 GN=PSMB6 PE=1 SV=4	0.35	0.09
A0A024RD93	Phosphoribosylaminoimidazole carboxylase, phosphoribosylaminoimidazole succinocarboxamide synthetase, isoform CRA_c GN=PAICS PE=3 SV=1	0.08	0.02
V9HWJ1	Glutathione synthetase GN=HEL-S-64p PE=2 SV=1	0.28	-0.07

P61457	Pterin-4-alpha-carbinolamine dehydratase GN=PCBD1 PE=1 SV=2	0.21	0.03
Q59FG9	Chondroitin sulfate proteoglycan 2 (Versican) variant (Fragment) PE=2 SV=1	1.37	0.33
A0A024RDE5	Ras-GTPase activating protein SH3 domain-binding protein 2, isoform CRA_a GN=G3BP2 PE=4 SV=1	0.69	-0.09
Q7Z4X0	MO25-like protein PE=2 SV=1	1.14	0.36
B2RBH2	cDNA, FLJ95508, highly similar to Homo sapiens 5'-nucleotidase, ecto (CD73) (NT5E), mRNA PE=2 SV=1	0.55	-0.17
P14324	Farnesyl pyrophosphate synthase GN=FDPS PE=1 SV=4	0.60	-0.07
H0YBX6	Ubiquitin-conjugating enzyme E2 variant 2 (Fragment) GN=UBE2V2 PE=1 SV=1	0.59	-0.10
Q96C19	EF-hand domain-containing protein D2 GN=EFHD2 PE=1 SV=1	0.19	-0.08
B0YIW6	Archain 1, isoform CRA_a GN=ARCN1 PE=1 SV=1	0.09	-0.04
P35268	60S ribosomal protein L22 GN=RPL22 PE=1 SV=2	1.52	0.23
P62888	60S ribosomal protein L30 GN=RPL30 PE=1 SV=2	0.42	0.20
Q9Y547	Intraflagellar transport protein 25 homolog GN=HSPB11 PE=1 SV=1	0.09	0.04
Q07666	KH domain-containing, RNA-binding, signal transduction-associated protein 1 GN=KHDRBS1 PE=1 SV=1	0.75	0.09
F6WQW2	Ran-specific GTPase-activating protein GN=RANBP1 PE=1 SV=1	2.33	0.20
P27487	Dipeptidyl peptidase 4 GN=DPP4 PE=1 SV=2	0.91	-0.19
P54136	Arginine--tRNA ligase, cytoplasmic GN=RARS PE=1 SV=2	0.50	0.08
F2Z3N3	Olfactomedin-like protein 2B GN=OLFML2B PE=1 SV=1	0.36	0.13
P29373	Cellular retinoic acid-binding protein 2 GN=CRABP2 PE=1 SV=2	0.00	0.00
O75822	Eukaryotic translation initiation factor 3 subunit J GN=EIF3J PE=1 SV=2	2.67	0.22
A0A024QZK8	Heterogeneous nuclear ribonucleoprotein H3 (2H9), isoform CRA_a GN=HNRPH3 PE=4 SV=1	0.24	0.05
Q9BS26	Endoplasmic reticulum resident protein 44 GN=ERP44 PE=1 SV=1	0.12	-0.05
Q9NR30	Nucleolar RNA helicase 2 GN=DDX21 PE=1 SV=5	2.23	0.21
Q0P5N8	TMSB4X protein (Fragment) GN=TMSB4X PE=2 SV=1	1.51	0.16
Q9Y2W1	Thyroid hormone receptor-associated protein 3 GN=THRAP3 PE=1 SV=2	0.15	-0.07
B4E284	cDNA FLJ51188, highly similar to N-acetylglucosamine-6-sulfatase (EC3.1.6.14) PE=2 SV=1	0.50	-0.19
P17936	Insulin-like growth factor-binding protein 3 GN=IGFBP3 PE=1 SV=2	0.06	-0.02
Q13443	Disintegrin and metalloproteinase domain-containing protein 9 GN=ADAM9 PE=1 SV=1	2.09	0.18
P61956	Small ubiquitin-related modifier 2 GN=SUMO2 PE=1 SV=3	0.97	0.18
P28838	Cytosol aminopeptidase GN=LAP3 PE=1 SV=3	0.43	0.13
P09497	Clathrin light chain B GN=CLTB PE=1 SV=1	1.81	0.30
Q5U043	S-(hydroxymethyl)glutathione dehydrogenase PE=2 SV=1	0.87	0.17
P49721	Proteasome subunit beta type-2 GN=PSMB2 PE=1 SV=1	0.57	0.04
P06132	Uroporphyrinogen decarboxylase GN=UROD PE=1 SV=2	0.57	-0.10
M0QXB4	Coatomer protein complex, subunit epsilon, isoform CRA_g GN=COPE PE=1 SV=1	0.49	-0.12
Q9UHL4	Dipeptidyl peptidase 2 GN=DPP7 PE=1 SV=3	0.36	0.07
Q6FIE5	PHP14 protein GN=PHP14 PE=2 SV=1	2.05	0.25
A0A024R5H0	Barrier to autointegration factor 1, isoform CRA_a GN=BANF1 PE=4 SV=1	1.75	0.31
J3KQ69	DNA replication licensing factor MCM3 GN=MCM3 PE=1 SV=2	2.10	0.18
B3KXM2	Serine/threonine-protein phosphatase PE=2 SV=1	0.11	0.03
Q9GZX9	Twisted gastrulation protein homolog 1 GN=TWSG1 PE=1 SV=1	2.62	0.19
A0A024R7U6	DNA helicase GN=MCM4 PE=3 SV=1	0.61	0.17
Q8WXX5	DnaJ homolog subfamily C member 9 GN=DNAJC9 PE=1 SV=1	0.34	0.08
O14737	Programmed cell death protein 5 GN=PDCD5 PE=1 SV=3	2.18	0.30
O75937	DnaJ homolog subfamily C member 8 GN=DNAJC8 PE=1 SV=2	1.42	0.19
Q59ET0	Glucan, branching enzyme 1 variant (Fragment) PE=2 SV=1	0.47	0.11
O00193	Small acidic protein GN=SMAP PE=1 SV=1	1.96	0.17
B2R4R9	HCG26477 GN=RPS28 PE=2 SV=1	1.82	0.34
P43251	Biotinidase GN=BTD PE=1 SV=2	0.11	0.03
P05204	Non-histone chromosomal protein HMG-17 GN=HMGN2 PE=1 SV=3	0.27	0.03
A0A024R6W2	Nudix (Nucleoside diphosphate linked moiety X)-type motif 21, isoform CRA_a GN=NUDT21 PE=4 SV=1	0.41	0.10
P23381	Tryptophan--tRNA ligase, cytoplasmic GN=WARS PE=1 SV=2	0.64	-0.16
P05556	Integrin beta-1 GN=ITGB1 PE=1 SV=2	0.05	-0.02

O75223	Gamma-glutamylcyclotransferase GN=GGCT PE=1 SV=1	0.10	0.03
B2R802	cDNA, FLJ93681, highly similar to Homo sapiens small nuclear ribonucleoprotein polypeptide A (SNRPA), mRNA PE=2 SV=1	0.11	-0.02
A0A024RAF1	Bridging integrator 1, isoform CRA_k GN=BIN1 PE=4 SV=1	3.19	0.24
K7ELC7	60S ribosomal protein L27 (Fragment) GN=RPL27 PE=1 SV=1	0.21	-0.06
A0A087WUT6	Eukaryotic translation initiation factor 5B GN=EIF5B PE=1 SV=1	1.48	0.28
J9R021	Eukaryotic translation initiation factor 3 subunit A GN=eIF3a PE=2 SV=1	0.07	-0.02
B7Z1Z5	cDNA FLJ57265, highly similar to Neurotrimin PE=2 SV=1	0.30	-0.11
Q14696	LDLR chaperone MESD GN=MESDC2 PE=1 SV=2	0.24	0.04
P15291	Beta-1,4-galactosyltransferase 1 GN=B4GALT1 PE=1 SV=5	0.08	0.01
A8K0I8	cDNA FLJ76207, highly similar to Homo sapiens delta-notch-like EGF repeat-containing transmembrane (DNER), mRNA PE=2 SV=1	0.37	0.05
A0A024R7T3	Heterogeneous nuclear ribonucleoprotein F, isoform CRA_a GN=HNRPF PE=4 SV=1	2.84	0.18
Q9NZM1	Myoferlin GN=MYOF PE=1 SV=1	0.30	0.07
P42126	Enoyl-CoA delta isomerase 1, mitochondrial GN=ECI1 PE=1 SV=1	0.07	-0.03
A8K7D9	Importin subunit alpha PE=2 SV=1	0.39	0.18
P41227	N-alpha-acetyltransferase 10 GN=NAA10 PE=1 SV=1	0.21	0.05
P35659	Protein DEK GN=DEK PE=1 SV=1	1.37	-0.87
Q99784	Noelin GN=OLFM1 PE=1 SV=4	0.50	0.14
Q13740	CD166 antigen GN=ALCAM PE=1 SV=2	0.14	-0.07
Q6NZI2	Caveolae-associated protein 1 GN=CAVIN1 PE=1 SV=1	1.88	0.31
B4DVA7	Beta-hexosaminidase PE=2 SV=1	1.19	0.22
P14174	Macrophage migration inhibitory factor GN=MIF PE=1 SV=4	0.03	-0.01
Q59EH3	Acid phosphatase 1 isoform c variant (Fragment) PE=2 SV=1	1.13	0.16
B2R6P3	cDNA, FLJ93047, highly similar to Homo sapiens matrix metallopeptidase 14 (membrane-inserted) (MMP14), mRNA PE=2 SV=1	2.01	0.20
O75643	U5 small nuclear ribonucleoprotein 200 kDa helicase GN=SNRNP200 PE=1 SV=2	0.62	0.14
Q8TDJ5	Tyrosine-protein kinase receptor GN=TFG/ALK fusion PE=2 SV=1	0.47	0.16
P51884	Lumican GN=LUM PE=1 SV=2	2.82	0.42
G8JLH6	Tetraspanin (Fragment) GN=CD9 PE=1 SV=1	0.82	-0.34
A8MU27	Small ubiquitin-related modifier 3 GN=SUMO3 PE=1 SV=1	1.97	0.12
A0A0A6YYL6	Protein RPL17-C18orf32 GN=RPL17-C18orf32 PE=3 SV=1	1.30	0.27
A0A024RAV0	Branched-chain-amino-acid aminotransferase GN=BCAT1 PE=3 SV=1	0.53	-0.22
P18827	Syndecan-1 GN=SDC1 PE=1 SV=3	0.18	0.04
P16104	Histone H2AX GN=H2AFX PE=1 SV=2	2.03	0.26
B1AKK2	Dimethylarginine dimethylaminohydrolase 1, isoform CRA_b GN=DDAH1 PE=2 SV=1	0.65	0.14
P13797	Plastin-3 GN=PLS3 PE=1 SV=4	0.35	-0.08
Q59HH3	Trifunctional purine biosynthetic protein adenosine-3 (Fragment) PE=2 SV=1	0.57	0.11
Q5JR05	Rho-related GTP-binding protein RhoC GN=RHOC PE=3 SV=1	0.09	-0.04
O60462	Neuropilin-2 GN=NRP2 PE=1 SV=2	0.13	0.04
H3BVE0	Uncharacterized protein (Fragment) PE=4 SV=1	2.26	0.17
V9HW90	Epididymis luminal protein 75 GN=HEL-75 PE=2 SV=1	0.35	-0.07
J3QRS3	Myosin regulatory light chain 12A GN=MYL12A PE=1 SV=1	1.07	0.35
P43034	Platelet-activating factor acetylhydrolase IB subunit alpha GN=PAFAH1B1 PE=1 SV=2	0.07	0.03
Q12792	Twinfilin-1 GN=TWF1 PE=1 SV=3	0.21	0.07
A8K8D9	Glucose-6-phosphate 1-dehydrogenase PE=2 SV=1	0.18	-0.05
D3DR24	Exostoses (Multiple) 2, isoform CRA_a GN=EXT2 PE=4 SV=1	0.20	-0.10
Q15182	Small nuclear ribonucleoprotein-associated protein GN=SNRPB PE=2 SV=1	2.01	0.35
A0A024R2A7	Lectin, mannose-binding, 1, isoform CRA_b GN=LMAN1 PE=4 SV=1	0.19	0.04
O60888	Protein CutA GN=CUTA PE=1 SV=2	0.78	0.18
A0A087X0X3	Heterogeneous nuclear ribonucleoprotein M GN=HNRNPM PE=1 SV=1	0.34	-0.11
Q32MZ4	Leucine-rich repeat flightless-interacting protein 1 GN=LRRFIP1 PE=1 SV=2	0.88	0.11
Q9UBS4	DnaJ homolog subfamily B member 11 GN=DNAJB11 PE=1 SV=1	1.08	0.27
Q92499	ATP-dependent RNA helicase DDX1 GN=DDX1 PE=1 SV=2	0.11	-0.06
Q4LE36	ACLY variant protein (Fragment) GN=ACLY variant protein PE=2 SV=1	0.24	-0.04
Q15370	Elongin-B GN=ELOB PE=1 SV=1	1.47	0.18
Q3MI39	HNRPA1 protein (Fragment) GN=HNRPA1 PE=2 SV=1	0.18	0.04

E9PF18	Hydroxyacyl-coenzyme A dehydrogenase, mitochondrial GN=HADH PE=1 SV=2	0.25	0.07
Q9NR45	Sialic acid synthase GN=NANS PE=1 SV=2	0.97	0.31
B4DWB5	cDNA FLJ53931, highly similar to Bifunctional 3'-phosphoadenosine5'-phosphosulfate synthetase 2 PE=2 SV=1	0.65	0.15
O43570	Carbonic anhydrase 12 GN=CA12 PE=1 SV=1	1.27	-0.53
Q86UA3	Chromosome 12 open reading frame 10 GN=C12orf10 PE=1 SV=1	1.11	0.13
O14561	Acyl carrier protein, mitochondrial GN=NDUFAB1 PE=1 SV=3	3.05	0.27
Q59GY2	Ribosomal protein L4 variant (Fragment) PE=2 SV=1	2.68	0.46
E5RJR5	S-phase kinase-associated protein 1 GN=SKP1 PE=1 SV=1	1.16	0.20
E9PQY2	Prefoldin subunit 4 GN=PFDN4 PE=1 SV=1	0.89	0.17
P08572	Collagen alpha-2(IV) chain GN=COL4A2 PE=1 SV=4	1.27	0.22
P51572	B-cell receptor-associated protein 31 GN=BCAP31 PE=1 SV=3	2.26	0.39
B3KQS9	cDNA PSEC0141 fis, clone PLACE1005913, highly similar to Deoxyribonuclease-2-alpha (EC 3.1.22.1) PE=2 SV=1	0.42	0.09
D3DWY7	Prefoldin subunit 3 GN=VBP1 PE=3 SV=1	1.58	0.23
Q13442	28 kDa heat- and acid-stable phosphoprotein GN=PDAP1 PE=1 SV=1	2.43	0.67
Q53G42	mRNA decapping enzyme variant (Fragment) PE=2 SV=1	0.32	-0.21
E7ETY2	Treacle protein GN=TCOF1 PE=1 SV=1	0.10	-0.05
Q96FJ2	Dynein light chain 2, cytoplasmic GN=DYNLL2 PE=1 SV=1	0.09	-0.04
X6R4W8	BUB3-interacting and GLEBS motif-containing protein ZNF207 GN=ZNF207 PE=1 SV=1	2.47	0.29
P30049	ATP synthase subunit delta, mitochondrial GN=ATP5D PE=1 SV=2	0.25	0.11
A0A024RAM4	Microtubule-associated protein 1B, isoform CRA_b GN=MAP1B PE=4 SV=1	0.55	-0.12
B1AKJ5	Nardilysin GN=NRDC PE=1 SV=1	2.89	0.29
B4DIS3	Dpy-30-like protein, isoform CRA_b GN=LOC84661 PE=2 SV=1	1.68	0.44
L0R599	Alternative protein CIRH1A GN=CIRH1A PE=4 SV=1	0.97	0.08
B2R6R6	Serine/threonine-protein phosphatase PE=2 SV=1	4.17	0.23
Q9NYU2	UDP-glucose:glycoprotein glucosyltransferase 1 GN=UGGT1 PE=1 SV=3	1.66	-0.20
Q10713	Mitochondrial-processing peptidase subunit alpha GN=PMPCA PE=1 SV=2	0.26	0.05
P78539	Sushi repeat-containing protein SRPX GN=SRPX PE=1 SV=1	0.04	0.02
P13473	Lysosome-associated membrane glycoprotein 2 GN=LAMP2 PE=1 SV=2	0.39	-0.10
O60869	Endothelial differentiation-related factor 1 GN=EDF1 PE=1 SV=1	0.71	0.12
B4E2L0	cDNA FLJ54730, highly similar to cAMP-dependent protein kinase, beta-2-catalytic subunit (EC 2.7.11.11) PE=2 SV=1	0.21	0.06
Q8WWM7	Ataxin-2-like protein GN=ATXN2L PE=1 SV=2	0.63	0.10
P60866	40S ribosomal protein S20 GN=RPS20 PE=1 SV=1	1.26	0.30
B2RBF5	cDNA, FLJ95483, highly similar to Homo sapiens chitobiase, di-N-acetyl- (CTBS), mRNA PE=2 SV=1	0.08	0.04
Q9NP84	Tumor necrosis factor receptor superfamily member 12A GN=TNFRSF12A PE=1 SV=1	1.11	0.44
Q59GM9	Alpha-1,4 glucan phosphorylase (Fragment) PE=2 SV=1	0.21	0.04
A8MXP9	Matrin-3 GN=MATR3 PE=1 SV=1	0.34	0.15
Q5JXB2	Putative ubiquitin-conjugating enzyme E2 N-like GN=UBE2NL PE=1 SV=1	0.36	-0.11
A0A0K0K1K7	6-phosphogluconolactonase, isoform CRA_b GN=HEL-S-304 PE=2 SV=1	0.03	0.02
Q86TI2	Dipeptidyl peptidase 9 GN=DPP9 PE=1 SV=3	0.62	-0.11
P46109	Crk-like protein GN=CRKL PE=1 SV=1	4.42	0.29
P62424	60S ribosomal protein L7a GN=RPL7A PE=1 SV=2	1.18	0.26
Q16630	Cleavage and polyadenylation specificity factor subunit 6 GN=CPSF6 PE=1 SV=2	1.05	0.23
Q14204	Cytoplasmic dynein 1 heavy chain 1 GN=DYNC1H1 PE=1 SV=5	0.03	-0.01
A0A087WTY6	Neuroblastoma suppressor of tumorigenicity 1 GN=NBL1 PE=1 SV=1	2.43	0.38
Q53FA7	Quinone oxidoreductase PIG3 GN=TP53I3 PE=1 SV=2	0.99	0.14
O00461	Golgi integral membrane protein 4 GN=GOLIM4 PE=1 SV=1	1.09	0.43
Q9Y3C6	Peptidyl-prolyl cis-trans isomerase-like 1 GN=PPIL1 PE=1 SV=1	0.55	0.21
B2RAU5	Sorting nexin PE=2 SV=1	0.30	-0.02
P62314	Small nuclear ribonucleoprotein Sm D1 GN=SNRPD1 PE=1 SV=1	0.34	0.06
Q9GZL7	Ribosome biogenesis protein WDR12 GN=WDR12 PE=1 SV=2	0.17	0.06
Q7Z6J2	General receptor for phosphoinositides 1-associated scaffold protein GN=GRASP PE=1 SV=1	3.48	0.55
A8K4W0	40S ribosomal protein S3a GN=RPS3A PE=2 SV=1	0.57	0.15

P13674	Prolyl 4-hydroxylase subunit alpha-1 GN=P4HA1 PE=1 SV=2	1.31	0.18
A0A024R172	Leukotriene B4 12-hydroxydehydrogenase, isoform CRA_a GN=LTB4DH PE=4 SV=1	0.36	-0.24
P49458	Signal recognition particle 9 kDa protein GN=SRP9 PE=1 SV=2	2.03	0.41
Q9NXF0	cDNA FLJ20288 fis, clone HEP04414 (Fragment) PE=2 SV=1	1.18	0.20
Q9Y678	Coatomer subunit gamma-1 GN=COPG1 PE=1 SV=1	0.08	0.04
P62633	Cellular nucleic acid-binding protein GN=CNBP PE=1 SV=1	1.51	0.16
Q4VC31	Coiled-coil domain-containing protein 58 GN=CCDC58 PE=1 SV=1	2.43	0.41
P61160	Actin-related protein 2 GN=ACTR2 PE=1 SV=1	0.33	0.11
O43252	Bifunctional 3'-phosphoadenosine 5'-phosphosulfate synthase 1 GN=PAPSS1 PE=1 SV=2	0.32	0.13
K7EQ73	DnaJ homolog subfamily C member 7 (Fragment) GN=DNAJC7 PE=1 SV=1	0.03	-0.02
A0A024RAE1	Ribosome assembly factor mrt4 GN=C1orf33 PE=3 SV=1	1.41	-0.13
Q9NQX4	Unconventional myosin-Vc GN=MYO5C PE=1 SV=2	0.57	0.15
A0A087WUB9	Beta-catenin-like protein 1 GN=CTNNBL1 PE=1 SV=1	0.68	-0.09
P62280	40S ribosomal protein S11 GN=RPS11 PE=1 SV=3	0.59	0.12
A0A0S2Z489	Proteasome (Prosome, macropain) 26S subunit, non-ATPase, 12, isoform CRA_a (Fragment) GN=PSMD12 PE=2 SV=1	0.81	0.20
P61970	Nuclear transport factor 2 GN=NUTF2 PE=1 SV=1	1.34	0.20
O43776	Asparagine--tRNA ligase, cytoplasmic GN=NARS PE=1 SV=1	1.09	0.62
A6NFX8	ADP-sugar pyrophosphatase GN=NUDT5 PE=1 SV=1	2.03	0.26
Q549M8	CLE7 GN=C14orf166 PE=2 SV=1	0.82	0.12
A0A0S2Z4R1	Tyrosine--tRNA ligase (Fragment) GN=YARS PE=2 SV=1	0.36	0.13
B2RB23	cDNA, FLJ95265, highly similar to Homo sapiens acetyl-Coenzyme A acyltransferase 2 (mitochondrial 3-oxoacyl-Coenzyme A thiolase) (ACAA2), nuclear gene encoding mitochondrial protein, mRNA PE=2 SV=1	0.99	0.15
A0A024R2W4	Dystroglycan 1 (Dystrophin-associated glycoprotein 1), isoform CRA_a GN=DAG1 PE=4 SV=1	2.55	0.27
A2RUR9	Coiled-coil domain-containing protein 144A GN=CCDC144A PE=2 SV=1	0.18	-0.06
B4DJ06	cDNA FLJ56620 PE=2 SV=1	0.80	0.15
Q5JWF2	Guanine nucleotide-binding protein G(s) subunit alpha isoforms XLas GN=GNAS PE=1 SV=2	0.92	-0.24
Q08209	Serine/threonine-protein phosphatase 2B catalytic subunit alpha isoform GN=PPP3CA PE=1 SV=1	0.09	0.03
O75452	Retinol dehydrogenase 16 GN=RDH16 PE=1 SV=2	0.23	0.05
Q14393	Growth arrest-specific protein 6 GN=GAS6 PE=1 SV=2	0.93	0.18
P20933	N(4)-(beta-N-acetylglucosaminyl)-L-asparaginase GN=AGA PE=1 SV=2	3.07	0.32
Q9UII2	ATPase inhibitor, mitochondrial GN=ATPIF1 PE=1 SV=1	1.28	0.27
B1AKZ4	Phosphoprotein enriched in astrocytes 15, isoform CRA_a GN=PEA15 PE=2 SV=1	0.88	0.24
P04424	Argininosuccinate lyase GN=ASL PE=1 SV=4	0.24	-0.05
P62081	40S ribosomal protein S7 GN=RPS7 PE=1 SV=1	1.17	0.16
Q9Y6H5	Synphilin-1 GN=SNCAIP PE=1 SV=2	0.54	0.15
P50897	Palmitoyl-protein thioesterase 1 GN=PPT1 PE=1 SV=1	0.56	0.22
A0A024R5U5	ADAM metallopeptidase domain 10, isoform CRA_b GN=ADAM10 PE=4 SV=1	3.64	0.53
O75340	Programmed cell death protein 6 GN=PDCD6 PE=1 SV=1	0.71	-0.11
Q5T5C7	Serine--tRNA ligase, cytoplasmic GN=SARS PE=1 SV=1	0.47	0.14
A8MUS3	60S ribosomal protein L23a GN=RPL23A PE=1 SV=1	0.89	0.13
P09661	U2 small nuclear ribonucleoprotein A' GN=SNRPA1 PE=1 SV=2	0.38	0.08
P14854	Cytochrome c oxidase subunit 6B1 GN=COX6B1 PE=1 SV=2	1.66	0.33
P25774	Cathepsin S GN=CTSS PE=1 SV=3	0.11	-0.05
B2RD79	cDNA, FLJ96494, highly similar to Homo sapiens ubiquitin specific peptidase 14 (tRNA-guanine transglycosylase) (USP14), mRNA PE=2 SV=1	0.72	0.19
P05023	Sodium/potassium-transporting ATPase subunit alpha-1 GN=ATP1A1 PE=1 SV=1	0.90	-0.58
P49773	Histidine triad nucleotide-binding protein 1 GN=HINT1 PE=1 SV=2	0.18	0.06
A4D2P0	Ras-related C3 botulinum toxin substrate 1 (Rho family, small GTP binding protein Rac1) GN=RAC1 PE=2 SV=1	0.39	-0.12
H7BY58	Protein-L-isoaspartate O-methyltransferase GN=PCMT1 PE=1 SV=1	2.15	0.24
Q8IYD1	Eukaryotic peptide chain release factor GTP-binding subunit ERF3B GN=GSPT2 PE=1 SV=2	0.43	0.09
A4D1T9	Probable inactive serine protease 37 GN=PRSS37 PE=2 SV=1	0.39	0.13

Q08945	FACT complex subunit SSRP1 GN=SSRP1 PE=1 SV=1	0.90	-0.08
Q9UHD0	Interleukin-19 GN=IL19 PE=1 SV=2	2.86	0.64
A0A024R814	Ribosomal protein L7, isoform CRA_a GN=RPL7 PE=4 SV=1	2.03	0.34
A0A024RBR3	Density-regulated protein GN=DENR PE=3 SV=1	1.94	0.18
Q9NU22	Midasin GN=MDN1 PE=1 SV=2	1.66	0.39
O14929	Histone acetyltransferase type B catalytic subunit GN=HAT1 PE=1 SV=1	0.05	-0.02
Q9NUJ1	Mycophenolic acid acyl-glucuronide esterase, mitochondrial GN=ABHD10 PE=1 SV=1	1.30	0.25
P20290	Transcription factor BTF3 GN=BTF3 PE=1 SV=1	1.91	0.32
Q7LBR1	Charged multivesicular body protein 1b GN=CHMP1B PE=1 SV=1	2.61	0.24
Q5JR94	40S ribosomal protein S8 GN=RPS8 PE=2 SV=1	1.38	0.23
P26885	Peptidyl-prolyl cis-trans isomerase FKBP2 GN=FKBP2 PE=1 SV=2	0.36	0.11
B8ZZD4	Tax1-binding protein 1 GN=TAX1BP1 PE=1 SV=1	0.76	-0.22
O60664	Perilipin-3 GN=PLIN3 PE=1 SV=3	0.36	-0.08
Q16394	Exostosin-1 GN=EXT1 PE=1 SV=2	0.26	0.04
E5RIM7	Copper transport protein ATOX1 GN=ATOX1 PE=1 SV=1	0.96	0.13
F5H450	Frizzled-10 GN=FZD10 PE=4 SV=1	1.03	0.31
B4DNE1	cDNA FLJ52708, highly similar to Basigin PE=2 SV=1	0.93	0.15
F5H8L0	Rab GTPase-activating protein 1-like GN=RABGAP1L PE=1 SV=1	0.95	0.17
Q6E0U4	Dermokine GN=DMKN PE=1 SV=3	0.65	0.15
Q5T6V5	UPF0553 protein C9orf64 GN=C9orf64 PE=1 SV=1	0.55	-0.18
A0A1W2PRB8	Uncharacterized protein PE=4 SV=1	0.33	0.09
A0A140VJZ4	Ubiquitin carboxyl-terminal hydrolase PE=2 SV=1	0.33	0.14
P18077	60S ribosomal protein L35a GN=RPL35A PE=1 SV=2	0.67	-0.14
Q99900	CD44 protein (Fragment) GN=CD44 PE=2 SV=1	0.29	0.11
P05198	Eukaryotic translation initiation factor 2 subunit 1 GN=EIF2S1 PE=1 SV=3	0.26	0.09
Q9Y3C8	Ubiquitin-fold modifier-conjugating enzyme 1 GN=UFC1 PE=1 SV=3	0.47	-0.13
Q4VCS5	Angiomotin GN=AMOT PE=1 SV=1	2.35	0.30
Q15043	Zinc transporter ZIP14 GN=SLC39A14 PE=1 SV=3	0.14	-0.06
Q96JQ0	Protocadherin-16 GN=DCHS1 PE=1 SV=1	0.80	0.19
Q12904	Aminoacyl tRNA synthase complex-interacting multifunctional protein 1 GN=AIMP1 PE=1 SV=2	1.22	0.20
Q68DE3	Basic helix-loop-helix domain-containing protein USF3 GN=USF3 PE=1 SV=3	0.72	-0.14
A0A140VJR2	Testicular tissue protein Li 138 PE=2 SV=1	0.37	-0.07
Q14686	Nuclear receptor coactivator 6 GN=NCOA6 PE=1 SV=3	0.47	-0.08
F5H1D4	Ankyrin repeat and LEM domain-containing protein 2 (Fragment) GN=ANKLE2 PE=1 SV=1	2.54	0.36
A8K0K0	cDNA FLJ77765, highly similar to Human glutamate receptor subunit (GluH1) mRNA PE=2 SV=1	2.75	0.20
Q6FGH5	RPS21 protein (Fragment) GN=RPS21 PE=2 SV=1	0.09	0.04
Q86U86	Protein polybromo-1 GN=PBRM1 PE=1 SV=1	4.09	-0.39
A0A140VJJ2	S-formylglutathione hydrolase GN=ESD PE=2 SV=1	0.60	-0.15
B2R4H6	cDNA, FLJ92093, highly similar to Homo sapiens polymerase (RNA) II (DNA directed) polypeptide F (POLR2F), mRNA PE=2 SV=1	2.55	0.21
Q13601	KRR1 small subunit processome component homolog GN=KRR1 PE=1 SV=4	1.54	0.26
B4DLN1	cDNA FLJ60124, highly similar to Mitochondrial dicarboxylate carrier PE=2 SV=1	1.14	0.27
Q4KWH8	1-phosphatidylinositol 4,5-bisphosphate phosphodiesterase eta-1 GN=PLCH1 PE=1 SV=1	0.76	-0.11
Q6ZVT0	Inactive polyglycylase TTLL10 GN=TTLL10 PE=1 SV=2	0.86	0.20
O60882	Matrix metalloproteinase-20 GN=MMP20 PE=1 SV=3	1.72	-0.34
B3KWI4	cDNA FLJ43122 fis, clone CTONG3003737, highly similar to Leucine-rich repeat-containing protein 15 PE=2 SV=1	0.81	-0.13
P22079	Lactoperoxidase GN=LPO PE=1 SV=2	0.22	-0.09

Appendix 4

Downregulated proteins in untreated hypoxia vs normoxia samples GN=Gene Name, PE=Protein Existence which is the numerical value describing the evidence for the existence of the protein, SV=Sequence Version which is the version number of the sequence.

Accession	Description	-log P	Diff.
P08123	Collagen alpha-2(I) chain GN=COL1A2 PE=1 SV=7	5.71	5.71
Q14766	Latent-transforming growth factor beta-binding protein 1 GN=LTBP1 PE=1 SV=4	1.93	1.93
P02452	Collagen alpha-1(I) chain GN=COL1A1 PE=1 SV=5	1.88	1.88
C9JD84	Latent-transforming growth factor beta-binding protein 1 GN=LTBP1 PE=1 SV=1	2.53	2.53
V9HWE1	Epididymis luminal protein 113 GN=HEL113 PE=2 SV=1	2.55	2.55
A0A024R498	Serpin peptidase inhibitor, clade E (Nexin, plasminogen activator inhibitor type 1), member 2, isoform CRA_b GN=SERPINE2 PE=3 SV=1	2.06	2.06
Q12841	Follistatin-related protein 1 GN=FSTL1 PE=1 SV=1	2.25	2.25
P02461	Collagen alpha-1(III) chain GN=COL3A1 PE=1 SV=4	3.86	3.86
P48307	Tissue factor pathway inhibitor 2 GN=TFPI2 PE=1 SV=1	1.48	1.48
A8K7Q1	cDNA FLJ77770, highly similar to Homo sapiens nucleobindin 1 (NUCB1), mRNA PE=2 SV=1	2.40	2.40
D3DQH8	Secreted protein, acidic, cysteine-rich (Osteonectin), isoform CRA_a GN=SPARC PE=4 SV=1	2.54	2.54
P19883	Follistatin GN=FST PE=1 SV=2	2.76	2.76
P22626	Heterogeneous nuclear ribonucleoproteins A2/B1 GN=HNRNPA2B1 PE=1 SV=2	2.95	2.95
P25786	Proteasome subunit alpha type-1 GN=PSMA1 PE=1 SV=1	2.41	2.41
Q6IAW5	CALU protein GN=CALU PE=2 SV=1	2.82	2.82
A0A024R755	Calumenin, isoform CRA_a GN=CALU PE=4 SV=1	2.64	2.64
Q09666	Neuroblast differentiation-associated protein AHNAK GN=AHNAK PE=1 SV=2	2.38	2.38
P20700	Lamin-B1 GN=LMNB1 PE=1 SV=2	2.06	2.06
A0A024RDB4	Heterogeneous nuclear ribonucleoprotein D (AU-rich element RNA binding protein 1, 37kDa), isoform CRA_c GN=HNRPD PE=4 SV=1	3.02	3.02
P19876	C-X-C motif chemokine 3 GN=CXCL3 PE=1 SV=1	3.18	3.18
P09382	Galectin-1 GN=LGALS1 PE=1 SV=2	2.91	2.91
B4DJQ8	cDNA FLJ55694, highly similar to Dipeptidyl-peptidase 1 (EC 3.4.14.1) PE=2 SV=1	2.34	2.34
Q53F64	Heterogeneous nuclear ribonucleoprotein AB isoform a variant (Fragment) PE=2 SV=1	1.99	1.99
P16035	Metalloproteinase inhibitor 2 GN=TIMP2 PE=1 SV=2	2.03	2.03
P07585	Decorin GN=DCN PE=1 SV=1	1.25	1.25
Q15293	Reticulocalbin-1 GN=RCN1 PE=1 SV=1	2.63	2.63
A0A024R9J4	Nephroblastoma overexpressed gene, isoform CRA_a GN=NOV PE=4 SV=1	3.22	3.22
P16403	Histone H1.2 GN=HIST1H1C PE=1 SV=2	1.67	1.67
Q16270	Insulin-like growth factor-binding protein 7 GN=IGFBP7 PE=1 SV=1	3.07	3.07
B7Z6Z4	Myosin light polypeptide 6 GN=MYL6 PE=1 SV=1	2.56	2.56
P63241	Eukaryotic translation initiation factor 5A-1 GN=EIF5A PE=1 SV=2	1.86	1.86
A0A109NGN6	Proteasome subunit alpha type PE=2 SV=1	1.82	1.82
A0A024R3W7	Eukaryotic translation elongation factor 1 beta 2, isoform CRA_a GN=EEF1B2 PE=3 SV=1	2.18	2.18
P09341	Growth-regulated alpha protein GN=CXCL1 PE=1 SV=1	3.40	3.40
P25788	Proteasome subunit alpha type-3 GN=PSMA3 PE=1 SV=2	1.89	1.89
P42830	C-X-C motif chemokine 5 GN=CXCL5 PE=1 SV=1	1.87	1.87
A0A087WSV8	Nucleobindin 2, isoform CRA_b GN=NUCB2 PE=1 SV=1	3.29	3.29
A0A024RDD9	C-X-C motif chemokine GN=CXCL2 PE=3 SV=1	2.63	2.63
P24592	Insulin-like growth factor-binding protein 6 GN=IGFBP6 PE=1 SV=1	1.95	1.95

P54727	UV excision repair protein RAD23 homolog B GN=RAD23B PE=1 SV=1	1.26	1.26
G3V3D1	Epididymal secretory protein E1 (Fragment) GN=NPC2 PE=1 SV=1	1.85	1.85
Q9UKY7	Protein CDV3 homolog GN=CDV3 PE=1 SV=1	1.94	1.94
A0A0K0K1J1	Cystatin GN=HEL-S-2 PE=2 SV=1	2.50	2.50
A6XND9	Beta-2-microglobulin PE=2 SV=1	2.77	2.77
P13500	C-C motif chemokine 2 GN=CCL2 PE=1 SV=1	4.22	4.22
D9IAI1	Epididymis secretory protein Li 34 GN=PEBP1 PE=2 SV=1	1.47	1.47
A0A024RDF6	Heterogeneous nuclear ribonucleoprotein D-like, isoform CRA_a GN=HNRPDL PE=4 SV=1	2.10	2.10
V9HW26	ATP synthase subunit alpha GN=HEL-S-123m PE=1 SV=1	1.86	1.86
Q00839	Heterogeneous nuclear ribonucleoprotein U GN=HNRNPU PE=1 SV=6	3.11	3.11
A0A023T787	RNA-binding protein 8A GN=RBM8 PE=2 SV=1	2.06	2.06
P22692	Insulin-like growth factor-binding protein 4 GN=IGFBP4 PE=1 SV=2	5.96	5.96
Q7Z7Q8	C-C motif chemokine GN=MCP-3 PE=3 SV=1	4.46	4.46
A0A087WYR3	Tumor protein D54 GN=TPD52L2 PE=1 SV=1	2.50	2.50
A0A140VJY2	Testicular tissue protein Li 209 PE=2 SV=1	1.81	1.81
P17987	T-complex protein 1 subunit alpha GN=TCP1 PE=1 SV=1	2.39	2.39
O43175	D-3-phosphoglycerate dehydrogenase GN=PHGDH PE=1 SV=4	1.99	1.99
P98066	Tumor necrosis factor-inducible gene 6 protein GN=TNFAIP6 PE=1 SV=2	2.68	2.68
A6XAA7	Gremlin GN=GREM1 PE=2 SV=1	2.04	2.04
A8KAQ5	cDNA FLJ77404, highly similar to Homo sapiens small nuclear ribonucleoprotein 70kDa polypeptide (RNP antigen) (SNRP70), transcript variant 1, mRNA PE=2 SV=1	2.12	2.12
P25398	40S ribosomal protein S12 GN=RPS12 PE=1 SV=3	1.28	1.28
Q08629	Testican-1 GN=SPOCK1 PE=1 SV=1	1.69	1.69
Q13344	Fus-like protein (Fragment) PE=2 SV=1	2.72	2.72
P09496	Clathrin light chain A GN=CLTA PE=1 SV=1	2.45	2.45
D3DPK5	SH3 domain binding glutamic acid-rich protein like 3, isoform CRA_a (Fragment) GN=SH3BGRL3 PE=4 SV=1	2.24	2.24
Q5T9B7	Adenylate kinase isoenzyme 1 GN=AK1 PE=1 SV=1	1.71	1.71
Q2VIR3	Putative eukaryotic translation initiation factor 2 subunit 3-like protein GN=EIF2S3L PE=5 SV=2	1.64	1.64
Q8NI22	Multiple coagulation factor deficiency protein 2 GN=MCFD2 PE=1 SV=1	1.72	1.72
Q59FG9	Chondroitin sulfate proteoglycan 2 (Versican) variant (Fragment) PE=2 SV=1	1.37	1.37
Q7Z4X0	MO25-like protein PE=2 SV=1	1.14	1.14
O75822	Eukaryotic translation initiation factor 3 subunit J GN=EIF3J PE=1 SV=2	2.67	2.67
P09497	Clathrin light chain B GN=CLTB PE=1 SV=1	1.81	1.81
Q6FIE5	PHP14 protein GN=PHP14 PE=2 SV=1	2.05	2.05
A0A024R5H0	Barrier to autointegration factor 1, isoform CRA_a GN=BANF1 PE=4 SV=1	1.75	1.75
O14737	Programmed cell death protein 5 GN=PDCD5 PE=1 SV=3	2.18	2.18
B2R4R9	HCG26477 GN=RPS28 PE=2 SV=1	1.82	1.82
A0A024RAF1	Bridging integrator 1, isoform CRA_k GN=BIN1 PE=4 SV=1	3.19	3.19
A0A087WUT6	Eukaryotic translation initiation factor 5B GN=EIF5B PE=1 SV=1	1.48	1.48
Q6NZI2	Caveolae-associated protein 1 GN=CAVIN1 PE=1 SV=1	1.88	1.88
P51884	Lumican GN=LUM PE=1 SV=2	2.82	2.82
P16104	Histone H2AX GN=H2AFX PE=1 SV=2	2.03	2.03
J3QRS3	Myosin regulatory light chain 12A GN=MYL12A PE=1 SV=1	1.07	1.07
Q15182	Small nuclear ribonucleoprotein-associated protein GN=SNRPB PE=2 SV=1	2.01	2.01
O14561	Acyl carrier protein, mitochondrial GN=NDUFAB1 PE=1 SV=3	3.05	3.05
Q59GY2	Ribosomal protein L4 variant (Fragment) PE=2 SV=1	2.68	2.68
P51572	B-cell receptor-associated protein 31 GN=BCAP31 PE=1 SV=3	2.26	2.26
Q13442	28 kDa heat- and acid-stable phosphoprotein GN=PDAP1 PE=1 SV=1	2.43	2.43

X6R4W8	BUB3-interacting and GLEBS motif-containing protein ZNF207 GN=ZNF207 PE=1 SV=1	2.47	2.47
B1AKJ5	Nardilysin GN=NRDC PE=1 SV=1	2.89	2.89
B4DIS3	Dpy-30-like protein, isoform CRA_b GN=LOC84661 PE=2 SV=1	1.68	1.68
B2R6R6	Serine/threonine-protein phosphatase PE=2 SV=1	4.17	4.17
P60866	40S ribosomal protein S20 GN=RPS20 PE=1 SV=1	1.26	1.26
Q9NP84	Tumor necrosis factor receptor superfamily member 12A GN=TNFRSF12A PE=1 SV=1	1.11	1.11
P46109	Crk-like protein GN=CRKL PE=1 SV=1	4.42	4.42
A0A087WTY6	Neuroblastoma suppressor of tumorigenicity 1 GN=NBL1 PE=1 SV=1	2.43	2.43
O00461	Golgi integral membrane protein 4 GN=GOLIM4 PE=1 SV=1	1.09	1.09
Q7Z6J2	General receptor for phosphoinositides 1-associated scaffold protein GN=GRASP PE=1 SV=1	3.48	3.48
P49458	Signal recognition particle 9 kDa protein GN=SRP9 PE=1 SV=2	2.03	2.03
Q4VC31	Coiled-coil domain-containing protein 58 GN=CCDC58 PE=1 SV=1	2.43	2.43
O43776	Asparagine--tRNA ligase, cytoplasmic GN=NARS PE=1 SV=1	1.09	1.09
A6NFX8	ADP-sugar pyrophosphatase GN=NUDT5 PE=1 SV=1	2.03	2.03
A0A024R2W4	Dystroglycan 1 (Dystrophin-associated glycoprotein 1), isoform CRA_a GN=DAG1 PE=4 SV=1	2.55	2.55
P20933	N(4)-(beta-N-acetylglucosaminyl)-L-asparaginase GN=AGA PE=1 SV=2	3.07	3.07
A0A024R5U5	ADAM metallopeptidase domain 10, isoform CRA_b GN=ADAM10 PE=4 SV=1	3.64	3.64
P14854	Cytochrome c oxidase subunit 6B1 GN=COX6B1 PE=1 SV=2	1.66	1.66
Q9UHD0	Interleukin-19 GN=IL19 PE=1 SV=2	2.86	2.86
A0A024R814	Ribosomal protein L7, isoform CRA_a GN=RPL7 PE=4 SV=1	2.03	2.03
Q9NU22	Midasin GN=MDN1 PE=1 SV=2	1.66	1.66
P20290	Transcription factor BTF3 GN=BTF3 PE=1 SV=1	1.91	1.91
Q7LBR1	Charged multivesicular body protein 1b GN=CHMP1B PE=1 SV=1	2.61	2.61
Q4VCS5	Angiomotin GN=AMOT PE=1 SV=1	2.35	2.35
F5H1D4	Ankyrin repeat and LEM domain-containing protein 2 (Fragment) GN=ANKLE2 PE=1 SV=1	2.54	2.54
B2R4H6	cDNA, FLJ92093, highly similar to Homo sapiens polymerase (RNA) II (DNA directed) polypeptide F (POLR2F), mRNA PE=2 SV=1	2.55	2.55
P08123	Collagen alpha-2(I) chain GN=COL1A2 PE=1 SV=7	5.71	5.71
Q14766	Latent-transforming growth factor beta-binding protein 1 GN=LTBP1 PE=1 SV=4	1.93	1.93
P02452	Collagen alpha-1(I) chain GN=COL1A1 PE=1 SV=5	1.88	1.88
C9JD84	Latent-transforming growth factor beta-binding protein 1 GN=LTBP1 PE=1 SV=1	2.53	2.53
V9HWE1	Epididymis luminal protein 113 GN=HEL113 PE=2 SV=1	2.55	2.55
A0A024R498	Serpin peptidase inhibitor, clade E (Nexin, plasminogen activator inhibitor type 1), member 2, isoform CRA_b GN=SERPINE2 PE=3 SV=1	2.06	2.06
Q12841	Follistatin-related protein 1 GN=FSTL1 PE=1 SV=1	2.25	2.25
P02461	Collagen alpha-1(III) chain GN=COL3A1 PE=1 SV=4	3.86	3.86
P48307	Tissue factor pathway inhibitor 2 GN=TFPI2 PE=1 SV=1	1.48	1.48
A8K7Q1	cDNA FLJ77770, highly similar to Homo sapiens nucleobindin 1 (NUCB1), mRNA PE=2 SV=1	2.40	2.40
D3DQH8	Secreted protein, acidic, cysteine-rich (Osteonectin), isoform CRA_a GN=SPARC PE=4 SV=1	2.54	2.54
P19883	Follistatin GN=FST PE=1 SV=2	2.76	2.76
P22626	Heterogeneous nuclear ribonucleoproteins A2/B1 GN=HNRNPA2B1 PE=1 SV=2	2.95	2.95
P25786	Proteasome subunit alpha type-1 GN=PSMA1 PE=1 SV=1	2.41	2.41
Q6IAW5	CALU protein GN=CALU PE=2 SV=1	2.82	2.82
A0A024R755	Calumenin, isoform CRA_a GN=CALU PE=4 SV=1	2.64	2.64
Q09666	Neuroblast differentiation-associated protein AHNAK GN=AHNAK PE=1 SV=2	2.38	2.38

P20700	Lamin-B1 GN=LMNB1 PE=1 SV=2	2.06	2.06
A0A024RDB4	Heterogeneous nuclear ribonucleoprotein D (AU-rich element RNA binding protein 1, 37kDa), isoform CRA_c GN=HNRPD PE=4 SV=1	3.02	3.02
P19876	C-X-C motif chemokine 3 GN=CXCL3 PE=1 SV=1	3.18	3.18
P09382	Galectin-1 GN=LGALS1 PE=1 SV=2	2.91	2.91
B4DJQ8	cDNA FLJ55694, highly similar to Dipeptidyl-peptidase 1 (EC 3.4.14.1) PE=2 SV=1	2.34	2.34
Q53F64	Heterogeneous nuclear ribonucleoprotein AB isoform a variant (Fragment) PE=2 SV=1	1.99	1.99
P16035	Metalloproteinase inhibitor 2 GN=TIMP2 PE=1 SV=2	2.03	2.03

Appendix 5

Proteins identified after data filtering in BEAM treated hypoxia vs normoxia samples, 1661 proteins were identified GN=Gene Name, PE=Protein Existence which is the numerical value describing the evidence for the existence of the protein, SV=Sequence Version which is the version number of the sequence.

Accession	Description	-log *P*	Diff.
A0A024R1N1	Myosin, heavy polypeptide 9, non-muscle, isoform CRA_a GN=MYH9 PE=3 SV=1	2.26	0.32
P21333	Filamin-A GN=FLNA PE=1 SV=4	1.57	0.21
Q15149	Plectin GN=PLEC PE=1 SV=3	1.83	0.23
A0A024R462	Fibronectin 1, isoform CRA_n GN=FN1 PE=4 SV=1	1.44	0.11
J3QSU6	Tenascin GN=TNC PE=1 SV=1	2.68	0.41
P01024	Complement C3 GN=C3 PE=1 SV=2	1.77	0.12
A7MBN2	TNC protein GN=TNC PE=2 SV=1	0.57	0.11
P12109	Collagen alpha-1(VI) chain GN=COL6A1 PE=1 SV=3	1.13	-0.08
A0A024R694	Actinin, alpha 1, isoform CRA_a GN=ACTN1 PE=4 SV=1	1.46	0.18
P13639	Elongation factor 2 GN=EEF2 PE=1 SV=4	2.97	0.39
A0A0S2Z3G9	Actinin alpha 4 isoform 1 (Fragment) GN=ACTN4 PE=2 SV=1	0.31	0.05
K9JA46	Epididymis luminal secretory protein 52 GN=EL52 PE=2 SV=1	1.88	0.25
A0A024RD80	Heat shock protein 90kDa alpha (Cytosolic), class B member 1, isoform CRA_a GN=HSP90AB1 PE=3 SV=1	1.48	0.19
V9HW22	Epididymis luminal protein 33 GN=HEL-S-72p PE=2 SV=1	2.44	0.28
A0A087WVQ6	Clathrin heavy chain GN=CLTC PE=1 SV=1	2.25	0.37
A0A1S5UZ07	Talin-1 GN=TLN1 PE=2 SV=1	1.79	0.20
V9HWB8	Pyruvate kinase GN=HEL-S-30 PE=1 SV=1	1.61	0.26
V9HWB4	Epididymis secretory sperm binding protein Li 89n GN=HEL-S-89n PE=2 SV=1	1.32	0.19
P06733	Alpha-enolase GN=ENO1 PE=1 SV=2	3.29	0.18
P34932	Heat shock 70 kDa protein 4 GN=HSPA4 PE=1 SV=4	2.33	0.27
P55072	Transitional endoplasmic reticulum ATPase GN=VCP PE=1 SV=4	0.83	0.17
A0A024R5Z9	Pyruvate kinase GN=PKM2 PE=3 SV=1	2.33	0.27
P03956	Interstitial collagenase GN=MMP1 PE=1 SV=3	0.69	0.04
A0A024R3X4	Heat shock 60kDa protein 1 (Chaperonin), isoform CRA_a GN=HSPD1 PE=2 SV=1	2.36	0.46
P07996	Thrombospondin-1 GN=THBS1 PE=1 SV=2	3.03	0.29
Q53G75	Matrix metalloproteinase 1 preproprotein variant (Fragment) PE=2 SV=1	1.48	-0.43
P02545	Prelamin-A/C GN=LMNA PE=1 SV=1	2.02	0.24
A0A0S2Z3H5	Collagen type I alpha 2 isoform 1 (Fragment) GN=COL1A2 PE=2 SV=1	5.38	0.63
B4DN15	cDNA FLJ55228, highly similar to Interstitial collagenase PE=2 SV=1	1.96	0.51
Q5CAQ5	Tumor rejection antigen (Gp96) 1 GN=TRA1 PE=2 SV=1	1.10	0.19
B4DW52	cDNA FLJ55253, highly similar to Actin, cytoplasmic 1 PE=2 SV=1	0.29	0.15
P43490	Nicotinamide phosphoribosyltransferase GN=NAMPT PE=1 SV=1	2.57	0.23
P04406	Glyceraldehyde-3-phosphate dehydrogenase GN=GAPDH PE=1 SV=3	1.89	0.22
P26038	Moesin GN=MSN PE=1 SV=3	2.49	0.21
Q09666	Neuroblast differentiation-associated protein AHNAK GN=AHNAK PE=1 SV=2	0.14	0.03
P18206	Vinculin GN=VCL PE=1 SV=4	1.44	0.16
A0A024RC65	HCG1991735, isoform CRA_a GN=hCG_1991735 PE=4 SV=1	2.40	0.24
V9HWF4	Phosphoglycerate kinase GN=HEL-S-68p PE=2 SV=1	1.04	-0.08
P22314	Ubiquitin-like modifier-activating enzyme 1 GN=UBA1 PE=1 SV=3	2.51	0.26
P29401	Transketolase GN=TKT PE=1 SV=3	4.30	0.20
P00338	L-lactate dehydrogenase A chain GN=LDHA PE=1 SV=2	0.76	0.08
P08670	Vimentin GN=VIM PE=1 SV=4	1.41	0.18
P68363	Tubulin alpha-1B chain GN=TUBA1B PE=1 SV=1	1.22	0.25
A0A024R321	Filamin B, beta (Actin binding protein 278), isoform CRA_a GN=FLNB PE=4 SV=1	0.27	0.05
Q53G35	Phosphoglycerate mutase (Fragment) PE=2 SV=1	1.55	0.11
Q71U36	Tubulin alpha-1A chain GN=TUBA1A PE=1 SV=1	0.92	0.23
P05120	Plasminogen activator inhibitor 2 GN=SERPINB2 PE=1 SV=2	2.07	0.25
B2R7Y0	cDNA, FLJ93654, highly similar to Homo sapiens serpin peptidase inhibitor, clade B (ovalbumin), member 2 (SERPINB2), mRNA PE=2 SV=1	1.19	0.10

B2RBR9	cDNA, FLJ95650, highly similar to Homo sapiens karyopherin (importin) beta 1 (KPNB1), mRNA PE=2 SV=1	2.57	0.32
P02452	Collagen alpha-1(I) chain GN=COL1A1 PE=1 SV=5	4.56	0.74
B2RDE8	cDNA, FLJ96580, highly similar to Homo sapiens hepatoma-derived growth factor (high-mobility group protein 1-like) (HDGF), mRNA PE=2 SV=1	3.42	0.24
P68032	Actin, alpha cardiac muscle 1 GN=ACTC1 PE=1 SV=1	1.64	0.27
D3DPU2	Adenylyl cyclase-associated protein GN=CAP1 PE=2 SV=1	1.83	0.20
P80723	Brain acid soluble protein 1 GN=BASP1 PE=1 SV=2	0.97	0.08
V9HWN7	Fructose-bisphosphate aldolase GN=HEL-S-87p PE=2 SV=1	0.43	-0.06
A0A024RDY0	RAN binding protein 5, isoform CRA_d GN=RANBP5 PE=4 SV=1	2.11	0.25
P49321	Nuclear autoantigenic sperm protein GN=NASP PE=1 SV=2	1.57	0.16
P07437	Tubulin beta chain GN=TUBB PE=1 SV=2	1.26	0.24
Q13813	Spectrin alpha chain, non-erythrocytic 1 GN=SPTAN1 PE=1 SV=3	0.72	0.07
P31946	14-3-3 protein beta/alpha GN=YWHAB PE=1 SV=3	2.18	0.20
A7BI36	p180/ribosome receptor GN=RRBP1 PE=2 SV=2	2.38	0.19
P55060	Exportin-2 GN=CSE1L PE=1 SV=3	2.65	0.30
A0A0G2JIW1	Heat shock 70 kDa protein 1B GN=HSPA1B PE=1 SV=1	2.63	0.23
P60174	Triosephosphate isomerase GN=TPI1 PE=1 SV=3	1.69	0.13
V9HW88	Calreticulin, isoform CRA_b GN=HEL-S-99n PE=2 SV=1	1.89	0.30
A0A024R6R4	Matrix metallopeptidase 2 (Gelatinase A, 72kDa gelatinase, 72kDa type IV collagenase), isoform CRA_a GN=MMP2 PE=3 SV=1	3.90	0.36
Q59E93	Aminopeptidase (Fragment) PE=2 SV=1	1.46	0.30
F5H5D3	Tubulin alpha chain GN=TUBA1C PE=1 SV=1	0.86	0.17
A0A024R4A0	Nucleolin, isoform CRA_b GN=NCL PE=4 SV=1	2.06	0.23
P07195	L-lactate dehydrogenase B chain GN=LDHB PE=1 SV=2	3.58	0.40
Q14766	Latent-transforming growth factor beta-binding protein 1 GN=LTBP1 PE=1 SV=4	4.40	0.25
P68371	Tubulin beta-4B chain GN=TUBB4B PE=1 SV=1	1.20	0.23
Q02952	A-kinase anchor protein 12 GN=AKAP12 PE=1 SV=4	1.28	-0.09
A0A024R8S5	Protein disulfide-isomerase GN=P4HB PE=2 SV=1	0.66	0.14
P38646	Stress-70 protein, mitochondrial GN=HSPA9 PE=1 SV=2	3.14	0.44
E7EVA0	Microtubule-associated protein GN=MAP4 PE=1 SV=1	2.62	0.24
A0A024RAM4	Microtubule-associated protein 1B, isoform CRA_b GN=MAP1B PE=4 SV=1	1.76	0.18
Q53G85	Elongation factor 1-alpha (Fragment) PE=2 SV=1	2.38	0.36
P12110	Collagen alpha-2(VI) chain GN=COL6A2 PE=1 SV=4	1.63	-0.09
Q12906	Interleukin enhancer-binding factor 3 GN=ILF3 PE=1 SV=3	1.01	0.20
D3DTX7	Collagen, type I, alpha 1, isoform CRA_a GN=COL1A1 PE=4 SV=1	0.01	0.00
P13797	Plastin-3 GN=PLS3 PE=1 SV=4	2.34	0.22
Q59ER5	WD repeat-containing protein 1 isoform 1 variant (Fragment) PE=2 SV=1	2.20	0.27
D0PNI1	Epididymis luminal protein 4 GN=YWHAZ PE=2 SV=1	1.53	0.15
P08254	Stromelysin-1 GN=MMP3 PE=1 SV=2	3.07	0.29
F4ZW66	NF110b PE=2 SV=1	2.40	0.27
P04179	Superoxide dismutase [Mn], mitochondrial GN=SOD2 PE=1 SV=3	0.81	0.12
A0A2R8Y5S7	Radixin GN=RDX PE=1 SV=1	2.14	0.17
V9HVZ7	Epididymis luminal protein 176 GN=HEL-176 PE=2 SV=1	2.84	0.32
B4DLV7	Rab GDP dissociation inhibitor PE=2 SV=1	2.38	0.26
Q12841	Follistatin-related protein 1 GN=FSTL1 PE=1 SV=1	2.92	0.12
V9HVY3	Protein disulfide-isomerase GN=HEL-S-269 PE=2 SV=1	2.24	0.29
E7EQR4	Ezrin GN=EZR PE=1 SV=3	2.16	0.20
B4DNA3	Adenylyl cyclase-associated protein PE=2 SV=1	2.07	0.37
P07602	Prosaposin GN=PSAP PE=1 SV=2	2.00	0.23
E9PK25	Cofilin-1 GN=CFL1 PE=1 SV=1	2.88	0.32
A0A087WUZ3	Spectrin beta chain GN=SPTBN1 PE=1 SV=1	1.38	0.11
P52209	6-phosphogluconate dehydrogenase, decarboxylating GN=PGD PE=1 SV=3	4.15	0.45
A0A0S2Z3X8	Rab GDP dissociation inhibitor (Fragment) GN=GDI1 PE=2 SV=1	3.59	0.25
Q14204	Cytoplasmic dynein 1 heavy chain 1 GN=DYNC1H1 PE=1 SV=5	1.65	0.28
P27348	14-3-3 protein theta GN=YWHAQ PE=1 SV=1	3.18	0.30
A0A2U3TZU2	Glucose-6-phosphate isomerase GN=GPI PE=1 SV=1	0.57	0.04

P05231	Interleukin-6 GN=IL6 PE=1 SV=1	1.22	0.05
V9HW31	ATP synthase subunit beta GN=HEL-S-271 PE=1 SV=1	1.91	0.32
A0A0C4DGB5	Calpastatin GN=CAST PE=1 SV=1	1.55	0.14
P35555	Fibrillin-1 GN=FBN1 PE=1 SV=3	0.78	0.06
V9HW96	Chaperonin containing TCP1, subunit 2 (Beta), isoform CRA_b GN=HEL-S-100n PE=1 SV=1	1.72	0.33
A0A024R5M9	Nuclear mitotic apparatus protein 1, isoform CRA_a GN=NUMA1 PE=4 SV=1	1.52	0.19
H0Y449	Nuclease-sensitive element-binding protein 1 (Fragment) GN=YBX1 PE=1 SV=1	1.41	0.14
Q9UKY7	Protein CDV3 homolog GN=CDV3 PE=1 SV=1	2.28	0.26
A0A024R4K3	Malate dehydrogenase GN=MDH2 PE=2 SV=1	3.95	0.45
P49327	Fatty acid synthase GN=FASN PE=1 SV=3	3.33	0.43
B5BUB5	Autoantigen La (Fragment) GN=SSB PE=2 SV=1	2.68	0.26
A0A024RAN2	Calpastatin, isoform CRA_a GN=CAST PE=4 SV=1	0.51	0.07
P35442	Thrombospondin-2 GN=THBS2 PE=1 SV=2	1.65	0.32
P37802	Transgelin-2 GN=TAGLN2 PE=1 SV=3	2.30	0.28
B4DJ30	cDNA FLJ61290, highly similar to Neutral alpha-glucosidase AB PE=2 SV=1	1.75	0.27
A0A024R498	Serpin peptidase inhibitor, clade E (Nexin, plasminogen activator inhibitor type 1), member 2, isoform CRA_b GN=SERPINE2 PE=3 SV=1	4.38	0.59
B2R983	cDNA, FLJ94267, highly similar to Homo sapiens glutathione S-transferase omega 1 (GSTO1), mRNA PE=2 SV=1	2.98	0.26
P50990	T-complex protein 1 subunit theta GN=CCT8 PE=1 SV=4	1.80	0.29
P26641	Elongation factor 1-gamma GN=EEF1G PE=1 SV=3	1.84	0.26
V9HW98	Epididymis luminal protein 2 GN=HEL2 PE=1 SV=1	1.40	0.18
P28838	Cytosol aminopeptidase GN=LAP3 PE=1 SV=3	3.31	0.43
A8K968	Band 4.1-like protein 3 GN=EPB41L3 PE=1 SV=1	1.53	0.20
V9HW37	Epididymis secretory protein Li 69 GN=HEL-S-69 PE=1 SV=1	1.80	0.34
V9HW74	Ubiquitin carboxyl-terminal hydrolase GN=HEL-117 PE=2 SV=1	2.36	0.26
P36871	Phosphoglucomutase-1 GN=PGM1 PE=1 SV=3	1.49	0.09
Q16658	Fascin GN=FSCN1 PE=1 SV=3	2.40	0.24
P20700	Lamin-B1 GN=LMNB1 PE=1 SV=2	2.04	0.23
A0A090N8Y2	Protein disulfide-isomerase A4 GN=ERP70 PE=2 SV=1	1.44	0.23
P23142	Fibulin-1 GN=FBLN1 PE=1 SV=4	1.85	0.09
A0A0A0MRA8	Band 4.1-like protein 3 GN=EPB41L3 PE=1 SV=1	0.79	0.08
A0A024R6W0	Aspartate aminotransferase GN=GOT2 PE=4 SV=1	3.75	0.35
P52907	F-actin-capping protein subunit alpha-1 GN=CAPZA1 PE=1 SV=3	2.38	0.34
O00299	Chloride intracellular channel protein 1 GN=CLIC1 PE=1 SV=4	2.77	0.29
P21291	Cysteine and glycine-rich protein 1 GN=CSRP1 PE=1 SV=3	1.99	0.18
A8K088	cDNA FLJ78614, highly similar to Homo sapiens eukaryotic translation initiation factor 4A, isoform 1 (EIF4A1), mRNA PE=2 SV=1	1.72	0.35
Q16719	Kynureninase GN=KYNU PE=1 SV=1	2.40	0.28
P37837	Transaldolase GN=TALDO1 PE=1 SV=2	3.26	0.31
A0A024RB85	Proliferation-associated 2G4, 38kDa, isoform CRA_a GN=PA2G4 PE=4 SV=1	3.01	0.34
Q32Q12	Nucleoside diphosphate kinase GN=NME1-NME2 PE=1 SV=1	1.69	0.24
P25786	Proteasome subunit alpha type-1 GN=PSMA1 PE=1 SV=1	2.37	0.27
Q02790	Peptidyl-prolyl cis-trans isomerase FKBP4 GN=FKBP4 PE=1 SV=3	3.28	0.27
A0A024RDR0	High-mobility group box 1, isoform CRA_a GN=HMGB1 PE=4 SV=1	3.60	0.23
A8K8U1	cDNA FLJ77762, highly similar to Homo sapiens cullin-associated and neddylation-dissociated 1 (CAND1), mRNA PE=2 SV=1	1.77	0.20
Q14566	DNA replication licensing factor MCM6 GN=MCM6 PE=1 SV=1	2.43	0.22
A0A024RAZ7	Heterogeneous nuclear ribonucleoprotein A1, isoform CRA_b GN=HNRPA1 PE=4 SV=1	1.90	0.22
P67936	Tropomyosin alpha-4 chain GN=TPM4 PE=1 SV=3	2.29	0.18
B4DUV1	Fibulin-1 PE=2 SV=1	1.15	0.17
Q9H1E3	Nuclear ubiquitous casein and cyclin-dependent kinase substrate 1 GN=NUCKS1 PE=1 SV=1	2.67	0.22
P40925	Malate dehydrogenase, cytoplasmic GN=MDH1 PE=1 SV=4	4.19	0.29
O00469	Procollagen-lysine,2-oxoglutarate 5-dioxygenase 2 GN=PLOD2 PE=1 SV=2	3.58	-0.84
P26639	Threonine--tRNA ligase, cytoplasmic GN=TARS PE=1 SV=3	2.14	0.26
A4UCS8	Enolase 1 (Fragment) PE=2 SV=1	1.41	0.25

P48307	Tissue factor pathway inhibitor 2 GN=TFPI2 PE=1 SV=1	3.31	0.45
Q14315	Filamin-C GN=FLNC PE=1 SV=3	1.55	0.20
A0A024R5Z7	Annexin GN=ANXA2 PE=3 SV=1	0.83	0.22
J3KQE5	GTP-binding nuclear protein Ran (Fragment) GN=RAN PE=1 SV=1	2.86	0.27
K7EJB9	Calreticulin (Fragment) GN=CALR PE=1 SV=1	0.78	-0.25
Q05682	Caldesmon GN=CALD1 PE=1 SV=3	1.78	0.15
A8K690	cDNA FLJ76863, highly similar to Homo sapiens stress-induced-phosphoprotein 1 (Hsp70/Hsp90-organizing protein) (STIP1), mRNA PE=2 SV=1	2.01	0.25
Q5TZP7	DNA-(apurinic or apyrimidinic site) lyase GN=APEX1 PE=2 SV=1	4.08	0.32
A0A1C7CYX9	Dihydropyrimidinase-related protein 2 GN=DPYSL2 PE=1 SV=1	2.18	0.20
A0A024QYT5	Serpin peptidase inhibitor, clade E (Nexin, plasminogen activator inhibitor type 1), member 1, isoform CRA_b GN=SERPINE1 PE=3 SV=1	1.66	-0.21
P22626	Heterogeneous nuclear ribonucleoproteins A2/B1 GN=HNRNPA2B1 PE=1 SV=2	2.75	0.22
Q8N7G1	Purine nucleoside phosphorylase PE=2 SV=1	1.11	0.13
B1AK88	Capping protein (Actin filament) muscle Z-line, beta, isoform CRA_d GN=CAPZB PE=1 SV=1	2.89	0.30
A0A024R895	SET translocation (Myeloid leukemia-associated), isoform CRA_b GN=SET PE=3 SV=1	1.97	0.19
P15121	Aldose reductase GN=AKR1B1 PE=1 SV=3	3.25	0.35
Q16531	DNA damage-binding protein 1 GN=DDB1 PE=1 SV=1	2.58	0.28
A0A087WTP3	Far upstream element-binding protein 2 GN=KHSRP PE=1 SV=1	1.57	0.16
Q9Y4L1	Hypoxia up-regulated protein 1 GN=HYOU1 PE=1 SV=1	2.03	0.27
Q15691	Microtubule-associated protein RP/EB family member 1 GN=MAPRE1 PE=1 SV=3	2.92	0.27
A0A024RAI1	ARP3 actin-related protein 3 homolog (Yeast), isoform CRA_a GN=ACTR3 PE=3 SV=1	2.44	0.31
P25705	ATP synthase subunit alpha, mitochondrial GN=ATP5F1A PE=1 SV=1	1.82	0.33
O75874	Isocitrate dehydrogenase [NADP] cytoplasmic GN=IDH1 PE=1 SV=2	3.46	0.29
P17987	T-complex protein 1 subunit alpha GN=TCP1 PE=1 SV=1	1.72	0.32
P12956	X-ray repair cross-complementing protein 6 GN=XRCC6 PE=1 SV=2	1.72	0.31
Q6FHV6	ENO2 protein GN=ENO2 PE=1 SV=1	3.17	-0.30
P23526	Adenosylhomocysteinase GN=AHCY PE=1 SV=4	2.30	0.29
Q562R1	Beta-actin-like protein 2 GN=ACTBL2 PE=1 SV=2	0.59	0.16
P07737	Profilin-1 GN=PFN1 PE=1 SV=2	2.77	0.36
Q59H77	T-complex protein 1 subunit gamma (Fragment) PE=2 SV=1	1.46	0.25
Q00839	Heterogeneous nuclear ribonucleoprotein U GN=HNRNPU PE=1 SV=6	1.30	0.22
P15531	Nucleoside diphosphate kinase A GN=NME1 PE=1 SV=1	0.97	0.23
P11047	Laminin subunit gamma-1 GN=LAMC1 PE=1 SV=3	2.22	0.24
J3KQ32	Obg-like ATPase 1 GN=OLA1 PE=1 SV=1	3.49	0.34
P09382	Galectin-1 GN=LGALS1 PE=1 SV=2	2.24	0.20
P25789	Proteasome subunit alpha type-4 GN=PSMA4 PE=1 SV=1	1.83	0.29
A0A024R1K7	Tyrosine 3-monooxygenase/tryptophan 5-monooxygenase activation protein, eta polypeptide, isoform CRA_b GN=YWHAH PE=3 SV=1	2.73	0.22
O14980	Exportin-1 GN=XPO1 PE=1 SV=1	2.75	0.34
Q01469	Fatty acid-binding protein 5 GN=FABP5 PE=1 SV=3	3.64	0.31
A0A024RDL1	Chaperonin containing TCP1, subunit 6A (Zeta 1), isoform CRA_a GN=CCT6A PE=3 SV=1	1.50	0.35
Q53HV2	Chaperonin containing TCP1, subunit 7 (Eta) variant (Fragment) PE=2 SV=1	1.36	0.22
B3KMZ6	cDNA FLJ13058 fis, clone NT2RP3001587, highly similar to Ubiquitin-like 1-activating enzyme E1B PE=2 SV=1	1.21	0.17
Q5VXV3	SET translocation (Myeloid leukemia-associated), isoform CRA_a GN=SET PE=2 SV=1	0.33	0.13
V9HWB5	Epididymis secretory sperm binding protein Li 66p GN=HEL-S-66p PE=2 SV=1	3.06	0.47
P35580	Myosin-10 GN=MYH10 PE=1 SV=3	0.60	0.12
P50454	Serpin H1 GN=SERPINH1 PE=1 SV=2	1.82	0.36
A2A274	Aconitate hydratase, mitochondrial GN=ACO2 PE=1 SV=1	4.67	0.34
A8K3C3	T-complex protein 1 subunit delta PE=2 SV=1	1.64	0.33
B7ZA86	cDNA, FLJ79100, highly similar to 14-3-3 protein epsilon (14-3-3E) PE=2 SV=1	2.87	0.45
P13489	Ribonuclease inhibitor GN=RNH1 PE=1 SV=2	2.29	0.24
B4DJQ5	cDNA FLJ59211, highly similar to Glucosidase 2 subunit beta PE=2 SV=1	1.35	0.21
A0A0S2Z4I4	Tropomyosin 3 isoform 3 (Fragment) GN=TPM3 PE=2 SV=1	1.19	0.15
P31939	Bifunctional purine biosynthesis protein PURH GN=ATIC PE=1 SV=3	2.95	0.36

A8K335	Gamma-glutamyl hydrolase PE=2 SV=1	1.27	0.13
B4DUQ1	cDNA FLJ54552, highly similar to Heterogeneous nuclear ribonucleoprotein K PE=2 SV=1	1.66	0.19
D3DQ69	SERPINE1 mRNA binding protein 1, isoform CRA_c GN=SERBP1 PE=4 SV=1	3.11	0.36
A0A140VK07	Testicular secretory protein Li 7 PE=2 SV=1	2.62	0.34
A8K7B7	Protein phosphatase 2 (Formerly 2A), regulatory subunit A (PR 65), alpha isoform GN=PPP2R1A PE=1 SV=1	1.97	0.28
A8K7Q1	cDNA FLJ77770, highly similar to Homo sapiens nucleobindin 1 (NUCB1), mRNA PE=2 SV=1	3.65	0.23
A8K329	cDNA FLJ76656, highly similar to Homo sapiens scaffold attachment factor B (SAFB), mRNA PE=2 SV=1	3.02	0.20
G3XAI2	Laminin subunit beta-1 GN=LAMB1 PE=1 SV=1	1.49	0.15
P04083	Annexin A1 GN=ANXA1 PE=1 SV=2	1.14	0.33
V9HWB7	Epididymis luminal protein 60 GN=HEL60 PE=2 SV=1	0.15	0.02
O00391	Sulfhydryl oxidase 1 GN=QSOX1 PE=1 SV=3	2.08	0.11
Q6IAW5	CALU protein GN=CALU PE=2 SV=1	1.86	0.22
A0A024R1Z6	Vesicle amine transport protein 1 homolog (T californica), isoform CRA_a GN=VAT1 PE=4 SV=1	2.09	0.24
O60664	Perilipin-3 GN=PLIN3 PE=1 SV=3	1.28	0.13
A0A087X1Z3	Proteasome activator complex subunit 2 GN=PSME2 PE=1 SV=1	2.25	0.26
Q4LE58	eIF4G1 variant protein (Fragment) GN=EIF4G1 variant protein PE=2 SV=1	3.15	0.31
A0A087X1N8	Serpin B6 GN=SERPINB6 PE=1 SV=1	2.90	0.25
Q15084	Protein disulfide-isomerase A6 GN=PDIA6 PE=1 SV=1	2.15	0.26
B4DPQ0	Complement C1r subcomponent GN=C1R PE=1 SV=1	3.63	0.76
P14866	Heterogeneous nuclear ribonucleoprotein L GN=HNRNPL PE=1 SV=2	2.81	0.34
P06748	Nucleophosmin GN=NPM1 PE=1 SV=2	2.44	0.23
Q59EQ5	Cysteine and glycine-rich protein 1 variant (Fragment) PE=2 SV=1	1.20	0.17
P52926	High mobility group protein HMGI-C GN=HMGA2 PE=1 SV=1	2.36	0.41
P17174	Aspartate aminotransferase, cytoplasmic GN=GOT1 PE=1 SV=3	2.86	0.27
A0A109NGN6	Proteasome subunit alpha type PE=2 SV=1	2.00	0.26
P23284	Peptidyl-prolyl cis-trans isomerase B GN=PPIB PE=1 SV=2	2.81	0.31
Q12888	TP53-binding protein 1 GN=TP53BP1 PE=1 SV=2	2.03	0.27
Q59EA2	Coronin (Fragment) PE=2 SV=1	2.99	0.23
P29966	Myristoylated alanine-rich C-kinase substrate GN=MARCKS PE=1 SV=4	1.38	0.15
O95373	Importin-7 GN=IPO7 PE=1 SV=1	2.79	0.30
E7EUF1	Ectonucleotide pyrophosphatase/phosphodiesterase family member 2 GN=ENPP2 PE=1 SV=1	2.89	0.22
Q96TA1	Niban-like protein 1 GN=FAM129B PE=1 SV=3	2.22	0.20
Q15075	Early endosome antigen 1 GN=EEA1 PE=1 SV=2	1.35	0.18
Q14240	Eukaryotic initiation factor 4A-II GN=EIF4A2 PE=1 SV=2	2.32	0.28
P61981	14-3-3 protein gamma GN=YWHAG PE=1 SV=2	2.36	0.18
P20618	Proteasome subunit beta type-1 GN=PSMB1 PE=1 SV=2	1.49	0.27
P19883	Follistatin GN=FST PE=1 SV=2	0.13	0.01
Q4LE36	ACLY variant protein (Fragment) GN=ACLY variant protein PE=2 SV=1	1.78	0.24
A0A0S2Z4C3	Fumarate hydratase isoform 1 (Fragment) GN=FH PE=2 SV=1	3.19	0.43
P63244	Receptor of activated protein C kinase 1 GN=RACK1 PE=1 SV=3	2.70	0.39
P11940	Polyadenylate-binding protein 1 GN=PABPC1 PE=1 SV=2	2.13	0.37
E7EMB3	Calmodulin-2 GN=CALM2 PE=1 SV=1	2.66	0.17
A0A024R374	Cathepsin B, isoform CRA_a GN=CTSB PE=3 SV=1	1.85	0.18
Q59FD4	Hexokinase 1 isoform HKI variant (Fragment) PE=2 SV=1	0.59	0.09
B2R6I6	cDNA, FLJ92965, highly similar to Homo sapiens stanniocalcin 1 (STC1), mRNA PE=2 SV=1	2.89	-0.30
Q92688	Acidic leucine-rich nuclear phosphoprotein 32 family member B GN=ANP32B PE=1 SV=1	2.51	0.21
Q9Y266	Nuclear migration protein nudC GN=NUDC PE=1 SV=1	3.92	0.29
A0A024RDF3	Heterogeneous nuclear ribonucleoprotein D (AU-rich element RNA binding protein 1, 37kDa), isoform CRA_d GN=HNRPD PE=4 SV=1	3.14	0.28
B5BU83	Stathmin GN=STMN1 PE=2 SV=1	2.02	0.17
Q4W4Y1	Dopamine receptor interacting protein 4 GN=DRIP4 PE=2 SV=1	1.71	0.23
A0A024RB75	Citrate synthase GN=CS PE=3 SV=1	3.41	0.44

B7Z8Z6	DNA helicase PE=2 SV=1	2.72	0.31
P13010	X-ray repair cross-complementing protein 5 GN=XRCC5 PE=1 SV=3	2.18	0.29
A4D2D2	Procollagen C-endopeptidase enhancer GN=PCOLCE PE=4 SV=1	2.85	0.43
P30041	Peroxiredoxin-6 GN=PRDX6 PE=1 SV=3	2.91	0.31
P49588	Alanine--tRNA ligase, cytoplasmic GN=AARS PE=1 SV=2	2.66	0.28
V9HWH9	Protein S100 GN=HEL-S-43 PE=2 SV=1	2.29	0.23
A0A024RCM3	DDX39B GN=hCG_2005638 PE=4 SV=1	2.52	0.25
E9KL48	Epididymis tissue sperm binding protein Li 18mP GN=GLUD1 PE=2 SV=1	2.25	0.37
P06703	Protein S100-A6 GN=S100A6 PE=1 SV=1	1.84	0.27
A0A024R6K8	Tryptophanyl-tRNA synthetase, isoform CRA_a GN=WARS PE=3 SV=1	2.65	0.39
P12004	Proliferating cell nuclear antigen GN=PCNA PE=1 SV=1	2.58	0.24
G3V5Z7	Proteasome subunit alpha type GN=PSMA6 PE=1 SV=1	2.77	0.30
P48594	Serpin B4 GN=SERPINB4 PE=1 SV=2	0.64	0.08
P28799	Granulins GN=GRN PE=1 SV=2	2.51	0.28
Q15582	Transforming growth factor-beta-induced protein ig-h3 GN=TGFBI PE=1 SV=1	0.05	-0.01
Q59EG8	Proteasome 26S non-ATPase subunit 2 variant (Fragment) PE=2 SV=1	1.74	0.32
A0A140VK27	Leukotriene A(4) hydrolase PE=2 SV=1	2.90	0.32
A0A024R755	Calumenin, isoform CRA_a GN=CALU PE=4 SV=1	0.93	0.13
P30084	Enoyl-CoA hydratase, mitochondrial GN=ECHS1 PE=1 SV=4	3.49	0.48
Q53F64	Heterogeneous nuclear ribonucleoprotein AB isoform a variant (Fragment) PE=2 SV=1	1.95	0.20
A0A0S2Z3Y1	Lectin galactoside-binding soluble 3 binding protein isoform 1 (Fragment) GN=LGALS3BP PE=2 SV=1	3.29	0.47
A8K9A4	cDNA FLJ75154, highly similar to Homo sapiens heterogeneous nuclear ribonucleoprotein C (C1/C2), mRNA PE=2 SV=1	2.40	0.35
A7XZE4	Beta tropomyosin isoform GN=TPM2 PE=1 SV=1	3.19	0.29
A8K8D9	Glucose-6-phosphate 1-dehydrogenase PE=2 SV=1	2.04	0.33
O43390	Heterogeneous nuclear ribonucleoprotein R GN=HNRNPR PE=1 SV=1	2.07	0.38
A0A024R3T8	Poly [ADP-ribose] polymerase GN=PARP1 PE=4 SV=1	2.62	0.35
B3KQF4	cDNA FLJ90373 fis, clone NT2RP2004606, highly similar to Metalloproteinase inhibitor 1 PE=2 SV=1	3.99	0.27
P55786	Puromycin-sensitive aminopeptidase GN=NPEPPS PE=1 SV=2	3.07	0.23
D3DQH8	Secreted protein, acidic, cysteine-rich (Osteonectin), isoform CRA_a GN=SPARC PE=4 SV=1	2.59	0.43
Q7Z406	Myosin-14 GN=MYH14 PE=1 SV=2	0.49	0.09
A3RJH1	ATP-dependent RNA helicase DDX1 GN=DDX1 PE=2 SV=1	2.22	0.33
A0A0F7NGI8	Leucine rich repeat (In FLII) interacting protein 1, isoform CRA_c GN=LRRFIP1 PE=2 SV=1	1.02	0.09
Q562L9	Actin-like protein (Fragment) GN=ACT PE=4 SV=1	1.58	0.25
Q96KP4	Cytosolic non-specific dipeptidase GN=CNDP2 PE=1 SV=2	3.01	0.29
V9HWC2	Epididymis secretory sperm binding protein Li 67p GN=HEL-S-67p PE=2 SV=1	2.82	0.28
Q9Y4K0	Lysyl oxidase homolog 2 GN=LOXL2 PE=1 SV=1	0.54	-0.03
Q9BUF5	Tubulin beta-6 chain GN=TUBB6 PE=1 SV=1	1.12	0.18
A0A0U1RRM4	Polypyrimidine tract-binding protein 1 GN=PTBP1 PE=1 SV=1	2.27	0.23
Q9NYU2	UDP-glucose:glycoprotein glucosyltransferase 1 GN=UGGT1 PE=1 SV=3	1.26	0.20
Q15293	Reticulocalbin-1 GN=RCN1 PE=1 SV=1	1.88	0.30
B2R8Z8	cDNA, FLJ94136, highly similar to Homo sapiens synaptotagmin binding, cytoplasmic RNA interacting protein (SYNCRIP), mRNA PE=2 SV=1	1.99	0.24
A4D1W7	Inhibin, beta A (Activin A, activin AB alpha polypeptide) GN=INHBA PE=1 SV=1	1.10	-0.08
Q13185	Chromobox protein homolog 3 GN=CBX3 PE=1 SV=4	3.10	0.31
P05387	60S acidic ribosomal protein P2 GN=RPLP2 PE=1 SV=1	1.73	0.27
P07814	Bifunctional glutamate/proline--tRNA ligase GN=EPRS PE=1 SV=5	1.31	0.23
P30050	60S ribosomal protein L12 GN=RPL12 PE=1 SV=1	1.38	0.20
P39687	Acidic leucine-rich nuclear phosphoprotein 32 family member A GN=ANP32A PE=1 SV=1	1.58	0.15
Q14019	Coactosin-like protein GN=COTL1 PE=1 SV=3	1.52	0.19
D6RER5	Septin-11 GN=SEPT11 PE=1 SV=1	0.49	0.10
P35556	Fibrillin-2 GN=FBN2 PE=1 SV=3	2.96	0.28
A0A087WUT6	Eukaryotic translation initiation factor 5B GN=EIF5B PE=1 SV=1	2.07	0.18
P63241	Eukaryotic translation initiation factor 5A-1 GN=EIF5A PE=1 SV=2	2.70	0.38

J3KN67	Tropomyosin alpha-3 chain GN=TPM3 PE=1 SV=1	1.73	0.15
Q6FIC5	Chloride intracellular channel protein GN=CLIC4 PE=2 SV=1	3.74	0.37
V9HWJ1	Glutathione synthetase GN=HEL-S-64p PE=2 SV=1	3.60	0.25
A0A0K0K1K4	Proteasome subunit alpha type GN=HEL-S-276 PE=2 SV=1	2.10	0.24
Q15436	Protein transport protein Sec23A GN=SEC23A PE=1 SV=2	3.05	0.31
Q549N0	Cofilin 2 (Muscle), isoform CRA_a GN=CFL2 PE=1 SV=1	1.65	0.19
B4DUP2	UTP--glucose-1-phosphate uridylyltransferase PE=2 SV=1	0.91	0.13
Q03252	Lamin-B2 GN=LMNB2 PE=1 SV=4	1.66	0.14
B4DRM3	cDNA FLJ54492, highly similar to Eukaryotic translation initiation factor 4B PE=2 SV=1	2.80	0.22
P19876	C-X-C motif chemokine 3 GN=CXCL3 PE=1 SV=1	0.14	0.04
A0A140VJL3	Hypoxanthine phosphoribosyltransferase PE=2 SV=1	1.90	0.20
Q7RU04	Aminopeptidase B GN=RNPEP PE=4 SV=1	2.56	0.32
Q15365	Poly(rC)-binding protein 1 GN=PCBP1 PE=1 SV=2	1.12	0.17
B8ZWD9	Diazepam binding inhibitor, splice form 1D(2) GN=DBI PE=2 SV=1	2.51	0.24
A2RUM7	Ribosomal protein L5, isoform CRA_c GN=RPL5 PE=2 SV=1	2.91	0.36
P26196	Probable ATP-dependent RNA helicase DDX6 GN=DDX6 PE=1 SV=2	3.11	0.20
P14868	Aspartate--tRNA ligase, cytoplasmic GN=DARS PE=1 SV=2	1.09	0.17
P11717	Cation-independent mannose-6-phosphate receptor GN=IGF2R PE=1 SV=3	0.29	0.04
Q12905	Interleukin enhancer-binding factor 2 GN=ILF2 PE=1 SV=2	2.36	0.29
A0A0K0K1L8	Epididymis secretory sperm binding protein Li 129m GN=HEL-S-129m PE=2 SV=1	2.72	0.28
B7Z809	cDNA FLJ56016, highly similar to C-1-tetrahydrofolate synthase, cytoplasmic PE=2 SV=1	2.51	0.29
A0A0C4DG17	40S ribosomal protein SA GN=RPSA PE=1 SV=1	2.51	0.44
A1KYQ7	Eukaryotic translation initiation factor 3 subunit C GN=EIF3C PE=2 SV=1	2.52	0.31
P46013	Proliferation marker protein Ki-67 GN=MKI67 PE=1 SV=2	4.07	0.20
P54727	UV excision repair protein RAD23 homolog B GN=RAD23B PE=1 SV=1	2.98	0.22
O60361	Putative nucleoside diphosphate kinase GN=NME2P1 PE=5 SV=1	2.49	0.19
B4DLC0	cDNA FLJ58476, highly similar to Poly(rC)-binding protein 2 PE=2 SV=1	0.03	0.02
C7DJS2	Glutathione S-transferase pi (Fragment) GN=GSTP1 PE=2 SV=1	1.66	0.28
Q9UNZ2	NSFL1 cofactor p47 GN=NSFL1C PE=1 SV=2	1.30	0.24
Q59ET0	Glucan, branching enzyme 1 variant (Fragment) PE=2 SV=1	0.82	0.10
Q6IBT1	Proteasome subunit beta type GN=PSMB7 PE=2 SV=1	2.41	0.29
B0YIW6	Archain 1, isoform CRA_a GN=ARCN1 PE=1 SV=1	1.58	0.29
P50502	Hsc70-interacting protein GN=ST13 PE=1 SV=2	2.48	0.32
B7Z3K9	Fructose-bisphosphate aldolase PE=2 SV=1	1.32	-0.12
P23246	Splicing factor, proline- and glutamine-rich GN=SFPQ PE=1 SV=2	3.40	0.31
A0A024R1A4	Ubiquitin-conjugating enzyme E2L 3, isoform CRA_a GN=UBE2L3 PE=3 SV=1	1.84	0.22
P23396	40S ribosomal protein S3 GN=RPS3 PE=1 SV=2	1.76	0.40
A8K651	cDNA FLJ75700, highly similar to Homo sapiens complement component 1, q subcomponent binding protein (C1QBP), nuclear gene encoding mitochondrial protein, mRNA PE=2 SV=1	3.80	0.43
V9HWE8	Epididymis secretory sperm binding protein Li 47e GN=HEL-S-47e PE=2 SV=1	2.11	0.22
P25788	Proteasome subunit alpha type-3 GN=PSMA3 PE=1 SV=2	2.51	0.32
P02795	Metallothionein-2 GN=MT2A PE=1 SV=1	1.96	0.12
P26583	High mobility group protein B2 GN=HMGB2 PE=1 SV=2	2.63	0.20
A0A024R7B7	CDC37 cell division cycle 37 homolog (S. cerevisiae), isoform CRA_a GN=CDC37 PE=4 SV=1	1.77	0.23
E7EQL5	Cytoplasmic dynein 1 intermediate chain 2 (Fragment) GN=DYNC1I2 PE=1 SV=1	1.75	0.29
P07686	Beta-hexosaminidase subunit beta GN=HEXB PE=1 SV=3	1.55	0.19
B4DPD5	Ubiquitin thioesterase PE=2 SV=1	3.76	0.25
O60701	UDP-glucose 6-dehydrogenase GN=UGDH PE=1 SV=1	1.97	0.21
Q8NE71	ATP-binding cassette sub-family F member 1 GN=ABCF1 PE=1 SV=2	1.81	0.18
Q9Y2W1	Thyroid hormone receptor-associated protein 3 GN=THRAP3 PE=1 SV=2	4.15	0.29
Q5STZ8	ATP-binding cassette sub-family F member 1 (Fragment) GN=ABCF1 PE=1 SV=9	0.55	0.09
Q8NBJ4	Golgi membrane protein 1 GN=GOLM1 PE=1 SV=1	4.57	0.15
Q15366	Poly(rC)-binding protein 2 GN=PCBP2 PE=1 SV=1	1.83	0.25
A8K3S1	Glucosamine-6-phosphate isomerase PE=2 SV=1	2.40	0.23
A0A024R1K8	Splicing factor 3a, subunit 1, 120kDa, isoform CRA_a GN=SF3A1 PE=4 SV=1	2.73	0.29

Q15046	Lysine--tRNA ligase GN=KARS PE=1 SV=3	2.87	0.27
A0A1B0GW77	Alpha-aminoadipic semialdehyde dehydrogenase GN=ALDH7A1 PE=1 SV=1	2.86	0.36
P52888	Thimet oligopeptidase GN=THOP1 PE=1 SV=2	2.51	0.26
Q16643	Drebrin GN=DBN1 PE=1 SV=4	1.07	0.13
O15144	Actin-related protein 2/3 complex subunit 2 GN=ARPC2 PE=1 SV=1	2.44	0.24
P09341	Growth-regulated alpha protein GN=CXCL1 PE=1 SV=1	2.90	0.38
O43143	Pre-mRNA-splicing factor ATP-dependent RNA helicase DHX15 GN=DHX15 PE=1 SV=2	2.38	0.28
O43765	Small glutamine-rich tetratricopeptide repeat-containing protein alpha GN=SGTA PE=1 SV=1	1.50	0.20
A0A0S2Z4Z9	Non-POU domain containing octamer-binding isoform 1 (Fragment) GN=NONO PE=2 SV=1	2.96	0.34
Q14247	Src substrate cortactin GN=CTTN PE=1 SV=2	2.39	0.13
F8W0W8	Serine/threonine-protein phosphatase GN=PPP1CC PE=1 SV=1	3.06	0.28
Q9UH65	Switch-associated protein 70 GN=SWAP70 PE=1 SV=1	1.88	0.21
Q13409	Cytoplasmic dynein 1 intermediate chain 2 GN=DYNC1I2 PE=1 SV=3	2.88	0.26
P15018	Leukemia inhibitory factor GN=LIF PE=1 SV=1	0.88	-0.06
Q9BZZ5	Apoptosis inhibitor 5 GN=API5 PE=1 SV=3	1.89	0.16
Q04760	Lactoylglutathione lyase GN=GLO1 PE=1 SV=4	2.92	0.29
Q08211	ATP-dependent RNA helicase A GN=DHX9 PE=1 SV=4	1.80	0.25
B4DR52	Histone H2B PE=2 SV=1	1.83	0.59
A0A024R3W7	Eukaryotic translation elongation factor 1 beta 2, isoform CRA_a GN=EEF1B2 PE=3 SV=1	1.95	0.30
Q53FN7	BZW1 protein variant (Fragment) PE=2 SV=1	2.40	0.22
P19875	C-X-C motif chemokine 2 GN=CXCL2 PE=1 SV=1	2.01	0.23
P54136	Arginine--tRNA ligase, cytoplasmic GN=RARS PE=1 SV=2	3.09	0.33
P51991	Heterogeneous nuclear ribonucleoprotein A3 GN=HNRNPA3 PE=1 SV=2	1.22	0.21
Q07954	Prolow-density lipoprotein receptor-related protein 1 GN=LRP1 PE=1 SV=2	0.87	0.06
P43034	Platelet-activating factor acetylhydrolase IB subunit alpha GN=PAFAH1B1 PE=1 SV=2	4.50	0.36
E9PRY8	Elongation factor 1-delta GN=EEF1D PE=1 SV=1	1.45	0.20
Q12931	Heat shock protein 75 kDa, mitochondrial GN=TRAP1 PE=1 SV=3	3.35	0.42
P61604	10 kDa heat shock protein, mitochondrial GN=HSPE1 PE=1 SV=2	3.91	0.42
D6REX3	Protein transport protein Sec31A GN=SEC31A PE=1 SV=1	2.23	0.23
Q6YHK3	CD109 antigen GN=CD109 PE=1 SV=2	0.80	0.09
P62140	Serine/threonine-protein phosphatase PP1-beta catalytic subunit GN=PPP1CB PE=1 SV=3	0.77	0.13
P10412	Histone H1.4 GN=HIST1H1E PE=1 SV=2	1.55	0.49
L0R849	Alternative protein EDARADD GN=EDARADD PE=3 SV=1	1.68	0.36
B7Z6Z4	cDNA FLJ56329, highly similar to Myosin light polypeptide 6 GN=MYL6 PE=1 SV=1	1.84	0.28
P62495	Eukaryotic peptide chain release factor subunit 1 GN=ETF1 PE=1 SV=3	3.55	0.30
P28074	Proteasome subunit beta type-5 GN=PSMB5 PE=1 SV=3	1.71	0.24
P68431	Histone H3.1 GN=HIST1H3A PE=1 SV=2	2.08	0.56
A0A024R084	Stromal cell derived factor 4, isoform CRA_c GN=SDF4 PE=4 SV=1	0.69	0.07
B4DT31	cDNA FLJ53425, highly similar to Far upstream element-binding protein 1 PE=2 SV=1	1.64	0.17
A0A024R4H0	Procollagen-lysine 1, 2-oxoglutarate 5-dioxygenase 1, isoform CRA_a GN=PLOD1 PE=4 SV=1	2.83	-0.39
P61160	Actin-related protein 2 GN=ACTR2 PE=1 SV=1	2.37	0.23
A5YM63	NEFM protein GN=NEFM PE=2 SV=1	2.07	0.22
O43491	Band 4.1-like protein 2 GN=EPB41L2 PE=1 SV=1	2.85	0.31
Q09028	Histone-binding protein RBBP4 GN=RBBP4 PE=1 SV=3	2.38	0.35
P16070	CD44 antigen GN=CD44 PE=1 SV=3	2.71	0.18
Q15019	Septin-2 GN=SEPT2 PE=1 SV=1	0.72	0.12
A0A024R3Q3	ADP-ribosylation factor 1, isoform CRA_a GN=ARF1 PE=3 SV=1	2.16	0.39
O75396	Vesicle-trafficking protein SEC22b GN=SEC22B PE=1 SV=4	1.38	0.29
A0A024RBE7	Thymopoietin, isoform CRA_c GN=TMPO PE=4 SV=1	2.75	0.25
P16152	Carbonyl reductase [NADPH] 1 GN=CBR1 PE=1 SV=3	5.24	0.42
P06899	Histone H2B type 1-J GN=HIST1H2BJ PE=1 SV=3	1.72	0.46
Q5T765	Interferon-induced protein with tetratricopeptide repeats 3, isoform CRA_a GN=IFIT3 PE=2 SV=1	1.88	0.50
Q14914	Prostaglandin reductase 1 GN=PTGR1 PE=1 SV=2	3.50	0.29

P41250	Glycine--tRNA ligase GN=GARS PE=1 SV=3	1.59	0.22
Q9Y5B9	FACT complex subunit SPT16 GN=SUPT16H PE=1 SV=1	3.16	0.38
Q9H2U2	Inorganic pyrophosphatase 2, mitochondrial GN=PPA2 PE=1 SV=2	2.96	0.41
Q59FF0	EBNA-2 co-activator variant (Fragment) PE=2 SV=1	2.34	0.31
P02461	Collagen alpha-1(III) chain GN=COL3A1 PE=1 SV=4	5.22	0.80
P14324	Farnesyl pyrophosphate synthase GN=FDPS PE=1 SV=4	2.41	0.30
A0A024RDS1	Heat shock 105kDa/110kDa protein 1, isoform CRA_c GN=HSPH1 PE=3 SV=1	3.02	0.49
D9IAI1	Epididymis secretory protein Li 34 GN=HEL-S-34 PE=2 SV=1	2.91	0.35
P49915	GMP synthase [glutamine-hydrolyzing] GN=GMPS PE=1 SV=1	0.78	0.10
B2R6S5	UMP-CMP kinase GN=CMPK PE=2 SV=1	2.94	0.39
Q59F66	DEAD box polypeptide 17 isoform p82 variant (Fragment) PE=2 SV=1	2.17	0.22
D3YTG3	Target of Nesh-SH3 GN=ABI3BP PE=1 SV=1	0.16	-0.01
O00193	Small acidic protein GN=SMAP PE=1 SV=1	0.77	0.14
B4DJQ8	cDNA FLJ55694, highly similar to Dipeptidyl-peptidase 1 PE=2 SV=1	2.86	0.39
Q9NR45	Sialic acid synthase GN=NANS PE=1 SV=2	1.65	0.24
E9PAV3	Nascent polypeptide-associated complex subunit alpha, muscle-specific form GN=NACA PE=1 SV=1	2.28	0.39
E7ETY2	Treacle protein GN=TCOF1 PE=1 SV=1	1.68	0.17
A0A024R821	Eukaryotic translation initiation factor 3 subunit B GN=EIF3S9 PE=3 SV=1	1.77	0.29
O43175	D-3-phosphoglycerate dehydrogenase GN=PHGDH PE=1 SV=4	2.04	0.30
A0A140VJY7	Testicular tissue protein Li 214 PE=2 SV=1	2.13	0.16
Q5U0I6	H.sapiens ras-related Hrab1A protein GN=RAB1A PE=2 SV=1	2.14	0.30
Q99873	Protein arginine N-methyltransferase 1 GN=PRMT1 PE=1 SV=3	2.31	0.29
Q9UHX1	Poly(U)-binding-splicing factor PUF60 GN=PUF60 PE=1 SV=1	1.59	0.21
P25787	Proteasome subunit alpha type-2 GN=PSMA2 PE=1 SV=2	2.27	0.23
M0QXB4	Coatomer protein complex, subunit epsilon, isoform CRA_g GN=COPE PE=1 SV=1	2.74	0.36
P42166	Lamina-associated polypeptide 2, isoform alpha GN=TMPO PE=1 SV=2	0.19	0.05
P34897	Serine hydroxymethyltransferase, mitochondrial GN=SHMT2 PE=1 SV=3	2.54	0.38
Q9P0L0	Vesicle-associated membrane protein-associated protein A GN=VAPA PE=1 SV=3	2.22	0.28
Q14151	Scaffold attachment factor B2 GN=SAFB2 PE=1 SV=1	1.94	0.07
A0A024R5Q7	Adenylosuccinate synthetase isozyme 2 GN=ADSS PE=3 SV=1	3.50	0.39
H0YFD6	Trifunctional enzyme subunit alpha, mitochondrial GN=HADHA PE=1 SV=2	1.73	0.33
Q9HAV7	GrpE protein homolog 1, mitochondrial GN=GRPEL1 PE=1 SV=2	2.44	0.32
P84090	Enhancer of rudimentary homolog GN=ERH PE=1 SV=1	2.32	0.23
A0A140VJI7	Testicular tissue protein Li 61 PE=2 SV=1	1.49	0.06
Q9Y678	Coatomer subunit gamma-1 GN=COPG1 PE=1 SV=1	2.24	0.39
B9EKV4	Aldehyde dehydrogenase 9 family, member A1 GN=ALDH9A1 PE=2 SV=1	2.72	0.29
O43583	Density-regulated protein GN=DENR PE=1 SV=2	2.91	0.23
A0A087WSV8	Nucleobindin 2, isoform CRA_b GN=NUCB2 PE=1 SV=1	2.35	0.28
A0A0B4J2C3	Translationally-controlled tumor protein GN=TPT1 PE=1 SV=1	2.91	0.41
E7EPK1	Septin-7 GN=SEPT7 PE=1 SV=2	1.93	0.23
H7BZJ3	Protein disulfide-isomerase A3 (Fragment) GN=PDIA3 PE=1 SV=1	1.36	0.28
P05198	Eukaryotic translation initiation factor 2 subunit 1 GN=EIF2S1 PE=1 SV=3	1.82	0.15
Q13011	Delta(3,5)-Delta(2,4)-dienoyl-CoA isomerase, mitochondrial GN=ECH1 PE=1 SV=2	0.92	0.12
A0A024R324	Ras homolog gene family, member A, isoform CRA_a GN=RHOA PE=4 SV=1	3.02	0.41
A0A024R7G8	RAD23 homolog A (S. cerevisiae), isoform CRA_a GN=RAD23A PE=4 SV=1	2.98	0.20
V9HWA6	Epididymis luminal protein 32 GN=HEL32 PE=2 SV=1	3.40	0.27
B2R9S4	cDNA, FLJ94534, highly similar to Homo sapiens capping protein (actin filament), gelsolin-like(CAPG), mRNA PE=2 SV=1	1.55	0.18
J9R021	Eukaryotic translation initiation factor 3 subunit A GN=eIF3a PE=2 SV=1	1.80	0.29
P83916	Chromobox protein homolog 1 GN=CBX1 PE=1 SV=1	1.54	0.15
A0A024R1U0	Ran GTPase activating protein 1, isoform CRA_d GN=RANGAP1 PE=4 SV=1	2.35	0.28
J3K000	PEPD protein GN=PEPD PE=2 SV=1	2.07	0.19
Q14847	LIM and SH3 domain protein 1 GN=LASP1 PE=1 SV=2	2.73	0.19
Q6BCY4	NADH-cytochrome b5 reductase 2 GN=CYB5R2 PE=1 SV=1	2.98	0.31
P05023	Sodium/potassium-transporting ATPase subunit alpha-1 GN=ATP1A1 PE=1 SV=1	0.98	0.19
E5RJD8	Tubulin-specific chaperone A GN=TBCA PE=1 SV=1	5.65	0.28

P12268	Inosine-5'-monophosphate dehydrogenase 2 GN=IMPDH2 PE=1 SV=2	1.24	0.46
P16403	Histone H1.2 GN=HIST1H1C PE=1 SV=2	0.18	-0.11
P25398	40S ribosomal protein S12 GN=RPS12 PE=1 SV=3	2.29	0.30
S4R3N1	HSPE1-MOB4 readthrough GN=HSPE1-MOB4 PE=3 SV=1	1.81	0.25
P05556	Integrin beta-1 GN=ITGB1 PE=1 SV=2	0.97	0.17
O00154	Cytosolic acyl coenzyme A thioester hydrolase GN=ACOT7 PE=1 SV=3	2.15	0.24
P46063	ATP-dependent DNA helicase Q1 GN=RECQL PE=1 SV=3	1.59	0.26
A0A077YIJ7	MHC class I antigen (Fragment) GN=HLA-A PE=3 SV=1	1.99	0.41
A0A024RAC5	Regulator of chromosome condensation 2, isoform CRA_a GN=RCC2 PE=4 SV=1	2.09	0.13
O00764	Pyridoxal kinase GN=PDXK PE=1 SV=1	2.22	0.20
P18085	ADP-ribosylation factor 4 GN=ARF4 PE=1 SV=3	1.27	0.34
O60763	General vesicular transport factor p115 GN=USO1 PE=1 SV=2	1.49	0.30
P16402	Histone H1.3 GN=HIST1H1D PE=1 SV=2	1.08	0.43
O75828	Carbonyl reductase [NADPH] 3 GN=CBR3 PE=1 SV=3	1.18	0.36
P12270	Nucleoprotein TPR GN=TPR PE=1 SV=3	1.73	0.20
Q96G03	Phosphoglucomutase-2 GN=PGM2 PE=1 SV=4	2.05	0.24
P24752	Acetyl-CoA acetyltransferase, mitochondrial GN=ACAT1 PE=1 SV=1	4.06	0.57
Q59EF6	Calpain 2, large [catalytic] subunit variant (Fragment) PE=2 SV=1	2.18	0.27
Q6NVY0	Calcyclin binding protein GN=CACYBP PE=2 SV=1	1.39	0.17
A0A140VK46	Proteasome subunit beta PE=2 SV=1	2.43	0.22
O75821	Eukaryotic translation initiation factor 3 subunit G GN=EIF3G PE=1 SV=2	2.63	0.34
Q1KMD3	Heterogeneous nuclear ribonucleoprotein U-like protein 2 GN=HNRNPUL2 PE=1 SV=1	2.76	0.25
Q96HE7	ERO1-like protein alpha GN=ERO1A PE=1 SV=2	0.17	-0.04
A8K566	cDNA FLJ78246, highly similar to Homo sapiens splicing factor 3a, subunit 3, 60kDa (SF3A3), mRNA PE=2 SV=1	2.21	0.22
Q9UJU6	Drebrin-like protein GN=DBNL PE=1 SV=1	3.05	0.29
B2R4R0	Histone H4 GN=HIST1H4L PE=2 SV=1	1.30	0.30
P0C0S5	Histone H2A.Z GN=H2AFZ PE=1 SV=2	1.85	0.41
P53621	Coatomer subunit alpha GN=COPA PE=1 SV=2	2.61	0.35
A0A024R563	Protein phosphatase 1, regulatory (Inhibitor) subunit 14B, isoform CRA_a GN=PPP1R14B PE=4 SV=1	1.08	0.13
A0A087WYR3	Tumor protein D54 GN=TPD52L2 PE=1 SV=1	0.86	0.13
P42224	Signal transducer and activator of transcription 1-alpha/beta GN=STAT1 PE=1 SV=2	3.36	0.61
Q59FR8	Galectin (Fragment) PE=2 SV=1	0.30	0.03
Q1HBJ4	Mitogen-activated protein kinase GN=MAPK1 PE=3 SV=1	2.78	0.25
O75643	U5 small nuclear ribonucleoprotein 200 kDa helicase GN=SNRNP200 PE=1 SV=2	3.04	0.36
A0A090N7T9	Secernin 1 GN=SCRN1 PE=4 SV=1	1.65	0.28
Q14444	Caprin-1 GN=CAPRIN1 PE=1 SV=2	2.44	0.29
Q5U0F4	Eukaryotic translation initiation factor 3 subunit I GN=EIF3S2 PE=2 SV=1	1.65	0.25
A0A0B4U5E3	Granulocyte-colony stimulating factor (Fragment) PE=2 SV=1	3.34	0.34
Q969H8	Myeloid-derived growth factor GN=MYDGF PE=1 SV=1	1.40	0.17
B2RBH2	cDNA, FLJ95508, highly similar to Homo sapiens 5'-nucleotidase, ecto (CD73) (NT5E), mRNA PE=2 SV=1	1.60	0.19
Q96P70	Importin-9 GN=IPO9 PE=1 SV=3	0.87	0.16
Q5U043	S-(hydroxymethyl)glutathione dehydrogenase PE=2 SV=1	2.50	0.32
A0A024R571	EH domain-containing protein 1 GN=EHD1 PE=1 SV=1	2.56	0.29
Q9BS26	Endoplasmic reticulum resident protein 44 GN=ERP44 PE=1 SV=1	1.41	0.21
O43776	Asparagine--tRNA ligase, cytoplasmic GN=NARS PE=1 SV=1	2.70	0.32
Q15631	Translin GN=TSN PE=1 SV=1	1.79	0.24
Q6FHC9	STC2 protein (Fragment) GN=STC2 PE=2 SV=1	5.52	-0.54
A8K4Z4	60S acidic ribosomal protein P0 PE=2 SV=1	1.93	0.33
P63208	S-phase kinase-associated protein 1 GN=SKP1 PE=1 SV=2	1.73	0.21
Q5U000	Cathepsin Z PE=2 SV=1	3.54	0.33
B4DDD6	cDNA FLJ59450, highly similar to Drebrin-like protein GN=DBNL PE=1 SV=1	2.95	0.36
Q13007	Interleukin-24 GN=IL24 PE=1 SV=1	0.79	-0.09
P49720	Proteasome subunit beta type-3 GN=PSMB3 PE=1 SV=2	1.27	0.21
A0A024R663	Kinectin 1 (Kinesin receptor), isoform CRA_a GN=KTN1 PE=4 SV=1	1.25	0.14

P35606	Coatomer subunit beta' GN=COPB2 PE=1 SV=2	2.27	0.31
B4E1U9	cDNA FLJ54776, highly similar to Cell division control protein 42 homolog PE=2 SV=1	3.69	0.36
O43493	Trans-Golgi network integral membrane protein 2 GN=TGOLN2 PE=1 SV=3	1.65	0.12
B3KSH1	Eukaryotic translation initiation factor 3 subunit F GN=EIF3F PE=2 SV=1	1.96	0.30
Q6FHX6	Flap endonuclease 1 GN=FEN1 PE=2 SV=1	2.86	0.35
A0A1W2PPZ5	Transcription elongation factor A protein 1 GN=TCEA1 PE=1 SV=1	2.06	0.23
A8K8F0	cDNA FLJ76436 PE=2 SV=1	3.05	0.30
P17096	High mobility group protein HMG-I/HMG-Y GN=HMGA1 PE=1 SV=3	1.97	0.37
A0A140VJF4	Biliverdin reductase A PE=2 SV=1	4.47	0.29
A0A024RBB7	Nucleosome assembly protein 1-like 1, isoform CRA_a GN=NAP1L1 PE=3 SV=1	1.71	0.27
P30044	Peroxiredoxin-5, mitochondrial GN=PRDX5 PE=1 SV=4	1.54	0.30
O14979	Heterogeneous nuclear ribonucleoprotein D-like GN=HNRNPDL PE=1 SV=3	2.36	0.32
P62316	Small nuclear ribonucleoprotein Sm D2 GN=SNRPD2 PE=1 SV=1	1.79	0.15
B2RD79	cDNA, FLJ96494, highly similar to Homo sapiens ubiquitin specific peptidase 14 (tRNA-guanine transglycosylase) (USP14), mRNA PE=2 SV=1	0.38	0.05
Q6I9S7	C-X-C motif chemokine GN=CXCL5 PE=1 SV=1	1.66	-0.07
B2R548	Prefoldin subunit 4 PE=2 SV=1	2.43	0.29
Q9Y3I0	tRNA-splicing ligase RtcB homolog GN=RTCB PE=1 SV=1	2.22	0.36
Q6FHQ0	RBBP7 protein (Fragment) GN=RBBP7 PE=2 SV=1	4.56	0.38
Q647J8	Granulocyte-macrophage colony stimulating factor 2 PE=2 SV=1	2.34	-0.89
B5BU01	Eukaryotic translation initiation factor 2 beta GN=EIF2S2 PE=2 SV=1	1.96	0.15
Q5TB52	3'-phosphoadenosine 5'-phosphosulfate synthase 2, isoform CRA_b GN=PAPSS2 PE=2 SV=1	1.63	0.24
Q9Y3F4	Serine-threonine kinase receptor-associated protein GN=STRAP PE=1 SV=1	2.82	0.29
O43684	Mitotic checkpoint protein BUB3 GN=BUB3 PE=1 SV=1	2.13	0.32
Q8IZ03	Interferon-induced protein with tetratricopeptide repeats 2 GN=IFIT2 PE=1 SV=2	2.35	0.39
P30405	Peptidyl-prolyl cis-trans isomerase F, mitochondrial GN=PPIF PE=1 SV=1	3.91	0.39
P00966	Argininosuccinate synthase GN=ASS1 PE=1 SV=2	1.76	0.24
Q71DI3	Histone H3.2 GN=HIST2H3A PE=1 SV=3	1.70	0.63
P52597	Heterogeneous nuclear ribonucleoprotein F GN=HNRNPF PE=1 SV=3	1.90	0.19
P09919	Granulocyte colony-stimulating factor GN=CSF3 PE=1 SV=1	2.67	0.37
P35659	Protein DEK GN=DEK PE=1 SV=1	1.49	0.16
Q76LA1	CSTB protein GN=CSTB PE=2 SV=1	1.21	0.07
B2R960	cDNA, FLJ94230, highly similar to Homo sapiens thioredoxin-like 1 (TXNL1), mRNA PE=2 SV=1	2.60	0.33
A8K3Q8	cDNA FLJ75069, highly similar to Homo sapiens serpin peptidase inhibitor, clade B (ovalbumin), member 7 (SERPINB7), mRNA PE=2 SV=1	1.44	-0.13
O00232	26S proteasome non-ATPase regulatory subunit 12 GN=PSMD12 PE=1 SV=3	2.30	0.26
Q9H2G2	STE20-like serine/threonine-protein kinase GN=SLK PE=1 SV=1	2.19	0.30
P38919	Eukaryotic initiation factor 4A-III GN=EIF4A3 PE=1 SV=4	2.39	0.25
X6R8A1	Carboxypeptidase GN=CTSA PE=1 SV=1	2.74	0.34
A0A024R3V8	Translin-associated factor X, isoform CRA_c GN=TSNAX PE=4 SV=1	0.37	0.06
A0A0A0MQS9	Laminin subunit alpha-4 GN=LAMA4 PE=1 SV=1	1.81	0.24
P01034	Cystatin-C GN=CST3 PE=1 SV=1	3.05	0.37
Q9UHV9	Prefoldin subunit 2 GN=PFDN2 PE=1 SV=1	2.18	0.26
A0A0K0K1I0	Epididymis secretory protein Li 265 GN=HEL-S-265 PE=2 SV=1	2.01	0.27
Q9C0C2	182 kDa tankyrase-1-binding protein GN=TNKS1BP1 PE=1 SV=4	1.31	0.13
Q13435	Splicing factor 3B subunit 2 GN=SF3B2 PE=1 SV=2	2.12	0.21
A0A024RD93	Phosphoribosylaminoimidazole carboxylase, phosphoribosylaminoimidazole succinocarboxamide synthetase, isoform CRA_c GN=PAICS PE=3 SV=1	0.62	0.11
A0A024R608	Ribosomal protein, large, P1, isoform CRA_a GN=RPLP1 PE=3 SV=1	1.01	0.18
A0A024R713	Dihydrolipoyl dehydrogenase GN=DLD PE=3 SV=1	2.27	0.30
D3DVC4	Nestin, isoform CRA_c GN=NES PE=3 SV=1	2.18	0.20
Q8WXX5	DnaJ homolog subfamily C member 9 GN=DNAJC9 PE=1 SV=1	2.95	0.30
B3KTJ9	cDNA FLJ38393 fis, clone FEBRA2007212 PE=2 SV=1	1.76	0.18
Q9Y6E3	HSPC027 PE=2 SV=1	2.01	0.29
A0A140VK83	Protein phosphatase 1, regulatory subunit 7, isoform CRA_b GN=PPP1R7 PE=2 SV=1	2.65	0.28

A0A0S2Z471	Creatine kinase brain isoform 2 (Fragment) GN=CKB PE=2 SV=1	1.94	0.29
P16401	Histone H1.5 GN=HIST1H1B PE=1 SV=3	1.68	0.32
P54577	Tyrosine--tRNA ligase, cytoplasmic GN=YARS PE=1 SV=4	1.82	0.29
A0A140VK08	Testicular secretory protein Li 8 PE=2 SV=1	1.17	0.18
A4D0V4	Capping protein (Actin filament) muscle Z-line, alpha 2 GN=CAPZA2 PE=2 SV=1	2.36	0.35
D9YZV7	Tropomyosin 1 (Alpha) isoform 6 GN=TPM1 PE=3 SV=1	1.96	0.25
Q96FQ6	Protein S100-A16 GN=S100A16 PE=1 SV=1	1.91	0.29
B2R7P6	cDNA, FLJ93543, highly similar to Homo sapiens phosphotidylinositol transfer protein, beta (PITPNB),mRNA PE=2 SV=1	1.28	0.11
Q15182	Small nuclear ribonucleoprotein-associated protein GN=SNRPB PE=2 SV=1	1.65	0.19
Q9H8K1	cDNA FLJ13518 fis, clone PLACE1005799 PE=2 SV=1	1.81	0.30
P13674	Prolyl 4-hydroxylase subunit alpha-1 GN=P4HA1 PE=1 SV=2	0.66	-0.11
A6NFX8	ADP-sugar pyrophosphatase GN=NUDT5 PE=1 SV=1	1.63	0.19
Q7Z4X0	MO25-like protein PE=2 SV=1	2.18	0.28
A0A024RBH2	Cytoskeleton-associated protein 4, isoform CRA_c GN=CKAP4 PE=4 SV=1	0.61	0.22
P32119	Peroxiredoxin-2 GN=PRDX2 PE=1 SV=5	2.30	0.22
P26368	Splicing factor U2AF 65 kDa subunit GN=U2AF2 PE=1 SV=4	2.29	0.23
O14974	Protein phosphatase 1 regulatory subunit 12A GN=PPP1R12A PE=1 SV=1	2.56	0.34
O75475	PC4 and SFRS1-interacting protein GN=PSIP1 PE=1 SV=1	2.26	0.33
P30740	Leukocyte elastase inhibitor GN=SERPINB1 PE=1 SV=1	1.82	0.22
A0A024R9D2	Metadherin, isoform CRA_a GN=MTDH PE=4 SV=1	3.85	0.23
B0QY89	Eukaryotic translation initiation factor 3 subunit L GN=EIF3L PE=1 SV=1	1.59	0.21
V9HW90	Glutathione reductase GN=HEL-75 PE=2 SV=1	1.72	0.22
P16035	Metalloproteinase inhibitor 2 GN=TIMP2 PE=1 SV=2	4.83	0.28
Q15369	Elongin-C GN=ELOC PE=1 SV=1	1.98	0.28
Q14112	Nidogen-2 GN=NID2 PE=1 SV=3	1.98	0.26
B2R5T5	Protein kinase, cAMP-dependent, regulatory, type I, alpha (Tissue specific extinguisher 1), isoform CRA_a GN=PRKAR1A PE=2 SV=1	2.80	0.30
A0A2U9QGI0	NAP1L4/NUTM1D fusion protein GN=NAP1L4 PE=2 SV=1	2.19	0.31
A0A024R5X2	HCG2001986, isoform CRA_a GN=hCG_2001986 PE=4 SV=1	1.03	0.35
B3KUY2	Prostaglandin E synthase 3 (Cytosolic), isoform CRA_c GN=PTGES3 PE=2 SV=1	3.67	0.28
O60832	H/ACA ribonucleoprotein complex subunit DKC1 GN=DKC1 PE=1 SV=3	3.12	0.26
A0A024QZ77	EF-hand domain family, member D2, isoform CRA_a GN=EFHD2 PE=2 SV=1	1.80	0.23
A0A024R572	Splicing factor 1, isoform CRA_h GN=SF1 PE=4 SV=1	1.68	0.17
V9HW41	Epididymis secretory protein Li 71 GN=HEL-S-71 PE=2 SV=1	1.48	0.15
Q9NQG5	Regulation of nuclear pre-mRNA domain-containing protein 1B GN=RPRD1B PE=1 SV=1	1.53	0.27
C6K6I9	MHC class I antigen GN=HLA-B PE=3 SV=1	3.17	0.52
B3KN28	Phosphoacetylglucosamine mutase PE=2 SV=1	2.03	0.25
P26022	Pentraxin-related protein PTX3 GN=PTX3 PE=1 SV=3	0.66	0.13
P29373	Cellular retinoic acid-binding protein 2 GN=CRABP2 PE=1 SV=2	1.61	0.20
P49767	Vascular endothelial growth factor C GN=VEGFC PE=1 SV=1	1.10	0.11
O43242	26S proteasome non-ATPase regulatory subunit 3 GN=PSMD3 PE=1 SV=2	1.90	0.29
Q16222	UDP-N-acetylhexosamine pyrophosphorylase GN=UAP1 PE=1 SV=3	0.13	-0.02
A0A0S2Z2Z6	Annexin (Fragment) GN=ANXA6 PE=2 SV=1	1.50	0.23
P61201	COP9 signalosome complex subunit 2 GN=COPS2 PE=1 SV=1	1.56	0.28
A0A023T6R1	Mago nashi protein GN=FLJ10292 PE=2 SV=1	2.63	0.32
Q9BXP5	Serrate RNA effector molecule homolog GN=SRRT PE=1 SV=1	1.96	0.25
A4D275	Actin-related protein 2/3 complex subunit GN=ARPC1B PE=2 SV=1	1.19	0.19
P62318	Small nuclear ribonucleoprotein Sm D3 GN=SNRPD3 PE=1 SV=1	1.37	0.18
B3KS98	Eukaryotic translation initiation factor 3 subunit H GN=EIF3H PE=1 SV=1	2.01	0.28
Q16881	Thioredoxin reductase 1, cytoplasmic GN=TXNRD1 PE=1 SV=3	2.15	0.26
M1VKI3	Tyrosine-protein kinase receptor GN=SDC4-ROS1_S4;R32 PE=2 SV=1	0.04	0.01
Q9UMS4	Pre-mRNA-processing factor 19 GN=PRPF19 PE=1 SV=1	2.47	0.27
A0A1U9X9A1	VARS PE=3 SV=2	2.22	0.27
F8VXU5	Vacuolar protein sorting-associated protein 29 GN=VPS29 PE=1 SV=1	4.15	0.37
P05362	Intercellular adhesion molecule 1 GN=ICAM1 PE=1 SV=2	0.71	-0.17
B2RBL3	Thymidine phosphorylase PE=2 SV=1	2.30	0.45

P24844	Myosin regulatory light polypeptide 9 GN=MYL9 PE=1 SV=4	1.58	0.28
P62906	60S ribosomal protein L10a GN=RPL10A PE=1 SV=2	1.23	0.24
A0A024R3P9	Acyl-Coenzyme A binding domain containing 3, isoform CRA_a GN=ACBD3 PE=4 SV=1	3.06	0.25
A8K2N0	cDNA FLJ77835, highly similar to Homo sapiens complement component 1, s subcomponent (C1S), transcript variant 2, mRNA PE=2 SV=1	3.42	0.71
H3BQQ9	SUMO-conjugating enzyme UBC9 (Fragment) GN=UBE2I PE=1 SV=1	3.18	0.27
A0A1W2PNV4	Uncharacterized protein PE=4 SV=1	2.80	0.21
J3KQ69	DNA replication licensing factor MCM3 GN=MCM3 PE=1 SV=2	0.97	0.12
P56537	Eukaryotic translation initiation factor 6 GN=EIF6 PE=1 SV=1	2.84	0.26
Q53HB3	Proteasome 26S ATPase subunit 1 variant (Fragment) PE=1 SV=1	1.18	0.22
A0A024R394	Cysteine and histidine-rich domain (CHORD)-containing 1, isoform CRA_c GN=CHORDC1 PE=4 SV=1	2.32	0.26
A0A158RFU3	Parathymosin GN=PTMS PE=2 SV=1	2.21	0.20
Q9UNF0	Protein kinase C and casein kinase substrate in neurons protein 2 GN=PACSIN2 PE=1 SV=2	1.35	0.13
P67775	Serine/threonine-protein phosphatase 2A catalytic subunit alpha isoform GN=PPP2CA PE=1 SV=1	2.00	0.25
P14550	Alcohol dehydrogenase [NADP(+)] GN=AKR1A1 PE=1 SV=3	0.98	0.10
I1W660	Dickkopf-like protein 1 GN=DKK1 PE=2 SV=1	0.39	0.04
A0A218KGR2	Amyloid beta A4 protein isoform a GN=APP PE=4 SV=1	2.29	0.13
J3QRS3	Myosin regulatory light chain 12A GN=MYL12A PE=1 SV=1	1.48	0.33
D3DPK5	SH3 domain binding glutamic acid-rich protein like 3, isoform CRA_a (Fragment) GN=SH3BGRL3 PE=4 SV=1	2.56	0.23
Q9Y520	Protein PRRC2C GN=PRRC2C PE=1 SV=4	1.71	0.26
P60228	Eukaryotic translation initiation factor 3 subunit E GN=EIF3E PE=1 SV=1	1.31	0.37
V9HW92	Epididymis secretory protein Li 112 GN=HEL-S-112 PE=2 SV=1	2.77	0.32
Q96EB3	EEF1A1 protein (Fragment) GN=EEF1A1 PE=2 SV=1	1.62	0.51
B2RBE5	cDNA, FLJ95468, highly similar to Homo sapiens transcriptional coactivator tubedown-100 (TBDN100),transcript variant 1, mRNA PE=2 SV=1	2.38	0.31
A0A024RDE8	PDZ and LIM domain 5, isoform CRA_c GN=PDLIM5 PE=4 SV=1	2.52	0.35
Q14157	Ubiquitin-associated protein 2-like GN=UBAP2L PE=1 SV=2	2.93	0.23
P01584	Interleukin-1 beta GN=IL1B PE=1 SV=2	0.14	0.04
Q9NQW7	Xaa-Pro aminopeptidase 1 GN=XPNPEP1 PE=1 SV=3	2.60	0.22
F6WQW2	Ran-specific GTPase-activating protein GN=RANBP1 PE=1 SV=1	3.42	0.26
Q14329	Farnesyl pyrophosphate synthetase like-4 protein (Fragment) PE=3 SV=1	2.02	0.76
Q5T6U8	High mobility group AT-hook 1 GN=HMGA1 PE=2 SV=1	2.60	0.30
Q01844	RNA-binding protein EWS GN=EWSR1 PE=1 SV=1	2.83	0.27
A0A024R152	HCG28765, isoform CRA_b GN=hCG_28765 PE=4 SV=1	1.06	0.09
Q07092	Collagen alpha-1(XVI) chain GN=COL16A1 PE=1 SV=2	1.26	0.24
A0A140VJP2	Methionine adenosyltransferase 2 subunit beta PE=2 SV=1	0.52	0.07
Q6LAF9	Cathepsin B (Fragment) PE=2 SV=1	1.14	0.20
C9JIF9	Acylamino-acid-releasing enzyme GN=APEH PE=1 SV=1	1.59	0.27
Q5VU77	Ubiquitin-associated protein 2-like (Fragment) GN=UBAP2L PE=1 SV=1	1.71	0.50
Q9ULC4	Malignant T-cell-amplified sequence 1 GN=MCTS1 PE=1 SV=1	2.25	0.36
A6NDG6	Glycerol-3-phosphate phosphatase GN=PGP PE=1 SV=1	1.48	0.32
Q14696	LRP chaperone MESD GN=MESD PE=1 SV=2	0.39	0.06
B4DZR0	cDNA FLJ55529, highly similar to Heat shock 70 kDa protein 4L PE=2 SV=1	1.47	-0.48
A8K669	cDNA FLJ78452, highly similar to Homo sapiens legumain (LGMN), transcript variant 2, mRNA PE=2 SV=1	2.50	0.37
P61026	Ras-related protein Rab-10 GN=RAB10 PE=1 SV=1	1.20	0.19
A0A024R6Q1	Eukaryotic translation initiation factor 5, isoform CRA_b GN=EIF5 PE=4 SV=1	2.41	0.34
A0A087WW66	26S proteasome non-ATPase regulatory subunit 1 GN=PSMD1 PE=1 SV=1	1.40	0.20
Q9NSE4	Isoleucine--tRNA ligase, mitochondrial GN=IARS2 PE=1 SV=2	3.11	0.45
G3V3D1	NPC intracellular cholesterol transporter 2 (Fragment) GN=NPC2 PE=1 SV=1	2.98	0.29
A0A024RDB0	Ubiquitin-activating enzyme E1-like 2, isoform CRA_a GN=UBE1L2 PE=4 SV=1	2.09	0.24
O00622	Protein CYR61 GN=CYR61 PE=1 SV=1	3.10	0.29
A0A140VJS3	Testicular tissue protein Li 149 PE=2 SV=1	1.70	0.32

P35268	60S ribosomal protein L22 GN=RPL22 PE=1 SV=2	0.52	0.11
Q5T9B7	Adenylate kinase isoenzyme 1 GN=AK1 PE=1 SV=1	2.03	0.31
P05114	Non-histone chromosomal protein HMG-14 GN=HMGN1 PE=1 SV=3	3.06	0.31
O15460	Prolyl 4-hydroxylase subunit alpha-2 GN=P4HA2 PE=1 SV=1	0.11	0.02
P61163	Alpha-centractin GN=ACTR1A PE=1 SV=1	2.63	0.40
P07585	Decorin GN=DCN PE=1 SV=1	3.56	0.42
P11233	Ras-related protein Ral-A GN=RALA PE=1 SV=1	1.35	0.24
Q3B790	High-mobility group nucleosome binding domain 1 GN=HMGN1 PE=2 SV=1	3.03	0.31
P33316	Deoxyuridine 5'-triphosphate nucleotidohydrolase, mitochondrial GN=DUT PE=1 SV=4	2.93	0.35
A0A140VJE3	Methionine aminopeptidase 2 GN=METAP2 PE=2 SV=1	0.71	0.12
Q99584	Protein S100-A13 GN=S100A13 PE=1 SV=1	3.87	0.27
A0A024R0R4	SUMO-1 activating enzyme subunit 1, isoform CRA_b GN=SAE1 PE=4 SV=1	1.79	0.22
Q07666	KH domain-containing, RNA-binding, signal transduction-associated protein 1 GN=KHDRBS1 PE=1 SV=1	4.22	0.36
Q9UKV3	Apoptotic chromatin condensation inducer in the nucleus GN=ACIN1 PE=1 SV=2	2.17	0.22
Q00688	Peptidyl-prolyl cis-trans isomerase FKBP3 GN=FKBP3 PE=1 SV=1	2.22	0.20
B3KML1	cDNA FLJ11308 fis, clone PLACE1010074, highly similar to Sorting nexin-2 PE=2 SV=1	2.85	0.37
P61221	ATP-binding cassette sub-family E member 1 GN=ABCE1 PE=1 SV=1	2.65	0.35
O14737	Programmed cell death protein 5 GN=PDCD5 PE=1 SV=3	2.25	0.31
O00148	ATP-dependent RNA helicase DDX39A GN=DDX39A PE=1 SV=2	1.10	0.37
P32321	Deoxycytidylate deaminase GN=DCTD PE=1 SV=2	2.03	0.24
O14929	Histone acetyltransferase type B catalytic subunit GN=HAT1 PE=1 SV=1	2.44	0.31
A0A140VK93	Adenylate kinase 2, mitochondrial GN=AK2 PE=2 SV=1	2.07	0.31
A0A0A0MRI2	Sorting nexin GN=SNX6 PE=1 SV=1	2.33	0.26
O75937	DnaJ homolog subfamily C member 8 GN=DNAJC8 PE=1 SV=2	1.42	0.23
P35318	ADM GN=ADM PE=1 SV=1	4.01	-0.47
Q10567	AP-1 complex subunit beta-1 GN=AP1B1 PE=1 SV=2	1.95	0.24
A8K4T6	cDNA FLJ76282, highly similar to Homo sapiens proteasome (prosome, macropain) 26S subunit, non-ATPase, 5 (PSMD5), mRNA PE=2 SV=1	1.85	0.25
P05161	Ubiquitin-like protein ISG15 GN=ISG15 PE=1 SV=5	3.27	0.53
P26373	60S ribosomal protein L13 GN=RPL13 PE=1 SV=4	1.29	0.32
A8K4W0	40S ribosomal protein S3a GN=RPS3A PE=2 SV=1	1.56	0.50
O15347	High mobility group protein B3 GN=HMGB3 PE=1 SV=4	2.85	0.24
G3V4P8	Glia maturation factor beta (Fragment) GN=GMFB PE=1 SV=1	2.48	0.23
V9HWF9	Epididymis luminal protein 20 GN=HEL20 PE=2 SV=1	2.45	0.27
P36957	Dihydrolipoyllysine-residue succinyltransferase component of 2-oxoglutarate dehydrogenase complex, mitochondrial GN=DLST PE=1 SV=4	1.18	0.29
P41091	Eukaryotic translation initiation factor 2 subunit 3 GN=EIF2S3 PE=1 SV=3	1.17	0.17
Q6IQ30	Polyadenylate-binding protein GN=PABPC4 PE=2 SV=1	2.18	0.35
Q15907	Ras-related protein Rab-11B GN=RAB11B PE=1 SV=4	3.41	0.27
P49721	Proteasome subunit beta type-2 GN=PSMB2 PE=1 SV=1	2.80	0.28
Q68D08	Uncharacterized protein DKFZp686B04128 GN=DKFZp686B04128 PE=2 SV=1	0.28	0.06
P51149	Ras-related protein Rab-7a GN=RAB7A PE=1 SV=1	3.61	0.23
Q15257	Serine/threonine-protein phosphatase 2A activator GN=PTPA PE=1 SV=3	1.78	0.24
Q9UBQ7	Glyoxylate reductase/hydroxypyruvate reductase GN=GRHPR PE=1 SV=1	1.18	0.22
A0A024R5H8	RAB6A, member RAS oncogene family, isoform CRA_b GN=RAB6A PE=4 SV=1	2.19	0.18
A4D2P0	Ras-related C3 botulinum toxin substrate 1 (Rho family, small GTP binding protein Rac1) GN=RAC1 PE=2 SV=1	2.62	0.29
Q08945	FACT complex subunit SSRP1 GN=SSRP1 PE=1 SV=1	2.14	0.30
Q969E4	Transcription elongation factor A protein-like 3 GN=TCEAL3 PE=1 SV=1	0.94	0.13
Q9UHL4	Dipeptidyl peptidase 2 GN=DPP7 PE=1 SV=3	1.22	0.19
A0A0U1RRH7	Histone H2A PE=3 SV=1	2.09	0.56
D6RBW1	Eukaryotic translation initiation factor 4E GN=EIF4E PE=1 SV=1	2.61	0.34
Q92973	Transportin-1 GN=TNPO1 PE=1 SV=2	3.33	0.31
Q59GM9	Alpha-1,4 glucan phosphorylase (Fragment) PE=2 SV=1	1.95	0.27
P16989	Y-box-binding protein 3 GN=YBX3 PE=1 SV=4	2.84	0.26
Q9UBC2	Epidermal growth factor receptor substrate 15-like 1 GN=EPS15L1 PE=1 SV=1	1.30	0.22

B5ME97	Septin 10, isoform CRA_c GN=SEPT10 PE=1 SV=2	1.50	0.26
Q53GG0	Epithelial protein lost in neoplasm beta variant (Fragment) PE=2 SV=1	1.23	0.20
O95218	Zinc finger Ran-binding domain-containing protein 2 GN=ZRANB2 PE=1 SV=2	2.34	0.22
P62304	Small nuclear ribonucleoprotein E GN=SNRPE PE=1 SV=1	1.76	0.22
Q5EBM0	UMP-CMP kinase 2, mitochondrial GN=CMPK2 PE=1 SV=3	4.13	0.61
Q53H88	Dynactin 2 variant (Fragment) PE=2 SV=1	2.60	0.28
B0I1S9	MYO1B variant protein GN=MYO1B PE=2 SV=1	1.63	0.28
D3DUW5	Dynamin 1-like, isoform CRA_c GN=DNM1L PE=3 SV=1	1.69	0.21
Q12996	Cleavage stimulation factor subunit 3 GN=CSTF3 PE=1 SV=1	2.28	0.25
B3KTS5	cDNA FLJ38670 fis, clone HSYRA2000190, highly similar to Voltage-dependent anion-selective channel protein 1 PE=2 SV=1	0.52	0.40
P0DN79	Cystathionine beta-synthase-like protein GN=CBSL PE=1 SV=1	1.27	0.14
Q9HBB3	60S ribosomal protein L6 PE=2 SV=1	2.06	0.46
Q13344	Fus-like protein (Fragment) PE=2 SV=1	0.38	0.08
O00487	26S proteasome non-ATPase regulatory subunit 14 GN=PSMD14 PE=1 SV=1	1.91	0.29
B4DHQ3	Phosphoserine aminotransferase PE=2 SV=1	2.67	0.37
Q53FA7	Quinone oxidoreductase PIG3 GN=TP53I3 PE=1 SV=2	2.20	0.30
A8K6Q8	cDNA FLJ75881, highly similar to Homo sapiens transferrin receptor (p90, CD71) (TFRC), mRNA PE=2 SV=1	1.61	0.20
A0A0S2Z3Q4	V-crk sarcoma virus CT10 oncogene-like protein isoform 1 (Fragment) GN=CRK PE=2 SV=1	2.03	0.19
Q9Y5S9	RNA-binding protein 8A GN=RBM8A PE=1 SV=1	1.26	0.18
Q5JR94	40S ribosomal protein S8 GN=RPS8 PE=2 SV=1	1.85	0.48
Q9NY27	Serine/threonine-protein phosphatase 4 regulatory subunit 2 GN=PPP4R2 PE=1 SV=3	2.79	0.27
A2A3R6	40S ribosomal protein S6 GN=RPS6 PE=2 SV=1	1.85	0.47
H7C2N1	Prothymosin alpha (Fragment) GN=PTMA PE=1 SV=1	0.40	0.28
B2R7D2	cDNA, FLJ93389, highly similar to Homo sapiens multiple inositol polyphosphate histidine phosphatase, 1 (MINPP1), mRNA PE=2 SV=1	0.60	-0.10
Q96CN7	Isochorismatase domain-containing protein 1 GN=ISOC1 PE=1 SV=3	2.50	0.18
P31153	S-adenosylmethionine synthase isoform type-2 GN=MAT2A PE=1 SV=1	3.44	0.29
A8K878	Mesencephalic astrocyte-derived neurotrophic factor GN=MANF PE=1 SV=1	1.10	0.22
P51572	B-cell receptor-associated protein 31 GN=BCAP31 PE=1 SV=3	1.74	0.13
P24592	Insulin-like growth factor-binding protein 6 GN=IGFBP6 PE=1 SV=1	2.73	0.33
P30048	Thioredoxin-dependent peroxide reductase, mitochondrial GN=PRDX3 PE=1 SV=3	3.00	0.41
Q16270	Insulin-like growth factor-binding protein 7 GN=IGFBP7 PE=1 SV=1	4.35	0.62
C9J8T6	Cytochrome c oxidase copper chaperone GN=COX17 PE=1 SV=1	0.37	0.06
P62280	40S ribosomal protein S11 GN=RPS11 PE=1 SV=3	1.56	0.43
B4DIS3	Dpy-30-like protein, isoform CRA_b GN=LOC84661 PE=2 SV=1	1.91	0.24
C1PHA2	Tyrosine-protein kinase receptor GN=KIF5B-ALK PE=2 SV=1	1.98	0.25
A0A140VJE8	AP complex subunit beta GN=AP2B1 PE=2 SV=1	1.63	0.36
P84243	Histone H3.3 GN=H3F3A PE=1 SV=2	2.57	0.59
B2R533	cDNA, FLJ92320, highly similar to Homo sapiens glutathione S-transferase theta 2 (GSTT2), mRNA PE=2 SV=1	1.98	0.23
Q6NZI2	Caveolae-associated protein 1 GN=CAVIN1 PE=1 SV=1	2.66	0.35
B7ZKY6	Membrane metallo-endopeptidase GN=MME PE=2 SV=1	0.49	0.08
Q5T5C7	Serine--tRNA ligase, cytoplasmic GN=SARS PE=1 SV=1	2.59	0.36
Q8TDQ7	Glucosamine-6-phosphate isomerase 2 GN=GNPDA2 PE=1 SV=1	0.74	0.18
O75533	Splicing factor 3B subunit 1 GN=SF3B1 PE=1 SV=3	0.96	0.08
Q9H6Z4	Ran-binding protein 3 GN=RANBP3 PE=1 SV=1	0.80	0.10
Q59EJ5	Glutathione S-transferase (Fragment) PE=2 SV=1	3.37	0.26
Q5UIP0	Telomere-associated protein RIF1 GN=RIF1 PE=1 SV=2	0.83	0.12
A5PLM9	Cathepsin L1 GN=CTSL1 PE=2 SV=1	0.92	0.14
B4DLN1	cDNA FLJ60124, highly similar to Mitochondrial dicarboxylate carrier PE=2 SV=1	2.54	0.44
Q8WW12	PEST proteolytic signal-containing nuclear protein GN=PCNP PE=1 SV=2	1.56	0.16
P35354	Prostaglandin G/H synthase 2 GN=PTGS2 PE=1 SV=2	0.05	-0.03
P14543	Nidogen-1 GN=NID1 PE=1 SV=3	2.05	0.10
P35080	Profilin-2 GN=PFN2 PE=1 SV=3	2.30	0.29

Q7Z4V5	Hepatoma-derived growth factor-related protein 2 GN=HDGFL2 PE=1 SV=1	2.01	0.24
Q59GY2	Ribosomal protein L4 variant (Fragment) PE=2 SV=1	1.65	0.35
A0A024RAM2	Glutaredoxin (Thioltransferase), isoform CRA_c GN=GLRX PE=4 SV=1	1.48	0.17
G3V180	Dipeptidyl peptidase 3 GN=DPP3 PE=1 SV=1	1.90	0.35
A0A024R8N6	Thymidine kinase GN=TK1 PE=3 SV=1	1.64	0.17
Q8WWM7	Ataxin-2-like protein GN=ATXN2L PE=1 SV=2	1.73	0.22
O75326	Semaphorin-7A GN=SEMA7A PE=1 SV=1	1.10	0.09
O95336	6-phosphogluconolactonase GN=PGLS PE=1 SV=2	1.92	0.24
Q9NPF4	Probable tRNA N6-adenosine threonylcarbamoyltransferase GN=OSGEP PE=1 SV=1	2.44	0.23
O15511	Actin-related protein 2/3 complex subunit 5 GN=ARPC5 PE=1 SV=3	1.87	0.27
Q96D15	Reticulocalbin-3 GN=RCN3 PE=1 SV=1	1.54	0.33
Q9NR30	Nucleolar RNA helicase 2 GN=DDX21 PE=1 SV=5	2.59	0.21
B8ZX62	Plasminogen activator GN=PLAT PE=2 SV=1	1.40	-0.13
Q9NYF8	Bcl-2-associated transcription factor 1 GN=BCLAF1 PE=1 SV=2	2.10	0.23
A0A024R814	Ribosomal protein L7, isoform CRA_a GN=RPL7 PE=4 SV=1	1.65	0.43
Q9UHD8	Septin-9 GN=SEPT9 PE=1 SV=2	1.53	0.18
A8MXP9	Matrin-3 GN=MATR3 PE=1 SV=1	0.74	0.09
O15212	Prefoldin subunit 6 GN=PFDN6 PE=1 SV=1	0.85	0.13
Q96I99	Succinate--CoA ligase [GDP-forming] subunit beta, mitochondrial GN=SUCLG2 PE=1 SV=2	3.21	0.39
V9HW48	SH3 domain-binding glutamic acid-rich-like protein GN=HEL-S-115 PE=2 SV=1	2.76	0.28
U5YKD2	MHC class I antigen (Fragment) GN=HLA-A PE=3 SV=1	2.79	0.50
O94985	Calsyntenin-1 GN=CLSTN1 PE=1 SV=1	0.81	0.22
Q02750	Dual specificity mitogen-activated protein kinase kinase 1 GN=MAP2K1 PE=1 SV=2	0.35	0.06
P61457	Pterin-4-alpha-carbinolamine dehydratase GN=PCBD1 PE=1 SV=2	2.44	0.20
A0A024R3C4	KDEL (Lys-Asp-Glu-Leu) containing 2, isoform CRA_a GN=KDELC2 PE=4 SV=1	1.19	0.21
P62424	60S ribosomal protein L7a GN=RPL7A PE=1 SV=2	1.54	0.42
Q08257	Quinone oxidoreductase GN=CRYZ PE=1 SV=1	2.52	0.32
D3DNI2	Profilin (Fragment) GN=PFN2 PE=3 SV=1	0.48	0.10
O60869	Endothelial differentiation-related factor 1 GN=EDF1 PE=1 SV=1	2.50	0.22
A8K2M0	Proteasome (Prosome, macropain) 26S subunit, ATPase, 4, isoform CRA_b GN=PSMC4 PE=2 SV=1	1.40	0.18
P09914	Interferon-induced protein with tetratricopeptide repeats 1 GN=IFIT1 PE=1 SV=2	2.05	0.70
Q9UNN8	Endothelial protein C receptor GN=PROCR PE=1 SV=1	3.40	0.39
P62314	Small nuclear ribonucleoprotein Sm D1 GN=SNRPD1 PE=1 SV=1	1.26	0.16
Q96EK6	Glucosamine 6-phosphate N-acetyltransferase GN=GNPNAT1 PE=1 SV=1	2.60	0.31
B0LPF3	Growth factor receptor-bound protein 2, isoform CRA_a GN=GRB2 PE=2 SV=1	2.51	0.23
Q13620	Cullin-4B GN=CUL4B PE=1 SV=4	1.04	0.15
A0A024RB87	RAP1B, member of RAS oncogene family, isoform CRA_a GN=RAP1B PE=4 SV=1	1.39	0.18
A0A024R6Y2	Nuclear transport factor 2, isoform CRA_a GN=NUTF2 PE=4 SV=1	2.82	0.28
Q549M8	CLE7 GN=C14orf166 PE=2 SV=1	2.16	0.28
Q92890	Ubiquitin recognition factor in ER-associated degradation protein 1 GN=UFD1 PE=1 SV=3	1.77	0.19
P17980	26S proteasome regulatory subunit 6A GN=PSMC3 PE=1 SV=3	1.92	0.36
A8K2W7	cDNA FLJ78119, highly similar to Homo sapiens G1 to S phase transition 1 (GSPT1), mRNA PE=2 SV=1	0.74	0.08
C9JEH3	Angio-associated migratory cell protein GN=AAMP PE=1 SV=1	2.18	0.26
Q5U0B9	Stem cell growth factor;lymphocyte secreted C-type lectin PE=2 SV=1	0.39	-0.05
K7EM18	Eukaryotic translation initiation factor 1 GN=EIF1 PE=1 SV=1	2.38	0.27
Q14008	Cytoskeleton-associated protein 5 GN=CKAP5 PE=1 SV=3	0.23	-0.02
B2R665	cDNA, FLJ92810, highly similar to Homo sapiens protein phosphatase 1G (formerly 2C), magnesium-dependent, gamma isoform (PPM1G), mRNA PE=2 SV=1	3.24	0.58
P08579	U2 small nuclear ribonucleoprotein B'' GN=SNRPB2 PE=1 SV=1	0.94	0.23
D6W4Z6	HCG23833, isoform CRA_b GN=hCG_23833 PE=4 SV=1	3.52	0.30
F8WCF6	Actin-related protein 2/3 complex subunit 4 GN=ARPC4-TTLL3 PE=3 SV=1	2.19	0.28
Q9NZM1	Myoferlin GN=MYOF PE=1 SV=1	1.53	0.28
M0R0R2	40S ribosomal protein S5 GN=RPS5 PE=1 SV=1	1.50	0.33
P27824	Calnexin GN=CANX PE=1 SV=2	0.78	0.34
P49753	Acyl-coenzyme A thioesterase 2, mitochondrial GN=ACOT2 PE=1 SV=6	3.50	0.42

Q9BVG4	Protein PBDC1 GN=PBDC1 PE=1 SV=1	0.89	0.16
Q8NI22	Multiple coagulation factor deficiency protein 2 GN=MCFD2 PE=1 SV=1	0.99	0.25
A0A024R5S5	Eukaryotic translation initiation factor 3 subunit J GN=EIF3S1 PE=3 SV=1	1.37	0.21
P58546	Myotrophin GN=MTPN PE=1 SV=2	2.77	0.33
A0A090N7V5	Chromosome 7 open reading frame 24 GN=C7orf24 PE=4 SV=1	2.22	0.34
A8K6V3	cDNA FLJ78677, highly similar to Homo sapiens splicing factor 3b, subunit 3, 130kDa (SF3B3), mRNA PE=2 SV=1	2.44	0.28
P30419	Glycylpeptide N-tetradecanoyltransferase 1 GN=NMT1 PE=1 SV=2	2.55	0.40
A0A024QZN9	Voltage-dependent anion channel 2, isoform CRA_a GN=VDAC2 PE=4 SV=1	0.85	0.35
P06132	Uroporphyrinogen decarboxylase GN=UROD PE=1 SV=2	2.13	0.26
P35244	Replication protein A 14 kDa subunit GN=RPA3 PE=1 SV=1	2.46	0.30
Q03405	Urokinase plasminogen activator surface receptor GN=PLAUR PE=1 SV=1	0.04	-0.01
P13500	C-C motif chemokine 2 GN=CCL2 PE=1 SV=1	5.88	0.99
Q16352	Alpha-internexin GN=INA PE=1 SV=2	2.10	0.26
E9PF18	Hydroxyacyl-coenzyme A dehydrogenase, mitochondrial GN=HADH PE=1 SV=2	3.67	0.47
H0YNJ6	GMP reductase GN=GMPR2 PE=1 SV=1	1.84	0.28
Q5SW79	Centrosomal protein of 170 kDa GN=CEP170 PE=1 SV=1	1.05	0.12
A8K168	Malic enzyme PE=2 SV=1	1.96	0.28
P62263	40S ribosomal protein S14 GN=RPS14 PE=1 SV=3	1.42	0.47
A0A024QZD5	Small nuclear ribonucleoprotein 70kDa polypeptide (RNP antigen), isoform CRA_b GN=SNRP70 PE=4 SV=1	3.36	0.32
P55084	Trifunctional enzyme subunit beta, mitochondrial GN=HADHB PE=1 SV=3	2.02	0.41
P53041	Serine/threonine-protein phosphatase 5 GN=PPP5C PE=1 SV=1	1.40	0.14
B7Z268	Single-stranded DNA binding protein 1, isoform CRA_c GN=SSBP1 PE=2 SV=1	1.74	0.28
Q15942	Zyxin GN=ZYX PE=1 SV=1	2.66	0.24
P62306	Small nuclear ribonucleoprotein F GN=SNRPF PE=1 SV=1	2.04	0.17
A0A024R962	HCG40889, isoform CRA_b GN=hCG_40889 PE=4 SV=1	2.78	0.19
F8VXC8	SWI/SNF complex subunit SMARCC2 GN=SMARCC2 PE=1 SV=1	0.24	0.04
Q59GE4	Ribosomal protein S10 variant (Fragment) PE=4 SV=1	1.80	0.40
Q8IUX7	Adipocyte enhancer-binding protein 1 GN=AEBP1 PE=1 SV=1	2.14	0.16
A0A024RCJ8	HCG1821276, isoform CRA_a GN=hCG_1821276 PE=4 SV=1	1.93	0.28
Q8NBS9	Thioredoxin domain-containing protein 5 GN=TXNDC5 PE=1 SV=2	2.04	0.26
O43818	U3 small nucleolar RNA-interacting protein 2 GN=RRP9 PE=1 SV=1	1.45	0.28
Q13740	CD166 antigen GN=ALCAM PE=1 SV=2	0.36	0.08
Q7Z460	CLIP-associating protein 1 GN=CLASP1 PE=1 SV=1	0.76	0.30
Q59FG9	Chondroitin sulfate proteoglycan 2 (Versican) variant (Fragment) PE=2 SV=1	4.80	0.32
A0A1U9X8E2	Proteasome subunit beta type PE=3 SV=1	2.22	0.35
D3DRR6	Inter-alpha (Globulin) inhibitor H2, isoform CRA_a GN=ITIH2 PE=4 SV=1	1.35	-0.53
B2RAH7	cDNA, FLJ94921, highly similar to Homo sapiens prolyl endopeptidase (PREP), mRNA PE=2 SV=1	1.41	0.15
P52788	Spermine synthase GN=SMS PE=1 SV=2	1.78	0.25
P49411	Elongation factor Tu, mitochondrial GN=TUFM PE=1 SV=2	2.30	0.44
D9ZGF2	Collagen, type VI, alpha 3 GN=COL6A3 PE=4 SV=1	2.14	-0.11
Q8TDJ5	Tyrosine-protein kinase receptor GN=TFG/ALK fusion PE=2 SV=1	3.03	0.21
O95292	Vesicle-associated membrane protein-associated protein B/C GN=VAPB PE=1 SV=3	3.98	0.44
P61956	Small ubiquitin-related modifier 2 GN=SUMO2 PE=1 SV=3	4.19	0.23
Q9UBQ5	Eukaryotic translation initiation factor 3 subunit K GN=EIF3K PE=1 SV=1	1.65	0.23
O76003	Glutaredoxin-3 GN=GLRX3 PE=1 SV=2	2.67	0.32
A0A024R7S3	Clathrin light chain GN=CLTB PE=3 SV=1	2.10	0.30
Q9UJ70	N-acetyl-D-glucosamine kinase GN=NAGK PE=1 SV=4	3.16	0.35
P32455	Guanylate-binding protein 1 GN=GBP1 PE=1 SV=2	3.40	0.43
Q96AY3	Peptidyl-prolyl cis-trans isomerase FKBP10 GN=FKBP10 PE=1 SV=1	0.96	0.25
P62750	60S ribosomal protein L23a GN=RPL23A PE=1 SV=1	1.23	0.25
Q96F85	CB1 cannabinoid receptor-interacting protein 1 GN=CNRIP1 PE=1 SV=1	0.63	0.14
O95817	BAG family molecular chaperone regulator 3 GN=BAG3 PE=1 SV=3	1.79	0.21
P49006	MARCKS-related protein GN=MARCKSL1 PE=1 SV=2	0.15	0.02
O15371	Eukaryotic translation initiation factor 3 subunit D GN=EIF3D PE=1 SV=1	1.94	0.45

A0A0A6YY92	Adenylosuccinate lyase GN=ADSL PE=1 SV=1	1.72	0.25
Q3MI39	HNRPA1 protein (Fragment) GN=HNRPA1 PE=2 SV=1	1.11	0.21
P27694	Replication protein A 70 kDa DNA-binding subunit GN=RPA1 PE=1 SV=2	1.60	0.20
B2RB23	cDNA, FLJ95265, highly similar to Homo sapiens acetyl-Coenzyme A acyltransferase 2 (mitochondrial 3-oxoacyl-Coenzyme A thiolase) (ACAA2), nuclear gene encoding mitochondrial protein, mRNA PE=2 SV=1	2.67	0.38
Q14767	Latent-transforming growth factor beta-binding protein 2 GN=LTBP2 PE=1 SV=3	2.04	0.35
P55735	Protein SEC13 homolog GN=SEC13 PE=1 SV=3	1.56	0.23
A0A140VJL8	Inositol-1-monophosphatase PE=2 SV=1	0.53	0.11
Q8TCD5	5'(3')-deoxyribonucleotidase, cytosolic type GN=NT5C PE=1 SV=2	0.61	0.26
A0A024R4M0	40S ribosomal protein S9 GN=RPS9 PE=1 SV=1	2.09	0.58
P38606	V-type proton ATPase catalytic subunit A GN=ATP6V1A PE=1 SV=2	2.73	0.31
P61086	Ubiquitin-conjugating enzyme E2 K GN=UBE2K PE=1 SV=3	1.14	0.10
B5BUE6	ATP-dependent RNA helicase DDX5 (Fragment) GN=DDX5 PE=2 SV=1	2.36	0.40
A0A024R9D3	Ribosomal protein L30, isoform CRA_b GN=RPL30 PE=3 SV=1	0.77	0.13
Q9Y3B8	Oligoribonuclease, mitochondrial GN=REXO2 PE=1 SV=3	1.97	0.21
Q15417	Calponin-3 GN=CNN3 PE=1 SV=1	0.03	0.01
A0A087WUF6	Fibroblast growth factor GN=FGF2 PE=1 SV=2	2.08	0.29
B2R4D5	Actin-related protein 2/3 complex subunit 3 PE=2 SV=1	1.63	0.22
E9PB61	THO complex subunit 4 GN=ALYREF PE=1 SV=1	2.75	0.27
P53992	Protein transport protein Sec24C GN=SEC24C PE=1 SV=3	0.68	0.13
B1AKJ5	Nardilysin (N-arginine dibasic convertase), isoform CRA_d GN=NRDC PE=1 SV=1	2.43	0.34
B2R491	40S ribosomal protein S4 GN=RPS4X PE=2 SV=1	1.07	0.38
A0A024RAF0	Bridging integrator 1, isoform CRA_c GN=BIN1 PE=4 SV=1	1.46	0.17
Q86TI2	Dipeptidyl peptidase 9 GN=DPP9 PE=1 SV=3	2.19	0.22
P15880	40S ribosomal protein S2 GN=RPS2 PE=1 SV=2	1.80	0.48
A8K070	COP9 signalosome complex subunit 1 GN=GPS1 PE=1 SV=1	1.41	0.17
Q9Y3C6	Peptidyl-prolyl cis-trans isomerase-like 1 GN=PPIL1 PE=1 SV=1	2.70	0.35
Q6EMK4	Vasorin GN=VASN PE=1 SV=1	1.86	0.24
Q6NUL6	PITPNA protein (Fragment) GN=PITPNA PE=2 SV=1	0.90	0.17
A0A024RAR8	Aminopeptidase GN=ARTS-1 PE=3 SV=1	2.03	0.27
Q16186	Proteasomal ubiquitin receptor ADRM1 GN=ADRM1 PE=1 SV=2	1.69	0.22
Q5T5H1	Alpha-endosulfine GN=ENSA PE=1 SV=1	2.18	0.13
Q99471	Prefoldin subunit 5 GN=PFDN5 PE=1 SV=2	3.23	0.33
Q16666	Gamma-interferon-inducible protein 16 GN=IFI16 PE=1 SV=3	1.75	0.44
Q6IBS0	Twinfilin-2 GN=TWF2 PE=1 SV=2	1.46	0.18
Q05DF2	SF3A2 protein (Fragment) GN=SF3A2 PE=2 SV=1	1.65	0.26
P55263	Adenosine kinase GN=ADK PE=1 SV=2	1.70	0.23
Q9NSD9	Phenylalanine--tRNA ligase beta subunit GN=FARSB PE=1 SV=3	2.37	0.27
F8W031	Uncharacterized protein (Fragment) PE=1 SV=1	0.43	0.13
Q9Y237	Peptidyl-prolyl cis-trans isomerase NIMA-interacting 4 GN=PIN4 PE=1 SV=1	0.41	0.09
Q597H1	Transformation-related protein 14 GN=TRG14 PE=2 SV=1	3.90	-0.67
P62081	40S ribosomal protein S7 GN=RPS7 PE=1 SV=1	2.14	0.45
O60271	C-Jun-amino-terminal kinase-interacting protein 4 GN=SPAG9 PE=1 SV=4	0.70	0.19
D6RFG8	Deoxycytidine kinase GN=DCK PE=1 SV=1	2.29	0.33
A0A087WY85	Ubiquitin-conjugating enzyme E2 D3 GN=UBE2D3 PE=1 SV=1	2.60	0.32
A0A140GPP7	Prolyl endopeptidase FAP PE=3 SV=1	1.46	0.39
P62633	Cellular nucleic acid-binding protein GN=CNBP PE=1 SV=1	0.47	0.14
A0A087WUB9	Beta-catenin-like protein 1 GN=CTNNBL1 PE=1 SV=1	2.68	0.36
A6XND9	Beta-2-microglobulin PE=2 SV=1	2.45	0.33
Q13162	Peroxiredoxin-4 GN=PRDX4 PE=1 SV=1	0.49	0.14
P62328	Thymosin beta-4 GN=TMSB4X PE=1 SV=2	1.09	0.09
A0A2R8YD14	40S ribosomal protein S24 GN=RPS24 PE=1 SV=1	1.92	0.47
P41227	N-alpha-acetyltransferase 10 GN=NAA10 PE=1 SV=1	1.46	0.27
A0A024R7U6	DNA helicase GN=MCM4 PE=3 SV=1	2.37	0.26
B3KQI5	cDNA FLJ90522 fis, clone NT2RP4000108, highly similar to Neurofilament triplet L protein PE=2 SV=1	0.83	0.15

A0A140VK41	Testicular secretory protein Li 41 PE=2 SV=1	4.47	0.41
P46776	60S ribosomal protein L27a GN=RPL27A PE=1 SV=2	1.34	0.33
Q59G75	Isoleucyl-tRNA synthetase, cytoplasmic variant (Fragment) PE=2 SV=1	2.14	0.38
A0A024R329	GDP-mannose pyrophosphorylase B, isoform CRA_a GN=GMPPB PE=4 SV=1	2.16	0.35
Q6UVK1	Chondroitin sulfate proteoglycan 4 GN=CSPG4 PE=1 SV=2	0.36	0.04
A0A024R4D1	COP9 constitutive photomorphogenic homolog subunit 8 (Arabidopsis), isoform CRA_a GN=COPS8 PE=4 SV=1	1.70	0.30
X5D2M8	Major vault protein isoform A (Fragment) GN=MVP PE=2 SV=1	1.65	0.30
B2R8Y9	Tissue factor pathway inhibitor PE=2 SV=1	1.28	0.26
P39023	60S ribosomal protein L3 GN=RPL3 PE=1 SV=2	1.53	0.43
A8K9B9	cDNA FLJ77391, highly similar to Homo sapiens EH-domain containing 4 (EHD4), mRNA PE=2 SV=1	1.29	0.42
P36551	Oxygen-dependent coproporphyrinogen-III oxidase, mitochondrial GN=CPOX PE=1 SV=3	2.01	0.27
A0A087WZT3	BolA-like protein 2 GN=BOLA2 PE=1 SV=2	0.04	0.01
B2R4C1	cDNA, FLJ92036, highly similar to Homo sapiens ribosomal protein L31 (RPL31), mRNA PE=2 SV=1	2.56	0.42
Q14320	Protein FAM50A GN=FAM50A PE=1 SV=2	1.37	0.16
P17812	CTP synthase 1 GN=CTPS1 PE=1 SV=2	2.83	0.43
Q9Y547	Intraflagellar transport protein 25 homolog GN=HSPB11 PE=1 SV=1	0.69	0.11
A8K5S3	cDNA FLJ78449 PE=2 SV=1	0.05	-0.01
O95433	Activator of 90 kDa heat shock protein ATPase homolog 1 GN=AHSA1 PE=1 SV=1	1.58	0.23
Q5U0Q1	Ras-GTPase-activating protein SH3-domain-binding protein, isoform CRA_a GN=DKFZp686L1159 PE=2 SV=1	1.39	0.23
P23497	Nuclear autoantigen Sp-100 GN=SP100 PE=1 SV=3	0.90	0.12
Q6FGY1	HPCAL1 protein GN=HPCAL1 PE=2 SV=1	1.69	0.17
O00233	26S proteasome non-ATPase regulatory subunit 9 GN=PSMD9 PE=1 SV=3	2.24	0.28
O14964	Hepatocyte growth factor-regulated tyrosine kinase substrate GN=HGS PE=1 SV=1	0.49	0.13
P47813	Eukaryotic translation initiation factor 1A, X-chromosomal GN=EIF1AX PE=1 SV=2	2.47	0.25
Q59G24	Activated RNA polymerase II transcription cofactor 4 variant (Fragment) PE=2 SV=1	0.53	0.17
O00273	DNA fragmentation factor subunit alpha GN=DFFA PE=1 SV=1	1.22	0.20
Q9UK45	U6 snRNA-associated Sm-like protein LSm7 GN=LSM7 PE=1 SV=1	1.74	0.22
O75832	26S proteasome non-ATPase regulatory subunit 10 GN=PSMD10 PE=1 SV=1	1.03	0.24
Q15437	Protein transport protein Sec23B GN=SEC23B PE=1 SV=2	2.39	0.28
O75663	TIP41-like protein GN=TIPRL PE=1 SV=2	2.08	0.26
Q9UNS2	COP9 signalosome complex subunit 3 GN=COPS3 PE=1 SV=3	1.25	0.29
H0YMD1	Low-density lipoprotein receptor GN=LDLR PE=1 SV=1	4.04	0.27
Q9BTY2	Plasma alpha-L-fucosidase GN=FUCA2 PE=1 SV=2	3.11	0.38
B4DP80	NAD(P)H-hydrate epimerase GN=APOA1BP PE=2 SV=1	0.14	0.03
Q15008	26S proteasome non-ATPase regulatory subunit 6 GN=PSMD6 PE=1 SV=1	2.49	0.28
Q58EY4	SWI/SNF related, matrix associated, actin dependent regulator of chromatin, subfamily c, member 1 GN=SMARCC1 PE=2 SV=1	1.40	0.44
P35998	26S proteasome regulatory subunit 7 GN=PSMC2 PE=1 SV=3	2.00	0.28
Q13501	Sequestosome-1 GN=SQSTM1 PE=1 SV=1	2.26	0.36
B4DN80	Peptidyl-prolyl cis-trans isomerase PE=2 SV=1	3.16	0.29
Q6FGH9	Dynein light chain GN=DNCL1 PE=2 SV=1	2.33	0.34
P53618	Coatomer subunit beta GN=COPB1 PE=1 SV=3	1.63	0.27
A0A024R3V7	NIF3-like protein 1 GN=NIF3L1 PE=3 SV=1	1.92	0.32
A0A2R8Y6X2	D-aminoacyl-tRNA deacylase GN=DTD1 PE=1 SV=1	2.53	0.28
P51668	Ubiquitin-conjugating enzyme E2 D1 GN=UBE2D1 PE=1 SV=1	1.34	0.59
Q15717	ELAV-like protein 1 GN=ELAVL1 PE=1 SV=2	1.78	0.26
B0QZ18	Copine-1 GN=CPNE1 PE=1 SV=1	0.55	0.08
P49792	E3 SUMO-protein ligase RanBP2 GN=RANBP2 PE=1 SV=2	1.85	0.23
P62917	60S ribosomal protein L8 GN=RPL8 PE=1 SV=2	1.11	0.44
Q01813	ATP-dependent 6-phosphofructokinase, platelet type GN=PFKP PE=1 SV=2	0.19	0.04
B3KNI2	cDNA FLJ14650 fis, clone NT2RP2002185, highly similar to Ubiquilin-1 PE=2 SV=1	1.76	0.24
Q5H9N4	Uncharacterized protein DKFZp686L20222 GN=DKFZp686L20222 PE=3 SV=1	1.27	0.46

A0A024R6W2	Nudix (Nucleoside diphosphate linked moiety X)-type motif 21, isoform CRA_a GN=NUDT21 PE=4 SV=1	2.04	0.21
Q06210	Glutamine--fructose-6-phosphate aminotransferase [isomerizing] 1 GN=GFPT1 PE=1 SV=3	1.36	0.34
Q02388	Collagen alpha-1(VII) chain GN=COL7A1 PE=1 SV=2	0.25	0.07
A8K8N7	Phosphoribosylformylglycinamidine synthase (FGAR amidotransferase), isoform CRA_b GN=PFAS PE=2 SV=1	1.28	0.27
B2R4C0	60S ribosomal protein L18a PE=2 SV=1	1.80	0.40
Q96ST2	Protein IWS1 homolog GN=IWS1 PE=1 SV=2	3.55	0.46
P17858	ATP-dependent 6-phosphofructokinase, liver type GN=PFKL PE=1 SV=6	0.34	0.13
A0A024RCW3	Ribosomal protein GN=RPL10A PE=3 SV=1	1.71	0.25
Q5T6V5	Queuosine salvage protein GN=C9orf64 PE=1 SV=1	0.29	0.05
Q12792	Twinfilin-1 GN=TWF1 PE=1 SV=3	1.31	0.21
Q99426	Tubulin-folding cofactor B GN=TBCB PE=1 SV=2	2.19	0.41
P28072	Proteasome subunit beta type-6 GN=PSMB6 PE=1 SV=4	1.85	0.24
E5KMI6	Lon protease homolog, mitochondrial GN=LONP1 PE=3 SV=1	0.92	0.28
O75942	Major prion protein GN=PRNP PE=3 SV=2	2.01	0.26
B4E3D4	cDNA FLJ56293, highly similar to Transmembrane glycoprotein NMB PE=2 SV=1	3.10	0.35
A0A024RDE5	Ras-GTPase activating protein SH3 domain-binding protein 2, isoform CRA_a GN=G3BP2 PE=4 SV=1	0.02	0.01
Q13596	Sorting nexin-1 GN=SNX1 PE=1 SV=3	0.60	0.18
B2RCM2	cDNA, FLJ96156, highly similar to Homo sapiens leucyl-tRNA synthetase (LARS), mRNA PE=2 SV=1	2.27	0.50
A2A2V4	Vascular endothelial growth factor A GN=VEGFA PE=1 SV=1	3.84	-0.56
Q8NBJ5	Procollagen galactosyltransferase 1 GN=COLGALT1 PE=1 SV=1	1.06	0.22
P04181	Ornithine aminotransferase, mitochondrial GN=OAT PE=1 SV=1	2.72	0.38
O14786	Neuropilin-1 GN=NRP1 PE=1 SV=3	0.14	0.02
Q96M27	Protein PRRC1 GN=PRRC1 PE=1 SV=1	3.53	0.27
O60888	Protein CutA GN=CUTA PE=1 SV=2	1.30	0.23
I3L0A0	HCG2044781 GN=TMEM189-UBE2V1 PE=4 SV=1	0.89	0.23
Q9BXV9	EKC/KEOPS complex subunit GON7 GN=GON7 PE=1 SV=2	1.71	0.27
Q86U42	Polyadenylate-binding protein 2 GN=PABPN1 PE=1 SV=3	2.04	0.28
D3DQU2	Tripeptidyl peptidase I, isoform CRA_a GN=TPP1 PE=4 SV=1	1.60	0.33
A8K7E0	Biglycan PE=2 SV=1	0.95	0.15
V9HW01	Epididymis secretory protein Li 310 GN=HEL-S-310 PE=2 SV=1	0.88	0.30
P25774	Cathepsin S GN=CTSS PE=1 SV=3	2.06	0.25
Q9NQR4	Omega-amidase NIT2 GN=NIT2 PE=1 SV=1	2.67	0.54
Q9H910	Jupiter microtubule associated homolog 2 GN=JPT2 PE=1 SV=1	1.27	0.13
A0A090N7U0	Cullin 1, isoform CRA_b GN=CUL1 PE=3 SV=1	2.33	0.28
B4DUM2	cDNA FLJ53891, highly similar to Adenylosuccinate lyase PE=2 SV=1	1.36	0.13
B4DJV9	cDNA FLJ60607, highly similar to Acyl-protein thioesterase 1 PE=2 SV=1	2.09	0.31
Q6IT96	Histone deacetylase GN=HDAC1 PE=1 SV=1	0.22	0.05
P98066	Tumor necrosis factor-inducible gene 6 protein GN=TNFAIP6 PE=1 SV=2	4.84	0.43
E9PR17	CD59 glycoprotein PE=1 SV=1	2.47	0.29
Q59F22	Interferon stimulated gene 20kDa variant (Fragment) PE=2 SV=1	1.90	0.24
Q13564	NEDD8-activating enzyme E1 regulatory subunit GN=NAE1 PE=1 SV=1	1.69	0.26
Q14203	Dynactin subunit 1 GN=DCTN1 PE=1 SV=3	1.67	0.31
P21283	V-type proton ATPase subunit C 1 GN=ATP6V1C1 PE=1 SV=4	1.05	0.16
B4E284	cDNA FLJ51188, highly similar to N-acetylglucosamine-6-sulfatase (EC3.1.6.14) PE=2 SV=1	2.02	0.30
C9JCC6	Dr1-associated corepressor GN=DRAP1 PE=1 SV=1	1.58	0.22
A0A024R056	Guanine nucleotide binding protein (G protein), beta polypeptide 1, isoform CRA_a GN=GNB1 PE=2 SV=1	0.76	0.20
Q53FI7	Four and a half LIM domains 1 variant (Fragment) PE=2 SV=1	2.44	0.29
Q9UHY7	Enolase-phosphatase E1 GN=ENOPH1 PE=1 SV=1	1.99	0.43
P61764	Syntaxin-binding protein 1 GN=STXBP1 PE=1 SV=1	1.49	0.28
K7ER00	Phenylalanine--tRNA ligase alpha subunit GN=FARSA PE=1 SV=1	0.82	-0.20

P53597	Succinate--CoA ligase [ADP/GDP-forming] subunit alpha, mitochondrial GN=SUCLG1 PE=1 SV=4	2.58	0.35
P23368	NAD-dependent malic enzyme, mitochondrial GN=ME2 PE=1 SV=1	2.46	0.34
Q53T99	Ribosome biogenesis protein WDR12 GN=WDR12 PE=2 SV=1	1.53	0.22
B3KUJ0	cDNA FLJ39996 fis, clone STOMA2002166, highly similar to Splicing factor 3B subunit 4 PE=2 SV=1	1.91	0.36
P54886	Delta-1-pyrroline-5-carboxylate synthase GN=ALDH18A1 PE=1 SV=2	1.18	0.31
P38117	Electron transfer flavoprotein subunit beta GN=ETFB PE=1 SV=3	2.08	0.32
A0A0C4DGG9	Chromodomain-helicase-DNA-binding protein 4 GN=CHD4 PE=1 SV=1	0.63	-0.14
Q96QK1	Vacuolar protein sorting-associated protein 35 GN=VPS35 PE=1 SV=2	2.36	0.49
B1AHD1	NHP2-like protein 1 GN=SNU13 PE=1 SV=1	0.56	0.20
P54920	Alpha-soluble NSF attachment protein GN=NAPA PE=1 SV=3	0.30	0.09
B3KY60	cDNA FLJ16777 fis, clone BRHIP2029567, highly similar to Cell division cycle 5-like protein PE=2 SV=1	3.17	0.25
Q96C23	Aldose 1-epimerase GN=GALM PE=1 SV=1	2.66	0.32
Q53G42	mRNA decapping enzyme variant (Fragment) PE=2 SV=1	2.41	0.29
A0A0A0MT60	Peptidylprolyl isomerase (Fragment) GN=FKBP15 PE=1 SV=1	0.47	0.05
P27635	60S ribosomal protein L10 GN=RPL10 PE=1 SV=4	1.29	0.44
Q7Z4Y4	GTP:AMP phosphotransferase AK3, mitochondrial GN=AK3 PE=2 SV=1	3.80	0.39
D3DWY7	Prefoldin subunit 3 GN=VBP1 PE=3 SV=1	0.67	0.08
B2R7E8	cDNA, FLJ93412, highly similar to Homo sapiens replication protein A2, 32kDa (RPA2), mRNA PE=2 SV=1	2.49	0.30
P60866	40S ribosomal protein S20 GN=RPS20 PE=1 SV=1	2.66	0.43
P17936	Insulin-like growth factor-binding protein 3 GN=IGFBP3 PE=1 SV=2	0.53	0.11
A8KAP3	cDNA FLJ78483, highly similar to Homo sapiens elongation factor Tu GTP binding domain containing 2 (EFTUD2), mRNA PE=2 SV=1	2.07	0.35
A0A024R216	Hepatoma-derived growth factor, related protein 3, isoform CRA_a GN=HDGFRP3 PE=1 SV=1	1.07	-0.06
Q06481	Amyloid-like protein 2 GN=APLP2 PE=1 SV=2	2.88	0.11
P42126	Enoyl-CoA delta isomerase 1, mitochondrial GN=ECI1 PE=1 SV=1	2.13	0.24
A0A0C4DGQ5	Calpain small subunit 1 GN=CAPNS1 PE=1 SV=1	2.83	0.33
A0A024R8E5	Collagen, type V, alpha 1, isoform CRA_a GN=COL5A1 PE=4 SV=1	1.68	0.07
P25685	DnaJ homolog subfamily B member 1 GN=DNAJB1 PE=1 SV=4	0.63	0.14
Q13045	Protein flightless-1 homolog GN=FLII PE=1 SV=2	0.44	0.10
B2R9H3	cDNA, FLJ94391, highly similar to Homo sapiens serine (or cysteine) proteinase inhibitor, clade B (ovalbumin), member 8 (SERPINB8), mRNA PE=2 SV=1	1.81	0.16
A0A0A0MRM9	Nucleolar and coiled-body phosphoprotein 1 (Fragment) GN=NOLC1 PE=1 SV=1	0.23	0.07
A0A140VJZ4	Ubiquitin carboxyl-terminal hydrolase PE=2 SV=1	1.27	0.24
P20809	Interleukin-11 GN=IL11 PE=1 SV=1	1.21	-0.09
P04899	Guanine nucleotide-binding protein G(i) subunit alpha-2 GN=GNAI2 PE=1 SV=3	0.63	0.15
P09661	U2 small nuclear ribonucleoprotein A' GN=SNRPA1 PE=1 SV=2	0.78	0.18
B3V096	BetaCstF-64 variant 2 GN=CSTF2 PE=2 SV=1	3.45	0.25
Q06124	Tyrosine-protein phosphatase non-receptor type 11 GN=PTPN11 PE=1 SV=2	2.98	0.37
B2R5T2	cDNA, FLJ92608, highly similar to Homo sapiens aldehyde dehydrogenase 1 family, member A3 (ALDH1A3), mRNA PE=2 SV=1	1.99	0.09
B2RCP7	cDNA, FLJ96197, highly similar to Homo sapiens connective tissue growth factor (CTGF), mRNA PE=2 SV=1	1.38	0.44
B0YIW2	Apolipoprotein C-III variant 1 GN=APOC3 PE=1 SV=1	0.09	0.04
P31942	Heterogeneous nuclear ribonucleoprotein H3 GN=HNRNPH3 PE=1 SV=2	1.98	0.25
A0A087WTY6	Neuroblastoma suppressor of tumorigenicity 1 GN=NBL1 PE=1 SV=1	0.52	0.50
Q9NZL4	Hsp70-binding protein 1 GN=HSPBP1 PE=1 SV=2	0.73	0.11
V9HW44	Epididymis secretory protein Li 303 GN=HEL-S-303 PE=2 SV=1	1.45	0.25
P78556	C-C motif chemokine 20 GN=CCL20 PE=1 SV=1	2.43	-0.42
P58107	Epiplakin GN=EPPK1 PE=1 SV=3	3.14	-0.53
A0A024R5X3	SAFB-like, transcription modulator, isoform CRA_b GN=SLTM PE=4 SV=1	1.27	0.21
O60565	Gremlin-1 GN=GREM1 PE=1 SV=1	1.63	0.25
B5BUB1	RuvB-like helicase (Fragment) GN=RUVBL1 PE=2 SV=1	1.68	0.30

P38159	RNA-binding motif protein, X chromosome GN=RBMX PE=1 SV=3	2.18	0.21
A0A024R0V4	Vasodilator-stimulated phosphoprotein isoform 1 GN=VASP PE=2 SV=1	0.13	-0.02
A0A286YFF7	Palmitoyl-protein thioesterase 1 GN=PPT1 PE=1 SV=1	2.33	0.23
Q8N543	Prolyl 3-hydroxylase OGFOD1 GN=OGFOD1 PE=1 SV=1	1.48	0.37
P55809	Succinyl-CoA:3-ketoacid coenzyme A transferase 1, mitochondrial GN=OXCT1 PE=1 SV=1	2.82	0.32
B2R825	Alpha-1,4 glucan phosphorylase PE=2 SV=1	0.51	0.07
A0A024R2Q2	Ubiquitin-conjugating enzyme E2E 2 (UBC4/5 homolog, yeast), isoform CRA_a GN=UBE2E2 PE=3 SV=1	2.18	0.28
P62277	40S ribosomal protein S13 GN=RPS13 PE=1 SV=2	2.16	0.47
P19957	Elafin GN=PI3 PE=1 SV=3	4.94	-0.79
B4DPV7	cDNA FLJ54534, highly similar to Homo sapiens cysteinyl-tRNA synthetase (CARS), transcript variant 3, mRNA PE=2 SV=1	1.40	0.10
Q15404	Ras suppressor protein 1 GN=RSU1 PE=1 SV=3	1.34	0.20
Q9P1F3	Costars family protein ABRACL GN=ABRACL PE=1 SV=1	1.52	0.21
Q6FIE5	PHP14 protein GN=PHP14 PE=2 SV=1	2.40	0.32
A8K3Q9	cDNA FLJ76611, highly similar to Homo sapiens ribosomal protein L14 (RPL14), mRNA PE=1 SV=1	0.97	0.15
Q13442	28 kDa heat- and acid-stable phosphoprotein GN=PDAP1 PE=1 SV=1	0.91	0.09
Q9BRF8	Serine/threonine-protein phosphatase CPPED1 GN=CPPED1 PE=1 SV=3	1.02	0.17
H3BQK0	ATP-dependent RNA helicase DDX19B GN=DDX19B PE=1 SV=1	2.25	0.44
B5MBZ0	Echinoderm microtubule-associated protein-like 4 GN=EML4 PE=1 SV=3	2.52	0.31
A0A024RA75	3-hydroxyisobutyrate dehydrogenase GN=HIBADH PE=3 SV=1	1.81	0.36
A0A140VK53	Testicular secretory protein Li 53 PE=2 SV=1	3.94	0.38
Q5VWC4	26S proteasome non-ATPase regulatory subunit 4 GN=PSMD4 PE=1 SV=1	2.29	0.27
Q05DB4	HEBP2 protein (Fragment) GN=HEBP2 PE=2 SV=1	2.59	0.14
M0QYS1	60S ribosomal protein L13a (Fragment) GN=RPL13A PE=1 SV=2	1.01	0.20
P33908	Mannosyl-oligosaccharide 1,2-alpha-mannosidase IA GN=MAN1A1 PE=1 SV=3	1.63	0.18
O00231	26S proteasome non-ATPase regulatory subunit 11 GN=PSMD11 PE=1 SV=3	2.07	0.27
B2RAU5	Sorting nexin PE=2 SV=1	1.19	0.24
Q9NR12	PDZ and LIM domain protein 7 GN=PDLIM7 PE=1 SV=1	0.33	0.08
P36542	ATP synthase subunit gamma, mitochondrial GN=ATP5F1C PE=1 SV=1	2.15	0.30
Q9NQC3	Reticulon-4 GN=RTN4 PE=1 SV=2	1.37	0.36
A8K6Y2	Serine/threonine-protein phosphatase 2A 56 kDa regulatory subunit PE=2 SV=1	2.56	0.34
O96019	Actin-like protein 6A GN=ACTL6A PE=1 SV=1	1.97	0.32
A8K0I8	cDNA FLJ76207, highly similar to Homo sapiens delta-notch-like EGF repeat-containing transmembrane (DNER), mRNA PE=2 SV=1	1.04	0.13
A0A096LPI6	Uncharacterized protein (Fragment) PE=4 SV=2	1.75	0.35
P37108	Signal recognition particle 14 kDa protein GN=SRP14 PE=1 SV=2	2.93	0.38
P09668	Pro-cathepsin H GN=CTSH PE=1 SV=4	1.40	0.24
Q8WZA0	Protein LZIC GN=LZIC PE=1 SV=1	1.37	0.21
A0A0G2JH68	Protein diaphanous homolog 1 GN=DIAPH1 PE=1 SV=1	1.59	0.32
E5KN59	Peptidyl-prolyl cis-trans isomerase D PE=4 SV=1	1.76	0.39
B2RD19	cDNA, FLJ96419, highly similar to Homo sapiens fructosamine-3-kinase-related protein (FN3KRP), mRNA PE=2 SV=1	1.66	0.33
P09496	Clathrin light chain A GN=CLTA PE=1 SV=1	1.77	0.26
Q9GZX9	Twisted gastrulation protein homolog 1 GN=TWSG1 PE=1 SV=1	0.09	-0.03
H0YHG0	Uncharacterized protein (Fragment) PE=1 SV=1	1.97	0.19
Q5T446	Uroporphyrinogen decarboxylase (Fragment) GN=UROD PE=1 SV=1	1.04	0.65
P62745	Rho-related GTP-binding protein RhoB GN=RHOB PE=1 SV=1	0.46	-0.09
A8K7D9	Importin subunit alpha PE=2 SV=1	3.59	0.41
A8K492	cDNA FLJ76789, highly similar to Homo sapiens methionine-tRNA synthetase (MARS), mRNA PE=2 SV=1	1.45	0.44
B2R802	cDNA, FLJ93681, highly similar to Homo sapiens small nuclear ribonucleoprotein polypeptide A (SNRPA), mRNA PE=2 SV=1	0.66	0.08
B7Z1Z5	cDNA FLJ57265, highly similar to Neurotrimin PE=2 SV=1	1.62	0.21
H3BN98	Uncharacterized protein (Fragment) PE=4 SV=2	2.33	0.41
P62913	60S ribosomal protein L11 GN=RPL11 PE=1 SV=2	1.90	0.42

D3DSY9	Farnesyltransferase, CAAX box, alpha, isoform CRA_a GN=FNTA PE=4 SV=1	3.51	0.18
Q13867	Bleomycin hydrolase GN=BLMH PE=1 SV=1	1.49	0.23
Q96CG8	Collagen triple helix repeat-containing protein 1 GN=CTHRC1 PE=1 SV=1	0.28	-0.01
H0YJ75	Serine/threonine-protein phosphatase 2A 56 kDa regulatory subunit gamma isoform (Fragment) GN=PPP2R5C PE=1 SV=1	2.03	0.36
Q9BY44	Eukaryotic translation initiation factor 2A GN=EIF2A PE=1 SV=3	2.43	0.27
H0YBX6	Ubiquitin-conjugating enzyme E2 variant 2 (Fragment) GN=UBE2V2 PE=1 SV=1	0.98	0.20
A8K6V0	cDNA FLJ78676, highly similar to Homo sapiens SEC24 related gene family, member D (SEC24D), mRNA PE=2 SV=1	1.23	0.31
Q8WWX9	Selenoprotein M GN=SELENOM PE=1 SV=3	0.39	0.09
Q9GZZ1	N-alpha-acetyltransferase 50 GN=NAA50 PE=1 SV=1	2.91	0.39
P30049	ATP synthase subunit delta, mitochondrial GN=ATP5F1D PE=1 SV=2	0.98	0.27
G3V5T9	Cyclin-dependent kinase 2, isoform CRA_c GN=CDK2 PE=1 SV=1	1.99	0.28
Q86UA3	Chromosome 12 open reading frame 10, isoform CRA_b GN=C12orf10 PE=1 SV=1	3.34	0.73
P35269	General transcription factor IIF subunit 1 GN=GTF2F1 PE=1 SV=2	0.64	0.10
Q9UMX5	Neudesin GN=NENF PE=1 SV=1	0.59	0.12
Q0VDC6	Peptidylprolyl isomerase GN=FKBP1A PE=1 SV=1	1.83	0.32
A0A0A6YYL6	Protein RPL17-C18orf32 GN=RPL17-C18orf32 PE=3 SV=1	1.57	0.37
Q96B97	SH3 domain-containing kinase-binding protein 1 GN=SH3KBP1 PE=1 SV=2	3.70	0.40
P46109	Crk-like protein GN=CRKL PE=1 SV=1	2.05	0.37
P45973	Chromobox protein homolog 5 GN=CBX5 PE=1 SV=1	0.16	0.03
O43488	Aflatoxin B1 aldehyde reductase member 2 GN=AKR7A2 PE=1 SV=3	1.63	0.36
P61106	Ras-related protein Rab-14 GN=RAB14 PE=1 SV=4	2.34	0.50
D3DVW9	Protein tyrosine phosphatase, non-receptor type substrate 1, isoform CRA_a GN=PTPNS1 PE=4 SV=1	0.32	0.05
Q96QR8	Transcriptional activator protein Pur-beta GN=PURB PE=1 SV=3	0.93	0.18
Q9HA77	Probable cysteine--tRNA ligase, mitochondrial GN=CARS2 PE=1 SV=1	3.81	0.47
P30040	Endoplasmic reticulum resident protein 29 GN=ERP29 PE=1 SV=4	1.72	0.43
A0A024R8A7	HCG31253, isoform CRA_a GN=hCG_31253 PE=4 SV=1	2.46	0.36
Q6FH49	NNMT protein GN=NNMT PE=2 SV=1	2.93	0.45
O00629	Importin subunit alpha-3 GN=KPNA4 PE=1 SV=1	1.50	0.20
P43155	Carnitine O-acetyltransferase GN=CRAT PE=1 SV=5	3.37	0.34
H3BQJ5	Nucleolar protein 3 (Fragment) GN=NOL3 PE=1 SV=2	1.52	0.36
Q8WZ82	Esterase OVCA2 GN=OVCA2 PE=1 SV=1	2.31	0.45
Q53FT3	Protein Hikeshi GN=HIKESHI PE=1 SV=2	0.09	-0.03
B3KPC7	Actin-related protein 2/3 complex subunit 5 PE=2 SV=1	1.07	0.37
Q32P28	Prolyl 3-hydroxylase 1 GN=P3H1 PE=1 SV=2	1.59	0.38
Q6PKG0	La-related protein 1 GN=LARP1 PE=1 SV=2	1.71	0.26
P18827	Syndecan-1 GN=SDC1 PE=1 SV=3	2.81	0.69
P41236	Protein phosphatase inhibitor 2 GN=PPP1R2 PE=1 SV=2	0.37	0.06
B2RBM8	cDNA, FLJ95596, highly similar to Homo sapiens activity-dependent neuroprotector (ADNP), mRNA PE=2 SV=1	0.86	0.14
Q5U5J2	CSNK2A1 protein GN=CSNK2A1 PE=1 SV=1	0.73	0.18
Q9UBB4	Ataxin-10 GN=ATXN10 PE=1 SV=1	1.81	0.24
Q9BZK7	F-box-like/WD repeat-containing protein TBL1XR1 GN=TBL1XR1 PE=1 SV=1	2.70	0.39
Q05048	Cleavage stimulation factor subunit 1 GN=CSTF1 PE=1 SV=1	2.55	0.44
A0A140VJZ1	Ubiquitin carboxyl-terminal hydrolase PE=2 SV=1	2.56	0.22
Q92769	Histone deacetylase 2 GN=HDAC2 PE=1 SV=2	0.94	0.16
Q92626	Peroxidasin homolog GN=PXDN PE=1 SV=2	0.86	0.10
P54105	Methylosome subunit pICln GN=CLNS1A PE=1 SV=1	1.70	0.45
A5Y5A3	PC1/MRPS28 fusion protein PE=2 SV=1	1.96	-0.25
Q9BZM5	UL16-binding protein 2 GN=ULBP2 PE=1 SV=1	1.12	0.30
P49458	Signal recognition particle 9 kDa protein GN=SRP9 PE=1 SV=2	1.58	0.21
O14561	Acyl carrier protein, mitochondrial GN=NDUFAB1 PE=1 SV=3	2.67	0.45
Q9H488	GDP-fucose protein O-fucosyltransferase 1 GN=POFUT1 PE=1 SV=1	0.59	0.17
A8K2Z3	cDNA FLJ76092, highly similar to Homo sapiens 5'-nucleotidase, cytosolic II-like 1 (NT5C2L1), mRNA PE=2 SV=1	3.77	0.37

P04733	Metallothionein-1F GN=MT1F PE=1 SV=1	1.22	0.09
J3KQ41	COP9 signalosome complex subunit 7b GN=COPS7B PE=1 SV=1	1.27	0.31
Q13630	GDP-L-fucose synthase GN=TSTA3 PE=1 SV=1	4.54	0.38
A8K6A7	Alpha-mannosidase PE=2 SV=1	2.61	0.26
Q8WVX7	Ribosomal protein S19 (Fragment) PE=2 SV=1	1.67	0.35
A0A024R7E3	DNA (cytosine-5)-methyltransferase GN=DNMT1 PE=3 SV=1	1.20	0.34
A0A024RDH8	Ribosomal protein L34, isoform CRA_a GN=RPL34 PE=4 SV=1	1.52	0.20
A0A0S2Z5H3	Clathrin interactor 1 isoform 2 (Fragment) GN=CLINT1 PE=2 SV=1	1.63	0.18
J3QQ67	60S ribosomal protein L18 (Fragment) GN=RPL18 PE=1 SV=1	0.96	0.45
A0A1B0GVH5	Alpha-ketoglutarate-dependent dioxygenase FTO GN=FTO PE=1 SV=1	1.66	0.39
Q08722	Leukocyte surface antigen CD47 GN=CD47 PE=1 SV=1	1.39	0.36
O00267	Transcription elongation factor SPT5 GN=SUPT5H PE=1 SV=1	1.90	0.16
O95831	Apoptosis-inducing factor 1, mitochondrial GN=AIFM1 PE=1 SV=1	2.35	0.29
Q6UX72	UDP-GlcNAc:betaGal beta-1,3-N-acetylglucosaminyltransferase 9 GN=B3GNT9 PE=2 SV=1	1.13	0.11
B2R6P3	cDNA, FLJ93047, highly similar to Homo sapiens matrix metallopeptidase 14 (membrane-inserted) (MMP14), mRNA PE=2 SV=1	2.18	0.29
U5IT74	MHC class I antigen (Fragment) GN=HLA-C PE=3 SV=1	2.29	0.38
A0A140VJL0	3-hydroxyisobutyryl-CoA hydrolase, mitochondrial PE=2 SV=1	2.18	0.36
A0A024R687	Pleckstrin homology domain containing, family C (With FERM domain) member 1, isoform CRA_b GN=PLEKHC1 PE=4 SV=1	1.60	0.14
Q9NZV1	Cysteine-rich motor neuron 1 protein GN=CRIM1 PE=1 SV=1	0.41	0.20
Q6MZT3	Uncharacterized protein DKFZp686C1054 GN=DKFZp686C1054 PE=2 SV=1	2.31	0.32
A8K2T7	Receptor protein-tyrosine kinase PE=2 SV=1	0.16	-0.04
Q16629	Serine/arginine-rich splicing factor 7 GN=SRSF7 PE=1 SV=1	0.91	0.34
Q15642	Cdc42-interacting protein 4 GN=TRIP10 PE=1 SV=3	1.34	0.15
A0A024R7J0	Protein kinase, cAMP-dependent, catalytic, alpha, isoform CRA_c GN=PRKACA PE=3 SV=1	2.68	0.37
P42574	Caspase-3 GN=CASP3 PE=1 SV=2	2.04	0.26
O75367	Core histone macro-H2A.1 GN=H2AFY PE=1 SV=4	1.85	0.31
Q9H1B7	Interferon regulatory factor 2-binding protein-like GN=IRF2BPL PE=1 SV=1	1.36	0.37
Q53XJ5	Peptidylprolyl isomerase GN=FKBP2 PE=2 SV=1	2.16	0.25
Q96DB5	Regulator of microtubule dynamics protein 1 GN=RMDN1 PE=1 SV=1	2.75	0.34
Q8NFH4	Nucleoporin Nup37 GN=NUP37 PE=1 SV=1	2.67	0.40
Q04941	Proteolipid protein 2 GN=PLP2 PE=1 SV=1	0.49	0.16
A0A024RAV0	Branched-chain-amino-acid aminotransferase GN=BCAT1 PE=3 SV=1	1.67	0.18
Q9NZD2	Glycolipid transfer protein GN=GLTP PE=1 SV=3	1.01	-0.17
A0A1B0GW23	ABHD14A-ACY1 readthrough (Fragment) GN=ABHD14A-ACY1 PE=4 SV=1	3.02	0.35
Q16831	Uridine phosphorylase 1 GN=UPP1 PE=1 SV=1	1.51	0.19
O94760	N(G),N(G)-dimethylarginine dimethylaminohydrolase 1 GN=DDAH1 PE=1 SV=3	1.39	0.21
P52434	DNA-directed RNA polymerases I, II, and III subunit RPABC3 GN=POLR2H PE=1 SV=4	1.45	0.14
A0A087X2I1	26S proteasome regulatory subunit 10B GN=PSMC6 PE=1 SV=1	1.35	0.23
Q59EI9	ADP,ATP carrier protein, liver isoform T2 variant (Fragment) PE=2 SV=1	0.95	0.38
B2RBA6	DNA replication licensing factor MCM7 GN=MCM7 PE=2 SV=1	1.40	0.24
P16298	Serine/threonine-protein phosphatase 2B catalytic subunit beta isoform GN=PPP3CB PE=1 SV=2	3.05	0.35
A0A024R0N6	Spectrin beta chain GN=SPTBN4 PE=3 SV=1	1.64	0.22
B3KWI4	cDNA FLJ43122 fis, clone CTONG3003737, highly similar to Leucine-rich repeat-containing protein 15 PE=2 SV=1	2.04	0.16
R9S3C3	p14ARF/p16INK4a fusion protein GN=p14ARF PE=2 SV=1	1.26	0.32
P60673	Profilin-3 GN=PFN3 PE=2 SV=1	2.91	0.47
Q4LE60	TNPO2 variant protein (Fragment) GN=TNPO2 variant protein PE=2 SV=1	1.21	0.32
Q5RKV6	Exosome complex component MTR3 GN=EXOSC6 PE=1 SV=1	0.08	-0.03
Q6UWP8	Suprabasin GN=SBSN PE=1 SV=2	3.17	0.40
Q53H82	Endoribonuclease LACTB2 GN=LACTB2 PE=1 SV=2	1.29	0.25
Q5VZU9	Tripeptidyl-peptidase 2 GN=TPP2 PE=1 SV=1	1.42	0.22
P11388	DNA topoisomerase 2-alpha GN=TOP2A PE=1 SV=3	2.86	0.60
Q10713	Mitochondrial-processing peptidase subunit alpha GN=PMPCA PE=1 SV=2	3.86	0.69
P02462	Collagen alpha-1(IV) chain GN=COL4A1 PE=1 SV=4	1.19	0.29

P61353	60S ribosomal protein L27 GN=RPL27 PE=1 SV=2	2.76	0.41
B7Z6S9	Glucosylceramidase PE=2 SV=1	1.73	0.17
Q9BY76	Angiopoietin-related protein 4 GN=ANGPTL4 PE=1 SV=2	1.12	-0.47
Q92990	Glomulin GN=GLMN PE=1 SV=2	1.57	0.28
B2R9W9	Craniofacial development protein 1 PE=2 SV=1	2.13	0.26
Q58FF9	Heat shock protein 90Af GN=HSP90Af PE=2 SV=1	2.13	0.41
O15231	Zinc finger protein 185 GN=ZNF185 PE=1 SV=3	0.55	-0.15
H3BNC9	Uncharacterized protein PE=3 SV=2	1.90	0.38
Q8NBF2	NHL repeat-containing protein 2 GN=NHLRC2 PE=1 SV=1	0.13	0.03
Q8N2S1	Latent-transforming growth factor beta-binding protein 4 GN=LTBP4 PE=1 SV=2	0.39	0.18
Q8N3D4	EH domain-binding protein 1-like protein 1 GN=EHBP1L1 PE=1 SV=2	0.96	-0.19
Q5HYL6	Uncharacterized protein DKFZp686E1899 GN=DKFZp686E1899 PE=2 SV=1	0.90	0.10
O75935	Dynactin subunit 3 GN=DCTN3 PE=1 SV=1	1.37	0.27
P13473	Lysosome-associated membrane glycoprotein 2 GN=LAMP2 PE=1 SV=2	2.04	0.20
B2R8D1	cDNA, FLJ93841, highly similar to Homo sapiens nitrilase 1 (NIT1), mRNA PE=2 SV=1	1.72	0.24
Q9H814	Phosphorylated adapter RNA export protein GN=PHAX PE=1 SV=1	0.87	-0.33
B2RAR3	Queuine tRNA-ribosyltransferase catalytic subunit 1 GN=QTRT1 PE=2 SV=1	2.21	0.42
B3KN49	cDNA FLJ13562 fis, clone PLACE1008080, highly similar to Homo sapiens hexamethylene bis-acetamide inducible 1 (HEXIM1), mRNA PE=2 SV=1	0.09	-0.03
O15400	Syntaxin-7 GN=STX7 PE=1 SV=4	0.32	0.07
B2RBP3	cDNA, FLJ95615, highly similar to Homo sapiens ubiquitin-activating enzyme E1C (UBA3 homolog, yeast)(UBE1C), mRNA PE=2 SV=1	1.38	0.20
Q9NRN7	L-aminoadipate-semialdehyde dehydrogenase-phosphopantetheinyl transferase GN=AASDHPPT PE=1 SV=2	2.39	0.34
Q8TAT6	Nuclear protein localization protein 4 homolog GN=NPLOC4 PE=1 SV=3	0.99	0.13
P10606	Cytochrome c oxidase subunit 5B, mitochondrial GN=COX5B PE=1 SV=2	1.98	0.42
A0A0N9MXA6	MHC class I antigen (Fragment) GN=HLA-A PE=3 SV=1	3.02	0.37
Q13443	Disintegrin and metalloproteinase domain-containing protein 9 GN=ADAM9 PE=1 SV=1	0.18	-0.04
J3KPP4	Cisplatin resistance-associated overexpressed protein, isoform CRA_b GN=LUC7L3 PE=1 SV=1	0.64	0.13
A0A0Y0J542	Vascular endothelial growth factor A121 (Fragment) PE=2 SV=1	2.83	-0.43
P49773	Histidine triad nucleotide-binding protein 1 GN=HINT1 PE=1 SV=2	3.36	0.37
A0A140VK39	Protein phosphatase methylesterase 1 PE=2 SV=1	1.50	0.23
B3KSH8	cDNA FLJ36241 fis, clone THYMU2001622, highly similar to Inositol polyphosphate 1-phosphatase PE=2 SV=1	2.31	0.37
V9HW87	Abhydrolase domain containing 14B, isoform CRA_a GN=HEL-S-299 PE=2 SV=1	0.50	0.08
Q9H074	Polyadenylate-binding protein-interacting protein 1 GN=PAIP1 PE=1 SV=1	2.05	0.33
F8VVA7	Coatomer subunit zeta-1 GN=COPZ1 PE=1 SV=1	0.18	0.04
Q9H773	dCTP pyrophosphatase 1 GN=DCTPP1 PE=1 SV=1	5.58	0.49
Q7Z7Q8	C-C motif chemokine GN=MCP-3 PE=3 SV=1	4.14	1.02
P62269	40S ribosomal protein S18 GN=RPS18 PE=1 SV=3	1.36	0.37
Q9H3H3	UPF0696 protein C11orf68 GN=C11orf68 PE=1 SV=2	0.26	0.07
A8K5C4	cDNA FLJ76290, highly similar to Homo sapiens TIA1 cytotoxic granule-associated RNA bindingprotein-like 1 (TIAL1), transcript variant 1, mRNA PE=2 SV=1	0.71	0.14
Q7Z6E9	E3 ubiquitin-protein ligase RBBP6 GN=RBBP6 PE=1 SV=1	1.54	0.15
Q71V07	Signal recognition particle subunit SRP72 PE=2 SV=1	0.21	0.03
I4AY87	Macrophage migration inhibitory factor (Fragment) GN=MIF PE=1 SV=1	0.37	0.05
P62879	Guanine nucleotide-binding protein G(I)/G(S)/G(T) subunit beta-2 GN=GNB2 PE=1 SV=3	0.61	0.10
A0A140VJT0	Serine/threonine-protein phosphatase 2A 55 kDa regulatory subunit B PE=2 SV=1	2.97	0.36
A8KAE0	cDNA FLJ78476, highly similar to Homo sapiens WD repeat and HMG-box DNA binding protein 1 (WDHD1), transcript variant 1, mRNA PE=2 SV=1	1.32	0.30
Q13541	Eukaryotic translation initiation factor 4E-binding protein 1 GN=EIF4EBP1 PE=1 SV=3	0.41	0.16
O95747	Serine/threonine-protein kinase OSR1 GN=OXSR1 PE=1 SV=1	4.42	0.55
Q9HCU0	Endosialin GN=CD248 PE=1 SV=1	3.38	0.43
J3KQ18	D-dopachrome decarboxylase GN=DDT PE=1 SV=1	0.55	0.09
B5BU08	U2 small nuclear RNA auxillary factor 1 isoform a GN=U2AF1 PE=2 SV=1	0.14	0.02

A0A024R7W9	COP9 constitutive photomorphogenic homolog subunit 5 (Arabidopsis), isoform CRA_a GN=COPS5 PE=2 SV=1	1.12	0.28
Q00325	Phosphate carrier protein, mitochondrial GN=SLC25A3 PE=1 SV=2	1.32	0.35
Q53Y06	ATPase, H+ transporting, lysosomal 31kDa, V1 subunit E isoform 1 GN=ATP6V1E1 PE=2 SV=1	0.26	-0.08
D3DV26	S100 calcium binding protein A10 (Annexin II ligand, calpactin I, light polypeptide (P11)), isoform CRA_b (Fragment) GN=S100A10 PE=4 SV=1	0.82	0.27
P55212	Caspase-6 GN=CASP6 PE=1 SV=2	0.79	0.25
A0A0G2JK23	Large proline-rich protein BAG6 GN=BAG6 PE=1 SV=1	1.15	0.25
Q13308	Inactive tyrosine-protein kinase 7 GN=PTK7 PE=1 SV=2	0.06	-0.01
A8K3A8	cDNA FLJ75085, highly similar to Homo sapiens glutaminyl-tRNA synthetase (QARS), mRNA PE=2 SV=1	2.38	0.32
Q92743	Serine protease HTRA1 GN=HTRA1 PE=1 SV=1	0.34	0.10
A0A024R203	Proteasome (Prosome, macropain) activator subunit 3 (PA28 gamma Ki), isoform CRA_a GN=PSME3 PE=4 SV=1	0.97	0.27
P48723	Heat shock 70 kDa protein 13 GN=HSPA13 PE=1 SV=1	0.78	0.14
Q7Z417	Nuclear fragile X mental retardation-interacting protein 2 GN=NUFIP2 PE=1 SV=1	1.86	0.27
A0A024R059	3-hydroxy-3-methylglutaryl coenzyme A synthase GN=HMGCS1 PE=3 SV=1	2.45	0.33
Q8N1G4	Leucine-rich repeat-containing protein 47 GN=LRRC47 PE=1 SV=1	1.48	0.13
Q53F47	Down-regulator of transcription 1 variant (Fragment) PE=2 SV=1	1.00	0.19
A0A0S2Z404	Regulator of chromosome condensation 1 isoform 2 (Fragment) GN=RCC1 PE=2 SV=1	2.04	0.34
A0A024R482	GDP-mannose pyrophosphorylase A, isoform CRA_a GN=GMPPA PE=4 SV=1	1.85	0.37
A0A0S2Z4Z6	Serine/arginine repetitive matrix 1 isoform 2 (Fragment) GN=SRRM1 PE=1 SV=1	0.05	0.02
P62857	40S ribosomal protein S28 GN=RPS28 PE=1 SV=1	1.64	0.35
A0A024R8U8	Calcium activated nucleotidase 1, isoform CRA_b GN=CANT1 PE=4 SV=1	0.64	0.07
Q9P0K7	Ankycorbin GN=RAI14 PE=1 SV=2	0.88	0.20
Q6DK41	Protein Wnt (Fragment) GN=WNT5A PE=2 SV=2	1.41	0.40
Q14232	Translation initiation factor eIF-2B subunit alpha GN=EIF2B1 PE=1 SV=1	0.98	0.06
K7ELG9	Protein LSM12 homolog GN=LSM12 PE=1 SV=1	1.02	0.27
B4DI08	cDNA FLJ60091, highly similar to Hypoxia-inducible factor 1 alpha inhibitor PE=2 SV=1	0.94	0.23
Q9NUL5	Repressor of yield of DENV protein GN=RYDEN PE=1 SV=2	1.75	0.29
Q5VW32	BRO1 domain-containing protein BROX GN=BROX PE=1 SV=1	2.15	0.28
O14618	Copper chaperone for superoxide dismutase GN=CCS PE=1 SV=1	0.55	0.10
Q12904	Aminoacyl tRNA synthase complex-interacting multifunctional protein 1 GN=AIMP1 PE=1 SV=2	0.97	0.20
A0A024R2T5	CUB domain containing protein 1, isoform CRA_a GN=CDCP1 PE=4 SV=1	0.65	-0.10
A8K588	cDNA FLJ76823, highly similar to Homo sapiens splicing factor, arginine/serine-rich 6 (SFRS6), mRNA PE=2 SV=1	1.19	0.24
Q14554	Protein disulfide-isomerase A5 GN=PDIA5 PE=1 SV=1	1.57	0.25
Q9H4A6	Golgi phosphoprotein 3 GN=GOLPH3 PE=1 SV=1	1.74	0.26
B2R761	cDNA, FLJ93299, highly similar to Homo sapiens sterol carrier protein 2 (SCP2), mRNA PE=2 SV=1	2.79	0.41
A0A0A0MQR2	Replication termination factor 2 GN=RTF2 PE=1 SV=1	1.71	0.32
Q59GW6	Acetyl-CoA acetyltransferase, cytosolic variant (Fragment) PE=2 SV=1	1.54	0.29
A0A024RDL9	Phosphoserine phosphatase, isoform CRA_b GN=PSPH PE=4 SV=1	1.16	0.26
P26447	Protein S100-A4 GN=S100A4 PE=1 SV=1	1.75	0.27
A1X283	SH3 and PX domain-containing protein 2B GN=SH3PXD2B PE=1 SV=3	2.19	0.29
Q96K17	Transcription factor BTF3 homolog 4 GN=BTF3L4 PE=1 SV=1	1.46	0.21
Q8WVY7	Ubiquitin-like domain-containing CTD phosphatase 1 GN=UBLCP1 PE=1 SV=2	0.82	0.16
B4DX46	cDNA FLJ52663, highly similar to SET and MYND domain-containing protein 5 PE=2 SV=1	1.70	0.57
Q13131	5'-AMP-activated protein kinase catalytic subunit alpha-1 GN=PRKAA1 PE=1 SV=4	1.71	0.31
A0A140VJC9	Lysophospholipase II, isoform CRA_f GN=LYPLA2 PE=2 SV=1	2.72	0.38
Q9BV57	1,2-dihydroxy-3-keto-5-methylthiopentene dioxygenase GN=ADI1 PE=1 SV=1	1.87	0.32
G5EA09	Syndecan binding protein (Syntenin), isoform CRA_a GN=SDCBP PE=1 SV=1	0.74	0.14
O76021	Ribosomal L1 domain-containing protein 1 GN=RSL1D1 PE=1 SV=3	1.77	0.32
E5RIM7	Copper transport protein ATOX1 GN=ATOX1 PE=1 SV=1	3.04	0.30
P62312	U6 snRNA-associated Sm-like protein LSm6 GN=LSM6 PE=1 SV=1	0.63	0.31

P11802	Cyclin-dependent kinase 4 GN=CDK4 PE=1 SV=2	1.21	0.29
A0A140VJJ2	S-formylglutathione hydrolase GN=ESD PE=2 SV=1	2.72	0.36
Q9NQL2	Ras-related GTP-binding protein D GN=RRAGD PE=1 SV=1	0.11	-0.03
Q6P2Q9	Pre-mRNA-processing-splicing factor 8 GN=PRPF8 PE=1 SV=2	0.85	0.32
P19525	Interferon-induced, double-stranded RNA-activated protein kinase GN=EIF2AK2 PE=1 SV=2	2.00	0.37
P62829	60S ribosomal protein L23 GN=RPL23 PE=1 SV=1	1.49	0.39
Q9NQ88	Fructose-2,6-bisphosphatase TIGAR GN=TIGAR PE=1 SV=1	2.38	0.43
D6RFN0	COP9 signalosome complex subunit 4 GN=COPS4 PE=1 SV=1	0.06	-0.02
A8K6T5	cDNA FLJ75144, highly similar to Homo sapiens ash2 (absent, small, or homeotic)-like (ASH2L), mRNA PE=2 SV=1	1.36	0.34
Q9Y6A4	Cilia- and flagella-associated protein 20 GN=CFAP20 PE=1 SV=1	0.67	0.17
P84098	60S ribosomal protein L19 GN=RPL19 PE=1 SV=1	2.45	0.46
O60711	Leupaxin GN=LPXN PE=1 SV=1	0.08	0.04
P61081	NEDD8-conjugating enzyme Ubc12 GN=UBE2M PE=1 SV=1	1.94	0.24
Q6PJT7	Zinc finger CCCH domain-containing protein 14 GN=ZC3H14 PE=1 SV=1	0.89	0.07
A0A024R9P6	Family with sequence similarity 82, member C, isoform CRA_a GN=FAM82C PE=4 SV=1	2.13	0.29
B2R679	cDNA, FLJ92825, highly similar to Homo sapiens SAR1a gene homolog 1 (S. cerevisiae) (SARA1), mRNA PE=2 SV=1	1.47	0.27
Q9Y5K6	CD2-associated protein GN=CD2AP PE=1 SV=1	2.06	0.33
Q7L9L4	MOB kinase activator 1B GN=MOB1B PE=1 SV=3	1.91	0.26
Q4VC31	Coiled-coil domain-containing protein 58 GN=CCDC58 PE=1 SV=1	1.92	0.21
Q13618	Cullin-3 GN=CUL3 PE=1 SV=2	1.00	0.15
Q16775	Hydroxyacylglutathione hydrolase, mitochondrial GN=HAGH PE=1 SV=2	0.94	0.18
A8K8F6	cDNA FLJ78417, highly similar to Homo sapiens low density lipoprotein receptor-related protein associated protein 1 (LRPAP1), mRNA PE=2 SV=1	2.10	0.34
Q96EI5	Transcription elongation factor A protein-like 4 GN=TCEAL4 PE=1 SV=2	0.07	0.01
Q8N1G2	Cap-specific mRNA (nucleoside-2'-O-)-methyltransferase 1 GN=CMTR1 PE=1 SV=1	1.20	0.23
A0MNN4	CDW3/SMU1 GN=SMU1 PE=2 SV=1	1.62	0.26
A0A024R6A5	Protein phosphatase 1A (Formerly 2C), magnesium-dependent, alpha isoform, isoform CRA_a GN=PPM1A PE=3 SV=1	1.50	0.41
Q9H6F5	Coiled-coil domain-containing protein 86 GN=CCDC86 PE=1 SV=1	2.16	0.31
E5RG17	Putative deoxyribonuclease TATDN1 (Fragment) GN=TATDN1 PE=1 SV=1	1.30	0.30
P20290	Transcription factor BTF3 GN=BTF3 PE=1 SV=1	1.14	0.24
Q96CS3	FAS-associated factor 2 GN=FAF2 PE=1 SV=2	2.59	0.37
O75436	Vacuolar protein sorting-associated protein 26A GN=VPS26A PE=1 SV=2	1.68	0.13
O00423	Echinoderm microtubule-associated protein-like 1 GN=EML1 PE=1 SV=3	2.83	0.57
B5BUC0	Glycogen synthase kinase-3 beta (Fragment) GN=GSK3B PE=2 SV=1	1.56	0.23
P36639	7,8-dihydro-8-oxoguanine triphosphatase GN=NUDT1 PE=1 SV=3	0.92	0.17
A0A024R4E5	High density lipoprotein binding protein (Vigilin), isoform CRA_a GN=HDLBP PE=1 SV=1	2.92	0.44
A0A2H4WPY8	MHC class I antigen GN=HLA-A PE=3 SV=1	0.14	0.04
G8JLH6	Tetraspanin GN=CD9 PE=1 SV=2	0.86	-0.14
O60264	SWI/SNF-related matrix-associated actin-dependent regulator of chromatin subfamily A member 5 GN=SMARCA5 PE=1 SV=1	3.27	0.26
Q00796	Sorbitol dehydrogenase GN=SORD PE=1 SV=4	1.35	0.25
Q5T178	Cyclin-dependent kinases regulatory subunit GN=CKS1B PE=2 SV=1	3.13	0.37
P30626	Sorcin GN=SRI PE=1 SV=1	2.36	0.44
B7Z9B1	cDNA FLJ52398, highly similar to Cadherin-13 PE=2 SV=1	1.99	0.30
B4DUC8	S-methyl-5'-thioadenosine phosphorylase GN=MTAP PE=1 SV=1	0.74	0.13
P07741	Adenine phosphoribosyltransferase GN=APRT PE=1 SV=2	0.42	0.05
Q9NX46	Poly(ADP-ribose) glycohydrolase ARH3 GN=ADPRHL2 PE=1 SV=1	0.42	0.19
Q13033	Striatin-3 GN=STRN3 PE=1 SV=3	0.93	0.10
A0A024R1U4	RAB5C, member RAS oncogene family, isoform CRA_a GN=RAB5C PE=4 SV=1	1.99	0.46
P46087	Probable 28S rRNA (cytosine(4447)-C(5))-methyltransferase GN=NOP2 PE=1 SV=2	2.14	0.35
B4DVA7	Beta-hexosaminidase PE=2 SV=1	0.82	0.14
B7Z9B8	cDNA FLJ56912, highly similar to Fibulin-2 PE=2 SV=1	1.56	0.32
J3KQN4	60S ribosomal protein L36a GN=RPL36A PE=1 SV=1	1.83	0.58

O00468	Agrin GN=AGRN PE=1 SV=6	3.59	0.46
Q53HB7	Diablo isoform 1 variant (Fragment) PE=2 SV=1	1.84	0.24
Q9NXJ5	Pyroglutamyl-peptidase 1 GN=PGPEP1 PE=1 SV=1	0.90	-0.76
Q15020	Squamous cell carcinoma antigen recognized by T-cells 3 GN=SART3 PE=1 SV=1	2.22	0.26
Q08623	Pseudouridine-5'-phosphatase GN=PUDP PE=1 SV=3	1.39	0.31
Q549H9	cAMP-dependent protein kinase inhibitor GN=PKIG PE=1 SV=1	2.10	0.20
E7ESC6	Exportin-7 GN=XPO7 PE=1 SV=1	0.99	0.21
Q7L5N1	COP9 signalosome complex subunit 6 GN=COPS6 PE=1 SV=1	1.28	0.31
P63220	40S ribosomal protein S21 GN=RPS21 PE=1 SV=1	2.75	0.45
Q59GK9	Ribosomal protein L21 variant (Fragment) PE=2 SV=1	0.49	0.18
P62851	40S ribosomal protein S25 GN=RPS25 PE=1 SV=1	0.55	0.17
B4DKQ5	cDNA FLJ54710, highly similar to Target of Myb protein 1 PE=2 SV=1	0.72	0.19
Q9UN70	Protocadherin gamma-C3 GN=PCDHGC3 PE=1 SV=1	2.15	0.35
X6R4W8	BUB3-interacting and GLEBS motif-containing protein ZNF207 GN=ZNF207 PE=1 SV=1	3.03	0.28
A0A024R7F4	Deoxyribonuclease II, lysosomal, isoform CRA_a GN=DNASE2 PE=4 SV=1	2.34	0.28
Q8N806	Putative E3 ubiquitin-protein ligase UBR7 GN=UBR7 PE=1 SV=2	0.47	0.18
P54709	Sodium/potassium-transporting ATPase subunit beta-3 GN=ATP1B3 PE=1 SV=1	0.37	-0.11
Q643R0	HCTP4 GN=HCTP4 PE=1 SV=1	2.22	0.40
Q13325	Interferon-induced protein with tetratricopeptide repeats 5 GN=IFIT5 PE=1 SV=1	1.59	0.40
Q96AT9	Ribulose-phosphate 3-epimerase GN=RPE PE=1 SV=1	2.42	0.21
A8K6K2	cDNA FLJ75877, highly similar to Homo sapiens 5'-nucleotidase, cytosolic II (NT5C2), mRNA PE=2 SV=1	0.94	0.17
Q4LE43	Phosphoinositide phospholipase C (Fragment) GN=PLCG1 variant protein PE=2 SV=1	1.27	0.27
Q9HCD5	Nuclear receptor coactivator 5 GN=NCOA5 PE=1 SV=2	1.12	0.23
O14776	Transcription elongation regulator 1 GN=TCERG1 PE=1 SV=2	2.19	0.35
P21912	Succinate dehydrogenase [ubiquinone] iron-sulfur subunit, mitochondrial GN=SDHB PE=1 SV=3	1.38	0.39
Q6NUR1	Non-SMC condensin I complex, subunit G GN=NCAPG PE=2 SV=1	1.37	0.71
Q14683	Structural maintenance of chromosomes protein 1A GN=SMC1A PE=1 SV=2	1.65	0.24
Q9P287	BRCA2 and CDKN1A-interacting protein GN=BCCIP PE=1 SV=1	2.54	0.43
P02458	Collagen alpha-1(II) chain GN=COL2A1 PE=1 SV=3	1.57	0.35
B2RD27	cDNA, FLJ96428, highly similar to Homo sapiens proteasome (prosome, macropain) 26S subunit, non-ATPase, 7 (Mov34 homolog) (PSMD7), mRNA PE=2 SV=1	1.16	0.20
Q5SSJ5	Heterochromatin protein 1-binding protein 3 GN=HP1BP3 PE=1 SV=1	3.42	0.25
A5PLM5	Exosome component 9 GN=EXOSC9 PE=2 SV=1	3.09	0.30
P62249	40S ribosomal protein S16 GN=RPS16 PE=1 SV=2	1.63	0.44
Q8WXF1	Paraspeckle component 1 GN=PSPC1 PE=1 SV=1	2.42	0.36
Q9Y230	RuvB-like 2 GN=RUVBL2 PE=1 SV=3	0.73	0.12
P04792	Heat shock protein beta-1 GN=HSPB1 PE=1 SV=2	1.02	0.35
A0A087X020	Ribosome maturation protein SBDS GN=SBDS PE=1 SV=1	0.94	0.18
Q96A33	Coiled-coil domain-containing protein 47 GN=CCDC47 PE=1 SV=1	2.40	0.40
A0A1L7NY41	Polypeptide N-acetylgalactosaminyltransferase GN=GALNT2 PE=2 SV=1	2.26	0.42
B7Z6F7	cDNA FLJ61705, highly similar to Symplekin PE=2 SV=1	0.49	0.21
A0A0A0MSS8	Aldo-keto reductase family 1 member C3 GN=AKR1C3 PE=1 SV=1	1.64	0.29
O14617	AP-3 complex subunit delta-1 GN=AP3D1 PE=1 SV=1	1.55	0.39
Q59GR1	Niemann-Pick disease, type C1 variant (Fragment) PE=4 SV=1	0.15	0.03
A0A0D9SF53	ATP-dependent RNA helicase DDX3X GN=DDX3X PE=1 SV=1	2.11	0.47
P29590	Protein PML GN=PML PE=1 SV=3	2.28	0.29
P52272	Heterogeneous nuclear ribonucleoprotein M GN=HNRNPM PE=1 SV=3	1.17	0.26
A0A024RA49	Anillin, actin binding protein (Scraps homolog, Drosophila), isoform CRA_e GN=ANLN PE=4 SV=1	1.56	0.27
A0A024RD15	Mitogen-activated protein kinase GN=MAPK14 PE=4 SV=1	2.28	0.38
P27487	Dipeptidyl peptidase 4 GN=DPP4 PE=1 SV=2	1.25	0.35
A8K683	cDNA FLJ75708, highly similar to Homo sapiens N-myc (and STAT) interactor (NMI), mRNA PE=2 SV=1	1.67	0.43
Q9BTE3	Mini-chromosome maintenance complex-binding protein GN=MCMBP PE=1 SV=2	2.73	0.29
P30530	Tyrosine-protein kinase receptor UFO GN=AXL PE=1 SV=4	1.60	0.18

H0UIC7	C-C motif chemokine GN=CCL8 PE=3 SV=1	2.22	0.77
Q9H832	Ubiquitin-conjugating enzyme E2 Z GN=UBE2Z PE=1 SV=2	1.75	0.22
A0A024R9J4	Nephroblastoma overexpressed gene, isoform CRA_a GN=NOV PE=4 SV=1	4.01	0.72
P22059	Oxysterol-binding protein 1 GN=OSBP PE=1 SV=1	0.57	0.17
P27708	CAD protein GN=CAD PE=1 SV=3	0.02	-0.01
Q07812	Apoptosis regulator BAX GN=BAX PE=1 SV=1	1.41	-0.34
O60462	Neuropilin-2 GN=NRP2 PE=1 SV=3	2.93	0.25
A0A1W2PNX8	Protein unc-45 homolog A GN=UNC45A PE=1 SV=1	2.00	0.35
F5H8L0	Rab GTPase-activating protein 1-like GN=RABGAP1L PE=1 SV=1	1.31	0.17
A0A024RAS8	Heme binding protein 1, isoform CRA_a GN=HEBP1 PE=4 SV=1	0.54	0.18
B2RB57	cDNA, FLJ95321, highly similar to Homo sapiens ATG7 autophagy related 7 homolog (S. cerevisiae) (ATG7), mRNA PE=2 SV=1	1.92	0.50
Q9Y2S6	Translation machinery-associated protein 7 GN=TMA7 PE=1 SV=1	0.66	0.11
A4D2J0	SNARE protein Ykt6, isoform CRA_a GN=YKT6 PE=1 SV=1	0.70	0.14
Q92917	G-patch domain and KOW motifs-containing protein GN=GPKOW PE=1 SV=2	0.01	0.00
Q4KWH8	1-phosphatidylinositol 4,5-bisphosphate phosphodiesterase eta-1 GN=PLCH1 PE=1 SV=1	1.60	0.22
A0A1S5UZH5	Mitochondrial thioredoxin GN=TXN PE=2 SV=1	0.66	-0.39
X6RAL5	Histone deacetylase complex subunit SAP18 GN=SAP18 PE=1 SV=1	2.25	0.34
B9EG90	Topoisomerase (DNA) I GN=TOP1 PE=2 SV=1	2.97	0.25
Q8NCN5	Pyruvate dehydrogenase phosphatase regulatory subunit, mitochondrial GN=PDPR PE=1 SV=2	1.37	0.38
P34896	Serine hydroxymethyltransferase, cytosolic GN=SHMT1 PE=1 SV=1	2.42	0.51
A0A024R4R3	CCR4-NOT transcription complex, subunit 3, isoform CRA_a GN=CNOT3 PE=4 SV=1	0.30	0.15
P40222	Alpha-taxilin GN=TXLNA PE=1 SV=3	1.59	0.18
Q09161	Nuclear cap-binding protein subunit 1 GN=NCBP1 PE=1 SV=1	1.52	0.26
P78539	Sushi repeat-containing protein SRPX GN=SRPX PE=1 SV=1	2.69	0.21
Q9NYV4	Cyclin-dependent kinase 12 GN=CDK12 PE=1 SV=2	0.48	-0.26
Q9UBG0	C-type mannose receptor 2 GN=MRC2 PE=1 SV=2	0.62	0.09
B3KP83	cDNA FLJ31382 fis, clone NHNPC2000187, highly similar to Docking protein 1 (Downstream of tyrosine kinase 1) PE=2 SV=1	2.03	0.43
A8K946	mRNA cap guanine-N7 methyltransferase PE=2 SV=1	0.62	0.04
B4DUT8	Calponin GN=CNN2 PE=1 SV=1	1.60	0.22
Q99700	Ataxin-2 GN=ATXN2 PE=1 SV=2	0.16	-0.02
P05204	Non-histone chromosomal protein HMG-17 GN=HMGN2 PE=1 SV=3	1.91	0.27
P50570	Dynamin-2 GN=DNM2 PE=1 SV=2	2.63	0.24
Q86V48	Leucine zipper protein 1 GN=LUZP1 PE=1 SV=2	0.43	0.10
A8K5K0	cDNA FLJ78309, highly similar to Homo sapiens heterogeneous nuclear ribonucleoprotein U-like 1 (HNRPUL1), transcript variant 1, mRNA PE=2 SV=1	1.61	0.22
A0A024R5K1	Coronin GN=CORO1B PE=3 SV=1	0.10	-0.02
A0A087WT44	Heme oxygenase 2 GN=HMOX2 PE=1 SV=1	1.80	0.32
B4E1C2	Kininogen 1, isoform CRA_b GN=KNG1 PE=2 SV=1	1.17	-0.63
A8K401	Prohibitin, isoform CRA_a GN=PHB PE=2 SV=1	2.11	0.35
A6NEM2	Host cell factor 1 GN=HCFC1 PE=1 SV=2	4.27	0.32
Q7Z3D7	Uncharacterized protein DKFZp686E2459 GN=DKFZp686E2459 PE=2 SV=1	0.40	0.06
A0A024R2W4	Dystroglycan 1 (Dystrophin-associated glycoprotein 1), isoform CRA_a GN=DAG1 PE=4 SV=1	0.88	-0.54
Q96PD2	Discoidin, CUB and LCCL domain-containing protein 2 GN=DCBLD2 PE=1 SV=1	0.47	0.08
Q9Y3Z3	Deoxynucleoside triphosphate triphosphohydrolase SAMHD1 GN=SAMHD1 PE=1 SV=2	1.97	0.69
Q6U8A4	Ubiquitin-specific protease 7 isoform (Fragment) PE=2 SV=1	0.61	0.23
O00228	Phosphoglycerate mutase (Fragment) PE=3 SV=1	1.20	0.68
P50238	Cysteine-rich protein 1 GN=CRIP1 PE=1 SV=3	1.47	0.17
A0A024RAW9	WW domain binding protein 11, isoform CRA_a GN=WBP11 PE=4 SV=1	1.36	0.27
Q15043	Zinc transporter ZIP14 GN=SLC39A14 PE=1 SV=3	1.09	0.20
A0A024RBF6	HCG26523, isoform CRA_a GN=hCG_26523 PE=4 SV=1	1.37	0.27
Q86X55	Histone-arginine methyltransferase CARM1 GN=CARM1 PE=1 SV=3	0.76	0.20
A8K3M3	Tyrosine-protein phosphatase non-receptor type GN=PTPN1 PE=2 SV=1	0.80	0.20
A0A024R5H0	Barrier to autointegration factor 1, isoform CRA_a GN=BANF1 PE=4 SV=1	2.78	0.30

O14562	Ubiquitin domain-containing protein UBFD1 GN=UBFD1 PE=1 SV=2	1.12	0.07
O95782	AP-2 complex subunit alpha-1 GN=AP2A1 PE=1 SV=3	0.97	0.14
A0A0S2Z3W7	Nucleotide diphosphatase (Fragment) GN=ITPA PE=2 SV=1	1.02	0.17
P33947	ER lumen protein-retaining receptor 2 GN=KDELR2 PE=1 SV=1	1.68	0.51
O95989	Diphosphoinositol polyphosphate phosphohydrolase 1 GN=NUDT3 PE=1 SV=1	0.16	0.08
Q9BX97	Plasmalemma vesicle-associated protein GN=PLVAP PE=2 SV=1	2.11	0.25
B4DPZ4	cDNA FLJ60782, highly similar to Rho-GTPase-activating protein 1 PE=2 SV=1	1.43	0.36
L8EC95	Alternative protein MMP1 GN=MMP1 PE=4 SV=1	2.26	0.37
O14672	Disintegrin and metalloproteinase domain-containing protein 10 GN=ADAM10 PE=1 SV=1	1.25	0.13
Q2TB10	Zinc finger protein 800 GN=ZNF800 PE=1 SV=1	0.60	0.15
A0A2P9ARY3	Membrane protein GN=BQ8482_380103 PE=4 SV=1	1.11	0.16
P61927	60S ribosomal protein L37 GN=RPL37 PE=1 SV=2	1.01	0.22
A0A0A6YYJ8	Putative RNA-binding protein Luc7-like 2 GN=LUC7L2 PE=4 SV=1	0.57	0.24
A0A2P9AM56	Dihydrodipicolinate synthetase GN=BQ8482_250079 PE=3 SV=1	1.63	0.35
A0A2P9ASH7	Uncharacterized protein GN=BQ8482_380309 PE=4 SV=1	2.01	0.31
Q9H8Y8	Golgi reassembly-stacking protein 2 GN=GORASP2 PE=1 SV=3	2.55	0.30
A8KAN3	Non-specific serine/threonine protein kinase PE=2 SV=1	4.27	1.86
P35611	Alpha-adducin GN=ADD1 PE=1 SV=2	0.85	-0.15
A8K521	DNA helicase PE=2 SV=1	1.04	0.18
Q13177	Serine/threonine-protein kinase PAK 2 GN=PAK2 PE=1 SV=3	1.30	0.14
A0A024QZY1	JTV1 gene, isoform CRA_a GN=JTV1 PE=4 SV=1	1.91	0.29
Q8WW59	SPRY domain-containing protein 4 GN=SPRYD4 PE=1 SV=2	1.94	0.41
J3KQJ1	Inactive C-alpha-formylglycine-generating enzyme 2 GN=SUMF2 PE=1 SV=1	1.68	0.33
B2RDD7	Protein arginine N-methyltransferase 5 PE=2 SV=1	1.59	0.41
P50479	PDZ and LIM domain protein 4 GN=PDLIM4 PE=1 SV=2	0.18	-0.03
A0A024R883	V-type proton ATPase subunit G GN=ATP6V1G1 PE=3 SV=1	2.82	0.39
Q86XI8	Uncharacterized protein ZSWIM9 GN=ZSWIM9 PE=1 SV=2	1.05	0.26
Q15102	Platelet-activating factor acetylhydrolase IB subunit gamma GN=PAFAH1B3 PE=1 SV=1	1.50	0.30
Q5BKZ1	DBIRD complex subunit ZNF326 GN=ZNF326 PE=1 SV=2	1.10	0.20
P62877	E3 ubiquitin-protein ligase RBX1 GN=RBX1 PE=1 SV=1	2.60	0.26
B7Z7F0	cDNA FLJ56420, highly similar to Aspartyl aminopeptidase PE=2 SV=1	1.72	0.24
Q53F55	Deoxythymidylate kinase (Thymidylate kinase) variant (Fragment) PE=2 SV=1	2.94	0.33
A0A024R0Z3	DEAD (Asp-Glu-Ala-Asp) box polypeptide 23, isoform CRA_b GN=DDX23 PE=4 SV=1	1.59	0.41
Q59HH3	Trifunctional purine biosynthetic protein adenosine-3 (Fragment) PE=2 SV=1	1.00	0.26
A8K3Y5	cDNA FLJ78186 PE=2 SV=1	1.42	0.30
I1E4Y6	GRB10-interacting GYF protein 2 GN=GIGYF2 PE=1 SV=1	0.35	0.11
A8K6A8	cDNA FLJ76304, highly similar to Homo sapiens ADAM metallopeptidase with thrombospondin type 1 motif, 4 (ADAMTS4), mRNA PE=2 SV=1	1.28	-0.26
B3KRW4	cDNA FLJ34980 fis, clone OCBBF2000522, highly similar to Rab GTPase-binding effector protein 2 PE=2 SV=1	0.38	0.09
B2RNR6	Zinc finger RNA binding protein GN=ZFR PE=2 SV=1	0.84	0.16
Q52LJ0	Protein FAM98B GN=FAM98B PE=1 SV=1	1.50	0.28
B3KQ07	Zinc finger protein 575, isoform CRA_b GN=ZNF575 PE=1 SV=1	0.97	0.17
B1AKZ4	Phosphoprotein enriched in astrocytes 15, isoform CRA_a GN=PEA15 PE=2 SV=1	0.36	0.09
Q7LBR1	Charged multivesicular body protein 1b GN=CHMP1B PE=1 SV=1	0.86	0.13
P51570	Galactokinase GN=GALK1 PE=1 SV=1	0.30	0.08
Q6IPI1	60S ribosomal protein L29 GN=RPL29 PE=2 SV=1	0.09	-0.02
Q9Y333	U6 snRNA-associated Sm-like protein LSm2 GN=LSM2 PE=1 SV=1	0.91	-0.14
Q9NU22	Midasin GN=MDN1 PE=1 SV=2	4.15	0.51
P40306	Proteasome subunit beta type-10 GN=PSMB10 PE=1 SV=1	0.78	-0.32
Q7Z3R0	Uncharacterized protein DKFZp686M03114 GN=DKFZp686M03114 PE=2 SV=1	0.80	0.09
Q9NUJ1	Mycophenolic acid acyl-glucuronide esterase, mitochondrial GN=ABHD10 PE=1 SV=1	2.77	0.32
B2RDI5	cDNA, FLJ96627, highly similar to Homo sapiens calpain 1, (mu/I) large subunit (CAPN1), mRNA PE=2 SV=1	0.53	0.12
Q01814	Plasma membrane calcium-transporting ATPase 2 GN=ATP2B2 PE=1 SV=2	1.13	-0.20
P27701	CD82 antigen GN=CD82 PE=1 SV=1	0.32	0.11

O60925	Prefoldin subunit 1 GN=PFDN1 PE=1 SV=2	1.59	0.16
O94888	UBX domain-containing protein 7 GN=UBXN7 PE=1 SV=2	0.57	-0.17
B2R791	cDNA, FLJ93335, highly similar to Homo sapiens PRP3 pre-mRNA processing factor 3 homolog (yeast) (PRPF3), mRNA PE=2 SV=1	2.37	0.50
O00159	Unconventional myosin-Ic GN=MYO1C PE=1 SV=4	1.25	0.30
A0A024R3C2	Uncharacterized protein GN=LOC57149 PE=3 SV=1	1.40	0.20
X5CMJ9	Proteasome subunit beta type GN=PSM8 PE=3 SV=1	1.18	0.26
A0A024R1U8	Insulin-like growth factor binding protein 4, isoform CRA_a GN=IGFBP4 PE=4 SV=1	2.81	0.44
P78318	Immunoglobulin-binding protein 1 GN=IGBP1 PE=1 SV=1	1.09	-0.09
Q96FJ2	Dynein light chain 2, cytoplasmic GN=DYNLL2 PE=1 SV=1	1.11	0.17
B2R5S9	cDNA, FLJ92604, highly similar to Homo sapiens paraneoplastic antigen MA3 (PNMA3), mRNA PE=2 SV=1	1.53	0.26
B4DM05	cDNA FLJ51241, highly similar to Nidogen-1 PE=2 SV=1	0.53	0.11
Q8TCS8	Polyribonucleotide nucleotidyltransferase 1, mitochondrial GN=PNPT1 PE=1 SV=2	0.82	0.13
A0A0A0MSG2	Four and a half LIM domains protein 2 GN=FHL2 PE=1 SV=1	1.17	0.39
Q9NRF9	DNA polymerase epsilon subunit 3 GN=POLE3 PE=1 SV=1	2.51	0.23
A0A2R8Y5Y7	60S ribosomal protein L9 GN=RPL9 PE=1 SV=1	1.65	0.43
Q9BUL8	Programmed cell death protein 10 GN=PDCD10 PE=1 SV=1	1.11	-0.16
A0A024R4Y2	HCG39762, isoform CRA_c GN=hCG_39762 PE=4 SV=1	0.28	0.07
A0A2P9ATI5	Uncharacterized protein GN=BQ8482_430018 PE=4 SV=1	1.00	0.22
F8VW96	Cysteine and glycine-rich protein 2 GN=CSRP2 PE=1 SV=1	0.42	0.10
A0A090N8P3	Peptidylprolyl isomerase GN=FKBP9 PE=4 SV=1	0.13	-0.03
Q96BP3	Peptidylprolyl isomerase domain and WD repeat-containing protein 1 GN=PPWD1 PE=1 SV=1	0.49	0.15
A0A0F7KYT8	Fragile X mental retardation autosomal homolog variant p2K GN=FXR1 PE=2 SV=1	1.48	0.36
A8K2X4	cDNA FLJ75401, highly similar to Homo sapiens endoglin (Osler-Rendu-Weber syndrome 1), mRNA PE=2 SV=1	0.60	0.20
Q9H8Y1	Vertnin GN=VRTN PE=1 SV=1	1.87	-0.93
J3KNQ4	Alpha-parvin GN=PARVA PE=1 SV=1	0.60	0.15
Q9BTL3	RNMT-activating mRNA cap methyltransferase subunit GN=RAMMET PE=1 SV=1	0.41	-0.11
Q00889	Pregnancy-specific beta-1-glycoprotein 6 GN=PSG6 PE=2 SV=1	0.53	0.13
Q4VCS5	Angiomotin GN=AMOT PE=1 SV=1	1.58	-0.61
H7BY58	Protein-L-isoaspartate O-methyltransferase GN=PCMT1 PE=1 SV=1	1.50	0.27
Q13206	Probable ATP-dependent RNA helicase DDX10 GN=DDX10 PE=1 SV=2	1.68	0.13
Q15276	Rab GTPase-binding effector protein 1 GN=RABEP1 PE=1 SV=2	1.13	0.29
A0A024R5Z5	Transcription initiation factor IIA subunit 2 GN=GTF2A2 PE=3 SV=1	2.25	0.14
B4DJM8	cDNA FLJ56534, highly similar to Protocadherin beta 13 PE=2 SV=1	1.05	0.22
Q93034	Cullin-5 GN=CUL5 PE=1 SV=4	2.20	0.27
Q9NXV6	CDKN2A-interacting protein GN=CDKN2AIP PE=1 SV=3	0.35	-0.03
A0A0S2Z410	Hydroxysteroid dehydrogenase 10 isoform 1 (Fragment) GN=HSD17B10 PE=2 SV=1	2.17	0.38
B2R9Y2	cDNA, FLJ94609 PE=2 SV=1	0.71	0.26
A0A2R8Y4V0	ATP-binding cassette sub-family C member 8 GN=ABCC8 PE=1 SV=1	1.46	0.35
B4DTK7	cDNA FLJ61387, highly similar to Homo sapiens conserved nuclear protein NHN1 (NHN1), mRNA PE=2 SV=1	0.16	0.02
A0A0C4DFN3	Monoglyceride lipase GN=MGLL PE=1 SV=1	1.51	0.21
A8K940	cDNA FLJ77630, highly similar to Homo sapiens BPY2 interacting protein 1, mRNA PE=1 SV=1	1.26	0.20
O75113	NEDD4-binding protein 1 GN=N4BP1 PE=1 SV=4	0.38	-0.13
F8WES2	S-methyl-5'-thioadenosine phosphorylase GN=MTAP PE=4 SV=1	1.21	0.20
Q96JB5	CDK5 regulatory subunit-associated protein 3 GN=CDK5RAP3 PE=1 SV=2	1.57	0.35
Q86WR0	Coiled-coil domain-containing protein 25 GN=CCDC25 PE=1 SV=2	1.88	0.31
A4D218	MAD1 mitotic arrest deficient-like 1 (Yeast) GN=MAD1L1 PE=4 SV=1	1.32	-0.57
A0A2P9AXN1	FAD-dependent pyridine nucleotide-disulphide oxidoreductase GN=BQ8482_90305 PE=4 SV=1	1.97	0.24
K7ELC2	40S ribosomal protein S15 GN=RPS15 PE=1 SV=1	1.33	0.60
Q8WUA2	Peptidyl-prolyl cis-trans isomerase-like 4 GN=PPIL4 PE=1 SV=1	1.26	0.29
A0A087WYC6	Dynein heavy chain 11, axonemal GN=DNAH11 PE=1 SV=1	1.20	-0.72

Q96CT7	Coiled-coil domain-containing protein 124 GN=CCDC124 PE=1 SV=1	1.81	0.30
Q8TEW0	Partitioning defective 3 homolog GN=PARD3 PE=1 SV=2	1.37	0.13
A0A024R7N7	Interferon, gamma-inducible protein 30, isoform CRA_b GN=IFI30 PE=4 SV=1	2.47	0.55
A6NGQ3	Obscurin GN=OBSCN PE=1 SV=5	0.66	0.08
A0A2P9AV54	Uncharacterized oxidoreductase Sfri_1503 GN=BQ8482_60029 PE=4 SV=1	1.73	0.17
B0I1S0	DYNC2H1 variant protein PE=2 SV=1	0.76	0.19
Q8NFC6	Biorientation of chromosomes in cell division protein 1-like 1 GN=BOD1L1 PE=1 SV=2	0.40	-0.14
P49247	Ribose-5-phosphate isomerase GN=RPIA PE=1 SV=3	3.14	0.35
A0A0C4ZLW1	CDK5RAP2 protein GN=CDK5RAP2 PE=2 SV=1	0.25	-0.06
Q13601	KRR1 small subunit processome component homolog GN=KRR1 PE=1 SV=4	0.48	0.12
A0A1U9X836	NEU1 PE=4 SV=1	0.73	0.12
P19623	Spermidine synthase GN=SRM PE=1 SV=1	1.19	0.33
Q6PIF6	Unconventional myosin-VIIb GN=MYO7B PE=1 SV=2	1.97	0.28
P42695	Condensin-2 complex subunit D3 GN=NCAPD3 PE=1 SV=2	2.24	0.48
P14854	Cytochrome c oxidase subunit 6B1 GN=COX6B1 PE=1 SV=2	0.65	0.11
A0A0J9YWP7	PRAME family member 18 GN=PRAMEF18 PE=4 SV=1	1.61	0.34
K7EQ73	DnaJ homolog subfamily C member 7 (Fragment) GN=DNAJC7 PE=1 SV=1	1.11	0.19
Q7Z6J2	General receptor for phosphoinositides 1-associated scaffold protein GN=GRASP PE=1 SV=1	1.64	0.23
B3KME2	cDNA FLJ10772 fis, clone NT2RP4000243, highly similar to Cartilage-associated protein PE=2 SV=1	0.59	0.13
Q4L180	Filamin A-interacting protein 1-like GN=FILIP1L PE=1 SV=2	0.71	0.14
Q2M2E5	Uncharacterized protein C5orf64 GN=C5orf64 PE=2 SV=2	2.18	0.11
F5H5T7	Probable C-mannosyltransferase DPY19L2 (Fragment) GN=DPY19L2 PE=4 SV=8	0.53	0.15
P98160	Basement membrane-specific heparan sulfate proteoglycan core protein GN=HSPG2 PE=1 SV=4	0.15	0.04
Q6ZMY3	SPOC domain-containing protein 1 GN=SPOCD1 PE=2 SV=1	0.91	0.28
B3KNF9	cDNA FLJ14522 fis, clone NT2RM1000883, highly similar to Homo sapiens nischarin (NISCH), mRNA PE=2 SV=1	1.10	0.17
Q15643	Thyroid receptor-interacting protein 11 GN=TRIP11 PE=1 SV=3	1.19	-0.60
P18583	Protein SON GN=SON PE=1 SV=4	1.83	0.33
Q5T4S7	E3 ubiquitin-protein ligase UBR4 GN=UBR4 PE=1 SV=1	2.87	0.37
B3KR97	cDNA FLJ33900 fis, clone CTONG2008262, highly similar to Low density lipoprotein receptor adapter protein 1 PE=2 SV=1	1.44	0.26
O95425	Supervillin GN=SVIL PE=1 SV=2	1.28	0.52
A2RUR9	Coiled-coil domain-containing protein 144A GN=CCDC144A PE=2 SV=1	1.10	0.15
Q8NHY5	Checkpoint protein HUS1B GN=HUS1B PE=1 SV=2	3.18	0.30
Q63ZY3	KN motif and ankyrin repeat domain-containing protein 2 GN=KANK2 PE=1 SV=1	2.11	0.31
B2R6F3	Splicing factor arginine/serine-rich 3 GN=SFRS3 PE=2 SV=1	1.71	0.42
A0A2P9AQ24	Uncharacterized protein GN=BQ8482_340170 PE=4 SV=1	1.46	0.37
B3KPA5	cDNA FLJ31518 fis, clone NT2RI2000064 PE=2 SV=1	2.81	0.30
Q9H306	Matrix metalloproteinase-27 GN=MMP27 PE=1 SV=2	1.01	0.44
A4D1W8	Ependymin related protein 1 (Zebrafish), isoform CRA_b GN=UCC1 PE=4 SV=1	0.13	0.04
Q9NTX5	Ethylmalonyl-CoA decarboxylase GN=ECHDC1 PE=1 SV=2	1.66	0.30
A0A024R231	Guanine deaminase, isoform CRA_b GN=GDA PE=4 SV=1	1.29	0.25
B3KVD6	cDNA FLJ16433 fis, clone BRACE3013936, highly similar to Cell death activator CIDE-B PE=2 SV=1	2.11	0.38
O94788	Retinal dehydrogenase 2 GN=ALDH1A2 PE=1 SV=3	0.54	0.09
A0A2P9AX55	Uncharacterized protein GN=BQ8482_90076 PE=4 SV=1	0.24	-0.09
A0A0S2Z5J4	Adaptor-related protein complex 3 beta 1 subunit isoform 1 (Fragment) GN=AP3B1 PE=2 SV=1	1.58	0.37
Q9NVN8	Guanine nucleotide-binding protein-like 3-like protein GN=GNL3L PE=1 SV=1	1.26	-0.66
A0A2P9ATT1	Uncharacterized protein GN=BQ8482_480060 PE=4 SV=1	1.59	0.25
B4DNE1	cDNA FLJ52708, highly similar to Basigin PE=2 SV=1	0.19	0.03
Q69YJ7	Uncharacterized protein DKFZp667H197 (Fragment) GN=DKFZp667H197 PE=2 SV=1	4.22	0.30
A0AVI9	WD repeat domain 78 GN=WDR78 PE=2 SV=1	1.06	0.22
A0A087X256	WASH complex subunit 4 GN=WASHC4 PE=1 SV=1	2.03	-0.63

Q8N122	Regulatory-associated protein of mTOR GN=RPTOR PE=1 SV=1	2.21	0.41
A0A2R8Y553	Mitochondrial glycine transporter GN=SLC25A38 PE=1 SV=1	0.92	0.18

Appendix 6

Downregulated 1049 proteins in BEAM treated hypoxia vs normoxia samples GN=Gene Name, PE=Protein Existence which is the numerical value describing the evidence for the existence of the protein, SV=Sequence Version which is the version number of the sequence.

Accession	Description	-log *p*	Diff.
A0A024R1N1	Myosin, heavy polypeptide 9, non-muscle, isoform CRA_a GN=MYH9 PE=3 SV=1	2.26	2.26
P21333	Filamin-A GN=FLNA PE=1 SV=4	1.57	1.57
Q15149	Plectin GN=PLEC PE=1 SV=3	1.83	1.83
J3QSU6	Tenascin GN=TNC PE=1 SV=1	2.68	2.68
P13639	Elongation factor 2 GN=EEF2 PE=1 SV=4	2.97	2.97
K9JA46	Epididymis luminal secretory protein 52 GN=EL52 PE=2 SV=1	1.88	1.88
V9HW22	Epididymis luminal protein 33 GN=HEL-S-72p PE=2 SV=1	2.44	2.44
A0A087WVQ6	Clathrin heavy chain GN=CLTC PE=1 SV=1	2.25	2.25
A0A1S5UZ07	Talin-1 GN=TLN1 PE=2 SV=1	1.79	1.79
V9HWB8	Pyruvate kinase GN=HEL-S-30 PE=1 SV=1	1.61	1.61
P06733	Alpha-enolase GN=ENO1 PE=1 SV=2	3.29	3.29
P34932	Heat shock 70 kDa protein 4 GN=HSPA4 PE=1 SV=4	2.33	2.33
A0A024R5Z9	Pyruvate kinase GN=PKM2 PE=3 SV=1	2.33	2.33
A0A024R3X4	Heat shock 60kDa protein 1 (Chaperonin), isoform CRA_a GN=HSPD1 PE=2 SV=1	2.36	2.36
P07996	Thrombospondin-1 GN=THBS1 PE=1 SV=2	3.03	3.03
P02545	Prelamin-A/C GN=LMNA PE=1 SV=1	2.02	2.02
A0A0S2Z3H5	Collagen type I alpha 2 isoform 1 (Fragment) GN=COL1A2 PE=2 SV=1	5.38	5.38
B4DN15	cDNA FLJ55228, highly similar to Interstitial collagenase PE=2 SV=1	1.96	1.96
P43490	Nicotinamide phosphoribosyltransferase GN=NAMPT PE=1 SV=1	2.57	2.57
P04406	Glyceraldehyde-3-phosphate dehydrogenase GN=GAPDH PE=1 SV=3	1.89	1.89
P26038	Moesin GN=MSN PE=1 SV=3	2.49	2.49
A0A024RC65	HCG1991735, isoform CRA_a GN=hCG_1991735 PE=4 SV=1	2.40	2.40
P22314	Ubiquitin-like modifier-activating enzyme 1 GN=UBA1 PE=1 SV=3	2.51	2.51
P29401	Transketolase GN=TKT PE=1 SV=3	4.30	4.30
P05120	Plasminogen activator inhibitor 2 GN=SERPINB2 PE=1 SV=2	2.07	2.07
B2RBR9	cDNA, FLJ95650, highly similar to Homo sapiens karyopherin (importin) beta 1 (KPNB1), mRNA PE=2 SV=1	2.57	2.57
P02452	Collagen alpha-1(I) chain GN=COL1A1 PE=1 SV=5	4.56	4.56
B2RDE8	cDNA, FLJ96580, highly similar to Homo sapiens hepatoma-derived growth factor (high-mobility group protein 1-like) (HDGF), mRNA PE=2 SV=1	3.42	3.42
P68032	Actin, alpha cardiac muscle 1 GN=ACTC1 PE=1 SV=1	1.64	1.64
D3DPU2	Adenylyl cyclase-associated protein GN=CAP1 PE=2 SV=1	1.83	1.83
A0A024RDY0	RAN binding protein 5, isoform CRA_d GN=RANBP5 PE=4 SV=1	2.11	2.11
P31946	14-3-3 protein beta/alpha GN=YWHAB PE=1 SV=3	2.18	2.18
A7BI36	p180/ribosome receptor GN=RRBP1 PE=2 SV=2	2.38	2.38
P55060	Exportin-2 GN=CSE1L PE=1 SV=3	2.65	2.65
A0A0G2JIW1	Heat shock 70 kDa protein 1B GN=HSPA1B PE=1 SV=1	2.63	2.63
V9HW88	Calreticulin, isoform CRA_b GN=HEL-S-99n PE=2 SV=1	1.89	1.89
A0A024R6R4	Matrix metallopeptidase 2 (Gelatinase A, 72kDa gelatinase, 72kDa type IV collagenase), isoform CRA_a GN=MMP2 PE=3 SV=1	3.90	3.90
Q59E93	Aminopeptidase (Fragment) PE=2 SV=1	1.46	1.46
A0A024R4A0	Nucleolin, isoform CRA_b GN=NCL PE=4 SV=1	2.06	2.06
P07195	L-lactate dehydrogenase B chain GN=LDHB PE=1 SV=2	3.58	3.58
Q14766	Latent-transforming growth factor beta-binding protein 1 GN=LTBP1 PE=1 SV=4	4.40	4.40
P38646	Stress-70 protein, mitochondrial GN=HSPA9 PE=1 SV=2	3.14	3.14
E7EVA0	Microtubule-associated protein GN=MAP4 PE=1 SV=1	2.62	2.62
Q53G85	Elongation factor 1-alpha (Fragment) PE=2 SV=1	2.38	2.38
P13797	Plastin-3 GN=PLS3 PE=1 SV=4	2.34	2.34
Q59ER5	WD repeat-containing protein 1 isoform 1 variant (Fragment) PE=2 SV=1	2.20	2.20
P08254	Stromelysin-1 GN=MMP3 PE=1 SV=2	3.07	3.07

F4ZW66	NF110b PE=2 SV=1	2.40	2.40
A0A2R8Y5S7	Radixin GN=RDX PE=1 SV=1	2.14	2.14
V9HVZ7	Epididymis luminal protein 176 GN=HEL-176 PE=2 SV=1	2.84	2.84
B4DLV7	Rab GDP dissociation inhibitor PE=2 SV=1	2.38	2.38
V9HVY3	Protein disulfide-isomerase GN=HEL-S-269 PE=2 SV=1	2.24	2.24
E7EQR4	Ezrin GN=EZR PE=1 SV=3	2.16	2.16
B4DNA3	Adenylyl cyclase-associated protein PE=2 SV=1	2.07	2.07
P07602	Prosaposin GN=PSAP PE=1 SV=2	2.00	2.00
E9PK25	Cofilin-1 GN=CFL1 PE=1 SV=1	2.88	2.88
P52209	6-phosphogluconate dehydrogenase, decarboxylating GN=PGD PE=1 SV=3	4.15	4.15
A0A0S2Z3X8	Rab GDP dissociation inhibitor (Fragment) GN=GDI1 PE=2 SV=1	3.59	3.59
Q14204	Cytoplasmic dynein 1 heavy chain 1 GN=DYNC1H1 PE=1 SV=5	1.65	1.65
P27348	14-3-3 protein theta GN=YWHAQ PE=1 SV=1	3.18	3.18
V9HW31	ATP synthase subunit beta GN=HEL-S-271 PE=1 SV=1	1.91	1.91
V9HW96	Chaperonin containing TCP1, subunit 2 (Beta), isoform CRA_b GN=HEL-S-100n PE=1 SV=1	1.72	1.72
Q9UKY7	Protein CDV3 homolog GN=CDV3 PE=1 SV=1	2.28	2.28
A0A024R4K3	Malate dehydrogenase GN=MDH2 PE=2 SV=1	3.95	3.95
P49327	Fatty acid synthase GN=FASN PE=1 SV=3	3.33	3.33
B5BUB5	Autoantigen La (Fragment) GN=SSB PE=2 SV=1	2.68	2.68
P35442	Thrombospondin-2 GN=THBS2 PE=1 SV=2	1.65	1.65
P37802	Transgelin-2 GN=TAGLN2 PE=1 SV=3	2.30	2.30
B4DJ30	cDNA FLJ61290, highly similar to Neutral alpha-glucosidase AB PE=2 SV=1	1.75	1.75
A0A024R498	Serpin peptidase inhibitor, clade E (Nexin, plasminogen activator inhibitor type 1), member 2, isoform CRA_b GN=SERPINE2 PE=3 SV=1	4.38	4.38
B2R983	cDNA, FLJ94267, highly similar to Homo sapiens glutathione S-transferase omega 1 (GSTO1), mRNA PE=2 SV=1	2.98	2.98
P50990	T-complex protein 1 subunit theta GN=CCT8 PE=1 SV=4	1.80	1.80
P26641	Elongation factor 1-gamma GN=EEF1G PE=1 SV=3	1.84	1.84
P28838	Cytosol aminopeptidase GN=LAP3 PE=1 SV=3	3.31	3.31
V9HW37	Epididymis secretory protein Li 69 GN=HEL-S-69 PE=1 SV=1	1.80	1.80
V9HW74	Ubiquitin carboxyl-terminal hydrolase GN=HEL-117 PE=2 SV=1	2.36	2.36
Q16658	Fascin GN=FSCN1 PE=1 SV=3	2.40	2.40
P20700	Lamin-B1 GN=LMNB1 PE=1 SV=2	2.04	2.04
A0A090N8Y2	Protein disulfide-isomerase A4 GN=ERP70 PE=2 SV=1	1.44	1.44
A0A024R6W0	Aspartate aminotransferase GN=GOT2 PE=4 SV=1	3.75	3.75
P52907	F-actin-capping protein subunit alpha-1 GN=CAPZA1 PE=1 SV=3	2.38	2.38
O00299	Chloride intracellular channel protein 1 GN=CLIC1 PE=1 SV=4	2.77	2.77
A8K088	cDNA FLJ78614, highly similar to Homo sapiens eukaryotic translation initiation factor 4A, isoform 1 (EIF4A1), mRNA PE=2 SV=1	1.72	1.72
Q16719	Kynureninase GN=KYNU PE=1 SV=1	2.40	2.40
P37837	Transaldolase GN=TALDO1 PE=1 SV=2	3.26	3.26
A0A024RB85	Proliferation-associated 2G4, 38kDa, isoform CRA_a GN=PA2G4 PE=4 SV=1	3.01	3.01
Q32Q12	Nucleoside diphosphate kinase GN=NME1-NME2 PE=1 SV=1	1.69	1.69
P25786	Proteasome subunit alpha type-1 GN=PSMA1 PE=1 SV=1	2.37	2.37
Q02790	Peptidyl-prolyl cis-trans isomerase FKBP4 GN=FKBP4 PE=1 SV=3	3.28	3.28
A0A024RDR0	High-mobility group box 1, isoform CRA_a GN=HMGB1 PE=4 SV=1	3.60	3.60
A8K8U1	cDNA FLJ77762, highly similar to Homo sapiens cullin-associated and neddylation-dissociated 1 (CAND1), mRNA PE=2 SV=1	1.77	1.77
Q14566	DNA replication licensing factor MCM6 GN=MCM6 PE=1 SV=1	2.43	2.43
A0A024RAZ7	Heterogeneous nuclear ribonucleoprotein A1, isoform CRA_b GN=HNRPA1 PE=4 SV=1	1.90	1.90
P67936	Tropomyosin alpha-4 chain GN=TPM4 PE=1 SV=3	2.29	2.29
Q9H1E3	Nuclear ubiquitous casein and cyclin-dependent kinase substrate 1 GN=NUCKS1 PE=1 SV=1	2.67	2.67
P40925	Malate dehydrogenase, cytoplasmic GN=MDH1 PE=1 SV=4	4.19	4.19
P26639	Threonine--tRNA ligase, cytoplasmic GN=TARS PE=1 SV=3	2.14	2.14
A4UCS8	Enolase 1 (Fragment) PE=2 SV=1	1.41	1.41
P48307	Tissue factor pathway inhibitor 2 GN=TFPI2 PE=1 SV=1	3.31	3.31
J3KQE5	GTP-binding nuclear protein Ran (Fragment) GN=RAN PE=1 SV=1	2.86	2.86

A8K690	cDNA FLJ76863, highly similar to Homo sapiens stress-induced-phosphoprotein 1 (Hsp70/Hsp90-organizing protein) (STIP1), mRNA PE=2 SV=1	2.01	2.01
Q5TZP7	DNA-(apurinic or apyrimidinic site) lyase GN=APEX1 PE=2 SV=1	4.08	4.08
A0A1C7CYX9	Dihydropyrimidinase-related protein 2 GN=DPYSL2 PE=1 SV=1	2.18	2.18
P22626	Heterogeneous nuclear ribonucleoproteins A2/B1 GN=HNRNPA2B1 PE=1 SV=2	2.75	2.75
B1AK88	Capping protein (Actin filament) muscle Z-line, beta, isoform CRA_d GN=CAPZB PE=1 SV=1	2.89	2.89
A0A024R895	SET translocation (Myeloid leukemia-associated), isoform CRA_b GN=SET PE=3 SV=1	1.97	1.97
P15121	Aldose reductase GN=AKR1B1 PE=1 SV=3	3.25	3.25
Q16531	DNA damage-binding protein 1 GN=DDB1 PE=1 SV=1	2.58	2.58
Q9Y4L1	Hypoxia up-regulated protein 1 GN=HYOU1 PE=1 SV=1	2.03	2.03
Q15691	Microtubule-associated protein RP/EB family member 1 GN=MAPRE1 PE=1 SV=3	2.92	2.92
A0A024RAI1	ARP3 actin-related protein 3 homolog (Yeast), isoform CRA_a GN=ACTR3 PE=3 SV=1	2.44	2.44
P25705	ATP synthase subunit alpha, mitochondrial GN=ATP5F1A PE=1 SV=1	1.82	1.82
O75874	Isocitrate dehydrogenase [NADP] cytoplasmic GN=IDH1 PE=1 SV=2	3.46	3.46
P17987	T-complex protein 1 subunit alpha GN=TCP1 PE=1 SV=1	1.72	1.72
P12956	X-ray repair cross-complementing protein 6 GN=XRCC6 PE=1 SV=2	1.72	1.72
P23526	Adenosylhomocysteinase GN=AHCY PE=1 SV=4	2.30	2.30
P07737	Profilin-1 GN=PFN1 PE=1 SV=2	2.77	2.77
Q59H77	T-complex protein 1 subunit gamma (Fragment) PE=2 SV=1	1.46	1.46
P11047	Laminin subunit gamma-1 GN=LAMC1 PE=1 SV=3	2.22	2.22
J3KQ32	Obg-like ATPase 1 GN=OLA1 PE=1 SV=1	3.49	3.49
P09382	Galectin-1 GN=LGALS1 PE=1 SV=2	2.24	2.24
P25789	Proteasome subunit alpha type-4 GN=PSMA4 PE=1 SV=1	1.83	1.83
A0A024R1K7	Tyrosine 3-monooxygenase/tryptophan 5-monooxygenase activation protein, eta polypeptide, isoform CRA_b GN=YWHAH PE=3 SV=1	2.73	2.73
O14980	Exportin-1 GN=XPO1 PE=1 SV=1	2.75	2.75
Q01469	Fatty acid-binding protein 5 GN=FABP5 PE=1 SV=3	3.64	3.64
A0A024RDL1	Chaperonin containing TCP1, subunit 6A (Zeta 1), isoform CRA_a GN=CCT6A PE=3 SV=1	1.50	1.50
V9HWB5	Epididymis secretory sperm binding protein Li 66p GN=HEL-S-66p PE=2 SV=1	3.06	3.06
P50454	Serpin H1 GN=SERPINH1 PE=1 SV=2	1.82	1.82
A2A274	Aconitate hydratase, mitochondrial GN=ACO2 PE=1 SV=1	4.67	4.67
A8K3C3	T-complex protein 1 subunit delta PE=2 SV=1	1.64	1.64
B7ZA86	cDNA, FLJ79100, highly similar to 14-3-3 protein epsilon (14-3-3E) PE=2 SV=1	2.87	2.87
P13489	Ribonuclease inhibitor GN=RNH1 PE=1 SV=2	2.29	2.29
P31939	Bifunctional purine biosynthesis protein PURH GN=ATIC PE=1 SV=3	2.95	2.95
D3DQ69	SERPINE1 mRNA binding protein 1, isoform CRA_c GN=SERBP1 PE=4 SV=1	3.11	3.11
A0A140VK07	Testicular secretory protein Li 7 PE=2 SV=1	2.62	2.62
A8K7B7	Protein phosphatase 2 (Formerly 2A), regulatory subunit A (PR 65), alpha isoform GN=PPP2R1A PE=1 SV=1	1.97	1.97
A8K7Q1	cDNA FLJ77770, highly similar to Homo sapiens nucleobindin 1 (NUCB1), mRNA PE=2 SV=1	3.65	3.65
A8K329	cDNA FLJ76656, highly similar to Homo sapiens scaffold attachment factor B (SAFB), mRNA PE=2 SV=1	3.02	3.02
P04083	Annexin A1 GN=ANXA1 PE=1 SV=2	1.14	1.14
Q6IAW5	CALU protein GN=CALU PE=2 SV=1	1.86	1.86
A0A024R1Z6	Vesicle amine transport protein 1 homolog (T californica), isoform CRA_a GN=VAT1 PE=4 SV=1	2.09	2.09
A0A087X1Z3	Proteasome activator complex subunit 2 GN=PSME2 PE=1 SV=1	2.25	2.25
Q4LE58	eIF4G1 variant protein (Fragment) GN=EIF4G1 variant protein PE=2 SV=1	3.15	3.15
A0A087X1N8	Serpin B6 GN=SERPINB6 PE=1 SV=1	2.90	2.90
Q15084	Protein disulfide-isomerase A6 GN=PDIA6 PE=1 SV=1	2.15	2.15
B4DPQ0	Complement C1r subcomponent GN=C1R PE=1 SV=1	3.63	3.63
P14866	Heterogeneous nuclear ribonucleoprotein L GN=HNRNPL PE=1 SV=2	2.81	2.81
P06748	Nucleophosmin GN=NPM1 PE=1 SV=2	2.44	2.44
P52926	High mobility group protein HMGI-C GN=HMGA2 PE=1 SV=1	2.36	2.36
P17174	Aspartate aminotransferase, cytoplasmic GN=GOT1 PE=1 SV=3	2.86	2.86
A0A109NGN6	Proteasome subunit alpha type PE=2 SV=1	2.00	2.00
P23284	Peptidyl-prolyl cis-trans isomerase B GN=PPIB PE=1 SV=2	2.81	2.81

Q12888	TP53-binding protein 1 GN=TP53BP1 PE=1 SV=2	2.03	2.03
Q59EA2	Coronin (Fragment) PE=2 SV=1	2.99	2.99
O95373	Importin-7 GN=IPO7 PE=1 SV=1	2.79	2.79
E7EUF1	Ectonucleotide pyrophosphatase/phosphodiesterase family member 2 GN=ENPP2 PE=1 SV=1	2.89	2.89
Q96TA1	Niban-like protein 1 GN=FAM129B PE=1 SV=3	2.22	2.22
Q14240	Eukaryotic initiation factor 4A-II GN=EIF4A2 PE=1 SV=2	2.32	2.32
P61981	14-3-3 protein gamma GN=YWHAG PE=1 SV=2	2.36	2.36
P20618	Proteasome subunit beta type-1 GN=PSMB1 PE=1 SV=2	1.49	1.49
Q4LE36	ACLY variant protein (Fragment) GN=ACLY variant protein PE=2 SV=1	1.78	1.78
A0A0S2Z4C3	Fumarate hydratase isoform 1 (Fragment) GN=FH PE=2 SV=1	3.19	3.19
P63244	Receptor of activated protein C kinase 1 GN=RACK1 PE=1 SV=3	2.70	2.70
P11940	Polyadenylate-binding protein 1 GN=PABPC1 PE=1 SV=2	2.13	2.13
E7EMB3	Calmodulin-2 GN=CALM2 PE=1 SV=1	2.66	2.66
Q92688	Acidic leucine-rich nuclear phosphoprotein 32 family member B GN=ANP32B PE=1 SV=1	2.51	2.51
Q9Y266	Nuclear migration protein nudC GN=NUDC PE=1 SV=1	3.92	3.92
A0A024RDF3	Heterogeneous nuclear ribonucleoprotein D (AU-rich element RNA binding protein 1, 37kDa), isoform CRA_d GN=HNRPD PE=4 SV=1	3.14	3.14
Q4W4Y1	Dopamine receptor interacting protein 4 GN=DRIP4 PE=2 SV=1	1.71	1.71
A0A024RB75	Citrate synthase GN=CS PE=3 SV=1	3.41	3.41
B7Z8Z6	DNA helicase PE=2 SV=1	2.72	2.72
P13010	X-ray repair cross-complementing protein 5 GN=XRCC5 PE=1 SV=3	2.18	2.18
A4D2D2	Procollagen C-endopeptidase enhancer GN=PCOLCE PE=4 SV=1	2.85	2.85
P30041	Peroxiredoxin-6 GN=PRDX6 PE=1 SV=3	2.91	2.91
P49588	Alanine--tRNA ligase, cytoplasmic GN=AARS PE=1 SV=2	2.66	2.66
V9HWH9	Protein S100 GN=HEL-S-43 PE=2 SV=1	2.29	2.29
A0A024RCM3	DDX39B GN=hCG_2005638 PE=4 SV=1	2.52	2.52
E9KL48	Epididymis tissue sperm binding protein Li 18mP GN=GLUD1 PE=2 SV=1	2.25	2.25
P06703	Protein S100-A6 GN=S100A6 PE=1 SV=1	1.84	1.84
A0A024R6K8	Tryptophanyl-tRNA synthetase, isoform CRA_a GN=WARS PE=3 SV=1	2.65	2.65
P12004	Proliferating cell nuclear antigen GN=PCNA PE=1 SV=1	2.58	2.58
G3V5Z7	Proteasome subunit alpha type GN=PSMA6 PE=1 SV=1	2.77	2.77
P28799	Granulins GN=GRN PE=1 SV=2	2.51	2.51
Q59EG8	Proteasome 26S non-ATPase subunit 2 variant (Fragment) PE=2 SV=1	1.74	1.74
A0A140VK27	Leukotriene A(4) hydrolase PE=2 SV=1	2.90	2.90
P30084	Enoyl-CoA hydratase, mitochondrial GN=ECHS1 PE=1 SV=4	3.49	3.49
Q53F64	Heterogeneous nuclear ribonucleoprotein AB isoform a variant (Fragment) PE=2 SV=1	1.95	1.95
A0A0S2Z3Y1	Lectin galactoside-binding soluble 3 binding protein isoform 1 (Fragment) GN=LGALS3BP PE=2 SV=1	3.29	3.29
A8K9A4	cDNA FLJ75154, highly similar to Homo sapiens heterogeneous nuclear ribonucleoprotein C (C1/C2), mRNA PE=2 SV=1	2.40	2.40
A7XZE4	Beta tropomyosin isoform GN=TPM2 PE=1 SV=1	3.19	3.19
A8K8D9	Glucose-6-phosphate 1-dehydrogenase PE=2 SV=1	2.04	2.04
O43390	Heterogeneous nuclear ribonucleoprotein R GN=HNRNPR PE=1 SV=1	2.07	2.07
A0A024R3T8	Poly [ADP-ribose] polymerase GN=PARP1 PE=4 SV=1	2.62	2.62
B3KQF4	cDNA FLJ90373 fis, clone NT2RP2004606, highly similar to Metalloproteinase inhibitor 1 PE=2 SV=1	3.99	3.99
P55786	Puromycin-sensitive aminopeptidase GN=NPEPPS PE=1 SV=2	3.07	3.07
D3DQH8	Secreted protein, acidic, cysteine-rich (Osteonectin), isoform CRA_a GN=SPARC PE=4 SV=1	2.59	2.59
A3RJH1	ATP-dependent RNA helicase DDX1 GN=DDX1 PE=2 SV=1	2.22	2.22
Q562L9	Actin-like protein (Fragment) GN=ACT PE=4 SV=1	1.58	1.58
Q96KP4	Cytosolic non-specific dipeptidase GN=CNDP2 PE=1 SV=2	3.01	3.01
V9HWC2	Epididymis secretory sperm binding protein Li 67p GN=HEL-S-67p PE=2 SV=1	2.82	2.82
A0A0U1RRM4	Polypyrimidine tract-binding protein 1 GN=PTBP1 PE=1 SV=1	2.27	2.27
Q15293	Reticulocalbin-1 GN=RCN1 PE=1 SV=1	1.88	1.88
B2R8Z8	cDNA, FLJ94136, highly similar to Homo sapiens synaptotagmin binding, cytoplasmic RNA interacting protein (SYNCRIP), mRNA PE=2 SV=1	1.99	1.99

Q13185	Chromobox protein homolog 3 GN=CBX3 PE=1 SV=4	3.10	3.10
P05387	60S acidic ribosomal protein P2 GN=RPLP2 PE=1 SV=1	1.73	1.73
P35556	Fibrillin-2 GN=FBN2 PE=1 SV=3	2.96	2.96
P63241	Eukaryotic translation initiation factor 5A-1 GN=EIF5A PE=1 SV=2	2.70	2.70
Q6FIC5	Chloride intracellular channel protein GN=CLIC4 PE=2 SV=1	3.74	3.74
V9HWJ1	Glutathione synthetase GN=HEL-S-64p PE=2 SV=1	3.60	3.60
A0A0K0K1K4	Proteasome subunit alpha type GN=HEL-S-276 PE=2 SV=1	2.10	2.10
Q15436	Protein transport protein Sec23A GN=SEC23A PE=1 SV=2	3.05	3.05
B4DRM3	cDNA FLJ54492, highly similar to Eukaryotic translation initiation factor 4B PE=2 SV=1	2.80	2.80
A0A140VJL3	Hypoxanthine phosphoribosyltransferase PE=2 SV=1	1.90	1.90
Q7RU04	Aminopeptidase B GN=RNPEP PE=4 SV=1	2.56	2.56
B8ZWD9	Diazepam binding inhibitor, splice form 1D(2) GN=DBI PE=2 SV=1	2.51	2.51
A2RUM7	Ribosomal protein L5, isoform CRA_c GN=RPL5 PE=2 SV=1	2.91	2.91
P26196	Probable ATP-dependent RNA helicase DDX6 GN=DDX6 PE=1 SV=2	3.11	3.11
Q12905	Interleukin enhancer-binding factor 2 GN=ILF2 PE=1 SV=2	2.36	2.36
A0A0K0K1L8	Epididymis secretory sperm binding protein Li 129m GN=HEL-S-129m PE=2 SV=1	2.72	2.72
B7Z809	cDNA FLJ56016, highly similar to C-1-tetrahydrofolate synthase, cytoplasmic PE=2 SV=1	2.51	2.51
A0A0C4DG17	40S ribosomal protein SA GN=RPSA PE=1 SV=1	2.51	2.51
A1KYQ7	Eukaryotic translation initiation factor 3 subunit C GN=EIF3C PE=2 SV=1	2.52	2.52
P46013	Proliferation marker protein Ki-67 GN=MKI67 PE=1 SV=2	4.07	4.07
P54727	UV excision repair protein RAD23 homolog B GN=RAD23B PE=1 SV=1	2.98	2.98
O60361	Putative nucleoside diphosphate kinase GN=NME2P1 PE=5 SV=1	2.49	2.49
C7DJS2	Glutathione S-transferase pi (Fragment) GN=GSTP1 PE=2 SV=1	1.66	1.66
Q9UNZ2	NSFL1 cofactor p47 GN=NSFL1C PE=1 SV=2	1.30	1.30
Q6IBT1	Proteasome subunit beta type GN=PSMB7 PE=2 SV=1	2.41	2.41
B0YIW6	Archain 1, isoform CRA_a GN=ARCN1 PE=1 SV=1	1.58	1.58
P50502	Hsc70-interacting protein GN=ST13 PE=1 SV=2	2.48	2.48
P23246	Splicing factor, proline- and glutamine-rich GN=SFPQ PE=1 SV=2	3.40	3.40
A0A024R1A4	Ubiquitin-conjugating enzyme E2L 3, isoform CRA_a GN=UBE2L3 PE=3 SV=1	1.84	1.84
P23396	40S ribosomal protein S3 GN=RPS3 PE=1 SV=2	1.76	1.76
A8K651	cDNA FLJ75700, highly similar to Homo sapiens complement component 1, q subcomponent binding protein (C1QBP), nuclear gene encoding mitochondrial protein, mRNA PE=2 SV=1	3.80	3.80
V9HWE8	Epididymis secretory sperm binding protein Li 47e GN=HEL-S-47e PE=2 SV=1	2.11	2.11
P25788	Proteasome subunit alpha type-3 GN=PSMA3 PE=1 SV=2	2.51	2.51
P26583	High mobility group protein B2 GN=HMGB2 PE=1 SV=2	2.63	2.63
A0A024R7B7	CDC37 cell division cycle 37 homolog (S. cerevisiae), isoform CRA_a GN=CDC37 PE=4 SV=1	1.77	1.77
E7EQL5	Cytoplasmic dynein 1 intermediate chain 2 (Fragment) GN=DYNC1I2 PE=1 SV=1	1.75	1.75
B4DPD5	Ubiquitin thioesterase PE=2 SV=1	3.76	3.76
O60701	UDP-glucose 6-dehydrogenase GN=UGDH PE=1 SV=1	1.97	1.97
Q9Y2W1	Thyroid hormone receptor-associated protein 3 GN=THRAP3 PE=1 SV=2	4.15	4.15
Q8NBJ4	Golgi membrane protein 1 GN=GOLM1 PE=1 SV=1	4.57	4.57
Q15366	Poly(rC)-binding protein 2 GN=PCBP2 PE=1 SV=1	1.83	1.83
A8K3S1	Glucosamine-6-phosphate isomerase PE=2 SV=1	2.40	2.40
A0A024R1K8	Splicing factor 3a, subunit 1, 120kDa, isoform CRA_a GN=SF3A1 PE=4 SV=1	2.73	2.73
Q15046	Lysine--tRNA ligase GN=KARS PE=1 SV=3	2.87	2.87
A0A1B0GW77	Alpha-aminoadipic semialdehyde dehydrogenase GN=ALDH7A1 PE=1 SV=1	2.86	2.86
P52888	Thimet oligopeptidase GN=THOP1 PE=1 SV=2	2.51	2.51
O15144	Actin-related protein 2/3 complex subunit 2 GN=ARPC2 PE=1 SV=1	2.44	2.44
P09341	Growth-regulated alpha protein GN=CXCL1 PE=1 SV=1	2.90	2.90
O43143	Pre-mRNA-splicing factor ATP-dependent RNA helicase DHX15 GN=DHX15 PE=1 SV=2	2.38	2.38
A0A0S2Z4Z9	Non-POU domain containing octamer-binding isoform 1 (Fragment) GN=NONO PE=2 SV=1	2.96	2.96
F8W0W8	Serine/threonine-protein phosphatase GN=PPP1CC PE=1 SV=1	3.06	3.06
Q9UH65	Switch-associated protein 70 GN=SWAP70 PE=1 SV=1	1.88	1.88
Q13409	Cytoplasmic dynein 1 intermediate chain 2 GN=DYNC1I2 PE=1 SV=3	2.88	2.88
Q04760	Lactoylglutathione lyase GN=GLO1 PE=1 SV=4	2.92	2.92
Q08211	ATP-dependent RNA helicase A GN=DHX9 PE=1 SV=4	1.80	1.80

B4DR52	Histone H2B PE=2 SV=1	1.83	1.83
A0A024R3W7	Eukaryotic translation elongation factor 1 beta 2, isoform CRA_a GN=EEF1B2 PE=3 SV=1	1.95	1.95
Q53FN7	BZW1 protein variant (Fragment) PE=2 SV=1	2.40	2.40
P19875	C-X-C motif chemokine 2 GN=CXCL2 PE=1 SV=1	2.01	2.01
P54136	Arginine--tRNA ligase, cytoplasmic GN=RARS PE=1 SV=2	3.09	3.09
P43034	Platelet-activating factor acetylhydrolase IB subunit alpha GN=PAFAH1B1 PE=1 SV=2	4.50	4.50
Q12931	Heat shock protein 75 kDa, mitochondrial GN=TRAP1 PE=1 SV=3	3.35	3.35
P61604	10 kDa heat shock protein, mitochondrial GN=HSPE1 PE=1 SV=2	3.91	3.91
D6REX3	Protein transport protein Sec31A GN=SEC31A PE=1 SV=1	2.23	2.23
P10412	Histone H1.4 GN=HIST1H1E PE=1 SV=2	1.55	1.55
L0R849	Alternative protein EDARADD GN=EDARADD PE=3 SV=1	1.68	1.68
B7Z6Z4	cDNA FLJ56329, highly similar to Myosin light polypeptide 6 GN=MYL6 PE=1 SV=1	1.84	1.84
P62495	Eukaryotic peptide chain release factor subunit 1 GN=ETF1 PE=1 SV=3	3.55	3.55
P28074	Proteasome subunit beta type-5 GN=PSMB5 PE=1 SV=3	1.71	1.71
P68431	Histone H3.1 GN=HIST1H3A PE=1 SV=2	2.08	2.08
P61160	Actin-related protein 2 GN=ACTR2 PE=1 SV=1	2.37	2.37
A5YM63	NEFM protein GN=NEFM PE=2 SV=1	2.07	2.07
O43491	Band 4.1-like protein 2 GN=EPB41L2 PE=1 SV=1	2.85	2.85
Q09028	Histone-binding protein RBBP4 GN=RBBP4 PE=1 SV=3	2.38	2.38
P16070	CD44 antigen GN=CD44 PE=1 SV=3	2.71	2.71
A0A024R3Q3	ADP-ribosylation factor 1, isoform CRA_a GN=ARF1 PE=3 SV=1	2.16	2.16
O75396	Vesicle-trafficking protein SEC22b GN=SEC22B PE=1 SV=4	1.38	1.38
A0A024RBE7	Thymopoietin, isoform CRA_c GN=TMPO PE=4 SV=1	2.75	2.75
P16152	Carbonyl reductase [NADPH] 1 GN=CBR1 PE=1 SV=3	5.24	5.24
P06899	Histone H2B type 1-J GN=HIST1H2BJ PE=1 SV=3	1.72	1.72
Q5T765	Interferon-induced protein with tetratricopeptide repeats 3, isoform CRA_a GN=IFIT3 PE=2 SV=1	1.88	1.88
Q14914	Prostaglandin reductase 1 GN=PTGR1 PE=1 SV=2	3.50	3.50
P41250	Glycine--tRNA ligase GN=GARS PE=1 SV=3	1.59	1.59
Q9Y5B9	FACT complex subunit SPT16 GN=SUPT16H PE=1 SV=1	3.16	3.16
Q9H2U2	Inorganic pyrophosphatase 2, mitochondrial GN=PPA2 PE=1 SV=2	2.96	2.96
Q59FF0	EBNA-2 co-activator variant (Fragment) PE=2 SV=1	2.34	2.34
P02461	Collagen alpha-1(III) chain GN=COL3A1 PE=1 SV=4	5.22	5.22
P14324	Farnesyl pyrophosphate synthase GN=FDPS PE=1 SV=4	2.41	2.41
A0A024RDS1	Heat shock 105kDa/110kDa protein 1, isoform CRA_c GN=HSPH1 PE=3 SV=1	3.02	3.02
D9IAI1	Epididymis secretory protein Li 34 GN=HEL-S-34 PE=2 SV=1	2.91	2.91
B2R6S5	UMP-CMP kinase GN=CMPK PE=2 SV=1	2.94	2.94
Q59F66	DEAD box polypeptide 17 isoform p82 variant (Fragment) PE=2 SV=1	2.17	2.17
B4DJQ8	cDNA FLJ55694, highly similar to Dipeptidyl-peptidase 1 PE=2 SV=1	2.86	2.86
Q9NR45	Sialic acid synthase GN=NANS PE=1 SV=2	1.65	1.65
E9PAV3	Nascent polypeptide-associated complex subunit alpha, muscle-specific form GN=NACA PE=1 SV=1	2.28	2.28
A0A024R821	Eukaryotic translation initiation factor 3 subunit B GN=EIF3S9 PE=3 SV=1	1.77	1.77
O43175	D-3-phosphoglycerate dehydrogenase GN=PHGDH PE=1 SV=4	2.04	2.04
Q5U0I6	H.sapiens ras-related Hrab1A protein GN=RAB1A PE=2 SV=1	2.14	2.14
Q99873	Protein arginine N-methyltransferase 1 GN=PRMT1 PE=1 SV=3	2.31	2.31
Q9UHX1	Poly(U)-binding-splicing factor PUF60 GN=PUF60 PE=1 SV=1	1.59	1.59
P25787	Proteasome subunit alpha type-2 GN=PSMA2 PE=1 SV=2	2.27	2.27
M0QXB4	Coatomer protein complex, subunit epsilon, isoform CRA_g GN=COPE PE=1 SV=1	2.74	2.74
P34897	Serine hydroxymethyltransferase, mitochondrial GN=SHMT2 PE=1 SV=3	2.54	2.54
Q9P0L0	Vesicle-associated membrane protein-associated protein A GN=VAPA PE=1 SV=3	2.22	2.22
A0A024R5Q7	Adenylosuccinate synthetase isozyme 2 GN=ADSS PE=3 SV=1	3.50	3.50
H0YFD6	Trifunctional enzyme subunit alpha, mitochondrial GN=HADHA PE=1 SV=2	1.73	1.73
Q9HAV7	GrpE protein homolog 1, mitochondrial GN=GRPEL1 PE=1 SV=2	2.44	2.44
P84090	Enhancer of rudimentary homolog GN=ERH PE=1 SV=1	2.32	2.32
Q9Y678	Coatomer subunit gamma-1 GN=COPG1 PE=1 SV=1	2.24	2.24
B9EKV4	Aldehyde dehydrogenase 9 family, member A1 GN=ALDH9A1 PE=2 SV=1	2.72	2.72

O43583	Density-regulated protein GN=DENR PE=1 SV=2	2.91	2.91
A0A087WSV8	Nucleobindin 2, isoform CRA_b GN=NUCB2 PE=1 SV=1	2.35	2.35
A0A0B4J2C3	Translationally-controlled tumor protein GN=TPT1 PE=1 SV=1	2.91	2.91
E7EPK1	Septin-7 GN=SEPT7 PE=1 SV=2	1.93	1.93
H7BZJ3	Protein disulfide-isomerase A3 (Fragment) GN=PDIA3 PE=1 SV=1	1.36	1.36
A0A024R324	Ras homolog gene family, member A, isoform CRA_a GN=RHOA PE=4 SV=1	3.02	3.02
A0A024R7G8	RAD23 homolog A (S. cerevisiae), isoform CRA_a GN=RAD23A PE=4 SV=1	2.98	2.98
V9HWA6	Epididymis luminal protein 32 GN=HEL32 PE=2 SV=1	3.40	3.40
J9R021	Eukaryotic translation initiation factor 3 subunit A GN=eIF3a PE=2 SV=1	1.80	1.80
A0A024R1U0	Ran GTPase activating protein 1, isoform CRA_d GN=RANGAP1 PE=4 SV=1	2.35	2.35
J3K000	PEPD protein GN=PEPD PE=2 SV=1	2.07	2.07
Q14847	LIM and SH3 domain protein 1 GN=LASP1 PE=1 SV=2	2.73	2.73
Q6BCY4	NADH-cytochrome b5 reductase 2 GN=CYB5R2 PE=1 SV=1	2.98	2.98
E5RJD8	Tubulin-specific chaperone A GN=TBCA PE=1 SV=1	5.65	5.65
P12268	Inosine-5'-monophosphate dehydrogenase 2 GN=IMPDH2 PE=1 SV=2	1.24	1.24
P25398	40S ribosomal protein S12 GN=RPS12 PE=1 SV=3	2.29	2.29
S4R3N1	HSPE1-MOB4 readthrough GN=HSPE1-MOB4 PE=3 SV=1	1.81	1.81
O00154	Cytosolic acyl coenzyme A thioester hydrolase GN=ACOT7 PE=1 SV=3	2.15	2.15
P46063	ATP-dependent DNA helicase Q1 GN=RECQL PE=1 SV=3	1.59	1.59
A0A077YIJ7	MHC class I antigen (Fragment) GN=HLA-A PE=3 SV=1	1.99	1.99
O00764	Pyridoxal kinase GN=PDXK PE=1 SV=1	2.22	2.22
P18085	ADP-ribosylation factor 4 GN=ARF4 PE=1 SV=3	1.27	1.27
O60763	General vesicular transport factor p115 GN=USO1 PE=1 SV=2	1.49	1.49
P16402	Histone H1.3 GN=HIST1H1D PE=1 SV=2	1.08	1.08
O75828	Carbonyl reductase [NADPH] 3 GN=CBR3 PE=1 SV=3	1.18	1.18
P12270	Nucleoprotein TPR GN=TPR PE=1 SV=3	1.73	1.73
Q96G03	Phosphoglucomutase-2 GN=PGM2 PE=1 SV=4	2.05	2.05
P24752	Acetyl-CoA acetyltransferase, mitochondrial GN=ACAT1 PE=1 SV=1	4.06	4.06
Q59EF6	Calpain 2, large [catalytic] subunit variant (Fragment) PE=2 SV=1	2.18	2.18
A0A140VK46	Proteasome subunit beta PE=2 SV=1	2.43	2.43
O75821	Eukaryotic translation initiation factor 3 subunit G GN=EIF3G PE=1 SV=2	2.63	2.63
Q1KMD3	Heterogeneous nuclear ribonucleoprotein U-like protein 2 GN=HNRNPUL2 PE=1 SV=1	2.76	2.76
A8K566	cDNA FLJ78246, highly similar to Homo sapiens splicing factor 3a, subunit 3, 60kDa (SF3A3), mRNA PE=2 SV=1	2.21	2.21
Q9UJU6	Drebrin-like protein GN=DBNL PE=1 SV=1	3.05	3.05
B2R4R0	Histone H4 GN=HIST1H4L PE=2 SV=1	1.30	1.30
P0C0S5	Histone H2A.Z GN=H2AFZ PE=1 SV=2	1.85	1.85
P53621	Coatomer subunit alpha GN=COPA PE=1 SV=2	2.61	2.61
P42224	Signal transducer and activator of transcription 1-alpha/beta GN=STAT1 PE=1 SV=2	3.36	3.36
Q1HBJ4	Mitogen-activated protein kinase GN=MAPK1 PE=3 SV=1	2.78	2.78
O75643	U5 small nuclear ribonucleoprotein 200 kDa helicase GN=SNRNP200 PE=1 SV=2	3.04	3.04
A0A090N7T9	Secernin 1 GN=SCRN1 PE=4 SV=1	1.65	1.65
Q14444	Caprin-1 GN=CAPRIN1 PE=1 SV=2	2.44	2.44
Q5U0F4	Eukaryotic translation initiation factor 3 subunit I GN=EIF3S2 PE=2 SV=1	1.65	1.65
A0A0B4U5E3	Granulocyte-colony stimulating factor (Fragment) PE=2 SV=1	3.34	3.34
Q5U043	S-(hydroxymethyl)glutathione dehydrogenase PE=2 SV=1	2.50	2.50
A0A024R571	EH domain-containing protein 1 GN=EHD1 PE=1 SV=1	2.56	2.56
O43776	Asparagine--tRNA ligase, cytoplasmic GN=NARS PE=1 SV=1	2.70	2.70
Q15631	Translin GN=TSN PE=1 SV=1	1.79	1.79
A8K4Z4	60S acidic ribosomal protein P0 PE=2 SV=1	1.93	1.93
P63208	S-phase kinase-associated protein 1 GN=SKP1 PE=1 SV=2	1.73	1.73
Q5U000	Cathepsin Z PE=2 SV=1	3.54	3.54
B4DDD6	cDNA FLJ59450, highly similar to Drebrin-like protein GN=DBNL PE=1 SV=1	2.95	2.95
P35606	Coatomer subunit beta' GN=COPB2 PE=1 SV=2	2.27	2.27
B4E1U9	cDNA FLJ54776, highly similar to Cell division control protein 42 homolog PE=2 SV=1	3.69	3.69
B3KSH1	Eukaryotic translation initiation factor 3 subunit F GN=EIF3F PE=2 SV=1	1.96	1.96
Q6FHX6	Flap endonuclease 1 GN=FEN1 PE=2 SV=1	2.86	2.86

A0A1W2PPZ5	Transcription elongation factor A protein 1 GN=TCEA1 PE=1 SV=1	2.06	2.06
A8K8F0	cDNA FLJ76436 PE=2 SV=1	3.05	3.05
P17096	High mobility group protein HMG-I/HMG-Y GN=HMGA1 PE=1 SV=3	1.97	1.97
A0A140VJF4	Biliverdin reductase A PE=2 SV=1	4.47	4.47
A0A024RBB7	Nucleosome assembly protein 1-like 1, isoform CRA_a GN=NAP1L1 PE=3 SV=1	1.71	1.71
P30044	Peroxiredoxin-5, mitochondrial GN=PRDX5 PE=1 SV=4	1.54	1.54
O14979	Heterogeneous nuclear ribonucleoprotein D-like GN=HNRNPDL PE=1 SV=3	2.36	2.36
B2R548	Prefoldin subunit 4 PE=2 SV=1	2.43	2.43
Q9Y3I0	tRNA-splicing ligase RtcB homolog GN=RTCB PE=1 SV=1	2.22	2.22
Q6FHQ0	RBBP7 protein (Fragment) GN=RBBP7 PE=2 SV=1	4.56	4.56
Q5TB52	3'-phosphoadenosine 5'-phosphosulfate synthase 2, isoform CRA_b GN=PAPSS2 PE=2 SV=1	1.63	1.63
Q9Y3F4	Serine-threonine kinase receptor-associated protein GN=STRAP PE=1 SV=1	2.82	2.82
O43684	Mitotic checkpoint protein BUB3 GN=BUB3 PE=1 SV=1	2.13	2.13
Q8IZ03	Interferon-induced protein with tetratricopeptide repeats 2 GN=IFIT2 PE=1 SV=2	2.35	2.35
P30405	Peptidyl-prolyl cis-trans isomerase F, mitochondrial GN=PPIF PE=1 SV=1	3.91	3.91
P00966	Argininosuccinate synthase GN=ASS1 PE=1 SV=2	1.76	1.76
Q71DI3	Histone H3.2 GN=HIST2H3A PE=1 SV=3	1.70	1.70
P52597	Heterogeneous nuclear ribonucleoprotein F GN=HNRNPF PE=1 SV=3	1.90	1.90
P09919	Granulocyte colony-stimulating factor GN=CSF3 PE=1 SV=1	2.67	2.67
B2R960	cDNA, FLJ94230, highly similar to Homo sapiens thioredoxin-like 1 (TXNL1), mRNA PE=2 SV=1	2.60	2.60
O00232	26S proteasome non-ATPase regulatory subunit 12 GN=PSMD12 PE=1 SV=3	2.30	2.30
Q9H2G2	STE20-like serine/threonine-protein kinase GN=SLK PE=1 SV=1	2.19	2.19
P38919	Eukaryotic initiation factor 4A-III GN=EIF4A3 PE=1 SV=4	2.39	2.39
X6R8A1	Carboxypeptidase GN=CTSA PE=1 SV=1	2.74	2.74
A0A0A0MQS9	Laminin subunit alpha-4 GN=LAMA4 PE=1 SV=1	1.81	1.81
P01034	Cystatin-C GN=CST3 PE=1 SV=1	3.05	3.05
Q9UHV9	Prefoldin subunit 2 GN=PFDN2 PE=1 SV=1	2.18	2.18
A0A0K0K1I0	Epididymis secretory protein Li 265 GN=HEL-S-265 PE=2 SV=1	2.01	2.01
Q13435	Splicing factor 3B subunit 2 GN=SF3B2 PE=1 SV=2	2.12	2.12
A0A024R713	Dihydrolipoyl dehydrogenase GN=DLD PE=3 SV=1	2.27	2.27
D3DVC4	Nestin, isoform CRA_c GN=NES PE=3 SV=1	2.18	2.18
Q8WXX5	DnaJ homolog subfamily C member 9 GN=DNAJC9 PE=1 SV=1	2.95	2.95
Q9Y6E3	HSPC027 PE=2 SV=1	2.01	2.01
A0A140VK83	Protein phosphatase 1, regulatory subunit 7, isoform CRA_b GN=PPP1R7 PE=2 SV=1	2.65	2.65
A0A0S2Z471	Creatine kinase brain isoform 2 (Fragment) GN=CKB PE=2 SV=1	1.94	1.94
P16401	Histone H1.5 GN=HIST1H1B PE=1 SV=3	1.68	1.68
P54577	Tyrosine--tRNA ligase, cytoplasmic GN=YARS PE=1 SV=4	1.82	1.82
A4D0V4	Capping protein (Actin filament) muscle Z-line, alpha 2 GN=CAPZA2 PE=2 SV=1	2.36	2.36
D9YZV7	Tropomyosin 1 (Alpha) isoform 6 GN=TPM1 PE=3 SV=1	1.96	1.96
Q96FQ6	Protein S100-A16 GN=S100A16 PE=1 SV=1	1.91	1.91
Q9H8K1	cDNA FLJ13518 fis, clone PLACE1005799 PE=2 SV=1	1.81	1.81
Q7Z4X0	MO25-like protein PE=2 SV=1	2.18	2.18
P32119	Peroxiredoxin-2 GN=PRDX2 PE=1 SV=5	2.30	2.30
P26368	Splicing factor U2AF 65 kDa subunit GN=U2AF2 PE=1 SV=4	2.29	2.29
O14974	Protein phosphatase 1 regulatory subunit 12A GN=PPP1R12A PE=1 SV=1	2.56	2.56
O75475	PC4 and SFRS1-interacting protein GN=PSIP1 PE=1 SV=1	2.26	2.26
P30740	Leukocyte elastase inhibitor GN=SERPINB1 PE=1 SV=1	1.82	1.82
A0A024R9D2	Metadherin, isoform CRA_a GN=MTDH PE=4 SV=1	3.85	3.85
B0QY89	Eukaryotic translation initiation factor 3 subunit L GN=EIF3L PE=1 SV=1	1.59	1.59
V9HW90	Glutathione reductase GN=HEL-75 PE=2 SV=1	1.72	1.72
P16035	Metalloproteinase inhibitor 2 GN=TIMP2 PE=1 SV=2	4.83	4.83
Q15369	Elongin-C GN=ELOC PE=1 SV=1	1.98	1.98
Q14112	Nidogen-2 GN=NID2 PE=1 SV=3	1.98	1.98
B2R5T5	Protein kinase, cAMP-dependent, regulatory, type I, alpha (Tissue specific extinguisher 1), isoform CRA_a GN=PRKAR1A PE=2 SV=1	2.80	2.80
A0A2U9QGI0	NAP1L4/NUTM1D fusion protein GN=NAP1L4 PE=2 SV=1	2.19	2.19

A0A024R5X2	HCG2001986, isoform CRA_a GN=hCG_2001986 PE=4 SV=1	1.03	1.03
B3KUY2	Prostaglandin E synthase 3 (Cytosolic), isoform CRA_c GN=PTGES3 PE=2 SV=1	3.67	3.67
O60832	H/ACA ribonucleoprotein complex subunit DKC1 GN=DKC1 PE=1 SV=3	3.12	3.12
A0A024QZ77	EF-hand domain family, member D2, isoform CRA_a GN=EFHD2 PE=2 SV=1	1.80	1.80
Q9NQG5	Regulation of nuclear pre-mRNA domain-containing protein 1B GN=RPRD1B PE=1 SV=1	1.53	1.53
C6K6I9	MHC class I antigen GN=HLA-B PE=3 SV=1	3.17	3.17
B3KN28	Phosphoacetylglucosamine mutase PE=2 SV=1	2.03	2.03
O43242	26S proteasome non-ATPase regulatory subunit 3 GN=PSMD3 PE=1 SV=2	1.90	1.90
A0A0S2Z2Z6	Annexin (Fragment) GN=ANXA6 PE=2 SV=1	1.50	1.50
P61201	COP9 signalosome complex subunit 2 GN=COPS2 PE=1 SV=1	1.56	1.56
A0A023T6R1	Mago nashi protein GN=FLJ10292 PE=2 SV=1	2.63	2.63
Q9BXP5	Serrate RNA effector molecule homolog GN=SRRT PE=1 SV=1	1.96	1.96
B3KS98	Eukaryotic translation initiation factor 3 subunit H GN=EIF3H PE=1 SV=1	2.01	2.01
Q16881	Thioredoxin reductase 1, cytoplasmic GN=TXNRD1 PE=1 SV=3	2.15	2.15
Q9UMS4	Pre-mRNA-processing factor 19 GN=PRPF19 PE=1 SV=1	2.47	2.47
A0A1U9X9A1	VARS PE=3 SV=2	2.22	2.22
F8VXU5	Vacuolar protein sorting-associated protein 29 GN=VPS29 PE=1 SV=1	4.15	4.15
B2RBL3	Thymidine phosphorylase PE=2 SV=1	2.30	2.30
P24844	Myosin regulatory light polypeptide 9 GN=MYL9 PE=1 SV=4	1.58	1.58
A0A024R3P9	Acyl-Coenzyme A binding domain containing 3, isoform CRA_a GN=ACBD3 PE=4 SV=1	3.06	3.06
A8K2N0	cDNA FLJ77835, highly similar to Homo sapiens complement component 1, s subcomponent (C1S), transcript variant 2, mRNA PE=2 SV=1	3.42	3.42
H3BQQ9	SUMO-conjugating enzyme UBC9 (Fragment) GN=UBE2I PE=1 SV=1	3.18	3.18
A0A1W2PNV4	Uncharacterized protein PE=4 SV=1	2.80	2.80
P56537	Eukaryotic translation initiation factor 6 GN=EIF6 PE=1 SV=1	2.84	2.84
A0A024R394	Cysteine and histidine-rich domain (CHORD)-containing 1, isoform CRA_c GN=CHORDC1 PE=4 SV=1	2.32	2.32
A0A158RFU3	Parathymosin GN=PTMS PE=2 SV=1	2.21	2.21
P67775	Serine/threonine-protein phosphatase 2A catalytic subunit alpha isoform GN=PPP2CA PE=1 SV=1	2.00	2.00
J3QRS3	Myosin regulatory light chain 12A GN=MYL12A PE=1 SV=1	1.48	1.48
D3DPK5	SH3 domain binding glutamic acid-rich protein like 3, isoform CRA_a (Fragment) GN=SH3BGRL3 PE=4 SV=1	2.56	2.56
Q9Y520	Protein PRRC2C GN=PRRC2C PE=1 SV=4	1.71	1.71
P60228	Eukaryotic translation initiation factor 3 subunit E GN=EIF3E PE=1 SV=1	1.31	1.31
V9HW92	Epididymis secretory protein Li 112 GN=HEL-S-112 PE=2 SV=1	2.77	2.77
Q96EB3	EEF1A1 protein (Fragment) GN=EEF1A1 PE=2 SV=1	1.62	1.62
B2RBE5	cDNA, FLJ95468, highly similar to Homo sapiens transcriptional coactivator tubedown-100 (TBDN100),transcript variant 1, mRNA PE=2 SV=1	2.38	2.38
A0A024RDE8	PDZ and LIM domain 5, isoform CRA_c GN=PDLIM5 PE=4 SV=1	2.52	2.52
Q14157	Ubiquitin-associated protein 2-like GN=UBAP2L PE=1 SV=2	2.93	2.93
Q9NQW7	Xaa-Pro aminopeptidase 1 GN=XPNPEP1 PE=1 SV=3	2.60	2.60
F6WQW2	Ran-specific GTPase-activating protein GN=RANBP1 PE=1 SV=1	3.42	3.42
Q14329	Farnesyl pyrophosphate synthetase like-4 protein (Fragment) PE=3 SV=1	2.02	2.02
Q5T6U8	High mobility group AT-hook 1 GN=HMGA1 PE=2 SV=1	2.60	2.60
Q01844	RNA-binding protein EWS GN=EWSR1 PE=1 SV=1	2.83	2.83
C9JIF9	Acylamino-acid-releasing enzyme GN=APEH PE=1 SV=1	1.59	1.59
Q5VU77	Ubiquitin-associated protein 2-like (Fragment) GN=UBAP2L PE=1 SV=1	1.71	1.71
Q9ULC4	Malignant T-cell-amplified sequence 1 GN=MCTS1 PE=1 SV=1	2.25	2.25
A6NDG6	Glycerol-3-phosphate phosphatase GN=PGP PE=1 SV=1	1.48	1.48
A8K669	cDNA FLJ78452, highly similar to Homo sapiens legumain (LGMN), transcript variant 2, mRNA PE=2 SV=1	2.50	2.50
A0A024R6Q1	Eukaryotic translation initiation factor 5, isoform CRA_b GN=EIF5 PE=4 SV=1	2.41	2.41
Q9NSE4	Isoleucine--tRNA ligase, mitochondrial GN=IARS2 PE=1 SV=2	3.11	3.11
G3V3D1	NPC intracellular cholesterol transporter 2 (Fragment) GN=NPC2 PE=1 SV=1	2.98	2.98
A0A024RDB0	Ubiquitin-activating enzyme E1-like 2, isoform CRA_a GN=UBE1L2 PE=4 SV=1	2.09	2.09
O00622	Protein CYR61 GN=CYR61 PE=1 SV=1	3.10	3.10

A0A140VJS3	Testicular tissue protein Li 149 PE=2 SV=1	1.70	1.70
Q5T9B7	Adenylate kinase isoenzyme 1 GN=AK1 PE=1 SV=1	2.03	2.03
P05114	Non-histone chromosomal protein HMG-14 GN=HMGN1 PE=1 SV=3	3.06	3.06
P61163	Alpha-centractin GN=ACTR1A PE=1 SV=1	2.63	2.63
P07585	Decorin GN=DCN PE=1 SV=1	3.56	3.56
P11233	Ras-related protein Ral-A GN=RALA PE=1 SV=1	1.35	1.35
Q3B790	High-mobility group nucleosome binding domain 1 GN=HMGN1 PE=2 SV=1	3.03	3.03
P33316	Deoxyuridine 5'-triphosphate nucleotidohydrolase, mitochondrial GN=DUT PE=1 SV=4	2.93	2.93
Q99584	Protein S100-A13 GN=S100A13 PE=1 SV=1	3.87	3.87
A0A024R0R4	SUMO-1 activating enzyme subunit 1, isoform CRA_b GN=SAE1 PE=4 SV=1	1.79	1.79
Q07666	KH domain-containing, RNA-binding, signal transduction-associated protein 1 GN=KHDRBS1 PE=1 SV=1	4.22	4.22
Q9UKV3	Apoptotic chromatin condensation inducer in the nucleus GN=ACIN1 PE=1 SV=2	2.17	2.17
Q00688	Peptidyl-prolyl cis-trans isomerase FKBP3 GN=FKBP3 PE=1 SV=1	2.22	2.22
B3KML1	cDNA FLJ11308 fis, clone PLACE1010074, highly similar to Sorting nexin-2 PE=2 SV=1	2.85	2.85
P61221	ATP-binding cassette sub-family E member 1 GN=ABCE1 PE=1 SV=1	2.65	2.65
O14737	Programmed cell death protein 5 GN=PDCD5 PE=1 SV=3	2.25	2.25
O00148	ATP-dependent RNA helicase DDX39A GN=DDX39A PE=1 SV=2	1.10	1.10
P32321	Deoxycytidylate deaminase GN=DCTD PE=1 SV=2	2.03	2.03
O14929	Histone acetyltransferase type B catalytic subunit GN=HAT1 PE=1 SV=1	2.44	2.44
A0A140VK93	Adenylate kinase 2, mitochondrial GN=AK2 PE=2 SV=1	2.07	2.07
A0A0A0MRI2	Sorting nexin GN=SNX6 PE=1 SV=1	2.33	2.33
O75937	DnaJ homolog subfamily C member 8 GN=DNAJC8 PE=1 SV=2	1.42	1.42
Q10567	AP-1 complex subunit beta-1 GN=AP1B1 PE=1 SV=2	1.95	1.95
A8K4T6	cDNA FLJ76282, highly similar to Homo sapiens proteasome (prosome, macropain) 26S subunit, non-ATPase, 5 (PSMD5), mRNA PE=2 SV=1	1.85	1.85
P05161	Ubiquitin-like protein ISG15 GN=ISG15 PE=1 SV=5	3.27	3.27
P26373	60S ribosomal protein L13 GN=RPL13 PE=1 SV=4	1.29	1.29
A8K4W0	40S ribosomal protein S3a GN=RPS3A PE=2 SV=1	1.56	1.56
O15347	High mobility group protein B3 GN=HMGB3 PE=1 SV=4	2.85	2.85
G3V4P8	Glia maturation factor beta (Fragment) GN=GMFB PE=1 SV=1	2.48	2.48
V9HWF9	Epididymis luminal protein 20 GN=HEL20 PE=2 SV=1	2.45	2.45
P36957	Dihydrolipoyllysine-residue succinyltransferase component of 2-oxoglutarate dehydrogenase complex, mitochondrial GN=DLST PE=1 SV=4	1.18	1.18
Q6IQ30	Polyadenylate-binding protein GN=PABPC4 PE=2 SV=1	2.18	2.18
Q15907	Ras-related protein Rab-11B GN=RAB11B PE=1 SV=4	3.41	3.41
P49721	Proteasome subunit beta type-2 GN=PSMB2 PE=1 SV=1	2.80	2.80
P51149	Ras-related protein Rab-7a GN=RAB7A PE=1 SV=1	3.61	3.61
Q15257	Serine/threonine-protein phosphatase 2A activator GN=PTPA PE=1 SV=3	1.78	1.78
A0A024R5H8	RAB6A, member RAS oncogene family, isoform CRA_b GN=RAB6A PE=4 SV=1	2.19	2.19
A4D2P0	Ras-related C3 botulinum toxin substrate 1 (Rho family, small GTP binding protein Rac1) GN=RAC1 PE=2 SV=1	2.62	2.62
Q08945	FACT complex subunit SSRP1 GN=SSRP1 PE=1 SV=1	2.14	2.14
A0A0U1RRH7	Histone H2A PE=3 SV=1	2.09	2.09
D6RBW1	Eukaryotic translation initiation factor 4E GN=EIF4E PE=1 SV=1	2.61	2.61
Q92973	Transportin-1 GN=TNPO1 PE=1 SV=2	3.33	3.33
Q59GM9	Alpha-1,4 glucan phosphorylase (Fragment) PE=2 SV=1	1.95	1.95
P16989	Y-box-binding protein 3 GN=YBX3 PE=1 SV=4	2.84	2.84
B5ME97	Septin 10, isoform CRA_c GN=SEPT10 PE=1 SV=2	1.50	1.50
O95218	Zinc finger Ran-binding domain-containing protein 2 GN=ZRANB2 PE=1 SV=2	2.34	2.34
P62304	Small nuclear ribonucleoprotein E GN=SNRPE PE=1 SV=1	1.76	1.76
Q5EBM0	UMP-CMP kinase 2, mitochondrial GN=CMPK2 PE=1 SV=3	4.13	4.13
Q53H88	Dynactin 2 variant (Fragment) PE=2 SV=1	2.60	2.60
B0I1S9	MYO1B variant protein GN=MYO1B PE=2 SV=1	1.63	1.63
D3DUW5	Dynamin 1-like, isoform CRA_c GN=DNM1L PE=3 SV=1	1.69	1.69
Q12996	Cleavage stimulation factor subunit 3 GN=CSTF3 PE=1 SV=1	2.28	2.28
Q9HBB3	60S ribosomal protein L6 PE=2 SV=1	2.06	2.06

O00487	26S proteasome non-ATPase regulatory subunit 14 GN=PSMD14 PE=1 SV=1	1.91	1.91
B4DHQ3	Phosphoserine aminotransferase PE=2 SV=1	2.67	2.67
Q53FA7	Quinone oxidoreductase PIG3 GN=TP53I3 PE=1 SV=2	2.20	2.20
A0A0S2Z3Q4	V-crk sarcoma virus CT10 oncogene-like protein isoform 1 (Fragment) GN=CRK PE=2 SV=1	2.03	2.03
Q5JR94	40S ribosomal protein S8 GN=RPS8 PE=2 SV=1	1.85	1.85
Q9NY27	Serine/threonine-protein phosphatase 4 regulatory subunit 2 GN=PPP4R2 PE=1 SV=3	2.79	2.79
A2A3R6	40S ribosomal protein S6 GN=RPS6 PE=2 SV=1	1.85	1.85
Q96CN7	Isochorismatase domain-containing protein 1 GN=ISOC1 PE=1 SV=3	2.50	2.50
P31153	S-adenosylmethionine synthase isoform type-2 GN=MAT2A PE=1 SV=1	3.44	3.44
P24592	Insulin-like growth factor-binding protein 6 GN=IGFBP6 PE=1 SV=1	2.73	2.73
P30048	Thioredoxin-dependent peroxide reductase, mitochondrial GN=PRDX3 PE=1 SV=3	3.00	3.00
Q16270	Insulin-like growth factor-binding protein 7 GN=IGFBP7 PE=1 SV=1	4.35	4.35
P62280	40S ribosomal protein S11 GN=RPS11 PE=1 SV=3	1.56	1.56
B4DIS3	Dpy-30-like protein, isoform CRA_b GN=LOC84661 PE=2 SV=1	1.91	1.91
C1PHA2	Tyrosine-protein kinase receptor GN=KIF5B-ALK PE=2 SV=1	1.98	1.98
A0A140VJE8	AP complex subunit beta GN=AP2B1 PE=2 SV=1	1.63	1.63
P84243	Histone H3.3 GN=H3F3A PE=1 SV=2	2.57	2.57
B2R533	cDNA, FLJ92320, highly similar to Homo sapiens glutathione S-transferase theta 2 (GSTT2), mRNA PE=2 SV=1	1.98	1.98
Q6NZI2	Caveolae-associated protein 1 GN=CAVIN1 PE=1 SV=1	2.66	2.66
Q5T5C7	Serine--tRNA ligase, cytoplasmic GN=SARS PE=1 SV=1	2.59	2.59
Q59EJ5	Glutathione S-transferase (Fragment) PE=2 SV=1	3.37	3.37
B4DLN1	cDNA FLJ60124, highly similar to Mitochondrial dicarboxylate carrier PE=2 SV=1	2.54	2.54
P35080	Profilin-2 GN=PFN2 PE=1 SV=3	2.30	2.30
Q7Z4V5	Hepatoma-derived growth factor-related protein 2 GN=HDGFL2 PE=1 SV=1	2.01	2.01
Q59GY2	Ribosomal protein L4 variant (Fragment) PE=2 SV=1	1.65	1.65
G3V180	Dipeptidyl peptidase 3 GN=DPP3 PE=1 SV=1	1.90	1.90
Q8WWM7	Ataxin-2-like protein GN=ATXN2L PE=1 SV=2	1.73	1.73
O95336	6-phosphogluconolactonase GN=PGLS PE=1 SV=2	1.92	1.92
Q9NPF4	Probable tRNA N6-adenosine threonylcarbamoyltransferase GN=OSGEP PE=1 SV=1	2.44	2.44
O15511	Actin-related protein 2/3 complex subunit 5 GN=ARPC5 PE=1 SV=3	1.87	1.87
Q96D15	Reticulocalbin-3 GN=RCN3 PE=1 SV=1	1.54	1.54
Q9NR30	Nucleolar RNA helicase 2 GN=DDX21 PE=1 SV=5	2.59	2.59
Q9NYF8	Bcl-2-associated transcription factor 1 GN=BCLAF1 PE=1 SV=2	2.10	2.10
A0A024R814	Ribosomal protein L7, isoform CRA_a GN=RPL7 PE=4 SV=1	1.65	1.65
Q96I99	Succinate--CoA ligase [GDP-forming] subunit beta, mitochondrial GN=SUCLG2 PE=1 SV=2	3.21	3.21
V9HW48	SH3 domain-binding glutamic acid-rich-like protein GN=HEL-S-115 PE=2 SV=1	2.76	2.76
U5YKD2	MHC class I antigen (Fragment) GN=HLA-A PE=3 SV=1	2.79	2.79
P61457	Pterin-4-alpha-carbinolamine dehydratase GN=PCBD1 PE=1 SV=2	2.44	2.44
P62424	60S ribosomal protein L7a GN=RPL7A PE=1 SV=2	1.54	1.54
Q08257	Quinone oxidoreductase GN=CRYZ PE=1 SV=1	2.52	2.52
O60869	Endothelial differentiation-related factor 1 GN=EDF1 PE=1 SV=1	2.50	2.50
P09914	Interferon-induced protein with tetratricopeptide repeats 1 GN=IFIT1 PE=1 SV=2	2.05	2.05
Q9UNN8	Endothelial protein C receptor GN=PROCR PE=1 SV=1	3.40	3.40
Q96EK6	Glucosamine 6-phosphate N-acetyltransferase GN=GNPNAT1 PE=1 SV=1	2.60	2.60
B0LPF3	Growth factor receptor-bound protein 2, isoform CRA_a GN=GRB2 PE=2 SV=1	2.51	2.51
A0A024R6Y2	Nuclear transport factor 2, isoform CRA_a GN=NUTF2 PE=4 SV=1	2.82	2.82
Q549M8	CLE7 GN=C14orf166 PE=2 SV=1	2.16	2.16
Q92890	Ubiquitin recognition factor in ER-associated degradation protein 1 GN=UFD1 PE=1 SV=3	1.77	1.77
P17980	26S proteasome regulatory subunit 6A GN=PSMC3 PE=1 SV=3	1.92	1.92
C9JEH3	Angio-associated migratory cell protein GN=AAMP PE=1 SV=1	2.18	2.18
K7EM18	Eukaryotic translation initiation factor 1 GN=EIF1 PE=1 SV=1	2.38	2.38
B2R665	cDNA, FLJ92810, highly similar to Homo sapiens protein phosphatase 1G (formerly 2C), magnesium-dependent, gamma isoform (PPM1G), mRNA PE=2 SV=1	3.24	3.24
D6W4Z6	HCG23833, isoform CRA_b GN=hCG_23833 PE=4 SV=1	3.52	3.52
F8WCF6	Actin-related protein 2/3 complex subunit 4 GN=ARPC4-TTLL3 PE=3 SV=1	2.19	2.19
Q9NZM1	Myoferlin GN=MYOF PE=1 SV=1	1.53	1.53

M0R0R2	40S ribosomal protein S5 GN=RPS5 PE=1 SV=1	1.50	1.50
P49753	Acyl-coenzyme A thioesterase 2, mitochondrial GN=ACOT2 PE=1 SV=6	3.50	3.50
P58546	Myotrophin GN=MTPN PE=1 SV=2	2.77	2.77
A0A090N7V5	Chromosome 7 open reading frame 24 GN=C7orf24 PE=4 SV=1	2.22	2.22
A8K6V3	cDNA FLJ78677, highly similar to Homo sapiens splicing factor 3b, subunit 3, 130kDa (SF3B3), mRNA PE=2 SV=1	2.44	2.44
P30419	Glycylpeptide N-tetradecanoyltransferase 1 GN=NMT1 PE=1 SV=2	2.55	2.55
P06132	Uroporphyrinogen decarboxylase GN=UROD PE=1 SV=2	2.13	2.13
P35244	Replication protein A 14 kDa subunit GN=RPA3 PE=1 SV=1	2.46	2.46
P13500	C-C motif chemokine 2 GN=CCL2 PE=1 SV=1	5.88	5.88
Q16352	Alpha-internexin GN=INA PE=1 SV=2	2.10	2.10
E9PF18	Hydroxyacyl-coenzyme A dehydrogenase, mitochondrial GN=HADH PE=1 SV=2	3.67	3.67
H0YNJ6	GMP reductase GN=GMPR2 PE=1 SV=1	1.84	1.84
A8K168	Malic enzyme PE=2 SV=1	1.96	1.96
P62263	40S ribosomal protein S14 GN=RPS14 PE=1 SV=3	1.42	1.42
A0A024QZD5	Small nuclear ribonucleoprotein 70kDa polypeptide (RNP antigen), isoform CRA_b GN=SNRP70 PE=4 SV=1	3.36	3.36
P55084	Trifunctional enzyme subunit beta, mitochondrial GN=HADHB PE=1 SV=3	2.02	2.02
B7Z268	Single-stranded DNA binding protein 1, isoform CRA_c GN=SSBP1 PE=2 SV=1	1.74	1.74
Q15942	Zyxin GN=ZYX PE=1 SV=1	2.66	2.66
A0A024R962	HCG40889, isoform CRA_b GN=hCG_40889 PE=4 SV=1	2.78	2.78
Q59GE4	Ribosomal protein S10 variant (Fragment) PE=4 SV=1	1.80	1.80
A0A024RCJ8	HCG1821276, isoform CRA_a GN=hCG_1821276 PE=4 SV=1	1.93	1.93
Q8NBS9	Thioredoxin domain-containing protein 5 GN=TXNDC5 PE=1 SV=2	2.04	2.04
O43818	U3 small nucleolar RNA-interacting protein 2 GN=RRP9 PE=1 SV=1	1.45	1.45
Q59FG9	Chondroitin sulfate proteoglycan 2 (Versican) variant (Fragment) PE=2 SV=1	4.80	4.80
A0A1U9X8E2	Proteasome subunit beta type PE=3 SV=1	2.22	2.22
P52788	Spermine synthase GN=SMS PE=1 SV=2	1.78	1.78
P49411	Elongation factor Tu, mitochondrial GN=TUFM PE=1 SV=2	2.30	2.30
Q8TDJ5	Tyrosine-protein kinase receptor GN=TFG/ALK fusion PE=2 SV=1	3.03	3.03
O95292	Vesicle-associated membrane protein-associated protein B/C GN=VAPB PE=1 SV=3	3.98	3.98
P61956	Small ubiquitin-related modifier 2 GN=SUMO2 PE=1 SV=3	4.19	4.19
Q9UBQ5	Eukaryotic translation initiation factor 3 subunit K GN=EIF3K PE=1 SV=1	1.65	1.65
O76003	Glutaredoxin-3 GN=GLRX3 PE=1 SV=2	2.67	2.67
A0A024R7S3	Clathrin light chain GN=CLTB PE=3 SV=1	2.10	2.10
Q9UJ70	N-acetyl-D-glucosamine kinase GN=NAGK PE=1 SV=4	3.16	3.16
P32455	Guanylate-binding protein 1 GN=GBP1 PE=1 SV=2	3.40	3.40
P62750	60S ribosomal protein L23a GN=RPL23A PE=1 SV=1	1.23	1.23
O95817	BAG family molecular chaperone regulator 3 GN=BAG3 PE=1 SV=3	1.79	1.79
O15371	Eukaryotic translation initiation factor 3 subunit D GN=EIF3D PE=1 SV=1	1.94	1.94
A0A0A6YY92	Adenylosuccinate lyase GN=ADSL PE=1 SV=1	1.72	1.72
P27694	Replication protein A 70 kDa DNA-binding subunit GN=RPA1 PE=1 SV=2	1.60	1.60
B2RB23	cDNA, FLJ95265, highly similar to Homo sapiens acetyl-Coenzyme A acyltransferase 2 (mitochondrial 3-oxoacyl-Coenzyme A thiolase) (ACAA2), nuclear gene encoding mitochondrial protein, mRNA PE=2 SV=1	2.67	2.67
Q14767	Latent-transforming growth factor beta-binding protein 2 GN=LTBP2 PE=1 SV=3	2.04	2.04
P55735	Protein SEC13 homolog GN=SEC13 PE=1 SV=3	1.56	1.56
A0A024R4M0	40S ribosomal protein S9 GN=RPS9 PE=1 SV=1	2.09	2.09
P38606	V-type proton ATPase catalytic subunit A GN=ATP6V1A PE=1 SV=2	2.73	2.73
B5BUE6	ATP-dependent RNA helicase DDX5 (Fragment) GN=DDX5 PE=2 SV=1	2.36	2.36
Q9Y3B8	Oligoribonuclease, mitochondrial GN=REXO2 PE=1 SV=3	1.97	1.97
A0A087WUF6	Fibroblast growth factor GN=FGF2 PE=1 SV=2	2.08	2.08
B2R4D5	Actin-related protein 2/3 complex subunit 3 PE=2 SV=1	1.63	1.63
E9PB61	THO complex subunit 4 GN=ALYREF PE=1 SV=1	2.75	2.75
B1AKJ5	Nardilysin (N-arginine dibasic convertase), isoform CRA_d GN=NRDC PE=1 SV=1	2.43	2.43
B2R491	40S ribosomal protein S4 GN=RPS4X PE=2 SV=1	1.07	1.07
Q86TI2	Dipeptidyl peptidase 9 GN=DPP9 PE=1 SV=3	2.19	2.19

P15880	40S ribosomal protein S2 GN=RPS2 PE=1 SV=2	1.80	1.80
Q9Y3C6	Peptidyl-prolyl cis-trans isomerase-like 1 GN=PPIL1 PE=1 SV=1	2.70	2.70
Q6EMK4	Vasorin GN=VASN PE=1 SV=1	1.86	1.86
A0A024RAR8	Aminopeptidase GN=ARTS-1 PE=3 SV=1	2.03	2.03
Q16186	Proteasomal ubiquitin receptor ADRM1 GN=ADRM1 PE=1 SV=2	1.69	1.69
Q99471	Prefoldin subunit 5 GN=PFDN5 PE=1 SV=2	3.23	3.23
Q16666	Gamma-interferon-inducible protein 16 GN=IFI16 PE=1 SV=3	1.75	1.75
Q05DF2	SF3A2 protein (Fragment) GN=SF3A2 PE=2 SV=1	1.65	1.65
P55263	Adenosine kinase GN=ADK PE=1 SV=2	1.70	1.70
Q9NSD9	Phenylalanine--tRNA ligase beta subunit GN=FARSB PE=1 SV=3	2.37	2.37
P62081	40S ribosomal protein S7 GN=RPS7 PE=1 SV=1	2.14	2.14
D6RFG8	Deoxycytidine kinase GN=DCK PE=1 SV=1	2.29	2.29
A0A087WY85	Ubiquitin-conjugating enzyme E2 D3 GN=UBE2D3 PE=1 SV=1	2.60	2.60
A0A140GPP7	Prolyl endopeptidase FAP PE=3 SV=1	1.46	1.46
A0A087WUB9	Beta-catenin-like protein 1 GN=CTNNBL1 PE=1 SV=1	2.68	2.68
A6XND9	Beta-2-microglobulin PE=2 SV=1	2.45	2.45
A0A2R8YD14	40S ribosomal protein S24 GN=RPS24 PE=1 SV=1	1.92	1.92
P41227	N-alpha-acetyltransferase 10 GN=NAA10 PE=1 SV=1	1.46	1.46
A0A024R7U6	DNA helicase GN=MCM4 PE=3 SV=1	2.37	2.37
A0A140VK41	Testicular secretory protein Li 41 PE=2 SV=1	4.47	4.47
P46776	60S ribosomal protein L27a GN=RPL27A PE=1 SV=2	1.34	1.34
Q59G75	Isoleucyl-tRNA synthetase, cytoplasmic variant (Fragment) PE=2 SV=1	2.14	2.14
A0A024R329	GDP-mannose pyrophosphorylase B, isoform CRA_a GN=GMPPB PE=4 SV=1	2.16	2.16
A0A024R4D1	COP9 constitutive photomorphogenic homolog subunit 8 (Arabidopsis), isoform CRA_a GN=COPS8 PE=4 SV=1	1.70	1.70
X5D2M8	Major vault protein isoform A (Fragment) GN=MVP PE=2 SV=1	1.65	1.65
B2R8Y9	Tissue factor pathway inhibitor PE=2 SV=1	1.28	1.28
P39023	60S ribosomal protein L3 GN=RPL3 PE=1 SV=2	1.53	1.53
A8K9B9	cDNA FLJ77391, highly similar to Homo sapiens EH-domain containing 4 (EHD4), mRNA PE=2 SV=1	1.29	1.29
P36551	Oxygen-dependent coproporphyrinogen-III oxidase, mitochondrial GN=CPOX PE=1 SV=3	2.01	2.01
B2R4C1	cDNA, FLJ92036, highly similar to Homo sapiens ribosomal protein L31 (RPL31), mRNA PE=2 SV=1	2.56	2.56
P17812	CTP synthase 1 GN=CTPS1 PE=1 SV=2	2.83	2.83
O95433	Activator of 90 kDa heat shock protein ATPase homolog 1 GN=AHSA1 PE=1 SV=1	1.58	1.58
O00233	26S proteasome non-ATPase regulatory subunit 9 GN=PSMD9 PE=1 SV=3	2.24	2.24
P47813	Eukaryotic translation initiation factor 1A, X-chromosomal GN=EIF1AX PE=1 SV=2	2.47	2.47
Q9UK45	U6 snRNA-associated Sm-like protein LSm7 GN=LSM7 PE=1 SV=1	1.74	1.74
Q15437	Protein transport protein Sec23B GN=SEC23B PE=1 SV=2	2.39	2.39
O75663	TIP41-like protein GN=TIPRL PE=1 SV=2	2.08	2.08
Q9UNS2	COP9 signalosome complex subunit 3 GN=COPS3 PE=1 SV=3	1.25	1.25
H0YMD1	Low-density lipoprotein receptor GN=LDLR PE=1 SV=1	4.04	4.04
Q9BTY2	Plasma alpha-L-fucosidase GN=FUCA2 PE=1 SV=2	3.11	3.11
Q15008	26S proteasome non-ATPase regulatory subunit 6 GN=PSMD6 PE=1 SV=1	2.49	2.49
Q58EY4	SWI/SNF related, matrix associated, actin dependent regulator of chromatin, subfamily c, member 1 GN=SMARCC1 PE=2 SV=1	1.40	1.40
P35998	26S proteasome regulatory subunit 7 GN=PSMC2 PE=1 SV=3	2.00	2.00
Q13501	Sequestosome-1 GN=SQSTM1 PE=1 SV=1	2.26	2.26
B4DN80	Peptidyl-prolyl cis-trans isomerase PE=2 SV=1	3.16	3.16
Q6FGH9	Dynein light chain GN=DNCL1 PE=2 SV=1	2.33	2.33
P53618	Coatomer subunit beta GN=COPB1 PE=1 SV=3	1.63	1.63
A0A024R3V7	NIF3-like protein 1 GN=NIF3L1 PE=3 SV=1	1.92	1.92
A0A2R8Y6X2	D-aminoacyl-tRNA deacylase GN=DTD1 PE=1 SV=1	2.53	2.53
P51668	Ubiquitin-conjugating enzyme E2 D1 GN=UBE2D1 PE=1 SV=1	1.34	1.34
Q15717	ELAV-like protein 1 GN=ELAVL1 PE=1 SV=2	1.78	1.78
P49792	E3 SUMO-protein ligase RanBP2 GN=RANBP2 PE=1 SV=2	1.85	1.85
P62917	60S ribosomal protein L8 GN=RPL8 PE=1 SV=2	1.11	1.11

B3KNI2	cDNA FLJ14650 fis, clone NT2RP2002185, highly similar to Ubiquilin-1 PE=2 SV=1	1.76	1.76
Q5H9N4	Uncharacterized protein DKFZp686L20222 GN=DKFZp686L20222 PE=3 SV=1	1.27	1.27
A0A024R6W2	Nudix (Nucleoside diphosphate linked moiety X)-type motif 21, isoform CRA_a GN=NUDT21 PE=4 SV=1	2.04	2.04
Q06210	Glutamine--fructose-6-phosphate aminotransferase [isomerizing] 1 GN=GFPT1 PE=1 SV=3	1.36	1.36
A8K8N7	Phosphoribosylformylglycinamidine synthase (FGAR amidotransferase), isoform CRA_b GN=PFAS PE=2 SV=1	1.28	1.28
B2R4C0	60S ribosomal protein L18a PE=2 SV=1	1.80	1.80
Q96ST2	Protein IWS1 homolog GN=IWS1 PE=1 SV=2	3.55	3.55
A0A024RCW3	Ribosomal protein GN=RPL10A PE=3 SV=1	1.71	1.71
Q99426	Tubulin-folding cofactor B GN=TBCB PE=1 SV=2	2.19	2.19
P28072	Proteasome subunit beta type-6 GN=PSMB6 PE=1 SV=4	1.85	1.85
O75942	Major prion protein GN=PRNP PE=3 SV=2	2.01	2.01
B4E3D4	cDNA FLJ56293, highly similar to Transmembrane glycoprotein NMB PE=2 SV=1	3.10	3.10
B2RCM2	cDNA, FLJ96156, highly similar to Homo sapiens leucyl-tRNA synthetase (LARS), mRNA PE=2 SV=1	2.27	2.27
P04181	Ornithine aminotransferase, mitochondrial GN=OAT PE=1 SV=1	2.72	2.72
Q96M27	Protein PRRC1 GN=PRRC1 PE=1 SV=1	3.53	3.53
Q9BXV9	EKC/KEOPS complex subunit GON7 GN=GON7 PE=1 SV=2	1.71	1.71
Q86U42	Polyadenylate-binding protein 2 GN=PABPN1 PE=1 SV=3	2.04	2.04
D3DQU2	Tripeptidyl peptidase I, isoform CRA_a GN=TPP1 PE=4 SV=1	1.60	1.60
P25774	Cathepsin S GN=CTSS PE=1 SV=3	2.06	2.06
Q9NQR4	Omega-amidase NIT2 GN=NIT2 PE=1 SV=1	2.67	2.67
A0A090N7U0	Cullin 1, isoform CRA_b GN=CUL1 PE=3 SV=1	2.33	2.33
B4DJV9	cDNA FLJ60607, highly similar to Acyl-protein thioesterase 1 PE=2 SV=1	2.09	2.09
P98066	Tumor necrosis factor-inducible gene 6 protein GN=TNFAIP6 PE=1 SV=2	4.84	4.84
E9PR17	CD59 glycoprotein PE=1 SV=1	2.47	2.47
Q59F22	Interferon stimulated gene 20kDa variant (Fragment) PE=2 SV=1	1.90	1.90
Q13564	NEDD8-activating enzyme E1 regulatory subunit GN=NAE1 PE=1 SV=1	1.69	1.69
Q14203	Dynactin subunit 1 GN=DCTN1 PE=1 SV=3	1.67	1.67
B4E284	cDNA FLJ51188, highly similar to N-acetylglucosamine-6-sulfatase (EC3.1.6.14) PE=2 SV=1	2.02	2.02
C9JCC6	Dr1-associated corepressor GN=DRAP1 PE=1 SV=1	1.58	1.58
Q53FI7	Four and a half LIM domains 1 variant (Fragment) PE=2 SV=1	2.44	2.44
Q9UHY7	Enolase-phosphatase E1 GN=ENOPH1 PE=1 SV=1	1.99	1.99
P61764	Syntaxin-binding protein 1 GN=STXBP1 PE=1 SV=1	1.49	1.49
P53597	Succinate--CoA ligase [ADP/GDP-forming] subunit alpha, mitochondrial GN=SUCLG1 PE=1 SV=4	2.58	2.58
P23368	NAD-dependent malic enzyme, mitochondrial GN=ME2 PE=1 SV=1	2.46	2.46
Q53T99	Ribosome biogenesis protein WDR12 GN=WDR12 PE=2 SV=1	1.53	1.53
B3KUJ0	cDNA FLJ39996 fis, clone STOMA2002166, highly similar to Splicing factor 3B subunit 4 PE=2 SV=1	1.91	1.91
P54886	Delta-1-pyrroline-5-carboxylate synthase GN=ALDH18A1 PE=1 SV=2	1.18	1.18
P38117	Electron transfer flavoprotein subunit beta GN=ETFB PE=1 SV=3	2.08	2.08
Q96QK1	Vacuolar protein sorting-associated protein 35 GN=VPS35 PE=1 SV=2	2.36	2.36
B3KY60	cDNA FLJ16777 fis, clone BRHIP2029567, highly similar to Cell division cycle 5-like protein PE=2 SV=1	3.17	3.17
Q96C23	Aldose 1-epimerase GN=GALM PE=1 SV=1	2.66	2.66
Q53G42	mRNA decapping enzyme variant (Fragment) PE=2 SV=1	2.41	2.41
P27635	60S ribosomal protein L10 GN=RPL10 PE=1 SV=4	1.29	1.29
Q7Z4Y4	GTP:AMP phosphotransferase AK3, mitochondrial GN=AK3 PE=2 SV=1	3.80	3.80
B2R7E8	cDNA, FLJ93412, highly similar to Homo sapiens replication protein A2, 32kDa (RPA2), mRNA PE=2 SV=1	2.49	2.49
P60866	40S ribosomal protein S20 GN=RPS20 PE=1 SV=1	2.66	2.66
A8KAP3	cDNA FLJ78483, highly similar to Homo sapiens elongation factor Tu GTP binding domain containing 2 (EFTUD2), mRNA PE=2 SV=1	2.07	2.07
P42126	Enoyl-CoA delta isomerase 1, mitochondrial GN=ECI1 PE=1 SV=1	2.13	2.13
A0A0C4DGQ5	Calpain small subunit 1 GN=CAPNS1 PE=1 SV=1	2.83	2.83

B3V096	BetaCstF-64 variant 2 GN=CSTF2 PE=2 SV=1	3.45	3.45
Q06124	Tyrosine-protein phosphatase non-receptor type 11 GN=PTPN11 PE=1 SV=2	2.98	2.98
B2RCP7	cDNA, FLJ96197, highly similar to Homo sapiens connective tissue growth factor (CTGF), mRNA PE=2 SV=1	1.38	1.38
P31942	Heterogeneous nuclear ribonucleoprotein H3 GN=HNRNPH3 PE=1 SV=2	1.98	1.98
V9HW44	Epididymis secretory protein Li 303 GN=HEL-S-303 PE=2 SV=1	1.45	1.45
O60565	Gremlin-1 GN=GREM1 PE=1 SV=1	1.63	1.63
B5BUB1	RuvB-like helicase (Fragment) GN=RUVBL1 PE=2 SV=1	1.68	1.68
P38159	RNA-binding motif protein, X chromosome GN=RBMX PE=1 SV=3	2.18	2.18
A0A286YFF7	Palmitoyl-protein thioesterase 1 GN=PPT1 PE=1 SV=1	2.33	2.33
Q8N543	Prolyl 3-hydroxylase OGFOD1 GN=OGFOD1 PE=1 SV=1	1.48	1.48
P55809	Succinyl-CoA:3-ketoacid coenzyme A transferase 1, mitochondrial GN=OXCT1 PE=1 SV=1	2.82	2.82
A0A024R2Q2	Ubiquitin-conjugating enzyme E2E 2 (UBC4/5 homolog, yeast), isoform CRA_a GN=UBE2E2 PE=3 SV=1	2.18	2.18
P62277	40S ribosomal protein S13 GN=RPS13 PE=1 SV=2	2.16	2.16
Q6FIE5	PHP14 protein GN=PHP14 PE=2 SV=1	2.40	2.40
H3BQK0	ATP-dependent RNA helicase DDX19B GN=DDX19B PE=1 SV=1	2.25	2.25
B5MBZ0	Echinoderm microtubule-associated protein-like 4 GN=EML4 PE=1 SV=3	2.52	2.52
A0A024RA75	3-hydroxyisobutyrate dehydrogenase GN=HIBADH PE=3 SV=1	1.81	1.81
A0A140VK53	Testicular secretory protein Li 53 PE=2 SV=1	3.94	3.94
Q5VWC4	26S proteasome non-ATPase regulatory subunit 4 GN=PSMD4 PE=1 SV=1	2.29	2.29
O00231	26S proteasome non-ATPase regulatory subunit 11 GN=PSMD11 PE=1 SV=3	2.07	2.07
P36542	ATP synthase subunit gamma, mitochondrial GN=ATP5F1C PE=1 SV=1	2.15	2.15
Q9NQC3	Reticulon-4 GN=RTN4 PE=1 SV=2	1.37	1.37
A8K6Y2	Serine/threonine-protein phosphatase 2A 56 kDa regulatory subunit PE=2 SV=1	2.56	2.56
O96019	Actin-like protein 6A GN=ACTL6A PE=1 SV=1	1.97	1.97
A0A096LPI6	Uncharacterized protein (Fragment) PE=4 SV=2	1.75	1.75
P37108	Signal recognition particle 14 kDa protein GN=SRP14 PE=1 SV=2	2.93	2.93
P09668	Pro-cathepsin H GN=CTSH PE=1 SV=4	1.40	1.40
A0A0G2JH68	Protein diaphanous homolog 1 GN=DIAPH1 PE=1 SV=1	1.59	1.59
E5KN59	Peptidyl-prolyl cis-trans isomerase D PE=4 SV=1	1.76	1.76
B2RD19	cDNA, FLJ96419, highly similar to Homo sapiens fructosamine-3-kinase-related protein (FN3KRP), mRNA PE=2 SV=1	1.66	1.66
P09496	Clathrin light chain A GN=CLTA PE=1 SV=1	1.77	1.77
H0YHG0	Uncharacterized protein (Fragment) PE=1 SV=1	1.97	1.97
Q5T446	Uroporphyrinogen decarboxylase (Fragment) GN=UROD PE=1 SV=1	1.04	1.04
A8K7D9	Importin subunit alpha PE=2 SV=1	3.59	3.59
A8K492	cDNA FLJ76789, highly similar to Homo sapiens methionine-tRNA synthetase (MARS), mRNA PE=2 SV=1	1.45	1.45
B7Z1Z5	cDNA FLJ57265, highly similar to Neurotrimin PE=2 SV=1	1.62	1.62
H3BN98	Uncharacterized protein (Fragment) PE=4 SV=2	2.33	2.33
P62913	60S ribosomal protein L11 GN=RPL11 PE=1 SV=2	1.90	1.90
D3DSY9	Farnesyltransferase, CAAX box, alpha, isoform CRA_a GN=FNTA PE=4 SV=1	3.51	3.51
Q13867	Bleomycin hydrolase GN=BLMH PE=1 SV=1	1.49	1.49
H0YJ75	Serine/threonine-protein phosphatase 2A 56 kDa regulatory subunit gamma isoform (Fragment) GN=PPP2R5C PE=1 SV=1	2.03	2.03
Q9BY44	Eukaryotic translation initiation factor 2A GN=EIF2A PE=1 SV=3	2.43	2.43
A8K6V0	cDNA FLJ78676, highly similar to Homo sapiens SEC24 related gene family, member D (SEC24D), mRNA PE=2 SV=1	1.23	1.23
Q9GZZ1	N-alpha-acetyltransferase 50 GN=NAA50 PE=1 SV=1	2.91	2.91
G3V5T9	Cyclin-dependent kinase 2, isoform CRA_c GN=CDK2 PE=1 SV=1	1.99	1.99
Q86UA3	Chromosome 12 open reading frame 10, isoform CRA_b GN=C12orf10 PE=1 SV=1	3.34	3.34
Q0VDC6	Peptidylprolyl isomerase GN=FKBP1A PE=1 SV=1	1.83	1.83
A0A0A6YYL6	Protein RPL17-C18orf32 GN=RPL17-C18orf32 PE=3 SV=1	1.57	1.57
Q96B97	SH3 domain-containing kinase-binding protein 1 GN=SH3KBP1 PE=1 SV=2	3.70	3.70
P46109	Crk-like protein GN=CRKL PE=1 SV=1	2.05	2.05
O43488	Aflatoxin B1 aldehyde reductase member 2 GN=AKR7A2 PE=1 SV=3	1.63	1.63

P61106	Ras-related protein Rab-14 GN=RAB14 PE=1 SV=4	2.34	2.34
Q9HA77	Probable cysteine--tRNA ligase, mitochondrial GN=CARS2 PE=1 SV=1	3.81	3.81
P30040	Endoplasmic reticulum resident protein 29 GN=ERP29 PE=1 SV=4	1.72	1.72
A0A024R8A7	HCG31253, isoform CRA_a GN=hCG_31253 PE=4 SV=1	2.46	2.46
Q6FH49	NNMT protein GN=NNMT PE=2 SV=1	2.93	2.93
P43155	Carnitine O-acetyltransferase GN=CRAT PE=1 SV=5	3.37	3.37
H3BQJ5	Nucleolar protein 3 (Fragment) GN=NOL3 PE=1 SV=2	1.52	1.52
Q8WZ82	Esterase OVCA2 GN=OVCA2 PE=1 SV=1	2.31	2.31
B3KPC7	Actin-related protein 2/3 complex subunit 5 PE=2 SV=1	1.07	1.07
Q32P28	Prolyl 3-hydroxylase 1 GN=P3H1 PE=1 SV=2	1.59	1.59
Q6PKG0	La-related protein 1 GN=LARP1 PE=1 SV=2	1.71	1.71
P18827	Syndecan-1 GN=SDC1 PE=1 SV=3	2.81	2.81
Q9UBB4	Ataxin-10 GN=ATXN10 PE=1 SV=1	1.81	1.81
Q9BZK7	F-box-like/WD repeat-containing protein TBL1XR1 GN=TBL1XR1 PE=1 SV=1	2.70	2.70
Q05048	Cleavage stimulation factor subunit 1 GN=CSTF1 PE=1 SV=1	2.55	2.55
A0A140VJZ1	Ubiquitin carboxyl-terminal hydrolase PE=2 SV=1	2.56	2.56
P54105	Methylosome subunit pICln GN=CLNS1A PE=1 SV=1	1.70	1.70
Q9BZM5	UL16-binding protein 2 GN=ULBP2 PE=1 SV=1	1.12	1.12
P49458	Signal recognition particle 9 kDa protein GN=SRP9 PE=1 SV=2	1.58	1.58
O14561	Acyl carrier protein, mitochondrial GN=NDUFAB1 PE=1 SV=3	2.67	2.67
A8K2Z3	cDNA FLJ76092, highly similar to Homo sapiens 5'-nucleotidase, cytosolic II-like 1 (NT5C2L1), mRNA PE=2 SV=1	3.77	3.77
J3KQ41	COP9 signalosome complex subunit 7b GN=COPS7B PE=1 SV=1	1.27	1.27
Q13630	GDP-L-fucose synthase GN=TSTA3 PE=1 SV=1	4.54	4.54
A8K6A7	Alpha-mannosidase PE=2 SV=1	2.61	2.61
Q8WVX7	Ribosomal protein S19 (Fragment) PE=2 SV=1	1.67	1.67
A0A024R7E3	DNA (cytosine-5)-methyltransferase GN=DNMT1 PE=3 SV=1	1.20	1.20
J3QQ67	60S ribosomal protein L18 (Fragment) GN=RPL18 PE=1 SV=1	0.96	0.96
A0A1B0GVH5	Alpha-ketoglutarate-dependent dioxygenase FTO GN=FTO PE=1 SV=1	1.66	1.66
Q08722	Leukocyte surface antigen CD47 GN=CD47 PE=1 SV=1	1.39	1.39
O95831	Apoptosis-inducing factor 1, mitochondrial GN=AIFM1 PE=1 SV=1	2.35	2.35
B2R6P3	cDNA, FLJ93047, highly similar to Homo sapiens matrix metallopeptidase 14 (membrane-inserted) (MMP14), mRNA PE=2 SV=1	2.18	2.18
U5IT74	MHC class I antigen (Fragment) GN=HLA-C PE=3 SV=1	2.29	2.29
A0A140VJL0	3-hydroxyisobutyryl-CoA hydrolase, mitochondrial PE=2 SV=1	2.18	2.18
Q6MZT3	Uncharacterized protein DKFZp686C1054 GN=DKFZp686C1054 PE=2 SV=1	2.31	2.31
A0A024R7J0	Protein kinase, cAMP-dependent, catalytic, alpha, isoform CRA_c GN=PRKACA PE=3 SV=1	2.68	2.68
P42574	Caspase-3 GN=CASP3 PE=1 SV=2	2.04	2.04
O75367	Core histone macro-H2A.1 GN=H2AFY PE=1 SV=4	1.85	1.85
Q9H1B7	Interferon regulatory factor 2-binding protein-like GN=IRF2BPL PE=1 SV=1	1.36	1.36
Q53XJ5	Peptidylprolyl isomerase GN=FKBP2 PE=2 SV=1	2.16	2.16
Q96DB5	Regulator of microtubule dynamics protein 1 GN=RMDN1 PE=1 SV=1	2.75	2.75
Q8NFH4	Nucleoporin Nup37 GN=NUP37 PE=1 SV=1	2.67	2.67
A0A1B0GW23	ABHD14A-ACY1 readthrough (Fragment) GN=ABHD14A-ACY1 PE=4 SV=1	3.02	3.02
Q59EI9	ADP,ATP carrier protein, liver isoform T2 variant (Fragment) PE=2 SV=1	0.95	0.95
B2RBA6	DNA replication licensing factor MCM7 GN=MCM7 PE=2 SV=1	1.40	1.40
P16298	Serine/threonine-protein phosphatase 2B catalytic subunit beta isoform GN=PPP3CB PE=1 SV=2	3.05	3.05
A0A024R0N6	Spectrin beta chain GN=SPTBN4 PE=3 SV=1	1.64	1.64
R9S3C3	p14ARF/p16INK4a fusion protein GN=p14ARF PE=2 SV=1	1.26	1.26
P60673	Profilin-3 GN=PFN3 PE=2 SV=1	2.91	2.91
Q4LE60	TNPO2 variant protein (Fragment) GN=TNPO2 variant protein PE=2 SV=1	1.21	1.21
Q6UWP8	Suprabasin GN=SBSN PE=1 SV=2	3.17	3.17
Q53H82	Endoribonuclease LACTB2 GN=LACTB2 PE=1 SV=2	1.29	1.29
P11388	DNA topoisomerase 2-alpha GN=TOP2A PE=1 SV=3	2.86	2.86
Q10713	Mitochondrial-processing peptidase subunit alpha GN=PMPCA PE=1 SV=2	3.86	3.86
P02462	Collagen alpha-1(IV) chain GN=COL4A1 PE=1 SV=4	1.19	1.19

P61353	60S ribosomal protein L27 GN=RPL27 PE=1 SV=2	2.76	2.76
Q92990	Glomulin GN=GLMN PE=1 SV=2	1.57	1.57
B2R9W9	Craniofacial development protein 1 PE=2 SV=1	2.13	2.13
Q58FF9	Heat shock protein 90Af GN=HSP90Af PE=2 SV=1	2.13	2.13
H3BNC9	Uncharacterized protein PE=3 SV=2	1.90	1.90
O75935	Dynactin subunit 3 GN=DCTN3 PE=1 SV=1	1.37	1.37
P13473	Lysosome-associated membrane glycoprotein 2 GN=LAMP2 PE=1 SV=2	2.04	2.04
B2R8D1	cDNA, FLJ93841, highly similar to Homo sapiens nitrilase 1 (NIT1), mRNA PE=2 SV=1	1.72	1.72
B2RAR3	Queuine tRNA-ribosyltransferase catalytic subunit 1 GN=QTRT1 PE=2 SV=1	2.21	2.21
Q9NRN7	L-aminoadipate-semialdehyde dehydrogenase-phosphopantetheinyl transferase GN=AASDHPPT PE=1 SV=2	2.39	2.39
P10606	Cytochrome c oxidase subunit 5B, mitochondrial GN=COX5B PE=1 SV=2	1.98	1.98
A0A0N9MXA6	MHC class I antigen (Fragment) GN=HLA-A PE=3 SV=1	3.02	3.02
P49773	Histidine triad nucleotide-binding protein 1 GN=HINT1 PE=1 SV=2	3.36	3.36
A0A140VK39	Protein phosphatase methylesterase 1 PE=2 SV=1	1.50	1.50
B3KSH8	cDNA FLJ36241 fis, clone THYMU2001622, highly similar to Inositol polyphosphate 1-phosphatase PE=2 SV=1	2.31	2.31
Q9H074	Polyadenylate-binding protein-interacting protein 1 GN=PAIP1 PE=1 SV=1	2.05	2.05
Q9H773	dCTP pyrophosphatase 1 GN=DCTPP1 PE=1 SV=1	5.58	5.58
Q7Z7Q8	C-C motif chemokine GN=MCP-3 PE=3 SV=1	4.14	4.14
P62269	40S ribosomal protein S18 GN=RPS18 PE=1 SV=3	1.36	1.36
A0A140VJT0	Serine/threonine-protein phosphatase 2A 55 kDa regulatory subunit B PE=2 SV=1	2.97	2.97
A8KAE0	cDNA FLJ78476, highly similar to Homo sapiens WD repeat and HMG-box DNA binding protein 1 (WDHD1), transcript variant 1, mRNA PE=2 SV=1	1.32	1.32
O95747	Serine/threonine-protein kinase OSR1 GN=OXSR1 PE=1 SV=1	4.42	4.42
Q9HCU0	Endosialin GN=CD248 PE=1 SV=1	3.38	3.38
A0A024R7W9	COP9 constitutive photomorphogenic homolog subunit 5 (Arabidopsis), isoform CRA_a GN=COPS5 PE=2 SV=1	1.12	1.12
Q00325	Phosphate carrier protein, mitochondrial GN=SLC25A3 PE=1 SV=2	1.32	1.32
A8K3A8	cDNA FLJ75085, highly similar to Homo sapiens glutaminyl-tRNA synthetase (QARS), mRNA PE=2 SV=1	2.38	2.38
Q7Z417	Nuclear fragile X mental retardation-interacting protein 2 GN=NUFIP2 PE=1 SV=1	1.86	1.86
A0A024R059	3-hydroxy-3-methylglutaryl coenzyme A synthase GN=HMGCS1 PE=3 SV=1	2.45	2.45
A0A0S2Z404	Regulator of chromosome condensation 1 isoform 2 (Fragment) GN=RCC1 PE=2 SV=1	2.04	2.04
A0A024R482	GDP-mannose pyrophosphorylase A, isoform CRA_a GN=GMPPA PE=4 SV=1	1.85	1.85
P62857	40S ribosomal protein S28 GN=RPS28 PE=1 SV=1	1.64	1.64
Q6DK41	Protein Wnt (Fragment) GN=WNT5A PE=2 SV=2	1.41	1.41
Q9NUL5	Repressor of yield of DENV protein GN=RYDEN PE=1 SV=2	1.75	1.75
Q5VW32	BRO1 domain-containing protein BROX GN=BROX PE=1 SV=1	2.15	2.15
Q14554	Protein disulfide-isomerase A5 GN=PDIA5 PE=1 SV=1	1.57	1.57
Q9H4A6	Golgi phosphoprotein 3 GN=GOLPH3 PE=1 SV=1	1.74	1.74
B2R761	cDNA, FLJ93299, highly similar to Homo sapiens sterol carrier protein 2 (SCP2), mRNA PE=2 SV=1	2.79	2.79
A0A0A0MQR2	Replication termination factor 2 GN=RTF2 PE=1 SV=1	1.71	1.71
Q59GW6	Acetyl-CoA acetyltransferase, cytosolic variant (Fragment) PE=2 SV=1	1.54	1.54
P26447	Protein S100-A4 GN=S100A4 PE=1 SV=1	1.75	1.75
A1X283	SH3 and PX domain-containing protein 2B GN=SH3PXD2B PE=1 SV=3	2.19	2.19
B4DX46	cDNA FLJ52663, highly similar to SET and MYND domain-containing protein 5 PE=2 SV=1	1.70	1.70
Q13131	5'-AMP-activated protein kinase catalytic subunit alpha-1 GN=PRKAA1 PE=1 SV=4	1.71	1.71
A0A140VJC9	Lysophospholipase II, isoform CRA_f GN=LYPLA2 PE=2 SV=1	2.72	2.72
Q9BV57	1,2-dihydroxy-3-keto-5-methylthiopentene dioxygenase GN=ADI1 PE=1 SV=1	1.87	1.87
O76021	Ribosomal L1 domain-containing protein 1 GN=RSL1D1 PE=1 SV=3	1.77	1.77
E5RIM7	Copper transport protein ATOX1 GN=ATOX1 PE=1 SV=1	3.04	3.04
P11802	Cyclin-dependent kinase 4 GN=CDK4 PE=1 SV=2	1.21	1.21
A0A140VJJ2	S-formylglutathione hydrolase GN=ESD PE=2 SV=1	2.72	2.72
P19525	Interferon-induced, double-stranded RNA-activated protein kinase GN=EIF2AK2 PE=1 SV=2	2.00	2.00
P62829	60S ribosomal protein L23 GN=RPL23 PE=1 SV=1	1.49	1.49

Q9NQ88	Fructose-2,6-bisphosphatase TIGAR GN=TIGAR PE=1 SV=1	2.38	2.38
A8K6T5	cDNA FLJ75144, highly similar to Homo sapiens ash2 (absent, small, or homeotic)-like (ASH2L), mRNA PE=2 SV=1	1.36	1.36
P84098	60S ribosomal protein L19 GN=RPL19 PE=1 SV=1	2.45	2.45
P61081	NEDD8-conjugating enzyme Ubc12 GN=UBE2M PE=1 SV=1	1.94	1.94
A0A024R9P6	Family with sequence similarity 82, member C, isoform CRA_a GN=FAM82C PE=4 SV=1	2.13	2.13
B2R679	cDNA, FLJ92825, highly similar to Homo sapiens SAR1a gene homolog 1 (S. cerevisiae) (SARA1), mRNA PE=2 SV=1	1.47	1.47
Q9Y5K6	CD2-associated protein GN=CD2AP PE=1 SV=1	2.06	2.06
Q7L9L4	MOB kinase activator 1B GN=MOB1B PE=1 SV=3	1.91	1.91
Q4VC31	Coiled-coil domain-containing protein 58 GN=CCDC58 PE=1 SV=1	1.92	1.92
A8K8F6	cDNA FLJ78417, highly similar to Homo sapiens low density lipoprotein receptor-related protein associated protein 1 (LRPAP1), mRNA PE=2 SV=1	2.10	2.10
A0MNN4	CDW3/SMU1 GN=SMU1 PE=2 SV=1	1.62	1.62
A0A024R6A5	Protein phosphatase 1A (Formerly 2C), magnesium-dependent, alpha isoform, isoform CRA_a GN=PPM1A PE=3 SV=1	1.50	1.50
Q9H6F5	Coiled-coil domain-containing protein 86 GN=CCDC86 PE=1 SV=1	2.16	2.16
E5RG17	Putative deoxyribonuclease TATDN1 (Fragment) GN=TATDN1 PE=1 SV=1	1.30	1.30
Q96CS3	FAS-associated factor 2 GN=FAF2 PE=1 SV=2	2.59	2.59
O00423	Echinoderm microtubule-associated protein-like 1 GN=EML1 PE=1 SV=3	2.83	2.83
B5BUC0	Glycogen synthase kinase-3 beta (Fragment) GN=GSK3B PE=2 SV=1	1.56	1.56
A0A024R4E5	High density lipoprotein binding protein (Vigilin), isoform CRA_a GN=HDLBP PE=1 SV=1	2.92	2.92
O60264	SWI/SNF-related matrix-associated actin-dependent regulator of chromatin subfamily A member 5 GN=SMARCA5 PE=1 SV=1	3.27	3.27
Q00796	Sorbitol dehydrogenase GN=SORD PE=1 SV=4	1.35	1.35
Q5T178	Cyclin-dependent kinases regulatory subunit GN=CKS1B PE=2 SV=1	3.13	3.13
P30626	Sorcin GN=SRI PE=1 SV=1	2.36	2.36
B7Z9B1	cDNA FLJ52398, highly similar to Cadherin-13 PE=2 SV=1	1.99	1.99
A0A024R1U4	RAB5C, member RAS oncogene family, isoform CRA_a GN=RAB5C PE=4 SV=1	1.99	1.99
P46087	Probable 28S rRNA (cytosine(4447)-C(5))-methyltransferase GN=NOP2 PE=1 SV=2	2.14	2.14
B7Z9B8	cDNA FLJ56912, highly similar to Fibulin-2 PE=2 SV=1	1.56	1.56
J3KQN4	60S ribosomal protein L36a GN=RPL36A PE=1 SV=1	1.83	1.83
O00468	Agrin GN=AGRN PE=1 SV=6	3.59	3.59
Q53HB7	Diablo isoform 1 variant (Fragment) PE=2 SV=1	1.84	1.84
Q15020	Squamous cell carcinoma antigen recognized by T-cells 3 GN=SART3 PE=1 SV=1	2.22	2.22
Q08623	Pseudouridine-5'-phosphatase GN=PUDP PE=1 SV=3	1.39	1.39
Q549H9	cAMP-dependent protein kinase inhibitor GN=PKIG PE=1 SV=1	2.10	2.10
Q7L5N1	COP9 signalosome complex subunit 6 GN=COPS6 PE=1 SV=1	1.28	1.28
P63220	40S ribosomal protein S21 GN=RPS21 PE=1 SV=1	2.75	2.75
Q9UN70	Protocadherin gamma-C3 GN=PCDHGC3 PE=1 SV=1	2.15	2.15
X6R4W8	BUB3-interacting and GLEBS motif-containing protein ZNF207 GN=ZNF207 PE=1 SV=1	3.03	3.03
A0A024R7F4	Deoxyribonuclease II, lysosomal, isoform CRA_a GN=DNASE2 PE=4 SV=1	2.34	2.34
Q643R0	HCTP4 GN=HCTP4 PE=1 SV=1	2.22	2.22
Q13325	Interferon-induced protein with tetratricopeptide repeats 5 GN=IFIT5 PE=1 SV=1	1.59	1.59
Q96AT9	Ribulose-phosphate 3-epimerase GN=RPE PE=1 SV=1	2.42	2.42
Q4LE43	Phosphoinositide phospholipase C (Fragment) GN=PLCG1 variant protein PE=2 SV=1	1.27	1.27
O14776	Transcription elongation regulator 1 GN=TCERG1 PE=1 SV=2	2.19	2.19
P21912	Succinate dehydrogenase [ubiquinone] iron-sulfur subunit, mitochondrial GN=SDHB PE=1 SV=3	1.38	1.38
Q6NUR1	Non-SMC condensin I complex, subunit G GN=NCAPG PE=2 SV=1	1.37	1.37
Q14683	Structural maintenance of chromosomes protein 1A GN=SMC1A PE=1 SV=2	1.65	1.65
Q9P287	BRCA2 and CDKN1A-interacting protein GN=BCCIP PE=1 SV=1	2.54	2.54
P02458	Collagen alpha-1(II) chain GN=COL2A1 PE=1 SV=3	1.57	1.57
Q5SSJ5	Heterochromatin protein 1-binding protein 3 GN=HP1BP3 PE=1 SV=1	3.42	3.42
A5PLM5	Exosome component 9 GN=EXOSC9 PE=2 SV=1	3.09	3.09
P62249	40S ribosomal protein S16 GN=RPS16 PE=1 SV=2	1.63	1.63
Q8WXF1	Paraspeckle component 1 GN=PSPC1 PE=1 SV=1	2.42	2.42

P04792	Heat shock protein beta-1 GN=HSPB1 PE=1 SV=2	1.02	1.02
Q96A33	Coiled-coil domain-containing protein 47 GN=CCDC47 PE=1 SV=1	2.40	2.40
A0A1L7NY41	Polypeptide N-acetylgalactosaminyltransferase GN=GALNT2 PE=2 SV=1	2.26	2.26
A0A0A0MSS8	Aldo-keto reductase family 1 member C3 GN=AKR1C3 PE=1 SV=1	1.64	1.64
O14617	AP-3 complex subunit delta-1 GN=AP3D1 PE=1 SV=1	1.55	1.55
A0A0D9SF53	ATP-dependent RNA helicase DDX3X GN=DDX3X PE=1 SV=1	2.11	2.11
P29590	Protein PML GN=PML PE=1 SV=3	2.28	2.28
A0A024RA49	Anillin, actin binding protein (Scraps homolog, Drosophila), isoform CRA_e GN=ANLN PE=4 SV=1	1.56	1.56
A0A024RD15	Mitogen-activated protein kinase GN=MAPK14 PE=4 SV=1	2.28	2.28
P27487	Dipeptidyl peptidase 4 GN=DPP4 PE=1 SV=2	1.25	1.25
A8K683	cDNA FLJ75708, highly similar to Homo sapiens N-myc (and STAT) interactor (NMI), mRNA PE=2 SV=1	1.67	1.67
Q9BTE3	Mini-chromosome maintenance complex-binding protein GN=MCMBP PE=1 SV=2	2.73	2.73
H0UIC7	C-C motif chemokine GN=CCL8 PE=3 SV=1	2.22	2.22
Q9H832	Ubiquitin-conjugating enzyme E2 Z GN=UBE2Z PE=1 SV=2	1.75	1.75
A0A024R9J4	Nephroblastoma overexpressed gene, isoform CRA_a GN=NOV PE=4 SV=1	4.01	4.01
O60462	Neuropilin-2 GN=NRP2 PE=1 SV=3	2.93	2.93
A0A1W2PNX8	Protein unc-45 homolog A GN=UNC45A PE=1 SV=1	2.00	2.00
B2RB57	cDNA, FLJ95321, highly similar to Homo sapiens ATG7 autophagy related 7 homolog (S. cerevisiae) (ATG7), mRNA PE=2 SV=1	1.92	1.92
Q4KWH8	1-phosphatidylinositol 4,5-bisphosphate phosphodiesterase eta-1 GN=PLCH1 PE=1 SV=1	1.60	1.60
X6RAL5	Histone deacetylase complex subunit SAP18 GN=SAP18 PE=1 SV=1	2.25	2.25
B9EG90	Topoisomerase (DNA) I GN=TOP1 PE=2 SV=1	2.97	2.97
Q8NCN5	Pyruvate dehydrogenase phosphatase regulatory subunit, mitochondrial GN=PDPR PE=1 SV=2	1.37	1.37
P34896	Serine hydroxymethyltransferase, cytosolic GN=SHMT1 PE=1 SV=1	2.42	2.42
Q09161	Nuclear cap-binding protein subunit 1 GN=NCBP1 PE=1 SV=1	1.52	1.52
P78539	Sushi repeat-containing protein SRPX GN=SRPX PE=1 SV=1	2.69	2.69
B3KP83	cDNA FLJ31382 fis, clone NHNPC2000187, highly similar to Docking protein 1 (Downstream of tyrosine kinase 1) PE=2 SV=1	2.03	2.03
B4DUT8	Calponin GN=CNN2 PE=1 SV=1	1.60	1.60
P05204	Non-histone chromosomal protein HMG-17 GN=HMGN2 PE=1 SV=3	1.91	1.91
P50570	Dynamin-2 GN=DNM2 PE=1 SV=2	2.63	2.63
A8K5K0	cDNA FLJ78309, highly similar to Homo sapiens heterogeneous nuclear ribonucleoprotein U-like 1 (HNRPUL1), transcript variant 1, mRNA PE=2 SV=1	1.61	1.61
A0A087WT44	Heme oxygenase 2 GN=HMOX2 PE=1 SV=1	1.80	1.80
A8K401	Prohibitin, isoform CRA_a GN=PHB PE=2 SV=1	2.11	2.11
A6NEM2	Host cell factor 1 GN=HCFC1 PE=1 SV=2	4.27	4.27
Q9Y3Z3	Deoxynucleoside triphosphate triphosphohydrolase SAMHD1 GN=SAMHD1 PE=1 SV=2	1.97	1.97
O00228	Phosphoglycerate mutase (Fragment) PE=3 SV=1	1.20	1.20
A0A024RAW9	WW domain binding protein 11, isoform CRA_a GN=WBP11 PE=4 SV=1	1.36	1.36
A0A024RBF6	HCG26523, isoform CRA_a GN=hCG_26523 PE=4 SV=1	1.37	1.37
A0A024R5H0	Barrier to autointegration factor 1, isoform CRA_a GN=BANF1 PE=4 SV=1	2.78	2.78
P33947	ER lumen protein-retaining receptor 2 GN=KDELR2 PE=1 SV=1	1.68	1.68
Q9BX97	Plasmalemma vesicle-associated protein GN=PLVAP PE=2 SV=1	2.11	2.11
B4DPZ4	cDNA FLJ60782, highly similar to Rho-GTPase-activating protein 1 PE=2 SV=1	1.43	1.43
L8EC95	Alternative protein MMP1 GN=MMP1 PE=4 SV=1	2.26	2.26
A0A2P9AM56	Dihydrodipicolinate synthetase GN=BQ8482_250079 PE=3 SV=1	1.63	1.63
A0A2P9ASH7	Uncharacterized protein GN=BQ8482_380309 PE=4 SV=1	2.01	2.01
Q9H8Y8	Golgi reassembly-stacking protein 2 GN=GORASP2 PE=1 SV=3	2.55	2.55
A8KAN3	Non-specific serine/threonine protein kinase PE=2 SV=1	4.27	4.27
A0A024QZY1	JTV1 gene, isoform CRA_a GN=JTV1 PE=4 SV=1	1.91	1.91
Q8WW59	SPRY domain-containing protein 4 GN=SPRYD4 PE=1 SV=2	1.94	1.94
J3KQJ1	Inactive C-alpha-formylglycine-generating enzyme 2 GN=SUMF2 PE=1 SV=1	1.68	1.68
B2RDD7	Protein arginine N-methyltransferase 5 PE=2 SV=1	1.59	1.59
A0A024R883	V-type proton ATPase subunit G GN=ATP6V1G1 PE=3 SV=1	2.82	2.82

Q15102	Platelet-activating factor acetylhydrolase IB subunit gamma GN=PAFAH1B3 PE=1 SV=1	1.50	1.50
P62877	E3 ubiquitin-protein ligase RBX1 GN=RBX1 PE=1 SV=1	2.60	2.60
B7Z7F0	cDNA FLJ56420, highly similar to Aspartyl aminopeptidase PE=2 SV=1	1.72	1.72
Q53F55	Deoxythymidylate kinase (Thymidylate kinase) variant (Fragment) PE=2 SV=1	2.94	2.94
A0A024R0Z3	DEAD (Asp-Glu-Ala-Asp) box polypeptide 23, isoform CRA_b GN=DDX23 PE=4 SV=1	1.59	1.59
A8K3Y5	cDNA FLJ78186 PE=2 SV=1	1.42	1.42
Q52LJ0	Protein FAM98B GN=FAM98B PE=1 SV=1	1.50	1.50
Q9NU22	Midasin GN=MDN1 PE=1 SV=2	4.15	4.15
Q9NUJ1	Mycophenolic acid acyl-glucuronide esterase, mitochondrial GN=ABHD10 PE=1 SV=1	2.77	2.77
B2R791	cDNA, FLJ93335, highly similar to Homo sapiens PRP3 pre-mRNA processing factor 3 homolog (yeast) (PRPF3), mRNA PE=2 SV=1	2.37	2.37
O00159	Unconventional myosin-Ic GN=MYO1C PE=1 SV=4	1.25	1.25
A0A024R1U8	Insulin-like growth factor binding protein 4, isoform CRA_a GN=IGFBP4 PE=4 SV=1	2.81	2.81
B2R5S9	cDNA, FLJ92604, highly similar to Homo sapiens paraneoplastic antigen MA3 (PNMA3), mRNA PE=2 SV=1	1.53	1.53
A0A0A0MSG2	Four and a half LIM domains protein 2 GN=FHL2 PE=1 SV=1	1.17	1.17
Q9NRF9	DNA polymerase epsilon subunit 3 GN=POLE3 PE=1 SV=1	2.51	2.51
A0A2R8Y5Y7	60S ribosomal protein L9 GN=RPL9 PE=1 SV=1	1.65	1.65
A0A0F7KYT8	Fragile X mental retardation autosomal homolog variant p2K GN=FXR1 PE=2 SV=1	1.48	1.48
H7BY58	Protein-L-isoaspartate O-methyltransferase GN=PCMT1 PE=1 SV=1	1.50	1.50
Q15276	Rab GTPase-binding effector protein 1 GN=RABEP1 PE=1 SV=2	1.13	1.13
Q93034	Cullin-5 GN=CUL5 PE=1 SV=4	2.20	2.20
A0A0S2Z410	Hydroxysteroid dehydrogenase 10 isoform 1 (Fragment) GN=HSD17B10 PE=2 SV=1	2.17	2.17
A0A2R8Y4V0	ATP-binding cassette sub-family C member 8 GN=ABCC8 PE=1 SV=1	1.46	1.46
A0A0C4DFN3	Monoglyceride lipase GN=MGLL PE=1 SV=1	1.51	1.51
Q96JB5	CDK5 regulatory subunit-associated protein 3 GN=CDK5RAP3 PE=1 SV=2	1.57	1.57
Q86WR0	Coiled-coil domain-containing protein 25 GN=CCDC25 PE=1 SV=2	1.88	1.88
A0A2P9AXN1	FAD-dependent pyridine nucleotide-disulphide oxidoreductase GN=BQ8482_90305 PE=4 SV=1	1.97	1.97
K7ELC2	40S ribosomal protein S15 GN=RPS15 PE=1 SV=1	1.33	1.33
Q8WUA2	Peptidyl-prolyl cis-trans isomerase-like 4 GN=PPIL4 PE=1 SV=1	1.26	1.26
Q96CT7	Coiled-coil domain-containing protein 124 GN=CCDC124 PE=1 SV=1	1.81	1.81
A0A024R7N7	Interferon, gamma-inducible protein 30, isoform CRA_b GN=IFI30 PE=4 SV=1	2.47	2.47
P49247	Ribose-5-phosphate isomerase GN=RPIA PE=1 SV=3	3.14	3.14
P19623	Spermidine synthase GN=SRM PE=1 SV=1	1.19	1.19
Q6PIF6	Unconventional myosin-VIIb GN=MYO7B PE=1 SV=2	1.97	1.97
P42695	Condensin-2 complex subunit D3 GN=NCAPD3 PE=1 SV=2	2.24	2.24
A0A0J9YWP7	PRAME family member 18 GN=PRAMEF18 PE=4 SV=1	1.61	1.61
Q7Z6J2	General receptor for phosphoinositides 1-associated scaffold protein GN=GRASP PE=1 SV=1	1.64	1.64
P18583	Protein SON GN=SON PE=1 SV=4	1.83	1.83
Q5T4S7	E3 ubiquitin-protein ligase UBR4 GN=UBR4 PE=1 SV=1	2.87	2.87
B3KR97	cDNA FLJ33900 fis, clone CTONG2008262, highly similar to Low density lipoprotein receptor adapter protein 1 PE=2 SV=1	1.44	1.44
O95425	Supervillin GN=SVIL PE=1 SV=2	1.28	1.28
Q8NHY5	Checkpoint protein HUS1B GN=HUS1B PE=1 SV=2	3.18	3.18
Q63ZY3	KN motif and ankyrin repeat domain-containing protein 2 GN=KANK2 PE=1 SV=1	2.11	2.11
B2R6F3	Splicing factor arginine/serine-rich 3 GN=SFRS3 PE=2 SV=1	1.71	1.71
A0A2P9AQ24	Uncharacterized protein GN=BQ8482_340170 PE=4 SV=1	1.46	1.46
B3KPA5	cDNA FLJ31518 fis, clone NT2RI2000064 PE=2 SV=1	2.81	2.81
Q9H306	Matrix metalloproteinase-27 GN=MMP27 PE=1 SV=2	1.01	1.01
Q9NTX5	Ethylmalonyl-CoA decarboxylase GN=ECHDC1 PE=1 SV=2	1.66	1.66
A0A024R231	Guanine deaminase, isoform CRA_b GN=GDA PE=4 SV=1	1.29	1.29
B3KVD6	cDNA FLJ16433 fis, clone BRACE3013936, highly similar to Cell death activator CIDE-B PE=2 SV=1	2.11	2.11
A0A0S2Z5J4	Adaptor-related protein complex 3 beta 1 subunit isoform 1 (Fragment) GN=AP3B1 PE=2 SV=1	1.58	1.58
A0A2P9ATT1	Uncharacterized protein GN=BQ8482_480060 PE=4 SV=1	1.59	1.59

Q69YJ7	Uncharacterized protein DKFZp667H197 (Fragment) GN=DKFZp667H197 PE=2 SV=1	4.22	4.22
Q8N122	Regulatory-associated protein of mTOR GN=RPTOR PE=1 SV=1	2.21	2.21

Appendix 7

Common proteins (519 proteins) to the two groups of samples (Untreated hypoxia vs normoxia) and (BEAM treated hypoxia vs normoxia). GN=Gene Name, PE=Protein Existence which is the numerical value describing the evidence for the existence of the protein, SV=Sequence Version which is the version number of the sequence.

Accession	Description
P12109	Collagen alpha-1(VI) chain GN=COL6A1 PE=1 SV=3
P03956	Interstitial collagenase GN=MMP1 PE=1 SV=3
A0A024R462	Fibronectin 1, isoform CRA_n GN=FN1 PE=4 SV=1
J3QSU6	Tenascin GN=TNC PE=1 SV=1
V9HWB4	Epididymis secretory sperm binding protein Li 89n GN=HEL-S-89n PE=2 SV=1
V9HW22	Epididymis luminal protein 33 GN=HEL-S-72p PE=2 SV=1
P06733	Alpha-enolase GN=ENO1 PE=1 SV=2
P21333	Filamin-A GN=FLNA PE=1 SV=4
P11047	Laminin subunit gamma-1 GN=LAMC1 PE=1 SV=3
Q14766	Latent-transforming growth factor beta-binding protein 1 GN=LTBP1 PE=1 SV=4
P02452	Collagen alpha-1(I) chain GN=COL1A1 PE=1 SV=5
G3XAI2	Laminin subunit beta-1 GN=LAMB1 PE=1 SV=1
P08254	Stromelysin-1 GN=MMP3 PE=1 SV=2
P12110	Collagen alpha-2(VI) chain GN=COL6A2 PE=1 SV=4
P13639	Elongation factor 2 GN=EEF2 PE=1 SV=4
P07996	Thrombospondin-1 GN=THBS1 PE=1 SV=2
A0A024R498	Serpin peptidase inhibitor, clade E (Nexin, plasminogen activator inhibitor type 1), member 2, isoform CRA_b GN=SERPINE2 PE=3 SV=1
P02545	Prelamin-A/C GN=LMNA PE=1 SV=1
P35556	Fibrillin-2 GN=FBN2 PE=1 SV=3
Q15149	Plectin GN=PLEC PE=1 SV=3
A0A024QYT5	Serpin peptidase inhibitor, clade E (Nexin, plasminogen activator inhibitor type 1), member 1, isoform CRA_b GN=SERPINE1 PE=3 SV=1
A0A0A0MQS9	Laminin subunit alpha-4 GN=LAMA4 PE=1 SV=1
V9HWB8	Pyruvate kinase GN=HEL-S-30 PE=1 SV=1
B2R7Y0	cDNA, FLJ93654, highly similar to Homo sapiens serpin peptidase inhibitor, clade B (ovalbumin), member 2 (SERPINB2), mRNA PE=2 SV=1
P35555	Fibrillin-1 GN=FBN1 PE=1 SV=3
D3DTX7	Collagen, type I, alpha 1, isoform CRA_a GN=COL1A1 PE=4 SV=1
P05120	Plasminogen activator inhibitor 2 GN=SERPINB2 PE=1 SV=2
V9HW88	Calreticulin, isoform CRA_b GN=HEL-S-99n PE=2 SV=1
O00391	Sulfhydryl oxidase 1 GN=QSOX1 PE=1 SV=3
E7EUF1	Ectonucleotide pyrophosphatase/phosphodiesterase family member 2 GN=ENPP2 PE=1 SV=1
Q59E93	Aminopeptidase (Fragment) PE=2 SV=1
Q12841	Follistatin-related protein 1 GN=FSTL1 PE=1 SV=1
P34932	Heat shock 70 kDa protein 4 GN=HSPA4 PE=1 SV=4
A0A0S2Z3Y1	Lectin galactoside-binding soluble 3 binding protein isoform 1 (Fragment) GN=LGALS3BP PE=2 SV=1
Q53G35	Phosphoglycerate mutase (Fragment) PE=2 SV=1
P26038	Moesin GN=MSN PE=1 SV=3
P60174	Triosephosphate isomerase GN=TPI1 PE=1 SV=3
P05231	Interleukin-6 GN=IL6 PE=1 SV=1
B5BUB5	Autoantigen La (Fragment) GN=SSB PE=2 SV=1
P35442	Thrombospondin-2 GN=THBS2 PE=1 SV=2
P23142	Fibulin-1 GN=FBLN1 PE=1 SV=4
A0A0G2JIW1	Heat shock 70 kDa protein 1B GN=HSPA1B PE=1 SV=1
P02461	Collagen alpha-1(III) chain GN=COL3A1 PE=1 SV=4
P68363	Tubulin alpha-1B chain GN=TUBA1B PE=1 SV=1
D3YTG3	Target of Nesh-SH3 GN=ABI3BP PE=1 SV=1
P48307	Tissue factor pathway inhibitor 2 GN=TFPI2 PE=1 SV=1
P49321	Nuclear autoantigenic sperm protein GN=NASP PE=1 SV=2

A0A024R8S5	Protein disulfide-isomerase GN=P4HB PE=2 SV=1
A8K7Q1	cDNA FLJ77770, highly similar to Homo sapiens nucleobindin 1 (NUCB1), mRNA PE=2 SV=1
P04406	Glyceraldehyde-3-phosphate dehydrogenase GN=GAPDH PE=1 SV=3
P26022	Pentraxin-related protein PTX3 GN=PTX3 PE=1 SV=3
D3DQH8	Secreted protein, acidic, cysteine-rich (Osteonectin), isoform CRA_a GN=SPARC PE=4 SV=1
B4DUV1	Fibulin-1 PE=2 SV=1
B2R983	cDNA, FLJ94267, highly similar to Homo sapiens glutathione S-transferase omega 1 (GSTO1), mRNA PE=2 SV=1
P67936	Tropomyosin alpha-4 chain GN=TPM4 PE=1 SV=3
B2R6I6	cDNA, FLJ92965, highly similar to Homo sapiens stanniocalcin 1 (STC1), mRNA PE=2 SV=1
P00338	L-lactate dehydrogenase A chain GN=LDHA PE=1 SV=2
P19883	Follistatin GN=FST PE=1 SV=2
E9PK25	Cofilin-1 GN=CFL1 PE=1 SV=1
O00299	Chloride intracellular channel protein 1 GN=CLIC1 PE=1 SV=4
A0A024R374	Cathepsin B, isoform CRA_a GN=CTSB PE=3 SV=1
B4DPQ0	Complement C1r subcomponent GN=C1R PE=1 SV=1
P61981	14-3-3 protein gamma GN=YWHAG PE=1 SV=2
P22626	Heterogeneous nuclear ribonucleoproteins A2/B1 GN=HNRNPA2B1 PE=1 SV=2
P26641	Elongation factor 1-gamma GN=EEF1G PE=1 SV=3
Q14112	Nidogen-2 GN=NID2 PE=1 SV=3
P27348	14-3-3 protein theta GN=YWHAQ PE=1 SV=1
B3KQF4	cDNA FLJ90373 fis, clone NT2RP2004606, highly similar to Metalloproteinase inhibitor 1 PE=2 SV=1
P07737	Profilin-1 GN=PFN1 PE=1 SV=2
P15121	Aldose reductase GN=AKR1B1 PE=1 SV=3
Q32Q12	Nucleoside diphosphate kinase GN=NME1-NME2 PE=1 SV=1
B4DLV7	Rab GDP dissociation inhibitor PE=2 SV=1
P80723	Brain acid soluble protein 1 GN=BASP1 PE=1 SV=2
Q16658	Fascin GN=FSCN1 PE=1 SV=3
A0A024RAZ7	Heterogeneous nuclear ribonucleoprotein A1, isoform CRA_b GN=HNRPA1 PE=4 SV=1
A0A024R4K3	Malate dehydrogenase GN=MDH2 PE=2 SV=1
V9HW31	ATP synthase subunit beta GN=HEL-S-271 PE=1 SV=1
P25786	Proteasome subunit alpha type-1 GN=PSMA1 PE=1 SV=1
Q6IAW5	CALU protein GN=CALU PE=2 SV=1
A0A024R755	Calumenin, isoform CRA_a GN=CALU PE=4 SV=1
Q09666	Neuroblast differentiation-associated protein AHNAK GN=AHNAK PE=1 SV=2
B4DJ30	cDNA FLJ61290, highly similar to Neutral alpha-glucosidase AB PE=2 SV=1
B7ZKY6	Membrane metallo-endopeptidase GN=MME PE=2 SV=1
F4ZW66	NF110b PE=2 SV=1
A0A024RB85	Proliferation-associated 2G4, 38kDa, isoform CRA_a GN=PA2G4 PE=4 SV=1
A0A0C4DGB5	Calpastatin GN=CAST PE=1 SV=1
P48594	Serpin B4 GN=SERPINB4 PE=1 SV=2
E7EQR4	Ezrin GN=EZR PE=1 SV=3
Q9Y4L1	Hypoxia up-regulated protein 1 GN=HYOU1 PE=1 SV=1
Q03252	Lamin-B2 GN=LMNB2 PE=1 SV=4
A0A087WVQ6	Clathrin heavy chain GN=CLTC PE=1 SV=1
P20700	Lamin-B1 GN=LMNB1 PE=1 SV=2
P13010	X-ray repair cross-complementing protein 5 GN=XRCC5 PE=1 SV=3
P37802	Transgelin-2 GN=TAGLN2 PE=1 SV=3
E7EMB3	Calmodulin-2 GN=CALM2 PE=1 SV=1
P39687	Acidic leucine-rich nuclear phosphoprotein 32 family member A GN=ANP32A PE=1 SV=1
A8K690	cDNA FLJ76863, highly similar to Homo sapiens stress-induced-phosphoprotein 1 (Hsp70/Hsp90-organizing protein) (STIP1), mRNA PE=2 SV=1
P28799	Granulins GN=GRN PE=1 SV=2
J3KQ32	Obg-like ATPase 1 GN=OLA1 PE=1 SV=1
P19876	C-X-C motif chemokine 3 GN=CXCL3 PE=1 SV=1
A0A024R1K7	Tyrosine 3-monooxygenase/tryptophan 5-monooxygenase activation protein, eta polypeptide, isoform CRA_b GN=YWHAH PE=3 SV=1

P09382	Galectin-1 GN=LGALS1 PE=1 SV=2
B4DJQ5	cDNA FLJ59211, highly similar to Glucosidase 2 subunit beta PE=2 SV=1
A0A024R895	SET translocation (Myeloid leukemia-associated), isoform CRA_b GN=SET PE=3 SV=1
O94985	Calsyntenin-1 GN=CLSTN1 PE=1 SV=1
P14543	Nidogen-1 GN=NID1 PE=1 SV=3
Q5U0B9	Stem cell growth factor;lymphocyte secreted C-type lectin PE=2 SV=1
P15531	Nucleoside diphosphate kinase A GN=NME1 PE=1 SV=1
P12004	Proliferating cell nuclear antigen GN=PCNA PE=1 SV=1
A0A024R4H0	Procollagen-lysine 1, 2-oxoglutarate 5-dioxygenase 1, isoform CRA_a GN=PLOD1 PE=4 SV=1
Q14767	Latent-transforming growth factor beta-binding protein 2 GN=LTBP2 PE=1 SV=3
P49767	Vascular endothelial growth factor C GN=VEGFC PE=1 SV=1
Q9Y4K0	Lysyl oxidase homolog 2 GN=LOXL2 PE=1 SV=1
B4DJQ8	cDNA FLJ55694, highly similar to Dipeptidyl-peptidase 1 (EC 3.4.14.1) PE=2 SV=1
P25789	Proteasome subunit alpha type-4 GN=PSMA4 PE=1 SV=1
P61604	10 kDa heat shock protein, mitochondrial GN=HSPE1 PE=1 SV=2
Q92626	Peroxidasin homolog GN=PXDN PE=1 SV=2
A0A0K0K1K4	Proteasome subunit alpha type GN=HEL-S-276 PE=2 SV=1
P23284	Peptidyl-prolyl cis-trans isomerase B GN=PPIB PE=1 SV=2
Q53F64	Heterogeneous nuclear ribonucleoprotein AB isoform a variant (Fragment) PE=2 SV=1
P07437	Tubulin beta chain GN=TUBB PE=1 SV=2
A0A024R962	HCG40889, isoform CRA_b GN=hCG_40889 PE=4 SV=1
Q92688	Acidic leucine-rich nuclear phosphoprotein 32 family member B GN=ANP32B PE=1 SV=1
P68371	Tubulin beta-4B chain GN=TUBB4B PE=1 SV=1
B2R8Z8	cDNA, FLJ94136, highly similar to Homo sapiens synaptotagmin binding, cytoplasmic RNA interacting protein (SYNCRIP), mRNA PE=2 SV=1
P16035	Metalloproteinase inhibitor 2 GN=TIMP2 PE=1 SV=2
Q01469	Fatty acid-binding protein, epidermal GN=FABP5 PE=1 SV=3
P07585	Decorin GN=DCN PE=1 SV=1
B8ZWD9	Diazepam binding inhibitor, splice form 1D(2) GN=DBI PE=2 SV=1
Q15293	Reticulocalbin-1 GN=RCN1 PE=1 SV=1
A0A024R9J4	Nephroblastoma overexpressed gene, isoform CRA_a GN=NOV PE=4 SV=1
Q9Y266	Nuclear migration protein nudC GN=NUDC PE=1 SV=1
Q59FF0	EBNA-2 co-activator variant (Fragment) PE=2 SV=1
Q13185	Chromobox protein homolog 3 GN=CBX3 PE=1 SV=4
P06899	Histone H2B type 1-J GN=HIST1H2BJ PE=1 SV=3
P16403	Histone H1.2 GN=HIST1H1C PE=1 SV=2
B4DR52	Histone H2B PE=2 SV=1
V9HWH9	Protein S100 GN=HEL-S-43 PE=2 SV=1
P20618	Proteasome subunit beta type-1 GN=PSMB1 PE=1 SV=2
Q16270	Insulin-like growth factor-binding protein 7 GN=IGFBP7 PE=1 SV=1
B7Z6Z4	Myosin light polypeptide 6 GN=MYL6 PE=1 SV=1
P21291	Cysteine and glycine-rich protein 1 GN=CSRP1 PE=1 SV=3
E9KL48	Epididymis tissue sperm binding protein Li 18mP GN=GLUD1 PE=2 SV=1
J3KQE5	GTP-binding nuclear protein Ran (Fragment) GN=RAN PE=1 SV=1
P63241	Eukaryotic translation initiation factor 5A-1 GN=EIF5A PE=1 SV=2
P23526	Adenosylhomocysteinase GN=AHCY PE=1 SV=4
Q14566	DNA replication licensing factor MCM6 GN=MCM6 PE=1 SV=1
E7EVA0	Microtubule-associated protein GN=MAP4 PE=1 SV=1
A0A1S5UZ07	Talin-1 GN=TLN1 PE=2 SV=1
P40925	Malate dehydrogenase, cytoplasmic GN=MDH1 PE=1 SV=4
B2RBR9	cDNA, FLJ95650, highly similar to Homo sapiens karyopherin (importin) beta 1 (KPNB1), mRNA PE=2 SV=1
Q59ER5	WD repeat-containing protein 1 isoform 1 variant (Fragment) PE=2 SV=1
A0A024R1A4	Ubiquitin-conjugating enzyme E2L 3, isoform CRA_a GN=UBE2L3 PE=3 SV=1
A0A087WTP3	Far upstream element-binding protein 2 GN=KHSRP PE=1 SV=1
Q15691	Microtubule-associated protein RP/EB family member 1 GN=MAPRE1 PE=1 SV=3
Q9BTY2	Plasma alpha-L-fucosidase GN=FUCA2 PE=1 SV=2
P68431	Histone H3.1 GN=HIST1H3A PE=1 SV=2

M1VKI3	Tyrosine-protein kinase receptor GN=SDC4-ROS1_S4;R32 PE=2 SV=1
Q6YHK3	CD109 antigen GN=CD109 PE=1 SV=2
Q15084	Protein disulfide-isomerase A6 GN=PDIA6 PE=1 SV=1
A0A109NGN6	Proteasome subunit alpha type PE=2 SV=1
P23246	Splicing factor, proline- and glutamine-rich GN=SFPQ PE=1 SV=2
O60361	Putative nucleoside diphosphate kinase GN=NME2P1 PE=5 SV=1
A0A0B4J2C3	Translationally-controlled tumor protein GN=TPT1 PE=1 SV=1
P52907	F-actin-capping protein subunit alpha-1 GN=CAPZA1 PE=1 SV=3
A5PLM9	Cathepsin L1 GN=CTSL1 PE=2 SV=1
P29966	Myristoylated alanine-rich C-kinase substrate GN=MARCKS PE=1 SV=4
A0A024R3W7	Eukaryotic translation elongation factor 1 beta 2, isoform CRA_a GN=EEF1B2 PE=3 SV=1
P09341	Growth-regulated alpha protein GN=CXCL1 PE=1 SV=1
P11717	Cation-independent mannose-6-phosphate receptor GN=IGF2R PE=1 SV=3
E9PAV3	Nascent polypeptide-associated complex subunit alpha, muscle-specific form GN=NACA PE=1 SV=1
P16070	CD44 antigen GN=CD44 PE=1 SV=3
Q549N0	Cofilin 2 (Muscle), isoform CRA_a GN=CFL2 PE=1 SV=1
P25788	Proteasome subunit alpha type-3 GN=PSMA3 PE=1 SV=2
A0A0B4U5E3	Granulocyte-colony stimulating factor (Fragment) PE=2 SV=1
O00622	Protein CYR61 GN=CYR61 PE=1 SV=1
P52209	6-phosphogluconate dehydrogenase, decarboxylating GN=PGD PE=1 SV=3
O43493	Trans-Golgi network integral membrane protein 2 GN=TGOLN2 PE=1 SV=2
P04083	Annexin A1 GN=ANXA1 PE=1 SV=2
B1AK88	Capping protein (Actin filament) muscle Z-line, beta, isoform CRA_d GN=CAPZB PE=1 SV=1
P41250	Glycine--tRNA ligase GN=GARS PE=1 SV=3
P06703	Protein S100-A6 GN=S100A6 PE=1 SV=1
A2RUM7	Ribosomal protein L5 GN=RPL5 PE=2 SV=1
A0A087WSV8	Nucleobindin 2, isoform CRA_b GN=NUCB2 PE=1 SV=1
O00468	Agrin GN=AGRN PE=1 SV=5
A8K9A4	cDNA FLJ75154, highly similar to Homo sapiens heterogeneous nuclear ribonucleoprotein C (C1/C2), mRNA PE=2 SV=1
A0A024R6W0	Aspartate aminotransferase GN=GOT2 PE=4 SV=1
G3V5Z7	Proteasome subunit alpha type GN=PSMA6 PE=1 SV=1
P16402	Histone H1.3 GN=HIST1H1D PE=1 SV=2
P07686	Beta-hexosaminidase subunit beta GN=HEXB PE=1 SV=3
P16401	Histone H1.5 GN=HIST1H1B PE=1 SV=3
A8K651	cDNA FLJ75700, highly similar to Homo sapiens complement component 1, q subcomponent binding protein (C1QBP), nuclear gene encoding mitochondrial protein, mRNA PE=2 SV=1
Q06481	Amyloid-like protein 2 GN=APLP2 PE=1 SV=2
Q16531	DNA damage-binding protein 1 GN=DDB1 PE=1 SV=1
A0A0C4DG17	40S ribosomal protein SA GN=RPSA PE=1 SV=1
B7Z8Z6	DNA helicase PE=2 SV=1
Q4W4Y1	Dopamine receptor interacting protein 4 GN=DRIP4 PE=2 SV=1
A8K2N0	cDNA FLJ77835, highly similar to Homo sapiens complement component 1, s subcomponent (C1S), transcript variant 2, mRNA PE=2 SV=1
E5RJD8	Tubulin-specific chaperone A GN=TBCA PE=1 SV=1
P24592	Insulin-like growth factor-binding protein 6 GN=IGFBP6 PE=1 SV=1
Q07954	Prolow-density lipoprotein receptor-related protein 1 GN=LRP1 PE=1 SV=2
Q6FIC5	Chloride intracellular channel protein GN=CLIC4 PE=2 SV=1
A8K329	cDNA FLJ76656, highly similar to Homo sapiens scaffold attachment factor B (SAFB), mRNA PE=2 SV=1
P30044	Peroxiredoxin-5, mitochondrial GN=PRDX5 PE=1 SV=4
A8K7E0	cDNA FLJ76911, highly similar to Homo sapiens biglycan (BGN), mRNA PE=2 SV=1
P05387	60S acidic ribosomal protein P2 GN=RPLP2 PE=1 SV=1
Q15582	Transforming growth factor-beta-induced protein ig-h3 GN=TGFBI PE=1 SV=1
P02795	Metallothionein-2 GN=MT2A PE=1 SV=1
P54727	UV excision repair protein RAD23 homolog B GN=RAD23B PE=1 SV=1
P30050	60S ribosomal protein L12 GN=RPL12 PE=1 SV=1
P28074	Proteasome subunit beta type-5 GN=PSMB5 PE=1 SV=3

Q14019	Coactosin-like protein GN=COTL1 PE=1 SV=3
P16152	Carbonyl reductase [NADPH] 1 GN=CBR1 PE=1 SV=3
O00469	Procollagen-lysine,2-oxoglutarate 5-dioxygenase 2 GN=PLOD2 PE=1 SV=2
G3V3D1	Epididymal secretory protein E1 (Fragment) GN=NPC2 PE=1 SV=1
A0A024R713	Dihydrolipoyl dehydrogenase GN=DLD PE=3 SV=1
Q96CG8	Collagen triple helix repeat-containing protein 1 GN=CTHRC1 PE=1 SV=1
Q59EA2	Coronin (Fragment) PE=2 SV=1
P52926	High mobility group protein HMGI-C GN=HMGA2 PE=1 SV=1
O14786	Neuropilin-1 GN=NRP1 PE=1 SV=3
A8K3S1	Glucosamine-6-phosphate isomerase PE=2 SV=1
Q6LAF9	Cathepsin B (Fragment) PE=2 SV=1
A0A024R5Z7	Annexin GN=ANXA2 PE=3 SV=1
B2R6S5	UMP-CMP kinase GN=CMPK PE=2 SV=1
Q9UKY7	Protein CDV3 homolog GN=CDV3 PE=1 SV=1
P26639	Threonine--tRNA ligase, cytoplasmic GN=TARS PE=1 SV=3
H0YMD1	Low-density lipoprotein receptor GN=LDLR PE=1 SV=1
O15460	Prolyl 4-hydroxylase subunit alpha-2 GN=P4HA2 PE=1 SV=1
V9HW37	Epididymis secretory protein Li 69 GN=HEL-S-69 PE=1 SV=1
Q6IQ30	Polyadenylate-binding protein GN=PABPC4 PE=2 SV=1
P55060	Exportin-2 GN=CSE1L PE=1 SV=3
Q9UNN8	Endothelial protein C receptor GN=PROCR PE=1 SV=1
V9HWA6	Epididymis luminal protein 32 GN=HEL32 PE=2 SV=1
A8K8F0	cDNA FLJ76436 PE=2 SV=1
P49720	Proteasome subunit beta type-3 GN=PSMB3 PE=1 SV=2
Q8N7G1	Purine nucleoside phosphorylase PE=2 SV=1
A8K335	cDNA FLJ76254, highly similar to Homo sapiens gamma-glutamyl hydrolase (GGH), mRNA PE=2 SV=1
A0A024RBB7	Nucleosome assembly protein 1-like 1, isoform CRA_a GN=NAP1L1 PE=3 SV=1
A0A023T6R1	Mago nashi protein GN=FLJ10292 PE=2 SV=1
P50990	T-complex protein 1 subunit theta GN=CCT8 PE=1 SV=4
E9PRY8	Elongation factor 1-delta GN=EEF1D PE=1 SV=1
A0A024R7B7	CDC37 cell division cycle 37 homolog (S. cerevisiae), isoform CRA_a GN=CDC37 PE=4 SV=1
P52888	Thimet oligopeptidase GN=THOP1 PE=1 SV=2
Q76LA1	CSTB protein GN=CSTB PE=2 SV=1
X6R8A1	Carboxypeptidase GN=CTSA PE=1 SV=1
A0A0S2Z4Z9	Non-POU domain containing octamer-binding isoform 1 (Fragment) GN=NONO PE=2 SV=1
A6XND9	Beta-2-microglobulin PE=2 SV=1
P15018	Leukemia inhibitory factor GN=LIF PE=1 SV=1
Q9BY76	Angiopoietin-related protein 4 GN=ANGPTL4 PE=1 SV=2
B4DRM3	cDNA FLJ54492, highly similar to Eukaryotic translation initiation factor 4B PE=2 SV=1
P26583	High mobility group protein B2 GN=HMGB2 PE=1 SV=2
A0A0K0K1L8	Epididymis secretory sperm binding protein Li 129m GN=HEL-S-129m PE=2 SV=1
P13500	C-C motif chemokine 2 GN=CCL2 PE=1 SV=1
Q16881	Thioredoxin reductase 1, cytoplasmic GN=TXNRD1 PE=1 SV=3
B7Z9B1	cDNA FLJ52398, highly similar to Cadherin-13 PE=2 SV=1
A0A024RDR0	High-mobility group box 1, isoform CRA_a GN=HMGB1 PE=4 SV=1
P17096	High mobility group protein HMG-I/HMG-Y GN=HMGA1 PE=1 SV=3
D9IAI1	Epididymis secretory protein Li 34 GN=PEBP1 PE=2 SV=1
Q5U000	Cathepsin Z PE=2 SV=1
B7Z6S9	Glucosylceramidase PE=2 SV=1
B3KUY2	Prostaglandin E synthase 3 (Cytosolic), isoform CRA_c GN=PTGES3 PE=2 SV=1
A2A274	Aconitate hydratase, mitochondrial GN=ACO2 PE=1 SV=1
Q96D15	Reticulocalbin-3 GN=RCN3 PE=1 SV=1
O75942	Major prion protein GN=PRNP PE=3 SV=2
P49588	Alanine--tRNA ligase, cytoplasmic GN=AARS PE=1 SV=2
B4DPD5	Ubiquitin thioesterase PE=2 SV=1
Q09028	Histone-binding protein RBBP4 GN=RBBP4 PE=1 SV=3
Q4LE58	eIF4G1 variant protein (Fragment) GN=EIF4G1 variant protein PE=2 SV=1

B4DHQ3	Phosphoserine aminotransferase PE=2 SV=1
P50454	Serpin H1 GN=SERPINH1 PE=1 SV=2
Q59FR8	Galectin (Fragment) PE=2 SV=1
P36957	Dihydrolipoyllysine-residue succinyltransferase component of 2-oxoglutarate dehydrogenase complex, mitochondrial GN=DLST PE=1 SV=4
O14980	Exportin-1 GN=XPO1 PE=1 SV=1
A0A024R608	Ribosomal protein, large, P1, isoform CRA_a GN=RPLP1 PE=3 SV=1
P35318	ADM GN=ADM PE=1 SV=1
B4DPV7	cDNA FLJ54534, highly similar to Homo sapiens cysteinyl-tRNA synthetase (CARS), transcript variant 3, mRNA PE=2 SV=1
A0A1C7CYX9	Dihydropyrimidinase-related protein 2 GN=DPYSL2 PE=1 SV=1
Q15631	Translin GN=TSN PE=1 SV=1
Q15019	Septin-2 GN=SEPT2 PE=1 SV=1
Q9HAV7	GrpE protein homolog 1, mitochondrial GN=GRPEL1 PE=1 SV=2
Q6EMK4	Vasorin GN=VASN PE=1 SV=1
Q8NBJ5	Procollagen galactosyltransferase 1 GN=COLGALT1 PE=1 SV=1
P30084	Enoyl-CoA hydratase, mitochondrial GN=ECHS1 PE=1 SV=4
P38159	RNA-binding motif protein, X chromosome GN=RBMX PE=1 SV=3
Q00839	Heterogeneous nuclear ribonucleoprotein U GN=HNRNPU PE=1 SV=6
Q13011	Delta(3,5)-Delta(2,4)-dienoyl-CoA isomerase, mitochondrial GN=ECH1 PE=1 SV=2
Q8NBS9	Thioredoxin domain-containing protein 5 GN=TXNDC5 PE=1 SV=2
P19957	Elafin GN=PI3 PE=1 SV=3
Q15366	Poly(rC)-binding protein 2 GN=PCBP2 PE=1 SV=1
B4DT31	cDNA FLJ53425, highly similar to Far upstream element-binding protein 1 PE=2 SV=1
P23396	40S ribosomal protein S3 GN=RPS3 PE=1 SV=2
Q9H1E3	Nuclear ubiquitous casein and cyclin-dependent kinase substrate 1 GN=NUCKS1 PE=1 SV=1
A2A2V4	Vascular endothelial growth factor A GN=VEGFA PE=1 SV=1
Q969H8	Myeloid-derived growth factor GN=MYDGF PE=1 SV=1
A0A087X1N8	Serpin B6 GN=SERPINB6 PE=1 SV=1
A0A087X1Z3	Proteasome activator complex subunit 2 GN=PSME2 PE=1 SV=1
P30048	Thioredoxin-dependent peroxide reductase, mitochondrial GN=PRDX3 PE=1 SV=3
P62316	Small nuclear ribonucleoprotein Sm D2 GN=SNRPD2 PE=1 SV=1
O75396	Vesicle-trafficking protein SEC22b GN=SEC22B PE=1 SV=4
Q15436	Protein transport protein Sec23A GN=SEC23A PE=1 SV=2
F8W031	Uncharacterized protein (Fragment) PE=1 SV=1
P34897	Serine hydroxymethyltransferase, mitochondrial GN=SHMT2 PE=1 SV=3
Q7Z7Q8	C-C motif chemokine GN=MCP-3 PE=3 SV=1
A0A087WYR3	Tumor protein D54 GN=TPD52L2 PE=1 SV=1
A0A140VJL8	Inositol-1-monophosphatase PE=2 SV=1
Q9UHV9	Prefoldin subunit 2 GN=PFDN2 PE=1 SV=1
Q8TDQ7	Glucosamine-6-phosphate isomerase 2 GN=GNPDA2 PE=1 SV=1
A0A087WUZ3	Spectrin beta chain GN=SPTBN1 PE=1 SV=1
B2R960	cDNA, FLJ94230, highly similar to Homo sapiens thioredoxin-like 1 (TXNL1), mRNA PE=2 SV=1
P17987	T-complex protein 1 subunit alpha GN=TCP1 PE=1 SV=1
Q15907	Ras-related protein Rab-11B GN=RAB11B PE=1 SV=4
O43175	D-3-phosphoglycerate dehydrogenase GN=PHGDH PE=1 SV=4
P98066	Tumor necrosis factor-inducible gene 6 protein GN=TNFAIP6 PE=1 SV=2
B9EKV4	Aldehyde dehydrogenase 9 family, member A1 GN=ALDH9A1 PE=2 SV=1
Q99584	Protein S100-A13 GN=S100A13 PE=1 SV=1
A0A0U1RRM4	Polypyrimidine tract-binding protein 1 GN=PTBP1 PE=1 SV=1
Q96AY3	Peptidyl-prolyl cis-trans isomerase FKBP10 GN=FKBP10 PE=1 SV=1
Q9UNZ2	NSFL1 cofactor p47 GN=NSFL1C PE=1 SV=2
P07814	Bifunctional glutamate/proline--tRNA ligase GN=EPRS PE=1 SV=5
Q00688	Peptidyl-prolyl cis-trans isomerase FKBP3 GN=FKBP3 PE=1 SV=1
P31153	S-adenosylmethionine synthase isoform type-2 GN=MAT2A PE=1 SV=1
O15347	High mobility group protein B3 GN=HMGB3 PE=1 SV=4
Q59G24	Activated RNA polymerase II transcription cofactor 4 variant (Fragment) PE=2 SV=1

D3DRR6	Inter-alpha (Globulin) inhibitor H2, isoform CRA_a GN=ITIH2 PE=4 SV=1
P0C0S5	Histone H2A.Z GN=H2AFZ PE=1 SV=2
J3KQ18	D-dopachrome decarboxylase GN=DDT PE=1 SV=1
P58546	Myotrophin GN=MTPN PE=1 SV=2
P05362	Intercellular adhesion molecule 1 GN=ICAM1 PE=1 SV=2
A8K6Q8	cDNA FLJ75881, highly similar to Homo sapiens transferrin receptor (p90, CD71) (TFRC), mRNA PE=2 SV=1
Q9P0L0	Vesicle-associated membrane protein-associated protein A GN=VAPA PE=1 SV=3
P41091	Eukaryotic translation initiation factor 2 subunit 3 GN=EIF2S3 PE=1 SV=3
Q53FN7	BZW1 protein variant (Fragment) PE=2 SV=1
P62495	Eukaryotic peptide chain release factor subunit 1 GN=ETF1 PE=1 SV=3
G3V180	Dipeptidyl peptidase 3 GN=DPP3 PE=1 SV=1
P25398	40S ribosomal protein S12 GN=RPS12 PE=1 SV=3
P62906	60S ribosomal protein L10a GN=RPL10A PE=1 SV=2
Q13344	Fus-like protein (Fragment) PE=2 SV=1
P09496	Clathrin light chain A GN=CLTA PE=1 SV=1
D3DPK5	SH3 domain binding glutamic acid-rich protein like 3, isoform CRA_a (Fragment) GN=SH3BGRL3 PE=4 SV=1
G5EA09	Syndecan binding protein (Syntenin), isoform CRA_a GN=SDCBP PE=1 SV=1
Q9HCU0	Endosialin GN=CD248 PE=1 SV=1
Q96FQ6	Protein S100-A16 GN=S100A16 PE=1 SV=1
P14866	Heterogeneous nuclear ribonucleoprotein L GN=HNRNPL PE=1 SV=2
P62304	Small nuclear ribonucleoprotein E GN=SNRPE PE=1 SV=1
Q99471	Prefoldin subunit 5 GN=PFDN5 PE=1 SV=2
Q5T9B7	Adenylate kinase isoenzyme 1 GN=AK1 PE=1 SV=1
Q9UN70	Protocadherin gamma-C3 GN=PCDHGC3 PE=1 SV=1
Q15257	Serine/threonine-protein phosphatase 2A activator GN=PTPA PE=1 SV=3
Q9Y3F4	Serine-threonine kinase receptor-associated protein GN=STRAP PE=1 SV=1
I3L0A0	HCG2044781 GN=TMEM189-UBE2V1 PE=3 SV=1
Q8NI22	Multiple coagulation factor deficiency protein 2 GN=MCFD2 PE=1 SV=1
A8K8U1	cDNA FLJ77762, highly similar to Homo sapiens cullin-associated and neddylation-dissociated 1 (CAND1), mRNA PE=2 SV=1
Q9H2G2	STE20-like serine/threonine-protein kinase GN=SLK PE=1 SV=1
B4E3D4	cDNA FLJ56293, highly similar to Transmembrane glycoprotein NMB PE=2 SV=1
B2RCP7	cDNA, FLJ96197, highly similar to Homo sapiens connective tissue growth factor (CTGF), mRNA PE=2 SV=1
P55786	Puromycin-sensitive aminopeptidase GN=NPEPPS PE=1 SV=2
Q59F66	DEAD box polypeptide 17 isoform p82 variant (Fragment) PE=2 SV=1
P28072	Proteasome subunit beta type-6 GN=PSMB6 PE=1 SV=4
A0A024RD93	Phosphoribosylaminoimidazole carboxylase, phosphoribosylaminoimidazole succinocarboxamide synthetase, isoform CRA_c GN=PAICS PE=3 SV=1
V9HWJ1	Glutathione synthetase GN=HEL-S-64p PE=2 SV=1
P61457	Pterin-4-alpha-carbinolamine dehydratase GN=PCBD1 PE=1 SV=2
Q59FG9	Chondroitin sulfate proteoglycan 2 (Versican) variant (Fragment) PE=2 SV=1
A0A024RDE5	Ras-GTPase activating protein SH3 domain-binding protein 2, isoform CRA_a GN=G3BP2 PE=4 SV=1
Q7Z4X0	MO25-like protein PE=2 SV=1
B2RBH2	cDNA, FLJ95508, highly similar to Homo sapiens 5'-nucleotidase, ecto (CD73) (NT5E), mRNA PE=2 SV=1
P14324	Farnesyl pyrophosphate synthase GN=FDPS PE=1 SV=4
H0YBX6	Ubiquitin-conjugating enzyme E2 variant 2 (Fragment) GN=UBE2V2 PE=1 SV=1
B0YIW6	Archain 1, isoform CRA_a GN=ARCN1 PE=1 SV=1
P35268	60S ribosomal protein L22 GN=RPL22 PE=1 SV=2
Q9Y547	Intraflagellar transport protein 25 homolog GN=HSPB11 PE=1 SV=1
Q07666	KH domain-containing, RNA-binding, signal transduction-associated protein 1 GN=KHDRBS1 PE=1 SV=1
F6WQW2	Ran-specific GTPase-activating protein GN=RANBP1 PE=1 SV=1
P27487	Dipeptidyl peptidase 4 GN=DPP4 PE=1 SV=2
P54136	Arginine--tRNA ligase, cytoplasmic GN=RARS PE=1 SV=2
P29373	Cellular retinoic acid-binding protein 2 GN=CRABP2 PE=1 SV=2
Q9BS26	Endoplasmic reticulum resident protein 44 GN=ERP44 PE=1 SV=1
Q9NR30	Nucleolar RNA helicase 2 GN=DDX21 PE=1 SV=5
Q9Y2W1	Thyroid hormone receptor-associated protein 3 GN=THRAP3 PE=1 SV=2

B4E284	cDNA FLJ51188, highly similar to N-acetylglucosamine-6-sulfatase (EC3.1.6.14) PE=2 SV=1
P17936	Insulin-like growth factor-binding protein 3 GN=IGFBP3 PE=1 SV=2
Q13443	Disintegrin and metalloproteinase domain-containing protein 9 GN=ADAM9 PE=1 SV=1
P61956	Small ubiquitin-related modifier 2 GN=SUMO2 PE=1 SV=3
P28838	Cytosol aminopeptidase GN=LAP3 PE=1 SV=3
Q5U043	S-(hydroxymethyl)glutathione dehydrogenase PE=2 SV=1
P49721	Proteasome subunit beta type-2 GN=PSMB2 PE=1 SV=1
P06132	Uroporphyrinogen decarboxylase GN=UROD PE=1 SV=2
M0QXB4	Coatomer protein complex, subunit epsilon, isoform CRA_g GN=COPE PE=1 SV=1
Q9UHL4	Dipeptidyl peptidase 2 GN=DPP7 PE=1 SV=3
Q6FIE5	PHP14 protein GN=PHP14 PE=2 SV=1
A0A024R5H0	Barrier to autointegration factor 1, isoform CRA_a GN=BANF1 PE=4 SV=1
J3KQ69	DNA replication licensing factor MCM3 GN=MCM3 PE=1 SV=2
Q9GZX9	Twisted gastrulation protein homolog 1 GN=TWSG1 PE=1 SV=1
A0A024R7U6	DNA helicase GN=MCM4 PE=3 SV=1
Q8WXX5	DnaJ homolog subfamily C member 9 GN=DNAJC9 PE=1 SV=1
O14737	Programmed cell death protein 5 GN=PDCD5 PE=1 SV=3
O75937	DnaJ homolog subfamily C member 8 GN=DNAJC8 PE=1 SV=2
Q59ET0	Glucan, branching enzyme 1 variant (Fragment) PE=2 SV=1
O00193	Small acidic protein GN=SMAP PE=1 SV=1
P05204	Non-histone chromosomal protein HMG-17 GN=HMGN2 PE=1 SV=3
A0A024R6W2	Nudix (Nucleoside diphosphate linked moiety X)-type motif 21, isoform CRA_a GN=NUDT21 PE=4 SV=1
P05556	Integrin beta-1 GN=ITGB1 PE=1 SV=2
B2R802	cDNA, FLJ93681, highly similar to Homo sapiens small nuclear ribonucleoprotein polypeptide A (SNRPA), mRNA PE=2 SV=1
A0A087WUT6	Eukaryotic translation initiation factor 5B GN=EIF5B PE=1 SV=1
J9R021	Eukaryotic translation initiation factor 3 subunit A GN=eIF3a PE=2 SV=1
B7Z1Z5	cDNA FLJ57265, highly similar to Neurotrimin PE=2 SV=1
Q14696	LDLR chaperone MESD GN=MESDC2 PE=1 SV=2
A8K0I8	cDNA FLJ76207, highly similar to Homo sapiens delta-notch-like EGF repeat-containing transmembrane (DNER), mRNA PE=2 SV=1
Q9NZM1	Myoferlin GN=MYOF PE=1 SV=1
P42126	Enoyl-CoA delta isomerase 1, mitochondrial GN=ECI1 PE=1 SV=1
A8K7D9	Importin subunit alpha PE=2 SV=1
P41227	N-alpha-acetyltransferase 10 GN=NAA10 PE=1 SV=1
P35659	Protein DEK GN=DEK PE=1 SV=1
Q13740	CD166 antigen GN=ALCAM PE=1 SV=2
Q6NZI2	Caveolae-associated protein 1 GN=CAVIN1 PE=1 SV=1
B4DVA7	Beta-hexosaminidase PE=2 SV=1
B2R6P3	cDNA, FLJ93047, highly similar to Homo sapiens matrix metallopeptidase 14 (membrane-inserted) (MMP14), mRNA PE=2 SV=1
O75643	U5 small nuclear ribonucleoprotein 200 kDa helicase GN=SNRNP200 PE=1 SV=2
Q8TDJ5	Tyrosine-protein kinase receptor GN=TFG/ALK fusion PE=2 SV=1
G8JLH6	Tetraspanin (Fragment) GN=CD9 PE=1 SV=1
A0A0A6YYL6	Protein RPL17-C18orf32 GN=RPL17-C18orf32 PE=3 SV=1
A0A024RAV0	Branched-chain-amino-acid aminotransferase GN=BCAT1 PE=3 SV=1
P18827	Syndecan-1 GN=SDC1 PE=1 SV=3
P13797	Plastin-3 GN=PLS3 PE=1 SV=4
Q59HH3	Trifunctional purine biosynthetic protein adenosine-3 (Fragment) PE=2 SV=1
O60462	Neuropilin-2 GN=NRP2 PE=1 SV=2
V9HW90	Epididymis luminal protein 75 GN=HEL-75 PE=2 SV=1
J3QRS3	Myosin regulatory light chain 12A GN=MYL12A PE=1 SV=1
P43034	Platelet-activating factor acetylhydrolase IB subunit alpha GN=PAFAH1B1 PE=1 SV=2
Q12792	Twinfilin-1 GN=TWF1 PE=1 SV=3
A8K8D9	Glucose-6-phosphate 1-dehydrogenase PE=2 SV=1
Q15182	Small nuclear ribonucleoprotein-associated protein GN=SNRPB PE=2 SV=1
O60888	Protein CutA GN=CUTA PE=1 SV=2

Q4LE36	ACLY variant protein (Fragment) GN=ACLY variant protein PE=2 SV=1
Q3MI39	HNRPA1 protein (Fragment) GN=HNRPA1 PE=2 SV=1
E9PF18	Hydroxyacyl-coenzyme A dehydrogenase, mitochondrial GN=HADH PE=1 SV=2
Q9NR45	Sialic acid synthase GN=NANS PE=1 SV=2
Q86UA3	Chromosome 12 open reading frame 10 GN=C12orf10 PE=1 SV=1
O14561	Acyl carrier protein, mitochondrial GN=NDUFAB1 PE=1 SV=3
Q59GY2	Ribosomal protein L4 variant (Fragment) PE=2 SV=1
P51572	B-cell receptor-associated protein 31 GN=BCAP31 PE=1 SV=3
D3DWY7	Prefoldin subunit 3 GN=VBP1 PE=3 SV=1
Q13442	28 kDa heat- and acid-stable phosphoprotein GN=PDAP1 PE=1 SV=1
Q53G42	mRNA decapping enzyme variant (Fragment) PE=2 SV=1
E7ETY2	Treacle protein GN=TCOF1 PE=1 SV=1
Q96FJ2	Dynein light chain 2, cytoplasmic GN=DYNLL2 PE=1 SV=1
X6R4W8	BUB3-interacting and GLEBS motif-containing protein ZNF207 GN=ZNF207 PE=1 SV=1
P30049	ATP synthase subunit delta, mitochondrial GN=ATP5D PE=1 SV=2
A0A024RAM4	Microtubule-associated protein 1B, isoform CRA_b GN=MAP1B PE=4 SV=1
B1AKJ5	Nardilysin GN=NRDC PE=1 SV=1
B4DIS3	Dpy-30-like protein, isoform CRA_b GN=LOC84661 PE=2 SV=1
Q9NYU2	UDP-glucose:glycoprotein glucosyltransferase 1 GN=UGGT1 PE=1 SV=3
Q10713	Mitochondrial-processing peptidase subunit alpha GN=PMPCA PE=1 SV=2
P78539	Sushi repeat-containing protein SRPX GN=SRPX PE=1 SV=1
P13473	Lysosome-associated membrane glycoprotein 2 GN=LAMP2 PE=1 SV=2
O60869	Endothelial differentiation-related factor 1 GN=EDF1 PE=1 SV=1
Q8WWM7	Ataxin-2-like protein GN=ATXN2L PE=1 SV=2
P60866	40S ribosomal protein S20 GN=RPS20 PE=1 SV=1
Q59GM9	Alpha-1,4 glucan phosphorylase (Fragment) PE=2 SV=1
A8MXP9	Matrin-3 GN=MATR3 PE=1 SV=1
Q86TI2	Dipeptidyl peptidase 9 GN=DPP9 PE=1 SV=3
P46109	Crk-like protein GN=CRKL PE=1 SV=1
P62424	60S ribosomal protein L7a GN=RPL7A PE=1 SV=2
Q14204	Cytoplasmic dynein 1 heavy chain 1 GN=DYNC1H1 PE=1 SV=5
A0A087WTY6	Neuroblastoma suppressor of tumorigenicity 1 GN=NBL1 PE=1 SV=1
Q53FA7	Quinone oxidoreductase PIG3 GN=TP53I3 PE=1 SV=2
Q9Y3C6	Peptidyl-prolyl cis-trans isomerase-like 1 GN=PPIL1 PE=1 SV=1
B2RAU5	Sorting nexin PE=2 SV=1
P62314	Small nuclear ribonucleoprotein Sm D1 GN=SNRPD1 PE=1 SV=1
Q7Z6J2	General receptor for phosphoinositides 1-associated scaffold protein GN=GRASP PE=1 SV=1
A8K4W0	40S ribosomal protein S3a GN=RPS3A PE=2 SV=1
P13674	Prolyl 4-hydroxylase subunit alpha-1 GN=P4HA1 PE=1 SV=2
P49458	Signal recognition particle 9 kDa protein GN=SRP9 PE=1 SV=2
Q9Y678	Coatomer subunit gamma-1 GN=COPG1 PE=1 SV=1
P62633	Cellular nucleic acid-binding protein GN=CNBP PE=1 SV=1
Q4VC31	Coiled-coil domain-containing protein 58 GN=CCDC58 PE=1 SV=1
P61160	Actin-related protein 2 GN=ACTR2 PE=1 SV=1
K7EQ73	DnaJ homolog subfamily C member 7 (Fragment) GN=DNAJC7 PE=1 SV=1
A0A087WUB9	Beta-catenin-like protein 1 GN=CTNNBL1 PE=1 SV=1
P62280	40S ribosomal protein S11 GN=RPS11 PE=1 SV=3
O43776	Asparagine--tRNA ligase, cytoplasmic GN=NARS PE=1 SV=1
A6NFX8	ADP-sugar pyrophosphatase GN=NUDT5 PE=1 SV=1
Q549M8	CLE7 GN=C14orf166 PE=2 SV=1
B2RB23	cDNA, FLJ95265, highly similar to Homo sapiens acetyl-Coenzyme A acyltransferase 2 (mitochondrial 3-oxoacyl-Coenzyme A thiolase) (ACAA2), nuclear gene encoding mitochondrial protein, mRNA PE=2 SV=1
A0A024R2W4	Dystroglycan 1 (Dystrophin-associated glycoprotein 1), isoform CRA_a GN=DAG1 PE=4 SV=1
A2RUR9	Coiled-coil domain-containing protein 144A GN=CCDC144A PE=2 SV=1
B1AKZ4	Phosphoprotein enriched in astrocytes 15, isoform CRA_a GN=PEA15 PE=2 SV=1
P62081	40S ribosomal protein S7 GN=RPS7 PE=1 SV=1
Q5T5C7	Serine--tRNA ligase, cytoplasmic GN=SARS PE=1 SV=1

P09661	U2 small nuclear ribonucleoprotein A' GN=SNRPA1 PE=1 SV=2
P14854	Cytochrome c oxidase subunit 6B1 GN=COX6B1 PE=1 SV=2
P25774	Cathepsin S GN=CTSS PE=1 SV=3
B2RD79	cDNA, FLJ96494, highly similar to Homo sapiens ubiquitin specific peptidase 14 (tRNA-guanine transglycosylase) (USP14), mRNA PE=2 SV=1
P05023	Sodium/potassium-transporting ATPase subunit alpha-1 GN=ATP1A1 PE=1 SV=1
P49773	Histidine triad nucleotide-binding protein 1 GN=HINT1 PE=1 SV=2
A4D2P0	Ras-related C3 botulinum toxin substrate 1 (Rho family, small GTP binding protein Rac1) GN=RAC1 PE=2 SV=1
H7BY58	Protein-L-isoaspartate O-methyltransferase GN=PCMT1 PE=1 SV=1
Q08945	FACT complex subunit SSRP1 GN=SSRP1 PE=1 SV=1
A0A024R814	Ribosomal protein L7, isoform CRA_a GN=RPL7 PE=4 SV=1
Q9NU22	Midasin GN=MDN1 PE=1 SV=2
O14929	Histone acetyltransferase type B catalytic subunit GN=HAT1 PE=1 SV=1
Q9NUJ1	Mycophenolic acid acyl-glucuronide esterase, mitochondrial GN=ABHD10 PE=1 SV=1
P20290	Transcription factor BTF3 GN=BTF3 PE=1 SV=1
Q7LBR1	Charged multivesicular body protein 1b GN=CHMP1B PE=1 SV=1
Q5JR94	40S ribosomal protein S8 GN=RPS8 PE=2 SV=1
O60664	Perilipin-3 GN=PLIN3 PE=1 SV=3
E5RIM7	Copper transport protein ATOX1 GN=ATOX1 PE=1 SV=1
B4DNE1	cDNA FLJ52708, highly similar to Basigin PE=2 SV=1
F5H8L0	Rab GTPase-activating protein 1-like GN=RABGAP1L PE=1 SV=1
Q5T6V5	UPF0553 protein C9orf64 GN=C9orf64 PE=1 SV=1
A0A140VJZ4	Ubiquitin carboxyl-terminal hydrolase PE=2 SV=1
P05198	Eukaryotic translation initiation factor 2 subunit 1 GN=EIF2S1 PE=1 SV=3
Q4VCS5	Angiomotin GN=AMOT PE=1 SV=1
Q15043	Zinc transporter ZIP14 GN=SLC39A14 PE=1 SV=3
Q12904	Aminoacyl tRNA synthase complex-interacting multifunctional protein 1 GN=AIMP1 PE=1 SV=2
A0A140VJJ2	S-formylglutathione hydrolase GN=ESD PE=2 SV=1
Q13601	KRR1 small subunit processome component homolog GN=KRR1 PE=1 SV=4
B4DLN1	cDNA FLJ60124, highly similar to Mitochondrial dicarboxylate carrier PE=2 SV=1
Q4KWH8	1-phosphatidylinositol 4,5-bisphosphate phosphodiesterase eta-1 GN=PLCH1 PE=1 SV=1
B3KWI4	cDNA FLJ43122 fis, clone CTONG3003737, highly similar to Leucine-rich repeat-containing protein 15 PE=2 SV=1
P12109	Collagen alpha-1(VI) chain GN=COL6A1 PE=1 SV=3